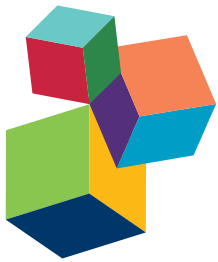


MOLECULAR AND BIOTECHNOLOGICAL ADVANCEMENTS IN *HYPERICUM* SPECIES

EDITED BY: Gregory Franklin, Ludger Beerhues and Eva Čellárová

PUBLISHED IN: Frontiers in Plant Science



Frontiers Copyright Statement

© Copyright 2007-2017 Frontiers Media SA. All rights reserved.

All content included on this site, such as text, graphics, logos, button icons, images, video/audio clips, downloads, data compilations and software, is the property of or is licensed to Frontiers Media SA ("Frontiers") or its licensees and/or subcontractors. The copyright in the text of individual articles is the property of their respective authors, subject to a license granted to Frontiers.

The compilation of articles constituting this e-book, wherever published, as well as the compilation of all other content on this site, is the exclusive property of Frontiers. For the conditions for downloading and copying of e-books from Frontiers' website, please see the Terms for Website Use. If purchasing Frontiers e-books from other websites or sources, the conditions of the website concerned apply.

Images and graphics not forming part of user-contributed materials may not be downloaded or copied without permission.

Individual articles may be downloaded and reproduced in accordance with the principles of the CC-BY licence subject to any copyright or other notices. They may not be re-sold as an e-book.

As author or other contributor you grant a CC-BY licence to others to reproduce your articles, including any graphics and third-party materials supplied by you, in accordance with the Conditions for Website Use and subject to any copyright notices which you include in connection with your articles and materials.

All copyright, and all rights therein, are protected by national and international copyright laws.

The above represents a summary only. For the full conditions see the Conditions for Authors and the Conditions for Website Use.

ISSN 1664-8714

ISBN 978-2-88945-117-3

DOI 10.3389/978-2-88945-117-3

About Frontiers

Frontiers is more than just an open-access publisher of scholarly articles: it is a pioneering approach to the world of academia, radically improving the way scholarly research is managed. The grand vision of Frontiers is a world where all people have an equal opportunity to seek, share and generate knowledge. Frontiers provides immediate and permanent online open access to all its publications, but this alone is not enough to realize our grand goals.

Frontiers Journal Series

The Frontiers Journal Series is a multi-tier and interdisciplinary set of open-access, online journals, promising a paradigm shift from the current review, selection and dissemination processes in academic publishing. All Frontiers journals are driven by researchers for researchers; therefore, they constitute a service to the scholarly community. At the same time, the Frontiers Journal Series operates on a revolutionary invention, the tiered publishing system, initially addressing specific communities of scholars, and gradually climbing up to broader public understanding, thus serving the interests of the lay society, too.

Dedication to Quality

Each Frontiers article is a landmark of the highest quality, thanks to genuinely collaborative interactions between authors and review editors, who include some of the world's best academicians. Research must be certified by peers before entering a stream of knowledge that may eventually reach the public - and shape society; therefore, Frontiers only applies the most rigorous and unbiased reviews.

Frontiers revolutionizes research publishing by freely delivering the most outstanding research, evaluated with no bias from both the academic and social point of view.

By applying the most advanced information technologies, Frontiers is catapulting scholarly publishing into a new generation.

What are Frontiers Research Topics?

Frontiers Research Topics are very popular trademarks of the Frontiers Journals Series: they are collections of at least ten articles, all centered on a particular subject. With their unique mix of varied contributions from Original Research to Review Articles, Frontiers Research Topics unify the most influential researchers, the latest key findings and historical advances in a hot research area! Find out more on how to host your own Frontiers Research Topic or contribute to one as an author by contacting the Frontiers Editorial Office: researchtopics@frontiersin.org

MOLECULAR AND BIOTECHNOLOGICAL ADVANCEMENTS IN *HYPERICUM* SPECIES

Topic Editors:

Gregory Franklin, Institute of Plant Genetics of the Polish Academy of Sciences, Poland
Ludger Beerhues, Braunschweig University of Technology, Germany
Eva Čellárová, Pavol Jozef Šafárik University in Košice, Slovakia



Hypericum perforatum inflorescence with flowers and floral buds containing characteristic hypericin glands at the periphery of petals.
Cover photo by G. Franklin

Hypericum is an important genus of the family Hypericaceae and includes almost 500 species of herbs, shrubs and trees. Being the home for many important bioactive compounds, these species have a long traditional value as medicinal plants. Currently, several species of this genus have been used in ailments as knowledge-based medicine in many countries. In the recent past, several pharmacological studies have been performed using crude extracts to evaluate the traditional knowledge. Results of those studies have revealed that *Hypericum* extract exert multiple pharmacological properties including antidepressant, antimicrobial, antitumor and wound healing effects. Phytochemical analyses revealed that these species produce a broad

spectrum of valuable compounds, mainly naphthodianthrones (hypericin and pseudohypericin), phloroglucinols (hyperforin and adhyperforin), flavonoids (hyperoside, rutin and quercitrin), benzophenones/xanthones (garcinol and gambogic acid), and essential oils.

Noticeably, *Hypericum perforatum* extracts have been used to treat mild to moderate depression from ancient to present times and the antidepressant efficacy of *Hypericum* extracts has been attributed to its hyperforin content, which is known to inhibit the re-uptake of aminergic transmitters such as serotonin and noradrenaline into synaptic nerve endings. Neurodegenerative diseases and inflammatory responses are also linked with Reactive Oxygen Species (ROS) production. A wide range of flavonoids present in *Hypericum* extracts, namely, rutin, quercetin, and quercitrin exhibit antioxidant/free radical scavenging activity. Hypericin, beside hyperforin, is the active molecule responsible for the antitumor ability of *Hypericum* extracts and is seen as a potent candidate to treat brain tumor. Recent attempts of using hypericin in patients with recurrent malignant brain tumors showed promising results. Collectively, *Hypericum* species contain multiple bioactive constituents, suggesting their potential to occupy a huge portion of the phytomedicine market.

Today, studies on medicinal plants are rapidly increasing because of the search for new active molecules, and for the improvement in the production of plants and molecules for the herbal pharmaceutical industries. In the post genomic era, application of molecular biology and genomic tools revolutionized our understanding of major biosynthetic pathways, phytochemistry and pharmacology of *Hypericum* species and individual compounds. This special issue mainly focuses on the recent advancements made in the understanding of biosynthetic pathways, application of biotechnology, molecular biology, genomics, pharmacology and related areas.

Citation: Franklin, G., Beerhues, L., Čellárová, E., eds. (2017). Molecular and Biotechnological Advancements in *Hypericum* Species. Lausanne: Frontiers Media. doi: 10.3389/978-2-88945-117-3

Table of Contents

- 06 Editorial: Molecular and Biotechnological Advancements in Hypericum Species**
Gregory Franklin, Ludger Beerhues and Eva Čellárová
- 08 Conservation Strategies in the Genus Hypericum via Cryogenic Treatment**
Katarína Bruňáková and Eva Čellárová
- 20 Neuroprotective Activity of Hypericum perforatum and Its Major Components**
Ana I. Oliveira, Cláudia Pinho, Bruno Sarmento and Alberto C. P. Dias
- 35 Hypericin in the Light and in the Dark: Two Sides of the Same Coin**
Zuzana Jendželovská, Rastislav Jendželovský, Barbora Kuchárová and Peter Fedoročko
- 55 Phloroglucinol and Terpenoid Derivatives from Hypericum cistifolium and H. galoides (Hypericaceae)**
Sara L. Crockett, Olaf Kunert, Eva-Maria Pferschy-Wenzig, Melissa Jacob, Wolfgang Schuehly and Rudolf Bauer
- 63 Polar Constituents and Biological Activity of the Berry-Like Fruits from Hypericum androsaemum L.**
Giovanni Caprioli, Alessia Alunno, Daniela Beghelli, Armandodoriano Bianco, Massimo Bramucci, Claudio Frezza, Romilde Iannarelli, Fabrizio Papa, Luana Quassinti, Gianni Sagratini, Bruno Tirillini, Alessandro Venditti, Sauro Vittori and Filippo Maggi
- 75 Metabolic Profile and Root Development of Hypericum perforatum L. In vitro Roots under Stress Conditions Due to Chitosan Treatment and Culture Time**
Elisa Brasili, Alfredo Miccheli, Federico Marini, Giulia Praticò, Fabio Sciubba, Maria E. Di Cocco, Valdir Filho Cechinel, Noemi Tocci, Alessio Valletta and Gabriella Pasqua
- 87 Molecular Cloning and Expression Analysis of hyp-1 Type PR-10 Family Genes in Hypericum perforatum**
Katja Karppinen, Emese Derzsó, Laura Jaakola and Anja Hohtola
- 99 Crystal Structure of Hyp-1, a Hypericum perforatum PR-10 Protein, in Complex with Melatonin**
Joanna Sliwiak, Zbigniew Dauter and Mariusz Jaskolski
- 109 Benzophenone Synthase and Chalcone Synthase Accumulate in the Mesophyll of Hypericum perforatum Leaves at Different Developmental Stages**
Asma K. Belkheir, Mariam Gaid, Benye Liu, Robert Hänsch and Ludger Beerhues
- 118 Alternative Oxidase Gene Family in Hypericum perforatum L.: Characterization and Expression at the Post-germinative Phase**
Isabel Velada, Hélia G. Cardoso, Carla Ragonezi, Amaia Nogales, Alexandre Ferreira, Vera Valadas and Birgit Arnholdt-Schmitt

134 Comparative Transcriptome Reconstruction of Four *Hypericum* Species Focused on Hypericin Biosynthesis

Miroslav Soták, Odeta Czeranková, Daniel Klein, Zuzana Jurčacková, Ling Li and Eva Čellárová

148 A Perspective on *Hypericum perforatum* Genetic Transformation

Weina Hou, Preeti Shakya and Gregory Franklin



Editorial: Molecular and Biotechnological Advancements in *Hypericum* Species

Gregory Franklin^{1*}, Ludger Beerhues² and Eva Čellárová³

¹ Department of Integrative Plant Biology, Institute of Plant Genetics of the Polish Academy of Sciences, Poznań, Poland,

² Institute of Pharmaceutical Biology, Technische Universität Braunschweig, Braunschweig, Germany, ³ Department of Genetics, Institute of Biology and Ecology, Faculty of Science, Pavol Jozef Šafárik University, Košice, Slovakia

Keywords: *Hypericum* spp., biosynthetic pathways, biotechnology, genomics, pharmacology

The Editorial on the Research Topic

Molecular and Biotechnological Advancements in *Hypericum* Species

This special issue on the genus *Hypericum* (family *Hypericaceae*) consists of 12 articles focusing on recent advancements related to biosynthetic pathways, biotechnology, molecular biology, genomics, pharmacology, and related disciplines. *Hypericum* is well-known for its medicinal properties. There are about 487 *Hypericum* spp., which are distributed across every continent except Antarctica. Although the Mediterranean basin was recognized as a hot spot for *Hypericum* spp., Asian and American continents also account for significant biodiversity of *Hypericum* spp., out of which many are endemic.

Due to anthropogenic exploitation and unsustainable collection practice, several *Hypericum* spp. have become critically rare/endangered and at least 17 species are included in the International Union for Conservation of Nature red list. The review by Bruňáková and Čellárová deals with conservation strategies in the genus *Hypericum* via cryogenic treatment. The authors discuss the recent advances in the conventional two-step and vitrification-based cryopreservation techniques in relation to the recovery rate and biosynthetic capacity of *Hypericum* spp. Moreover, freezing tolerance as a necessary pre-condition for successful post-cryogenic recovery of *Hypericum* spp. is proposed.

Within the genus, *H. perforatum* is the most important species, which is used in the treatment of mild to moderate depression since ancient times. Oliveira et al. comprehensively review the neuroprotective properties of *H. perforatum* in terms of its main biologically active compounds, their chemistry, pharmacological activities, drug interactions, and adverse reactions. They also discuss how *H. perforatum* extracts and its major components protect neurons from toxic insults either directly or indirectly as antioxidants.

Hypericin is a characteristic constituent of the genus *Hypericum*, which can countervail complex diseases. Importantly, hypericin is a natural photosensitizing pigment and its photoexcitation properties are under intensive investigation with the aim of its utilization as a fluorescent diagnostic tool and anti-cancer agent for photodynamic therapy (PDT). Jendželovská et al. review the benefits of photoactivated and non-activated hypericin in preclinical and clinical applications focusing on multidrug resistance mechanisms.

The demand of the pharmaceutical industry for new active compounds and drug leads is the driving force behind phytochemical analysis of medicinal plants. Although *H. perforatum* is phytochemically well-characterized, several other species still need to be elucidated for their chemical profiles. Crockett et al. report the isolation of a new phloroglucinol derivative, 1-(6-hydroxy-2,4-dimethoxyphenyl)-2-methyl-1-propanone, from *H. cistifolium* and *H. galiodoides*. They

OPEN ACCESS

Edited and reviewed by:
Kazuki Saito,
RIKEN Center for Sustainable
Resource Science and Chiba
University, Japan

***Correspondence:**
Gregory Franklin
fgre@lgr.poznan.pl

Specialty section:

This article was submitted to
Plant Metabolism and Chemodiversity,
a section of the journal
Frontiers in Plant Science

Received: 03 October 2016
Accepted: 26 October 2016
Published: 11 November 2016

Citation:

Franklin G, Beerhues L and
Čellárová E (2016) Editorial: Molecular
and Biotechnological Advancements
in *Hypericum* Species.
Front. Plant Sci. 7:1687.
doi: 10.3389/fpls.2016.01687

also detect two new terpenoid derivatives in the later species. In addition to establishing the chemical structures of these new compounds using 2D-NMR spectroscopy and mass spectrometry, the *in vitro* antimicrobial and anti-inflammatory activities are analyzed.

In spite of many reports on the phytochemistry of *H. androsaemum*, the chemical composition of its red berries remained unknown. The study by Caprioli et al. reveals that a new tetraoxigenated-type xanthone is responsible for the red color of the berries. In addition, the authors observe high amounts of phenolic compounds in the red berries and show their cytotoxicity in human tumor cell lines.

Changes in the metabolome of *H. perforatum* root cultures in response to time of culture and chitosan treatment are reported by Brasili et al. For example, increases in biomass correlated with increases in phenolic compounds, such as xanthones including brasili xanthone B. Histological studies reveal that chitosan-treated roots undergo marked swelling of the root apex, which is mainly due to hypertrophy of the first two sub-epidermal layers and periclinal cell divisions.

Although hypericin is a major active compound of *Hypericum* spp., identified and characterized a century back, its biosynthesis is still not fully understood. *HYP1* was thought to be involved in the final stages of hypericin biosynthesis. There are two articles on *HYP1* in this issue. Karppinen et al. show that expression of *HYP1* genes is relatively high in leaves and increases after wounding and treatment with defense signaling compounds, such as salicylic and abscisic acids. *HYP1* transcripts mainly occur in vascular tissues of root and stem and in leaves in mesophyll cells as well, as indicated by *in situ* hybridization.

Sliwiak et al. report the crystal structure of the *HYP1* protein in complex with melatonin. This structure confirms the conserved protein fold and the presence of three unusual ligand-binding sites, two of which are in internal chambers, while the third one is formed as an invagination of the protein surface. Altogether, the studies of *HYP1* reveal that it may be involved, as a *PR10* gene, in plant defense responses, however, its role in hypericin biosynthesis is questioned.

Xanthones and flavonoids also contribute to the medicinal effects of *H. perforatum* extracts. Belkheir et al. analyze regulatory mechanisms underlying flavonoid and xanthone biosyntheses in *H. perforatum* using immunofluorescence localization and histochemical staining (Belkheir et al.). They observe that both chalcone synthase (CHS) and benzophenone synthase (BPS) are located in the mesophyll. However, CHS and BPS accumulate at different stages of leaf development, with CHS accumulation occurring earlier than that of BPS. Flavonoids were detected in the mesophyll, indicating that the sites of biosynthesis and accumulation coincide.

Transcriptome profiling is an unbiased approach for gene prediction. Using this tool, Velada et al. identify and characterize the alternative oxidase (AOX) protein family of *H. perforatum* during post-germination seedling development. Analysis of the intron regions of *AOX* reveals miRNA coding sequence polymorphisms with functional significance in regulation of gene expression at the posttranscriptional level. Moreover, the presence of a transposable element in the *AOX* intron region with still unidentified function is elucidated by *in silico* analysis.

Besides *H. perforatum*, *de novo* transcriptome profiling of four other *Hypericum* spp. namely, *H. annulatum*, *H. tomentosum*, *H. kalmianum*, and *H. androsaemum*, is reported by Soták et al. for the first time. The next-generation sequencing-acquired data provide a source of information for subsequent studies toward the search for candidate genes involved in the biosynthesis of hypericin. Comparative analysis of differentially expressed genes between hypericin-producing and hypericin-lacking species and tissues reveals more than 100 differentially upregulated contigs. These include new sequences with homology to octaketide synthase and enzymes that catalyze phenolic oxidative coupling reactions.

In spite of the recent advances in the understanding of biosynthesis-related gene expression in *H. perforatum*, functional genomics is still in its infancy, mainly due to its recalcitrance against *Agrobacterium tumefaciens* and low efficiencies of the reported transformation methods. Hou et al. propose a perspective on possible ways to achieve efficient transformation and hence improvements *via* metabolic engineering.

AUTHOR CONTRIBUTIONS

All the authors contributed equally to the manuscript, and approved it for publication.

ACKNOWLEDGMENTS

We acknowledge all the authors for their insightful contributions, reviewers for their valuable comments and Frontiers editorial team for their constant support.

Conflict of Interest Statement: The authors declare that the research was conducted in the absence of any commercial or financial relationships that could be construed as a potential conflict of interest.

Copyright © 2016 Franklin, Beerhues and Čellárová. This is an open-access article distributed under the terms of the Creative Commons Attribution License (CC BY). The use, distribution or reproduction in other forums is permitted, provided the original author(s) or licensor are credited and that the original publication in this journal is cited, in accordance with accepted academic practice. No use, distribution or reproduction is permitted which does not comply with these terms.



Conservation Strategies in the Genus *Hypericum* via Cryogenic Treatment

Katarína Bruňáková* and Eva Čellárová

Institute of Biology and Ecology, Faculty of Science, Pavol Jozef Šafárik University in Košice, Košice, Slovakia

In the genus *Hypericum*, cryoconservation offers a strategy for maintenance of remarkable biodiversity, emerging from large inter- and intra-specific variability in morphological and phytochemical characteristics. Long-term cryostorage thus represents a proper tool for preservation of genetic resources of endangered and threatened *Hypericum* species or new somaclonal variants with unique properties. Many representatives of the genus are known as producers of pharmacologically important polyketides, namely naphthodianthrone and phloroglucinols. As a part of numerous *in vitro* collections, the nearly cosmopolitan *Hypericum perforatum* – Saint John's wort – has become a suitable model system for application of biotechnological approaches providing an attractive alternative to the traditional methods for secondary metabolite production. The necessary requirements for efficient cryopreservation include a high survival rate along with an unchanged biochemical profile of plants regenerated from cryopreserved cells. Understanding of the processes which are critical for recovery of *H. perforatum* cells after the cryogenic treatment enables establishment of cryopreservation protocols applicable to a broad number of *Hypericum* species. Among them, several endemic taxa attract a particular attention due to their unique characteristics or yet unrevealed spectrum of bioactive compounds. In this review, recent advances in the conventional two-step and vitrification-based cryopreservation techniques are presented in relation to the recovery rate and biosynthetic capacity of *Hypericum* spp. The pre-cryogenic treatments which were identified to be crucial for successful post-cryogenic recovery are discussed. Being a part of genetic predisposition, the freezing tolerance as a necessary precondition for successful post-cryogenic recovery is pointed out. Additionally, a beneficial influence of cold stress on modulating naphthodianthrone biosynthesis is outlined.

OPEN ACCESS

Edited by:

Thomas Vogt,
Leibniz Institute of Plant Biochemistry,
Germany

Reviewed by:

Courtney M. Starks,
Sequoia Sciences, USA
Raquel Folgado,
The Huntington Library, Art
Collections and Botanical Gardens,
USA

*Correspondence:

Katarína Bruňáková
katarina.brunakova@upjs.sk

Specialty section:

This article was submitted to
Plant Metabolism
and Chemodiversity,
a section of the journal
Frontiers in Plant Science

Received: 26 February 2016

Accepted: 11 April 2016

Published: 27 April 2016

Citation:

Bruňáková K and Čellárová E (2016)
Conservation Strategies in the Genus
Hypericum via Cryogenic Treatment.

Front. Plant Sci. 7:558.

doi: 10.3389/fpls.2016.00558

INTRODUCTION

The genus *Hypericum* encompassing nearly 500 species is one of the most diverse plant genera in the angiosperms (Nürk and Blattner, 2010). The representatives of the genus are distributed throughout nearly all continents with an exception of the poles, deserts, and low-altitude tropical areas (Robson, 1996). Among them, *H. perforatum* L. is a perennial herb native to Europe, originally used as a folk remedy for the treatment of depression. The 'Saint John's wort' became a subject of the British Herbal Pharmacopoeia (1996), the American Herbal Pharmacopoeia (1997),

and the European Pharmacopoeia (2008) representing the most important and commercially recognized species of the genus *Hypericum*. Several groups of bioactive natural products involving naphthodianthrones (e.g., hypericin and pseudohypericin), phloroglucinols (e.g., hyperforin and adhyperforin), flavonol derivatives (e.g., isoquercitrin and hyperoside), biflavones, xanthones, proanthocyanidins, amino acids, and essential oil constituents have been identified in the crude drug of *H. perforatum*, *Hyperici herba* (Nahrstedt and Butterweck, 1997).

In the context of traditional medicine, recent pharmacological research confirmed anti-depressive activity and dermatological applications of *H. perforatum* extracts based on their antimicrobial (Saddiqe et al., 2010) and anti-inflammatory (Wölfle et al., 2014) effects. Recently, the naphthodianthrones hypericin and pseudohypericin have received most of the attention due to their antitumour (Penjweini et al., 2013) and antiviral (Arumugam et al., 2013) action. These compounds are concentrated in the clusters of specialized cells, so-called 'dark nodules' distributed on the leaves, stems, petals, sepals, stamens and ovules of many *Hypericum* taxa (Crockett and Robson, 2011). In plants, hypericin and its congener pseudohypericin are present mainly in protoforms which convert to their naphthodianthrone analogs upon activation by visible light (Rückert et al., 2006). It has been reported that the biosynthetic potential of *Hypericum* plants grown in outdoor conditions depends on environmental factors, mainly temperature and water stress (Gray et al., 2003; Zobayed et al., 2005). Therefore, development of *in vitro* culture systems for perspective biotechnological applications is indispensable.

In addition to the clonal multiplication procedure designed for *H. perforatum* (Čellárová et al., 1992), the *in vitro* systems involving both, other wide-spread cosmopolitan, and endemic *Hypericum* species have been established for *H. erectum* (Yazaki and Okuda, 1990), *H. canariense* (Mederos Molina, 1991), *H. brasiliense* (Cardoso and de Oliveira, 1996), *H. balearicum*, *H. glandulosum*, *H. tomentosum*, *H. maculatum*, *H. olympicum*, and *H. bithynicum* (Kartnig et al., 1996), *H. foliosum* (Moura, 1998), *H. patulum* (Baruah et al., 2001), *H. androsaemum* (Guedes et al., 2003), *H. heterophyllum* (Ayan and Cirak, 2006), *H. polyanthemum* (Bernardi et al., 2007), *H. hookerianum* (Padmesh et al., 2008), *H. mysorense*, (Shilpashree and Ravishankar Rai, 2009), *H. frondosum*, *H. kalmianum*, and *H. galoides* (Meyer et al., 2009), *H. triquetrifolium* (Karakas et al., 2009; Oluk and Orhan, 2009), *H. retusum* (Namli et al., 2010), *H. rumeliacum*, *H. tetrapterum*, *H. calycinum* (Danova, 2010), *H. richeri* ssp. *transsilvanicum*, *H. umbellatum* A. Kern. (Coste et al., 2012), *H. cordatum* (Vell. Conc.) N. Robson (Bianchi and Chu, 2013), etc.

While the advances in the tissue culture techniques enable breeding of plants outside their natural habitat, genetic and epigenetic alterations increasing the potential of somaclonal variability in course of serial sub-culturing may occur (Kaepller et al., 2000). To provide a more reliable method for saving rare or endangered taxa, the cryogenic storage represents a safe and long-term conservation opportunity for the plant specimens. In principle, the plant parts are stored in liquid

nitrogen (LN) below the glass transition temperature (T_g) at which the cell solution forms an amorphous solid or glass. Under these conditions, the sample is biologically inert and can be maintained indefinitely (Bajaj, 1995; Butler and Pegg, 2012). Nevertheless, the viability of cells, tissues and organs is retained and regeneration of plants is acquired after the rewarming.

Despite an extensive research has been exerted in the course of total synthesis and semi-synthesis of hypericin (Huang et al., 2014), numerous *in vitro* studies indicate that shoot cultures of *Hypericum* spp. remain a reliable source of hypericin and other unique constituents. Concurrently, various cryopreservation techniques have been successfully applied to several *Hypericum* species maintaining the genetic features and biosynthetic capacity in the regenerated shoot tissues. Therefore, the aim of this review is to summarize advances in long-term conservation of *Hypericum* species by cryopreservation, and to analyze the relation between endo- and exogenous preconditions and post-cryogenic recovery and ability to synthesize unique bioactive substances.

CRYOPRESERVATION APPROACHES AND POST-CRYOGENIC RECOVERY IN *HYPERICUM* SPP.

The earliest cryopreservation study of *H. perforatum* was carried out by Kimáková et al. (1996) who used the encapsulation-dehydration procedure. Isolated apical meristems were encapsulated in calcium alginate beads, osmoprotected with sugar solutions, partially dehydrated by exposure to a flow of dry air and directly immersed into LN. The first protocols resulted in a low, up to 10% survival (Kimáková et al., 1996), and the need for a more efficient long-term storage method for *H. perforatum* has arisen.

Later both, the controlled cooling and vitrification-based techniques were adopted for the cryoconservation of *Hypericum* spp. In principle, the controlled (slow) cooling method is based on crystallization induced in the extracellular solution, thus the probability of intracellular ice formation is minimized (Karlsson and Toner, 1996). Generally, the plants or their parts are pre-cultured under special conditions, such as low but above-freezing temperature, treated with growth regulators and/or osmotically active compounds, and exposed to cryoprotectants. Subsequently, the explants are subjected to slow cooling rates reaching the homogenous ice nucleation at -35 to -40°C and plunged into LN (Benson, 2008). After cryostorage, the samples are thawed rapidly in a 40 to 50°C water bath, and the cryoprotective chemicals are removed from the system by dilution. Usually, the incubation of explants in 1.2 mol L^{-1} sucrose for 10 to 20 min at room temperature is used (Shibli et al., 2006). On the other hand, the vitrification procedure performed by a direct immersion of the specimen into LN (so-called 'rapid cooling') is based on the complete elimination of ice formation throughout the entire sample (Karlsson and Toner, 1996). The protocols are based on cell dehydration performed by a standard sequence of steps involving: (i) exposure of the

explants to diluted vitrification solutions such as loading solution (LS; Nishizawa et al., 1993), (ii) dehydration of the tissues performed by highly concentrated mixtures of cryoprotective agents, mostly plant vitrification solutions like the PVS2 or PVS3 (Nishizawa et al., 1993), (iii) direct immersion into LN, and (iv) rapid re-warming of the specimens followed by unloading phase at which the cryoprotectants are washed out of the cells.

Applying the controlled cooling for cryopreservation of *H. perforatum*, the isolated shoot tips were pre-treated with mannitol or abscisic acid (ABA), loaded in a mixture of cryoprotectants containing 10% (w/v) glycerol, 20% (w/v) sucrose, and 10% (w/v) ME₂SO and exposed to gradual decrease of temperature (Urbanová et al., 2002, 2006). Cooling was performed in the programmed freezer up to -40°C followed by immersion into LN. The recovery after re-warming varied between 10 and 50% depending on genotype. Using the modified cooling regime by Skyba et al. (2011), the mean recovery varying in the interval from 0 to 34% was positively influenced by lowering the cooling rate.

According to the vitrification protocol published by Skyba et al. (2010), *H. perforatum* shoot tips were exposed to two different additives, either sucrose or ABA. Subsequently, the explants were loaded with LS and transferred to the cryovials filled with the PVS2 or PVS3. The samples were equilibrated on ice and immersed into LN. The post-cryogenic survival was strongly influenced by the genotype varying in the range from 0 to 62%. However, the highest mean recovery rate of 27% was recorded for the explants treated with ABA and subsequently exposed to PVS3. A comparably extensive variation of the mean recovery of *H. perforatum* shoot tips cryoconserved by a vitrification-based method was observed by Petijová et al. (2012). Despite a significant genotype-dependent variation, the post-cryogenic survival linearly increased in relation to extension of the pre-culture time. For instance, the prolongation of incubation of ABA-treated *H. perforatum* shoot tips in PVS3 resulted in an increased mean regeneration percentage reaching the maximum between 59 and 71% (Bruňáková et al., 2011).

Beside the 'model' *H. perforatum*, the vitrification protocol published by Skyba et al. (2010) was adopted for cryopreservation of *H. rumeliacum*, a species restricted to the Balkan region (Danova et al., 2012), and further optimized for several *Hypericum* species of different provenances involving both, cosmopolitan and endemic representatives. The post-cryogenic variation in the regeneration rate of *H. humifusum* L., *H. kalmianum* L., *H. annulatum* Moris., *H. tomentosum* L., *H. tetrapterum* Fries., *H. pulchrum* L., *H. kouytchense* Lév., *H. canariense* L., and *H. rumeliacum* Boiss., was in the interval from 0 to 26% corresponding well with the inter-specific variability in the tolerance against freezing stress (Petijová et al., 2014).

For *H. richeri* ssp. *transsilvanicum* and *H. umbellatum*, the rare species found in Transylvania, a droplet-vitrification procedure was designed by Coste et al. (2012). Combining a ME₂SO-droplet method and vitrification, less time for cryoprotection of the explants in a very small volume of cryoprotectant mixture is needed and substantially higher rate of cooling is

achieved (Schäfer-Menuhr et al., 1997; Sakai and Engelmann, 2007). The post-thaw recovery depended on the type of explant, sucrose concentration in the pre-culture medium, and dehydration duration. The highest mean post-cryogenic recovery was obtained for axillary buds reaching 68 and 71% for *H. richeri* and *H. umbellatum*, respectively.

Moreover, the slow cooling and vitrification methods were successfully applied for undifferentiated cell suspensions of *H. perforatum* in order to find a possible relation between the ability of cryoprotective mixtures to decrease temperature of crystallization (TC) and post-cryogenic viability of the cells (Mišianiková et al., 2016). Among 13 cryoprotectant mixtures, the highest portion of viable cells exceeding 58% was reached in *H. perforatum* cell suspensions cryoprotected with a mixture containing 30% (w/v) sucrose, 30% (w/v) glycerol, 5% (w/v) ME₂SO, and 20% (w/v) ethylene glycol and subjected to a controlled cooling. The results revealed that the highest cell viability correlated well with the lowest TC.

Although the genotypic effects may have contributed to the broad variation in post-thaw survival of *Hypericum* spp., the regrowth capability of cryopreserved meristems and cell suspensions was predominantly influenced by the pre-cryogenic sample preparation, mainly by the type and duration of the pre-culture, cryoprotection and rate of cooling.

CRUCIAL PROCESSES FOR SUCCESSFUL CRYOPRESERVATION IN *HYPERICUM* SPP.

The efficient cryopreservation protocol comprises series of procedures which enable the meristematic tissues to maintain the viability and regeneration potential at the freezing temperatures. Several processes have been recognized to be essential for post-cryogenic survival of *H. perforatum*. Among them, modifications of anatomical, morphological, and physiological status of the shoot apices in relation to the current views on structural changes occurring in the meristematic cells during preconditioning, and freezing-induced dehydration and phase transitions during cooling are further discussed.

Effects of Preconditioning on Morphology, Anatomy, and Physiology of Shoot-Tip Meristems

The optimal preconditioning of plants or their parts is crucial for post-cryogenic survival and commonly includes chemical pre-treatments with exogenously applied growth regulators, osmotically active chemicals such as saccharides or saccharide alcohols, or subjecting to cold acclimation prior to cryopreservation. Among the plant growth regulators, ABA is involved in mediation of many physiological processes including adaptation responses to environmental conditions comprising dehydration, osmotic, and cold stresses (Chandler and Robertson, 1994). The increasing level of endogenous ABA was observed under dehydration stress and cold treatment performed by the exposure of *in vitro* grown *H. perforatum*

plants to subfreezing temperature of -4°C (Bruňáková et al., 2015). The phytohormone ABA is known to induce freezing resistance in many winter annual and perennial species (Bravo et al., 1998) and was shown to contribute to acquisition of the tolerance to cryopreservation, e.g., in *Triticum aestivum* L. (Chen et al., 1985), *Bromus inermis* Leyss., *Medicago sativa* L. (Reaney and Gusta, 1987), *Daucus carota* L. (Thierry et al., 1999), etc. Despite the exogenously applied ABA did not improve the resistance of *H. perforatum* shoot tips against freezing, the 3.5-fold higher level of endogenous ABA was observed in the freezing-tolerant *H. perforatum*, when compared with freezing-sensitive *H. canariense* (Bruňáková et al., 2015).

The pre-treatment with ABA is routinely used in numerous plant cryopreservation protocols (Buritt, 2008; Lu et al., 2009). In *Hypericum* cryoprotection, ABA is obviously used alone (Skyba et al., 2012) or in combination with sucrose or mannitol (Coste et al., 2012; Danova et al., 2012; Petijová et al., 2012). In addition to morphological alterations of the apical meristems expressed by an increased size of the meristematic domes (Petijová et al., 2012), a significant dehydration effect of ABA during preconditioning of *H. perforatum* shoot tips has been observed. Pre-treatment with ABA substantially affected total water content in the cryoprotected shoot apices. When compared to the hydration level of explants excised from cold acclimated plants, the shoot tips isolated from non-acclimated control group that was pre-cultured with ABA displayed a significantly lower amount of both, the total water content and the proportion of so-called ‘freezable water’ that can crystallize (Bruňáková et al., 2011). According to Danova (2010) and Danova et al. (2012), the extended period of ABA pre-treatment positively influenced the physiological state of *H. rumeliacum* apical meristems by decreasing the level of oxidative stress which consequently improved the status of plants regenerated after cryopreservation.

Despite ambiguous interactions between the plant hormone ABA and cytokinins have been reported in higher plants (Reed, 1993; Baldwin et al., 1998; Tran et al., 2007; Werner and Schmülling, 2009), the supplementation of media with cytokinins is usually used for micropropagation of plant material prior to cryopreservation and for increasing the proportion of proliferating meristems (Helliot et al., 2002). In *Hypericum* spp. cryopreservation, shoot tips are isolated from individually growing *Hypericum* plants or clusters of shoots developing on BA-enriched medium (Urbanová et al., 2006; Coste et al., 2012; Danova et al., 2012; Petijová et al., 2012). However, a long-acting influence of BA may reduce the post-cryogenic survival by alterations of morphological and physiological status of meristematic tissues (Petijová et al., 2012).

The longitudinal sections of *H. perforatum* shoot apices isolated from clusters revealed the meristematic domes uncovered with the leaf primordia which normally protect the proliferating cells from injurious effects of cryoprotectants. On the other side, the normal position of the first pair of leaves, compactness of apical meristem and increased mitotic activity in meristematic regions have been attributed to a synergic effect of ABA and BA during the short-term pre-culture of

shoot tips before cryoprotection treatment (Petijová et al., 2012). In contrast, long-term culturing of the donor plants on media enriched with BA negatively influenced survival of shoot tips after cryopreservation. The results indicate that long-term exposure of plants to BA can delay the protective effect of ABA during preconditioning; the reduced tolerance to low temperatures may be attributed to the morphological alterations of the shoot tip meristematic regions isolated from BA-induced clusters of shoots (Petijová et al., 2012). At the physiological level, ABA and BA antagonized each other influencing the hydration status of *H. perforatum* meristems during preconditioning; while a massive accumulation of water was observed in the shoot tips solely pre-cultured in liquid BA-enriched media, the pre-treatment of explants with ABA resulted in a subsequent dehydration (Bruňáková et al., 2011).

Along with the phytohormone ABA, the saccharides are involved in freezing tolerance (FT) and are often used for preparation of plant tissues before cryopreservation (Dereuddre and Tannoury, 1995; Cho et al., 2000; Pâques et al., 2002; Shatnawi et al., 2011). Exogenously applied sucrose is known to stimulate the saccharide metabolism (Gibson, 2000), stabilize the native conformation of biomembranes (Kent et al., 2010), and reduce the proportion of freezable water which is important for minimizing the injurious effects of ice formation (Fang et al., 2009). Besides, the saccharides and saccharide alcohols prevent cryoinjury by increasing the osmotic pressure and reducing the size of treated cells (Cho et al., 2000). In *Hypericum* cryopreservation, pre-treatment of the explants in media supplemented with high concentration of sucrose was proved to be essential for post-cryogenic survival of *H. richeri* and *H. umbellatum* (Coste et al., 2012). In this work, incubation of the shoot apices or axillary buds in PVS2 without any previous saccharide pre-treatment of the explants did not provide enough protection from the lethal effects of LN. Using sucrose and mannitol as the pre-culture agents improved the post-thaw survival of *H. perforatum* shoot tips (Urbanová et al., 2002; Skyba et al., 2010, 2011; Coste et al., 2012; Petijová et al., 2012).

Another way in which the cryoprotectant agents relate to restoration of the viability after cryostorage is preservation of the photosynthetic apparatus. The protective roles of ABA and mannitol were confirmed on cellular and sub-cellular levels by transmission electron microscopy (TEM) in *H. perforatum* and *H. rumeliacum* plants (Stoyanova-Koleva et al., 2013, 2015). The effect of ABA depended on the species, duration of the treatment and cooling regime; in *H. perforatum*, although no deleterious post-cryogenic alterations of the internal membrane system under 10-day pre-treatment with ABA followed by slow-cooling were seen, the destruction of the chloroplast membranes was observed after vitrification (Stoyanova-Koleva et al., 2015). In *H. rumeliacum* shoot tips cryopreserved by vitrification, an optimal efficacy of the ABA-treatment was already observed after 3-day pre-culture (Stoyanova-Koleva et al., 2013). The positive influence of the saccharide alcohol mannitol was represented by the native structure of chloroplasts with a typical thylakoid arrangement in the palisade parenchyma cells

in post-cryogenic *H. perforatum* regenerants (Stoyanova-Koleva et al., 2013).

Natural resistance to low temperatures can also be induced by subjection of plants to low but above-freezing temperatures in the process of cold acclimation (Thomashow, 1999). Cold-induced tolerance to freezing is effective in the preparation of plant meristems before cryopreservation, and was successfully applied for preconditioning treatment of the species originated from temperate regions such as *Cynodon dactylon* L. or *Allium sativum* L. (Volk et al., 2004; Reed et al., 2006). As a consequence, the anatomical and physiological changes of the tissues induced by cold-acclimation contributed to overall plant tolerance to cryogenic temperatures (Thinh, 1997). It has been observed that the exposure of freezing-tolerant *H. perforatum* or *H. rumeliacum* to a temperature of 4°C could entirely substitute the effect of ABA treatment during the pre-cryogenic phase (Bruňáková et al., 2014). These conditions resulted in almost 45% recovery in *H. perforatum* and led to 1.3- and 1.5-fold increase in the content of ABA in *H. perforatum* and *H. canariense* (Bruňáková et al., 2015). As a part of a cold-acclimation response, the elevated level of endogenous ABA is in agreement with a slight and transient increase of the hormone level in the model *Arabidopsis thaliana* (Lang et al., 1994).

Apart from the external factors that were shown to improve the cold tolerance of several *Hypericum* species, the physiological status of meristematic tissues *in vitro* was significantly influenced by genetically predetermined endogenous processes. The results of Skyba et al. (2011) predicted an existence of seasonal biorhythm altering the capability of *H. perforatum* shoot tips to regenerate after cryopreservation. In this study, the recovery rates depended on the season when the cryopreservation of *in vitro* initiated seedlings was performed; the nearly fourfold higher post-thaw regeneration favored the shoot tips cryopreserved in March in comparison with October.

Freezing-Induced Dehydration and Phase Transitions during Cooling

Apart from the preconditioning, the cooling step represents a component of cryopreservation protocol having a significant influence on post-cryogenic cell survival. In the slowly cooled systems, the explants are exposed to specific cooling rates ranging from 0.1 to 5.0°C min⁻¹ when ice is primarily initiated in the extracellular space. The optimal rate of freezing is a vital point of this process at which the damaging osmotic effects are minimized and the mechanical destruction of the cell organelles induced by intracellular crystallization is prevented (Kartha and Engelmann, 1994). Before subjection to freezing, the tissues are dehydrated by incubation in media supplemented with highly concentrated osmoregulants such as sucrose. However, for retaining the post-cryogenic viability, the plant organs should contain an optimal content of water varying from 0.25 to 0.4 g H₂O g⁻¹ dry weight (DW; Vertucci et al., 1991; Dereuddre and Kaminski, 1992; Wesley-Smith et al., 1992).

The analyses performed by differential scanning calorimetry (DSC) showed that the amount of freezable water in the shoot tips of *H. perforatum* which were cryoprotected with the mixture

consisting of 10% (w/v) glycerol, 10% (w/v) ME₂SO and 0.5 mol L⁻¹ sucrose for 60 min remained high referring to 52% (3.05 g H₂O g⁻¹ DW; Skyba et al., 2011). In the partially hydrated biological systems such as seeds or embryos containing more than 0.25 g freezable H₂O g⁻¹ DW, the cooling velocity is known to critically affect post-cryogenic survival (Liebo and Mazur, 1971; Vertucci, 1989). Lowering the rates of cooling in the interval from 0.1 to 2.0°C min⁻¹, the post-cryogenic recovery of *H. perforatum* shoot tips increased, reaching maximum of 34% at 0.3°C min⁻¹ (Skyba et al., 2011). At the lower cooling rates, the improved survival of *H. perforatum* meristems corresponded well with the significantly higher compactness of cryopreserved apical domes when compared to disintegrated meristematic tissues of the shoot tips cooled at higher velocities. Based on the analyses of thermal gradients in the cryovials, the positive effect of slower cooling predominantly consisted in more homogenous temperature distribution in the sample during freezing resulting in a moderate and non-invasive growth of ice crystals.

The positive influence of the prolonged dehydration interval related to the lower rates of cooling was also confirmed for mesophyll cells of *H. perforatum* plants regenerated after cryopreservation (Stoyanova-Koleva et al., 2013). TEM analyses revealed the increasing protective effect of mannitol at lower cooling velocities. The pre-treatments of *H. perforatum* with 0.3 mol L⁻¹ mannitol followed by the cryoprotection and cooling at 0.2°C min⁻¹ resulted in a sustentative ultrastructure of the chloroplasts and other organelles in post-cryogenic regenerants.

On the other hand, cryopreservation of plants by vitrification completely eliminates formation of ice inside and outside the cell by combination of dehydration and rapid cooling. The critical viscosity of cytoplasm, at which the ice nucleation is inhibited and an amorphous, glassy solid is formed, is achieved by subjection of the explants to highly concentrated mixtures of cryoprotectants at non-freezing temperatures (Sakai et al., 1991). Although the precise mechanism by which the cryoprotectant compounds prevent the cells from freezing injury remains ambiguous, the loading time is an essential prerequisite for post-cryogenic recovery. It is necessary to apply an adequately long period of time to achieve sufficient dehydration and penetration of cryoprotectants inside the cell (Volk and Walters, 2006). However, the tissues overexposed to vitrification solutions may be severely impaired by the toxic nature of cryoprotectant agents and excessive dehydration.

Using vitrification method, the survival of cryostored *H. perforatum* shoot tips significantly increased with the enhancing dehydration and prolongation of the loading phase. However, the maximum mean recovery rate reaching nearly 70% was reported even if the freezable water up to 0.4% of the total water content (0.005 g freezable H₂O g⁻¹ DW) was present in the cryopreserved tissues (Bruňáková et al., 2011). In meristematic cells of *H. perforatum*, the incidence of small endothermal transitions proportional up to 3.5% of freezable water (0.05 g freezable H₂O g⁻¹ DW) was shown to have no lethal effects on the post-cryogenic recovery. This observation indicates an existence of other protective mechanisms preventing the freezing injury during cryopreservation.

POST-CRYOGENIC RECOVERY IN RELATION TO FREEZING TOLERANCE IN *HYPERICUM* SPP.

Along with the influence of external factors, the genetic predetermination of cold response affecting the post-cryogenic survival within the genus *Hypericum* should be highlighted. More than 450 *Hypericum* species have been found predominantly in a variety of biotopes connected to the temperate regions and high elevation in the tropics (Crockett and Robson, 2011). Apart from dehydration, osmotic and high-temperature stresses, low temperature represents a limiting factor for the species distribution as well. In general, plants adapt to freezing by the 'tolerance' or 'avoidance' strategies (Levitt, 1980). The freezing response is a complex mechanism reflecting the biology of water and its interactions with cellular components at low temperatures (Olien and Livingston, 2006). The cold-tolerant species can overcome sudden decreases of the temperatures below 0°C and improve their ability to survive potentially damaging temperatures after cold acclimation (Levitt, 1980). During the adaptation process, plants accumulate endogenous cryoprotective substances that prevent cell injury by stabilizing the membranes and proteins under dehydration conditions, inhibiting the growth of ice crystals, preventing re-crystallization, interacting with other molecules to scavenge the reactive oxygen species (ROS), etc., (Gusta and Wisniewski, 2013). On the other hand, the freezing avoidance means that plants do not tolerate ice formation in their tissues and avoid crystallization, e.g., by supercooling.

Freezing Tolerance Based on Frost-Killing Temperature LT₅₀

The results concerning FT in the *Hypericum* genus are based on assessment of the extent of freezing injury performed by measurement of the electrolyte leakage. The FT of several *Hypericum* species was estimated according to the temperature at which 50 percent of the shoot tips were lethally damaged (LT₅₀; Petijová et al., 2014). Among the studied taxa, *H. perforatum* L. and *H. kalmianum* were proved to be the most freezing-tolerant species tolerating the temperatures up to -9°C when acclimated at 4°C for 7 days. The capacity to increase the tolerance to low temperatures depends on several factors, e.g., the temperature and regime of acclimation as well as the quantity and intensity of light (Levitt, 1980; Monroy et al., 1993). In the model *H. perforatum*, a greater enhancement of the FT was observed upon exposure to gradually decreasing temperature from 22°C up to 4°C at a rate of 1°C day⁻¹ (Bruňáková et al., 2015). Based on the three-fold depress of the LT₅₀ value, *H. perforatum* was shown to possess the protective mechanisms associated with two major components: the constitutive FT expressed by LT₅₀ = -5.6°C, and cold-acclimation capacity to increase FT reaching LT₅₀ = -16.2°C. Considering the nearly cosmopolitan distribution of *H. perforatum* and the endemic occurrence of *H. kalmianum* in the cold area of USA and Canada adjacent to the Great Lakes and the Ottawa River (Robson, 1996), the extent of FT reflected the ecological demands of these species.

While the processes associated with FT are based rather on biochemical adaptations, the freezing avoidance is more connected to physical attributes of plants which determine the preferential sites of ice accumulation through the presence or absence of ice nucleators, anatomical ice barriers, lowering the freezing point or supercooling (Gusta and Wisniewski, 2013). However, freezing avoidance is only safe under conditions of mild frost that lasts short period of time, e.g., in tropical high mountains or during the spring frost periods (Wisniewski et al., 2009). As an example for the avoidance strategy in preventing freezing injury, *H. canariense* as the endemic species of Canary Island and Madeira (Robson, 1996) could be mentioned. No significant difference in the LT₅₀ value was registered for the meristems excised from the control plants cultured under room temperature and plants exposed to 4°C showing the LT₅₀ = -2.3°C and LT₅₀ = -3.5°C, respectively (Bruňáková et al., 2015). However, *H. canariense* avoided freezing by supercooling when LT₅₀ dropped up to -8.2°C.

The natural ability to acclimate represents a suitable alternative for preconditioning of plant tissues without any side effects that may result from the incubation on media supplemented with high concentration of cryoprotectants, such as sucrose, glycerol or ME₂SO. Among herbaceous plants, cold exposure was shown to induce FT and improve the post-cryogenic recovery of cryopreserved meristems in *Solanum commersonii* (Folgado et al., 2015), *Lolium L.* and *Zoysia Willd*, grass cultivars (Chang et al., 2000), *Cynodon* spp. (Reed et al., 2006) and others. In *H. perforatum*, the exposure of plants to 4°C alone or in combination with ABA significantly enhanced the recovery of shoot tips cryopreserved by LS and PVS3 and immersed directly into LN (Bruňáková et al., 2014). It has been reported that FT represented by the LT₅₀ were concurred with the geographical distribution and post-thaw survival of *Hypericum* species involved in the study of Petijová et al. (2014). While the highest post-cryogenic regeneration of 26% was registered for *H. kalmianum* as the most freeze-tolerant species, the cold-sensitive species growing in the tropical and subtropical areas such as *H. canariense* and *H. kouytchense* did not survive the cryogenic treatment at all.

Structural and Physiological Markers of Freezing Tolerance

To obtain additional information on the FT in plants, the extent of freezing injury in terms of the integrity of photosynthetic apparatus has been intensively investigated at both, functional and structural levels (Rumich-Bayer and Krause, 1986; He et al., 2002; Su et al., 2015). Based on histological and TEM examination of the effect of freezing temperature on leaf tissue organization and chloroplast ultrastructure of seven *Hypericum* species differing in the LT₅₀ values (Petijová et al., 2014; Stoyanova-Koleva et al., 2015), no plausible connection between the predicted FT and response to cryoinjury was observed. Under the experimental conditions including a 10-day ABA preculture, cryoprotection with PVS3 and rapid cooling by direct immersion into LN, the well-developed leaves with regularly structured mesophyll in post-cryogenic regenerants of *H. annulatum*, *H. tomentosum*, *H. rumeliacum*, *H. humifusum*, and *H. kalmianum*

possessing a various extent of the FT were seen. A partial damage of chloroplasts ultrastructure was only observed in the freezing-tolerant *H. perforatum*. However, a remarkably increased thickness of the leaf assimilation parenchyma indicates a possible compensatory mechanism to overcome the low-temperature stress in that species (Stoyanova-Koleva et al., 2015).

Apart from the species-specific structural modifications observed in post-cryogenic regenerants of *Hypericum* spp., differences in the extent of oxidative damage are also documented at physiological level. Along with the natural enzymatic defense represented by ROS-scavenging enzymes that are known to accumulate in cryopreserved cells and tissues (Reed, 2014; Chen et al., 2015), the non-enzymatic physiological markers including chlorophylls, carotenoids, proline, phenolics, and flavonoids have been investigated (Skyba et al., 2010; Danova et al., 2012; Georgieva et al., 2014).

Molecular and biochemical aspects of the FT in *H. perforatum* were documented by Skyba et al. (2010, 2012). In post-cryogenic regenerants exhibiting deleterious damage of thylakoid membranes in a substantial proportion of chloroplasts, the elevated level of mRNA transcripts of catalase (*hp-cat*) and superoxide dismutase (*hp-sod*) genes followed by the increased activity of CAT and SOD enzymes were detected. In *H. rumeliacum*, markedly increased both, enzymatic and non-enzymatic antioxidant activities indicating an extensive ROS-production persisted during the regeneration phase for several months (Danova et al., 2012). While post-cryogenic regenerants of *H. rumeliacum* displayed several morphological and physiological deviations comprising shorter stems, decreased number of leaves, poorly developed root system and slower growth rate (Georgieva et al., 2014), no substantial modifications in the developmental pattern of *H. perforatum* were observed (Skyba et al., 2012). When compared with *H. rumeliacum*, the ability of *H. perforatum* to eliminate the phenotypic expression of an increased oxidative status, substantially lower LT₅₀ value and increased post-cryogenic regeneration potential (Petijová et al., 2014) indicates *H. perforatum* as more tolerant to the freezing process.

On the other hand, no significant differences in the physiological state of post-cryogenic regenerants in another *Hypericum* representative – *H. tetapterum* – were noticed (Georgieva et al., 2014). Although the lower degree of oxidative damage expressed by both, enzymatic and non-enzymatic physiological markers might suggest that the species is more tolerant to freezing, the potential of the species to withstand cryogenic treatment was much reduced when compared to *H. perforatum*. Although a successful post-cryogenic regeneration of *H. tetapterum* was reported by Georgieva et al. (2014), the recovery of this species after cryopreservation was not confirmed in our laboratory under the same experimental conditions (Bruňáková et al., 2014; Petijová et al., 2014).

Apart from the inter-specific variation in avoiding the freezing injury among the *Hypericum* species (Petijová et al., 2012), a considerable intra-specific variability in the tolerance to cryogenic treatment using the physiological markers malondialdehyde (MDA), CAT, SOD, H₂O₂, total free proline, carotenoid, and hypericins content was reported (Skyba et al.,

2010). In addition to the differences in biochemical status of the individual genotypes of *H. perforatum* before and after cryostorage, several molecular techniques including RAPD fingerprinting and VNTR minisatellite analysis were used to assess the genetic background for genotype-determined variability (Urbanová et al., 2006; Skyba et al., 2010; Skyba et al., 2012). While a marked variation within the species was repeatedly confirmed, no differences in RAPD/VNTR amplification profiles of the analyzed control and cryopreserved pairs of plantlets were reported (Skyba et al., 2012). However, the data concerning DNA primary structure analyses based on RAPD and minisatellite markers should be interpreted with regard to only a small fraction of diploid *H. perforatum* genome they reveal which is estimated to represent 0.003 and 0.001% of the genome, respectively. The genetic integrity was proved at cytogenetic level by chromosome counts and ploidy level in recovered plants of *H. perforatum* which were shown to preserve the original chromosomal number (2n = 2x = 16; Urbanová et al., 2006).

In general, an increased oxidative status referring to a cryoinjury primarily denotes a reduced tolerance of the species toward the freezing. However, activation of antioxidant mechanism might reflect genetically predetermined capability of the species to detoxify the ROS. Therefore, the overall tolerance of the plant species to low-temperature stress accompanying cryopreservation seems to be a multifactorial trait and should be evaluated in a complex manner.

IS COLD STRESS A POSSIBLE ELICITOR OF NAPHTHODIANTHRONES BIOSYNTHESIS?

In higher plants, the products of secondary metabolic pathways mediate plant adaptation to changing environment and function as the signal molecules during ontogenesis (Broun, 2005; Zhao et al., 2005). The cold response of the overwintering plants consists in three consecutive phases involving: (i) exposure to temperatures above freezing ranging from 2 to 5°C, (ii) exposition to mild freezing from -2 to -5°C, and (iii) post-freezing recovery (Li et al., 2008). As a part of cold acclimation at above-zero temperatures, plant metabolism diverts to synthesize various metabolites involving saccharides, saccharide alcohols, low-molecular weight nitrogenous compounds proline and glycine-betaine, cold-regulated (COR) proteins, antioxidant enzymes, endogenous jasmonates, phenolics, flavonoids, polyamines and other substances exhibiting cryoprotective characteristics (Ramakrishna and Ravishankar, 2011; Espevig et al., 2012; Bhandari and Nayyar, 2014). During the second phase, the full degree of tolerance is achieved by the exposition of plants to mild freezing which is commonly associated with ice formation in apoplast and dehydration of plant cells (Steponkus and Lynch, 1989). In the post-freezing phase, the plant undergoes thawing, rehydration of the cells, and restoration of cell structures and functions (Li et al., 2008).

Naphthodianthrones are secondary metabolites known to be used by plants for defense (Kainulainen et al., 1996). It has

been found that variability in the content of naphthodianthrones including hypericin, pseudohypericin and their protoforms (so-called ‘total hypericins’ or ‘total naphthodianthrones’) is determined genetically, and can be modulated by environmental parameters such as light conditions and temperature (Kirakosyan et al., 2004). In the context of temperature stress, the yield of total naphthodianthrones in *H. perforatum* was found to be positively influenced by enhancing the temperature up to 35°C (Zobayed et al., 2005). In response to low temperatures, the accumulation of hypericins was found to depend predominantly on the physiological status of the plants as well as on the cold treatment applying: (i) cold acclimation, (ii) cold-shock caused by subfreezing at -4°C and (iii) cryopreservation procedure.

With an exception of *H. tetrapterum*, the total hypericin content was unchanged or decreased upon exposure to 4°C for 7 days in several other *Hypericum* species, including *H. humifusum*, *H. annulatum*, *H. tomentosum*, and *H. rumeliacum* (Petijová et al., 2014). Exposure of plants to gradual temperature decrease significantly lowered the amount of total hypericins in the vegetative parts of the treated plants (Petijová et al., 2014; Bruňáková et al., 2015). Considering the fact that the period of cold acclimation of *H. perforatum* was shown to be accompanied by a decrease in the total water content (Bruňáková et al., 2011), the drop in the content of hypericins might be influenced by the increase in DW in the cold-acclimated plants. Similarly, during the period of cold acclimation of *Arabidopsis* ecotype Columbia plants, the rise of DW accompanied with the accumulation of sugars and proline was observed (Wanner and Junntila, 1999).

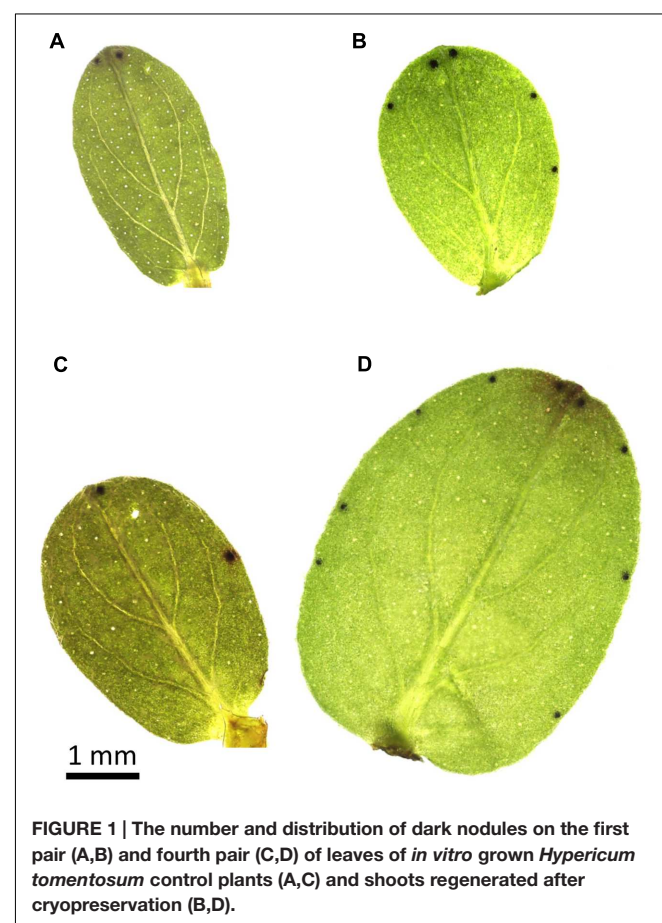
On the other side, a beneficial effect of the cold shock on the stimulation of naphthodianthrones biosynthesis in *H. perforatum* was shown by Bruňáková et al. (2015). In contrast to the unchanged level of total hypericins in cold-acclimated *H. perforatum* plants subjected to -4°C, the 48-h subfreezing treatment of the controlled, non-acclimated plants resulted in the 1.6-fold increase of the total naphthodianthrones content. In the same study, the significant enhancement of the carotenoids in non-acclimated *H. perforatum* plants serves as another evidence for the stimulatory effect of the cold-shock treatment.

It has been evidenced that total hypericins amount in the post-cryogenic regenerants depended on the physiological status of the explants entering the cryopreservation that could be manipulated by the pre-cryogenic conditions, e.g., the preconditioning with ABA or cold treatment (Danova et al., 2012). Based on the HPLC analyses, the enhanced total hypericins content was seen in *H. rumeliacum* shoots regenerated from the cryopreserved shoot tips that were exposed to ABA pre-treatment for the period of 7 days. In contrast, a shorter exposure did not show any stimulatory effect on hypericins biosynthesis (Danova et al., 2012; Bruňáková et al., 2014; Georgieva et al., 2014; Petijová et al., 2014). On the other side, the higher level of total hypericins reaching 3.1 and 1.6-fold increase, respectively, was found in *H. perforatum* and *H. rumeliacum* regenerants initiated from the cryopreserved shoot apices isolated from cold-acclimated plants (Bruňáková et al., 2014). Although the induction effect of cryo-environment on the formation of dark nodules is ambiguous (Petijová et al., 2014), an increased number of these hypericins

reservoirs on the leaves in post-cryogenic regenerants of some *Hypericum* species was evidenced (Figure 1). Considering the fact that accumulation of hypericins and total phenolics in *Hypericum* species was reported to be positively influenced by extreme conditions of the higher altitudes including low temperatures (Rahnavard et al., 2012), the enhancement of the constitutive FT by a process of cold acclimation prior to cryopreservation treatment may potent biosynthesis of these compounds as a part of natural plant defense. Along with naphthodianthrones, the cold stress was shown to enhance the flavonoids content in the post-cryogenic *H. rumeliacum* and *H. tetrapterum* regenerants (Danova et al., 2012).

CONCLUSION

Apart from the model *H. perforatum*, several *Hypericum* species involving *H. rumeliacum*, *H. kalmianum*, *H. annulatum*, *H. humifusum*, *H. tomentosum*, *H. tetrapterum*, *H. pulchrum*, *H. richeri* ssp. *Transsilvanicum*, and *H. umbellatum* have been successfully cryopreserved applying encapsulation-dehydration, droplet-vitrification, slow cooling and vitrification methods. Over the last 20 years, an intensive research has been conducted on the evaluation of critical factors affecting post-cryogenic survival. Among them, the physiological status of donor plants



as a source of shoot tips as well as external parameters, e.g., optimal dehydration of meristems in course of slow cooling and minimization of the intensity of phase transitions during vitrification were identified.

The protection effects of ABA were proved at physiological and structural levels by lowering the water content including the proportion of freezeable water, preservation of the meristematic tissue integrity and stabilization of internal membrane system of photosynthetic apparatus. Although some differences in intra- and interspecific responses in relation to the exposure time and cooling regime were observed, application of ABA, sucrose and/or mannitol during the pre-culture treatment positively influenced the recovery after cryopreservation.

On the other side, applying the uniform cryopreservation conditions to *Hypericum* species of various provenances resulting in a broad variability in post-cryogenic recovery pointed out the significance of genetically predetermined ability to resist the cryogenic injury. In the freezing-tolerant species, the exposure of donor plants to temperature of 4°C prior to cryoprotection was shown to completely substitute the effects of ABA and resulted in an improved survival and regeneration of shoots from the cryopreserved meristems. Applying a slow-cooling regime, the improved survival could be attributed to higher integrity of meristematic domes at lower rates of cooling. Using the vitrification-based protocols, the recovery rates depended on length of the loading phase which was proved to be critical for survival balancing the dehydration and toxic effects of cryoprotectants.

Apart from structural changes in the leaf tissue organization and chloroplast ultrastructure, several physiological markers indicating the freezing injury in post-cryogenic regenerants were assessed. The increased activity of ROS-scavenging enzymes CAT, SOD indicated that higher oxidative stress

persisted in regenerated shoot tissues of some *Hypericum* species in spite of the fact that no substantial alteration of the phenotype was present. The increased content of proline, green pigments, carotenoids, phenolics, and flavonoids observed in the shoot tissues regenerated from cryopreserved meristems of *Hypericum* spp. are in consent with an overall plant response to extreme abiotic conditions. Similarly, an enhanced accumulation of naphthodianthrones hypericin, pseudohypericin, and their protoforms under low-temperature stress could be considered as a part of natural mechanisms of a systemic defense in the freezing-tolerant hypericin-producing species.

In conclusion, to achieve an improved post-cryogenic survival along with maintenance of the physiological functions and biochemical potential of the post-cryogenic regenerants of *Hypericum* spp., the modifications of the cryoconservation protocol with respect to the species-specific plant responses to low-temperature treatment in the context of predetermined FT are inevitable.

AUTHOR CONTRIBUTIONS

This review was conceived and supervised by EČ. The concept of the review was worked out by both EČ and KB. Author of the manuscript draft, photographs and figure image was KB. The manuscript was revised and finally approved by EČ.

ACKNOWLEDGMENT

This work was supported by the Scientific Grant Agency of the Slovak Ministry of Education No. 1/0090/15.

REFERENCES

- American Herbal Pharmacopoeia (1997). *St. John's Wort. Hypericum perforatum. Quality Control, Analytical and Therapeutic Monograph*. Texas: American Botanical Council.
- Arumugam, M., Lulu, S., Kumari, S., and Kumari, N. V. D. (2013). Computational screening and evaluation of bioactive compounds against NS3 helicase of HCV. *Int. J. Pharm. Pharm. Sci.* 5, 370–376.
- Ayan, A.K., and Cirak, C. (2006). In vitro multiplication of *Hypericum heterophyllum* an endemic Turkish species. *Am. J. Plant Pathol.* 1, 76–81.
- Bajaj, Y.P.S. (1995) "Cryopreservation of plant cells, tissues and organ cultures for the conservation of germplasm and biodiversity," in *Biotechnology in Agriculture and Forestry 32, Cryopreservation of Plant Germplasm I*, ed. Y. P. S. Bajaj (Berlin: Springer-Verlag), 3–28.
- Baldwin, B. D., Bandara, M. S., and Tanino, K. K. (1998). Is tissue culture a viable system with which to examine environmental and hormonal regulation of cold acclimation in woody plants? *Physiol. Plant.* 102, 201–209. doi: 10.1034/j.1399-3054.1998.1020207.x
- Baruah, A., Sarma, D., Saud, J., and Singh, R.S. (2001). In vitro regeneration of *Hypericum patulum* Thunb. – a medicinal plant. *Indian J. Exp. Biol.* 39, 947–949.
- Benson, E.E. (2008). "Cryopreservation theory," in *Plant Cryopreservation: A Practical Guide*, ed. B.M. Reed (New York, NY: Springer Science + Business Media, LLC), 15–32.
- Bernardi, A. P. M., Maurmann, N., Rech, S. B., and von Poser, G. (2007). Benzopyrans in *Hypericum polyanthemum* Klotzsch ex Reichardt cultured in vitro. *Acta Physiol. Plant* 29, 165–170. doi: 10.1007/s11738-006-0021-2
- Bhandari, K., and Nayyar, H. (2014). "Low temperature stress in plants: an overview of roles of cryoprotectants in defense," in *Physiological Mechanisms and Adaptation Strategies in Plants Under Changing Environment*, Vol. 1, eds P. Ahmad, and M. R. Wani (New York, NY: Springer), 193–265.
- Bianchi, B.R., and Chu, E.P. (2013). In vitro propagation of *Hypericum cordatum* (Vell. Conc.) N. Robson (Clusiaceae) and phytochemical analysis of its secondary compounds. *Rev. Bras. Plantas Med.* 15:1. doi: 10.1590/S1516-05722013000100003.
- Bravo, L. A., Zuniga, G. E., Alberdi, M., and Corcuera, L. J. (1998). The role of ABA in freezing tolerance and cold acclimation in barley. *Physiol. Plant.* 103, 17–23. doi: 10.1034/j.1399-3054.1998.1030103.x
- British Herbal Pharmacopoeia (1996). *British Herbal Pharmacopoeia*. Surrey: British Herbal Medicine Association.
- Broun, P. (2005). Transcriptional control of flavonoid biosynthesis: a complex network of conserved regulators involved in multiple aspects of differentiation in *Arabidopsis*. *Curr. Opin. Plant Biol.* 8, 272–279. doi: 10.1016/j.pbi.2005.03.006
- Bruňáková, K., Petijová, L., and Čellárová, E. (2014). "Strategies of freezing-injury avoidance – the basis for long-term storage in *Hypericum* spp.," in *Proceeding of the 50th Anniversary Celebration, Annual Scientific Conference & AGM - Freezing Biological Time*. Kew: The Royal Botanic Gardens, 33.
- Bruňáková, K., Petijová, L., Zámečník, J., Turečková, V., and Čellárová, E. (2015). The role of ABA in the freezing injury avoidance in two *Hypericum* species differing in frost tolerance and potential to synthesize hypericins. *Plant Cell Tiss. Org.* 122, 45–56. doi: 10.1007/s11240-015-0748-9
- Bruňáková, K., Zámečník, J., Urbanová, M., and Čellárová, E. (2011). Dehydration status of ABA-treated and cold-acclimated *Hypericum perforatum* L. shoot

- tips subjected to cryopreservation. *Thermochim. Acta* 525, 62–70. doi: 10.1016/j.tca.2011.07.022
- Burritt, D. J. (2008). Efficient cryopreservation of adventitious shoots of *Begonia x erythrophylla* using encapsulation-dehydration requires pretreatment with both ABA and proline. *Plant Cell Tiss. Org.* 95, 209–215. doi: 10.1007/s11240-008-9434-5
- Butler, S., and Pegg, D. (2012). “Precision in cryopreservation – equipment and control,” in *Current Frontiers in Cryobiology*, ed. I. Katkov (Rijeka: In Tech Europe), 507–526.
- Cardoso, N. A., and de Oliveira, D. E. (1996). Tissue culture of *Hypericum brasiliense* Choisy: shoot multiplication and callus induction. *Plant Cell Tiss. Org.* 44, 91–94. doi: 10.1007/BF00048184
- Čellárová, E., Kimáková, K., and Brutovská, R. (1992). Multiple shoot formation and phenotypic changes of R0 regenerants in *Hypericum perforatum* L. *Acta Biotechnol.* 12, 445–452. doi: 10.1002/abio.370120602
- Chandler, P. M., and Robertson, M. (1994). Gene expression regulated by abscisic acid and its relation to stress tolerance. *Annu. Rev. Plant Phys.* 45, 113–141. doi: 10.1146/annurev.pp.45.060194.000553
- Chang, Y., Barker, R. E., and Reed, B. M. (2000). Cold acclimation improves recovery of cryopreserved grass (*Zoysia* and *Lolium* sp.). *CryoLetters* 21, 107–116.
- Chen, G. Q., Ren, L., Zhang, J., Reed, B. M., Zhang, D., and Shen, X. H. (2015). Cryopreservation affects ROS-induced oxidative stress and antioxidant response in *Arabidopsis* seedlings. *Cryobiology* 70, 38–47. doi: 10.1016/j.cryobiol.2014.11.004
- Chen, T. H. H., Kartha, K. K., and Gusta, L. V. (1985). Cryopreservation of wheat suspension culture and regenerable callus. *Plant Cell Tiss. Org.* 4, 101–109. doi: 10.1007/BF00042268
- Cho, J. S., Chun, S. H., Lee, S. J., Kim, I. H., and Kim D. I. (2000). Development of cell line preservation method for research and industry producing useful metabolites by plant cell culture. *Biotechnol. Bioprocess Eng.* 5, 372–378. doi: 10.1007/BF02942215
- Coste, A., Halmagyi, A., Butiuc-Keul, A. L., Deliu, C., Coldea, G., and Hurdu, B. (2012). In vitro propagation and cryopreservation of Romanian endemic and rare *Hypericum* species. *Plant Cell Tiss. Org.* 110, 213–226. doi: 10.1007/s11240-012-0144-7
- Crockett, S. L., and Robson, N. K. B. (2011). Taxonomy and chemotaxonomy of the genus *Hypericum*. *Med. Aromat. Plant Sci. Biotechnol.* 5, 1–13.
- Danova, K. (2010). Production of polyphenolic compounds in shoot cultures of *Hypericum* species characteristic for the Balkan flora. *Bot. Serb.* 34, 29–36.
- Danova, K., Nikolova-Damianova, B., Denev, R., and Markovska, Y. (2012). Impact of pre-culture on short- and long-term in vitro recovery of the biosynthetic potential and enzymatic and non-enzymatic antioxidant defense of *Hypericum rumeliacum* Boiss. after cryostorage. *Plant Growth Regul.* 68, 447–457. doi: 10.1007/s10725-012-9733-z
- Dereuddre, J., and Kaminski, M. (1992). Applications of thermal analysis in cryopreservation of plant cells and organs. *J. Therm. Anal.* 38, 1965–1978. doi: 10.1007/BF01979606
- Dereuddre, J., and Tannoury, M. (1995). “Cryopreservation of Germplasm of Carnation (*Dianthus caryophyllus* L.),” in *Biotechnology in Agriculture and Forestry 32, Cryopreservation of Plant Germplasm I*, 2nd Edn, ed. Y.P.S. Bajaj (Berlin: Springer-Verlag), 458–475.
- Espevig, T., Xu, C. H., Aamlid, T. S., DaCosta, M., and Huang, B. (2012). Proteomic responses during cold acclimation in association with freezing tolerance of velvet bentgrass. *J. Am. Soc. Hort. Sci.* 137, 391–399.
- European Pharmacopoeia (2008). *European Pharmacopoeia*, 6th Edn. Strasbourg: Council of Europe.
- Fang, J. Y., Sacande, M., Pritchard, H., and Wetten, A. (2009). Influence of freezable/non-freezable water and sucrose on the viability of *Theobroma cacao* somatic embryos following desiccation and freezing. *Plant Cell Rep.* 28, 883–889. doi: 10.1007/s00299-009-0691-5
- Folgado, R., Panis, B., Sergeant, K., Renaud, J., Swennen, R., and Hausman, J. F. (2015). Unravelling the effect of sucrose and cold pretreatment on cryopreservation of potato through sugar analysis and proteomics. *Cryobiology* 71, 432–441. doi: 10.1016/j.cryobiol.2015.09.006
- Georgieva, E., Petrova, D., Yordanova, Z., Kapchina-Toteva, V., Čellárová, E., and Chaneva, G. (2014). Influence of cryopreservation on the antioxidative activity of in vitro cultivated *Hypericum* species. *Biotechnol. Biotechnol. Equip.* 28, 863–870. doi: 10.1080/13102818.2014.946805
- Gibson, S. I. (2000). Plant sugar-response pathways. part of a complex regulatory web. *Plant Physiol.* 124, 1532–1539. doi: 10.1104/pp.124.4.1532
- Gray D. E., Pallardy, S. G., Garrett, H. E., and Rottinghaus G. E. (2003). Effect of acute drought stress and time of harvest on phytochemistry and dry weight of St. John’s wort leaves and flowers. *Planta Med.* 69, 1024–1030. doi: 10.1055/s-2003-45150
- Guedes, A. P., Amorim, L. R., Vicente, A. M. S., Ramos, G., and Ferreira, M. F. (2003). Essential oils from plants and in vitro shoots of *Hypericum androsaemum* L. *J. Agric. Food Chem.* 51, 1399–1404. doi: 10.1021/jf020872f
- Gusta L. V., and Wisniewski, M. (2013). Understanding plant cold hardness: an opinion *Physiol. Plantarum* 147, 4–14. doi: 10.1111/j.1399-3054.2012.01611.x
- He, L., Nada, K., Kasukabe, Y., and Tachibana, S. (2002). Enhanced susceptibility of photosynthesis to low-temperature photoinhibition due to interruption of chill-induced increase of S-adenosylmethionine decarboxylase activity in leaves of spinach (*Spinacia oleracea* L.). *Plant Cell Physiol.* 43, 196–206. doi: 10.1093/pcp/pcf021
- Helliott, B., Panis, B., Poumay, Z., Swennen, R., Lepoivre, P., and Frison, E. (2002). Cryopreservation for the elimination of cucumber mosaic and banana streak viruses from banana (*Musa* spp.). *Plant Cell Rep.* 20, 1117–1122. doi: 10.1007/s00299-002-0458-8
- Huang, L. F., Wang, Z. H., and Chen, S. L. (2014). Hypericin: chemical synthesis and biosynthesis. *Chin. J. Nat. Med.* 12, 81–88. doi: 10.1016/S1875-5364(14)60014-5
- Kaeppler, S. M., Kaeplle, H. F., and Rhee, Y. (2000). Epigenetic aspects of somaclonal variation in plants. *Plant Mol. Biol.* 43, 179–188. doi: 10.1023/A:1006423110134
- Kainulainen, P., Holopainen, J. K., Palomaki, V., and Holopainen, T. (1996). Effect of nitrogen fertilization on secondary chemistry and ectomycorrhizal state of Scots pine seedlings and on growth of grey pine aphid. *J. Chem. Ecol.* 22, 617–636. doi: 10.1007/BF02033574
- Karakas, O., Toker, Z., Tilkat, E., Ozen, H. C., and Onay, A. (2009). Effect of different concentrations of benzylaminopurine on shoot regeneration and hypericin content in *Hypericum triquetrifolium* Turra. *Nat. Prod. Res.* 23, 1459–1465. doi: 10.1080/14786410701664528
- Karlsson, J. O. M., and Toner, M. (1996). Long-term storage of tissues by cryopreservation: critical issues. *Biomaterials* 17, 243–256. doi: 10.1016/0142-9612(96)85562-1
- Kartha, K.K., and Engelmann, F. (1994). “Cryopreservation and germplasm storage,” in *Plant Cell and Tissue Culture*, eds I. K. Vasil, and T. A. Thorpe, (Dordrecht: Kluwer), 195–230.
- Kartnig, T., Göbel, I., and Heydel, B. (1996). Production of hypericin, pseudohypericin and flavonoids in cell cultures of various *Hypericum* species and their chemotypes. *Planta Med.* 62, 51–53. doi: 10.1055/s-2006-957796
- Kent, B., Garvey, C. J., Lenne, T., Porcar, L., Garamus, V. M., and Bryant, G. (2010). Measurement of glucose exclusion from the fully hydrated DOPE inverse hexagonal phase. *Soft Matter* 6, 1197–1202. doi: 10.1039/b919086d
- Kimáková, K., Čellárová, E., and Hončariv, R. (1996). A study of regeneration capacity of encapsulated meristems of *Hypericum perforatum* L. after cryopreservation. *Biotologia* 51:83.
- Kirakosyan, A., Sirvent, T. M., Gibson, D. M., and Kaufman, P. B. (2004). The production of hypericins and hyperforin by in vitro cultures of *Hypericum perforatum* (Review). *Biotechnol. Appl. Biochem.* 39, 71–81. doi: 10.1042/BA20030144
- Lang, V., Mantyla, E., Welin, B., Sundberg, B., and Palva, E. T. (1994). Alterations in water status, endogenous abscisic acid content, and expression of rab18 gene during the development of freezing tolerance in *Arabidopsis thaliana*. *Plant Physiol.* 104, 1341–1349.
- Levitt, J. (1980). *Responses of Plants to Environmental Stress, Chilling, Freezing, and High Temperature Stresses*, 2nd Edn, Vol. 1. New York: Academic Press.
- Li, W., Wang, R., Li, M., Li, L., Wang, C., Welti, R., et al. (2008). Differential degradation of extraplastidic and plastidic lipids during freezing and post-freezing recovery in *Arabidopsis thaliana*. *J. Biol. Chem.* 283, 461–468. doi: 10.1074/jbc.M706692200
- Liebo, S. P., and Mazur, P. (1971). The role of cooling rates in low temperature preservation. *Cryobiology* 8, 447–452. doi: 10.1016/0011-2240(71)90035-6

- Lu, Z. W., Popova, E. V., Wu, C. H., Lee, E. J., Hahn, E. J., and Paek, K. Y. (2009). Cryopreservation of *Ginkgo biloba* cell culture: effect of pretreatment with sucrose and ABA. *CryoLetters* 30, 232–243.
- Mederos Molina, S. (1991). In vitro growth and multiplication of *Hypericum canariense* L. *Acta Hortic.* 289, 133–134. doi: 10.17660/ActaHortic.1991.289.30
- Meyer, E.M., Touchell, D.H., and Ranney, T.G. (2009). In vitro shoot regeneration and polyploidy induction from leaves of *Hypericum* species. *Hortscience* 44, 1957–1961.
- Mišianiková, A., Zubrická, D., Petijová, L., Bruňáková, K., and Čellárová, E. (2016). Effect of composition of cryoprotectants and cooling rate on temperature of crystallisation in cryopreserved *Hypericum perforatum* cell suspension cultures. *CryoLetters* 37.
- Monroy, A. F., Sarhan, F., and Dhindsa, R. S. (1993). Cold-induced changes in freezing tolerance, protein phosphorylation, and gene expression. *Plant Physiol.* 102, 1227–1235.
- Moura, M. (1998). Conservation of *Hypericum foliosum* aiton, an endemic azorean species, by micropropagation. *In Vitro Cell.* 34, 244–248. doi: 10.1007/BF02822715
- Nahrstedt, A., and Butterweck, V. (1997). Biologically active and other chemical constituents of the herb of *Hypericum perforatum* L. *Pharmacopsychiatry* 30, 129–134. doi: 10.1055/s-2007-979533
- Namlí S., Akbas, F., Isikalan, C., Tilkat, E. A., and Basaran, D. (2010). The effect of different plant hormones (PGRs) on multiple shoots of *Hypericum retusum* Aucher. *Plant Omics J.* 3, 12–17.
- Nishizawa, S., Sakai, A., Amano, Y., and Matsuzawa, T. (1993). Cryopreservation of asparagus (*Asparagus officinalis* L.) embryogenic suspension cells and subsequent plant regeneration by vitrification. *Plant Sci.* 91, 67–73. doi: 10.1016/0168-9452(93)90189-7
- Nürk, N. M., and Blattner, F. R. (2010). Cladistic analysis of morphological characters in *Hypericum* (Hypericaceae). *Taxon* 59, 1495–1507.
- Olien, C., and Livingston, D. P. (2006). Understanding freeze stress in biological tissues: Thermodynamics of interfacial water. *Thermochim. Acta* 451, 52–56. doi: 10.1016/j.tca.2006.08.014
- Olkuk, E. A., and Orhan, S. (2009). Thidiazuron induced micropropagation of *Hypericum triquetrifolium* Turra. *Afr. J. Biotechnol.* 8, 3506–3510.
- Padmash, P., Seeni, S., Reji, J. V., and Nair, G. M. (2008). A Novel Process for the Production of Hypericin from Shoot and Callus Cultures of *Hypericum Hookerianum* Wight and Arn, Indian Patent 224656.
- Páques, M., Monod, V., and Dereuddre, J. (2002). “Cryopreservation of Eucalyptus sp. shoot tips by the encapsulation-dehydration procedure,” in *Biotechnology in Agriculture and Forestry, Cryopreservation of Plant Germplasm II* Vol. 50, eds L.E. Towill, and Y.P.S. Bajaj (Berlin: Springer-Verlag), 234–244.
- Penjweini, R., Loew, H. G., Breit, P., and Kratky, K. W. (2013). Optimizing the antitumor selectivity of PVP-Hypericin re A549 cancer cells and HLF normal cells through pulsed blue light. *Photodiagn. Photodyn.* 10, 591–599. doi: 10.1016/j.pdpdt.2013.06.005
- Petijová, L., Bruňáková, K., Zubrická, D., Mišianiková, A., Kimáková, K., and Čellárová, E. (2014). Relation between frost tolerance and post-cryogenic recovery in *Hypericum* spp. *Cryoletters* 35, 171–179.
- Petijová, L., Skyba, M., and Čellárová, E. (2012). Genotype-dependent response of St. John’s wort (*Hypericum perforatum* L.) shoot tips to cryogenic treatment: effect of pre-culture conditions on post-thaw recovery. *Plant Omics J.* 5, 291–297.
- Rahnardav, A., Daneshian, J., Heravan, E., Valadabadi, S., and Golein, B. (2012). Investigation of the most important secondary metabolites of St. John’s wort (*Hypericum perforatum* L.) in Caspian climate. *J. Food Agric. Environ.* 10, 375–381.
- Ramakrishna, A., and Ravishankar, G. A. (2011). Influence of abiotic stress signals on secondary metabolites in plants. *Plant Signal. Behav.* 6, 1720–1731. doi: 10.4161/psb.6.11.17613
- Reaney, M. J. T., and Gusta, L. V. (1987). Factors influencing the induction of freezing tolerance by abscisic acid in cell suspension cultures of *Bromus inermis* Leyss and *Medicago sativa* L. *Plant Physiol.* 83, 423–427. doi: 10.1104/pp.83.2.423
- Reed, B. (1993). Responses to ABA and cold acclimation are genotype dependent for cryopreserved blackberry and raspberry meristems. *Cryobiology* 30, 179–184. doi: 10.1006/cryo.1993.1017
- Reed, B. M. (2014). Antioxidants and cryopreservation, the new normal? *Acta Hortic.* 1039, 41–48. doi: 10.17660/ActaHortic.2014.1039.3
- Reed, B. M., Schumacher, L., Wang, N., D’Achino, J., and Barker, R. E. (2006). Cryopreservation of bermudagrass germplasm by encapsulation dehydration. *Crop Sci.* 46, 6–11. doi: 10.2135/cropsci2004.0620
- Robson, N. K. B. (1996). Studies in the genus *Hypericum* L. (Guttiferae). 6. Sections 20. *Myriandra* to 28. *Elodes*. *Bull. Br. Museum Nat. Hist.* 26:75.
- Rückert, U., Eggenreich, K., Likussar, W., Wintersteiger, R., and Michelitsch, A. (2006). A high-performance liquid chromatography with electrochemical detection for the determination of total hypericin in extracts of St. John’s Wort. *Phytochem. Anal.* 17, 162–167. doi: 10.1002/pcba.908
- Rumich-Bayer, S., and Krause, G. H. (1986). Freezing damage and frost tolerance of the photosynthetic apparatus studied with isolated mesophyll protoplasts of *Valerianella locusta* L. *Photosynth. Res.* 8, 161–174. doi: 10.1007/BF00035246
- Saddique, Z., Naeem, I., and Maimoona, A. (2010). A review of the antibacterial activity of *Hypericum perforatum* L. *J. Ethnopharmacol.* 131, 511–521. doi: 10.1016/j.jep.2010.07.034
- Sakai, A., and Engelmann, F. (2007). Vitrification, encapsulation-vitrification and droplet vitrification: a review. *CryoLetters* 28, 151–172.
- Sakai, A., Kobayashi, S., and Oiyama, I. (1991). Survival by vitrification of nucellar cells of navel orange *Citrus sinensis* var. brasiliensis tanaka cooled to -196°C. *J. Plant Physiol.* 137, 465–470. doi: 10.1007/BF00232130
- Schäfer-Menuhr, A., Mix-Wagner, G., and Schumacher, H. M. (1997). Cryopreservation of potato cultivars—design of a method for routine application in genebanks. *Acta Hortic.* 447, 477–483. doi: 10.17660/ActaHortic.1997.447.97
- Shatnawi, M. A., Shibli, R. A., Abu-Romman, S. M., Al-Mazraawi, M. S., Al Ajlouni, Z. I., Shatanawi, W. A., et al. (2011). Clonal propagation and cryogenic storage of the medicinal plant Stevia rebaudiana. *Span. J. Agric. Res.* 9, 213–220. doi: 10.5424/sjar/20110901-021-10
- Shibli, R., Shatnawi, M., Subaikh, W., and Ajlouni, M. (2006). In vitro conservation and cryopreservation of plant genetic resources: a review. *World J. Agricult. Sci.* 2, 372–382.
- Shilpasree, H. P., and Ravishankar Rai, V. (2009). In vitro plant regeneration and accumulation of flavonoids in *Hypericum mysorense*. *Int. J. Integr. Biol.* 8, 43–49.
- Skyba, M., Faltus, M., Zámečník, J., and Čellárová, E. (2011). Thermal analysis of cryopreserved *Hypericum perforatum* L. shoot tips: cooling regime dependent dehydration and ice growth. *Thermochim. Acta* 514, 22–27. doi: 10.1016/j.tca.2010.11.027
- Skyba, M., Petijová, L., Košuth, J., Petrova Koleva, D., Gancheva Ganeva, T., Kapchina-Toteva, V. M., et al. (2012). Oxidative stress and antioxidant response in *Hypericum perforatum* L. plants subjected to low temperature treatment. *J. Plant Physiol.* 169, 955–964. doi: 10.1016/j.jplph.2012.02.017
- Skyba, M., Urbanová, M., Kapchina-Toteva, V., Košuth, J., Harding, K., and Čellárová, E. (2010). Physiological, biochemical and molecular characteristics of cryopreserved *Hypericum perforatum* L. shoot tips. *Cryoletters* 31, 249–260.
- Steponkus, P. L., and Lynch, D. V. (1989). Freeze/thaw-induced destabilization of the plasma membrane and the effects of cold acclimation. *J. Bioenerg. Biomembr.* 21, 21–41. doi: 10.1007/BF00762210
- Stoyanova-Koleva, D., Stefanova, M., Čellárová, E., and Kapchina-Toteva, V. (2013). Chloroplast ultrastructure of *Hypericum perforatum* plants regenerated in vitro after cryopreservation. *Biol. Plant.* 57, 793–796. doi: 10.1007/s10535-013-0357-6
- Stoyanova-Koleva, D., Stefanova, M., Ganeva, T. S., and Čellárová, E. (2015). Structural modifications in the mesophyll associated with cryopreservation of seven *Hypericum* species. *Biol. Plant.* 59, 214–220. doi: 10.1007/s10535-015-0528-8
- Su, F., Jacquard, C., Villaume, S., Michel, J., Rabenoelina, F., Clément, C., et al. (2015). *Burkholderia phytophaga* PsJN reduces impact of freezing temperatures on photosynthesis in *Arabidopsis thaliana*. *Front. Plant Sci.* 6:810. doi: 10.3389/fpls.2015.00810
- Thierry, C., Florin, B., and Pétiard, V. (1999). Changes in protein metabolism during the acquisition of tolerance to cryopreservation of carrot somatic embryos. *Plant Physiol. Biochem.* 37, 145–154. doi: 10.1016/S0981-9428(99)80076-X
- Thin, N. T. (1997). *Cryopreservation of Germplasm of Vegetatively Propagated Tropical Monocots by Vitrification*, Dissertation thesis, Kobe University, Kobe.

- Thomashow, M. F. (1999). Plant cold acclimation: freezing tolerance genes and regulatory mechanisms. *Annu. Rev. Plant Physiol. Plant Mol. Biol.* 50, 571–599. doi: 10.1146/annurev.arplant.50.1.571
- Tran, L. S. P., Urao, T., Qin, F., Maruyama, K., Kakimoto, T., Shinozaki, K., et al. (2007). Functional analysis of AHK1/ATHK1 and cytokinin receptor histidine kinases in response to abscisic acid, drought, and salt stress in *Arabidopsis*. *Proc. Natl. Acad. Sci. U.S.A.* 104, 20623–20628. doi: 10.1073/pnas.0706547105
- Urbanová, M., Čellárová, E., and Kimáková, K. (2002). Chromosome number stability and mitotic activity of cryopreserved *Hypericum perforatum* L. meristems. *Plant Cell Rep.* 20, 1082–1086. doi: 10.1007/s00299-002-0447-y
- Urbanová, M., Košuth, J., and Čellárová, E. (2006). Genetic and biochemical analysis of *Hypericum perforatum* L. plants regenerated after cryopreservation. *Plant Cell Rep.* 25, 140–147. doi: 10.1007/s00299-005-0050-0
- Vertucci, C. W. (1989). Effects of cooling rate on seeds exposed to liquid nitrogen temperatures. *Plant Physiol.* 90, 1478–1485. doi: 10.1104/pp.90.4.1478
- Vertucci, C. W., Berjak, P., Pammenter, N. W., and Crane, J. (1991). Cryopreservation of embryonic axes of an homoiohydrous (recalcitrant) seed in relation to calorimetric properties of tissue water. *CryoLetters* 12, 339–350.
- Volk, G. M., Maness, N., and Rotindo, K. (2004). Cryopreservation of garlic (*Allium sativum* L.) using plant vitrification solution 2. *CryoLetters* 25, 219–226.
- Volk, G. M., and Walters, C. (2006). Plant vitrification solution 2 lowers water content and alters freezing behavior in shoot tips during cryoprotection. *Cryobiology* 52, 48–61. doi: 10.1016/j.cryobiol.2005.09.004
- Wanner, L. A., and Junttila, O. (1999). Cold-induced freezing tolerance in *Arabidopsis*. *Plant Physiol.* 120, 391–399. doi: 10.1104/pp.120.2.391
- Werner, T., and Schmülling, T. (2009). Cytokinin action in plant development. *Curr. Opin. Plant Biol.* 12, 527–538. doi: 10.1016/j.pbi.2009.07.002
- Wesley-Smith, J., Vertucci, C. W., Berjak, P., Pammenter, N. W., and Crane, J. (1992). Cryopreservation of desiccation-sensitive axes of *Camellia sinensis* in relation to dehydration, freezing rate, and the thermal properties of tissue water. *J. Plant Physiol.* 140, 596–604. doi: 10.1016/S0176-1617(11)80795-9
- Wisniewski, M., Gusta, L.V., Fuller, M.P., and Karlson, D. (2009). “Ice nucleation, propagation and deep supercooling: the lost tribes of freezing studies,” in *Plant Cold Hardiness: From the Laboratory to the Field*, eds L. V. Gusta, M. E. Wisniewski, and K. K. Tanino (Cambridge: CABI), 73–97.
- Wölflé, U., Seelinger, G., and Schempp, C.M. (2014). Topical Application of St. John’s Wort (*Hypericum perforatum*). *Planta Med.* 80, 109–120.
- Yazaki, K., and Okuda, T. (1990). Procyanidins in callus and multiple shoot cultures of *Hypericum erectum*. *Planta Med.* 56, 490–491. doi: 10.1055/s-2006-961020
- Zhao, J., Davis, L. C., and Verpoorte, R. (2005). Elicitor signal transduction leading to production of plant secondary metabolites. *Biotechnol. Adv.* 23, 283–333. doi: 10.1016/j.biotechadv.2005.01.003
- Zobayed, S. M. A., Afreen, F., and Kozai, T. (2005). Temperature stress can alter the photosynthetic efficiency and secondary metabolite concentrations in St. John’s wort. *Plant Physiol. Biochem.* 43, 977–984. doi: 10.1016/j.plaphy.2005.07.013

Conflict of Interest Statement: The authors declare that the research was conducted in the absence of any commercial or financial relationships that could be construed as a potential conflict of interest.

Copyright © 2016 Bruňáková and Čellárová. This is an open-access article distributed under the terms of the Creative Commons Attribution License (CC BY). The use, distribution or reproduction in other forums is permitted, provided the original author(s) or licensor are credited and that the original publication in this journal is cited, in accordance with accepted academic practice. No use, distribution or reproduction is permitted which does not comply with these terms.



Neuroprotective Activity of *Hypericum perforatum* and Its Major Components

Ana I. Oliveira^{1,2}, Cláudia Pinho^{1,2}, Bruno Sarmento^{3,4,5} and Alberto C. P. Dias^{2*}

¹ Nucleo de Investigação e Informação em Farmácia, Centro de Investigação em Saúde e Ambiente, Escola Superior de Tecnologia de Saúde do Porto – Instituto Politécnico do Porto, Vila Nova de Gaia, Portugal, ² Agrobioplant Group (CITAB-UM), Department of Biology, University of Minho, Braga, Portugal, ³ Cooperativa de Ensino Superior Politécnico e Universitário, Instituto de Investigação e Formação Avançada em Ciências e Tecnologias da Saúde, Gandra PRD, Portugal, ⁴ Instituto de Investigação e Inovação em Saúde, Porto, Portugal, ⁵ Instituto de Engenharia Biomédica, Porto, Portugal

OPEN ACCESS

Edited by:

Eva Cellarova,
Pavol Jozef Safarik University
in Kosice, Slovakia

Reviewed by:

Nibaldo C. Inestrosa,
Pontifical Catholic University of Chile,
Chile

Edmar Miyoshi,
Ponta Grossa State University, Brazil

***Correspondence:**

Alberto C. P. Dias
acpdias@bio.uminho.pt

Specialty section:

This article was submitted to
Plant Metabolism
and Chemodiversity,
a section of the journal
Frontiers in Plant Science

Received: 15 March 2016

Accepted: 27 June 2016

Published: 11 July 2016

Citation:

Oliveira AI, Pinho C, Sarmento B and
Dias ACP (2016) Neuroprotective
Activity of *Hypericum perforatum*
and Its Major Components.
Front. Plant Sci. 7:1004.
doi: 10.3389/fpls.2016.01004

Hypericum perforatum is a perennial plant, with worldwide distribution, commonly known as St. John's wort. It has been used for centuries in traditional medicine for the treatment of several disorders, such as minor burns, anxiety, and mild to moderate depression. In the past years, its antidepressant properties have been extensively studied. Despite that, other *H. perforatum* biological activities, as its neuroprotective properties have also been evaluated. The present review aims to provide a comprehensive summary of the main biologically active compounds of *H. perforatum*, as for its chemistry, pharmacological activities, drug interactions and adverse reactions and gather scattered information about its neuroprotective abilities. As for this, it has been demonstrated that *H. perforatum* extracts and several of its major molecular components have the ability to protect against toxic insults, either directly, through neuroprotective mechanisms, or indirectly, through its antioxidant properties. *H. perforatum* has therefore the potential to become an effective neuroprotective therapeutic agent, despite further studies that need to be carried out.

Keywords: *Hypericum perforatum*, extracts, compounds, neuroprotection, antioxidant activity

INTRODUCTION

Hypericum perforatum, also known as St. John's wort, hypericum or millepertuis is a member of the family Hypericaceae and a herbaceous perennial plant native Europe, western Asia, and northern Africa. Nowadays it has a worldwide distribution. The crude drug, called herba hyperici, consists of the upper aerial parts of the plant collected just before or during the flowering period (Barnes et al., 2001; Greeson et al., 2001; Patocka, 2003).

Hypericum perforatum has been used as a medicinal plant for centuries, for the treatment of external and internal disorders. Externally, oily preparations of the plant may be applied to treat minor burns, wounds, skin inflammation, and nerve pain (Barnes et al., 2001; Greeson et al., 2001; Patocka, 2003). Internally, it is indicated for the treatment of anxiety and mild to moderately severe depression (Barnes et al., 2001; Greeson et al., 2001; Patocka, 2003; Butterweck and Schmidt, 2007) competing for status as a standard antidepressant therapy and being the only herbal alternative to synthetic antidepressants (Wurglis and Schubert-Zsilavecz, 2006).

Hypericum perforatum contains several classes of biologically active compounds. These constituents often vary in its concentration, due to genetic variation within the species and/or adulteration, ecological factors, time of harvesting, preparation and processing of sample

material and storage conditions, such as exposure to light, time of harvesting. Important bioactive components are concentrated in buds, blossoms, and tips of twigs. Despite this variation, it is known that around 20% of the plant extract is comprised of bioactive compounds (Nahrstedt and Butterweck, 1997; Patocka, 2003; Wurglics and Schubert-Zsilavecz, 2006; Linde, 2009).

PHARMACOLOGICAL ACTIVITY OF *Hypericum perforatum*

St John's wort most investigated pharmacological activity has been its antidepressant properties. There are several reports of higher *H. perforatum* effectiveness compared to placebo intake and a similar activity, when comparing to several antidepressant drugs. The exact mechanism of *H. perforatum*'s antidepressant activity is still unclear, as to which are the most relevant constituents. Early *in vitro* research suggested an antidepressant activity due to hypericin, through the inhibition of the monoamine oxidase (MAO) enzyme (Suzuki et al., 1984; De Vry et al., 1999; Gaster and Holroyd, 2000; Behnke et al., 2002; Linde et al., 2005; Linde, 2009; Rahimi et al., 2009). However, its concentration was too low to explain the clinical effects (Butterweck, 2003) detected. Further studies showed that hyperforin was capable of inhibiting the reuptake of serotonin, dopamine, noradrenaline, GABA, and L-glutamate (Chatterjee et al., 1998). Antidepressive activity was also reported in several flavonoids. Taking all these results in consideration and the fact that the mechanisms underlying depression are still not well understood, it is more likely that *H. perforatum*'s antidepressant activity is due to a multiplicity of bioactive compounds and not to a single constituent and/or mechanism of action (Greeson et al., 2001; Butterweck and Schmidt, 2007; Nahrstedt and Butterweck, 2010).

Hypericum perforatum also presents antimicrobial properties. Regarding the antibacterial activity, crude plant extracts of the aerial parts of the plant, fractions and isolated compounds have been tested, demonstrating positive results. Concerning specific compounds, hyperforin is reported to present antibacterial activity against *Staphylococcus aureus* and Gram-positive bacteria, such as *Streptococcus pyogenes* and *Corynebacterium diphtheriae* being considered the antibacterial agent of *H. perforatum*. As for antifungal properties the flavonoids quercitrin, hyperoside, avicularin, rutin, quercetin, and kaempferol were reported to present antifungal activity against *Helminthosporium sativum* (Schempp et al., 1999; Reichling et al., 2001; Saddiqe et al., 2010). Another compound extensively studied, in what concerns its antimicrobial, more specifically, antiviral activity, is hypericin. This naphtodianthrone has demonstrated *in vitro* antiviral activity against a variety of viruses, light and oxygen influenced (Kubin et al., 2005). The *in vivo* studies did not, however, retrieve as promising results, possibly due to differences in terms of light irradiation (Karioti and Bilia, 2010) in many regions of the human body.

Besides its antiviral properties, hypericin has aroused interest in the scientific community for its antitumoral activity. Since hypericin is probably the most powerful photosensitizer

found in nature and for its specific properties, such as a strong absorption at longer wavelength, minimal dark toxicity, certain tumor selectivity and much higher clearance rate from the host body than hematoporphyrins, its potential for antitumoral photodynamic therapy has been explored in several studies (Agostinis et al., 2002; Miskovsky, 2002; Martinez-Poveda et al., 2005b). Hyperforin and its stable, hydrosoluble derivate, aristoforin has also been reported to possess antitumoral activity, namely anticarcinogenic, antiproliferative, proapoptotic, antiinvasive, antimetastatic, and antiangiogenic effects (Hostanska et al., 2003; Schwarz et al., 2003; Dona et al., 2004; Martarelli et al., 2004; Gartner et al., 2005; Martinez-Poveda et al., 2005a; Rothley et al., 2009).

Anti-inflammatory, wound healing and anti-nociceptive effects have also been associated with *H. perforatum* (Motallebnejad et al., 2008; Suntar et al., 2010).

Hypericum perforatum–Drug Interactions and Adverse Reactions

A number of clinically significant pharmacokinetic and pharmacodynamic interactions have been reported (Henderson et al., 2002) over the years suggesting that *H. perforatum* use concomitantly with several other drugs may represent its most relevant risk (Knuppel and Linde, 2004). These interactions are possibly due to a modulation of isoenzymes of the cytochrome P450 (CYP; Borrelli and Izzo, 2009), which metabolizes a series of pharmaceutical substances and an induction of P-glycoprotein, which is responsible for an increase of drugs' excretion from the organism (Muller, 2003). **Table 1** summarizes the most known interactions.

As to what adverse reactions concerns, *H. perforatum* is referred to as generally well tolerated. When side effects occur they are considered mild and transient. The most common are gastrointestinal symptoms, dizziness, confusion, fatigue and/or sedation, skin reactions, restlessness or anxiety, headache, dry mouth and allergic reactions. These may occur in 1–3% of patients taking *H. perforatum*. There have also been described rare adverse reactions that include phototoxicity. Symptoms indicative of phototoxicity include dermal erythema, rash, and pruritus. These adverse reactions have been attributed to naphthodianthrone. Other rare adverse reactions described comprehend alopecia, neuropathy and mania (Barnes et al., 2001; Greeson et al., 2001; Hammerness et al., 2003; Schulz, 2006; Wurglics and Schubert-Zsilavecz, 2006; Russo et al., 2013).

NEUROPROTECTIVE ACTIVITY AND *Hypericum perforatum*

The Central Nervous System (CNS) is known for being particularly sensitive to oxidative stress, which can be described as an imbalance between generation and elimination of reactive oxygen species (ROS) and reactive nitrogen species (RNS). This particular susceptibility of the brain is caused by a high metabolic rate, a low concentration of glutathione and antioxidant enzyme catalase (CAT) and a high proportion of polyunsaturated fatty acids. The general inability of neurons to divide explains some

TABLE 1 | *Hypericum perforatum*-drug interactions.

Drug	Possible interaction	Type of interaction	Reference
Warfarin	Induction of CYP1A2 and CYP2C9	Pharmacokinetic	Karminsky and Zhang, 1997; Hamerness et al., 2003
Cyclosporin	Induction of CYP3A4 and P-glycoprotein transport	Pharmacokinetic	Henderson et al., 2002; Hamerness et al., 2003
Oral contraceptives	Risk of transplant rejection Induction CYP1A2 and CYP3A4	Pharmacodynamic Pharmacokinetic	Muller, 2003 Ball et al., 1990; Schmider et al., 1997
Theophylline	Inhibition of CYP2C9 and CYP2C19 Induction of CYP1A2 and CYP2C9 and P-glycoprotein transport	Pharmacokinetic	Pfrunder et al., 2003 Henderson et al., 2002; Hamerness et al., 2003; Wurglics and Schubert-Zsilavecz, 2006
Digoxin	Induction of CYP2C9, CYP2D6, CYP3A4, CYP1A2, CYP2C19, affecting P-glycoprotein transport, and reduction of drug's plasmatic concentration	Pharmacokinetic	Barnes et al., 2001; Greeson et al., 2001; Henderson et al., 2002
HIV protease inhibitors	Induction of CYP3A4	Pharmacokinetic	Piscitelli et al., 2000
HIV non-nucleoside reverse transcriptase inhibitors	Induction of CYP3A4	Pharmacokinetic	Henderson et al., 2002; Hamerness et al., 2003
Anticonvulsivants	Induction of CYP2C9, CYP3A4, CYP1A2, and affecting P-glycoprotein transport	Pharmacokinetic	Barnes et al., 2001; Henderson et al., 2002
Phenprocoumon	Induction of CYP2C9, CYP2D6, CYP3A4, CYP1A2, CYP2C19, and affecting P-glycoprotein transport	Pharmacokinetic	Barnes et al., 2001
Nifedipin	Induction of CYP3A4;	Pharmacokinetic	Hamerness et al., 2003
Statins	Induction of CYP3A4; Induction of P-glycoprotein transport	Pharmacokinetic	Wang et al., 2007 Hamerness et al., 2003
Midazolam	Induction of CYP3A4;	Pharmacokinetic	Hamerness et al., 2003
Verapamil	Induction of first-pass CYP3A4 metabolism	Pharmacokinetic	Russo et al., 2013
Omeprazol, esomeprazole, and pantoprazole	Induction of CYP2C19	Pharmacokinetic	Wang et al., 2004
Loperamide	Theoretical induction of monoamine oxidase inhibitor-drug reaction	Pharmacokinetic	Khawaja et al., 1999
Ibuprofen	Increase of expression of glycoprotein G	Pharmacokinetic	Russo et al., 2013
Dexamethasone, prednisone, and budesonide	Induction of CYP3A4	Pharmacokinetic	Russo et al., 2013
Methadone and pethidine	Induction of CYP2D2	Pharmacokinetic	Dostalek et al., 2005
Dextromethorphan and oxycodone	Induction of CYP3A4	Pharmacokinetic	Nieminen et al., 2010
Voriconazole	Induction of CYP3A4, CYP2C19, and CYP2C9	Pharmacokinetic	Borrelli and Izzo, 2009
Erythromycin	Induction of CYP3A4	Pharmacokinetic	Borrelli and Izzo, 2009
Imatinib	Induction of CYP3A4 and P-gp	Pharmacokinetic	Smith et al., 2004
Triptans	Risk of increased serotonergic effects with the possibility of an increased risk of adverse reactions	Pharmacodynamic	Barnes et al., 2001; Henderson et al., 2002; Hamerness et al., 2003
Selective serotonin reuptake inhibitors	Risk of increased serotonergic effects with the possibility of an increased risk of adverse reactions	Pharmacodynamic	Barnes et al., 2001; Greeson et al., 2001; Henderson et al., 2002; Hamerness et al., 2003
Antineoplastic drugs directed against to topoisomerase II alpha	May antagonize therapeutic activity of the drugs	Pharmacodynamic	Hamerness et al., 2003
Thyroid agents	Increase in thyroid-stimulating hormone	Pharmacodynamic	Ferro and Levine, 2001; Russo et al., 2013

aging and neurodegenerative disease related loss of function, as neurons die, without chance to be replaced. Apoptosis and excitotoxicity are among the mechanisms that cause neuronal death, involving ROS and RNS. Therefore oxidative stress plays an important role in the development of neurodegenerative

diseases, such as Alzheimer's and Parkinson's disease and stroke. In order to prevent these cause-dependent diseases it is important to preserve redox environment and mitochondrial function of the cell. This can be achieved by avoiding the causes of oxidative stress and strengthen the defenses with the usage endogenous

antioxidants and the intake of others. Endogenous antioxidants include enzymatic and non-enzymatic defenses. Enzymatic antioxidants react with reactive species and are, subsequently, efficiently recycled, preventing most of the formation of the toxic free radicals. Only small amounts of these enzymes are therefore needed to offer protection. Relevant enzymatic antioxidants are Se-glutathione peroxidase (GPx), CAT, and superoxide dismutase (SOD) that metabolizes superoxide, hydrogen peroxide (H_2O_2), and lipid peroxides. Non-enzymatic defenses can be divided in hydrophobic and hydrophilic antioxidants. Lipophilic antioxidants comprise α -tocopherol, carotenoids, and ubiquinone-10 and are mostly present in membranes and lipoproteins. Hydrophilic antioxidants include glutathione, histone-peptides, the iron-binding proteins transferring and ferritin, dihydrolipoic acid, melatonin, uric acid, and ascorbic acid. They can be found in cytosolic, mitochondrial, and nuclear aqueous compartments. These defense mechanisms are complementary to each other, due to the different species and cellular compartments that they act against. Exogenous antioxidants include several vitamins, such as A, E, and C, carotenoids and polyphenolic compounds, such as flavonoids (Pietta, 2000; Emerit et al., 2004; Silva et al., 2005; Zhao, 2005; Silva B.A. et al., 2008; Butterfield et al., 2007; Boots et al., 2008; Ansari et al., 2009).

Besides their usage in the prevention of neurodegenerative diseases, antioxidants could also be relevant on its treatment, as a single compound or in supplementary combination with drugs targeting other pathogenic mechanisms (Behl, 1999).

Neuroprotective Activity of *Hypericum perforatum* Extracts

Lu et al. (2004) reported a neuroprotective effect of standard *H. perforatum* extracts on H_2O_2 trauma induced by an optimum concentration of 200 μM in rat pheochromocytome cell line PC12 (cell line widely used in *in vitro* model of neuronal injury and oxidative stress (Sasaki et al., 2003; Zou et al., 2010) within 24 h treatment. The extract improved the survival rate of neural cells, in a dose-dependent manner, at concentrations of 1 ~40 $\mu g/mL$, with a 133% improvement at 40 $\mu g/mL$. In extract concentrations ranging from 60 to 100 $\mu g/mL$, a decrease in cell viability was reported, maintaining, however, higher viability levels, when comparing to control ($p < 0.05$). *H. perforatum* extract, at concentrations of 1~100 $\mu g/mL$ also decreased intra- and extracellular ROS levels, at 71 and 50%, respectively, when comparing to the control group. This is indicative of a limitation in the intracellular ROS generation during cell aerobic metabolism and of the extract's entrance in the cells, with a consequent reduction of ROS levels. There also was reported a block in DNA fragmentation of H_2O_2 -induced apoptosis (which reflects the endonuclease activity characteristic of apoptosis) at concentrations of 10 to 100 $\mu g/mL$ (Lu et al., 2004; Zou et al., 2010). These results are in accordance with those described by Benedi et al. (2004) but with an insult of 300 μM H_2O_2 . Pre-treatment with the standardized extract also attenuated caspase-3 activity, increased by H_2O_2 insult. Caspases, of which caspase-3 is the most widely studied, are a class of cysteine proteases, considered of extreme importance in the

apoptotic process, triggering a proteolytic cleavage cascade in mammalian cells (Cohen, 1997).

Using the same biological model and insult, a flavonoid-rich extract, particularly in rutin, hyperoside, isoquercetin, avicularin, and quercitrin (Zou et al., 2004), proven significant protective effects against induced apoptosis, in the studied concentrations above 6.25 $\mu g/mL$ (Zou et al., 2010). Similar results (regarding induced-apoptosis protection and attenuation of caspase 3-activity) have been described for a *H. perforatum*'s methanolic dried extract in human neuroblastoma cell line SK-N-MC. There was also observed, under the phase-contrast microscope, that cells treated with H_2O_2 (at a concentration of 10⁻¹⁰ mM) for 5 h were detached from the dish, with cell rounding, cytoplasmic blebbing, and irregularity in shape. All of the morphological alterations described were less frequent among cells pre-treated with *H. perforatum*. The DAPI assay revealed nuclear condensation, DNA fragmentation, and perinuclear apoptotic bodies under the same treatment conditions with H_2O_2 . The appearance of cells pre-treated with *H. perforatum* was, like described above, closer to that of control (Jang et al., 2002). *H. perforatum* standardized extract has also been described to have the ability to protect against enzymatic and non-enzymatic lipid peroxidation in rat brain, inhibiting NADPH-dependent lipid peroxidation and attenuating of non-enzymatic Fe²⁺/ascorbate-dependent lipid peroxidation in cerebral cortex mitochondria. Inhibition of lipid peroxidation was reported to be the results of the extract's scavenging effect on NADPH and Fe²⁺/ascorbate generated free radicals (Benedi et al., 2004).

Glutamate, a neurotransmitter, which extracellular accumulation leads to overstimulation of postsynaptic glutamate receptors, with consequent inhibition of intracellular glutathione synthesis and Ca²⁺ overload, can act as a toxic, leading to cell death (Ankarcrona et al., 1995; Breyer et al., 2007). Taking this in consideration Breyer et al. (2007) investigated the neuroprotective activity of *H. perforatum* extract in glutamate-induced cell death in hippocampal HT22 nerve cell line. Pre-incubation for 2–25 h with the extract and/or simultaneous incubation with glutamate and extract-incubation of the cells up to 8 h after glutamate exposition prevented cell death. There is no statistically significant difference between the control cells and the cells pre and co-incubated with the extract, whereas the glutamate-exposure cells decrease in cell viability more than 80%. It was also demonstrated that *H. perforatum* extract was able to counteract the energy losses induced by the glutamate. The authors concluded that the extract protected HT22 cells from glutamate-induced cytotoxicity by reducing or attenuating glutathione loss, calcium fluxes, energy status, and ROS-mediated cell death, but only up to 8 h after glutamate exposition.

Alzheimer's disease is characterized by neuronal degeneration, particularly of pyramidal hippocampal neurons, entorhinal cortex, and other neocortical areas, which include the specific loss of cholinergic neurons in the median forebrain (Bains and Shaw, 1997). Besides that, two hallmarks of this neurodegenerative disorder are neurofibrillary tangles and senile plaques (Silva et al., 2004), the last mainly constituted by amyloid protein fibers, derived from an amyloid precursor protein, arranged in a so-called cross- β -pleated sheet conformation. This heterogeneous

peptide in size is proven to be neurotoxic and this general toxicity appears mediated in some part by oxidative stress (Behl, 1999; Behl and Moosmann, 2002; Ansari et al., 2009). In fact, amyloid- β -induced toxicity on neuronal cells is proposed as a main route to neuronal loss in Alzheimer's disease (Butterfield et al., 2007). Taking this in consideration and the protective characteristics of *H. perforatum* extracts, Silva et al. (2004) studied its potential neuroprotective action in β -amyloid-induced cell toxicity, through lipid peroxidation and Syto-13/PI assay. After incubating hippocampal wistar rat neurons with non-toxic concentrations of ethanolic extract *H. perforatum* and fractions, a significant inhibition of ascorbate/Fe²⁺-induced lipid peroxidation was observed on the fractions containing caffeoylquinic acids and flavonol glycosides, flavonol glycosides (quercetin-type), flavonol and biflavone aglycones and several phenols (19, 21 ($p < 0.05$), 77, and 98% ($p < 0.001$), respectively). *H. perforatum* extract and the fractions containing bianthraquinones, flavonol glycosides and flavonol and biflavone aglycones significantly inhibited lipid peroxidation, after cell incubation with β -amyloid_(25–35) 25 μM ($p < 0.001$), with levels lower than the control basal peroxidation. Cell viability was determined by Syto-13/PI assay. *H. perforatum* ethanolic extract and fractions containing flavonol glycosides, flavonol, and biflavone aglycones reduced cell death [65, 58, and 59%, respectively, when comparing to control ($p < 0.001$)]. Morphological analysis with cells stained with cresyl violet showed that after cell exposure to amyloid β -peptide a pattern of neuronal death was observed, specifically by a decrease in cell volume, nuclear condensation, appearance of apoptotic bodies and dendritic retraction. These alterations were not evident in the presence of *H. perforatum* extract and fractions containing bianthraquinones and flavonol glycosides. Accordingly with these results, the authors concluded that *H. perforatum* alcoholic extract and studied fractions have neuroprotective activity, which can be of relevance on preventing amyloid- β peptide neuronal degeneration. The senile plaques, in Alzheimer's disease, are also enriched with reactive microglia and astrocytes (Akiyama et al., 2000). As immunocompetent cells of the brain, the microglia are able to counteract the deleterious effects of amyloid- β in Alzheimer's disease. Taking this in consideration and amyloid β -peptide toxicity described above, Kraus et al. (2007) investigated the effects of the peptide on cell viability of microglia and a possible protective mode of action of *H. perforatum* extract by studying the influence of a pretreatment on cell survival. In BV2 and N11 cells (microglial cell lines) pretreated with *H. perforatum* ethanolic extract 50–100 $\mu\text{g/mL}$, the cell death evoked by treatment with amyloid- β _(25–35) and amyloid- β _(1–40) was significantly attenuated in a dose-dependent manner. It was concluded that treatment with *H. perforatum* ethanolic extract may restore or improve microglial viability, attenuating amyloid- β mediated toxicity in Alzheimer's disease. Regarding biochemical and neurotransmitter alterations in the brain, this neurodegenerative disorder is characterized by a loss of cholinergic markers butyrylcholine and acetylcholine that are hydrolyzed butyrylcholinesterase and acetylcholinesterase, respectively. Cholinesterases are an ubiquitous class of serine hydrolases that hydrolyze choline esters with various efficiency

(Talesa, 2001). The inhibitory effects of ethyl acetate, methanol and water *H. perforatum* extracts against butyrylcholinesterase and acetylcholinesterase were, therefore, investigated. Methanol extract was the one that, from the three tested, exerted the highest acetylcholinesterase inhibition (49.54 ± 4.44%), while the ethyl acetate extract had the best inhibition toward butyrylcholinesterase (50.79 ± 3.07%). The water extract presented no inhibitory effect in the tested concentrations (50–200 $\mu\text{g/mL}$). Another enzyme that has become a research target in neurodegenerative diseases investigation has been tyrosinase, a multifunctional enzyme, involved in neuromelanin production and damaged neurons associated with Parkinson's disease. The three *H. perforatum* extracts described above were also tested against tyrosinase, and only the methanol extract was found to have a low inhibitory effect (19.21 ± 1.44%; Asanuma et al., 2003; Altun et al., 2013).

Hypericum perforatum's neuroprotective activity has also been investigated in association with other compounds. For instance, a drug commonly used for the treatment of Parkinson's disease is bromocriptine, which is reported to have strong free radical scavenging action *in vivo* and potent neuroprotective actions (Muralikrishnan and Mohanakumar, 1998; Mohanasundari et al., 2006). Due to several adverse effects of bromocriptine monotherapy, Mohanasundari et al. (2006) evaluated the combined effect of bromocriptine and *H. perforatum* alcoholic extract against 1-Methyl-4-phenyl-1,2,3,6-tetrahydropyridine (MPTP), a neurotoxin, in mice. Lipid peroxidation increased in the MPTP-treated group when compared to the control (in 91%). *H. perforatum* extract and bromocriptine alone lowered lipid peroxidation ($p < 0.05$) and the combined treatment showed even better results, when comparing with all the other groups (control, *H. perforatum* and MPTP-treated groups; $p < 0.05$). A mixture of *Panax quinquefolius*, *Ginkgo biloba*, and *H. perforatum* was proven to enhance retinal ganglion cell survival after axotomy, increasing the number of regenerating retinal ganglion cell in 87%, 21 days after optic nerve transaction. Effects of the herbal extracts mixture on the survival of axotomized retinal ganglion cells 7 days after axotomy showed a delay in cell death, offering, therefore, significant neuroprotection ($p < 0.01$) versus optical nerve transaction (Cheung et al., 2002). Axotomy-induced retinal ganglion cell death has been adopted as an animal model in the investigation of neuronal death in the CNS. It is known to be related to the activation of apoptotic pathways (Cheung et al., 2008), like caspase-3 and -9 (Cheung et al., 2004). When investigating the mechanisms underlying a neuroprotective activity of the herbal mixture described, Cheung et al. (2008) verified an apoptotic property, through the inhibition of cell's nuclear fragmentation, with no effect on caspase-3 action, suggesting that the reduction of nuclear fragmentation was not achieved by the limitation of caspase-3 activation. The mixture, nonetheless, reduced the percentage of caspase-3-negative fragmented nuclei, though with no effect in caspase-3-dependent nuclear fragmentation, suggesting an inhibition by a caspase-3 independent pathway. Additionally, an intravitreal injection with wortmannin, a phosphoinositide-3 kinase (PI3K) inhibitor, abolished the neuroprotective effect of the herbal mixture, indicating, according to the authors, that this

effect was PI3K-dependent. It's important to refer that PI3K–Akt (Akt: protein kinase identified in the AKT virus [also known as protein kinase B]) signaling pathway plays a critical role in mediating survival signals in a wide range of neuronal cell types (Brunet et al., 2001).

Since the removal of excessive ROS or suppression of their generation by antioxidants may be effective in the prevention of oxidative cell damage (Benedi et al., 2004), having therefore a neuroprotective effect, the protective antioxidant properties of *H. perforatum* will also be described.

El-Sherbiny et al. (2003) studied the effect of a dried ethanolic *H. perforatum* extract on brain oxidative status of naïve rats upon the administration of an amnesic dose of scopolamine. When in doses equivalent to the ones used to treat depression, the extract proven to inhibit brain malondialdehyde (MDA) formation, modulating also the activity of GPx and the glutathione levels without any alteration on any of the measured oxidative stress indices, suggesting that low doses of *H. perforatum* extract have antioxidant properties, protecting rat brain from elevated oxidative status due to the administration of antidepressants. These protective activities have also been reported in a hydroethanolic standardized and ethanolic (Benedi et al., 2004; Silva et al., 2005; Silva B.A. et al., 2008) extracts of *H. perforatum* through a direct radical scavenging activity on 1,1-diphenyl-2-pycryl-hydrazyl (DPPH) radical [$EC_{50} = 109 \mu\text{g/mL}$ (Benedi et al., 2004), $49.3 \pm 1.05 \mu\text{g/dwb/mL}$ (Silva B.A. et al., 2008), and $21 \mu\text{g/dwb/mL}$ (Silva et al., 2005)] and inhibition of xanthine oxidase (XO) activity (at a concentration of $5 \mu\text{g/mL}$ the reported inhibition of XO activity was by 16% with an $IC_{50} = 68.3 \mu\text{g/mL}$), which may also contribute to the scavenging action of the O_2^- radical by *H. perforatum*. According to these findings, *H. perforatum* may have the ability to bind iron ions and a moderate to high direct scavenging action for hydroxyl radical, independent of any enzymatic activity (Benedi et al., 2004; Silva et al., 2005; Silva B.A. et al., 2008). Besides these properties, *H. perforatum* ethanolic and aqueous extracts has the ability to inhibit stress induced by 2,2'-azo-bis(2-methylpropionamidine) dihydrochloride (AAPH), an inductor of lipid peroxidation by formation of peroxy radicals [$IC_{50} = 50.4 \pm 2.57 \mu\text{g/dwb/mL}$ (Silva B.A. et al., 2008) and $16.77 \mu\text{mol}$ of Trolox equivalent/g of fresh weight (Zheng and Wang, 2001)] and scavenge nitric oxide (NO) [through nitrite measurement, used as an estimate for the NO content (Cheung et al., 2008; Silva B.A. et al., 2008)] ($10 \mu\text{g/dwb/mL}$ extract showed $78.7 \pm 1.3\%$ reduction of release of nitrite) and hypochlorous acid (through the reduction of 5-thio-2-nitrobenzoic acid (TNB; $50 \mu\text{g/dwb/mL}$ extract showed $17.1 \pm 1.3\%$ reduction in TNB oxidation; Silva B.A. et al., 2008).

As stated previously, Parkinson's a neurodegenerative disease. In patients suffering from this pathology a reduction of mitochondrial complex I activity has been reported. Rotenone, a pesticide and specific inhibitor of this complex, causes tissue damage due to its toxic effect (Sanchez-Reus et al., 2007), with an involvement of oxidative damage (Sherer et al., 2003). Taken this in consideration, the potential antioxidant protective effect of a standardized extract of *H. perforatum* against rotenone-exposed rats was investigated. The extract was tested on brain MDA, GPx, CAT, MnSOD, and CuZnSOD expression and activities.

Pretreatment of rats with *H. perforatum* extract before insult with rotenone resulted in an antioxidant activity with a decrease in brain MDA formation and an increase of SOD, CAT, and GPx levels. Regarding enzyme activities, *H. perforatum* extract recovered brain mRNA levels of SOD and GPx, altered by rotenone. In the case of CAT, pretreatment with the extract also revealed an antioxidant effect reducing mRNA levels of the enzyme elevated after rotenone administration, but this result was different from those of activity (Sanchez-Reus et al., 2007). This could be explained by an up-regulation of the relevant gene expression, protecting therefore the cell from rotenone toxicity (Alia et al., 2006).

Similarly to neuroprotective, also antioxidant properties of *H. perforatum* extracts have been tested in combined treatment regimens. When in simultaneous administration with bromocriptine and after an insult with MPTP, restoration of CAT, SOD, reduced glutathione (GSH), and GPx levels (CAT – 0.19 ± 0.01 to 0.57 ± 0.02 ; SOD – 1.97 ± 0.12 to 3.51 ± 0.08 ; GSH – 0.28 ± 0.02 to 0.53 ± 0.02 ; GPx – 8.6 ± 0.02 to 12.0 ± 0.07) to near normal (CAT – 0.58 ± 0.01 ; SOD – 3.83 ± 0.02 ; GSH – 0.62 ± 0.01 ; GPx – 12.21 ± 0.17) was verified (Mohanansundari et al., 2006). The herbal mixture of *P. quinquefolius*, *G. biloba*, and *H. perforatum* described previously also exhibited antioxidant activity, mainly NO scavenging property, by lowering NO content in axotomized retinas [treatment with 30 mg of the mixture significantly lowered the amount of nitrite ($p < 0.05$) versus PBS-treated control group] without affecting NO synthase activity (Cheung et al., 2008).

Neuroprotective Activity of *Hypericum perforatum* Major Compounds

Hypericum perforatum's major compounds are described as neuroprotective in several studies, being this activity related with direct pathways, such as an *in vitro* and *in vivo* cytoprotective effect and indirect pathways, particularly through its antioxidant properties.

Quercetin

Quercetin, whose ability to interact with multiple cellular targets is likely the basis of its therapeutic activity (Dajas, 2012) has been described to protect against several insults, such as H_2O_2 (Dok-Go et al., 2003; Arredondo et al., 2004, 2010; Heo and Lee, 2004; Suematsu et al., 2011), linoleic acid hydroperoxide (LOOH; Sasaki et al., 2003), 6-hydroxydopamine (6-OHDA; Zhang et al., 2011), and *tert*-butylhydroperoxide (*t*-BOOH; Silva J.P. et al., 2008), in PC12 cells (Sasaki et al., 2003; Arredondo et al., 2004; Heo and Lee, 2004; Silva J.P. et al., 2008; Zhang et al., 2011), primary cultured rat cortical cells (Dok-Go et al., 2003) and rat cerebellar granule neurons (Arredondo et al., 2010) and human neuronal SH-SY5Y cells (Suematsu et al., 2011). In the first case, it's described a cytoprotective action of quercetin 25 and $50 \mu\text{M}$ and $30\text{--}100 \mu\text{M}$ against H_2O_2 200 and $400 \mu\text{M}$ (Arredondo et al., 2004; Heo and Lee, 2004), respectively, in PC12 cells. Similar effects were described, for primary cultured rat cortical cells, with quercetin at concentrations of 3 and $10 \mu\text{g/mL}$, facing a H_2O_2 -injury at $100 \mu\text{M}$ ($IC_{50} = 4.1 \mu\text{g/mL}$; Dok-Go et al., 2003). In primary rat cerebellar granule neurons a pretreatment with

quercetin 25 μM significantly protected ($p < 0.001$) the cells from H_2O_2 -injury at 60 μM . These findings were supported by morphological analysis of the cells (Arredondo et al., 2010). Heo and Lee (2004) also studied quercetin's ability to block H_2O_2 -induced membrane damage, verifying a significantly protective effect of this flavonol ($p < 0.05$). In human neuronal SH-SY5Y cells, quercetin increased the viability of H_2O_2 -treated cells in a concentration dependent manner, becoming about 67% of that of the vehicle-treated ones at 100 μM . There were also suppressed H_2O_2 -induced apoptotic features, such as DNA fragmentation, by co-treatment with quercetin, in a concentration dependent manner. In addition, quercetin suppressed the caspase cascade and pro-apoptotic Bax gene expression and increased anti-apoptotic Bcl-2 gene expression (Suematsu et al., 2011). Regarding LOOH insult, protective effects were reported in undifferentiated and differentiated PC12 cells with quercetin 25 and 50 μM , respectively, in pre- and co-incubation regimens (Sasaki et al., 2003). Pretreatment with quercetin 12.5–200 μM protected PC12 cells against 6-OHDA-induced damage (at a concentration of 1 mM) in a dose-dependent manner and significantly reduced ($p < 0.05$) the LDH leakage caused by the neurotoxin. Likewise, quercetin prevented 6-OHDA-induced cell apoptosis and attenuated 6-OHDA-induced NO over-production and iNOS over-expression. Morphological analysis of the cells treated with 6-OHDA revealed the presence of bright condensed dots, apoptotic bodies. There was also verified a reduction in colony density and cell size. Pretreatment with quercetin 25, 50, and 100 μM significantly attenuated nuclear condensation and at higher concentrations (50 and 100 μM) inhibited 6-OHDA-induced colony reduction and cell shrinkage (Zhang et al., 2011). Regarding NO production, it's believed that its augment and consequent iNOS induction plays an important role in the initial phase of 6-OHDA-induced neuro-damage in *in vitro* and *in vivo* models (Lin et al., 2007). Taking this in consideration, Zhang et al. (2011) with a mechanistic study, tested the effect of quercetin on 6-OHDA-induced NO over-production and iNOS over-expression in PC12 cells, concluding that quercetin attenuated NO over-production via down-regulation of iNOS over-expression in 6-OHDA-treated cells. Silva J.P. et al. (2008) studied the protective effect of quercetin against *t*-BOOH-induced strand breaks. When added simultaneously with the insult, quercetin's protective effect was significantly increased ($p \leq 0.001$, compared with *t*-BOOH 200 μM), when comparing with a co-incubation regimen ($p \leq 0.01$).

Likewise, pretreatment of HT22 cells with quercetin 5 and 10 μM significantly attenuated amyloid- $\beta_{(1-42)}$ -induced cytotoxicity ($p < 0.001$) and decreased 4-hydroxynonenal levels (an index of lipid peroxidation), in comparison to control ($p < 0.001$). Low doses of quercetin (5 and 10 μM) also mitigated morphological alterations induced by amyloid- $\beta_{(1-42)}$, characterized by vacuolated soma and fragmented neurites, membrane blebblings and cell shrinkage, inhibiting, therefore amyloid- $\beta_{(1-42)}$ -induced apoptotic cell death (Ansari et al., 2009).

Liu et al. (2013) studied the effect of quercetin in the neurovascular unit (NVU) and its underlying mechanisms. The NVU comprises cerebral blood vessels and surrounding

cells, such as astrocytes, neurons, and pericytes (Abbott, 2002) where the receptor for advanced glycation end products (RAGE) and low density lipoprotein receptor related protein-1 play an important role in the control of amyloid- β levels in the brain (Deane et al., 2009), maintaining it. After injecting amyloid- $\beta_{(25-35)}$, quercetin, in concentrations from 5 to 40 mg/kg, was orally administrated, in male Kunming mice, for 8 days. Quercetin treatment improved the learning and memory capabilities and conferred neurovascular coupling protection, involving maintenance of the NVU integrity, reduction of neurovascular oxidation, modulation of microvascular function, improvement of cholinergic system, and regulation of neurovascular RAGE signaling pathway. The authors conclude on a possible quercetin mechanism through reduction of oxidative damage, inactivation of RAGE-mediated pathway and preservation of cholinergic neurons (Liu et al., 2013).

Silva B. et al. (2008) investigated the effects of *H. perforatum*'s phenolic compounds, such as quercetin, against neuronal excitotoxicity and mitochondrial dysfunction. Quercetin 10 μM significantly reduced neuronal death due to kainate and NMDA-insult ($p < 0.05$). The authors correlated this protection with prevention of toxic-induced delayed calcium deregulation and the maintenance of mitochondrial electric potential. Quercetin 10 μM was also able to reduce mitochondrial lipid peroxidation and loss of mitochondrial transmembrane electric potential caused by oxidative stress ADP plus Fe-induced.

In Sprague-Dawley rats, with Parkinsonism induced by the neurotoxin 6-OHDA, a 14 days treatment with quercetin significantly increased the striatal dopamine ($p < 0.05$) by 34.56% and decreased the striatal protein carbonyl level ($p < 0.05$) by 49.69% compared with levels found in the 6-OHDA treated group (Haleagrahara et al., 2011). The increase of protein carbonyls is a proof of oxidatively damaged proteins, characteristic of Parkinson's disease (McNaught et al., 2003). In zebrafish, considered a good model to study disorders of the dopaminergic system (Rink and Wullimann, 2001), co-treatment with quercetin (6 or 12 μM) significantly inhibited 6-OHDA-induced dopaminergic neuron loss ($p < 0.05$). However, there was no reversion of the neuron loss by quercetin after a 48 h exposure to 6-OHDA, what could be attributed to the poor permeability of quercetin across the blood-brain-barrier (Ossola et al., 2009; Zhang et al., 2011).

Regarding its antioxidant properties, quercetin has been shown to have an excellent *in vitro* antioxidant activity and it is considered the most potent scavenger of ROS, RNS, and peroxynitrite of the flavonoid family (Boots et al., 2008). In human hepatoma HepG₂ cell line, quercetin 50 and 100 μM evoked a significant increase of intracellular GSH ($76 \pm 6 \text{ ng/mg/protein}$ and $83 \pm 7 \text{ ng/mg/protein}$, respectively), after 4 h treatment ($p < 0.05$; Alia et al., 2006), which can be expected, assuming the preparation of the cell against a potential oxidative insult (Myhrstad et al., 2002). This flavonol was also able to inhibit significantly ROS generation ($p < 0.05$), after insult with *t*-BOOH, therefore preventing or delaying conditions which favor oxidative stress in the cell (Alia et al., 2006). Increase of intracellular GSH has also been reported in rat primary cerebellar

granule neurons, after a 24 h quercetin 25 μM pretreatment ($146.3 \pm 12\%$, in comparison to control; Arredondo et al., 2010). Regarding GSH synthesis, it's important to refer the role of the Nuclear factor erythroid 2 related factor 2 (Nrf2)-dependent cytoprotective pathway in the induction of gene expression of enzymes involved in it. Taking into account that Nrf2 is a translocation factor, it is essential that it translocates to the nucleus in order to transactivate (Myhrstad et al., 2002; Zhang et al., 2013). Consequently, Liu et al. (2013) studied the activity of quercetin in nuclear translocation of Nrf2 in neurons. By the use of immunocytochemistry, there was verified that quercetin-treated cultures presented a major Nrf2 signal in both cytoplasm and, particularly, nucleus. The authors conclude that quercetin has the ability to cause nuclear translocation of Nrf2 in neuronal cultures, therefore activating the Nrf2 cytoprotective signaling pathway. Similarly, quercetin's protective activity was verified by the inhibition of the oxidative injury induced by xanthine/XO in primary cultured rat cortical cells (quercetin 10 $\mu\text{g}/\text{mL}$ and $\text{IC}_{50} = 5.5 \mu\text{g}/\text{mL}$; Dok-Go et al., 2003).

Quercetin prevents DNA single strand breakage and cytotoxicity, in U937 lymphoblast human cell line, caused by *t*-BOOH through its iron chelation properties. In fact, quercetin 100 μM and desferroxamine, an iron chelator (used as a control for this activity) prevented DNA cleavage generated by H_2O_2 , whereas antioxidants trolox and *N,N'*-diphenyl-1,4-phenylenediamine were not efficient (Sestili et al., 1998). Metallic ions chelating is also involved in quercetin's ability to diminish and prevent the oxidative hepatic damage produced by ethanol, besides interrupting the chain reaction that takes place on the lipid membrane. Pre-treatment with quercetin in mice treated with chronic doses of ethanol is more effective for CAT, selenium dependent-GPx, total GPx and GSH, which can be explained by a possible promotion of the antioxidant endogenous defenses (Molina et al., 2003).

According to Inal and Kahraman (2000), quercetin may be useful in reducing or preventing photobiologic damage, caused by ultraviolet A light, since it significantly decreases MDA levels ($p < 0.05$ and $p < 0.001$) and increases antioxidant defenses, namely SOD and CAT activities ($p < 0.001$), in Sprague-Dawley rats. In the same animal model, with Parkinsonism induced by 6-OHDA, a 14 days treatment with quercetin partially restored GSH levels, increasing it by 97.88% as compared with GSH in rats treated only with 6-OHDA ($p < 0.05$; Haleagrahara et al., 2011).

Antioxidant activities of quercetin have also been reported through its antiradical activity on DPPH [$\text{EC}_{50} = 8.30 \pm 1.03 \mu\text{M}$ (Silva B.A. et al., 2008), $11.34 \pm 0.04 \mu\text{M}$ (Ramos et al., 2008) and $10.37 \pm 1.53 \mu\text{g}/\text{mL}$ (Dok-Go et al., 2003)] and AAPH [$\text{EC}_{50} = 29.4 \pm 2.29 \mu\text{M}$], lipid peroxidation inhibition potential [$\text{EC}_{50} = 0.08 \pm 1.90 \mu\text{M}$; Silva B.A. et al., 2008] and inhibitory effect on NO synthase in a concentration-dependent manner, determined in rat cerebral homogenate and blood ($\text{IC}_{50} = 63.06$ and $57.54 \mu\text{M}$, respectively; Luo et al., 2004).

Despite its beneficial activities, quercetin has also been reported to have toxic effects (Dok-Go et al., 2003; Arredondo et al., 2004, 2010; Boots et al., 2008; Ansari et al., 2009), being consequently important, to define, the therapeutical concentration of this compound (Ansari et al., 2009), for

different pathologies, in order to maximize positive and minimize deleterious effects. It's also relevant to refer that studies of *in vivo* quercetin's neuroprotective activity remains controversial which can be due to the failure to examine prolonged exposures to micromolar levels of the flavonol and a required unattainable *in vivo* concentration (Ossola et al., 2009; Dajas, 2012).

Hyperoside

Hyperoside is the main active component of *H. perforatum* (Silva B.A. et al., 2008). Despite this, its neuroprotective activity has not been explored. Liu et al. (2005) evaluated hyperoside's ability to prevent ROS generation and diminishing neuronal damage, in PC12 cells. Alone, hyperoside promoted the growth rate of the cells among the concentrations of 10–180 $\mu\text{g}/\text{mL}$, markedly between 10 and 120 $\mu\text{g}/\text{mL}$. As for its cytoprotective activity, hyperoside was effective preventing *t*-BOOH- and H_2O_2 -induced toxicity, in a dose dependent manner, with the best improvement for 175% of control group at 160 $\mu\text{g}/\text{mL}$ and 177% of control group at 100 $\mu\text{g}/\text{mL}$. These results were concordant to those of flow cytometry assay, where apoptotic cells formed via *t*-BOOH- and H_2O_2 -induced toxicity were measured (sub-G1 peak). Hyperoside (160 and 100 $\mu\text{g}/\text{mL}$) attenuated cell death via apoptosis to 1.0 and 1.3%, respectively (Abbott, 2002). Protective properties of hyperoside in amyloid- $\beta_{(25-35)}$ -induced toxicity, in primary cortical rat neurons, were also studied. After exposure to amyloid- $\beta_{(25-35)}$ (20 μM) for 24 h cell viability decreased to $63.1 \pm 3.2\%$. Pretreatment for 30 min with hyperoside 5, 10, and 20 μM significantly increased cell viability [$p < 0.05$ for 5 and 10 μM and $p < 0.01$ for 20 μM , in comparison with amyloid- $\beta_{(25-35)}$ treatment group]. Morphological analysis of the cells supported these results, with an effective reversion of amyloid- $\beta_{(25-35)}$ neurite injury (observed as neurite loss and cleavage) after pretreatment with hyperoside (2.5, 5, 10, and 20 μM). Apoptosis was also reverted in a dose dependent manner, after pretreatment with hyperoside, by reversing the amyloid- β -induced mitochondrial dysfunction, including mitochondrial membrane potential decrease, ROS production, and mitochondrial release of cytochrome *c*. Caspase-9 and caspase-3 activities were also significantly inhibited ($p < 0.01$), after pretreatment with hyperoside (5, 10, and 20 μM) and amyloid- $\beta_{(25-35)}$ -induced injury. Further study indicated that hyperoside can activate PI3K/Akt signaling, resulting in inhibition of Bad-Bcl_{XL} interaction, without intervening in Bad-Bcl-2 interaction. It was concluded that hyperoside can protect amyloid- $\beta_{(25-35)}$ -induced injury in primary cultured cortical neurons via PI3K/Akt/Bad/Bcl_{XL}-regulated mitochondrial apoptotic pathway (Zeng et al., 2011). In the same biological model, the neuroprotective activity of hyperoside was investigated, by using an *in vitro* ischemic model of oxygen-glucose deprivation followed by reperfusion (OGD-R). Pretreatment with hyperoside (3, 10, 30, and 100 μM) for 24 h was able to significantly protect cultured cortical neurons from OGD-R injury ($p < 0.05$ for 3 μM and $p < 0.01$ for 10, 30, and 100 μM , in comparison to OGD-R group). In order to investigate the protective effect of hyperoside in neuronal excitotoxicity that can occur after OGD-R injury, cultured cortical neurons were exposed to glutamate 200 μM combined with glycine

10 μM for 2 h, followed by 24 h reperfusion. Pretreatment with hyperoside 24 h prior to the glutamate-exposure reversed the degradation of cell viability in a concentration dependent manner and significantly increased the neuronal survival rate ($p < 0.05$ for 1 μM and $p < 0.01$ for 3, 10, 30, and 100 μM in comparison to glutamate-exposure group). Hyperoside (10 μM) also relieved NMDA receptor-induced $[\text{Ca}^{2+}]_i$ elevation ($p < 0.01$, compared to NMDA group). NMDA receptor mediates Ca^{2+} influx, which is responsible for excitotoxicity (Liu et al., 2012). As for possible related mechanisms, the authors describe attenuation of CaMKII phosphorylation caused by OGD-R lesions. Hyperoside also lessened iNOS expression induced by OGD-R via inhibition of Nf- κB activation and ameliorated extracellular signal-regulated kinase, c-Jun NH₂-terminal kinase, and Bcl-2 family-related apoptotic signaling pathways (Liu et al., 2012), related to NO signaling pathway.

As for its antioxidant activity, hyperoside is known for its ROS scavenging activity (Liu et al., 2005). It has active antiradical activity on DPPH ($\text{EC}_{50} = 6.38 \pm 1.06 \mu\text{M}$) and APPH ($\text{EC}_{50} = 11.5 \pm 1.76 \mu\text{M}$), lipid peroxidation inhibition potential ($\text{EC}_{50} = 5.37 \pm 1.05 \mu\text{M}$; Silva B.A. et al., 2008) and inhibitory effect on NO synthase in a concentration-dependent manner, determined in rat cerebral homogenate and blood ($\text{IC}_{50} = 56.23$ and 158.49 μM , respectively; Luo et al., 2004).

Quercitrin

Quercitrin is thought to possibly overcome quercetin in its antioxidant and neuroprotective activity due to its high bioavailability in the digestive track (Hollman et al., 1995). Despite this, few studies have been published focusing on the neuroprotective activity of quercitrin. Rattanajarasroj and Unchern (2010) studied the neuroprotective effects of quercitrin on amyloid- $\beta_{(25-35)}$ -induced injury in cultured hippocampal rat neurons, as well as its possible mechanisms. Co-incubation of quercitrin (50 and 100 μM) and amyloid- $\beta_{(25-35)}$ for 72 h significantly increased cell viability ($p < 0.01$), in comparison to cells only subjected to amyloid- $\beta_{(25-35)}$ injury. These results were supported by the analysis of cell death, through LDH leakage assay. Here and in all experimental conditions, the magnitude of cell death was correlated with the percentage of cell viability in a complementary manner. Neuroprotective potential of quercitrin, using a rat primary-isolated retinal ganglion cells cultured under three types of stress conditions: hypoxia, excessive glutamate levels, and oxidative stress, was also evaluated. After 12 h of hypoxia stress, the retinal ganglion cells survival rate was reduced in cells without quercitrin to $55.5 \pm 10\%$. Treatment with quercitrin 100 nM and 1 μM significantly increased retinal ganglion cell viability ($p < 0.05$; Nakayama et al., 2011). Regarding glutamate-induced cell death similar results were verified, with the quercitrin-treated retinal ganglion cells [increase in cell viability, in the same concentrations referred above ($p < 0.05$)].

As for its antioxidant activity, co-exposure of quercitrin (50 and 100 μM) and amyloid- $\beta_{(25-35)}$ for 72 h significantly decreased cellular lipid peroxidation in a concentration dependent manner ($p < 0.05$, compared to amyloid- $\beta_{(25-35)}$ -exposure group). There were, however, no significant effects

on amyloid- $\beta_{(25-35)}$ -induced ROS accumulation. It was hypothesized that a long exposure of cells to quercitrin could alter intracellular antioxidant defense system, including the production of GSH, SOD, and GPx. However, only GPx significantly increased its activity after co-exposure to quercitrin and amyloid- $\beta_{(25-35)}$ ($p < 0.05$; Rattanajarasroj and Unchern, 2010).

Antioxidant activities of quercitrin have also been reported through its antiradical activity on DPPH ($\text{EC}_{50} = 13.0 \pm 1.10 \mu\text{M}$) and lipid peroxidation inhibition potential (Wagner et al., 2006; Silva B.A. et al., 2008; $\text{EC}_{50} = 7.33 \pm 1.16 \mu\text{M}$; Silva B.A. et al., 2008).

Rutin

Neuroprotective properties of rutin, a flavonoid with a wide range of biological activities, have been investigated. Wang et al. (2012) studied the interference of rutin in the pathogenic factors of Alzheimer's disease. Morphological analysis of amyloid- β fibrillization revealed that amyloid- β_{42} co-incubation with rutin 200 μM inhibited by more than 95% fibril formation. In SH-SY5Y cells rutin 20 μM significantly inhibited amyloid- β_{42} cytotoxicity ($p < 0.05$), also restoring cells fluorescent intensity ratio value in a concentration-dependent manner, which is, according to the authors, indicative of an attenuation of amyloid- β_{42} -induced mitochondrial dysfunction. In order to determine rutin's ability to protect against an oxidative damage, SH-SY5Y cells were treated with amyloid- β_{42} , in the presence and absence of rutin. The flavonoid decreased amyloid- β_{42} -induced ROS production in a concentration dependent-manner, with a significant inhibition when rutin 8 μM was employed ($p < 0.05$). Likewise, MDA levels were significantly decreased with rutin 0.8 and 8 μM ($p < 0.05$). Regarding the regulatory effect of rutin on GSH content, rutin 0.8 and 8 μM increased, in a concentration-dependent manner, GSH content of BV-2 microglial cells and decreased GSSG levels. The GSH/GSSG ratios were also decreased by amyloid- β_{42} and increased with the addition of rutin 8 μM ($p < 0.05$). Rutin's effects on aldehyde dehydrogenase 2 (enzyme which metabolizes acetaldehyde into non-toxic acetate; ALDH2) activity in HT22 cells were also studied. Pretreatment with rutin 1 $\mu\text{g/mL}$, significantly inhibited ethanol-induced cell death ($p < 0.01$). Co-treatment with rutin also significantly reversed ethanol-increased Bax ($p < 0.05$, compared with ethanol), caspase 3 activity, and decreased Bcl-2 and Bcl-xL protein expression ($p < 0.01$, compared with ethanol). In order to clarify the mechanisms involved in rutin's protective effects, an ALDH2 inhibitor, daidizin, was employed. Taking into account that pretreatment with rutin also lowered cytochrome *c* expression (involved in ethanol-induced apoptosis in HT22 cells; $p < 0.01$) and increased ALDH2 expression, it is concluded that rutin protects HT22 cells against ethanol-induced neurotoxicity by increasing ALDH2 activity (Song et al., 2014). Nakayama et al. also investigated the effects of rutin under the three types of stress conditions mentioned above. Regarding hypoxia stress, the retinal ganglion cells survival rate was reduced in cells without rutin $56.0 \pm 3.1\%$. Treatment with rutin 1, 10, and 100 nM significantly increased retinal ganglion cell viability ($p < 0.05$). As for glutamate-induced cell death similar results

were verified [increase in cell viability, in the same concentrations referred above ($p < 0.05$)]. Under oxidative stress conditions, the activity of caspase-3 and calpain were studied, in order to investigate the effect of rutin in apoptotic and necrotic cell death signaling, respectively. Calpains are a family of cytosolic cysteine proteinases whose enzymatic activities depend on Ca^{2+} and are believed to function in various biological processes, including cell death, more specifically, necrosis. Rutin at final concentrations of 1, 10, and 100 nM showed significant reduction of caspase-3 activity under hypoxia and by glutamate stress ($p < 0.05$) and of calpain activity by oxidative stress ($p < 0.05$; Goll et al., 2003; Nakayama et al., 2011).

Khan et al. (2009) investigated the protective effects of rutin on cerebral ischemia on Wistar rats. Pretreatment with rutin (25 mg/kg, for 21 days) protected the animals from motor deficit and lead to recovered motor coordination ($p < 0.05$, in comparison with the lesion group), improving, therefore, the neurological outcomes. It was also verified a significant attenuation ($p < 0.05$) on thiobarbituric acid reactive species, H_2O_2 levels and protein carbonyl content, in comparison to lesioned rats. Morphological analysis of rats' brains revealed that activation of p53 up-regulation (associated with neuronal cell death in cerebral ischemia) was also attenuated by rutin. These results lead the authors to conclude that rutin offered significant protection on middle cerebral artery occlusion rats, probably due to inhibition of neurological deficit, lipid peroxidation, p53 expression and increase in endogenous antioxidant defense enzymes (data shown downward), evoking neuroprotection to the degenerating dopaminergic neurons (Khan et al., 2012). Taking the previous results into consideration, Khan et al. (2012) investigated the neuroprotective activity of rutin on 6-OHDA-induced Parkinson's disease in rats. Similar results were obtained concerning the rutin's protective activity, leading the authors to suggest that the consumption of rutin may have positive effects on the prevention on neurological disorders, such as Parkinson's disease. Regarding Alzheimer's disease and in following the study of Wang et al. (2012) and Xu et al. (2014) investigated the effects of rutin on APPswe/PS1dE9 transgenic mice. These animals overproduce human amyloid- β_{40} and amyloid- β_{42} , also developing progressive cerebral β -amyloid deposit and learning and memory impairment, being considered animal models for Alzheimer's disease (Garcia-Alloza et al., 2006). Oral administration of rutin (100 mg/kg for 6 weeks) significantly attenuated memory deficits, associated with the reduction in β -amyloid oligomer formation. It also improved spatial memory ($p < 0.05$, compared with disease's control group) in transgenic mice. Similarly to *in vitro* studies performed by Wang et al. (2012), there was also reported a protective activity by rutin in the attenuation on β -amyloid-induced oxidative stress and lipid peroxidation. Rutin was also able to reduce neuro-inflammation in transgenic mice by attenuating microgliosis and astrocytosis (Xu et al., 2014).

Rutin is considered to have powerful antioxidant capacity against several antioxidant *in vitro* systems, being a concentration dependent property (Yang et al., 2008). Alike quercetin, in HepG₂ cells, rutin 100 μM significantly increased intracellular GSH ($52 \pm 2 \text{ ng/mg/protein}$; $p < 0.05$). Despite its similar effects, rutin

demonstrated to be less active than quercetin, which could be related to its lower bioavailability (Alia et al., 2006).

As to *in vivo* studies, antioxidant activities have also been reported (La Casa et al., 2000; Kamalakkannan and Stanely Mainzen Prince, 2006; Khan et al., 2009; Xu et al., 2014). Pre-treating Wistar rats with rutin (25 mg/kg, for 21 days) significantly restored ($p < 0.05$) GSH, GPx, GR, SOD, and CAT in hippocampus (GPx – from -35.69 to 31.31%; GR – from -45.12 to 48.65%; SOD – from -45.18 to 39.42%; CAT – from -54.28 to 66.96%) and frontal cortex (GPx – from -41.53 to 45.56%; GR – from -46.36 to 36.53%; SOD – from -50.51 to 68.73%; CAT – from -55.95 to 43.80%), in comparison to lesioned rats (Khan et al., 2009).

Antioxidant activities of rutin have also been reported through its antiradical activity on DPPH [Ramos et al., 2008; Silva B.A. et al., 2008; Yang et al., 2008; EC₅₀ = 11.3 \pm 1.06 μM (Silva B.A. et al., 2008) IC₅₀ = 18.27 \pm 0.62 μM (Ramos et al., 2008)], AAPH [EC₅₀ = 31.5 \pm 4.93 μM (Silva B.A. et al., 2008)], lipid peroxidation inhibition potential (EC₅₀ = 8.98 \pm 1.03 μM) and scavenging of superoxide radicals (IC₅₀ = 0.13 mg/mL) and hydrogen peroxide (IC₅₀ = 24 $\mu\text{g/mL}$; Yang et al., 2008).

Hypericin

The effect of hypericin (neuroprotection or apoptosis) on the transcription factor NF- κ B, which is involved in regulation of genes relevant in several cellular processes, like neuronal survival and inflammatory response, has been accessed (Kaltschmidt et al., 2002). One hour treatment of cerebellar granule cells with 0.1 μM hypericin resulted in activation of NF- κ B, which is further enhanced with 1 or 10 μM hypericin. Despite of the hypothesis that long-lasting activation of the transcription factor would result in neuroprotection, a 24 h treatment with different hypericin concentrations lead to a loss of the NF- κ B activation previously observed. Basing on these results the authors investigated the effect of hypericin in Fe²⁺ ion-induced cell death. While low concentrations of hypericin (0.1 and 1 μM) had no effect on cell survival, 10 μM exerted cell death up to 100% after 24 h treatment, having therefore a synergistic effect with Fe²⁺. It was concluded that stimulus like hypericin, depending on the gene promoters that are activated, may have a neuroprotective therefore anti- or apoptotic activity (Kaltschmidt et al., 2002).

Low antioxidant activity of hypericin have been reported through its lipid peroxidation inhibition potential (EC₅₀ = 21.0 \pm 2.86 μM ; Silva B.A. et al., 2008).

Kaempferol

Filomeni et al. (2012) studied the ability of kaempferol to protect SH-SY5Y cells and primary neurons from rotenone-induced toxicity. Pre-treating cells with kaempferol 30 μM for 1 h prior to a 1 μM rotenone-insult significantly counteracted rotenone-induced toxicity ($p < 0.01$). Microscopic morphologic analysis indicated that kaempferol was able to inhibit rotenone-induced round shape phenotype and cell detachment, characteristics of apoptotic process. At a molecular level, kaempferol was proven to significantly inhibit rotenone-induced caspase-3 and -9 cleavage ($p < 0.001$). Kaempferol was also able to preserve and restore mitochondrial function upon rotenone-mediated challenge, at

least if provided before caspases activation, within upon 12 h. Underlying kaempferol protective activity was its autophagic's ability, prior demonstrated in carcinoma cells by altering cellular energetics. The authors conclude that this maintained at lower doses and protects neuronal cells against from rotenone-induced toxicity. Note that autophagy has been observed to be deregulated in Parkinson's disease (Chu et al., 2009; Filomeni et al., 2010, 2012).

Kaempferol was also investigated for its ability to protect neurons from excitotoxicity and mitochondrial dysfunction. Results were similar to those of quercetin, what lead the authors to conclude for a possible neuroprotective activity induced by the antioxidant properties of these compounds (Silva B. et al., 2008).

Antioxidant activities of kaempferol have been reported through its antiradical activity on DPPH ($EC_{50} = 21.3 \pm 1.04 \mu\text{M}$) and lipid peroxidation inhibition potential ($EC_{50} = 0.69 \pm 1.62 \mu\text{M}$; Silva B.A. et al., 2008).

Biapigenin

Biapigenin is a sparingly studied compound for its possible neuroprotective activity. It was studied (as well as quercetin and kaempferol) its ability to protect neurons from excitotoxicity and mitochondrial dysfunction. Besides the results already described, that were similar for biapigenin, this biflavone significantly affects mitochondrial bioenergetics ($p < 0.001$, in comparison to insult) and decreased the mitochondria's ability to accumulate calcium ($p < 0.05$, in comparison to control; Silva B. et al., 2008). Biapigenin modulates the mitochondrial permeability transition pore, reducing calcium burden and contributing against excitotoxic insults (Silva et al., 2010).

Antioxidant activities of biapigenin have been reported through its lipid peroxidation inhibition potential ($EC_{50} = 5.10 \pm 1.11 \mu\text{M}$; Silva B.A. et al., 2008).

Hyperforin

Hyperforin is the major lipophilic constituent of *H. perforatum* (Albert et al., 2002) and considered the major active compound for the anti-depressant activity (Singer et al., 1999).

Dinamarca et al. (2008) studied the ability of a hyperforin synthetic analog, tetrahydroperforin (IDN 5706) on the reduction of β -amyloid deposition and the improvement of spatial learning acquisition, destabilizing amyloid β -acetylcholinesterase interaction. It is important to refer that *in vivo* and *in vitro* studies are indicative of an enhancement of amyloid β aggregation and amyloid fibril formation by acetylcholinesterase (Dinamarca et al., 2008). This study showed that IDN 5706 decreased the formation of β -amyloid fibrils *in vitro*, depolymerizing them.

An oral administration of 1.25 mg/kg/day, for 7 days, in rats, improved learning ability from the second day onward. Additionally the memory of the learned responses acquired during the administration time and training was retained after 9 days without further treatment or training. Klusa et al. (2001) also verified that on mice, a single dose of 1.25 mg/kg of hyperforin improved memory acquisition and consolidation and completely reversed scopolamine-induced amnesia. The authors concluded that hyperforin possesses memory enhancing

properties, being potentially considered as an antidementia compound (Klusa et al., 2001).

In vivo and in transgenic mice, Dinamarca et al. (2008) verified that IDN 5706 was able to remove the acetylcholinesterase present in the plaques and improved the animal behavior, indicating that the presence of the enzyme was correlated to the behavioral impairment observed.

In a subsequent work, Inestrosa et al. (2011) studied the *in vivo* effects of IDN 5706 on β -amyloid neurotoxicity using young transgenic mice. Five months old mice were treated for 10 weeks, tested for spatial memory and their brains analyzed through several techniques. The authors reported that IDN 5706 significantly reduced spatial memory impairments, tau hyperphosphorylation, β -amyloid oligomer accumulation and increased long-term potentiation, suggesting that this compounds could be a novel pharmacological tool for the treatment of Alzheimer's disease (Inestrosa et al., 2011).

CONCLUSION

Hypericum perforatum has been used in traditional medicine for several hundred years. Despite of not fully studied or understood, the extract and isolated compounds of this plant have demonstrated neuroprotective activities. Neuroprotection can be achieved by a direct action on one or several mechanisms, such as an anti-apoptotic effect, or indirectly, through antioxidant properties. Chemically, structure-activity relationships suggest that sugar side chain of flavonoids might be important for neuroprotective activities (Nakayama et al., 2011) and multiple hydroxyl groups confer these compounds substantial antioxidant properties (Heim et al., 2002). Taken together, the data collected suggests a protective effect of *H. perforatum* and some of its major compounds in neurotoxicity, thus a possible beneficial activity in neurodegenerative disorders, such as Alzheimer's and Parkinson's disease. Nonetheless, further studies are needed to fully understand and characterize the activity of this plant and its compounds and its possible therapeutic activity.

AUTHOR CONTRIBUTIONS

All authors contributed on the conception and design of the work. AO and CP specifically intervened on the acquisition and interpretation of data and AO, BS, and AD collaborated on the structure of the work. AO was the main responsible for drafting. CP, BS, and AD critically revised it. All authors approved the final version of this work and agree to be accountable for all aspects of the work.

ACKNOWLEDGMENTS

This work was supported by Fundação para a Ciência e Tecnologia (FCT), projects PTDC/AGR-ALI/105169/2008, PEst-OE/AGR/UI4033/2014. AO was supported by Escola Superior de Tecnologia da Saúde do Porto and Instituto Politécnico do Porto (Programa de Formação Avançada de Docentes).

REFERENCES

- Abbott, N. J. (2002). Astrocyte-endothelial interactions and blood-brain barrier permeability. *J. Anat.* 200, 629–638. doi: 10.1046/j.1469-7580.2002.00064.x
- Agostinini, P., Vantieghem, A., Merlevede, W., and de Witte, P. A. (2002). Hypericin in cancer treatment: more light on the way. *Int. J. Biochem. Cell Biol.* 34, 221–241. doi: 10.1016/S1357-2725(01)00126-1
- Akiyama, H., Barger, S., Barnum, S., Bradt, B., Bauer, J., Cole, G. M., et al. (2000). Inflammation and Alzheimer's disease. *Neurobiol. Aging* 21, 383–421. doi: 10.1016/S0197-4580(00)00124-X
- Albert, D., Zundorf, I., Dingermann, T., Muller, W. E., Steinhilber, D., and Werz, O. (2002). Hyperforin is a dual inhibitor of cyclooxygenase-1 and 5-lipoxygenase. *Biochem. Pharmacol.* 64, 1767–1775. doi: 10.1016/S0006-2952(02)01387-4
- Alia, M., Mateos, R., Ramos, S., Lecumberri, E., Bravo, L., and Goya, L. (2006). Influence of quercetin and rutin on growth and antioxidant defense system of a human hepatoma cell line (HepG2). *Eur. J. Nutr.* 45, 19–28. doi: 10.1007/s00394-005-0558-7
- Altun, M. L., Yilmaz, B. S., Orhan, I. E., and Citoglu, G. S. (2013). Assessment of cholinesterase and tyrosinase inhibitory and antioxidant effects of *Hypericum perforatum* L. (St. John's wort). *Ind. Crops Prod.* 43, 87–92. doi: 10.1016/j.indcrop.2012.07.017
- Ankarcrone, M., Dypbukt, J. M., Bonfoco, E., Zhivotovsky, B., Orrenius, S., Lipton, S. A., et al. (1995). Glutamate-induced neuronal death: a succession of necrosis or apoptosis depending on mitochondrial function. *Neuron* 15, 961–973. doi: 10.1016/0896-6273(95)90186-8
- Ansari, M. A., Abdul, H. M., Joshi, G., Opie, W. O., and Butterfield, D. A. (2009). Protective effect of quercetin in primary neurons against Abeta(1–42): relevance to Alzheimer's disease. *J. Nutr. Biochem.* 20, 269–275. doi: 10.1016/j.jnutbio.2008.03.002
- Arredondo, F., Echeverry, C., Abin-Carriquiry, J. A., Blasina, F., Antunez, K., Jones, D. P., et al. (2010). After cellular internalization, quercetin causes Nrf2 nuclear translocation, increases glutathione levels, and prevents neuronal death against an oxidative insult. *Free Radic. Biol. Med.* 49, 738–747. doi: 10.1016/j.freeradbiomed.2010.05.020
- Arredondo, M. F., Blasina, F., Echeverry, C., Morquio, A., Ferreira, M., Abin-Carriquiry, J. A., et al. (2004). Cytoprotection by *Achyrocline satureoides* (Lam.) D.C. and some of its main flavonoids against oxidative stress. *J. Ethnopharmacol.* 91, 13–20. doi: 10.1016/j.jep.2003.11.012
- Asanuma, M., Miyazaki, I., and Ogawa, N. (2003). Dopamine- or L-DOPA-induced neurotoxicity: the role of dopamine quinone formation and tyrosinase in a model of Parkinson's disease. *Neurotox. Res.* 5, 165–176. doi: 10.1007/BF03033137
- Bains, J. C., and Shaw, C. A. (1997). Neurodegenerative disorders in humans: the role of glutathione in oxidative stress-mediated neuronal death. *Brain Res. Rev.* 25, 335–358. doi: 10.1016/S0165-0173(97)00045-3
- Ball, S. E., Forrester, L. M., Wolf, C. R., and Back, D. J. (1990). Differences in the cytochrome P-450 isoenzymes involved in the 2-hydroxylation of oestradiol and 17 alpha-ethinyloestradiol. Relative activities of rat and human liver enzymes. *Biochem. J.* 267, 221–226. doi: 10.1042/bj2670221
- Barnes, J., Anderson, L. A., and Phillipson, J. D. (2001). St John's wort (*Hypericum perforatum* L.): a review of its chemistry, pharmacology and clinical properties. *J. Pharm. Pharmacol.* 53, 583–600. doi: 10.1211/0022357011775910
- Behl, C. (1999). Alzheimer's disease and oxidative stress: implications for novel therapeutic approaches. *Prog. Neurobiol.* 57, 301–323. doi: 10.1016/S0301-0082(98)00055-0
- Behl, C., and Moosmann, B. (2002). Antioxidant neuroprotection in Alzheimer's disease as preventive and therapeutic approach. *Free Radic. Biol. Med.* 33, 182–191. doi: 10.1016/S0891-5849(02)00883-3
- Behnke, K., Jensen, G. S., Graubaum, H. J., and Gruenwald, J. (2002). *Hypericum perforatum* versus fluoxetine in the treatment of mild to moderate depression. *Adv. Ther.* 19, 43–52. doi: 10.1007/BF02850017
- Benedi, J., Arroyo, R., Romero, C., Martin-Aragon, S., and Villar, A. M. (2004). Antioxidant properties and protective effects of a standardized extract of *Hypericum perforatum* on hydrogen peroxide-induced oxidative damage in PC12 cells. *Life Sci.* 75, 1263–1276. doi: 10.1016/j.lfs.2004.05.001
- Boots, A. W., Haenen, G. R., and Bast, A. (2008). Health effects of quercetin: from antioxidant to nutraceutical. *Eur. J. Pharmacol.* 585, 325–337. doi: 10.1016/j.ejphar.2008.03.008
- Borrelli, F., and Izzo, A. A. (2009). Herb-drug interactions with St John's wort (*Hypericum perforatum*): an update on clinical observations. *AAPS J.* 11, 710–727. doi: 10.1208/s12248-009-9146-8
- Breyer, A., Elstner, M., Gillessen, T., Weiser, D., and Elstner, E. (2007). Glutamate-induced cell death in neuronal HT22 cells is attenuated by extracts from St. John's wort (*Hypericum perforatum* L.). *Phytomedicine* 14, 250–255. doi: 10.1016/j.phymed.2007.02.001
- Brunet, A., Datta, S. R., and Greenberg, M. E. (2001). Transcription-dependent and -independent control of neuronal survival by the PI3K-Akt signaling pathway. *Curr. Opin. Neurobiol.* 11, 297–305. doi: 10.1016/S0959-4388(00)00211-7
- Butterfield, D. A., Reed, T., Newman, S. F., and Sultana, R. (2007). Roles of amyloid beta-peptide-associated oxidative stress and brain protein modifications in the pathogenesis of Alzheimer's disease and mild cognitive impairment. *Free Radic. Biol. Med.* 43, 658–677. doi: 10.1016/j.freeradbiomed.2007.05.037
- Butterweck, V. (2003). Mechanism of action of St John's wort in depression : what is known? *CNS Drugs* 17, 539–562. doi: 10.2165/00023210-200317080-00001
- Butterweck, V., and Schmidt, M. (2007). St. John's wort: role of active compounds for its mechanism of action and efficacy. *Wien Med Wochenschr* 157, 356–361. doi: 10.1007/s10354-007-0440-8
- Chatterjee, S. S., Bhattacharya, S. K., Wonnemann, M., Singer, A., and Muller, W. E. (1998). Hyperforin as a possible antidepressant component of hypericum extracts. *Life Sci.* 63, 499–510. doi: 10.1016/S0024-3205(98)00299-9
- Cheung, Z. H., Chan, Y. M., Siu, F. K., Yip, H. K., Wu, W., Leung, M. C., et al. (2004). Regulation of caspase activation in axotomized retinal ganglion cells. *Mol. Cell. Neurosci.* 25, 383–393. doi: 10.1016/j.mcn.2003.11.001
- Cheung, Z. H., Leung, M. C., Yip, H. K., Wu, W., Siu, F. K., and So, K. F. (2008). A neuroprotective herbal mixture inhibits caspase-3-independent apoptosis in retinal ganglion cells. *Cell Mol. Neurobiol.* 28, 137–155. doi: 10.1007/s10571-007-9175-8
- Cheung, Z. H., So, K. F., Lu, Q., Yip, H. K., Wu, W., Shan, J. J., et al. (2002). Enhanced survival and regeneration of axotomized retinal ganglion cells by a mixture of herbal extracts. *J. Neurotrauma* 19, 369–378. doi: 10.1089/089771502753594936
- Chu, Y., Dodiya, H., Aebischer, P., Olanow, C. W., and Kordower, J. H. (2009). Alterations in lysosomal and proteasomal markers in Parkinson's disease: relationship to alpha-synuclein inclusions. *Neurobiol. Dis.* 35, 385–398. doi: 10.1016/j.nbd.2009.05.023
- Cohen, G. M. (1997). Caspases: the executioners of apoptosis. *Biochem. J.* 326 (Pt 1), 1–16. doi: 10.1042/bj3260001
- Dajas, F. (2012). Life or death: neuroprotective and anticancer effects of quercetin. *J. Ethnopharmacol.* 143, 383–396. doi: 10.1016/j.jep.2012.07.005
- De Vry, J., Maurel, S., Schreiber, R., de Beun, R., and Jentzsch, K. R. (1999). Comparison of hypericum extracts with imipramine and fluoxetine in animal models of depression and alcoholism. *Eur. Neuropsychopharmacol.* 9, 461–468. doi: 10.1016/S0929-477X(99)00005-X
- Deane, R., Bell, R. D., Sagare, A., and Zlokovic, B. V. (2009). Clearance of amyloid-beta peptide across the blood-brain barrier: implication for therapies in Alzheimer's disease. *CNS Neurol. Disord. Drug Targets* 8, 16–30. doi: 10.2174/187152709787601867
- Dinamarca, M. C., Arrázola, M., Toledo, E., Cerpa, W. F., Hancke, J., Inestrosa, N. C., et al. (2008). Release of acetylcolinesterase (AChE) from β-amyloid plaques assemblies te spatial memory impairments in APP-transgenic mice. *Chem. Biol. Interact.* 175, 142–149. doi: 10.1016/j.cbi.2008.05.026
- Dok-Go, H., Lee, K. H., Kim, H. J., Lee, E. H., Lee, J., Song, Y. S., et al. (2003). Neuroprotective effects of antioxidant flavonoids, quercetin, (+) dihydroquercetin and quercetin 3-methyl ether, isolated from *Opuntia ficus-indica* var. saboten. *Brain Res.* 965, 130–136. doi: 10.1016/S0006-8993(02)04150-1
- Dona, M., Dell'Aica, I., Pezzato, E., Sartor, L., Calabrese, F., Della Barbera, M., et al. (2004). Hyperforin inhibits cancer invasion and metastasis. *Cancer Res.* 64, 6225–6232. doi: 10.1158/0008-5472.CAN-04-0280
- Dostalek, M., Pistovcakova, J., Jurica, J., Tomandl, J., Linhart, I., Sulcova, A., et al. (2005). Effect of St John's wort (*Hypericum perforatum*) on cytochrome P-450 activity in perfused rat liver. *Life Sci.* 78, 239–244. doi: 10.1016/j.lfs.2005.04.055
- El-Sherbiny, D. A., Khalifa, A. E., Attia, A. S., and Eldenshary Eel, D. (2003). *Hypericum perforatum* extract demonstrates antioxidant properties against elevated rat brain oxidative status induced by amnestic dose of scopolamine. *Pharmacol. Biochem. Behav.* 76, 525–533. doi: 10.1016/j.pbb.2003.09.014

- Emerit, J., Edeas, M., and Bricaire, F. (2004). Neurodegenerative diseases and oxidative stress. *Biomed. Pharmacother.* 58, 39–46. doi: 10.1016/j.biopha.2003.11.004
- Ferko, N., and Levine, M. A. (2001). Evaluation of the association between St. John's wort and elevated thyroid-stimulating hormone. *Pharmacotherapy* 21, 1574–1578. doi: 10.1592/phco.21.20.1574.34483
- Filomeni, G., Desideri, E., Cardaci, S., Graziani, I., Piccirillo, S., Rotilio, G., et al. (2010). Carcinoma cells activate AMP-activated protein kinase-dependent autophagy as survival response to kaempferol-mediated energetic impairment. *Autophagy* 6, 202–216. doi: 10.4161/auto.6.2.10971
- Filomeni, G., Graziani, I., De Zio, D., Dini, L., Centonze, D., Rotilio, G., et al. (2012). Neuroprotection of kaempferol by autophagy in models of rotenone-mediated acute toxicity: possible implications for Parkinson's disease. *Neurobiol. Aging* 33, 767–785. doi: 10.1016/j.neurobiolaging.2010.05.021
- Garcia-Alloza, M., Robbins, E. M., Zhang-Nunes, S. X., Purcell, S. M., Betensky, R. A., Raju, S., et al. (2006). Characterization of amyloid deposition in the APPswe/PS1dE9 mouse model of Alzheimer disease. *Neurobiol. Dis.* 24, 516–524. doi: 10.1016/j.nbd.2006.08.017
- Gartner, M., Muller, T., Simon, J. C., Giannis, A., and Sleeman, J. P. (2005). Aristoforin, a novel stable derivative of hyperforin, is a potent anticancer agent. *Chembiochem* 6, 171–177. doi: 10.1002/cbic.200400195
- Gaster, B., and Holroyd, J. (2000). St John's wort for depression: a systematic review. *Arch. Intern. Med.* 160, 152–156. doi: 10.1001/archinte.160.2.152
- Goll, D. E., Thompson, V. F., Li, H., Wei, W., and Cong, J. (2003). The calpain system. *Physiol. Rev.* 83, 731–801. doi: 10.1152/physrev.00029.2002
- Greeson, J. M., Sanford, B., and Monti, D. A. (2001). St. John's wort (*Hypericum perforatum*): a review of the current pharmacological, toxicological, and clinical literature. *Psychopharmacology (Berl.)* 153, 402–414. doi: 10.1007/s002130000625
- Haleagrahara, N., Siew, C. J., Mitra, N. K., and Kumari, M. (2011). Neuroprotective effect of bioflavonoid quercetin in 6-hydroxydopamine-induced oxidative stress biomarkers in the rat striatum. *Neurosci. Lett.* 500, 139–143. doi: 10.1016/j.neulet.2011.06.021
- Hammerstein, P., Basch, E., Ulbricht, C., Barrette, E. P., Foppa, I., Basch, S., et al. (2003). St John's wort: a systematic review of adverse effects and drug interactions for the consultation psychiatrist. *Psychosomatics* 44, 271–282. doi: 10.1176/appi.psy.44.4.271
- Heim, K. E., Tagliaferro, A. R., and Bobilya, D. J. (2002). Flavonoid antioxidants: chemistry, metabolism and structure-activity relationships. *J. Nutr. Biochem.* 13, 572–584. doi: 10.1016/S0955-2863(02)00208-5
- Henderson, L., Yue, Q. Y., Bergquist, C., Gerden, B., and Arlett, P. (2002). St John's wort (*Hypericum perforatum*): drug interactions and clinical outcomes. *Br. J. Clin. Pharmacol.* 54, 349–356. doi: 10.1046/j.1365-2125.2002.01683.x
- Heo, H. J., and Lee, C. Y. (2004). Protective effects of quercetin and vitamin C against oxidative stress-induced neurodegeneration. *J. Agric. Food Chem.* 52, 7514–7517. doi: 10.1021/jf049243r
- Hollman, P. C., de Vries, J. H., van Leeuwen, S. D., Mengelers, M. J., and Katan, M. B. (1995). Absorption of dietary quercetin glycosides and quercetin in healthy ileostomy volunteers. *Am. J. Clin. Nutr.* 62, 1276–1282.
- Holtzman, C. W., Wiggins, B. S., and Spinler, S. A. (2006). Role of P-glycoprotein in statin drug interactions. *Pharmacotherapy* 26, 1601–1607. doi: 10.1592/phco.26.11.1601
- Hostanska, K., Reichling, J., Bommer, S., Weber, M., and Saller, R. (2003). Hyperforin a constituent of St John's wort (*Hypericum perforatum* L.) extract induces apoptosis by triggering activation of caspases and with hypericin synergistically exerts cytotoxicity towards human malignant cell lines. *Eur. J. Pharm. Biopharm.* 56, 121–132. doi: 10.1016/S0939-6411(03)00046-8
- Inal, M. E., and Kahraman, A. (2000). The protective effect of flavonol quercetin against ultraviolet induced oxidative stress in rats. *Toxicology* 154, 21–29. doi: 10.1016/S0300-483X(00)00268-7
- Inestrosa, N. C., Tapia-Rojas, C., Griffith, T. N., Carvajal, F. J., Benito, M. J., Rivera-Dictter, A., et al. (2011). Tetrahydrohyperforin prevents cognitive deficits, $\text{A}\beta$ deposition, tau phosphorylation and synaptotoxicity in the APPswe/PSEN Δ E9 model of Alzheimer's disease: a possible effect on APP processing. *Transl. Psychiatry* 1:e20. doi: 10.1038/tp.2011.19
- Jang, M. H., Lee, T. H., Shin, M. C., Bahn, G. H., Kim, J. W., Shin, D. H., et al. (2002). Protective effect of *Hypericum perforatum* Linn (St. John's wort) against hydrogen peroxide-induced apoptosis on human neuroblastoma cells. *Neurosci. Lett.* 329, 177–180. doi: 10.1016/S0304-3940(02)00644-4
- Kaltschmidt, B., Heinrich, M., and Kaltschmidt, C. (2002). Stimulus-dependent activation of NF-kappaB specifies apoptosis or neuroprotection in cerebellar granule cells. *Neuromol. Med.* 2, 299–309. doi: 10.1385/NMM:2:3:299
- Kamalakkannan, N., and Stanely Mainzen Prince, P. (2006). Rutin improves the antioxidant status in streptozotocin-induced diabetic rat tissues. *Mol. Cell. Biochem.* 293, 211–219. doi: 10.1007/s11010-006-9244-1
- Karioti, A., and Bilia, A. R. (2010). Hypericins as potential leads for new therapeutics. *Int. J. Mol. Sci.* 11, 562–594. doi: 10.3390/ijms11020562
- Karminsky, L. S., and Zhang, Z. Y. (1997). Human P450 metabolism of warfarin. *Pharmacol. Ther.* 73, 67–74. doi: 10.1016/S0163-7258(96)00140-4
- Khan, M. M., Ahmad, A., Ishrat, T., Khuwaja, G., Srivastava, P., Khan, M. B., et al. (2009). Rutin protects the neural damage induced by transient focal ischemia in rats. *Brain Res.* 1292, 123–135. doi: 10.1016/j.brainres.2009.07.026
- Khan, M. M., Raza, S. S., Javed, H., Ahmad, A., Khan, A., Islam, F., et al. (2012). Rutin protects dopaminergic neurons from oxidative stress in an animal model of Parkinson's disease. *Neurotox. Res.* 22, 1–15. doi: 10.1007/s12640-011-9295-2
- Khawaja, I. S., Marotta, R. F., and Lippmann, S. (1999). Herbal medicines as a factor in delirium. *Psychiatr. Serv.* 50, 969–970. doi: 10.1176/ps.50.7.969a
- Klusa, V., Germane, S., Noldner, M., and Chaterjee, S. S. (2001). Hypericum extract and hyperforin: memory – enhancing properties in rodents. *Pharmacopsychiatry* 34(Suppl. 1), S61–S69. doi: 10.1055/s-2001-15451
- Knuppel, L., and Linde, K. (2004). Adverse effects of St. John's Wort: a systematic review. *J. Clin. Psychiatry* 65, 1470–1479. doi: 10.4088/JCP.v65n1105
- Kraus, B., Wolff, H., Heilmann, J., and Elstner, E. F. (2007). Influence of *Hypericum perforatum* extract and its single compounds on amyloid-beta mediated toxicity in microglial cells. *Life Sci.* 81, 884–894. doi: 10.1016/j.lfs.2007.07.020
- Kubin, A., Wierrani, F., Burner, U., Alth, G., and Grunberger, W. (2005). Hypericin—the facts about a controversial agent. *Curr. Pharm. Des.* 11, 233–253. doi: 10.2174/1381612053382287
- La Casa, C., Villegas, I., Alarcon de la Lastra, C., Motilva, V., and Martin Calero, M. J. (2000). Evidence for protective and antioxidant properties of rutin, a natural flavone, against ethanol induced gastric lesions. *J. Ethnopharmacol.* 71, 45–53. doi: 10.1016/S0378-8741(99)00174-9
- Lin, Y. C., Uang, H. W., Lin, R. J., Chen, I. J., and Lo, Y. C. (2007). Neuroprotective effects of glyceryl nonivamide against microglia-like cells and 6-hydroxydopamine-induced neurotoxicity in SH-SY5Y human dopaminergic neuroblastoma cells. *J. Pharmacol. Exp. Ther.* 323, 877–887. doi: 10.1124/jpet.107.125955
- Linde, K. (2009). St. John's wort - an overview. *Forsch. Komplementmed.* 16, 146–155. doi: 10.1159/000209290
- Linde, K., Berner, M., Egger, M., and Mulrow, C. (2005). St John's wort for depression: meta-analysis of randomised controlled trials. *Br. J. Psychiatry* 186, 99–107. doi: 10.1192/bj.p.186.2.99
- Liu, R., Zhang, T. T., Zhou, D., Bai, X. Y., Zhou, W. L., Huang, C., et al. (2013). Quercetin protects against the Abeta(25–35)-induced amnesia injury: involvement of inactivation of rage-mediated pathway and conservation of the NVU. *Neuropharmacology* 67, 419–431. doi: 10.1016/j.neuropharm.2012.11.018
- Liu, R. L., Xiong, Q. J., Shu, Q., Wu, W. N., Cheng, J., Fu, H., et al. (2012). Hyperoside protects cortical neurons from oxygen-glucose deprivation-reperfusion induced injury via nitric oxide signal pathway. *Brain Res.* 1469, 164–173. doi: 10.1016/j.brainres.2012.06.044
- Liu, Z., Tao, X., Zhang, C., Lu, Y., and Wei, D. (2005). Protective effects of hyperoside (quercetin-3-O-galactoside) to PC12 cells against cytotoxicity induced by hydrogen peroxide and tert-butyl hydroperoxide. *Biomed. Pharmacother.* 59, 481–490. doi: 10.1016/j.biopha.2005.06.009
- Lu, Y. H., Du, C. B., Liu, J. W., Hong, W., and Wei, D. Z. (2004). Neuroprotective effects of *Hypericum perforatum* on trauma induced by hydrogen peroxide in PC12 cells. *Am. J. Chin. Med.* 32, 397–405. doi: 10.1142/S0192415X04002053
- Luo, L., Sun, Q., Mao, Y. Y., Lu, Y. H., and Tan, R. X. (2004). Inhibitory effects of flavonoids from *Hypericum perforatum* on nitric oxide synthase. *J. Ethnopharmacol.* 93, 221–225. doi: 10.1016/j.jep.2004.03.042
- Martarelli, D., Martarelli, B., Pediconi, D., Nabissi, M. I., Perfumi, M., and Pompei, P. (2004). *Hypericum perforatum* methanolic extract inhibits growth of human prostatic carcinoma cell line orthotopically implanted in nude mice. *Cancer Lett.* 210, 27–33. doi: 10.1016/j.canlet.2004.01.031

- Martinez-Poveda, B., Quesada, A. R., and Medina, M. A. (2005a). Hyperforin, a bio-active compound of St. John's Wort, is a new inhibitor of angiogenesis targeting several key steps of the process. *Int. J. Cancer* 117, 775–780. doi: 10.1002/ijc.21246
- Martinez-Poveda, B., Quesada, A. R., and Medina, M. A. (2005b). Hypericin in the dark inhibits key steps of angiogenesis in vitro. *Eur. J. Pharmacol.* 516, 97–103. doi: 10.1016/j.ejphar.2005.03.047
- McNaught, K. S., Belizaire, R., Isacson, O., Jenner, P., and Olanow, C. W. (2003). Altered proteasomal function in sporadic Parkinson's disease. *Exp. Neurol.* 179, 38–46. doi: 10.1006/exnr.2002.8050
- Miskovsky, P. (2002). Hypericin—a new antiviral and antitumor photosensitizer: mechanism of action and interaction with biological macromolecules. *Curr. Drug Targets* 3, 55–84. doi: 10.2174/1389450023348091
- Mohanasundari, M., Srinivasan, M. S., Sethupathy, S., and Sabesan, M. (2006). Enhanced neuroprotective effect by combination of bromocriptine and *Hypericum perforatum* extract against MPTP-induced neurotoxicity in mice. *J. Neurol. Sci.* 249, 140–144. doi: 10.1016/j.jns.2006.06.018
- Molina, M. F., Sanchez-Reus, I., Iglesias, I., and Benedi, J. (2003). Quercetin, a flavonoid antioxidant, prevents and protects against ethanol-induced oxidative stress in mouse liver. *Biol. Pharm. Bull.* 26, 1398–1402. doi: 10.1248/bpp.26.1398
- Motallebjnejad, M., Moghadamnia, A., and Talei, M. (2008). The efficacy of *Hypericum perforatum* extract on recurrent aphthous ulcers. *J. Med. Sci.* 8, 39–43. doi: 10.3923/jms.2008.39.43
- Muller, W. E. (2003). Current St John's wort research from mode of action to clinical efficacy. *Pharmacol. Res.* 47, 101–109. doi: 10.1016/S1043-6618(02)00266-9
- Muralikrishnan, D., and Mohanakumar, K. P. (1998). Neuroprotection by bromocriptine against 1-methyl-4-phenyl-1,2,3,6-tetrahydropyridine-induced neurotoxicity in mice. *FASEB J.* 12, 905–912.
- Myhrstad, M. C., Carlsen, H., Nordstrom, O., Blomhoff, R., and Moskaug, J. O. (2002). Flavonoids increase the intracellular glutathione level by transactivation of the gamma-glutamylcysteine synthetase catalytic subunit promoter. *Free Radic. Biol. Med.* 32, 386–393. doi: 10.1016/S0891-5849(01)00812-7
- Nahrstedt, A., and Butterweck, V. (1997). Biologically active and other chemical constituents of the herb of *Hypericum perforatum* L. *Pharmacopsychiatry* 30(Suppl. 2), 129–134. doi: 10.1055/s-2007-979533
- Nahrstedt, A., and Butterweck, V. (2010). Lessons learned from herbal medicinal products: the example of St. John's Wort (perpendicular). *J. Nat. Prod.* 73, 1015–1021. doi: 10.1021/np1000329
- Nakayama, M., Aihara, M., Chen, Y. N., Araie, M., Tomita-Yokotani, K., and Iwashina, T. (2011). Neuroprotective effects of flavonoids on hypoxia-, glutamate-, and oxidative stress-induced retinal ganglion cell death. *Mol. Vis.* 17, 1784–1793.
- Nieminen, T. H., Hagelberg, N. M., Saari, T. I., Neuvonen, M., Laine, K., Neuvonen, P. J., et al. (2010). St John's wort greatly reduces the concentrations of oral oxycodone. *Eur. J. Pain* 14, 854–859. doi: 10.1016/j.ejpain.2009.12.007
- Ossola, B., Kaariainen, T. M., and Mannisto, P. T. (2009). The multiple faces of quercetin in neuroprotection. *Exp. Opin. Drug Saf.* 8, 397–409. doi: 10.1517/14740330903026944
- Patocka, J. (2003). The chemistry, pharmacology, and toxicology of the biologically active constituents of the herb *Hypericum perforatum* L. *J. Appl. Biomed.* 1, 61–70.
- Pfrunder, A., Schiesser, M., Gerber, S., Haschke, M., Bitzer, J., and Drewe, J. (2003). Interaction of St John's wort with low-dose oral contraceptive therapy: a randomized controlled trial. *Br. J. Clin. Pharmacol.* 56, 683–690. doi: 10.1046/j.1365-2125.2003.02005.x
- Pietta, P. G. (2000). Flavonoids as antioxidants. *J. Nat. Prod.* 63, 1035–1042. doi: 10.1021/np9904509
- Piscitelli, S. C., Burstein, A. H., Chaitt, D., Alfaro, R. M., and Falloon, J. (2000). Indinavir concentrations and St John's wort. *Lancet* 355, 547–548. doi: 10.1016/S0140-6736(99)05712-8
- Rahimi, R., Nikfar, S., and Abdollahi, M. (2009). Efficacy and tolerability of *Hypericum perforatum* in major depressive disorder in comparison with selective serotonin reuptake inhibitors: a meta-analysis. *Prog. Neuropsychopharmacol. Biol. Psychiatry* 33, 118–127. doi: 10.1016/j.pnpbp.2008.10.018
- Ramos, A. A., Lima, C. F., Pereira, M. L., Fernandes-Ferreira, M., and Pereira-Wilson, C. (2008). Antigenotoxic effects of quercetin, rutin and ursolic acid on HepG2 cells: evaluation by the comet assay. *Toxicol. Lett.* 177, 66–73. doi: 10.1016/j.toxlet.2008.01.001
- Rattanajarasroj, S., and Unchern, S. (2010). Comparable attenuation of Abeta(25–35)-induced neurotoxicity by quercitrin and 17beta-estradiol in cultured rat hippocampal neurons. *Neurochem. Res.* 35, 1196–1205. doi: 10.1007/s11064-010-0175-6
- Reichling, J., Weseler, A., and Saller, R. (2001). A current review of the antimicrobial activity of *Hypericum perforatum* L. *Pharmacopsychiatry* 34(Suppl. 1), S116–S118. doi: 10.1055/s-2001-15514
- Rink, E., and Wullimann, M. F. (2001). The teleostean (zebrafish) dopaminergic system ascending to the subpallium (striatum) is located in the basal diencephalon (posterior tuberculum). *Brain Res.* 889, 316–330. doi: 10.1016/S0006-8993(00)03174-7
- Rothley, M., Schmid, A., Thiele, W., Schacht, V., Plaumann, D., Gartner, M., et al. (2009). Hyperforin and aristoforin inhibit lymphatic endothelial cell proliferation in vitro and suppress tumor-induced lymphangiogenesis in vivo. *Int. J. Cancer* 125, 34–42. doi: 10.1002/ijc.24295
- Russo, E., Scicchitano, F., Whalley, B. J., Mazzitello, C., Ciriaco, M., Esposito, S., et al. (2013). *Hypericum perforatum*: pharmacokinetic, mechanism of action, tolerability, and clinical drug-drug interactions. *Phytother. Res.* 28, 643–655. doi: 10.1002/ptr.5050
- Saddique, Z., Naeem, I., and Maimoona, A. (2010). A review of the antibacterial activity of *Hypericum perforatum* L. *J. Ethnopharmacol.* 131, 511–521. doi: 10.1016/j.jep.2010.07.034
- Sanchez-Reus, M. I., Gomez del Rio, M. A., Iglesias, I., Elorza, M., Slowing, K., and Benedi, J. (2007). Standardized *Hypericum perforatum* reduces oxidative stress and increases gene expression of antioxidant enzymes on rotenone-exposed rats. *Neuropharmacology* 52, 606–616. doi: 10.1016/j.neuropharm.2006.09.003
- Sasaki, N., Toda, T., Kaneko, T., Baba, N., and Matsuo, M. (2003). Protective effects of flavonoids on the cytotoxicity of linoleic acid hydroperoxide toward rat pheochromocytoma PC12 cells. *Chem. Biol. Interact.* 145, 101–116. doi: 10.1016/S0009-2797(02)00248-X
- Schempp, C. M., Pelz, K., Wittmer, A., Schopf, E., and Simon, J. C. (1999). Antibacterial activity of hyperforin from St John's wort, against multiresistant *Staphylococcus aureus* and gram-positive bacteria. *Lancet* 353, 2129. doi: 10.1016/S0140-6736(99)00214-7
- Schmider, J., Greenblatt, D. J., von Moltke, L. L., Karsov, D., Vena, R., Friedman, H. L., et al. (1997). Biotransformation of mestranol to ethinyl estradiol in vitro: the role of cytochrome P-450 2C9 and metabolic inhibitors. *J. Clin. Pharmacol.* 37, 193–200. doi: 10.1002/j.1552-4604.1997.tb04781.x
- Schulz, V. (2006). Safety of St. John's Wort extract compared to synthetic antidepressants. *Phytomedicine* 13, 199–204. doi: 10.1016/j.phymed.2005.07.005
- Schwarz, D., Kissilev, P., and Roots, I. (2003). St. John's wort extracts and some of their constituents potently inhibit ultimate carcinogen formation from benzo[a]pyrene-7,8-dihydrodiol by human CYP1A1. *Cancer Res.* 63, 8062–8068.
- Sestili, P., Guidarelli, A., Dacha, M., and Cantoni, O. (1998). Quercetin prevents DNA single strand breakage and cytotoxicity caused by tert-butylhydroperoxide: free radical scavenging versus iron chelating mechanism. *Free Radic. Biol. Med.* 25, 196–200. doi: 10.1016/S0891-5849(98)00040-9
- Sherer, T. B., Betarbet, R., Testa, C. M., Seo, B. B., Richardson, J. R., Kim, J. H., et al. (2003). Mechanism of toxicity in rotenone models of Parkinson's disease. *J. Neurosci.* 23, 10756–10764.
- Silva, B., Oliveira, P. J., Dias, A., and Malva, J. O. (2008). Quercetin, kaempferol and biapigenin from *Hypericum perforatum* are neuroprotective against excitotoxic insults. *Neurotox. Res.* 13, 265–279. doi: 10.1007/BF03033510
- Silva, B. A., Dias, A. C. P., Ferreres, F., Malva, J. O., and Oliveira, C. R. (2004). Neuroprotective effect of *H. perforatum* extracts on B-amyloid-induced neurotoxicity. *Neurotox. Res.* 6, 119–130. doi: 10.1007/BF03033214
- Silva, B. A., Ferreres, F., Malva, J. O., and Dias, A. C. P. (2005). Phytochemical and antioxidant characterization of *Hypericum perforatum* alcoholic extracts. *Food Chem.* 90, 157–167. doi: 10.1016/j.foodchem.2004.03.049
- Silva, B. A., Malva, J. O., and Dias, A. C. P. (2008). St John's Wort (*Hypericum perforatum*) extracts and isolated phenolic compounds are effective antioxidants in several in vitro models of oxidative stress. *Food Chem.* 110, 611–619. doi: 10.1016/j.foodchem.2008.02.047

- Silva, B. A., Oliveira, P. J., Cristóvão, A., Dias, A. C. P., and Malva, J. (2010). Biapigenin modulates the activity of the adenine nucleotide translocator in isolated rat brain mitochondria. *Neurotox Res.* 17, 75–90. doi:10.1007/s12640-009-9082-5
- Silva, J. P., Gomes, A. C., and Coutinho, O. P. (2008). Oxidative DNA damage protection and repair by polyphenolic compounds in PC12 cells. *Eur. J. Pharmacol.* 601, 50–60. doi: 10.1016/j.ejphar.2008.10.046
- Singer, A., Wonnemann, M., and Müller, W. E. (1999). Hyperforin, a major antidepressant constituent of St. John's Wort, inhibits serotonin uptake by elevating free intracellular Na^{+1} . *J. Pharmacol. Exp. Ther.* 290, 1363–1368.
- Smith, P., Bullock, J. M., Booker, B. M., Haas, C. E., Berenson, C. S., and Jusko, W. J. (2004). The influence of St. John's wort on the pharmacokinetics and protein binding of imatinib mesylate. *Pharmacotherapy* 24, 1508–1514. doi: 10.1592/phco.24.16.1508.50958
- Song, K., Kim, S., Na, J. Y., Park, J. H., Kim, J. K., Kim, J. H., et al. (2014). Rutin attenuates ethanol-induced neurotoxicity in hippocampal neuronal cells by increasing aldehyde dehydrogenase 2. *Food Chem. Toxicol.* 72, 228–233. doi: 10.1016/j.fct.2014.07.028
- Suematsu, N., Hosoda, M., and Fujimori, K. (2011). Protective effects of quercetin against hydrogen peroxide-induced apoptosis in human neuronal SH-SY5Y cells. *Neurosci. Lett.* 504, 223–227. doi: 10.1016/j.neulet.2011.09.028
- Suntar, I. P., Akkol, E. K., Yilmazer, D., Baykal, T., Kirmizibekmez, H., Alper, M., et al. (2010). Investigations on the in vivo wound healing potential of *Hypericum perforatum* L. *J. Ethnopharmacol.* 127, 468–477. doi: 10.1016/j.jep.2009.10.011
- Suzuki, O., Katsumata, Y., Oya, M., Bladt, S., and Wagner, H. (1984). Inhibition of monoamine oxidase by hypericin. *Planta Med.* 50, 272–274. doi: 10.1055/s-2007-969700
- Talesa, V. N. (2001). Acetylcholinesterase in Alzheimer's disease. *Mech. Ageing Dev.* 122, 1961–1969. doi: 10.1016/S0047-6374(01)00309-8
- Wagner, C., Fachinetto, R., Dalla Corte, C. L., Brito, V. B., Severo, D., de Oliveira Costa Dias, G., et al. (2006). Quercitrin, a glycoside form of quercetin, prevents lipid peroxidation in vitro. *Brain Res.* 1107, 192–198. doi: 10.1016/j.brainres.2006.05.084
- Wang, L. S., Zhu, B., Abd El-Aty, A. M., Zhou, G., Li, Z., Wu, J., et al. (2004). The influence of St. John's Wort on CYP2C19 activity with respect to genotype. *J. Clin. Pharmacol.* 44, 577–581. doi: 10.1177/0091270004265642
- Wang, S. W., Wang, Y. J., Su, Y. J., Zhou, W. W., Yang, S. G., Zhang, R., et al. (2012). Rutin inhibits beta-amyloid aggregation and cytotoxicity, attenuates oxidative stress, and decreases the production of nitric oxide and proinflammatory cytokines. *Neurotoxicology* 33, 482–490. doi: 10.1016/j.neuro.2012.03.003
- Wang, X. D., Li, J. L., Lu, Y., Chen, X., Huang, M., Chowbay, B., et al. (2007). Rapid and simultaneous determination of nifedipine and dehydronifedipine in human plasma by liquid chromatography-tandem mass spectrometry: application to a clinical herb-drug interaction study. *J. Chromatogr. B Analyt. Technol. Biomed. Life Sci.* 852, 534–544. doi: 10.1016/j.jchromb.2007.02.026
- Wurglics, M., and Schubert-Zsilavecz, M. (2006). *Hypericum perforatum*: a 'modern' herbal antidepressant: pharmacokinetics of active ingredients. *Clin. Pharmacokinet.* 45, 449–468. doi: 10.2165/00003088-200645050-00002
- Xu, P. X., Wang, S. W., Yu, X. L., Su, Y. J., Wang, T., Zhou, W. W., et al. (2014). Rutin improves spatial memory in Alzheimer's disease transgenic mice by reducing Abeta oligomer level and attenuating oxidative stress and neuroinflammation. *Behav. Brain Res.* 264, 173–180. doi: 10.1016/j.bbr.2014.02.002
- Yang, J., Guo, J., and Yuan, J. (2008). In vitro antioxidant properties of rutin. *LWT* 41, 1060–1066. doi: 10.1016/j.lwt.2007.06.010
- Zeng, K. W., Wang, X. M., Ko, H., Kwon, H. C., Cha, J. W., and Yang, H. O. (2011). Hyperoside protects primary rat cortical neurons from neurotoxicity induced by amyloid beta-protein via the PI3K/Akt/Bad/Bcl(XL)-regulated mitochondrial apoptotic pathway. *Eur. J. Pharmacol.* 672, 45–55. doi: 10.1016/j.ejphar.2011.09.177
- Zhang, M., An, C., Gao, Y., Leak, R. K., Chen, J., and Zhang, F. (2013). Emerging roles of Nrf2 and phase II antioxidant enzymes in neuroprotection. *Prog. Neurobiol.* 100, 30–47. doi: 10.1016/j.pneurobio.2012.09.003
- Zhang, Z. J., Cheang, L. C., Wang, M. W., and Lee, S. M. (2011). Quercetin exerts a neuroprotective effect through inhibition of the iNOS/NO system and pro-inflammation gene expression in PC12 cells and in zebrafish. *Int. J. Mol. Med.* 27, 195–203. doi: 10.3892/ijmm.2010.571
- Zhao, B. (2005). Natural antioxidants for neurodegenerative diseases. *Mol. Neurobiol.* 31, 283–293. doi: 10.1385/MN:31:1-3:283
- Zheng, W., and Wang, S. Y. (2001). Antioxidant activity and phenolic compounds in selected herbs. *J. Agric. Food Chem.* 49, 5165–5170. doi: 10.1021/jf010697n
- Zou, Y., Lu, Y., and Wei, D. (2004). Antioxidant activity of a flavonoid-rich extract of *Hypericum perforatum* L. in vitro. *J. Agric. Food Chem.* 52, 5032–5039. doi: 10.1021/jf049571r
- Zou, Y. P., Lu, Y. H., and Wei, D. Z. (2010). Protective effects of a flavonoid-rich extract of *Hypericum perforatum* L. against hydrogen peroxide-induced apoptosis in PC12 cells. *Phytother. Res.* 24(Suppl. 1), S6–S10. doi: 10.1002/ptr.2852

Conflict of Interest Statement: The authors declare that the research was conducted in the absence of any commercial or financial relationships that could be construed as a potential conflict of interest.

Copyright © 2016 Oliveira, Pinho, Sarmento and Dias. This is an open-access article distributed under the terms of the Creative Commons Attribution License (CC BY). The use, distribution or reproduction in other forums is permitted, provided the original author(s) or licensor are credited and that the original publication in this journal is cited, in accordance with accepted academic practice. No use, distribution or reproduction is permitted which does not comply with these terms.



Hypericin in the Light and in the Dark: Two Sides of the Same Coin

Zuzana Jendželovská, Rastislav Jendželovský, Barbora Kuchárová and Peter Fedoročko *

Department of Cellular Biology, Faculty of Science, Pavol Jozef Šafárik University in Košice, Košice, Slovakia

OPEN ACCESS

Edited by:

Gregory Franklin,
Polish Academy of Sciences, Poland

Reviewed by:

Jiřina Hofmanová,
Academy of Sciences of the Czech
Republic, Czech Republic
Lester M. Davids,
University of Cape Town, South Africa
Abhishek D. Garg,
KU Leuven, Belgium

*Correspondence:

Peter Fedoročko
peter.fedorocko@upjs.sk

Specialty section:

This article was submitted to
Plant Metabolism and Chemodiversity,
a section of the journal
Frontiers in Plant Science

Received: 12 February 2016

Accepted: 11 April 2016

Published: 06 May 2016

Citation:

Jendželovská Z, Jendželovský R,
Kuchárová B and Fedoročko P (2016)
Hypericin in the Light and in the Dark:
Two Sides of the Same Coin.

Front. Plant Sci. 7:560.

doi: 10.3389/fpls.2016.00560

Hypericin (4,5,7,4',5',7'-hexahydroxy-2,2'-dimethylnaphthodianthrone) is a naturally occurring chromophore found in some species of the genus *Hypericum*, especially *Hypericum perforatum* L. (St. John's wort), and in some basidiomycetes (*Dermocybe* spp.) or endophytic fungi (*Thielavia subthermophila*). In recent decades, hypericin has been intensively studied for its broad pharmacological spectrum. Among its antidepressant and light-dependent antiviral actions, hypericin is a powerful natural photosensitizer that is applicable in the photodynamic therapy (PDT) of various oncological diseases. As the accumulation of hypericin is significantly higher in neoplastic tissue than in normal tissue, it can be used in photodynamic diagnosis (PDD) as an effective fluorescence marker for tumor detection and visualization. In addition, light-activated hypericin acts as a strong pro-oxidant agent with antineoplastic and antiangiogenic properties, since it effectively induces the apoptosis, necrosis or autophagy of cancer cells. Moreover, a strong affinity of hypericin for necrotic tissue was discovered. Thus, hypericin and its radiolabeled derivatives have been recently investigated as potential biomarkers for the non-invasive targeting of tissue necrosis in numerous disorders, including solid tumors. On the other hand, several light-independent actions of hypericin have also been described, even though its effects in the dark have not been studied as intensively as those of photoactivated hypericin. Various experimental studies have revealed no cytotoxicity of hypericin in the dark; however, it can serve as a potential antimetastatic and antiangiogenic agent. On the contrary, hypericin can induce the expression of some ABC transporters, which are often associated with the multidrug resistance (MDR) of cancer cells. Moreover, the hypericin-mediated attenuation of the cytotoxicity of some chemotherapeutics was revealed. Therefore, hypericin might represent another St. John's wort metabolite that is potentially responsible for negative herb–drug interactions. The main aim of this review is to summarize the benefits of photoactivated and non-activated hypericin, mainly in preclinical and clinical applications, and to uncover the “dark side” of this secondary metabolite, focusing on MDR mechanisms.

Keywords: hypericin, St. John's wort, anticancer activities, photodynamic therapy, photodynamic diagnosis, drug resistance

INTRODUCTION

Hypericin (4,5,7,4',5',7'-hexahydroxy-2,2'-dimethylnaphthodianthrone) is a naturally occurring compound synthesized by some species of the genus *Hypericum*. Hypericin was first isolated from *Hypericum perforatum* L. (Brockmann et al., 1939), commonly known as St. John's wort, which is one of the best characterized and most important representatives of this genus, because of its broad pharmacological activity (antidepressant, antimicrobial, anticancer, anti-inflammatory, wound healing, etc.) (reviewed in Kasper et al., 2010; Wölflé et al., 2014). Hypericin and its derivatives are accumulated in special morphological structures, so called dark nodules, occurring in the aerial parts of hypericin-producing *Hypericum* species. The newest data on interspecific variation in localization of hypericins and spatial chemo-profiling of hypericin in some *Hypericum* species were published recently (Kusari et al., 2015; Kucharikova et al., 2016).

In addition to St. John's wort, this secondary metabolite was found in several other *Hypericum* species (Kitanov, 2001; Ayan et al., 2004) and in some basidiomycetes (*Dermocybe* spp.) (Dewick, 2002; Garnica et al., 2003) or endophytic fungi growing in *Hypericum perforatum* (*Thielavia subthermophila*) (Kusari et al., 2008, 2009). As hypericin is a bioactive compound that is applicable in several medicinal approaches, its content has been evaluated in *in vitro* grown *Hypericum perforatum* and in its transgenic clones (Čellárová et al., 1997; Košuth et al., 2003; Koperdáková et al., 2009), or in *Hypericum* cultures exposed to various biotechnological applications that focused on their preservation or stimulation of secondary metabolite production (Urbanová et al., 2006; Bruňáková et al., 2015; reviewed in: Čellárová, 2011).

Hypericin is well-known as a potent natural photosensitizing agent with great potential in anticancer photodynamic therapy (PDT) and photodynamic diagnosis (PDD). Besides its antineoplastic action, light-dependent *in vitro* fungicidal (Rezusta et al., 2012; Paz-Cristobal et al., 2014) and bactericidal effects (Kashef et al., 2013; García et al., 2015) have also been reported. In addition, light-activated hypericin is considered

Abbreviations: $^1\text{O}_2$, singlet oxygen; ^{64}Cu -bis-DOTA-hypericin, ^{64}Cu -Labeled bis-1,4,7,10-tetraazacyclododecane-N,N',N,N'-tetraacetic acid conjugated hypericin; ABC, ATP-binding cassette; AK, actinic keratosis; BCC, basal cell carcinoma; BCRP, breast cancer resistance protein; BD, Bowen's disease; CA4P, combretastatin A4 phosphate; Cdk4, cyclin-dependent kinase 4; CIS, carcinoma *in situ*; CLE, confocal laser endomicroscopy; CYP3A4, cytochrome P450 3A4; DAMPs, damage-associated molecular patterns; DLI, drug-light interval; EGFR, epidermal growth factor receptor; FE, fluorescence endoscopy; Hsp90, heat shock protein 90; HY-PDD, hypericin-mediated photodynamic diagnosis; HY-PDT, hypericin-mediated photodynamic therapy; ICD, immunogenic cell death; INF- α , interferon- α ; LIF, laser-induced fluorescence; MDR, multidrug resistance; MF, mycosis fungoides; MRPI, multidrug resistance-associated protein 1; NACA, necrosis-avid contrast agent; O_2^- , superoxide anion; p53, phosphoprotein p53, tumor suppressor p53, tumor protein p53; PDD, photodynamic diagnosis; PDT, photodynamic therapy; P-gp, P-glycoprotein; Plk, Polo-like kinase; PVP, polyvinylpyrrolidone; Raf-1, serine/threonine kinase; Raf-1 proto-oncogene; ROS, reactive oxygen species; SCC, squamous cell carcinoma; Ser, serine; SN-38, 7-Ethyl-10-hydroxy-camptothecin; TCC, transitional cell carcinoma; Thr, threonine; TNF- α , tumor necrosis factor- α ; TNT, tumor necrosis therapy; VEGF, vascular endothelial growth factor; WLE, white-light endoscopy.

to be an effective antiviral agent (Hudson et al., 1993; Prince et al., 2000). However, some clinical studies have revealed that high doses of hypericin can induce phototoxic skin reactions without showing any detectable antiviral or antiretroviral activity in patients with viral infections (Gulick et al., 1999; Jacobson et al., 2001). The controversy concerning the virucidal effect of hypericin was summarized in detail by Kubin et al. (2005).

However, the potential use of this secondary metabolite in medicine might be broader than currently thought. Although hypericin has been extensively studied mainly because of its photodynamic and photocytotoxic properties, it also possesses various positive or negative biological activities without being activated by light.

LIGHT-ACTIVATED HYPERICIN

Hypericin possesses several properties that make it a powerful fluorescent photosensitizer that is suitable for PDT and PDD—attractive applications for the treatment and detection of tumors. It possesses minimal or no toxicity in the dark (Thomas and Pardini, 1992; Vandebogaerde et al., 1997; Miadokova et al., 2010; Jendželovská et al., 2014; Feruszová et al., 2016), accumulates preferentially in neoplastic tissues (Kamuhabwa et al., 2002; Noell et al., 2011) and generates reactive oxygen species (ROS) in the presence of light (at wavelengths around 600 nm) and oxygen (Diwu and Lown, 1993). Thus, hypericin represents a potent natural alternative to chemically synthesized photosensitizers.

Hypericin in Photodynamic Therapy

PDT represents a non-invasive therapeutic approach that is beneficial in the treatment of various cancerous (reviewed in Agostinis et al., 2011) and even non-cancerous lesions and disorders (reviewed in Kim et al., 2015). In general, it is based on the combined action of a photosensitizer, light and molecular oxygen. PDT involves the administration of a non-toxic photosensitizer that preferentially accumulates in the target tissue, followed by its local illumination with harmless visible light of an appropriate wavelength, to activate and excite the photosensitizer. These photoreactions lead to the oxygen-dependent generation of cytotoxic ROS, resulting in cell death and tissue destruction. However, PDT is a multifactorial process and the degree of cellular photodamage depends on many factors, including cell permeability, the subcellular localization of the photosensitizer, the quantity of molecular oxygen, the light dose, the types of generated ROS and the attributes of cancer cells.

The exact mechanisms of cellular hypericin uptake are still unclear and require further investigation, but the results indicate that hypericin might be transported into or through cells via temperature-dependent diffusion (Thomas and Pardini, 1992; Sattler et al., 1997), partitioning, pinocytosis or endocytosis (Siboni et al., 2002). Concerning its subcellular redistribution, the co-labeling of cancer cells with hypericin and fluorescent dyes specific for cell organelles revealed that hypericin accumulates in the membranes of the endoplasmic reticulum, the Golgi apparatus, lysosomes and mitochondria (Agostinis et al., 2002; Ali and Olivo, 2002; Galanou et al., 2008; Mikeš et al., 2011).

However, the cellular uptake and subcellular localization of hypericin might be affected by its lipophilicity, incubation concentrations and/or interaction with serum lipoproteins (Crnolatac et al., 2005; Galanou et al., 2008; Kascakova et al., 2008). In brief, upon light-activation, hypericin is efficient primarily in the generation of singlet oxygen (${}^1\text{O}_2$; type II mechanism) and superoxide anion (O_2^- ; type I mechanism) (Thomas et al., 1992; Diwu and Lown, 1993), which can ultimately lead to necrosis (Du et al., 2003b; Mikeš et al., 2007, 2009), apoptosis (Ali and Olivo, 2002; Mikeš et al., 2009), autophagy-associated cell death (Buytaert et al., 2006; Rubio et al., 2012) or even to immunogenic cell death (ICD) (Garg et al., 2012a). As type II ICD inducer (Garg et al., 2015a), HY-PDT represents a promising form of active immunotherapy (Galluzzi et al., 2014) owing to spatiotemporally defined emission of damage-associated molecular patterns (DAMPs) (Garg et al., 2012b, 2015b, 2016; Zheng et al., 2016).

The photocytotoxicity of hypericin is strongly oxygen-dependent, as no such effects are present in hypoxic conditions (Thomas and Pardini, 1992; Delaey et al., 2000). Nevertheless, the final response of hypericin-mediated PDT (HY-PDT) might also be affected by the ability of cells to overcome oxidative stress through the activity of various cytoprotective mechanisms, including cellular redox systems (Mikeš et al., 2011; Mikešová et al., 2013). Furthermore, the light-dependent inhibitory effect of hypericin against various enzymes engaged in the regulation of cell survival and proliferation (Ser/Thr kinases, tyrosine kinases, etc.) has been reported (reviewed in Kubin et al., 2005). These activities might also contribute to the cytotoxic and antiproliferative effects of HY-PDT. The exact mechanisms of action and the cellular aspects of HY-PDT have been outlined and summarized in several reviews (Agostinis et al., 2002; Theodossiou et al., 2009; Mikeš et al., 2013; Garg and Agostinis, 2014).

Preclinical and Clinical Assessment of HY-PDT

Efficacy and Suitable Conditions

Many *in vitro* studies have demonstrated the cytotoxicity of photoactivated hypericin in various cancer cell types (Xie et al., 2001; Head et al., 2006; Sacková et al., 2006; Mikeš et al., 2007; Koval et al., 2010; Mikešová et al., 2013; Kleemann et al., 2014). Moreover, recent *in vivo*, preclinical and clinical studies have indicated that HY-PDT might be an effective and relevant approach in the treatment of some skin tumors, carcinomas and sarcomas. In general, the depth of tumor destruction after PDT commonly ranges from a few mm to 1 cm, due to limited photosensitizer and light penetration through the tissues. Thus, PDT is effective mostly against superficial lesions and small tumors.

Clinical studies to test HY-PDT efficacy

To our knowledge, three clinical trials of HY-PDT applied to various skin tumors have been published to date (Table 1). In the first study, Alecu et al. (1998) tested the intralesional injection of hypericin with subsequent photoactivation with visible light in the treatment of basal cell carcinoma (BCC) (eleven patients) and squamous cell carcinoma (SCC) (eight

patients) and found that HY-PDT was effective in the treatment of both skin disorders. A reduction in tumor size and the generation of a new epithelium at the surface of lesions following HY-PDT were observed. Moreover, as no necrosis or cell loss was evident in the surrounding healthy tissues and no side effects were observed, with the exception of mild erythema in five cases (two patients with SCC, three patients with BCC), HY-PDT-mediated tumor targeting was selective. The treatment resulted in a complete clinical response in one SCC patient and two BCC patients, but in the remaining patients, only a partial clinical response was observed. Thus, the efficacy of HY-PDT appeared to be dependent on the initial lesion size, the total dose of hypericin, or the frequency and duration of the therapy (Alecu et al., 1998). Several years later, the potential use of HY-PDT in the treatment of non-melanoma skin cancers was explored (Kacerovská et al., 2008). A complete clinical response was observed in 50% of patients with actinic keratosis (AK) 3 months after HY-PDT, and in 22% of patients with superficial BCC and 40% of patients with Bowen's disease (BD) 6 months after HY-PDT. However, in the case of AK, the percentage reduced to 29% 6 months after HY-PDT and only partial remission was observed in patients with nodular BCC. On the other hand, complete histological remission was evident in 80% of patients with BD (Kacerovská et al., 2008). Only the partial response rate and suboptimal success of HY-PDT could be caused by the limited penetration of the skin by hypericin and by its low concentration in the final extraction product. In the third clinical trial, Rook et al. (2010) tested HY-PDT as a potentially well-tolerated and effective therapeutic modality for the treatment of lymphocyte-mediated skin disorders: malignant mycosis fungoïdes (MF; the most common type of cutaneous T-cell lymphoma) and non-cancerous autoimmune psoriasis. The results were promising for both diseases. In the case of MF, HY-PDT led to an improvement in the treated lesions (a size reduction by at least 50%) in the majority of patients, whereas the placebo was ineffective. Moreover, hypericin was well tolerated by the patients, with only mild to moderate phototoxic skin reactions occurring after exposure to visible light. No serious adverse effects or events were observed (Rook et al., 2010). However, the authors themselves recommended a phase III study with a greater number of patients. All these clinical data indicate that topically applied hypericin, combined with its photoactivation, might be a promising and safe alternative for the treatment of some cancerous and non-cancerous skin disorders. However, as the effectiveness of HY-PDT depends on the hypericin concentration, its total dose, its rate of tissue penetration, the frequency and duration of the therapy, or on the grade of malignancy, more clinical trials are necessary to define the optimal conditions for the whole procedure.

Preclinical *in vivo* studies to test HY-PDT effects and conditions

Many further studies to test HY-PDT efficacy have been performed using mouse or rat animal models (Table 2). Several *in vivo* studies indicate that HY-PDT might be a promising approach in the treatment of bladder carcinomas. Kamuhabwa et al. (2002) reported selective hypericin uptake

TABLE 1 | Clinical studies to test HY-PDT efficacy.

Disease/No. of patients	Hypericin administration	Hypericin dosage	Light dose/Fluence rate	HY-PDT efficacy	References
Squamous cell carcinoma/8	Intralesional injection	40–100 µg 3–5 times per week for 2–4 weeks;	86 J/cm ² /24 mW/cm ²	Reduction in tumor size, re-epithelialization at the borders of the lesion, complete clinical remission in the case of one patient;	Alecu et al., 1998
Basal cell carcinoma/11		40–200 µg 3–5 times per week for 2–6 weeks		Reduction in tumor size, complete clinical remission in the case of two patients, no evident signs of tumor recurrence after 5 months	
Actinic keratosis/8 Basal cell carcinoma/21	On the lesion	Weekly for 6 weeks on average	75 J/cm ²	50% complete clinical response (AK) 28% complete clinical response (superficial BCC) 11% complete histological response (superficial BCC) 67% partial clinical response (nodular BCC)	Kacerovská et al., 2008
Bowen's disease/5				40% complete clinical response (BD) 80% complete histological response (BD)	
Mycosis fungoïdes (T-cell lymphoma)/12	On the lesion	0.005–0.025 mg/cm ² twice-weekly for 6 weeks	8–20 J/cm ²	58.3% of responsive patients (reduction in MF lesion size by 50% or more)	Rook et al., 2010
Psoriasis/11				54.6% of responsive patients	

AK, actinic keratosis; BCC, basal cell carcinoma; BD, Bowen's disease; MF, mycosis fungoïdes.

in bladder tumors and subsequently, even HY-PDT-mediated tumor damage was observed without the destruction of normal tissue (Kamuhabwa et al., 2003). In both studies, female Fisher rats with an orthotopic superficial transitional cell carcinoma (TCC) were used as an experimental model and hypericin was administered directly into the bladder via the catheter. The instilled hypericin accumulated selectively in the bladder urothelial tumors and the normal urothelium (in a ratio of 12:1), but no hypericin was detected in normal bladder submucosa and muscle layers, which is an important factor to avoid underlying tissue damage. In addition, no hypericin was detected in plasma; thus, systemic side-effects should not appear (Kamuhabwa et al., 2002).

Furthermore, photoactivated hypericin resulted in selective urothelial tumor damage, with tumor cells shrinking and detaching from the bladder wall, indicating that HY-PDT might be beneficial in the treatment of superficial carcinomas and premalignant changes in the bladder. The HY-PDT that was performed under suitable light conditions had no significant effects on the other bladder layers; nevertheless, 2–5% of tumor cells survived and were responsible for tumor regrowth (Kamuhabwa et al., 2003). However, following the results of *in vitro* study based on TCC-derived spheroids, the same authors suggested that hyperoxigenation could overcome this problem and might enhance the efficacy of HY-PDT (Huygens et al., 2005). In addition to the orthotopic tumor model, Liu et al. (2000) also used a xenograft model in their experiments. Human MiaPaCa-2 pancreatic adenocarcinoma cells were injected subcutaneously and orthotopically into the pancreatic bed of nude, athymic mice. To allow hypericin photoactivation in orthotopic pancreatic tumor nodules, mice underwent a laparotomy that was necessary for the positioning of the optical fiber. A significant decrease in growth of subcutaneous

shoulder tumors ($91.2\% \pm 2.3\%$) and even pancreatic tumor nodules ($42.2\% \pm 8.1\%$) was observed 4 weeks after HY-PDT, indicating that intratumor hypericin and laser therapy might also be beneficial in the treatment of unresectable pancreatic cancer (Liu et al., 2000).

However, instead of more clinically relevant orthotopic tumor models, more *in vivo* studies have been performed to test the efficacy, conditions or responses of HY-PDT after the treatment, only in the murine or rat xenograft or allograft models of subcutaneous carcinomas or sarcomas. Various positive effects of HY-PDT involving the inhibition of tumor growth, a prolonged survival time of the treated animals, tumor necrosis, apoptosis or damage to the tumor vasculature were observed in mice bearing human epidermoid carcinoma (Vandenbogaerde et al., 1996), human prostate adenocarcinoma cells (Xie et al., 2001), human nasopharyngeal carcinoma cells (Du et al., 2003a,b; Thong et al., 2006), human squamous carcinoma cells (Head et al., 2006), human bladder carcinoma cells (Bhuvaneswari et al., 2008), human rhabdomyosarcoma cells (Urla et al., 2015), murine lymphoma cells (Chen and de Witte, 2000), murine colon adenocarcinoma cells (Blank et al., 2002; Sanovic et al., 2011), murine fibrosarcoma cells (Čavarga et al., 2001, 2005; Chen et al., 2001, 2002a,b; Bobrov et al., 2007) or murine Ehrlich ascites carcinoma cells (Lukšienė and De Witte, 2002) and in rats bearing rat bladder transitional bladder carcinoma (Zupkó et al., 2001) or rat pituitary adenoma cells (Cole et al., 2008) (Table 2). In addition, Blank et al. (2002) demonstrated the dependence of HY-PDT efficacy on the irradiation conditions (light dose and wavelength). Tumor necrosis was much more pronounced at 590 nm than at 550 nm and even increased when the light dose was raised from 60 to 120 J/cm²; however, the maximum depth of tumor necrosis was 9.9 ± 0.8 mm at 590 nm (Blank et al., 2002). Considering the relationship

TABLE 2 | Preclinical *in vivo* studies to test HY-PDT effects and conditions.

Experimental model/Type of tumor (cell line)	Hypericin administration	Hypericin dose	Light dose/Fluence rate	HY-PDT effects	References
Athymic nude mice/Epidermoid carcinoma (A431)	Intraperitoneal injection	2.5 mg/kg, 5 mg/kg	180 J/cm ²	Tumor growth inhibition, reduced tumor mass	Vandenbogaerde et al., 1996
Athymic nude mice/Pancreatic carcinoma (MiaPaCa-2)	Intratumoral Injection	10 µg/mouse	2 doses of 200 J	Suppressed growth of subcutaneous and orthotopic tumors	Liu et al., 2000
DBA/2 mice/Lymphoma (P388)	Intraperitoneal injection	2, 5 or 20 mg/kg	120 J/cm ² /100 mW/cm ²	Reduced tumor mass and tumor size, prolonged survival time	Chen and de Witte, 2000
Nude mice/Prostate carcinoma (LNCaP)	Oral	5 mg/kg	30 mW	Tumor growth inhibition	Xie et al., 2001
C3H/Km mice/Fibrosarcoma (RIF-1)	Intravenous injection	5 mg/kg	120 J/cm ² /100 mW/cm ²	Tumor vasculature damage after 0.5 h DLI PDT resulting in complete tumor cure, apoptosis as a main form of cell death	Chen et al., 2001, 2002a,b
Fischer CDF (F344)/CrIBR rats/Bladder carcinoma (AY-27)	Intravenous injection	1 or 5 mg/kg	120 J/cm ² /100 mW/cm ²	Reduced tumor size, no measurable tumor mass 9–10 days after 0.5 h DLI PDT	Zupkó et al., 2001
C3H/DiSn mice/Fibrosarcoma (G5:1:13)	Intratumoral or intraperitoneal injection	5 mg/kg	180 J/cm ² /150 mW/cm ²	Reduced tumor volume, prolonged survival time, complete remission in smaller lesions (3 mm or less in size)	Čavarga et al., 2001
	Intraperitoneal injection	1 × 5 mg/kg, 2 × 2.5 mg/kg	168 J/cm ² /70 mW/cm ²	Higher efficiency of fractionated dose Vascular damage, formation of necrotic areas	Čavarga et al., 2005; Bobrov et al., 2007
Balb/c mice/Colon carcinoma (C26)	Intraperitoneal injection	5 mg/kg	60, 90 or 120 J/cm ² /100 mW/cm ²	Vascular damage, tumor necrosis (the depth of tumor necrosis increased with increased light dose)	Blank et al., 2002
Balb/c mice/Ehrlich ascites carcinoma	Intraperitoneal injection	40 mg/kg	50 mW/cm ²	Prolonged survival time (75% of mice), no tumor recurrence (25% of survived mice)	Lukšienė and De Witte, 2002
Fischer rats/Bladder carcinoma (AY-27)	Instillation into the bladder	30 µM	6–48 J/cm ² /25–50 mW/cm ²	Selective urothelial tumor damage without destructive effects on detrusor musculature	Kamuhabwa et al., 2003
Balb/c nude mice/Nasopharyngeal carcinoma (HK-1)	Intravenous injection	2 mg/kg	120 J/cm ² /226 mW/cm ²	Inhibited tumor growth, tumor shrinkage, necrosis as a main form of cell death	Du et al., 2003a,b
		2 or 5 mg/kg	30 J/cm ² /25 mW/cm ²	Increased apoptosis and lower serum levels of VEGF after 6 h DLI PDT	Thong et al., 2006
Athymic nude mice/Squamous carcinoma (SNU1)	Intratumoral injection	10 µg per mg tumor	0–60 J/cm ²	Regression of smaller tumors (under 400 mm ³)	Head et al., 2006

(Continued)

TABLE 2 | Continued

Experimental model/Type of tumor (cell line)	Hypericin administration	Hypericin dose	Light dose/Fluence rate	HY-PDT effects	References
Balb/c nude mice/Bladder carcinoma (MGH)	Intravenous injection	5 mg/kg	120 J/cm ² /100 mW/cm ²	Vascular damage after 0.5 h DLI PDT resulting in reduced tumor volume, increased expression of some angiogenic proteins after 6 h DLI PDT	Bhuvaneswari et al., 2008
Wistar-Furth rats/Pituitary adenoma (GH4C1)	Intraperitoneal injection	4 × 1 mg/kg	105–130 J/m ²	Inhibited growth of smaller tumors (under 1 cm ³), formation of apoptotic clusters	Cole et al., 2008
NMRI – HR-HR hairless mice/UV-induced small skin tumors	Topical application	0.1% in gelcream	40 J/cm ² /20 mW/cm ²	Full lesional necrosis resulting in total lesional clearance (44%), replacement of atypical AK cells by normal keratinocytes	Boiy et al., 2010
Balb/c mice/Colon carcinoma (CT26)	Intravenous injection	2.5 or 10 mg/kg	14 or 60 J/cm ² /27 or 50 mW/cm ²	Vascular damage after "low power PDT" resulting in complete tumor regression, prevention of new tumor growth after the re-challenge of cured mice with CT26 cells	Sanovic et al., 2011
NOD/LtSz-scid IL2R γ null mice/Rhabdomyosarcoma (Rh30)	Intravenous injection	100 µg/mouse	--	Induction of apoptosis in tumor cells	Urla et al., 2015
Balb/c mice/Colon carcinoma (CT26)	Subcutaneous injection of HY-PDT treated cells	150 nM	2.70 J/cm ²	Tumor-rejecting anticancer vaccination effect after the re-challenge of cured mice with CT26 cells	Garg et al., 2012a, 2015b, 2016
Fischer 344 rats/Rat bladder carcinoma (AY27)	Subcutaneous injection of HY-PDT treated cells	150 nM	2.70 J/cm ²	Absence of tumor-rejecting anticancer vaccination effect after the re-challenge of cured rats with AY27 cells	Garg et al., 2015b
C57BL/6 mice/Lewis lung carcinoma (LLC), Dendritic cells (DC) co-cultured with PDT-LLCs	Subcutaneous injection of HY-PDT treated cells	0.25 µM	1.85 J/cm ²	Tumor-rejecting anticancer vaccination effect after the re-challenge of cured mice with LLC-Luc cells	Zheng et al., 2016

AK, actinic keratosis; DLI, drug-light interval; VEGF, vascular endothelial growth factor; --, the parameter was not provided by the authors.

between HY-PDT efficacy and tumor volume, similar results were obtained in other studies. Head et al. (2006) and Cole et al. (2008) observed a regression or reduction in tumor size only in tumors smaller than 0.4 or 1 cm³, respectively, whereas larger tumors showed only a partial response followed by their regrowth (Head et al., 2006), or did not respond to the treatment (Cole et al., 2008). Thus, light penetration into the tissue appeared to be a limiting factor. However, Cole et al. (2008) also concluded that HY-PDT can be effective in the elimination of small solid tumor residues. Čavarga et al. (2001) also determined complete remission only in

smaller tumors (3 mm or less in height), but the main aim of their study was to compare the impact of intraperitoneal and intratumoral hypericin injection on the effectiveness of HY-PDT. Both schedules of hypericin administration significantly reduced tumor volume and increased the survival rate of animals. However, considering the complete response, a higher HY-PDT efficacy was observed for hypericin that was administered intraperitoneally (44.4%) compared to intratumorally (33.3%) (Čavarga et al., 2001). Moreover, it was later demonstrated that a better therapeutic response was obtained after fractionated hypericin administration (two 2.5 mg/kg doses; 6 and 1 h before

irradiation) than after a single hypericin dose (5 mg/kg; 1 or 6 h before irradiation) (Čavarga et al., 2005).

Furthermore, Chen et al. (2001) reported the correlation between hypericin biodistribution, HY-PDT efficacy and various administration–irradiation time intervals (drug–light intervals—DLIs). It was found that shortly (0.5 h) after the intravenous administration of hypericin (5 mg/kg), the photosensitizer was located preferentially within tumor blood vessels. At 6 h after injection, maximum intratumoral hypericin content was evident and only poor fluorescence was detected in the tumor vasculature. Despite high tumor hypericin levels, no tumor cure was observed after longer DLI HY-PDT (6 h) treatment. However, the efficacy of PDT was maximal (100% tumor cure) when irradiation was performed at 0.5 h after hypericin administration (short DLI), indicating strong HY-PDT-induced damage to the tumor vasculature (Chen et al., 2001). Similar results were obtained by Zupkó et al. (2001). In TCC tumors, the outcome of HY-PDT was highly dependent on DLI (0.5, 6, or 24 h). The strongest effect, which resulted in no tumor regrowth in some rats, was evident after 0.5 h DLI PDT. At the same time, the highest hypericin concentration was detected in the plasma, indicating that PDT-mediated tumor vascular damage was responsible for its antineoplastic action (Zupkó et al., 2001). The antivascular and strong antitumoral effects of short DLI HY-PDT were also subsequently confirmed in the murine fibrosarcoma model (Chen et al., 2002a,b). Damage to tumor vessels was also detected following long DLI HY-PDT treatments, but many viable tumor cells were present, especially at the tumor periphery, indicating that this PDT modality only induced partial vascular collapse (Chen et al., 2002a). In agreement with these results, Bobrov et al. (2007) also observed primary vascular damage after HY-PDT with either a single dose (5 mg/kg; 1 or 6 h before irradiation) or fractionated hypericin administration (two 2.5 mg/kg doses; 6 and 1 h before irradiation), which subsequently progressed to tumor tissue necrosis. The preference of HY-PDT-mediated vasculature or cellular damage appears to be dependent on the distribution and accumulation of the photosensitizer; thus, greater vascular destruction is expected after short DLI PDT and more direct killing of tumor cells is expected after long DLI PDT. However, because the damage to tumor vessels can have devastating consequences for whole tumor mass, the targeting of the tumor vasculature via short DLI PDT might be more effective in the treatment of solid tumors than a long DLI PDT. Moreover, apoptosis was the main form of cell death responsible for tumor eradication following short DLI HY-PDT (Chen et al., 2002b). In contrast, Thong et al. (2006) observed significantly more apoptosis after long DLI PDT (6 h) compared to short DLI PDT (1 h). However, different irradiation conditions and tumor models were used in both studies: whereas Chen et al. (2002b) photoactivated hypericin with a light dose of 120 J/cm² delivered at a fluence rate of 100 mW/cm², a lower fluence rate HY-PDT (light dose of 30 J/cm², fluence rate of 25 mW/cm²) was applied by Thong et al. (2006). The results indicate that long DLI PDT might also be effective in the induction of programmed cell death, but only under low fluence rate conditions. Moreover, lower serum levels of vascular endothelial growth factor (VEGF) were detected after

HY-PDT using a long DLI and a low fluence rate, which can reduce the risk of new tumor vasculature formation (Thong et al., 2006).

As PDT-mediated tissue damage can lead to various cellular and molecular responses, Bhuvaneswari et al. (2008) examined the potential anti-angiogenic vs. angiogenic properties of short (0.5 h) and long (6 h) DLI HY-PDT. Both HY-PDT scenarios led to a reduction in tumor volume, but the effect was much more pronounced for a short DLI. These findings agree with the above-mentioned results (Chen et al., 2001, 2002a,b) and suggest the destruction of the tumor vasculature after short DLI HY-PDT. However, in addition to its antitumor activities, cellular-targeted long DLI HY-PDT induced the expression of some angiogenic proteins in tumor tissue, including VEGF, tumor necrosis growth factor-α (TNF-α) and interferon-α (INF-α), which potentially lead to the formation of new vessels (Bhuvaneswari et al., 2008). In subsequent studies, the efficacy of HY-PDT was enhanced using monoclonal antibodies against VEGF and the epidermal growth factor receptor (EGFR) (Bhuvaneswari et al., 2010, 2011). For short DLI HY-PDT, similar results were obtained by Sanovic et al. (2011) in mice bearing CT26 colon carcinoma cells. Complete tumor regression was observed after “low-power HY-PDT” (a hypericin dose of 2.5 mg/kg, a short DLI of 0.5 h, a light dose of 14 J/cm² and a fluence rate of 27 mW/cm²), as no visible or palpable tumors were detected for at least 60 days after the treatment. In contrast, all mice exposed to “high-power HY-PDT” (a hypericin dose of 10 mg/kg, a short DLI of 1 h, a light dose of 60 J/cm² and a fluence rate of 50 mW/cm²) died 2 days after the treatment as a consequence of internal bleeding. Thus, both HY-PDT modalities with short DLIs appeared to preferentially target the vessels, but a higher hypericin concentration and light dose produced a much stronger response. These results suggest that “low-power HY-PDT” is strong enough to completely eliminate tumors by damaging their vasculature. Moreover, the re-challenge of cured mice with tumorigenic CT26 cells did not result in new tumor growth, indicating the HY-PDT-mediated induction of the antitumor immune response (Sanovic et al., 2011). HY-PDT-mediated induction of anticancer immunity was also observed in the studies utilizing different *in vivo* experimental models. Immunization of BALB/c mice with “dying or dead” colon carcinoma CT26 cells prevented the tumor growth at the rechallenge site treated with live CT26 tumor cells. Approximately 70–85% of the mice immunized with HY-PDT treated CT26 cells efficiently rejected the formation of CT26-derived tumors at challenge site (Garg et al., 2012a, 2015b, 2016). Activation of adaptive immune system was also detected in immunocompetent C57BL/6 mice immunized with HY-PDT treated Lewis lung carcinoma (LLC) cells and LLC cells co-cultured with dendritic cells (Zheng et al., 2016). The results of these three independent experimental groups suggest great potential of HY-PDT in development of anticancer vaccines.

Similar results as in the case of partial remission in patients with nodular BCC (Kacerovská et al., 2008) were obtained in an *in vivo* study using hairless mice with UV-induced non-melanoma skin tumors (AK, SCC) as an experimental model (Boiy et al., 2010). Photoactivated hypericin induced a total and partial response in 44 and 22% of lesions (diameter of 1–2 mm),

respectively, with evident lesional necrosis and the replacement of atypical AK cells for normal keratinocytes. However, 33% of lesions were non-responsive to HY-PDT. Tumor penetration and the selectivity of topically applied hypericin was also limited by mouse skin, as the accumulation of hypericin was highest in the outermost epidermal layer and lower hypericin levels were detected in the rest of the epidermis and the dermis (Boiy et al., 2010).

Some preclinical and clinical results gave relatively disappointing results and in some cases, the efficacy of HY-PDT was not as high as expected. The above-mentioned studies contributed to a better understanding of HY-PDT-induced responses and highlighted the importance of optimizing the conditions, such as suitable hypericin administration, light dose, fluence rate, or time intervals and implicated HY-PDT as a promising anticancer therapeutic approach; however, more clinically relevant studies and trials are required for the implementation of HY-PDT into clinical practice.

Hypericin in Photodynamic Diagnosis

In addition to their therapeutic abilities, most photosensitizers are also potent diagnostic agents. The main principle and relevance of PDD is to enhance the contrast between neoplastic and surrounding healthy tissue, which should contribute to the surgical clearance of the whole tumor mass or its small residues. Due to the fluorescent properties of hypericin and its specificity for neoplastic tissue, hypericin-mediated PDD (HY-PDD) is being tested for various clinical uses, including optical tumor imaging, and the targeting, monitoring or detection of tumor stages and grades. To date, fluorescence diagnosis using hypericin has been clinically tested in bladder, head and neck cancers or gliomas (Table 3).

HY-PDD in the Detection and Identification of Bladder Cancer

In most published clinical studies, HY-PDD was applied to bladder tumors. As already mentioned in the HY-PDT section, Kamuhabwa et al. (2002) (Table 4) revealed selective hypericin uptake in rat bladder tumors using *in situ* laser-induced fluorescence (LIF) and fluorescence microscopy. The results suggest that hypericin is very beneficial in visualization and distinguishing the tumor mass from normal tissue using various fluorescent techniques. Thus, hypericin could be used not only in PDT, but also in the PDD of superficial bladder tumors.

At about the same time, the first clinical studies were performed by D'Hallewin et al. (2000, 2002), who examined the fluorescence-based detection of flat bladder carcinomas *in situ* (CIS) and in papillary non-invasive bladder tumors after the intravesical instillation of hypericin (at least 2 h). The fluorescence emission was induced using fluorescence endoscopy (FE) under blue-light illumination. Hypericin accumulated selectively in tumor cells and papillary and flat lesions showed red fluorescence, whereas no fluorescence was evident in the normal bladder tissue. Subsequently, biopsies were taken from fluorescent regions for microscopic analyses. The results of both clinical studies suggested that HY-PDD has a high sensitivity and specificity for the detection of bladder cancer (D'Hallewin

et al., 2000, 2002). Moreover, the results obtained by confocal microscopy, white-light endoscopy (WLE) and histopathology revealed that the intensity of hypericin fluorescence increased with the stage and grade of bladder cancer (normal bladder tissue < inflammation in the bladder < grade 1 TCC < grade 2 TCC < CIS < grade 3 TCC) (Olivo et al., 2003b). Therefore, HY-PDD could be used as a diagnostic aid to the histopathology of bladder tumors.

Nowadays, bladder lesions are conventionally diagnosed under WLE followed by biopsies that are necessary for the histological examination of suspicious tissues. However, in previous studies, some lesions were barely visible or were absent in white light (D'Hallewin et al., 2000, 2002), thus, WLE appears not to be sensitive enough to reveal all CIS lesions and leads to a high risk of missing the tumor. Therefore, another clinical study compared the WLE and HY-PDD methods (Sim et al., 2005). Hypericin was instilled into the bladder (for 2 h) and immediately after WLE, FE (violet light) was used to induce fluorescence emission in the same bladder regions. Despite the comparable specificity of both approaches (91% for HY-PDD, 98% for WLE), HY-PDD was more sensitive (82%) than WLE (62%) (Sim et al., 2005), suggesting that hypericin might be very potent in the labeling and early detection of flat superficial bladder tumors. Similar results were obtained by Kubin et al. (2008) using polyvinylpyrrolidone (PVP) bound to hypericin as a new water-soluble formula for the improvement of hypericin-mediated bladder cancer detection and diagnosis. Hypericin-PVP was intravesically instilled 1–2 h prior to FE. The overall sensitivity of PDD with PVP-hypericin (95%) was significantly higher than WLE (85%). The maximum contrast in sensitivity was evident in the case of CIS (100% for PDD vs. 33% for WLE) and dysplasia (85% for PDD vs. 31% for WLE) (Kubin et al., 2008).

As the PVP-hypericin complex represents a potent water-soluble PDD agent without the necessity of binding to serum proteins, its biodistribution (Vandepitte et al., 2010) and optimal dosage and instillation time were evaluated (Straub et al., 2015) in tumor-bearing rats and in patients with bladder cancer, respectively. Vandepitte et al. (2010) (Table 4) demonstrated the uniform distribution of instilled PVP-hypericin in all cell layers of the malignant urothelium, whereas its penetration into the normal bladder epithelium was very limited. Straub et al. (2015) tested various combinations of PVP-hypericin dosage (75 and 225 µg) and instillation time (15, 30, 60, and 120 min) to identify the optimal PDD conditions. Even though the fluorescence of 225 µg PVP-hypericin instilled for 120 and 60 min was very strong, the shorter instillation time (30 min) for 225 µg PVP-hypericin was evaluated as optimal. A lower photosensitizer dose (75 µg) and 15 min with a dose of 225 µg were insufficient to detect the lesions (Straub et al., 2015). The authors established the most suitable dosage and instillation time of PDD with PVP-hypericin, but they suggest a larger phase IIB study should be performed to determine the sensitivity and specificity of these optimal conditions.

All the above-mentioned results indicate that HY-PDD is highly sensitive in the detection of early bladder cancer

TABLE 3 | Clinical studies to test HY-PDD efficacy, sensitivity and specificity.

No. of patients	Hypericin administration	Hypericin dose	Fluorescence excitation	HY-PDD efficacy	References
BLADDER CANCER					
40	Instillation into the bladder	8 μM (40 ml)	FE/blue light	93% sensitivity and 98.5% specificity (for CIS)	D'Hallewin et al., 2000
87	Instillation into the bladder	8 μM (40 ml)	FE/blue light	94% sensitivity and 95% specificity (for CIS)	D'Hallewin et al., 2002
30	Instillation into the bladder	8 μM (50 ml)	FE/blue light	Fluorescence intensity increased with the stage and grade of cancer (normal < inflammation < grade 1 TCC < grade 2 TCC < CIS < grade 3 TCC)	Olivo et al., 2003b
41	Instillation into the bladder	8 μM (40 ml)	FE/violet light	Higher sensitivity (82%) compared to conventional WLE (62%)	Sim et al., 2005
57	Instillation into the bladder	0.25 mg HY + 25 mg PVP (50 ml)	FE/blue light	Higher overall sensitivity (95%) compared to conventional WLE (85%), fewer overlooked malignant lesions compared to WLE, sensitivity increased with the grade of cancer	Kubin et al., 2008
40	Instillation into the bladder	75 or 225 μg PVP-hypericin (50 ml)	FE/blue light	very strong fluorescence of 225 μg PVP-hypericin (120 and 60 min), optimal fluorescence of 225 μg PVP-hypericin instilled for 30 min, insufficient fluorescence of 75 μg and 225 μg PVP-hypericin (15 min)	Straub et al., 2015
8	Instillation into the bladder	8 μM (40 ml)	FM/380–425 nm	<i>Ex vivo</i> urine fluorescence cytology—fluorescence detected in all eight tumor cases	Pytel and Schmeller, 2002
29 urine samples	<i>Ex vivo</i> staining of sediment extracted from voided urine	Concentration not given (1 ml)	CFM/488 nm Argon laser	Higher fluorescence intensity in tumor cells than in cells from normal urine and in high-grade tumors than in low-grade tumors	Olivo et al., 2003a
21	<i>Ex vivo</i> staining of sediment extracted from voided urine	Concentration not given (1 ml)	CFM/488 nm Argon laser	Higher fluorescence intensity in tumor cells than in cells from normal urine	Fu et al., 2007
GLIOMA					
5	Intravenous injection	0.1 mg/kg	NM/blue light	Tumor fluorescence clearly distinguishable from normal brain tissue, high specificity (100 and 90%) and sensitivity (91 and 94%)	Ritz et al., 2012
HEAD AND NECK CANCER					
23	Oral rinsing	8 μM (100 ml)	FE/blue light	Distinguishing between various types of oral cancer (red-to-blue ratio), 90% and higher specificity and sensitivity (red-to-blue ratio)	Thong et al., 2009

(Continued)

TABLE 3 | Continued

No. of patients	Hypericin administration	Hypericin dose	Fluorescence excitation	HY-PDD efficacy	References
2	Oral rinsing	8 μM (100 ml)	CLE/488 nm Argon laser	3-D visualization of human buccal mucosa at the surface and approximately 15 μm below the surface	Thong et al., 2012
27	Ex vivo tissue staining	8 μM	pCLE/568 nm laser diode	longer time interval for sufficient ex vivo staining (at least 30 min), the anomalies of keratinization not stained	Abbacì et al., 2015

CIS, carcinoma *in situ*; CFM, confocal fluorescence microscopy; CLE, confocal laser endomicroscopy; FE, fluorescence endoscopy; FM, fluorescence microscopy; HY, hypericin; NM, neurosurgical microscopy; pCLE, probe-based CLE; PVP, polyvinylpyrrolidone; TCC, transitional cell carcinoma; WLE, white-light endoscopy.

TABLE 4 | Preliminary data for clinical HY-PDD applications and *in vivo* studies concerning hypericin accumulation.

Experimental model/Type of tumor (cell line)	Hypericin administration	Hypericin dose	Fluorescence excitation	Hypericin accumulation and fluorescence	References
Fischer rats/Bladder carcinoma (AY-27)	Instillation into the bladder	8 or 30 μM	LIF/410 nm Krypton laser FM/525/50 nm	Intense fluorescence in tumor tissue and faint fluorescence in normal bladder tissue (ratio 12:1), no fluorescence in submucosa and muscle layers	Kamuhabwa et al., 2002
		30 μM PVP-hypericin	FM/510–560 nm	Higher accumulation (3.5-fold more) in malignant tissue than in normal urothelium	Vandepitte et al., 2010
Wistar rats/Glioma (C6)	Intravenous injection	5 mg/kg	FM/510–550 nm	Higher accumulation in glioma than in normal brain tissue and infiltration zone	Noell et al., 2011
VMDk mice/Glioma (SMA-560)	Intravenous injection	2.5 mg/kg	FM/510–550 nm FME/405 nm	Time-dependent accumulation in glioma cells (maximal uptake—6 h after administration), FME—fluorescence detection also in intracerebral and extracranial gliomas and in brain vessels	Noell et al., 2013
NOD/LtSz-scid IL2R ^{γnull} mice/Rhabdomyosarcoma (Rh30)	Intravenous injection	100 μg/mouse	FL/blue light	Tumor fluorescence clearly distinguishable from normal healthy tissue	Urla et al., 2015

CLE, confocal laser endomicroscopy; FL, fluorescence laparoscopy; FM, fluorescence microscopy; FME, fluorescence microendoscopy; LIF, laser-induced fluorescence technique.

and could be routinely used as a diagnostic approach. Moreover, no photobleaching during FE and resection or side effects were detected (D’Hallewin et al., 2002; Olivo et al., 2003b; Sim et al., 2005; Kubin et al., 2008). Kamuhabwa et al. (2005) also conclude that either photosensitization or systemic side-effects should not be expected in patients after intravesical hypericin administration, as the hypericin concentration in plasma was below the detection limit (<6 nM).

Another common method used for bladder cancer diagnosis is *ex vivo* urine cytology, which microscopically analyzes the exfoliated bladder cells from voided urine. This diagnostic technique is non-invasive and less time-consuming than taking biopsy specimens. However, its sensitivity to detect early-stage or low-grade cancer is relatively low. Thus, several teams have focused on a technique that combines HY-PDD and urine cytology (Pytel and Schmeller, 2002; Olivo et al., 2003a; Fu

et al., 2007). In the first study conducted by Pytel and Schmeller (2002), voided urine was analyzed in eight patients following intravesically instilled hypericin (for at least 1 h). Even though the number of patients was quite low, hypericin fluorescence was detected in all cases of bladder cancer. On the contrary, Olivo et al. (2003a) and Fu et al. (2007) performed HY-PDD-mediated urine cytology without intravesical instillation of hypericin. In both studies, sediments extracted from patient urine samples were incubated with hypericin in the dark for 15 min and were subsequently analyzed using confocal fluorescence microscopy. The overall fluorescence intensity of the urothelial cells was significantly higher in urine from early-grade TCC than in normal samples, which enabled the differentiation between normal and early bladder cancer specimens (Olivo et al., 2003a). This finding was later confirmed through a diagnostic algorithm (Fu et al., 2007). Moreover, fluorescence was even higher in high-grade tumors than in low-grade tumors (Olivo et al.,

2003a). The results indicate that *ex vivo* fluorescence cytology using hypericin might be a promising diagnostic method for the detection and identification of early and low-grade bladder cancer.

HY-PDD in the Detection of Gliomas

It is well-known that malignant gliomas are tumors with a very poor prognosis and their complete resection significantly improves and extends the survival of patients. Thus, in these cases, the enhancement of the contrast between tumor and surrounding healthy tissue would be very beneficial for surgeons.

In the first *in vivo* study, Noell et al. (2011) (**Table 4**) investigated the accumulation of hypericin in tumors arising from intracerebrally implanted C6 glioma cells, in the zones surrounding the tumors and in healthy brain tissue. Hypericin was injected intravenously and its uptake was maximal 24 h after injection. Considering tissue autofluorescence, the ratios of fluorescence intensities were as follows: tumor:infiltration zone:normal tissue = 19.8:2.5:1.0. Because hypericin accumulation was significantly higher in the tumor than in normal tissue, it could be effectively used as a fluorescence marker for glioma detection (Noell et al., 2011). According to these promising preliminary results, the hypericin-mediated visualization of tumor tissue during its surgical resection was examined in five patients with recurrent glioblastomas (Ritz et al., 2012). Hypericin was injected intravenously 6 h prior to the surgical procedure, which was performed using a neurosurgical microscope under switchable white- and blue-light modes. Malignant tumor tissue (red fluorescence) was clearly distinguishable from the healthy brain tissue (blue color) in all patients and the margins of the tumors showed weaker pink fluorescence. Moreover, specimens were taken for histological evaluation, which was carried out by two neuropathologists and showed 100 and 90% specificity and 91 and 94% sensitivity. The obtained results suggest that HY-PDD is well-tolerated and represents a method that is sufficiently sensitive and specific for the intraoperative visualization of malignant gliomas (Ritz et al., 2012).

Furthermore, time-dependent hypericin uptake was investigated and observed in a subcutaneous glioma mouse model using microendoscopy, an approach that is not designed for microsurgical tumor resection, but is very useful for applications such as the visualization of different tissue compartments, the identification of vessels or the detection of optimal regions for biopsy. To verify the potential to detect intracerebral gliomas using microendoscopy, tumor cells were also implanted into the brain. After craniotomy, hypericin fluorescence was detected in intracerebral and extracranial gliomas and also in the vessels located in the cortical surface of the contralateral hemisphere (Noell et al., 2013) (**Table 4**).

HY-PDD in the Detection and Visualization of Other Types of Malignancies

In addition to the above-mentioned studies, HY-PDD was also examined in mice bearing rhabdomyosarcoma (Urla et al., 2015)

and in patients with various types of head and neck cancer (Thong et al., 2009, 2012; Abbaci et al., 2015) (**Tables 3, 4**).

Similarly to bladder cancer, lesions in the oral cavity are conventionally diagnosed using WLE and histopathology. However, the results obtained by Thong et al. (2009) demonstrate the great potential of hypericin for the diagnosis of various oral cancer types (hyperplasia, cellular pleomorphic adenoma of the palate, dysplasia, SCC). After oral rinsing with hypericin solution (over 30 min), FE was performed and the captured images were analyzed using several parameters. Firstly, the selective uptake of hypericin in tumor tissue was confirmed. Moreover, an increase in the red-to-blue fluorescence intensity ratio was evaluated from normal tissue (0.3) to hyperplasia (1.0) to SCC (2.0), which makes this parameter suitable for distinguishing between these tissue types with high specificity and sensitivity (over 90%) (Thong et al., 2009). Subsequently, the endomicroscopy imaging technique was improved by the same research team (Thong et al., 2012). Preliminary study already suggested that confocal laser endomicroscopy (CLE) might be a potent approach for the surface and subsurface imaging of oral cavity tissues using various fluorescent dyes in both animal and human models (Thong et al., 2007). Recently, a computing system was interfaced to CLE, which enables the 3-D fluorescence visualization of the oral cavity in real-time (Thong et al., 2012). This system could be integrated into current techniques for oral cancer diagnosis and might ultimately lead to better clinical outcomes.

The fluorescent properties of hypericin and four additional fluorescent dyes were also tested for their ability to characterize normal and cancerous head and neck tissue; however, the staining procedure was performed *ex vivo* on fresh samples obtained from head and neck surgeries (glossectomy, pharyngolaryngectomy, laryngectomy, etc.). Hypericin accumulated in the cytoplasm of normal and tumor cells, but was the only fluorescent dye that did not stain the anomalies of keratinization. Thus, the authors conclude that hypericin might not be a suitable photosensitizer for use in such head and neck specimens (Abbaci et al., 2015).

However, more promising *in vivo* results were obtained for intra-operative HY-PDD of rhabdomyosarcoma. In the preclinical study conducted by Urla et al. (2015), mice were injected intraperitoneally with human alveolar rhabdomyosarcoma cells and 3 weeks later, hypericin was administered intravenously. After 24 h, conventional and fluorescence laparoscopy were performed and the tumors were surgically resected using hypericin-mediated red fluorescence as guidance. Tumor specimens were processed for histological analyses. Conventional laparoscopy revealed 24 tumors (ranging in size from 1.6 to 13.5 mm) and 28 tumors were detected only by fluorescence laparoscopy (0.5–11 mm). The results indicate that intraoperative HY-PDD is more sensitive than conventional laparoscopy and can clearly distinguish rhabdomyosarcoma from healthy tissue (Urla et al., 2015). Moreover, the authors inform about clinical trial that will be initiated in children with advanced-stage rhabdomyosarcoma.

HYPERICIN IN DARK CONDITIONS OR THE EFFECTS OF HYPERICIN WITHOUT LIGHT-ACTIVATION

Although hypericin has been extensively studied mainly because of its photodynamic and photocytotoxic properties, it also possesses various positive and negative biological activities without light-activation.

As some *in vitro* studies revealed cytotoxic or growth-inhibitory effects of non-activated hypericin (Blank et al., 2001, 2003; Berlanda et al., 2010; Besic Gyenge et al., 2012) and antiproliferative (Blank et al., 2001) and antimetastatic (Blank et al., 2004) activities *in vivo* and antiangiogenic actions *in vitro* (Martínez-Poveda et al., 2005) have been described, hypericin might also show antitumor potential in the absence of light. Moreover, one clinical study has demonstrated antglioma activity of hypericin in dark conditions (Couldwell et al., 2011). However, the potential use of this natural compound in medicine might be broader. Regarding its avidity to necrotic tissues, the radiolabeled hypericin derivative ($[^{123}\text{I}]$ iodohypericin) can be used for radio-imaging of numerous necrosis-related pathologies (acute myocardial infarction, liver infarction) (Ni et al., 2006; Fonge et al., 2008), including solid tumors (Van de Putte et al., 2012).

On the other hand, hypericin can be associated with a decrease in the chemosensitivity of cancer cells because of its ability to induce the expression of some ATP-binding cassette (ABC) transporters, which are well-known multidrug resistance (MDR) components (Jendželovský et al., 2009; Jendželovská et al., 2014; Kuchárová et al., 2015). In addition, the hypericin-mediated attenuation of the cytotoxicity of some chemotherapeutic agents was demonstrated (Jendželovská et al., 2014).

Non-Activated Hypericin and Its Potential Antitumor Activity

Hypericin-mediated photocytotoxic effects have always been a relevant and attractive issue for researchers in the field of oncology; however, the abilities of hypericin in the absence of light-activation have not been studied as intensively. Although several studies indicate that hypericin might possess some anticancer activities even in dark conditions (Table 5).

It has been found that non-activated hypericin possesses no cytotoxicity toward various cancer cell lines at concentrations sufficient for its photocytotoxic action (Thomas and Pardini, 1992; Hadjur et al., 1996; Vandebogaerde et al., 1997). However, some *in vitro* studies have shown that hypericin can act as a cytotoxic or antiproliferative agent even in the dark (Blank et al., 2001, 2003; Berlanda et al., 2010; Besic Gyenge et al., 2012). The presence or absence of these effects often strongly depends on the hypericin concentration (higher concentrations are required than for HY-PDT-mediated toxicity), treatment conditions, the applied experimental methods, as well as on the type, origin and sensitivity of cancer cells. Moreover, most *in vitro* studies have tested the cytotoxicity of non-activated hypericin following its single dose or during relatively short time intervals; however, the

situation after multiple fractionated hypericin dosages or during a long-term investigation might be completely different.

Firstly, Blank et al. (2001) demonstrated the cytotoxic and antiproliferative effect of non-activated hypericin both *in vitro* and *in vivo*. Hypericin significantly decreased the viability of highly metastatic murine breast adenocarcinoma (DA3^{HI}) and SCC (SQ2) cells. Moreover, the anticancer potential of hypericin was observed even *in vivo* in DA3^{HI}- and SQ2-derived tumors. Even though hypericin slightly accelerated death in mice with DA3^{HI}-derived tumor development that was very rapid, intraperitoneal hypericin administration (6 declining doses) in other animals led to the inhibition of tumor growth, which was accompanied by prolonged survival time. Moreover, the hypericin-mediated improvement of survival was also evident in mice with high-grade SCC tumors (Blank et al., 2001). Subsequently, Blank et al. (2004) examined the antimetastatic potential of non-activated hypericin and evaluated its influence on long-term survival (up to 300 days). Again, mice with breast adenocarcinoma or SCC tumors, which develop metastases predominantly in the lungs, were used as experimental models. To evaluate the impact of hypericin only on metastases, primary tumors were surgically excised at a stage when micrometastases already existed. Hypericin was administered intraperitoneally in multiple declining dosages (up to 6 doses of hypericin at 5-day intervals). In both cases of tumor origin, hypericin therapy together with the resection of primary tumors resulted in a significant increase in long-term animal survival compared to the untreated control or to those animals that received surgery alone. Moreover, the complete destruction of several, but not all lung metastases, was evident 72 h after hypericin treatment. The results indicate that a single hypericin dose was insufficient to prolong the survival of animals, but fractionated hypericin doses could prevent animal death when administered shortly after the resection of the primary tumor (Blank et al., 2004). Similarly, multiple hypericin doses were applied in a previous study to obtain positive anticancer therapeutic results (Blank et al., 2001).

Considering the potential of hypericin to destroy metastases (Blank et al., 2004), the results are consistent with previous *in vitro* findings, where a decrease in the viability of DA-3^{HI} and SQ2 cells was also evident 72 h after treatment (Blank et al., 2001). However, no hypericin-mediated induction of apoptosis in the dark was observed. The inhibition of DNA synthesis indicated that the anticancer action of non-activated hypericin in these cell lines was more cytostatic than cytotoxic (Blank et al., 2001). Nevertheless, another *in vitro* experiment conducted by the same research group established mitotic cell death as the mechanism of hypericin-mediated cytotoxicity. Hypericin was responsible for the enhanced ubiquitinylation of the Hsp90 chaperone, resulting in the destabilization of its client proteins engaged in the regulation of cell proliferation, including p53, Cdk4, Plk, and Raf-1. Ultimately, cytostasis and a decrease in cell viability with no apoptosis were observed. Mitotic cell death is generally characterized by cell-cycle arrest in the G2/M phase, increased cell volume and multinucleation. All these phenotypes were evident in DA3 and SQ2 cells and even in B16.F10 melanoma cells after hypericin treatment (Blank et al., 2003). Thus, mitotic

TABLE 5 | Anticancer effects of hypericin in dark conditions.

Experimental model	Hypericin doses and administration	Effects of non-activated hypericin	References
IN VITRO STUDIES			
Murine breast adenocarcinoma cell line (DA3)	0.065–10 µM (24 h), 0.2–20 µM (72 h), 0.6 and 6 µM	Mild decrease in cell viability detected by MTT assay (24 h, SQ2 cells), Significant decrease in cell viability detected by Hemacolor assay (72 h), Decrease in DNA synthesis detected by ³ H-thymidine incorporation (72 h)	Blank et al., 2001
Murine anaplastic SCC cell line (SQ2)			
Murine melanoma cell line (B16.F10)	1–40 µM	Cytostasis detected by BrdU incorporation assay (72 h; doses ≤ 10 µM), Reduced cell viability detected by Hemacolor assay (72 h; doses > 10 µM); G2/M cell cycle arrest, formation of enlarged polynucleated cells and no evidence of apoptosis indicating mitotic cell death; enhanced ubiquitinylation of Hsp90 resulting in increased destabilization of its client proteins (p53, Cdk4, Plk, Raf-1)	Blank et al., 2003
Bovine aorta endothelial cells (BAE)	Range of concentrations, 5, 10 or 20 µM	Inhibition of some key steps of angiogenesis (decrease in urokinase extracellular level; inhibition of: endothelial cells proliferation, endothelial tube formation, migration and invasive capability of endothelial cells)	Martínez-Poveda et al., 2005
Human epidermoid carcinoma cell line (A431)	Range of concentrations (up to 100 µM)	Antiproliferative and/or cytotoxic effect detected by MTT assay (concentrations higher than 3.13 µM)	Berlanda et al., 2010
Human head and neck SCC carcinoma cell lines (UMB-SCC 745, UMB-SCC 969)	0.6–10 µg/ml	Antiproliferative effect detected by BrdU cell proliferation assay (all applied concentrations), no influence on RNA integrity, initial DNA damage (recovered after 3 h)	Besic Gyenge et al., 2012
IN VIVO STUDIES			
Balb/c mice/Murine breast carcinoma (DA3)	200, 100 and 50 µM; intraperitoneal injection	Reduced volume of DA3-derived tumors (66% at 20 days after beginning of treatment), prolonged survival time (both DA3 and SQ2 models)	Blank et al., 2001
Murine SCC (SQ2)			
	5, 2.5, and 1.25 mg/kg, 10 mg/kg; intraperitoneal injection	Increase in long-term (300 days) animal survival (together with surgery), complete destruction of several DA3-derived metastatic foci in lungs (10 mg/kg, 72 h)	Blank et al., 2004
CLINICAL STUDIES			
Glioblastoma (35 patients)	0.05–0.50 mg/kg; oral administration	Stabilization or slight reduction of tumor volume (7 of 42 patients = 17%), partial clinical response (> 50% tumor reduction; 2 of 42 patients = 2%), mild adverse effects (photosensitivity, erythema, vomiting, diarrhea, etc.)	Couldwell et al., 2011
Anaplastic astrocytoma (7 patients)			

BrdU, 5-bromo-2'-deoxyuridine; MTT, 3-(4,5-dimethylthiazol-2-yl)-2,5-diphenyltetrazolium bromide; SCC, squamous cell carcinoma.

cell death might participate in the tumoricidal and antimetastatic functions of hypericin in the absence of light.

Martínez-Poveda et al. (2005) described another mechanism that might be implicated in the anticancer effects of hypericin in the dark. The results of several *in vitro* assays indicated that hypericin can inhibit several key steps of angiogenesis, including the proliferation, migration and invasion of endothelial cells, extracellular matrix-degrading urokinase or tubular formation on Matrigel (Martínez-Poveda et al., 2005). All these effects might be beneficial in the prevention of tumor neovascularization.

To our knowledge, one clinical trial has investigated the impact of hypericin on recurrent malignant gliomas (anaplastic astrocytoma and glioblastoma) and has monitored the tolerance

of the patients to this treatment. Hypericin was administered orally at gradually increasing dosages ranging from 0.05 to 0.5 mg/kg (once each morning for up to 3 months) and was well-tolerated (mean maximum tolerated daily dose of 0.40 ± 0.098 mg/kg), although some mild skin or gastrointestinal side effects were observed. More importantly, hypericin stabilized or slightly reduced tumor volume (in seven out of 42 patients). In addition, a partial response (>50% reduction of tumor volume) was observed in two patients (Couldwell et al., 2011). These results indicate that synthetic orally administered hypericin can be moderately effective as an adjuvant therapy in cases of malignant glioma; however, further clinical studies are required.

Hypericin as a Necrosis-Avid Agent in Oncology

In addition to its preferential accumulation in tumors compared to in normal healthy tissue, hypericin also has a specific strong affinity toward necrotic tissue (Van de Putte et al., 2008a,b,c). The mechanisms of this phenomenon have not yet been fully elucidated; although some hypotheses already exist that consider the binding of hypericin to specific constituents in the necrotic space. Several radiolabeled hypericin derivatives, particularly [¹²³I]iodohypericin (Fonge et al., 2007) and [¹³¹I]iodohypericin (Li et al., 2011), possess similar necrosis avidity; thus, hypericin can be used as a potent necrosis-avid contrast agent (NACA) for the non-invasive detection and imaging of various necrosis-related pathologies and diseases or to assess tissue viability and therapeutic responses. Moreover, iodohypericins as NACAs might also be effective in relatively new approaches that combine both tumor diagnosis and therapy, so-called “theranostic” modalities (Table 6).

In a few initial *in vivo* studies, hypericin was investigated as a potential indicator of therapeutic responses, following various necrosis-inducing anticancer treatments. Mice bearing intrahepatic fibrosarcoma tumors were used as an experimental model and hypericin was injected intravenously 1 h before, or 24 h after intratumoral ethanol injection (Van de Putte et al., 2008b) or radiofrequency ablation (Van de Putte et al., 2008c), which both induced tumor necrosis. Fluoromicroscopic and fluoromicroscopic examinations confirmed that hypericin accumulated preferentially in necrotic tissue. In the cases of necrosis, mean fluorescence densities were about 4.5- and 5-fold higher than in viable tumor tissue and 14- and 12-fold higher than in normal liver tissue. These results demonstrate the ability of hypericin to enhance the imaging contrast between necrotic and viable tissues and ultimately, its potential role in the early assessment of the therapeutic response (Van de Putte et al., 2008b,c). At about the same time, tumor uptake of radiolabeled hypericin (mono-[¹²³I]iodohypericin) and protohypericin (mono-[¹²³I]iodoprotohypericin) derivatives were tested and compared, because of the applicability of tomographic imaging techniques instead of fluorescence-based techniques. Radioactivity was measured using a gamma counter. Both radiolabeled compounds were retained by the tumors, but mono-[¹²³I]iodohypericin appeared to be a more suitable tumor diagnostic agent, due to its faster clearance from healthy organs (Fonge et al., 2007). Another radiolabeled derivate, ⁶⁴Cu-bis-DOTA-hypericin, was also applicable in the early determination of the therapeutic response as its accumulation was significantly lower in non-treated tumors than in those treated by photothermal ablation therapy, inducing necrosis (Song et al., 2011).

As necrotic tissue represents 30–80% of the solid tumor mass and is rarely present in normal healthy tissue and organs, it is a suitable target not only for cancer diagnosis, but also for anticancer therapy. The strong avidity of iodohypericins for necrotic tissue makes these compounds very potent in the imaging of tumor necrosis. Furthermore, as hypericin can persist in necrotic tumor areas much longer (up to 72 h) than in

viable tumor tissue (up to 24 h) (Van de Putte et al., 2012), its radiolabeled derivatives could be also used for so-called tumor necrosis therapy (TNT). This therapy is based on the destruction of adjacent viable tumor cells by the deposition and accumulation of radiation energy. In other words, attached radioactive iodine “bombards” the neighboring living tumor cells with radiation. Each successive treatment kills more tumor cells, thus, increasing the necrotic region, which allows higher efficacy with each treatment. As three injections of [¹³¹I]iodohypericin reduced the volume of RIF-1-derived tumors, this radiolabeled derivate might have potential in TNT (Van de Putte et al., 2012). In addition, similar results, especially the intense retention of [¹³¹I]iodohypericin in necrotic tumor tissue (over 168 h) and inhibited tumor growth after a single dose, were obtained by Liu et al. (2015) in mice bearing hepatomas or sarcomas.

Moreover, the approach of a necrosis-based anticancer treatment has been expanded into a dual-targeting theranostic strategy by administering the vascular-disrupting agent prior to the hypericin iododerivate. Firstly, a vascular-disrupting agent, such as combretastatin A4 phosphate (CA4P), targets the tumor microenvironment and subsequently, iodine radioactivity kills residual cancer cells. Several preclinical studies have demonstrated that dual-targeting using CA4P with [¹³¹I]iodohypericin was much more effective than single treatments. A reduced tumor volume, a prolonged tumor doubling time, an increase in radiation-induced cell death and intratumoral necrosis or prolonged survival time were reported in rats bearing liver rhabdomyosarcomas (Li et al., 2011, 2012), in mice bearing fibrosarcomas (Li et al., 2013) and in rabbits with liver and muscular VX2 tumors (Shao et al., 2015). Thus, the dual-targeting theranostic approach appears to be well tolerated and can enhance the therapeutic response, encouraging further development for other preclinical and even clinical applications.

Non-Activated Hypericin and Its Potential Negative Impact on Cancer Treatment

All the above-mentioned preclinical and clinical results suggest that hypericin offers great potential in tumor diagnosis as well as in anticancer therapy. However, this secondary metabolite might also cause some other effects that would not be beneficial for therapeutic outcomes. It is well-known that the efficacy of commonly used anticancer treatment modalities is often limited by intrinsic or acquired MDR—a multifactorial phenomenon of the increased tolerance of cancer cells to various tumoricidal agents. A number of cellular mechanisms can contribute to MDR (reviewed in Stavrovskaya, 2000; Zahreddine and Borden, 2013), including the increased elimination of anticancer drugs by tumor cells, which is mostly linked to the elevated expression and/or activity of several ABC transporters. It has been shown that non-activated hypericin can modulate some of these efflux pumps. *In vitro* experiments conducted by our research group (Jendželovský et al., 2009; Jendželovská et al., 2014; Kuchárová et al., 2015) have revealed an increased expression of multidrug resistance-associated protein 1 (MRP1) and breast cancer resistance protein (BCRP) in colorectal HT-29 cells or in ovarian A2780 and A2780cis cells following hypericin treatment

TABLE 6 | Preclinical *in vivo* studies to test hypericin as a necrosis-avid agent.

Experimental model/Type of tumor (cell line)	Hypericin derivate	Detection method	Effects	References
C3H mice/Fibrosarcoma (RIF-1)	[¹²³ I]MIH	Gamma counter	Retention by the tumors and rapid clearance from healthy organs (faster clearance than [¹²³ I]protoH)	Fonge et al., 2007
C3H/Km mice/Fibrosarcoma (RIF-1)	hypericin	FM imaging	Accumulation in intratumoral necrosis (4 h after administration)	Van de Putte et al., 2008a
		UV ₃₆₅ and Tungsten light, FM imaging	Preferential accumulation in intratumoral necrosis (intratumoral necrosis > viable tumor > normal liver tissue), enhanced contrast between necrotic and viable tissue = early assessment of therapeutic response (diagnosis)	Van de Putte et al., 2008b,c
Nude mice/Mammary cancer (BT474)	⁶⁴ CuBDH	PET, autoradiography	Higher accumulation in treated than in non-treated tumors = assessment of therapeutic response (diagnosis)	Song et al., 2011
Balb/c mice/Fibrosarcoma (RIF-1)	hypericin, [¹²³ I]MIH, [¹³¹ I]MIH	FM, PET, autoradiography, scintigraphy	Longer persistence of tracers in necrotic than in viable tumor, stabilization of tumor growth and reduced tumor volume (3 injections of [¹³¹ I]MIH) = potential in TNT	Van de Putte et al., 2012
WAG/Rij rats/Rhabdomyosarcoma (R1)	[¹³¹ I]MIH	MRI, CT scan, scintigraphy, Gamma counter, autoradiography	Reduced tumor volume, prolonged tumor doubling time and inhibited tumor regrowth (dual-targeting with CA4P)	Li et al., 2011
	[¹²³ I]MIH, [¹³¹ I]MIH		Accumulation in intratumoral necrosis (¹²³ I)MIH); reduced tumor volume, prolonged tumor doubling time and increased intratumoral necrosis = tumoricidal effect (dual-targeting - [¹³¹ I]MIH with CA4P)	Li et al., 2012
SCID mice/Fibrosarcoma (RIF-1)	[¹³¹ I]MIH	MRI, scintiscan, autoradiography	Accumulation in intratumoral necrosis (over 120 h); prolonged survival time, marked radiation-induced cell death, reduced tumor volume, prolonged tumor doubling time (dual-targeting with CA4P)	Li et al., 2013
New Zealand white rabbits/VX2 tumors	[¹³¹ I]MIH	MRI, SPECT, autoradiography	High targetability to tumor necrosis; reduced tumor growth and prolonged tumor doubling time (dual-targeting with CA4P)	Shao et al., 2015
Kunming (KM) mice/Hepatoma (H22) Sarcoma (S180)	[¹³¹ I]MIH	FM, SPECT, autoradiography	Prolonged retention by the tumors, limited systemic toxicity, tumor growth delay = therapeutic efficacy	Liu et al., 2015

[¹²³I]MIH, mono-[¹²³I]iodohypericin; [¹²³I]protoH, mono-[¹²³I]iodoprotopyericin; [¹³¹I]MIH, mono-[¹³¹I]iodohypericin; ⁶⁴CuBDH, ⁶⁴Cu-bis-DOTA-hypericin; CA4P, combretastatin A4 phosphate; CT, computed tomography; FM, fluorescence microscopy; MRI, magnetic resonance imaging; PET, positron emission tomography; SPECT, single-photon emission computed tomography; TNT, tumor necrosis therapy.

in the dark. In A2780 and A2780cis cells, 0.5 μM hypericin elevated MRP1 protein levels already 6 h after the treatment (Jendželovská et al., 2014). For HT-29 cells, an even lower hypericin concentration (0.1 μM) was sufficient to increase MRP1 and BCRP expression (16 h after hypericin addition) (Jendželovský et al., 2009; Kuchárová et al., 2015). Therefore, because many chemotherapeutic agents and photosensitizers are substrates of the above-mentioned transporters (reviewed in Nies et al., 2007; Robey et al., 2007), the hypericin-mediated stimulation of efflux systems might lead to a decrease in the efficacy of these therapeutic approaches when they are applied at the same time or shortly following hypericin treatment.

Wada et al. (2002) evaluated the impact of hypericin on the action of several anticancer drugs, using the cervical HeLa cell line and its resistant subline Hvr100-6 that overexpress another MDR-related ABC transporter, P-glycoprotein (P-gp), but no effect was observed. Several studies suggest that hypericin can neither modulate P-gp expression nor its activity (Wada et al., 2002; Tian et al., 2005; Jendželovský et al., 2009), which explains its poor ability to influence the cytotoxicity and transport of P-gp substrates, such as paclitaxel, daunorubicin, doxorubicin or vinblastin (Wada et al., 2002). On the other hand, 24 h pre-treatment with hypericin resulted in the attenuation of mitoxantrone cytotoxicity in HL-60 cells and cisplatin cytotoxicity in sensitive A2780 and resistant A2780cis cells

(Jendželovská et al., 2014). However, this effect was probably not caused by modulation of the analyzed ABC transporters. However, the results suggest that hypericin in the dark might have a negative impact on the onset or progress of cell death induced by some anticancer agents, possibly by affecting some other mechanisms. Further studies are required, to elucidate the specific mechanisms responsible for the above-mentioned changes and *in vivo* studies will be necessary to verify the impact of non-activated hypericin on the outcome of chemotherapy.

Moreover, some MDR mechanisms, including ABC transporters, are also involved in drug pharmacokinetics. The modulation of these mechanisms can affect the absorption, distribution or clearance and ultimately, the action of the administered xenobiotics, resulting in negative drug interactions. Several clinical trials have demonstrated the interactions between some chemotherapeutic agents and St. John's wort extract, which is often taken by oncological patients as an antidepressant. In the first study, the enhanced metabolism of irinotecan and consequently, decreased plasma levels of its active metabolite (SN-38) were evaluated in cancer patients following St. John's wort treatment (Mathijssen et al., 2002). Furthermore, Frye et al. (2004) and Smith et al. (2004) examined the effect of St. John's wort extract on the pharmacokinetics of imatinib mesylate in healthy adult volunteers. In both studies, imatinib was administered before and after the treatment with St. John's wort (300 mg three times daily for 2 weeks) and its clearance and half-life was significantly increased or decreased, respectively, by the herb extract. Similar results were obtained by Goey et al. (2014) using a similar experimental design. Besides the enhanced clearance and decreased plasma concentrations of docetaxel in cancer patients, St. John's wort lowered the incidence of docetaxel-mediated toxicities. Thus, due to the risk of potential undertreatment, combining anticancer therapeutic approaches with St. John's wort extracts should not be recommended to oncological patients.

The probable reason for these effects is the induction of the metabolic enzyme (CYP3A4) and/or the P-gp transporter by hyperforin (Komoroski et al., 2004; Tian et al., 2005), another St. John's wort metabolite. However, considering the potential of hypericin to induce the expression of some ABC efflux pumps, this secondary metabolite might also contribute to negative drug interactions with St. John's wort. Therefore, a much broader spectrum of antineoplastic drugs might exist, including various chemotherapeutic agents or photosensitizers, whose action might be altered due to the presence of hypericin.

REFERENCES

- Abbaci, M., Casiraghi, O., Temam, S., Ferchiou, M., Bosq, J., Dartigues, P., et al. (2015). Red and far-red fluorescent dyes for the characterization of head and neck cancer at the cellular level. *J. Oral Pathol. Med.* 44, 831–841. doi: 10.1111/jop.12316
- Agostinis, P., Berg, K., Cengel, K. A., Foster, T. H., Girotti, A. W., Gollnick, S. O., et al. (2011). Photodynamic therapy of cancer: an update. *CA Cancer J. Clin.* 61, 250–281. doi: 10.3322/caac.20114
- Agostinis, P., Vantieghem, A., Merlevede, W., and de Witte, P. A. (2002). Hypericin in cancer treatment: more light on the way. *Int. J. Biochem. Cell Biol.* 34, 221–241. doi: 10.1016/S1357-2725(01)00126-1
- Alecu, M., Ursaciuc, C., Hălălău, F., Coman, G., Merlevede, W., Waelkens, E., et al. (1998). Photodynamic treatment of basal cell carcinoma and squamous cell carcinoma with hypericin. *Cancer Res.* 18, 4651–4654.
- Ali, S. M., and Olivo, M. (2002). Bio-distribution and subcellular localization of Hypericin and its role in PDT induced apoptosis in cancer cells. *Int. J. Oncol.* 21, 531–540. doi: 10.3892/ijo.21.3.531

SUMMARY

In this review, we have summarized the medicinal applications of light-activated and non-activated hypericin in the field of oncology. We have preferentially highlighted the “primary beneficial side” of this secondary metabolite concerning its anticancer potential, but have also outlined its “second non-beneficial side,” which was revealed by preliminary *in vitro* studies.

The vast majority of the results summarized here suggest that hypericin in light and dark conditions might be a very potent agent in cancer treatment and diagnosis. Besides the well-known and intensively investigated HY-PDT and HY-PDD, some new and promising approaches using hypericin as NACA are becoming the focus of various research groups. Moreover, some tested modalities, including dual-targeting, might even improve the clinical outcome of cancer treatments. However, in the dark, hypericin might be responsible for the limited efficacy of conventionally applied chemotherapy or even PDT, due to its ability to induce the expression of some ABC transporters. Moreover, there is a suspicion that non-activated hypericin possesses much broader biological activity. Thus, the chronic usage of St. John's wort extracts as an antidepressant by oncological patients undergoing anticancer treatment should be avoided.

AUTHOR CONTRIBUTIONS

ZJ designed the concept and issue of the review, studied the literature, contributed to all chapters and summarized the bulk of the text, revised the text after it was completed and also following English revision and approved the final version. RJ discussed the concept of the review with first author, studied the literature and contributed to the chapters about HY-PDT and non-activated hypericin, revised the text and approved the final version. BK studied the literature and contributed to the chapters about HY-PDT and non-activated hypericin, revised the text and approved the final version. PF discussed the concept of the review with first author, revised the text and approved the final version.

ACKNOWLEDGMENTS

This work was supported by the Slovak Research and Development Agency under contract No. APVV-14-0154 and the Scientific Grant Agency of the Ministry of Education of the Slovak Republic under contract No. VEGA 1/0147/15.

- Ayan, A. K., Cirak, C., Kevseroglu, K., and Ozen, T. (2004). Hypericin in some *Hypericum* species from Turkey. *Asian J. Plant Sci.* 3, 200–202. doi: 10.3923/ajps.2004.200.202
- Berlanda, J., Kiesslich, T., Engelhardt, V., Krammer, B., and Plaetzer, K. (2010). Comparative *in vitro* study on the characteristics of different photosensitizers employed in PDT. *J. Photochem. Photobiol. B. Biol.* 100, 173–180. doi: 10.1016/j.jphotobiol.2010.06.004
- Besic Gyenge, E., Forny, P., Lüscher, D., Laass, A., Walt, H., and Maake, C. (2012). Effects of hypericin and a chlorin based photosensitizer alone or in combination in squamous cell carcinoma cells in the dark. *Photodiagnosis Photodyn. Ther.* 9, 321–331. doi: 10.1016/j.pdpt.2012.03.006
- Bhuvaneswari, R., Gan, Y. Y., Lucky, S. S., Chin, W. W., Ali, S. M., Soo, K. C., et al. (2008). Molecular profiling of angiogenesis in hypericin mediated photodynamic therapy. *Mol. Cancer.* 7:56. doi: 10.1186/1476-4598-7-56
- Bhuvaneswari, R., Thong, P. S., Gan, Y. Y., Soo, K. C., and Olivo, M. (2010). Evaluation of hypericin-mediated photodynamic therapy in combination with angiogenesis inhibitor bevacizumab using *in vivo* fluorescence confocal endomicroscopy. *J. Biomed. Opt.* 15:011114. doi: 10.1117/1.3281671
- Bhuvaneswari, R., Yuen, G. Y., Chee, S. K., and Olivo, M. (2011). Antiangiogenesis agents avastin and erbitux enhance the efficacy of photodynamic therapy in a murine bladder tumor model. *Lasers Surg. Med.* 43, 651–662. doi: 10.1002/lsm.21109
- Blank, M., Kostenich, G., Lavie, G., Kimel, S., Keisari, Y., and Orenstein, A. (2002). Wavelength-dependent properties of photodynamic therapy using hypericin *in vitro* and in an animal model. *Photochem. Photobiol.* 76, 335–340. doi: 10.1562/0031-8655(2002)0760335WDPPT2.0.CO2
- Blank, M., Lavie, G., Mandel, M., Hazan, S., Orenstein, A., Meruelo, D., et al. (2004). Antimetastatic activity of the photodynamic agent hypericin in the dark. *Int. J. Cancer.* 111, 596–603. doi: 10.1002/ijc.20285
- Blank, M., Mandel, M., Hazan, S., Keisari, Y., and Lavie, G. (2001). Anti-cancer activities of hypericin in the dark. *Photochem. Photobiol.* 74, 120–125. doi: 10.1562/0031-8655(2001)0740120ACAOH12.0.CO2
- Blank, M., Mandel, M., Keisari, Y., Meruelo, D., and Lavie, G. (2003). Enhanced ubiquitylation of heat shock protein 90 as a potential mechanism for mitotic cell death in cancer cells induced with hypericin. *Cancer Res.* 63, 8241–8247.
- Bobrov, N., Cavarga, I., Longauer, F., Rybárová, S., Fedorocko, P., Brezání, P., et al. (2007). Histomorphological changes in murine fibrosarcoma after hypericin-based photodynamic therapy. *Phytomedicine* 14, 172–178. doi: 10.1016/j.phymed.2006.09.017
- Boiy, A., Roelandts, R., and de Witte, P. A. (2010). Photodynamic therapy using topically applied hypericin: comparative effect with methyl-aminolevulinic acid on UV induced skin tumours. *J. Photochem. Photobiol. B. Biol.* 102, 123–131. doi: 10.1016/j.jphotobiol.2010.09.012
- Brockmann, H., Haschad, M. N., Maier, K., and Pohl, F. (1939). Über das Hypericin, den photodynamisch wirksamen Farbstoff aus *Hypericum perforatum*. *Naturwissenschaften* 27, 550. doi: 10.1007/BF01495453
- Bruňáková, K., Petrijová, L., Zámečník, J., Turecková, V., and Čellárová, E. (2015). The role of ABA in the freezing injury avoidance in two *Hypericum* species differing in frost tolerance and potential to synthesize hypericins. *Plant Cell Tissue Organ Cult.* 122, 45–56. doi: 10.1007/s11240-015-0748-9
- Buytaert, E., Callewaert, G., Hendrickx, N., Scorrano, L., Hartmann, D., Missiaen, L., et al. (2006). Role of endoplasmic reticulum depletion and multidomain proapoptotic BAX and BAK proteins in shaping cell death after hypericin-mediated photodynamic therapy. *FASEB J.* 20, 756–758. doi: 10.1096/fj.05-4305fje
- Cavarga, I., Brezání, P., Čekanová-Figurová, M., Solár, P., and Fedorocko, P., Miskovský, P. (2001). Photodynamic therapy of murine fibrosarcoma with topical and systemic administration of hypericin. *Phytomedicine* 8, 325–330. doi: 10.1017/0944-7113-00057
- Cavarga, I., Brezání, P., Fedorocko, P., Miskovský, P., and Bobrov, N., Longauer, F., et al. (2005). Photoinduced antitumour effect of hypericin can be enhanced by fractionated dosing. *Phytomedicine* 12, 680–683. doi: 10.1016/j.phymed.2004.02.011
- Čellárová, E. (2011). "Effect of exogenous morphogenetic signals on differentiation *in vitro* and secondary metabolite formation in the genus *Hypericum*," in *Medicinal and Aromatic Plant Science and Biotechnology 5 (Special Issue 1)*, eds M. S. Odabas and C. Çirak (Ikenobe: Global Science Books), 62–69.
- Čellárová, E., Brutovská, R., Daxnerová, Z., Bruňáková, K., and Weigel, R. C. (1997). Correlation between hypericin content and the ploidy of somaclones of *Hypericum perforatum* L. *Acta Biotechnol.* 17, 83–90. doi: 10.1002/abio.370170111
- Chen, B., and de Witte, P. A. (2000). Photodynamic therapy efficacy and tissue distribution of hypericin in a mouse P388 lymphoma tumor model. *Cancer Lett.* 150, 111–117. doi: 10.1016/S0304-3835(99)00381-X
- Chen, B., Roskams, T., and de Witte, P. A. (2002a). Antivascular tumor eradication by hypericin-mediated photodynamic therapy. *Photochem. Photobiol.* 76, 509–513. doi: 10.1562/0031-8655(2002)0760509ATEBHM2.0.CO2
- Chen, B., Roskams, T., Xu, Y., Agostinis, P., and de Witte, P. A. (2002b). Photodynamic therapy with hypericin induces vascular damage and apoptosis in the RIF-1 mouse tumor model. *Int. J. Cancer.* 98, 284–290. doi: 10.1002/ijc.10175
- Chen, B., Xu, Y., Roskams, T., Delaey, E., Agostinis, P., Vandenheede, J. R., et al. (2001). Efficacy of antitumoral photodynamic therapy with hypericin: relationship between biodistribution and photodynamic effects in the RIF-1 mouse tumor model. *Int. J. Cancer.* 93, 275–282. doi: 10.1002/ijc.1324
- Cole, C. D., Liu, J. K., Sheng, X., Chin, S. S., Schmidt, M. H., Weiss, M. H., et al. (2008). Hypericin-mediated photodynamic therapy of pituitary tumors: preclinical study in a GH4C1 rat tumor model. *J. Neurooncol.* 87, 255–261. doi: 10.1007/s11060-007-9514-0
- Couldwell, W. T., Surnock, A. A., Tobia, A. J., Cabana, B. E., Stillerman, C. B., Forsyth, P. A., et al. (2011). A phase 1/2 study of orally administered synthetic hypericin for treatment of recurrent malignant gliomas. *Cancer* 117, 4905–4915. doi: 10.1002/cncr.26123
- Crnolatac, I., Huygens, A., van Aerstschot, A., Busson, R., Rozenski, J., and de Witte, P. A. (2005). Synthesis, *in vitro* cellular uptake and photo-induced antiproliferative effects of lipophilic hypericin acid derivatives. *Bioorg. Med. Chem.* 13, 6347–6353. doi: 10.1016/j.bmc.2005.09.003
- Delaey, E., Vandenbogaerde, A., Merlevede, W., and de Witte, P. (2000). Photocytotoxicity of hypericin in normoxic and hypoxic conditions. *J. Photochem. Photobiol. B. Biol.* 56, 19–24. doi: 10.1016/S1011-1344(00)00051-8
- Dewick, P. M. (2002). *Medicinal Natural Products: A Biosynthetic Approach*, 2nd Edn. Chichester: John Wiley & Sons Ltd.
- D'Hallewin, M. A., De Witte, P. A., Waelkens, E., Merlevede, W., and Baert, L. (2000). Fluorescence detection of flat bladder carcinoma *in situ* after intravesical instillation of hypericin. *J. Urol.* 164, 349–351. doi: 10.1016/S0022-5347(05)67357-0
- D'Hallewin, M. A., Kamuhawwa, A. R., Roskams, T., De Witte, P. A., and Baert, L. (2002). Hypericin-based fluorescence diagnosis of bladder carcinoma. *BJU Int.* 89, 760–763. doi: 10.1046/j.1464-410X.2002.02690.x
- Diwu, Z., and Lown, J. W. (1993). Photosensitization with anticancer agents. 17. EPR studies of photodynamic action of hypericin: formation of semiquinone radical and activated oxygen species on illumination. *Free Radic. Biol. Med.* 14, 209–215. doi: 10.1016/0891-5849(93)90012-J
- Du, H. Y., Bay, B. H., and Olivo, M. (2003a). Biodistribution and photodynamic therapy with hypericin in a human NPC murine tumor model. *Int. J. Oncol.* 22, 1019–1024. doi: 10.3892/ijo.22.5.1019
- Du, H. Y., Olivo, M., Tan, B. K., and Bay, B. H. (2003b). Hypericin-mediated photodynamic therapy induces lipid peroxidation and necrosis in nasopharyngeal cancer. *Int. J. Oncol.* 23, 1401–1405. doi: 10.3892/ijo.23.5.1401
- Feruszová, J., Imreová, P., Bodnárová, K., Ševčovičová, A., Kyzek, S., Chalupa, I., et al. (2016). Photoactivated hypericin is not genotoxic. *Gen. Physiol. Biophys.* 35, 223–230. doi: 10.4149/gpb_2015045
- Fonge, H., Van de Putte, M., Huyghe, D., Bormans, G., Ni, Y., de Witte, P., et al. (2007). Evaluation of tumor affinity of mono-[¹²³I]iodohypericin and mono-[¹²³I]iodoprotohypericin in a mouse model with a RIF-1 tumor. *Contrast Media Mol. Imaging.* 2, 113–119. doi: 10.1002/cmmi.136
- Fonge, H., Vunckx, K., Wang, H., Feng, Y., Mortelmans, L., Nuyts, J., et al. (2008). Non-invasive detection and quantification of acute myocardial infarction in rabbits using mono-[¹²³I]iodohypericin microSPECT. *Eur. Heart J.* 29, 260–269. doi: 10.1093/eurheartj/ehm588
- Frye, R. F., Fitzgerald, S. M., Lagattuta, T. F., Hruska, M. W., and Egorin, M. J. (2004). Effect of St John's wort on imatinib mesylate pharmacokinetics. *Clin. Pharmacol. Ther.* 76, 323–329. doi: 10.1016/j.clpt.2004.06.007

- Fu, C. Y., Ng, B. K., Razul, S. G., Chin, W. W., Tan, P. H., Lau, W. K., et al. (2007). Fluorescence detection of bladder cancer using urine cytology. *Int. J. Oncol.* 31, 525–530. doi: 10.3892/ijo.31.3.525
- Galanou, M. C., Theodossiou, T. A., Tsiorvas, D., Sideratou, Z., and Paleos, C. M. (2008). Interactive transport, subcellular relocation and enhanced phototoxicity of hypericin encapsulated in guanidinylated liposomes via molecular recognition. *Photochem. Photobiol.* 84, 1073–1083. doi: 10.1111/j.1751-1097.2008.00392.x
- Galluzzi, L., Vacchelli, E., Bravo-San Pedro, J. M., Buqué, A., Senovilla, L., Baracco, E. E., et al. (2014). Classification of current anticancer immunotherapies. *Oncotarget* 5, 12472–12508. doi: 10.18632/oncotarget.2998
- García, I., Ballesta, S., Gilaberte, Y., Rezusta, A., and Pascual, A. (2015). Antimicrobial photodynamic activity of hypericin against methicillin-susceptible and resistant *Staphylococcus aureus* biofilms. *Future Microbiol.* 10, 347–356. doi: 10.2217/fmb.14.114
- Garg, A. D., and Agostinis, P. (2014). ER stress, autophagy and immunogenic cell death in photodynamic therapy-induced anti-cancer immune responses. *Photochem. Photobiol. Sci.* 13, 474–487. doi: 10.1039/c3pp50333j
- Garg, A. D., Elsen, S., Krysko, D. V., Vandenabeele, P., de Witte, P., and Agostinis, P. (2015b). Resistance to anticancer vaccination effect is controlled by a cancer cell-autonomous phenotype that disrupts immunogenic phagocytic removal. *Oncotarget* 6, 26841–26860. doi: 10.18632/oncotarget.4754
- Garg, A. D., Galluzzi, L., Apetoh, L., Baert, T., Birge, R. B., Bravo-San Pedro, J. M., et al. (2015a). Molecular and translational classifications of DAMPs in immunogenic cell death. *Front. Immunol.* 6:588. doi: 10.3389/fimmu.2015.00588
- Garg, A. D., Krysko, D. V., Vandenabeele, P., and Agostinis, P. (2012b). Hypericin-based photodynamic therapy induces surface exposure of damage-associated molecular patterns like HSP70 and calreticulin. *Cancer Immunol. Immunother.* 61, 215–221. doi: 10.1007/s00262-011-1184-2
- Garg, A. D., Krysko, D. V., Vandenabeele, P., and Agostinis, P. (2016). Extracellular ATP and P₂X₇ receptor exert context-specific immunogenic effects after immunogenic cancer cell death. *Cell Death Dis.* 7, e2097. doi: 10.1038/cddis.2015.411
- Garg, A. D., Krysko, D. V., Verfaillie, T., Kaczmarek, A., Ferreira, G. B., Marysael, T., et al. (2012a). A novel pathway combining calreticulin exposure and ATP secretion in immunogenic cancer cell death. *EMBO J.* 31, 1062–1079. doi: 10.1038/embj.2011.497
- Garnica, S., Weiss, M., and Oberwinkler, F. (2003). Morphological and molecular phylogenetic studies in South American *Cortinarius* species. *Mycol. Res.* 107, 1143–1156. doi: 10.1017/S0953756203008414
- Goey, A. K., Meijerman, I., Rosing, H., Marchetti, S., Mergui-Roelvink, M., Keessen, M., et al. (2014). The effect of St John's wort on the pharmacokinetics of docetaxel. *Clin. Pharmacokinet.* 53, 103–110. doi: 10.1007/s40262-013-0102-5
- Gulick, R. M., McAuliffe, V., Holden-Wiltse, J., Crumpacker, C., Liebes, L., Stein, D. S., et al. (1999). Phase I studies of hypericin, the active compound in St. John's Wort, as an antiretroviral agent in HIV-infected adults. AIDS Clinical Trials Group Protocols 150 and 258. *Ann Intern Med.* 130, 510–514. doi: 10.7326/0003-4819-130-6-199903160-00015
- Hadjur, C., Richard, M. J., Parat, M. O., Jardon, P., and Favier, A. (1996). Photodynamic effects of hypericin on lipid peroxidation and antioxidant status in melanoma cells. *Photochem. Photobiol.* 64, 375–381. doi: 10.1111/j.1751-1097.1996.tb02474.x
- Head, C. S., Luu, Q., Sercarz, J., and Saxton, R. (2006). Photodynamic therapy and tumor imaging of hypericin-treated squamous cell carcinoma. *World J. Surg. Oncol.* 4:87. doi: 10.1186/1477-7819-4-87
- Hudson, J. B., Harris, L., and Towers, G. H. (1993). The importance of light in the anti-HIV effect of hypericin. *Antiviral Res.* 20, 173–178. doi: 10.1016/0166-3542(93)90006-5
- Huygens, A., Kamuhabwa, A. R., Van Laethem, A., Roskams, T., Van Cleynenbreugel, B., Van Poppel, H., et al. (2005). Enhancing the photodynamic effect of hypericin in tumour spheroids by fractionated light delivery in combination with hyperoxigenation. *Int. J. Oncol.* 26, 1691–1697. doi: 10.3892/ijo.26.6.1691
- Jacobson, J. M., Feinman, L., Liebes, L., Ostrow, N., Koslowski, V., Tobia, A., et al. (2001). Pharmacokinetics, safety, and antiviral effects of hypericin, a derivative of St. John's wort plant, in patients with chronic hepatitis C virus infection. *Antimicrob. Agents Chemother.* 45, 517–524. doi: 10.1128/AAC.45.2.517-524.2001
- Jendželovská, Z., Jendželovský, R., Hil'ovská, L., Koval', J., Mikeš, J., and Fedoročko, P. (2014). Single pre-treatment with hypericin, a St. John's wort secondary metabolite, attenuates cisplatin- and mitoxantrone-induced cell death in A2780, A2780cis and HL-60 cells. *Toxicol. In vitro* 28, 1259–1273. doi: 10.1016/j.tiv.2014.06.011
- Jendželovský, R., Mikes, J., Koval', J., Soucek, K., Procházková, J., Kello, M., et al. (2009). Drug efflux transporters, MRP1 and BCRP, affect the outcome of hypericin-mediated photodynamic therapy in HT-29 adenocarcinoma cells. *Photochem. Photobiol. Sci.* 8, 1716–1723. doi: 10.1039/b9pp0086k
- Kacerovská, D., Pizinger, K., Majer, F., and Smíd, F. (2008). Photodynamic therapy of nonmelanoma skin cancer with topical *Hypericum perforatum* extract—a pilot study. *Photochem. Photobiol.* 84, 779–785. doi: 10.1111/j.1751-1097.2007.00260.x
- Kamuhabwa, A. A., Cosserat-Gerardin, I., Didelon, J., Notter, D., Guillemin, F., Roskams, T., et al. (2002). Biodistribution of hypericin in orthotopic transitional cell carcinoma bladder tumors: implication for whole bladder wall photodynamic therapy. *Int. J. Cancer.* 97, 253–260. doi: 10.1002/ijc.1594
- Kamuhabwa, A. A., Di Mavungu, J. D., Baert, L., D'Hallewin, M. A., Hoogmartens, J., and de Witte, P. A. (2005). Determination of hypericin in human plasma by high-performance liquid chromatography after intravesical administration in patients with transitional cell carcinoma of the bladder. *Eur. J. Pharm. Biopharm.* 59, 469–474. doi: 10.1016/j.ejpb.2004.09.013
- Kamuhabwa, A. A., Roskams, T., D'Hallewin, M. A., Baert, L., Van Poppel, H., and de Witte, P. A. (2003). Whole bladder wall photodynamic therapy of transitional cell carcinoma rat bladder tumors using intravesically administered hypericin. *Int. J. Cancer.* 107, 460–467. doi: 10.1002/ijc.11396
- Kascakova, S., Nadova, Z., Mateasik, A., Mikes, J., Huntosova, V., Refregiers, M., et al. (2008). High level of low-density lipoprotein receptors enhance hypericin uptake by U-87 MG cells in the presence of LDL. *Photochem. Photobiol.* 84, 120–127. doi: 10.1111/j.1751-1097.2007.00207.x
- Kashef, N., Borghei, Y. S., and Djavid, G. E. (2013). Photodynamic effect of hypericin on the microorganisms and primary human fibroblasts. *Photodiagnosis Photodyn. Ther.* 10, 150–155. doi: 10.1016/j.pdpt.2012.11.007
- Kasper, S., Caraci, F., Forti, B., Drago, F., and Aguglia, E. (2010). Efficacy and tolerability of *Hypericum* extract for the treatment of mild to moderate depression. *Eur. Neuropsychopharmacol.* 20, 747–765. doi: 10.1016/j.euroneuro.2010.07.005
- Kim, M., Jung, H. Y., and Park, H. J. (2015). Topical PDT in the treatment of benign skin diseases: principles and new applications. *Int. J. Mol. Sci.* 16, 23259–23278. doi: 10.3390/ijms161023259
- Kitanov, G. M. (2001). Hypericin and pseudohypericin in some *Hypericum* species. *Biochem. Syst. Ecol.* 29, 171–178. doi: 10.1016/S0305-1978(00)00032-6
- Kleemann, B., Loos, B., Scriba, T. J., Lang, D., and Davids, L. M. (2014). St John's Wort (*Hypericum perforatum L.*) photomedicine: hypericin-photodynamic therapy induces metastatic melanoma cell death. *PLoS ONE* 9:e103762. doi: 10.1371/journal.pone.0103762
- Komoroski, B. J., Zhang, S., Cai, H., Hutzler, J. M., Frye, R., Tracy, T. S., et al. (2004). Induction and inhibition of cytochromes P450 by the St. John's wort constituent hyperforin in human hepatocyte cultures. *Drug Metab. Dispos.* 32, 512–518. doi: 10.1124/dmd.32.5.512
- Koperdáková, J., Komarovská, H., Koštúth, J., Giovannini, A., and Čellárová, E. (2009). Characterization of hairy root-phenotype in transgenic *Hypericum perforatum L.* clones. *Acta Physiol. Plant.* 31, 351–358. doi: 10.1007/s11738-008-0241-8
- Koštúth, J., Koperdáková, J., Tolonen, A., Hohtola, A., and Čellárová, E. (2003). The content of hypericins and phloroglucinols in *Hypericum perforatum L.* seedlings at early stage of development. *Plant Sci.* 165, 515–521. doi: 10.1016/S0168-9452(03)00210-3
- Koval, J., Mikes, J., Jendželovský, R., Kello, M., Solár, P., and Fedoročko, P. (2010). Degradation of HER2 receptor through hypericin-mediated photodynamic therapy. *Photochem. Photobiol.* 86, 200–205. doi: 10.1111/j.1751-1097.2009.00639.x
- Kubin, A., Meissner, P., Wierrani, F., Burner, U., Bodenteich, A., Pytel, A., et al. (2008). Fluorescence diagnosis of bladder cancer with new water

- soluble hypericin bound to polyvinylpyrrolidone: PVP-hypericin. *Photochem. Photobiol.* 84, 1560–1563. doi: 10.1111/j.1751-1097.2008.00384.x
- Kubin, A., Wieranni, F., Burner, U., Alth, G., and Grünberger, W. (2005). Hypericin—the facts about a controversial agent. *Curr. Pharm. Des.* 11, 233–253. doi: 10.2174/1381612053382287
- Kucharikova, A., Kimakova, K., and Janfelt, C., and Čellarova, E. (2016). Interspecific variation in localization of hypericins and phloroglucinols in the genus *Hypericum* as revealed by Desorption Electrospray Ionization Mass Spectrometry imaging. *Physiol Plant.* 157, 2–12. doi: 10.1111/ppl.12422
- Kuchárová, B., Mikeš, J., Jendželovský, R., Vargová, J., Mikešová, L., Jendželovská, Z., et al. (2015). Potentiation of hypericin-mediated photodynamic therapy cytotoxicity by MK-886: focus on ABC transporters, GDF-15 and redox status. *Photodiagnosis Photodyn. Ther.* 12, 490–503. doi: 10.1016/j.pdpt.2015.04.008
- Kusari, S., Lamshöft, M., Zühlke, S., and Spiteller, M. (2008). An endophytic fungus from *Hypericum perforatum* that produces hypericin. *J. Nat. Prod.* 71, 159–162. doi: 10.1021/np070669k
- Kusari, S., Sezgin, S., Nigutová, K., Čellárová, E., and Spiteller, M. (2015). Spatial chemo-profiling of hypericin and related phytochemicals in *Hypericum* species using MALDI-HRMS imaging. *Anal. Bioanal. Chem.* 407, 4779–4791. doi: 10.1007/s00216-015-8682-6
- Kusari, S., Zühlke, S., Koštúth, J., Čellárová, E., and Spiteller, M. (2009). Light-independent metabolomics of endophytic *Thielavia subthermophila* provides insight into microbial hypericin biosynthesis. *J. Nat. Prod.* 72, 1825–1835. doi: 10.1021/np9002977
- Li, J., Cona, M. M., Chen, F., Feng, Y., Zhou, L., Yu, J., et al. (2012). Exploring theranostic potentials of radioiodinated hypericin in rodent necrosis models. *Theranostics* 2, 1010–1019. doi: 10.7150/thno.4924
- Li, J., Cona, M. M., Chen, F., Feng, Y., Zhou, L., Zhang, G., et al. (2013). Sequential systemic administrations of combretastatin A4 Phosphate and radioiodinated hypericin exert synergistic targeted theranostic effects with prolonged survival on SCID mice carrying bifocal tumor xenografts. *Theranostics* 3, 127–137. doi: 10.7150/thno.5790
- Li, J., Sun, Z., Zhang, J., Shao, H., Cona, M. M., Wang, H., et al. (2011). A dual-targeting anticancer approach: soil and seed principle. *Radiology* 260, 799–807. doi: 10.1148/radiol.11102120
- Liu, C. D., Kwan, D., Saxton, R. E., and McFadden, D. W. (2000). Hypericin and photodynamic therapy decreases human pancreatic cancer *in vitro* and *in vivo*. *J. Surg. Res.* 93, 137–143. doi: 10.1006/jsre.2000.5949
- Liu, W., Zhang, D., Feng, Y., Li, Y., Huang, D., Jiang, C., et al. (2015). Biodistribution and anti-tumor efficacy of intratumorally injected necrosis-avid theranostic agent radioiodinated hypericin in rodent tumor models. *J. Drug Target.* 23, 371–379. doi: 10.3109/1061186X.2014.1000337
- Luksienė, Ž., and De Witte, P. (2002). Hypericin-based photodynamic therapy: I. Comparative antitumor activity uptake studies in Ehrlich ascite tumor. *Acta Med Litu.* 9, 195–199.
- Martínez-Poveda, B., Quesada, A. R., and Medina, M. A. (2005). Hypericin in the dark inhibits key steps of angiogenesis *in vitro*. *Eur. J. Pharmacol.* 516, 97–103. doi: 10.1016/j.ejphar.2005.03.047
- Mathijssen, R. H., Verweij, J., de Brujin, P., Loos, W. J., and Sparreboom, A. (2002). Effects of St. John's wort on irinotecan metabolism. *J. Natl. Cancer Inst.* 94, 1247–1249. doi: 10.1093/jnci/94.16.1247
- Miadokova, E., Chalupa, I., Vlčková, V., Sevcovicova, A., Nadova, S., Kopaskova, M., et al. (2010). Genotoxicity and antigenotoxicity evaluation of non-photoactivated hypericin. *Phytother. Res.* 24, 90–95. doi: 10.1002/ptr.2901
- Mikeš, J., Hýdžalová, M., Kočí, L., Jendželovský, R., Koval', J., Vaculová, A., et al. (2011). Lower sensitivity of FHC fetal colon epithelial cells to photodynamic therapy compared to HT-29 colon adenocarcinoma cells despite higher intracellular accumulation of hypericin. *Photochem. Photobiol. Sci.* 10, 626–632. doi: 10.1039/c0pp00359j
- Mikeš, J., Jendželovský, R., and Fedoročko, P. (2013). “Cellular aspects of photodynamic therapy with hypericin,” in *Photodynamic Therapy: New Research*, ed M. L. T. Elsaie (New York, NY: Nova Science Publishers), 111–147.
- Mikeš, J., Kleban, J., Sacková, V., Horváth, V., Jamborová, E., Vaculová, A., et al. (2007). Necrosis predominates in the cell death of human colon adenocarcinoma HT-29 cells treated under variable conditions of photodynamic therapy with hypericin. *Photochem. Photobiol. Sci.* 6, 758–766. doi: 10.1039/B700350A
- Mikeš, J., Koval', J., Jendželovský, R., Sacková, V., Uhrinová, I., Kello, M., et al. (2009). The role of p53 in the efficiency of photodynamic therapy with hypericin and subsequent long-term survival of colon cancer cells. *Photochem. Photobiol. Sci.* 8, 1558–1567. doi: 10.1039/b9pp0021f
- Mikešová, L., Mikeš, J., Koval', J., Gyurászová, K., Culka, L., Vargová, J., et al. (2013). Conjunction of glutathione level, NAD(P)H/FAD redox status and hypericin content as a potential factor affecting colon cancer cell resistance to photodynamic therapy with hypericin. *Photodiagnosis Photodyn. Ther.* 10, 470–483. doi: 10.1016/j.pdpt.2013.04.003
- Ni, Y., Huyghe, D., Verbeke, K., de Witte, P. A., Nuyts, J., Mortelmans, L., et al. (2006). First preclinical evaluation of mono-[123I]iodohypericin as a necrosis-avid tracer agent. *Eur. J. Nucl. Med. Mol. Imaging* 33, 595–601. doi: 10.1007/s00259-005-0013-2
- Nies, A. T., Rius, M., and Keppler, D. (2007). “Multidrug resistance proteins of the ABCC subfamily,” in *Drug Transporters: Molecular Characterization and Role in Drug Disposition*, eds G. You and M. E. Morris (New Jersey, NJ: John Wiley & Sons, Inc.), 223–262.
- Noell, S., Feigl, G. C., Serifi, D., Mayer, D., Naumann, U., Göbel, W., et al. (2013). Microendoscopy for hypericin fluorescence tumor diagnosis in a subcutaneous glioma mouse model. *Photodiagnosis Photodyn. Ther.* 10, 552–560. doi: 10.1016/j.pdpt.2013.06.001
- Noell, S., Mayer, D., Strauss, W. S., Tatagiba, M. S., and Ritz, R. (2011). Selective enrichment of hypericin in malignant glioma: pioneering *in vivo* results. *Int. J. Oncol.* 38, 1343–1348. doi: 10.3892/ijo.2011.1968
- Olivo, M., Lau, W., Manivasager, V., Bhuvaneswari, R., Wei, Z., Soo, K. C., et al. (2003a). Novel photodynamic diagnosis of bladder cancer: *ex vivo* fluorescence cytology using hypericin. *Int. J. Oncol.* 23, 1501–1504. doi: 10.3892/ijo.23.6.1501
- Olivo, M., Lau, W., Manivasager, V., Tan, P. H., Soo, K. C., and Cheng, C. (2003b). Macro-microscopic fluorescence of human bladder cancer using hypericin fluorescence cystoscopy and laser confocal microscopy. *Int. J. Oncol.* 23, 983–990. doi: 10.3892/ijo.23.4.983
- Paz-Cristobal, M. P., Gilaberte, Y., Alejandre, C., Pardo, J., Revillo, M. J., and Rezusta, A. (2014). *In vitro* fungicidal photodynamic effect of hypericin on *Trichophyton* spp. *Mycopathologia* 178, 221–225. doi: 10.1007/s11046-014-9797-6
- Prince, A. M., Pascual, D., Meruelo, D., Liebes, L., Mazur, Y., Dubovi, E., et al. (2000). Strategies for evaluation of enveloped virus inactivation in red cell concentrates using hypericin. *Photochem. Photobiol.* 71, 188–195. doi: 10.1562/0031-8655(2000)0710188SFOEV2.0.CO2
- Pytel, A., and Schmeller, N. (2002). New aspect of photodynamic diagnosis of bladder tumors: fluorescence cytology. *Urology* 59, 216–219. doi: 10.1016/S0090-4295(01)01528-X
- Rezusta, A., López-Chicón, P., Paz-Cristobal, M. P., Alemany-Ribes, M., Royo-Díez, D., Agut, M., et al. (2012). *In vitro* fungicidal photodynamic effect of hypericin on *Candida* species. *Photochem. Photobiol.* 88, 613–619. doi: 10.1111/j.1751-1097.2011.01053.x
- Ritz, R., Daniels, R., Noell, S., Feigl, G. C., Schmidt, V., Bornemann, A., et al. (2012). Hypericin for visualization of high grade gliomas: first clinical experience. *Eur. J. Surg. Oncol.* 38, 352–360. doi: 10.1016/j.ejsco.2011.12.021
- Robey, R. W., Polgar, O., Deeken, J., To, K. K. W., and Bates, S. (2007). “Breast cancer resistance protein,” in *Drug Transporters: Molecular Characterization and Role in Drug Disposition*, eds G. You and M. E. Morris (New Jersey, NJ: John Wiley & Sons, Inc.), 319–358. doi: 10.1002/9780470140505.ch12
- Rook, A. H., Wood, G. S., Duvic, M., Vonderheid, E. C., Tobia, A., and Cabana, B. (2010). A phase II placebo-controlled study of photodynamic therapy with topical hypericin and visible light irradiation in the treatment of cutaneous T-cell lymphoma and psoriasis. *J. Am. Acad. Dermatol.* 63, 984–990. doi: 10.1016/j.jaad.2010.02.039
- Rubio, N., Coupienne, I., Di Valentin, E., Heirman, I., Grooten, J., Piette, J., et al. (2012). Spatiotemporal autophagic degradation of oxidatively damaged organelles after photodynamic stress is amplified by mitochondrial reactive oxygen species. *Autophagy* 8, 1312–1324. doi: 10.4161/auto.20763

- Sacková, V., Fedorocko, P., Szilárdiová, B., Mikes, J., and Kleban, J. (2006). Hypericin-induced photocytotoxicity is connected with G2/M arrest in HT-29 and S-phase arrest in U937 cells. *Photochem. Photobiol.* 82, 1285–1291. doi: 10.1562/2006-02-22-RA-806
- Sanovic, R., Verwanger, T., Hartl, A., and Krammer, B. (2011). Low dose hypericin-PDT induces complete tumor regression in BALB/c mice bearing CT26 colon carcinoma. *Photodiagnosis Photodyn. Ther.* 8, 291–296. doi: 10.1016/j.pdpdt.2011.04.003
- Sattler, S., Schaefer, U., Schneider, W., Hoelzl, J., and Lehr, C. M. (1997). Binding, uptake, and transport of hypericin by Caco-2 cell monolayers. *J. Pharm. Sci.* 86, 1120–1126. doi: 10.1021/jspk.970004a
- Shao, H., Zhang, J., Sun, Z., Chen, F., Dai, X., Li, Y., et al. (2015). Necrosis targeted radiotherapy with iodine-131-labeled hypericin to improve anticancer efficacy of vascular disrupting treatment in rabbit VX2 tumor models. *Oncotarget* 6, 14247–14259. doi: 10.18632/oncotarget.3679
- Siboni, G., Weitman, H., Freeman, D., Mazur, Y., Malik, Z., and Ehrenberg, B. (2002). The correlation between hydrophilicity of hypericins and helianthrone: internalization mechanisms, subcellular distribution and photodynamic action in colon carcinoma cells. *Photochem. Photobiol. Sci.* 1, 483–491. doi: 10.1039/b202884k
- Sim, H. G., Lau, W. K., Olivo, M., Tan, P. H., and Cheng, C. W. (2005). Is photodynamic diagnosis using hypericin better than white-light cystoscopy for detecting superficial bladder carcinoma? *BJU Int.* 95, 1215–1218. doi: 10.1111/j.1464-410X.2005.05508.x
- Smith, P., Bullock, J. M., Booker, B. M., Haas, C. E., Berenson, C. S., and Jusko, W. J. (2004). The influence of St. John's wort on the pharmacokinetics and protein binding of imatinib mesylate. *Pharmacotherapy* 24, 1508–1514. doi: 10.1592/phco.24.16.1508.50958
- Song, S., Xiong, C., Zhou, M., Lu, W., Huang, Q., Ku, G., et al. (2011). Small-animal PET of tumor damage induced by photothermal ablation with 64Cu-bis-DOTA-hypericin. *J. Nucl. Med.* 52, 792–799. doi: 10.2967/jnumed.110.086116
- Stavrovskaya, A. A. (2000). Cellular mechanisms of multidrug resistance of tumor cells. *Biochemistry Mosc.* 65, 95–106.
- Straub, M., Russ, D., Horn, T., Gschwend, J. E., and Abrahamsberg, C. (2015). A phase IIA dose-finding study of PVP-hypericin fluorescence cystoscopy for detection of nonmuscle-invasive bladder cancer. *J. Endourol.* 29, 216–222. doi: 10.1089/end.2014.0282
- Theodossiou, T. A., Hothersall, J. S., De Witte, P. A., Pantos, A., and Agostinis, P. (2009). The multifaceted photocytotoxic profile of hypericin. *Mol. Pharm.* 6, 1775–1789. doi: 10.1021/mp900166q
- Thomas, C., MacGill, R. S., Miller, G. C., and Pardini, R. S. (1992). Photoactivation of hypericin generates singlet oxygen in mitochondria and inhibits succinoxidase. *Photochem. Photobiol.* 55, 47–53. doi: 10.1111/j.1751-1097.1992.tb04208.x
- Thomas, C., and Pardini, R. S. (1992). Oxygen dependence of hypericin-induced phototoxicity to EMT6 mouse mammary carcinoma cells. *Photochem. Photobiol.* 55, 831–837. doi: 10.1111/j.1751-1097.1992.tb08531.x
- Thong, P. S., Kho, K. W., Zheng, W., Harris, M., Soo, K. C., and Olivo, M. (2007). Development of a laser confocal endomicroscope for *in vivo* fluorescence imaging. *J. Mech. Med. Biol.* 7, 11–18. doi: 10.1142/S0219519407002108
- Thong, P. S., Olivo, M., Chin, W. W., Bhuvaneswari, R., Mancer, K., and Soo, K. C. (2009). Clinical application of fluorescence endoscopic imaging using hypericin for the diagnosis of human oral cavity lesions. *Br. J. Cancer.* 101, 1580–1584. doi: 10.1038/sj.bjc.6605357
- Thong, P. S., Tandjung, S. S., Movania, M. M., Chiew, W. M., Olivo, M., Bhuvaneswari, R., et al. (2012). Toward real-time virtual biopsy of oral lesions using confocal laser endomicroscopy interfaced with embedded computing. *J. Biomed. Opt.* 17:056009. doi: 10.1117/1.JBO.17.5.056009
- Thong, P. S., Watt, F., Ren, M. Q., Tan, P. H., Soo, K. C., and Olivo, M. (2006). Hypericin-photodynamic therapy (PDT) using an alternative treatment regime suitable for multi-fraction PDT. *J. Photochem. Photobiol. B. Biol.* 82, 1–8. doi: 10.1016/j.jphotoobiol.2005.08.002
- Tian, R., Koyabu, N., Morimoto, S., Shoyama, Y., Ohtani, H., and Sawada, Y. (2005). Functional induction and de-induction of P-glycoprotein by St. John's wort and its ingredients in a human colon adenocarcinoma cell line. *Drug Metab. Dispos.* 33, 547–554. doi: 10.1124/dmd.104.002485
- Urbanová, M., Košuth, J., and Čellárová, E. (2006). Genetic and biochemical analysis of *Hypericum perforatum* L. plants regenerated after cryopreservation. *Plant Cell Rep.* 25, 140–147. doi: 10.1007/s00299-005-0050-0
- Urla, C., Armeanu-Ebinger, S., Fuchs, J., and Seitz, G. (2015). Successful *in vivo* tumor visualization using fluorescence laparoscopy in a mouse model of disseminated alveolar rhabdomyosarcoma. *Surg. Endosc.* 29, 1105–1114. doi: 10.1007/s00464-014-3770-9
- Vandenbogaerde, A. L., Cuveele, J. F., Proot, P., Himpens, B. E., Merlevede, W. J., and de Witte, P. A. (1997). Differential cytotoxic effects induced after photosensitization by hypericin. *J. Photochem. Photobiol. B. Biol.* 38, 136–142. doi: 10.1016/S1011-1344(96)07446-5
- Vandenbogaerde, A. L., Geboes, K. R., Cuveele, J. F., Agostinis, P. M., Merlevede, W. J., and De Witte, P. A. (1996). Antitumour activity of photosensitized hypericin on A431 cell xenografts. *Anticancer Res.* 16, 1619–1625.
- Vandepitte, J., Van Cleynenbreugel, B., Hettinger, K., Van Poppel, H., and de Witte, P. A. (2010). Biodistribution of PVP-hypericin and hexaminolevulinate-induced PpIX in normal and orthotopic tumor-bearing rat urinary bladder. *Cancer Chemother. Pharmacol.* 67, 775–781. doi: 10.1007/s00280-010-1375-0
- Van de Putte, M., Marysael, T., Fonge, H., Roskams, T., Cona, M. M., Li, J., et al. (2012). Radiolabeled iodohypericin as tumor necrosis avid tracer: diagnostic and therapeutic potential. *Int. J. Cancer.* 131, E129–E137. doi: 10.1002/ijc.26492
- Van de Putte, M., Ni, Y., and De Witte, P. A. (2008a). Exploration of the mechanism underlying the tumor necrosis avidity of hypericin. *Oncol. Rep.* 19, 921–926. doi: 10.3892/or.19.4.921
- Van de Putte, M., Wang, H., Chen, F., de Witte, P. A., and Ni, Y. (2008b). Hypericin as a marker for determination of tissue viability after intratumoral ethanol injection in a murine liver tumor model. *Acad. Radiol.* 15, 107–113. doi: 10.1016/j.acra.2007.08.008
- Van de Putte, M., Wang, H., Chen, F., De Witte, P. A., and Ni, Y. (2008c). Hypericin as a marker for determination of tissue viability after radiofrequency ablation in a murine liver tumor model. *Oncol. Rep.* 19, 927–932. doi: 10.3892/or.19.4.927
- Wada, A., Sakaeda, T., Takara, K., Hirai, M., Kimura, T., Ohmoto, N., et al. (2002). Effects of St John's wort and hypericin on cytotoxicity of anticancer drugs. *Drug Metab. Pharmacokinet.* 17, 467–474. doi: 10.2133/dmpk.17.467
- Wölflé, U., Seelinger, G., and Schempp, C. M. (2014). Topical application of St. John's wort (*Hypericum perforatum*). *Planta Med.* 80, 109–120. doi: 10.1055/s-0033-1351019
- Xie, X., Hudson, J. B., and Guns, E. S. (2001). Tumor-specific and photodependent cytotoxicity of hypericin in the human LNCaP prostate tumor model. *Photochem. Photobiol.* 74, 221–225. doi: 10.1562/0031-8655(2001)0740221TSAPCO2.0.CO2
- Zahreddine, H., and Borden, K. L. (2013). Mechanisms and insights into drug resistance in cancer. *Front. Pharmacol.* 4:28. doi: 10.3389/fphar.2013.00028
- Zheng, Y., Yin, G., Le, V., Zhang, A., Chen, S., Liang, X., et al. (2016). Photodynamic-therapy activates immune response by disrupting immunity homeostasis of tumor cells, which generates vaccine for cancer therapy. *Int. J. Biol. Sci.* 12, 120–132. doi: 10.7150/ijbs.12852
- Zupkó, I., Kamuhabwa, A. R., D'Hallewin, M. A., Baert, L., and De Witte, P. A. (2001). *In vivo* photodynamic activity of hypericin in transitional cell carcinoma bladder tumors. *Int. J. Oncol.* 18, 1099–1105. doi: 10.3892/ijo.18.5.1099
- Conflict of Interest Statement:** The authors declare that the research was conducted in the absence of any commercial or financial relationships that could be construed as a potential conflict of interest.
- Copyright © 2016 Jendželovská, Jendželovský, Kuchárová and Fedoročko. This is an open-access article distributed under the terms of the Creative Commons Attribution License (CC BY). The use, distribution or reproduction in other forums is permitted, provided the original author(s) or licensor are credited and that the original publication in this journal is cited, in accordance with accepted academic practice. No use, distribution or reproduction is permitted which does not comply with these terms.*



Phloroglucinol and Terpenoid Derivatives from *Hypericum cistifolium* and *H. galiooides* (Hypericaceae)

Sara L. Crockett^{1*†}, Olaf Kunert², Eva-Maria Pferschy-Wenzig¹, Melissa Jacob³, Wolfgang Schuehly^{1†} and Rudolf Bauer¹

¹ Department of Pharmacognosy, Institute of Pharmaceutical Sciences, University of Graz, Graz, Austria, ² Department of Pharmaceutical Chemistry, Institute of Pharmaceutical Sciences, University of Graz, Graz, Austria, ³ National Center for Natural Products Research, Research Institute of Pharmaceutical Sciences, School of Pharmacy, University of Mississippi, University, MS, USA

OPEN ACCESS

Edited by:

Eva Cellarova,
Pavol Jozef Safarik University
in Kosice, Slovakia

Reviewed by:

Guolin Zhang,
Chengdu Institute of Biology, China
Souvik Kusari,
Technical University of Dortmund,
Germany

*Correspondence:

Sara L. Crockett
sara.crockett@uni-graz.at

†Present address:

Sara Crockett,
Institute of Systems Sciences,
Innovation and Sustainability
Research, University of Graz, Graz,
Austria;
Wolfgang Schuehly,
Institute of Zoology, University
of Graz, Graz, Austria

Specialty section:

This article was submitted to
Plant Metabolism
and Chemodiversity,
a section of the journal
Frontiers in Plant Science

Received: 10 March 2016

Accepted: 15 June 2016

Published: 04 July 2016

Citation:

Crockett SL, Kunert O, Pferschy-Wenzig E-M, Jacob M, Schuehly W and Bauer R (2016)
Phloroglucinol and Terpenoid Derivatives from *Hypericum cistifolium* and *H. galiooides* (Hypericaceae).
Front. Plant Sci. 7:961.
doi: 10.3389/fpls.2016.00961

A new simple phloroglucinol derivative characterized as 1-(6-hydroxy-2,4-dimethoxyphenyl)-2-methyl-1-propanone (**1**) was isolated from *Hypericum cistifolium* (Hypericaceae) as a major constituent of the non-polar plant extract. Minor amounts of this new compound, in addition to two known structurally related phloroglucinol derivatives (**2** and **3**), and two new terpenoid derivatives characterized, respectively, as 2-benzoyl-3,3-dimethyl-4R,6S-bis-(3-methylbut-2-enyl)-cyclohexanone (**4a**) and 2-benzoyl-3,3-dimethyl-4S,6R-bis-(3-methylbut-2-enyl)-cyclohexanone (**4b**), were isolated from a related species, *H. galiooides* Lam. The chemical structures were established using 2D-NMR spectroscopy and mass spectrometry. These compounds were evaluated *in vitro* for antimicrobial activity against a panel of pathogenic microorganisms and anti-inflammatory activity through inhibition of COX-1, COX-2, and 5-LOX catalyzed LTB₄ formation.

Keywords: *Hypericum*, Hypericaceae, section *Myriandra*, anti-inflammatory, anti-bacterial, phloroglucinol, terpenoid

INTRODUCTION

The genus *Hypericum* L. (St. John's wort, Hypericaceae), one of the 100 largest flowering plant genera worldwide, contains to date 490 species that have been divided into 36 taxonomic sections (Hypericum Online, 2016). More than 50 native species of *Hypericum* occur in North America, of which 29 belong to the taxonomic section *Myriandra* (Sprach) R. Keller (Robson, 2003). These species, which are distributed from eastern Canada southward to Honduras and Barbados and westward to Iowa, all possess clear- to amber-colored punctate glands concentrated on the stem, leaf, sepal and petal margins. Clusters of cells that contain waxy hydrocarbons and the naphthodianthrone pigments (i.e., pseudohypericin and hypericin) and appear as minute, reddish- to black-colored glands are present in many other *Hypericum* species, including the medicinally important species *H. perforatum* L. (common St. John's wort), but are lacking in species of section *Myriandra* (Robson, 1996). A carefully detailed anatomical study of these dark "glands" in *H. perforatum* has been conducted by Ciccarelli et al. (2001). The translucent

Abbreviations: CD, circular dichroism; COSY, correlation spectroscopy; COX, cyclooxygenase; DAD, diode array; DFQ, double quantum-filled; ESI, electrospray ionization; FTIR, fourier transform infrared; HMBC, heteronuclear multiple bond correlation; LOX, lipoxygenase; LTB₄, leukotriene B₄; NOE, nuclear overhauser effect.

glands, meanwhile, have been identified as the accumulation sites of acylphloroglucinol derivatives (i.e., hyperforin), compounds of significant interest due to their antidepressant, antibacterial, and anti-inflammatory activities (Beerhues, 2006; Soelberg et al., 2007).

Hypericum cistifolium Lam. is a shrubby or sub-shrubby representative of *Hypericum* section *Myriandra*, which branches only in its inflorescence and possesses numerous, bright-yellow flowers that are up to 12 mm in diameter. The plant is found in moist soil in pine flatwoods; along bog, swamp and marsh margins; in roadside ditches; along road embankments and generally occurs in sandy soils throughout the coastal plain of the United States from North Carolina to Louisiana. On the basis of morphological evidence, it is considered to be derived from *H. prolificum* L., a species found on calcareous and granitic soils in the eastern US. *H. galiooides* Lam. is a more highly branching shrub with a rounded aspect, which is distributed in wet habitats such as stream banks, river and lake margins, swamps, flood plains, roadside ditches and low-lying pine forests throughout the coastal plain south of North Carolina and extending west to eastern Texas. Morphologically, *H. galiooides* is most similar to *H. densiflorum* Pursh, a wetland plant that occurs throughout the Appalachian mountain range (Robson, 1996).

Molecular studies using sequences of the internal transcribed spacer (ITS) region of nuclear ribosomal DNA have indicated that, within *Hypericum*, species of section *Myriandra* are most closely related to those of section *Brathys sensu lato* (Mutis ex L.f.) Choisy. Species in these sections generally display shrubby or herbaceous habits, with only a few annual members represented, and possess the shared morphological characteristics of a stellate corolla, yellow petals (persistent in *H. sect. Brathys*, but deciduous in *H. sect. Myriandra*), strictly pale glands, parietal placentation (incompletely axile in some *H. sect. Myriandra* species) and stamens in a ring (narrow or with modifications in *H. sect. Brathys*, but broad in *H. sect. Myriandra*). Members of both sections lack staminodes (Nürk et al., 2012). In two separate studies, both a parsimony analysis (using *Clusia rosea* L. as an outgroup taxon) and a Bayesian analysis (including outgroup taxa from *Vismia* Vand., *Harungana* Lam. and *Cratoxylum* Blume) of ITS sequence data grouped *H. cistifolium* in a clade with *H. hypericoides* (L.) Cr., *H. tetrapetalum* Lam., *H. microsepalum* (Torrey & Gray) A. Gray ex S. Watson, *H. nudiflorum* Michx. ex Willd. and *H. apocynifolium* Small (Crockett et al., 2004; Nürk et al., 2012). Nürk et al. (2012) assigned *H. galiooides* to a broader clade that contained numerous other species of section *Myriandra*, with lower bootstrap support, but indicated a sister group relationship between this species and *H. adpressum* W.P.C.Barton. Evidence for this same sister relationship had also previously been demonstrated by Crockett et al. (2004).

Relatively few chemical investigations for the purpose of elucidating taxonomic relationships within *Hypericum* have been published, and the phytochemistry of species belonging to section *Myriandra* is, in general, poorly known. The caffeoylquinic acids neochlorogenic acid, chlorogenic acid and 4-O-caffeoylequinic acid and the flavonoids hyperoside and isoquercitrin have been detected using HPLC in samples of fresh vegetative

material of *H. cistifolium* collected in Liberty County, FL, USA, while neochlorogenic acid, rutin, isoquercitrin, quercitrin, and quercetin were detected in fresh floral material (Crockett, unpub. results). Interestingly, the caffeoylequinic acids, but not the flavonoids, were detected in an extract from dried material collected in Tallahassee County, FL, USA (Crockett et al., 2005, and Crockett, unpub. results). Compounds have not been previously isolated from this species.

When fresh vegetative material of *H. galiooides* was analyzed using HPLC for these compounds, all three caffeoylequinic acids, rutin, isoquercitrin, and quercitrin were detected in samples collected from one population growing in Bryan County, GA, USA, but the caffeoylequinic acids were absent from a neighboring population growing a few miles away in the same county. Neochlorogenic acid, 4-O-caffeoylequinic acid and the flavonoids found in the vegetative material, as well as hyperoside, were detected in fresh floral material collected from both these populations (Crockett, unpub. results). These results highlight the difficulties inherent in the use of caffeoylequinic acids as biomarkers in *Hypericum*. Quercimeritin, hyperoside, isoquercitrin, and quercetin have been detected in extracts of dried material of *H. galiooides* (Shakirova et al., 1972; Crockett et al., 2005). In an examination of the volatile constituents of the aerial material, caryophyllene oxide (12.9%) and guai-6,10(14)-dien-4β-ol (18.5%) were identified as major components of the distilled volatiles (Crockett et al., 2008a). Again, however, compounds have not been previously isolated from this species. During the study by Crockett et al. (2005), several late-eluting peaks were observed that had UV spectral pattern characteristics compatible with those of phloroglucinol derivatives, prompting the current investigation (pers. obs.). The high level of structural diversity inherent among phloroglucinol derivatives, coupled with their bioactivities, makes this class of substances an interesting target of phytochemical research.

Considering the known bioactivities of reported phloroglucinol derivatives, the anti-inflammatory potentials of extracts and isolated compounds from *H. cistifolium* and *H. galiooides* were determined using *in vitro* assays that measured the inhibition of COX and 5-LOX product formation. COX-1, COX-2, and 5-LOX are the key enzymes of arachidonic acid metabolism that lead to the production of important mediators of inflammation. COX-1 and -2 catalyze the first two steps in prostaglandin synthesis and 5-LOX catalyzes the oxygenation of arachidonic acid in the first step of the leukotriene pathway. In addition, antimicrobial screening using an *in vitro* microplate assay was conducted to target extracts and fractions with antibacterial and/or antifungal activity. This work resulted in the characterization of one new phloroglucinol and two new terpenoid derivatives.

MATERIALS AND METHODS

General Experimental Procedures

Polarimetry was performed on a Perkin-Elmer 241-MC polarimeter, in a 10-cm microcuvette. FTIR data were acquired using a Perkin-Elmer spectrometer, model-spectrum BX-series,

in cm^{-1} (PerkinElmer, USA). CD measurements in MeOH were carried out on a Jasco J-715 spectropolarimeter (Welltech Enterprises, Inc., USA) using a 0.1 cm path-length cell (λ_{range} 200–400 nm, resolution 0.2 nm, scan speed 50 nm/min, T 25°C, five scans averaged). ^1H -, ^{13}C -, and 2D-NMR experiments (HSQC, HMBC, DQF-COSY) were performed with Varian Unity Inova –400 and –600 MHz spectrometers. Chemical shift values (δ) were reported in ppm relative to tetramethylsilane (TMS, $\delta = 0$) as an internal standard and coupling constants (J -values) are given in Hertz (Hz). The compounds **1–4** were dissolved in CDCl_3 and spectra were recorded at 25°C. Experimental parameters were as published in Seebacher et al. (2003). HPLC-DAD/ESI-MS (neg.) data were obtained on a Thermo Finnigan Surveyor LC instrument with Thermo Quest Surveyor DAD, autosampler, and MS pump, and a Thermo Finnigan LCQ-XP mass detector equipped with an ESI source run by Xcalibur software (Thermo Finnigan, USA). Analytical HPLC was performed using a Zorbax SB RP-18 column (3 μm , 2.1 \times 150 mm; Agilent Technologies), flow rate 250 $\mu\text{L}/\text{min}$, gradient elution $\text{H}_2\text{O}/\text{MeOH}$ (25:75 to 0:100 over 20 min, 10 min at 0:100, 10 min equilibration). Mass spectra were detected and recorded (scan range = m/z 50–1000, transfer capillary temperature = 350°C, spray voltage = 5.00 kV, sheath gas flow = 70 units). VLC was performed on either fine-grade silica gel 60 (230–400 mesh ASTM; Merck) or medium-grade silica gel 60 (70–230 mesh ASTM; Merck). Analytical TLC was performed on silica gel 60 F₂₅₄ plates (Merck), eluting with hexane/EtOAc 75:25, visualization by spraying with H_2SO_4 (10% solution v/v in 95% aq. EtOH) and then vanillin (5% solution w/v in 95% aq. EtOH) reagents, then heating at 150° for 45 s and detecting under UV/VIS light at 254 and 365 nm. Preparative HPLC and detection of UV spectra (λ_{max} in nm) were performed on an Agilent 1100 Separations Module equipped with a photodiode array detector (Agilent Technologies, USA), using a LiChroCART RP-18 column (LiChrospher, 7 μm , 10 \times 250 mm; Merck), flow rate 2 mL/min, MeCN:H₂O gradient system (50:50 to 100:0 over 30 min), detection at 254 and 280 nm.

Plant Material

Aerial material of *H. cistifolium* Lam. (Hypericaceae) was collected from Tallahassee County, FL, USA. A voucher specimen (Crockett-H65) has been deposited at the University of Georgia (UGA) Herbarium in Athens, GA. Aerial material of *H. galoides* Lam. was collected from Liberty County, FL, USA. A voucher specimen (Crockett-152B) has been deposited at the University of Mississippi (UMISS) Herbarium in Oxford, MS, USA. The aerial material (flowers, inflorescence bracts, and upper stems) was collected while plants were in full flower, and plants were identified by S. Crockett. Material was dried in darkened, ventilated cabinets to a moisture content of less than 2% prior to grinding.

Extraction and Isolation

Hypericum cistifolium: 800 g aerial material was ground and extracted in a maceration tank with CH_2Cl_2 (4 L, 5 days). 12.5 g extract was further investigated due to interesting TLC features (i.e., a bright orange band, following spraying and heating). 10 g

of the CH_2Cl_2 extract was subjected to VLC using fine-grade silica (100 g), eluting with a hexane-EtOAc gradient (5% steps, 200 mL/step, 25 mL fractions). A bright yellow band eluted from the column with the first 400 mL solvent (<5% EtOAc in hexane). Upon sitting overnight, a clear crystalline material precipitated from these initial fractions. This substance was purified by repeated crystallization from hexane, yielding 985 mg (~10.2% w/w yield) of compound **1**. *H. galoides*: 940 g aerial material was ground and extracted in a maceration tank with *n*-hexane (5 L, 5 days), yielding 13.5 g extract. TLC examination of this extract revealed several bright orange- and blue-staining bands upon spraying with a vanillin/sulphuric acid reagent and heating. 13 g of this extract was subjected to VLC on fine-grade silica (150 g), eluting with a hexane-EtOAc gradient (5% steps, 300 mL/step, 150 mL fractions) to yield six fractions (after combining on the basis of TLC similarities). A bright yellow visible band was observed eluting from the column with 20% EtOAc, and this fraction (ca. 1 g) was further purified by VLC on medium-grade silica (100 g), using a hexane-Et₂O gradient (10% steps, 200 mL/step, 25 mL fractions), yielding 10 fractions. The MeCN-soluble portion of merged fractions 3–5 were further purified by preparative RP-HPLC, resulting in the isolation of one new (**1**) and two known (**2** and **3**) phloroglucinol derivatives, in amounts of 3.5, 12, and 2 mg, respectively. In addition, 4 mg of a known compound (4,12,12-trimethyl-9-methylene-5-oxatricyclo[8.2.0.0.4,6] dodecane or β -caryophyllene oxide) was isolated. This compound was identified by comparison of its ^1H - and ^{13}C -NMR and mass values with those cited in literature (Harper et al., 1998).

On the basis of interesting TLC bands (yellow-green fluorescence under UV_{366} , turning blue when sprayed and heated), the fraction eluting from the original VLC column with 30% EtOAc was additionally selected for further purification. This extract (ca. 1 g) was subjected to VLC on medium-grade silica (100 g), eluting with a hexane-EtOAc gradient (5% steps, 200 mL/step, 25 mL fractions), to yield 10 fractions. Fractions 3–5 were merged on the basis of TLC similarities and repeated crystallization from hexane:EtOAc (75:25) yielded compound **4** (16 mg, 0.02% w/w), which was subsequently characterized as a racemic mixture of two new terpenoid derivatives (**4a** and **4b**).

1-(6-Hydroxy-2,4-dimethoxy-phenyl)-2-methyl-1-propanone (**1**) Clear crystalline solid; UV (CH_2Cl_2) λ_{max} ($\log \epsilon$): 287 (5.47) nm; IR (thin film) ν_{max} 3447, 2977, 1626, 1222 cm^{-1} ; ^1H -NMR and ^{13}C -NMR (MeOH-d4): see Table 1; ESI-MS (m/z): 224.1 (calc. for $\text{C}_{11}\text{H}_{14}\text{O}_4$, 224.1049).

2-Benzoyl-3,3-dimethyl-4R,6S-bis-(3-methylbut-2-enyl)-cyclohexanone (**4a**) and **2-Benzoyl-3,3-dimethyl-4S,6R-bis-(3-methylbut-2-enyl)-cyclohexanone** (**4b**) Pale yellow solid; UV (CH_2Cl_2) λ_{max} ($\log \epsilon$): 243 (3.55) nm; IR (thin film) ν_{max} 3395, 2922, 1718, 1655, 1463 cm^{-1} ; ^1H -NMR and ^{13}C -NMR (CDCl_3): see Table 2; ESI-MS (m/z): 398.3 (calc. for $\text{C}_{27}\text{H}_{42}\text{O}_2$, 398.3185).

BIOASSAY TESTING

In vitro assays for COX-1 and COX-2 enzymatic inhibitory activity were performed in a 96-well-plate format with purified

TABLE 1 | ^1H and ^{13}C NMR chemical shifts (ppm) of compounds **1 – 3** in MeOH-d₄ at 25°C, TMS as internal standard, J in Hz.

Atom	1		2		3	
	δC	δH	δC	δH	δC	δH
1	106.4	—	106.9	—	110.3	—
2	167.7	—	168.1	—	161.1	—
3	91.9	6.07 s	92.1	6.06 s	112.7	—
4	164.1	—	164.6	—	165.4	—
5	95.3	6.06 s	95.3	6.06 s	96.8	6.28 s
6	168.1	—	168.1	—	163.9	—
2-OMe	56.1	3.82 s	56.2	3.82 s	63.0	3.68 s
3-Me					19.0	2.04 s
4-OMe	56.3	3.88 s	56.4	3.88 s	56.1	3.83 s
1'	211.7	—	207.4	—	212.3	—
2'	40.8	3.76 sept., J = 6.6	47.4	2.96 t, J = 7.2	40.5	3.76 sept., J = 6.6
3'	19.6	1.12 d, J = 6.6	19.7	1.67 sext., J = 7.2	20.0	1.12 d, J = 6.6
4'	19.6	1.12 d, J = 6.6	14.6	0.98 t, J = 7.2	20.0	1.12 d, J = 6.6

TABLE 2 | ^1H and ^{13}C NMR chemical shifts (ppm) of compound **4** in CDCl₃ at 25°C, TMS as internal standard, J in Hz.

Atom	δC	δH	atom	δC	δH
1	207.8	—	1'	196.7	—
2	67.3	4.39 s	2'	138.8	—
3	44.6	—	3'	127.7	7.78 d, J = 7.8
4	48.8	1.70	4'	128.5	7.42 t, J = 7.8
5	35.4	1.25, 2.20 ddd, J = 14.2, 6.4, 3.5	5'	132.7	7.52 t, J = 7.6
6	51.4	2.51 sext., J = 6.4	6'	128.5	7.42 t, J = 7.8
7	26.8	1.13 s	7'	127.7	7.78 d, J = 7.8
8	16.1	1.15 s			
1''	27.9	1.72 m, 2.26 m	1'''	27.7	1.97 dtr, J = 14.8, 6.5, 2.41 dtr, J = 14.6, 6.0
2''	123.2	5.17 t, J = 6.8	2'''	121.6	5.09 t, J = 6.8
3''	132.8	—	3'''	133.2	—
4''	17.9	1.62 s	4'''	17.9	1.60 s
5''	25.8	1.74 s	5'''	25.8	1.68 s

prostaglandin H synthase (PGHS)-1 from ram seminal vesicles for COX-1 and purified PGHS-2 from sheep placental cotyledons for COX-2 (both Cayman Chemical Company, Ann Arbor, MI, USA). The bioassay for inhibition of leukotriene formation was carried out in 96-well-plate format using polymorphic leukocytes with 5-LOX activity, isolated from venous human blood. Further details of the bioassays for anti-inflammatory activity are described in Crockett et al. (2008b). Antimicrobial testing using an *in vitro* microplate assay were performed as reported in Samoylenko et al. (2009).

RESULTS AND DISCUSSION

As part of our continuing phytochemical investigation of the genus *Hypericum*, and in particular, the identification and elucidation of chemotaxonomic markers in species of section *Myriandra*, the non-polar extracts of *H. cistifolium* and *H. galiooides* were targeted on basis of interesting TLC, UV,

and HPLC characteristics. Previously, we had observed that simple phloroglucinols and filicinic acid derivatives generally display red to orange colors during TLC analysis upon spraying and heating, while more complex structures (e.g., those with bicyclo[3.3.1]nonane base structures) display blue to purple colors (Crockett, pers. obs.). These characteristics aided the chromatographic fractionation and purification of phloroglucinol and terpenoid derivatives, namely, three new (**1**, **4a**, and **4b**) and two known compounds (**2** and **3**), which were subsequently identified from these two *Hypericum* species (**Figure 1**).

Despite the structurally simple nature of compound **1**, it has not been previously reported in the scientific literature to our knowledge. This compound occurred as a major component of the non-polar extract of *H. cistifolium* (>10% w/w) and was isolated from *H. galiooides* as a minor constituent (0.03% w/w) as a clear, crystalline solid with a pleasant odor. Its structure was established through NMR spectroscopy. The ^1H - and ^{13}C -NMR spectra indicated an asymmetrically tetrasubstituted

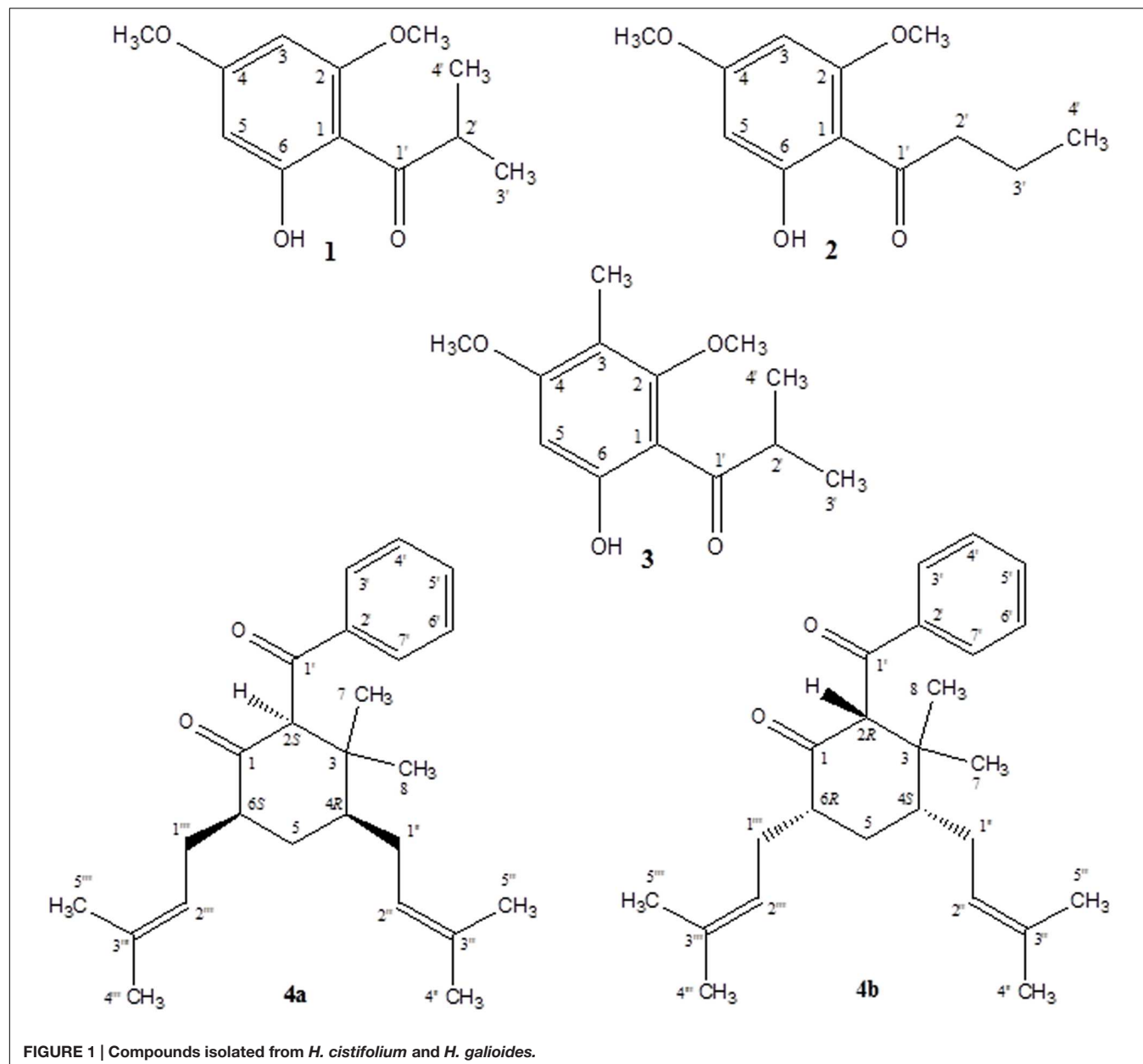


FIGURE 1 | Compounds isolated from *H. cistifolium* and *H. galloides*.

phenyl group with two methoxy, one hydroxyl and one isobutyryl moiety, with methoxy and hydroxyl groups on alternating carbons. The relative positions of the substituents were determined using HMBC correlations. Both aromatic protons coupled to C-1 (106 ppm), but only the one at 6.07 ppm coupled to both carbons attached to the methoxy groups.

Compound 2 (0.09% w/w) has been both synthesized (Carter et al., 1931) and isolated from a natural plant source as a pale, crystalline substance with no remarkable scent from two species of *Dysophylla* (Lamiaceae) (Joshi and Ravindranath, 1977; Nanda et al., 1983). Interestingly, this compound is used as a starting reagent in the synthesis of (+)-calanolide-A, a coumarin that was originally isolated from another member of

Calophyllaceae (Clusiaceae *sensu lato*), *Calophyllum lanigerum* var. *austrocoriaceum*, and that has been investigated as a potential anti-HIV drug candidate in the USA (Tanaka et al., 2000). Compound 3 (0.02% w/w) was identified as a known substance that has been previously synthesized (Schiemann et al., 1985) and isolated from the leaf oils of several species in the plant family Myrtaceae including *Thryptomene saxicola* (Dastlik et al., 1989), *Austromyrtus dulcis* (Brophy et al., 1995), *Eucalyptus miniata* (Ireland et al., 2004), and *Xanthostemon eucalyptoides* (Brophy et al., 2006). This substance has been given the informal name isobaeckeol and has been described in previous literature as a light pink substance with a faint pleasant odor. The identities of compounds 2 and 3 were verified by comparison with values reported in the literature (2: Joshi and

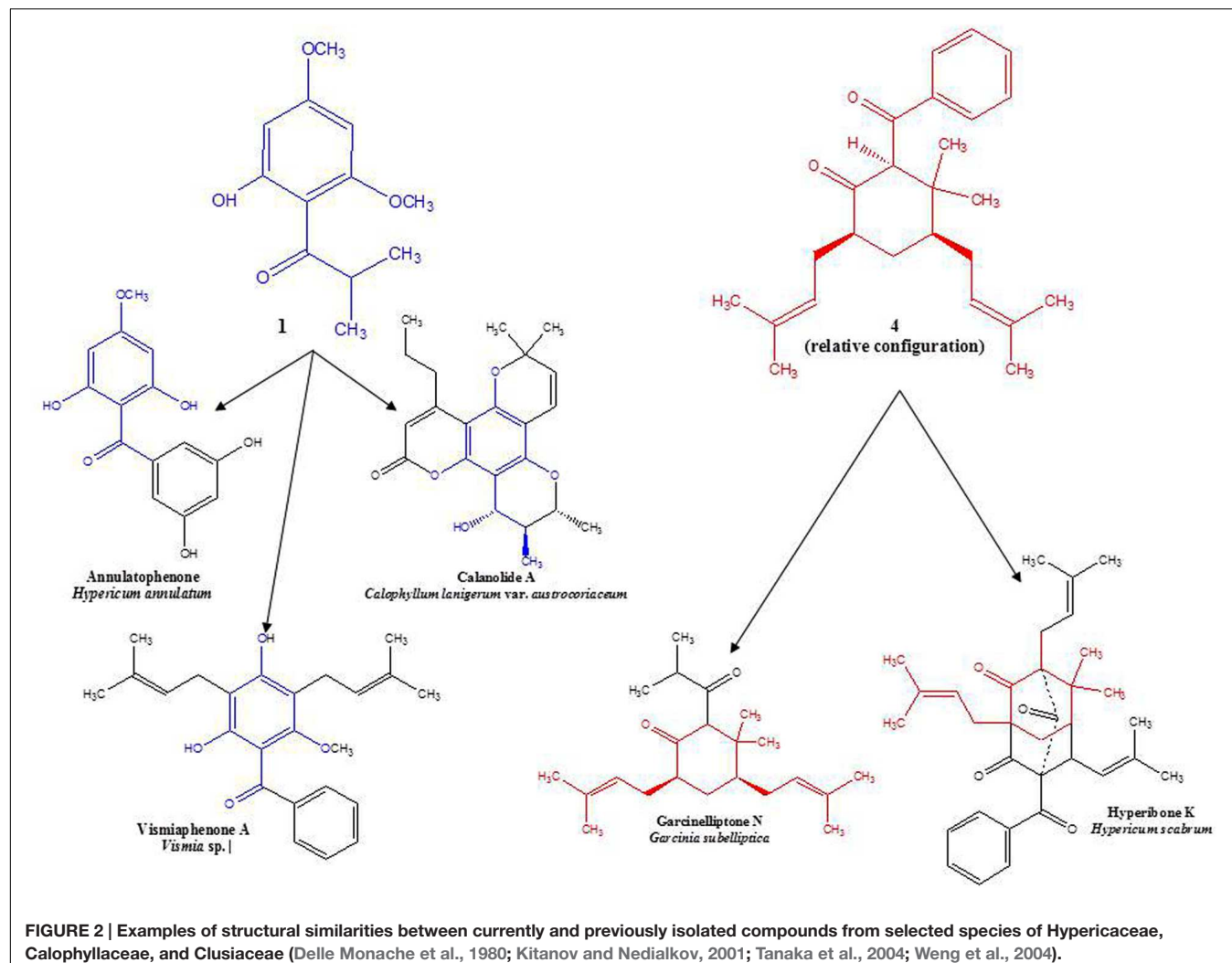


FIGURE 2 | Examples of structural similarities between currently and previously isolated compounds from selected species of Hypericaceae, Calophyllaceae, and Clusiaceae (Delle Monache et al., 1980; Kitanov and Nedialkov, 2001; Tanaka et al., 2004; Weng et al., 2004).

Ravindranath, 1977; Åyras and Widén, 1978 and 3: Schiemenz et al., 1985; Ireland et al., 2004). Because complete data sets for these compounds have not been previously published, we include a comparison of the values for compounds 1–3 here in Table 1.

A simple acylphloroglucinol with a very similar structure to compounds 1–3 has also been isolated from *H. beanii* N. Robson (section *Ascyreia*, Shiu and Gibbons, 2006). While this compound demonstrated moderate activity (MIC = 16–32 µg/mL) against a panel of multidrug-resistant strains of *Staphylococcus aureus*, compound 1 tested in the same panel (data not shown) displayed no anti-staphylococcal activity. The compound isolated from *H. beanii* differs from compound 1 only in that it possesses a hydroxyl group at C-5 (rather than a methoxy group) and a methylation at C-6 (see Figure 1), indicating that modification at these positions have the potential to influence anti-staphylococcal activity. Interestingly, prenylated phloroglucinol derivatives that contain sub-structures of compounds 1–3 have been previously isolated from a Jamaican collection of *H. hypericoides*, which has been hypothesized to be closely related to *H. cistifolium*

(Christian et al., 2008; Nürk et al., 2012). An analysis of other species in the section *Myriandra* revealed the presence of peaks eluting in or near the same region as compound 1 (e.g., *H. brachyphyllum*, *H. densiflorum*, *H. edisonianum*, *H. hypericoides*, *H. lissophloeus*, *H. lobocarpum*, *H. prolificum*, *H. suffruticosum*), and further chemical investigations of these species have the potential to yield additional phloroglucinol derivatives (Crockett et al., 2005; Henry et al., 2006).

Compounds 4a and 4b have not been previously reported as natural products isolated from *Hypericum* or another plant species to our knowledge. These compounds were isolated as a mixture, a pale-yellow odorless solid, representing minor constituents (0.02% w/w) of the lipophilic extract of *H. galiodes*. ¹H- and ¹³C-NMR spectral analyses revealed that compound 4 consisted of a six-membered ring with a benzophenone group at C-2, two methyl groups at C-3, and isoprenyl groups at C-4 and C-6. C-1 was represented by a keto group and C-5, by a methylene group. The relative configurations at the stereogenic centers were determined through analysis of cross-peaks in COSY and enhancements in selective 1D NOE spectra. Selective inversion

of H-2 (4.39 ppm) led to NOEs at H-4 and H-6, indicating an axial orientation for all these protons. An additional NOE between H-2 and a signal at 1.15 ppm allowed the assignments of the methyl groups bound to C-3. Evidence for the equatorial orientation of H-5 (1.25 ppm) is supported by the coupling constants ($J = 3.5, 6.4$, and 14.2 Hz), although the multiplicity of the signal was obscured by methylene resonances from a minor fatty acid constituent in the sample. The axial orientations of H-4 and H-6 were confirmed by strong COSY cross-peaks to the equatorial proton H-5. The ‘sexet’ reported for H-6 arises from the superposition of a doublet ($J \approx 13$ Hz) of quadruplets ($J \approx 6.5$ Hz) with relative intensities of 1:3:4:4:3:1. A comparison with NOE-derived data (not shown) was performed to assign the resonances of the methyl groups in the isoprene side-chains.

Circular dichroism spectra were taken to determine the absolute configuration at C-2, -4, and -6 in the molecule. However, no CD signal was detected, indicating the presence of a racemic mixture of **4a** and **4b**. Interestingly, this structure occurs wholly or in part as a sub-structure within other phloroglucinol derivatives that have been isolated from certain members of the family, Clusiaceae, which is related to Hypericaceae. A similar observation may be made for the base structure of compounds **1–3** (see Figure 2). Along with data from literature, these findings support hypotheses for biogenetic links among several sections of *Hypericum*, as well as between *Hypericum* and other currently recognized tribes in Hypericaceae (i.e., Vismieae and Cratoxyleae), and between Hypericaceae and other related families, namely Clusiaceae nom. cons. and Calophyllaceae, within the broader plant order Malpighiales.

As several phloroglucinol derivatives isolated from *Hypericum* species are known to possess anti-inflammatory and antibacterial activities, the crude CH_2Cl_2 extracts as well as the isolated new compounds were subjected to antibacterial and anti-inflammatory *in vitro* testing: CH_2Cl_2 extracts of *H. cistifolium* and *H. galoides* were submitted to the National Center for Natural Products Research (NCNPR, Oxford, MS, USA) for bioassay testing against a variety of pathogenic microorganisms including the fungi *Candida albicans*, *C. glabrata*, *C. krusei*, *Cryptococcus neoformans*, *Aspergillus fumigatus*, and the bacteria *Mycobacterium intracellulare*, *Pseudomonas aeruginosa*, *S. aureus*, and methicillin-resistant *S. aureus* (MRSA). Only the extract of *H. cistifolium* displayed a marginal activity against *S. aureus* (MRSA) and *C. neoformans* with IC_{50} s of 100–150 $\mu\text{g}/\text{mL}$. In addition, when tested at 50 μM *in vitro* against enzymes involved in arachidonic acid metabolism, compounds **1** and **4a/b** displayed negligible or only very weak bioactivity against COX-1, COX-2, and 5-LOX product formation.

The new compounds isolated from two species of *Hypericum* section *Myriandra* displayed relatively low bioactivity levels in the bioassays selected, although structurally similar compounds isolated from other species have demonstrated higher levels of activity, and the evidence collected thus far seems to indicate that the degree of hydroxylation and methylation, as well as the positions of these moieties, can strongly influence

bioactivity. Commercially, *H. cistifolium* and *H. galoides* occupy a very small niche market within the horticultural industry and are sold as ornamental landscaping plants, primarily in the southeastern United States (Huxley et al., 1992). Because established cultivation methods for these species exist, however, larger-scale production for the purposes of phytochemical isolation of these compounds could be rapidly established.

While phloroglucinol derivatives have been previously isolated as both major and minor constituents from many species of *Hypericum*, as well as related genera within Clusiaceae *sensu lato*, their ecological roles in the plants are still poorly understood. Hypotheses suggesting that such compounds act as attractive (for pollinators) and/or defensive (against herbivores) substances in the plant have been proposed, but further studies are needed (Gronquist et al., 2001). The potential ecological role of such compounds as compound **1**, produced in such high amounts by *H. cistifolium*, is an area of considerable research interest for our group. Phylogenetic hypotheses have been proposed regarding relationships between and among species in section *Myriandra* on the basis of morphological and molecular evidence (Robson, 1996; Crockett et al., 2004; Nürk et al., 2012). Steadily accumulating evidence from phytochemical investigations indicates that acylated and prenylated phloroglucinol derivatives are not only compounds of significant interest due to their respective bioactivities, but also have the potential to be used as chemotaxonomic markers in *Hypericum*. Future directions of research include the phytochemical investigation of species (i.e., *H. hypericoides*, *H. tetrapetalum*, *H. microsepalum*, *H. nudiflorum*, *H. apocynifolium*, and *H. adpressum*) closely allied to those in the current investigation.

AUTHOR CONTRIBUTIONS

SC, plant collection, compound isolation (TLC and CC), HPLC-DAD/ESI-MS analysis, manuscript preparation and revision; OK, NMR; EP and RB, *in vitro* assays for assessing COX-1 and COX-2 enzymatic inhibitory activity and inhibition of leukotriene formation (5-LOX activity); MJ, *in vitro* antimicrobial testing; WS, circular dichroism measurements.

FUNDING

Funds for antimicrobial testing were provided by the NIH, NIAID, Division of AIDS, Grant No. AI 27094 and the USDA Agricultural Research Service Specific Cooperative Agreement No. 58-6408-2-0009. Funding for SC were provided through a Lise-Meitner Stipend (M844-B05) from the Fonds zur Förderung der Wissenschaftlichen Forschung (FWF) in Austria.

ACKNOWLEDGMENTS

The authors thank Ing. Elke Prettner for carrying out polarimetry experiments, Ms. Andrea Fleck and Mr. Robert Alex for NMR sample assistance, Dr. Simon Gibbons for anti-staphylococcal testing and Ms. Marsha Wright for antimicrobial testing.

REFERENCES

- Äyras, P., and Widén, C. J. (1978). NMR spectroscopy of naturally occurring phloroglucinol derivatives. Part II. Use of the additivity of substituent parameters in carbon-13 NMR spectral analysis of mono- and dimethyl ethers of methyl- and acyl-substituted phloroglucinols. *Finn. Chem. Lett.* 8, 264–266.
- Beerhues, L. (2006). Molecules of interest – hyperforin. *Phytochemistry* 67, 2201–2207. doi: 10.1016/j.phytochem.2006.08.017
- Brophy, J. J., Goldsack, R. J., Fookes, C. J. R., and Forster, P. I. (1995). The essential oils of Australian *Austromyrtus* sensu lato Part I. The *Austromyrtus dulcis* group. *Flav. Fragr. J.* 10, 69–73. doi: 10.1002/ffj.2730100203
- Brophy, J. J., Goldsack, R. J., and Forster, P. I. (2006). A preliminary examination of the leaf oils of the genus *Xanthostemon* (Myrtaceae) in Australia. *J. Essent. Oil Res.* 18, 222–230. doi: 10.1080/10412905.2006.9699071
- Canter, F. W., Curd, F. H., and Robertson, A. (1931). Hydroxy-carbonyl compounds. II. benzoylation of ketones derives from phloroglucinol. *J. Chem. Soc.* 165, 1245–1255. doi: 10.1039/JR9310001245
- Christian, O. E., McLean, S., Reynolds, W. F., and Jacobs, H. (2008). Prenylated benzophenones from *Hypericum hypericoides*. *Nat. Prod. Commun.* 3, 1781–1786.
- Ciccarelli, D., Andreucci, A. C., and Pagni, A. M. (2001). The “black nodules” of *Hypericum perforatum* L. subsp. *perforatum*: morphological, anatomical, and histochemical studies during the course of ontogenesis. *Israel J. Plant Sci.* 49, 33–40. doi: 10.1560/46y5-afwd-tcy0-kfgf
- Crockett, S. L., Demirci, B., Baser, K. H. C., and Khan, I. A. (2008a). Volatile constituents of *Hypericum* L. section *Myriandra* (Clusiaceae): species of the *H. fasciculatum* Lam. Alliance. *J. Essent. Oil Res.* 20, 244–249. doi: 10.1080/10412905.2008.9700003
- Crockett, S. L., Douglas, A. W., Scheffler, B. E., and Khan, I. A. (2004). Genetic profiling of *Hypericum* (St. John’s wort) species by nuclear ribosomal ITS sequence analysis. *Planta Med.* 70, 929–935. doi: 10.1055/s-2004-832619
- Crockett, S. L., Schaneberg, B., and Khan, I. A. (2005). Phytochemical profiling of new and old world *Hypericum* (St. John’s wort) species. *Phytochem. Anal.* 16, 479–485. doi: 10.1002/pca.875
- Crockett, S. L., Wenzig, E.-M., Kunert, O., and Bauer, R. (2008b). Anti-inflammatory phloroglucinol derivatives from *Hypericum empetrifolium*. *Phytochem. Lett.* 1, 37–43. doi: 10.1016/j.phytol.2007.12.003
- Dastlik, K. A., Ghisalberti, E. L., and Jefferies, P. R. (1989). Phloroacylphenones in the essential oil of *Thryptomene saxicola*. *Phytochemistry* 28, 3543–3544. doi: 10.1016/0031-9422(89)80388-7
- Delle Monache, G., Gonzalez, J., Delle Monache, F., and Marini Bettolo, G. B. (1980). Chemistry of the *Vismia* genus. Part VI. prenylated benzophenones from *Vismia decipiens*. *Phytochemistry* 19, 2025–2028. doi: 10.1016/0031-9422(80)83030-5
- Gronquist, M., Bezzerezides, A., Attygalle, A., Meinwald, J., Eisner, M., and Eisner, T. (2001). Attractive and defensive functions of the ultraviolet pigments of a flower (*Hypericum calycinum*). *Proc. Natl. Acad. Sci. U.S.A.* 98, 13745–13750. doi: 10.1073/pnas.231471698
- Harper, J. K., McGeorge, G., and Grant, D. M. (1998). Solid-state ¹³C chemical shift tensors in terpenes. Part I. Spectroscopic methods and chemical shift structure correlations in caryophyllene oxide. *Magn. Reson. Chem.* 36, S135–S144. doi: 10.1002/(SICI)1097-458X(199806)36:13<S135::AID-OMR312>3.0.CO;2-9
- Henry, G. E., Raithore, S., Zhang, Y., Jayaprakasam, B., Nair, M. G., Heber, D., et al. (2006). Acylphloroglucinol derivatives from *Hypericum prolificum*. *J. Nat. Prod.* 69, 1645–1648. doi: 10.1021/np060356+
- Huxley, A., Griffiths, M., and Levy, M. (eds) (1992). *The New Royal Horticultural Society Dictionary of Gardening*. Vol. 2. New York, NY: Stockton Press.
- Hypericum Online* (2016). *Hypericum Online*—A Site Dedicated to *Hypericum* – The St. John’s Worts. Available at: <http://hypericum.myspecies.info/>
- Ireland, B. F., Goldsack, R. J., Brophy, J. J., Fookes, C. J. R., and Clarkson, J. R. (2004). The leaf essential oils of *Eucalyptus miniata* and its allies. *J. Essent. Oil Res.* 16, 89–94. doi: 10.1080/10412905.2004.9698659
- Joshi, B. S., and Ravindranath, K. R. (1977). Isolation and identification of two phenolic ketones and a chromone from *Dysophylla stellata* Benth. *J. Chem. Soc. Perkin. Trans. 1* 4, 433–436. doi: 10.1039/p19770004433
- Kitanov, G. M., and Nedialkov, P. T. (2001). Benzophenone O-glucoside, a biogenic precursor of 1,3,7-trioxygenated xanthones in *Hypericum annulatum*. *Phytochemistry* 57, 1237–1243. doi: 10.1016/S0031-9422(01)00194-7
- Nanda, B., Patwardhan, S. A., and Gupta, A. S. (1983). Chemical examination of *Dysophylla tomentosa*. *Indian J. Chem.* 22B, 185–186.
- Nürk, N. M., Mandriñán, S., Carine, M. A., Chase, M. W., and Blattner, F. R. (2012). Molecular phylogenetics and morphological evolution of St. John’s Wort (*Hypericum*; *Hypericaceae*). *Mol. Phylogenet. Evol.* 66, 1–16. doi: 10.1016/j.ympev.2012.08.022
- Robson, N. K. B. (1996). Studies in the genus *Hypericum* L. (Guttiferae). 3. Sections 20. *Myriandra to Elodes*. *Bull. Br. Mus. Nat. Hist. (Bot.)* 26, 75–217.
- Robson, N. K. B. (2003). “Hypericum botany,” in *Hypericum: The Genus Hypericum*, ed. E. Ernst (New York, NY: Taylor and Francis), 1–22.
- Samoylenko, V., Ashfaq, M. K., Jacob, M. R., Takwani, B. L., Khan, S. I., Manley, S. P., et al. (2009). Indolizidine, antiinfective and antiparasitic compounds from *Prosopis glandulosa* var. *glandulosa*. *J. Nat. Prod.* 72, 92–98. doi: 10.1021/np800653z
- Schiemenz, G. P., Behrens, H., Ebert, C. P., Maienschein, K., and Schroeder, J. M. (1985). Trimethoxyphenyl compounds, XI. Constituents of *Hagenia abyssinica*, 2: synthesis of phloracylphenones containing one phloroglucinol unit. *Z. Naturforsch. B* 40B, 681–692.
- Seebacher, W., Simic, N., Weis, R., Saf, R., and Kunert, O. (2003). Complete assignments of 1H and 13C NMR resonances of oleanolic acid, 18 α -oleanic acid, ursolic acid and their 11-oxo derivatives. *Magn. Reson. Chem.* 41, 636–638. doi: 10.1002/mrc.1214
- Shakirova, K. K., Bandyukovam, V. A., Kalmatov, K. K., and Khazanovich, R. L. (1972). Flavonoids of several species of St. John’s Wort. *Mater Yubileinoi. Resp. Nauchn. Konf. Farm. Posvyashch. 50-Letiyu. Obraz. SSSR* 40–41.
- Shiu, W. K. P., and Gibbons, S. (2006). Anti-staphylococcal acylphloroglucinols from *Hypericum beanii*. *Phytochemistry* 67, 2568–2572. doi: 10.1016/j.phytochem.2006.09.037
- Soelberg, J., Jørgensen, L. B., and Jäger, A. K. (2007). Hyperforin accumulates in the translucent glands of *Hypericum perforatum*. *Ann. Bot.* 99, 1097–1100. doi: 10.1093/aob/mcm057
- Tanaka, T., Kumamoto, T., and Ishikawa, T. (2000). Enantioselective total synthesis of anti HIV-1 active (+)-calanolide A through a quinine-catalyzed asymmetric intramolecular oxo-Michael addition. *Tetrahedron Lett.* 41, 10229–10232. doi: 10.1016/S0040-4039(00)01820-7
- Tanaka, N., Takaishi, Y., Shikishima, Y., Nakanishi, Y., Bastow, K., Lee, K.-H., et al. (2004). Prenylated benzophenones and xanthones from *Hypericum scabrum*. *J. Nat. Prod.* 67, 1870–1875. doi: 10.1021/np040024+
- Weng, J.-R., Tsao, L.-T., Wang, J.-P., Wu, R.-R., and Lin, C.-N. (2004). Anti-inflammatory phloroglucinols and terpenoids from *Garcinia subelliptica*. *J. Nat. Prod.* 67, 1796–1799. doi: 10.1021/np049811x
- Conflict of Interest Statement:** The authors declare that the research was conducted in the absence of any commercial or financial relationships that could be construed as a potential conflict of interest.
- Copyright © 2016 Crockett, Kunert, Pferschy-Wenzig, Jacob, Schuehly and Bauer. This is an open-access article distributed under the terms of the Creative Commons Attribution License (CC BY). The use, distribution or reproduction in other forums is permitted, provided the original author(s) or licensor are credited and that the original publication in this journal is cited, in accordance with accepted academic practice. No use, distribution or reproduction is permitted which does not comply with these terms.*



Polar Constituents and Biological Activity of the Berry-Like Fruits from *Hypericum androsaemum* L.

Giovanni Caprioli^{1†}, Alessia Alunno², Daniela Beghelli³, Armandodoriano Bianco⁴, Massimo Bramucci¹, Claudio Frezza⁵, Romilde Iannarelli^{1†}, Fabrizio Papa⁶, Luana Quassinti¹, Gianni Sagratini¹, Bruno Tirillini⁷, Alessandro Venditti^{4,5}, Sauro Vittori¹ and Filippo Maggi^{1*}

¹ School of Pharmacy, University of Camerino, Camerino, Italy, ² Rheumatology Unit, Department of Medicine, University of Perugia, Perugia, Italy, ³ School of Bioscience and Veterinary Medicine, University of Camerino, Camerino, Italy, ⁴ Department of Chemistry, Sapienza University of Rome, Rome, Italy, ⁵ Department of Environmental Biology, Sapienza University of Rome, Rome, Italy, ⁶ School of Science and Technology, University of Camerino, Camerino, Italy, ⁷ Department of Biomolecular Sciences, University of Urbino, Urbino, Italy

OPEN ACCESS

Edited by:

Gregory Franklin,
Polish Academy of Sciences, Poland

Reviewed by:

Akira Oikawa,
Yamagata University, Japan
Laxminarain Misra,
Retired from CSIR-CIMAP, India

*Correspondence:

Filippo Maggi
filippo.maggi@unicam.it

[†]These authors have contributed equally to this work.

Specialty section:

This article was submitted to
Plant Metabolism and Chemodiversity,
a section of the journal
Frontiers in Plant Science

Received: 10 December 2015

Accepted: 11 February 2016

Published: 01 March 2016

Citation:

Caprioli G, Alunno A, Beghelli D, Bianco A, Bramucci M, Frezza C, Iannarelli R, Papa F, Quassinti L, Sagratini G, Tirillini B, Venditti A, Vittori S and Maggi F (2016) Polar Constituents and Biological Activity of the Berry-Like Fruits from *Hypericum androsaemum* L. *Front. Plant Sci.* 7:232.
doi: 10.3389/fpls.2016.00232

Hypericum androsaemum, also known as Tutsan, is a small evergreen shrub common in the Mediterranean basin where it is traditionally used as diuretic and hepatoprotective herbal drug. This plant possesses the peculiarity to produce fleshy and berry-like fruits that ripen from red to shiny black. In the present work, the chemical constituents of methanolic extracts and infusions of red and black fruits were analyzed by HPLC, and correlated with their antioxidant properties which were evaluated by the DPPH, β-Carotene/linoleic acid, and hypochlorous acid tests. In addition, the red pigment of the fruit was isolated by column chromatography and structurally elucidated by NMR. Results showed that *H. androsaemum* fruits contain high amounts of shikimic and chlorogenic acids, while their color was given by a tetraoxygenated-type xanthone, reported for the first time in *Hypericum* species. The red berries infusion gave the highest content of total phenolic compounds, DPPH, and hypochlorous acid scavenging activity, and β-carotene bleaching. Cytotoxicity of the berries extracts on three human tumor cell lines (malignant melanoma, breast adenocarcinoma, and colon carcinoma) was evaluated by MTT assay, and relevant inhibition on colon carcinoma cells (IC_{50} value of 8.4 μg/mL) was found. Finally, the effects of red berries extract on the immune system were evaluated by peripheral blood mononuclear cell (PBMC) proliferation assay that revealed a strong stimulation on lymphocytes at low doses (0.4–6 μg/mL).

Keywords: *Hypericum androsaemum*, berry-like fruits, phytochemicals, antioxidant, cytotoxicity, immunomodulatory

INTRODUCTION

H. androsaemum [Hypericaceae, sect. *Androsaemum* (Duhamel) Godr.], well known as “tutsan,” is a small evergreen shrub fairly common in damp woods and hedgerows (100–1400 m of altitude) within the Mediterranean Basin, mainly in Western and Southern Europe, South-Western Asia, North Africa, while it has been introduced elsewhere (Allen and Hatfield, 2004). The plant possesses big, opposite, sessile, ovate and slightly aromatic leaves bearing translucent glands, but lacking black nodules which are the secretory structures storing naphtodiantrones (Perrone et al., 2013).

The flowers are large, yellow, with small clearer spots on the petals. Among *Hypericum* species, the plant has the peculiarity to produce capsules that are not dry at ripening, but become more or less fleshy and berry-like. The ease of cultivation of the plant and the natural color variation in the fresh capsules has been exploited through directed breeding and line selection, resulting in economically highly successful cultivars.

H. androsaemum is used as an important traditional medicine in Europe. For instance, in Portugal its leaves are used as diuretic and to treat liver, kidney and bladder ailments (Valentão et al., 2002). In England, they are mixed with lard to produce an ointment for dressing cuts and wounds (Phillips, 1977; Allen and Hatfield, 2004).

So far, much of the phytochemical and pharmacological studies focused on leaves, revealing the presence of several flavonoids and phenolic acids, mainly chlorogenic acids, and quercetin derivatives which are responsible for the plant hepatoprotective properties (Valentão et al., 2002, 2004). However, scientific works on the showy tutsan's berries were not yet provided. Interestingly, the pigment giving the reddish-black color to the capsular tissue has not yet been identified.

Searching for new fruits with healthy properties, in the present work we reported a comprehensive analysis on the polar constituents and biological activities, namely the antioxidant power, cytotoxicity on tumor cells, and immunomodulatory capacities of *H. androsaemum* berries collected from spontaneous and cultivated plants in central Italy. On the above, we identified the balsamic period during which the berries are richer in active constituents.

MATERIALS AND METHODS

Plant Material

Fleshy red and black capsules of *H. androsaemum* were collected in July–August 2014 from cultivated and wild-growing plants from different localities of central Italy belonging to Emilia-Romagna, Marche, and Abruzzo regions (Table 1). Voucher specimens were authenticated and deposited in the *Herbarium Universitatis Camerinensis* (CAME, included in the online edition of Index Herbariorum c/o School of Biosciences and Veterinary Medicine, University of Camerino, Italy), and archived in the anArchive system for botanical data (anArchive system, <http://www.anarchive.it>).

Reagents and Standards

The analytical standards of polyphenols, hypericin, hyperforin, and ascorbic acid were purchased from Sigma-Aldrich (Milano, Italy) and individual stock solutions and standard working solutions were prepared in methanol. HPLC-grade methanol, acetonitrile, acetone, ethyl acetate ($\geq 99.9\%$) and phosphoric acid were purchased from Sigma-Aldrich (Milano, Italy). HPLC-grade formic acid was supplied by Merck (Darmstadt, Germany). All solvents and solutions were filtered through $0.45\text{-}\mu\text{m}$ PTFE filters purchased from Phenomenex (Bologna, Italy). For antioxidant assays, 1,1-diphenyl-2-picrylhydrazyl radical (DPPH), butylated hydroxytoluene (BHT), 6-hydroxy-2,5,7,8-tetramethylchroman-2-carboxylic acid (Trolox), Tween 20, β -carotene, linoleic acid, sodium hypochlorite, taurine, phosphate buffer saline (PBS),

and potassium iodide were purchased from Sigma-Aldrich-Fluka (Milan, Italy). Potassium hydroxide, hexane and ethanol were purchased from Sigma-Aldrich (Milan, Italy). Supelco 37 Component FAME Mix was purchased from Supelco (Bellefonte, PA, USA). Anhydrous sodium sulfate was purchased from Fluka-Riedel-deHaën (Milano, Italy) and methanol from Panreac Quimica SA (Barcelona, Spain). Deionized water ($>18\text{ M}\Omega\text{ cm}$ resistivity) was obtained from a Milli-Q SP Reagent Water System (Millipore, Bedford, MA, USA).

Preparation of Extracts and Infusions

The fresh fruits of *H. androsaemum* were grinded using liquid nitrogen. The finely powdered material (500 mg) was extracted with 5 mL of methanol by sonication (60 min, at ambient temperature). After centrifugation at 5000 rpm for 10 min, the extracts were transferred to volumetric flask, which was then filled up to 5 mL with extraction solvent. The sample solutions were filtered through a $0.45\text{ }\mu\text{m}$ pore size nylon membrane filter (Phenex, Phenomenex, Torrance, CA, USA) before injection into HPLC-DAD. All samples were stored in a refrigerator at the temperature of 4°C until analysis. Each sample was analyzed in triplicate. For tea preparation (water infusion), 5 g of fresh red and black capsules were treated with boiling water (100 mL), and infused for 15 min. The obtained liquid was then filtered and cooled. The volume was adjusted to 100 mL in a volumetric flask. An aliquot of the infusion was then filtered through a $0.45\text{ }\mu\text{m}$ membrane and used for HPLC analysis. Each sample was analyzed in triplicate.

HPLC-DAD Analysis

Analysis of Polyphenols

HPLC-DAD studies were performed using a Hewlett-Packard HP-1090 Series II (Palo Alto, CA, USA), equipped with a vacuum degasser, a binary pump, an autosampler and a model 1046A HP photodiode array detector (DAD). Chromatographic separation was accomplished on a Synergi Polar-RP C18 ($4.6 \times 150\text{ mm}$, $4\text{ }\mu\text{m}$) analytical column from Phenomenex (Cheshire, UK). The column was preceded by a security cartridge. The mobile phase for HPLC-DAD (diode array detector) analyses was a mixture of (A) water with 0.1% formic acid (v/v) and (B) methanol, flowing at 0.7 mL/min in isocratic conditions: 60% A, 40% B. The injection volume was $5\text{ }\mu\text{L}$. UV spectra were recorded in the range 210–350 nm for 11 compounds, where 210 nm was used for quantification of shikimic acid, gallic acid, (+)-catechin hydrate, (-)-epicatechin; 310 nm for *p*-coumaric acid, and *trans*-resveratrol; 325 for caffeic acid and *trans*-ferulic acid, 3-O-caffeoylequinic acid, 5-O-caffeoylequinic acid, and 3,5-di-O-caffeoylequinic acid.

Analysis of Flavonoids, Hypericin, and Hyperforin

Each extract was chromatographed in reverse phase by an HPLC HP 1090 equipped with an autosampler HP series 1090, ternary pump and DAD detector, following a method previously developed in our research group (Zorzetto et al., 2015). UV/Vis spectra were recorded in the range 210–650 nm, where 210 nm was used for quantification of rutin, hyperoside, isoquercitrin,

TABLE 1 | Main information on the investigated “berry-like” fruits of *Hypericum androsaemum*.

Color	Sample N.	Region	Collection site	GPS coordinates	Altitude (m a.s.l.)	Voucher number ^a	Habitat
Red	1	Emilia Romagna	Il Giardino delle Erbe (Casola Valsenio)	N 44°13'48"; E 11°37'26"	265	CAME 26763	Cultivated
	2	Marche	Torrone (Camerino)	N 43°15'72"; E 13°10'36"	675	CAME 26708	<i>Castanea sativa</i> old coppice
	3	Marche	Paganico (Camerino)	N 43°07'38"; E 13°06'30	620	CAME 26934	<i>Castanea sativa</i> old coppice
Black	4	Marche	University Botanical Garden (Camerino)	N 43°08'06"; E 13°04'09"	638	CAME 26757	Cultivated
	5	Marche	Torrone (Camerino)	N 43°15'72"; E 13°10'36"	675	CAME 26708	<i>Castanea sativa</i> old coppice and conifers reforestation
	6	Marche	Gorgovivo (Serra San Quirico)	N 43°26'01"; E 13°01'05"	160	CAME 26754	<i>Orno-ostryetum</i> s.l. old coppice
	7	Abruzzo	Monte Morrone (Pratola Peligna)	N 42°07'16"; E 13°55'05"	1005	CAME 26755	Between <i>Quercus cerris</i> forest and conifers reforestation

^aCAME, Herbarium Universitatis Camerinensis, School of Biosciences and Veterinary Medicine, Sect. of Botany and Ecology, University of Camerino (Italy).

quercetin, and quercitrin, 270 nm for hyperforin, and 590 nm for hypericin.

Evaluation of Anthocyanins and Betacyanins Occurrence

The freeze-dried powder (1 g) of *H. androsaemum* fruits (sample 4) was extracted at room temperature under stirring, twice with 30 mL of 70% EtOH adjusted to pH 2.0 by HCOOH, over 1 h as total time. The supernatant was filtered, dried under vacuum, and redissolved with 5–10 mL (exactly measured) of the following mixture: acidic water/acetonitrile/methanol 8:1:1, final pH 2.0, giving a red-brownish color. Sample was then directly analyzed by HPLC/DAD (Mulinacci et al., 2008), but the analyses of the chromatographic profile at 520 nm, the wavelength of choice for monitoring of anthocyanins excluded the presence of this class of compounds. Furthermore, an extraction was carried out with ethanol/water 60:40 on the lyophilized sample; the extract obtained was red-brownish, but once again the analyses in HPLC/DAD excluded the presence of betacyanins.

Method Validation

Polyphenols

Calibration curves of the 11 analyzed compounds (linear range 0.5–100 mg/L), correlation coefficient and LODs and LOQs are reported in Table S1. The obtained recoveries for all compounds, evaluated spiking the samples at two different level of concentration (10 and 50 mg/L) with a standard mixture of the 11 compounds, were in the range 92–97 and 99–102%, respectively, with a % RSDs <12% ($n = 5$) in all cases. Retention time stability was utilized to demonstrate the specificity of the HPLC-DAD method. Reproducibility of the chromatographic retention time for each compound was examined five times per day over a 5-day period ($n = 25$). The retention times using this method were stable with a percent RSD value of $\leq 1.89\%$.

Flavonoids, Hypericin, and Hyperforin

Calibration curves of the eight analyzed compounds (linear range 5–100 mg/L), correlation coefficient, LODs, and LOQs

are reported in Table S1. Retention time stability was used to demonstrate the specificity of the HPLC-DAD method. Reproducibility of the chromatographic retention time for each compound was examined five times per day over a 5-day period ($n = 25$). The retention times using this method were stable with a percent RSD value of $\leq 2.52\%$.

Estimation of the Total Amount of Phenolic Compounds and Flavonoids

A modified method of Folin-Ciocalteu, according to Singleton and Rossi (1965) was used for determination of the total amount of phenolics. Seven milliliter of distilled water, 0.5 mL of Folin-Ciocalteu reagent and 0.5 mL of extract (or standard solution of gallic acid) were mixed. After 3 min, 2 mL of 20% Na₂CO₃ were added and incubated in darkness at room temperature for 90 min. The absorbance was measured at 685 nm and the results expressed in mg of gallic acid/kg fresh fruit. All measures were repeated three times and averaged. The flavonoids content was estimated by the AlCl₃ method (Lamaison and Carnat, 1990). One mL of methanol extract solution was added to 1 mL of 2% methanolic AlCl₃ 6H₂O. The absorbance was measured 10 min later at 430 nm comparatively to a rutin standard. The results were expressed as mg rutin/kg fresh fruit. All measures were repeated three times and the results were averaged.

Isolation and Structural Elucidation of the Fruit Pigment

The red berries (20.0 g, sample 2) were exhaustively extracted with ethanol 96% (3 × 250 mL) for 48 h and the extracts were gathered altogether and concentrated under reduced pressure obtaining an aqueous sunspension which was further freeze-dried to recover finally 3.0 g of crude extract. A portion of the crude extract (2.0 g) was subjected to a first column chromatography (CC) on silica gel (60.0 g) using *n*-butanol saturated with water (BuOH/H₂O 82:18 v/v) as eluting system. From this chromatographic run, five compounds were directly identified, i.e., 1,2,3,5-tetrahydroxyxanthone [Fr. 3] (3.9 mg; Trong Tuan et al., 2012), isoquercitrin (Manguro et al., 2003;

Han et al., 2004), and 7-O-glucosyl luteolin (Lu and Foo, 2000; Chung, 2003) in mixture (3:1) [Fr. 4-9] (42.7 mg), chlorogenic acid (Scarpati et al., 1957; Han et al., 2006), and shikimic acid in mixture (2:1) [Fr. 10-68] (98.0 mg; Xiao et al., 2008). A second column chromatography was, later, performed on the assembly of [Fr.10-68] deriving from this first separation using, this time, as eluting system, a mixture of chloroform/methanol at different concentrations also raising the polarity of the solution during the run in order to elute the most polar compounds which, otherwise, would be left attached to the silica gel. The initial concentration of the mixture was $\text{CHCl}_3/\text{MeOH}$ 85:15 v/v and then it was passed respectively to 8:2 v/v, 7:3 v/v, and lastly to 6:4 v/v. From this run, shikimic acid [Fr. 4-25] (40.3 mg; Xiao et al., 2008) and chlorogenic acid [Fr. 39-100] (66.8 mg; Scarpati et al., 1957; Han et al., 2006) were better separated each other. The isolated compounds were identified by comparison of experimental NMR spectra with literature data and/or direct comparison with pure compounds available in our laboratory. NMR spectra were recorded on a Varian Mercury 300 MHz and/or on a Bruker Avance II 400 MHz instrument using CDCl_3 , CD_3OD , or D_2O as deuterated solvents; the chemical shift was expressed in ppm from TMS. MS spectra were performed on a Q-TOF MICRO spectrometer (Micromass, now Waters, Manchester, UK) equipped with an ESI source, that was operated in the negative and/or positive ion mode. The flow rate of sample infusion was $10 \mu\text{L}/\text{min}$ with 100 acquisitions per spectrum. Data were analyzed using the MassLynx software developed by Waters.

1,2,3,5-tetrahydroxyxanthone: ^1H NMR (300 MHz, CD_3OD) δ : 7.92 (1H, d, $J = 7.8 \text{ Hz}$, H-8), 7.63 (1H, m, H-7), 7.44 (1H, d, $J = 7.8 \text{ Hz}$, H-6), 6.33 (1H, s, H-4). ESI-MS: m/z [M-H] $^-$ 259.07.

isoquercitrin: ^1H NMR (300 MHz, CD_3OD) δ : 7.89 (1H, s, H-2'), 7.67 (1H, d, $J = 8.0 \text{ Hz}$, H-6'), 6.82 (1H, d, $J = 8.0 \text{ Hz}$, H-5'), 6.46 (1H, br s, H-8), 6.17 (1H, br s, H-6), 5.15 (1H, d, $J = 7.6 \text{ Hz}$, H-1''), 3.96 (1H, d, $J = 12.0 \text{ Hz}$, H-6 α''), 3.74 (1H, dd $J = 12.0, 5.8 \text{ Hz}$, H-6 β''). ESI-MS: m/z [M+Na] $^+$ 486.87.

7-O-glucosyl luteolin: ^1H NMR (300 MHz, CD_3OD) δ : 7.39 (1H, br s, H-2'), 7.58 (1H, br s, H-5'), 7.07 (1H, d, $J = 8.5 \text{ Hz}$, H-6'), 6.87 (1H, s, H-6), 6.46 (1H, br s, H-8), 5.34 (1H, d, $J = 5.4 \text{ Hz}$, H-1''). ESI-MS: m/z [M+K] $^+$ 486.95.

chlorogenic acid: ^1H NMR (CD_3OD a 300 MHz) δ : 7.57 (1H, d, $J = 15.9 \text{ Hz}$, H-10), 7.03 (1H, br s, H-12), 6.93 (2H, m, H-15 to H-16), 6.28 (1H, d, $J = 15.9 \text{ Hz}$, H-9), 5.35 (1H, m, H-3), 4.37 (1H, m, H-4), 3.67 (1H, m, H-5), 2.37-1.86 (4H, m, H-2 to H-6). ESI-MS: m/z [M+Na] $^+$ 376.98; m/z [M-H] $^-$ 353.21.

shikimic acid: ^1H NMR (300 MHz, CD_3OD), δ : 6.63 (1H, m, H-2), 4.32 (1H, br t, $J = 3.9 \text{ Hz}$, H-3), 3.94 (1H, ddd, $J = 7.6, 6.3, 5.2, \text{ Hz}$, H-5), 3.59 (1H, dd, $J = 7.6, 3.9 \text{ Hz}$, H-4), 2.77 (1H, dd, $J = 17.7, 5.2 \text{ Hz}$, H-6 α), 2.18 (1H, dd, $J = 17.7, 6.3, \text{ Hz}$ H-6 β). ESI-MS: m/z [M-H] $^-$ 173.11.

Determination of the Antioxidant Activity

1,1-diphenyl-2-picrylhydrazyl (DPPH)

Radical-Scavenging Activity

The antiradical activity was determined by the DPPH radical-scavenging method (Peterson et al., 2002). Each sample was mixed with $900 \mu\text{L}$ of 100 mM Tris-HCl buffer, pH 7.4, and then added to 1 mL of 0.5 mM DPPH in methanol ($250 \mu\text{M}$ in

the reaction mixture). The control sample was prepared using methanol. Trolox was employed as a standard antioxidant to examine the radical-scavenging activities. Absorbances of the mixtures were measured at 517 nm. The activity was calculated as IC_{50} . All tests and analyses were run in triplicate and averaged.

β -Carotene/Linoleic Acid Assay

In this assay, the antioxidant capacity was determined by measuring the inhibition of the volatile organic compounds and the conjugated diene hydroperoxides arising from linoleic acid oxidation (Dapkevicius et al., 1998). A stock solution of β -carotene/linoleic acid mixture was prepared as follows: 0.5 mg of β -carotene was dissolved in 1 mL of chloroform, then $25 \mu\text{L}$ of linoleic acid and 200 mg of Tween 40 were added. Then, 100 mL distilled water saturated with oxygen (30 min, 100 mL/min) was added; 2.5 mL of this reaction mixture were dispensed into test tubes and $100 \mu\text{L}$ portions of variable concentrations of the samples were added; the emulsion system was incubated for up to 48 h at 37°C . The same procedure was repeated with the synthetic antioxidant butylated hydroxytoluene (BHT) and Trolox as positive controls, and the blank. After incubation, absorbances of the mixtures were measured at 490 nm. The activity was calculated as IC_{50} . All tests and analyses were run in triplicate and averaged.

Hypochlorous Acid Scavenging (HOCl)

The amount of HOCl was measured by the chlorination of taurine (Weiss et al., 1982). One hundred microliters of sodium hypochlorite (600 mM) were added to $100 \mu\text{L}$ of taurine (150 mM) and $100 \mu\text{L}$ of variable concentrations of sample in PBS at pH 7.4. Absorbance was measured at 350 nm after the addition of $100 \mu\text{L}$ of 2 M potassium iodide. The activity was calculated as IC_{50} . Trolox was used as the positive control. All tests and analyses were run in triplicate and averaged.

Cytotoxic Activity

A375 (human malignant melanoma cells) and MDA-MB 231 cells (human breast adenocarcinoma cells) were cultured in Dulbecco's Modified Eagle's Medium (DMEM) with 2 mM L-glutamine, 100 IU/mL penicillin, 100 $\mu\text{g}/\text{mL}$ streptomycin, and supplemented with 10% heat-inactivated fetal bovine serum (HI-FBS). HCT116 cells (human colon carcinoma cells), were cultured in RPMI1640 medium with 2 mM L-glutamine, 100 IU/mL penicillin, 100 $\mu\text{g}/\text{mL}$ streptomycin, and supplemented with 10% HI-FBS. Cells medium and solutions were from PAA Laboratories GmbH, Austria. Cells were cultured in a humidified atmosphere at 37°C in presence of 5% CO_2 . The MTT assay was used as a relative measure of cell viability. Cell-viability assays were carried out as described (Quassinti et al., 2013). Briefly, cells were seeded at the density of 2×10^4 cells/mL. After 24 h, samples were exposed to different concentrations of *H. androsaemum* fruits methanolic extracts (1.56–200 $\mu\text{g}/\text{mL}$). Cells were incubated for 72 h in a humidified atmosphere of 5% CO_2 at 37°C . Cisplatin (Sigma) was used as the positive control. At the end of incubation, each well received $10 \mu\text{L}$ of 3-(4,5-dimethyl-2-thiazolyl)-2,5-diphenyl-2H-tetrazoliumbromide (MTT) (5 mg/mL in phosphate-buffered

saline, PBS) and the plates were incubated for 4 h at 37°C. The extent of MTT reduction was measured spectrophotometrically at 540 nm using a Titertek Multiscan microElisa (Labsystems, FI-Helsinki). Experiments were conducted in triplicate. Cytotoxicity is expressed as the concentration of berries extract inhibiting cell growth by 50% (IC_{50}). The IC_{50} values were determined with GraphPad Prism 4 computer program (GraphPad Software, S. Diego, CA, USA).

Immunomodulatory Activity

Peripheral blood mononuclear cell (PBMC) proliferation assay was performed by flow cytometry on pig lymphocytes isolated from fresh heparinized blood samples (20 mL/pig).

The blood donors (Danish pigs, weighing 80–90 kg) were conventionally reared in a hilly area of Umbria (Rustici Farm, Parco del Subasio, Assisi, Italy) and the same were not subjected to none experimental protocol. For this reason this study is exempt from the ethics committee approval (DL 2014/26, Art. 2, comma 1,f). However, the blood samplings have been collected (only one time) with the farmer's consent, handling the animals in accordance with the recommendations of the Directive 2010/63/EU of the European Parliament and of the Council of the European Union for the protection of animals used for scientific purposes. The number of live lymphocytes, suspended in complete RPMI-1640 medium (Euroclone[®]) that contained 10% heat-inactivated pig serum, L-glutamine (2 mM; Euroclone[®]), penicillin (100 U/mL; Biochrom^{AG}, Berlin), and streptomycin (100 µg/mL; Biochrom^{AG}, Berlin), was determined using a counting chamber and a trypan blue dye exclusion procedure. The final concentration of live cells was adjusted to 2×10^6 /mL in complete medium and 100 µL of suspension/well (2×10^5 live cells) were dispensed in flat bottom 96-well tissue culture plates (Becton Dickinson, Lincoln Park, NJ). For the measurement of cell proliferation, the PBMC were prestained with carboxyfluorescein diacetate succinimidyl ester (CFSE) cell tracer (BioLegend, San Diego, CA) and cultured for 5 days at 37°C in 5% CO₂. Proliferation stimuli were 1 µg/mL of pokeweed mitogen (PWM, it stimulates the B lymphocyte only in the presence of T cells; Sigma-Aldrich) or 1.2 µg/mL of phytohemagglutinin (PHA, a polyclonal T-cell activator; Biochrom^{AG}, Berlin) in presence or absence of different dilutions of methanolic extract from red berries. The first assay was conducted analysing three different concentrations of red berries methanolic extract, starting from its IC_{50} higher dosage (i.e., 20, 10, and 6 µg/mL, respectively). The second assay was conducted further analyzing lower concentrations of *H. androsaemum* extract (i.e., 1.2, 0.8, and 0.4 µg/mL, respectively). Each culture condition was repeated in triplicate. The fruit extract was initially diluted 1:100 (v/v) in ethanol, and further dilutions were made in HBSS (Gibco[®], Life Technologies Italia). Finally, medium volume was adjusted to 200 µL/well. A negative control was represented by PBMC cultured without any mitogen/activator (CTR), so that the base proliferation could be estimated (Liu et al., 1996). With each cell division, the intensity of CFSE staining is reduced of a half and lymphocyte proliferation is calculated as frequency of CFSE^{low} cells within gated cell population compared to intensity of parent population. Flow cytometry

analyses were performed on a standard FACSCalibur™ flow cytometer (Becton Dickinson, Mountain View, CA) operated by the CELLQuestPro™ software. Within a tight lymphocyte gate, 10,000 cells were acquired and the data were saved in the list mode. Cells from each culture condition were pooled and analyzed together. The percentage of increased proliferation vs. the basal values (PI) were calculated by the following formula:

$$(B - A)/A * 100$$

where, B is represented by the percentage of proliferation obtained by cells stimulated with the mitogen/activator ± fruit extract (the CTR-B was stimulated only with fruit extract), whereas A is represented by the percentage of proliferation obtained by cells stimulated or not (CTR) with the mitogen/activator, without fruit extract.

RESULTS AND DISCUSSION

Analysis of Polar Constituents in *H. androsaemum* Fruit and Infusions

From the analysis of *H. androsaemum* fruits methanolic extracts performed with the first method developed, we identified and quantified simultaneously 11 compounds, mainly polyphenols, i.e., shikimic acid, gallic acid, catechin hydrate, epicatechin, *p*-coumaric acid, *trans*-resveratrol, caffeoic acid, *trans*-ferulic acid, chlorogenic acid, neochlorogenic acid, and 3,5-di-O-caffeoquinic acid, meanwhile with the second method, we identified and quantified simultaneously seven compounds among flavonoids naphtodianthrones and phloroglucinols, i.e., rutin, quercetin, quercitrin, isoquercitrin, hyperoside, hypericin, and hyperforin.

In Table 2, the quantitative determination of the 18 analyzed compounds in the seven *H. androsaemum* fruit samples and in two infusions obtained from red and black "berry-like" capsules is reported. Shikimic acid, chlorogenic acid, rutin, and hyperoside, were present in all samples analyzed meanwhile neochlorogenic acid and isoquercetrin were not found only in black sample 5. Catechin was present only in the three red samples analyzed and in one black fruit sample (7), while epicatechin was present in the three red fruits but also in one black sample (6), even if in a very low concentration. Shikimic acid was found at high levels in all samples, ranging from 0.805 to 12.799 mg/g dry weight. It was found in higher concentration in red fruits (8.187–12.799 mg/g) than in black ones (0.805–5.988 mg/g). This compound is the biosynthetic precursor of aromatic amino acids and phenolic compounds and is endowed with important biological properties such as antiviral, anti-inflammatory, antiplatelet aggregation, and prevention of brain damage after ischemia. Shikimic acid was never reported in *H. androsaemum* leaves in previous studies.

Chlorogenic acid was the second most abundant fruit constituent, ranging from 0.099 to 14.553 mg/g. The lowest amount was detected in black fruit (0.099 mg/g in sample 5) and the highest amount in the three red fruit samples, i.e., 14.553 mg/g in sample 1, 7.035 mg/g in sample 2, and 6.811 mg/g in sample 3. The high levels of chlorogenic acid found in this

TABLE 2 | Quantitative determination of the analyzed compounds in six *H. androsaemum* fruit samples (mg/g dry weight) and in two infusions (mg/L) obtained from red and black “berry-like” capsules; relative standard deviations were in a range from 0.10 to 5.88 (*n* = 3).

Constituent (mg/g dry fruit)	Fruits (mg/g)							Infusion (mg/L)	
	Red			Black				Red (2)	Black (5)
	1	2	3	4	5	6	7		
Shikimic acid	12.799	10.203	8.187	1.235	1.182	0.805	5.988	208.0	29.5
Gallic acid	nd	nd	nd	nd	0.044	nd	0.032	nd	4.6
Caffeic acid	nd	nd	nd	nd	nd	nd	nd	nd	nd
Cumaric acid	nd	nd	nd	nd	nd	nd	nd	nd	nd
Ferulic acid	nd	nd	nd	nd	nd	nd	0.123	15.0	nd
Chlorogenic acid	14.553	7.035	6.811	2.029	0.099	0.441	0.887	422.0	8.4
Neochlorogenic acid	6.587	0.662	0.122	0.312	nd	0.008	0.035	nd	0.6
3,5-dicaffeoylquinic acid	0.208	0.340	nd	nd	nd	nd	nd	nd	nd
Catechin	0.114	0.063	0.083	nd	nd	nd	0.068	nd	23.2
Epicatechin	0.521	0.680	0.300	nd	nd	0.001	nd	25.0	nd
Rutin	0.233	0.662	0.008	0.039	0.014	0.023	0.011	27.0	nd
Hyperoside	0.662	0.053	0.004	0.247	0.015	0.012	0.029	21.6	nd
Isoquercetin	0.179	0.106	0.004	0.078	nd	0.007	0.063	8.76	nd
Quercitrin	nd	0.113	0.017	nd	0.005	0.012	0.132	9.38	3.57
Quercetin	nd	nd	nd	nd	nd	nd	nd	nd	nd
Resveratrol	nd	nd	nd	nd	nd	nd	nd	nd	nd
Hyperforin	nd	nd	nd	nd	nd	nd	nd	nd	nd
Hypericin	nd	nd	nd	nd	nd	nd	nd	nd	nd

nd, not detected.

study are of great interest for a potential application of the berries of *H. androsaemum* as a functional food. Chlorogenic acid is a hydroxycinnamic acid derivative widespread in plants, fruits and vegetables, among which coffee beans are the main source. This compound has attracted attention of nutritionists because it has been proven to inhibit carcinogenesis, to protect against oxidative stress, to improve the glucose metabolism, to reduce the risk of cardiovascular disease, and to exhibit anti-obesity effects (Cho et al., 2010). Moreover, its abundance may also confirm the traditional uses of the plant as a wound healing agent (Allen and Hatfield, 2004). In fact, Chen et al. (2013) have demonstrated that topical application of chlorogenic acid can accelerate the process of excision wound healing by its ability to increase collagen synthesis through up-regulation of key players such as tumor necrosis factor- α and transforming growth factor- β 1 in different phases of wound healing as well as by its antioxidant potential. Among the other compounds of chlorogenic acid family, neochlorogenic acid was quite abundant, ranging from 0.008 to 6.587 mg/g in the seven fruit samples. The lowest amount was detected in black fruits (sample 6) and the highest in red fruits (sample 1). Instead, 3,5-dicaffeoylquinic acid was only present in red fruits (0.208 mg/g in sample 1 and 0.340 mg/g in sample 2). The concentrations of the caffeoylquinic acids found in the berries extracts were slightly lower with respect to those reported for water infusions of leaves (Valentão et al., 2004). In particular the latter showed neochlorogenic acid more abundant than chlorogenic acid, and high level of quercetin, which instead was missing in berries.

As mentioned above, catechin was present only in the three red fruits analyzed, ranging from 0.066 mg/g in sample 2 to 0.114 mg/g in sample 1, and in one sample (7) of black fruits (0.068 mg/g). Epicatechin amounts ranged from 0.001 mg/g in black fruits (sample 6) to 0.680 mg/g in red fruits (sample 2). The highest levels of these two flavanols, which are believed to possess strong antioxidant activity, were comparable with those previously found in the leaves (Dopico-Garcia et al., 2011).

Among flavonoids, rutin was abundant in red fruits, ranging from 0.008 in sample 3 to 0.662 mg/g in sample 2. On the contrary, it was present in low amount in black fruits, ranging from 0.011 in sample 7 to 0.039 mg/g in sample 4. Although high, these levels were lower than those reported in other *Hypericum* species such as *H. perforatum* (4.25–9.23 mg/g), and *H. hyssopifolium* (12.42 mg/g), both growing in central Italy (Sagrati et al., 2008). This flavonoid was not reported in leaves of *H. androsaemum*.

Also hyperoside and isoquercitrin were present at high levels in red fruits, especially in sample 1 (0.662 and 0.179 mg/g, respectively), and in sample 2 (0.053 and 0.106 mg/g, respectively). These metabolites were already detected in leaves, although in trace amounts (Valentão et al., 2002). By the way, their levels were lower with respect to those found in other species belonging to the sect. *Androsaemum* like *H. grandifolium* (1.7 mg/g) and *H. hircinum* (1.3 mg/g; Bonkanka et al., 2008; Sagrati et al., 2008).

Quercitrin was found in two red fruit samples, such as sample 2 (0.113 mg/g) and sample 3 (0.017 mg/g), and in three black fruit

samples, such as sample 5 (0.005 mg/g), sample 6 (0.012 mg/g), and sample 7 (0.132 mg/g). Also this compound was never detected in *H. androsaemum* leaves.

The HPLC-DAD method employed did not allow to detect both hypericin and hyperforin in the *H. androsaemum* fruits. The absence of hypericin, and of naphtodianthrones in general, is supported by the lack of black nodules which are the secretory structures storing naphtodianthrones. As a matter of fact, hypericin was never detected in the whole plant as well (Kitanov, 2001). Regarding hyperforin, other studies confirmed its absence from *H. androsaemum* (Aziz et al., 2006).

The performed analysis clearly showed that red fruits contained more constituents and in higher amount with respect to black ones, although some differences among samples according to the geographical origin were evidenced (Table 2). Samples 1, 2, and 3 of red fruits contained 9, 10, and 9 of the investigated analytes, respectively. Among black fruits, sample 7 was the richer with seven compounds. Overall, the fruits of *H. androsaemum* showed to be a rich source of shikimic acid. Moreover, they were richer in chlorogenic acid and poorer in neo-chlorogenic acid with respect to leaves previously analyzed (Valentão et al., 2004), while they lack quercetin which instead was found as the most abundant flavonoid in leaves (Dopico-Garcia et al., 2011). On the other hand, fruits showed levels of the flavanols catechin and epicatechin comparable to those of leaves (Dopico-Garcia et al., 2011).

From the analyses of the two infusions obtained from red and black “berry-like” capsules, it emerged that the former contained a high number of the investigated analytes (8 out of the 18 monitored) and at a quite high level (Table 2). In fact, the infusion obtained from red fruits was rich in chlorogenic acid (422 mg/L) and shikimic acid (208 mg/L), followed by rutin (27 mg/L), epicatechin (25 mg/L), and hyperoside (21.6 mg/L), while ferulic acid, quercitrin, and isoquercitrin were found at low concentrations (≤ 15 mg/L). On the other hand, the infusions obtained from black berries contained a lower number of the investigated analytes (6 out of 18 compounds) and in a very low level (< 30 mg/L). In black berries infusion shikimic acid was the most abundant compound with a concentration of 29.5 mg/L. Surprisingly, catechin but not epicatechin was detected (23.2 mg/L). Overall, the analysis of infusions supported those performed on methanolic extracts and confirmed that red berries of *H. androsaemum* are to be preferred to black ones as a source of shikimic acid and phenolic compounds. The level of chlorogenic acid found in the infusion from red berries is particular interesting, since the concentration (422 mg/L) was comparable to that obtained in a cup of espresso coffee (Caprioli et al., 2013), in which it ranged from 394.9 to 555.8 mg/L, depending on the different ways of preparation. Also when compared with berry fruits such as blueberries, blackberries, and raspberries, tutsan fruits showed higher levels of chlorogenic acids (Clifford, 1999).

Determination of the Fruit Pigment

The chromatographic separation of the ethanolic extract obtained from the red berries of *H. androsaemum* confirmed that chlorogenic and shikimic acids were the most abundant polar

compounds. On the other hand, among the minor components we evidenced several molecules with aromatic structure such as glycosidic flavonoids (i.e., isoquercitrin and 7-O-glucosyl luteolin) and a xanthone never reported before in *Hypericum* species. The latter was identified as 1,2,3,5-tetrahydroxyxanthone (Figure 1), and its presence in *H. androsaemum* could be of taxonomic interest. This compound was previously found in *Polygala karensium* (Trong Tuan et al., 2012), a species belonging to Polygalaceae family. Previously, hydroxy and methoxy substituted xanthones were isolated from roots of *H. androsaemum* (Nielsen and Arends, 1979), while in calli and suspended cells cultures of the same species 1,3,5,6 and 1,3,6,7 oxygenated xanthones (Dias et al., 2000), along with prenylated xanthone aglycones and their glucosides were characterized (Schmidt et al., 2000). Therefore, the occurrence of this xanthone in the genus *Hypericum* is remarkable. Although xanthones are less abundant in the genus *Hypericum* and more in general in nature in comparison with other phenolic compounds, they showed several biological properties, such as strong and selective inhibition of MAO-A, *in vitro* toxicity, *in vivo* antitumor activity, as well as anti-inflammatory, antibacterial, and antifungal activities (Demirkiran, 2007).

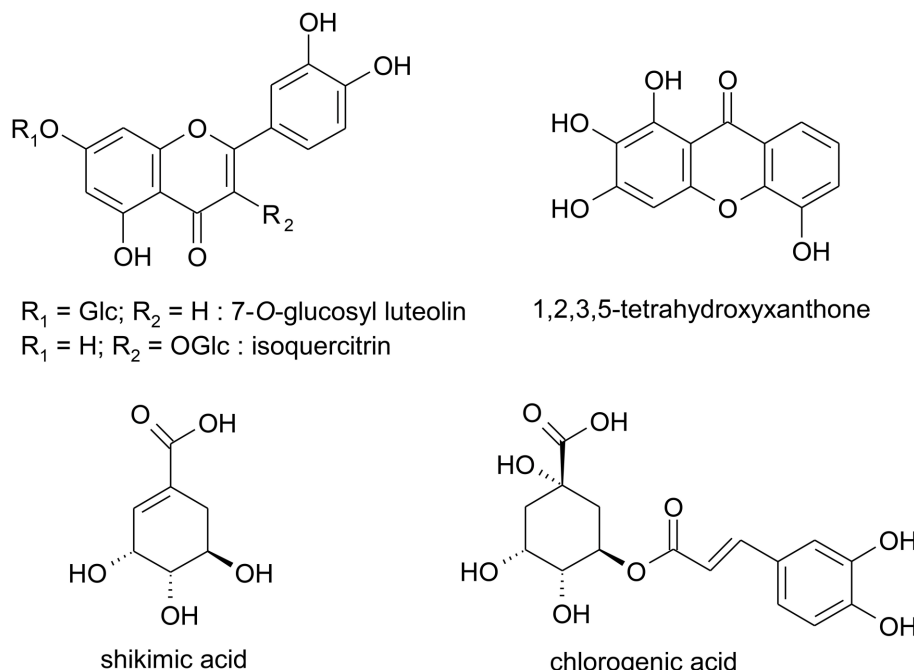
The presence of mixture of all these aromatic compounds (i.e., flavonoids and xanthone) in the fruit pericarp, may contribute to the observed color of the fleshy capsule and extracts of *H. androsaemum*.

Determination of Total Phenolics and Flavonoids Content, and of Antioxidant Capacity of *H. androsaemum* Berries

The methanolic extracts from berries of *H. androsaemum* in almost all cases exhibited a significant high content in phenolics ranging from 1448 mg gallic acid equivalent (GAE)/kg in black fruits (sample 5) to 8530 mg GAE/kg in red berries (sample 2; Table 3). Much higher was the phenol content in tea infusions, with values of 8744 mg GAE/kg for black berries and, more important, of 18145 mg GAE/kg for red berries. The total phenols and the total flavonoids were “extracted” better with an infusion procedure than with a methanolic extraction. Therefore, the red fruits showed higher amounts of phenols and flavonoids than black ones, i.e., ripening lowered the phenolic content.

On the basis of classification of fruits and vegetables depending on the total phenolic content, namely high (> 2000 mg GAE/kg), medium (1000–2000 mg GAE/kg) and low (< 1000 mg GAE/kg), the examined samples of berries fruits took place mainly in the first group. Interestingly, in almost all cases the total phenolic content of tutsan berries was higher than that of strawberry (1127 mg GAE/kg), mandarin (1161 mg GAE/kg), blueberry (2196 mg GAE/kg), and sour cherry (2560 mg GAE/kg; Dragović-Uzelac et al., 2009).

The chemical complexity of the extracts or infusions, often mixtures of many compounds with differences in functional groups, polarity, and chemical behavior, could lead to scattered results, depending on the antioxidant test employed. Therefore, an approach with multiple assays in screening work is highly advisable. The *H. androsaemum* berries were screened for

FIGURE 1 | Structures of polar compounds isolated from the red berries of *Hypericum androsaemum*.TABLE 3 | Antioxidant activity, total phenols, and total flavonoids in methanolic extracts and infusions of red and black berries of *H. androsaemum*.

Sample	Color	DPPH $\mu\text{g/mL}$	Linoleic Test $\mu\text{g/mL}$	Hypochlorous acid $\mu\text{g/mL}$	Total Phenols mg gallic acid Eq/kg fw	Total Flavonoids mg rutin Eq/kg fw
METHANOLIC EXTRACTS						
2	Red	27.7 \pm 2.5bc*	11.7 \pm 1.1bc	45.5 \pm 4.1e	8530 \pm 773b	1748 \pm 158d
3	Red	29.5 \pm 2.5cd	21.3 \pm 1.8f	9.5 \pm 0.8a	2158 \pm 186a	1289 \pm 111c
4	Black	33.9 \pm 2.3cd	9.6 \pm 0.7bc	20.1 \pm 1.4bc	3114 \pm 215a	676 \pm 46ab
5	Black	32.1 \pm 2.8cd	13.0 \pm 1.1cd	16.9 \pm 1.5b	1448 \pm 126a	367 \pm 32a
7	Black	36.5 \pm 3.0d	23.7 \pm 2.0f	23.3 \pm 1.9c	2317 \pm 194a	960 \pm 80bc
INFUSIONS						
2	Red	21.4 \pm 1.8b	7.9 \pm 0.7b	37.0 \pm 3.1d	18145 \pm 1510c	2463 \pm 205e
5	Black	52.8 \pm 4.5e	17.1 \pm 1.5e	10.6 \pm 0.9a	8744 \pm 738b	1140 \pm 96c
POSITIVE CONTROL						
Trolox		6.3 \pm 0.6a	16.6 \pm 1.5de	10.6 \pm 1.0a		
BHT			3.4 \pm 0.3a			

*Values within a column for each sample having different letters are significantly different from each other using Tukey's LSD test ($p < 0.05$).

their possible antioxidant activity by three non-enzymatic test systems: 1,1-diphenyl-2-picrylhydrazyl (DPPH) radical-scavenging, β -carotene/linoleic acid assay, and hypochlorous acid scavenging (HOCl). All methanolic extracts and tea infusions of berry-like fruits of *H. androsaemum* showed a significant radical scavenging activity with IC_{50} values in the range 21.4–52.8 $\mu\text{g/mL}$ (Table 3). Methanolic extracts displayed similar inhibition on DPPH. Compared with activity of Trolox, the methanolic extracts showed an activity only 4.4–5.8 lower than that of the positive control. Water infusion from red berries was by far the most active with an IC_{50} value of 21.4 $\mu\text{g/mL}$, only 3.4 times higher than that of Trolox. This activity seemed to be

related to the higher content of total phenolics (18145 mg GA Eq/kg).

The antioxidant activity of tutsan berries was evaluated by the β -carotene-linoleic acid test, using BHT as positive control. For the methanolic extracts we obtained IC_{50} values in the range 9.6–23.7 $\mu\text{g/mL}$ which were 2.8–6.9 times higher than that of BHT. This activity did not depend on the ripening rate, but appeared to be correlated to the different geographic origin of the samples. Instead, water infusions displayed the same kind of inhibition seen on DPPH, with those prepared with red berries (IC_{50} value of 7.9 $\mu\text{g/mL}$) being more active than those made with black berries (IC_{50} value of 17.1 $\mu\text{g/mL}$). Opposite situation was found

in the hypochlorous acid test where methanolic extracts showed in almost all cases a more potent scavenging activity (IC_{50} values in the range 9.5–45.5 $\mu\text{g/mL}$) with respect to the infusion made with red berries (IC_{50} value of 37.0 $\mu\text{g/mL}$). On the contrary, the black berries tea exhibited a good activity with an IC_{50} value of 10.6 $\mu\text{g/mL}$ (Table 3).

H. androsaemum is a medicinal plant species containing many polyphenolic compounds, namely flavonoids, and phenolic acids and traditionally employed in the preparation of an infusion used for its diuretic and hepatoprotective activities (Valentão et al., 2004). A previous report investigated the ability of *H. androsaemum* leaf infusion to act as a scavenger of reactive oxygen species (superoxide radical, hydroxyl radical, and hypochlorous acid). The tested infusion mainly exhibited a potent scavenging effect on superoxide radicals, although a non-competitive inhibitory effect on xanthine oxidase was also observed. The infusion also acted as a moderate scavenger of hydroxyl radicals and hypochlorous acid (Valentão et al., 2002). Also our results supported the use of *H. androsaemum* in folk medicine to prepare teas with diuretic and antihepatotoxic activities.

Cytotoxic Activity

The cytotoxic activity of methanolic extracts of *H. androsaemum* fruits were evaluated on tumor cell lines by MTT assay. Three human cell lines, a malignant melanoma cell line (A375), a breast adenocarcinoma cell line (MDA-MB 231), and colon carcinoma cell line (HCT116), were treated with different concentrations of extracts for 72 h. As shown in Table 4, extracts were active against all three tumor cell lines tested and induced a concentration-dependent inhibitory effect in the dilution range 1.56–200 $\mu\text{g/mL}$. Results showed that the highest activity was observed on HCT116 cell line, with a IC_{50} value of 8.40 $\mu\text{g/mL}$ for black berries extract, while red berries extract resulted less active on all cell lines tested (IC_{50} values in the range 19.40–32.29 $\mu\text{g/mL}$). Analysis of secondary metabolites put in evidence the presence of polyphenols, especially shikimic acid, chlorogenic acid, neochlorogenic acid, and 3,5-di-O-caffeoquinic acid as the main components of fruit methanolic extracts. Chlorogenic acid is reported cytotoxic on human oral tumor cell lines but at high concentrations (HSG, HSC-2, and HGF; IC_{50} values of 1.4, 1.3, and 2.3 mM, respectively; Jiang et al., 2000). The same low cytotoxic activity was reported for shikimic acid on CHO, 3T3, and NRK cell lines (Ngomuo and Jones, 1996). 3,5-Dicaffeoylquinic acid inhibited proliferation in a dose-dependent manner as detected by MTT assays using Hela cells (Hu et al., 2014). Also flavonoids present in fruit extracts as catechin, epicatechin, and rutin were able to inhibit MDA-MB 231 and HCT116 proliferation at concentrations higher than 100 μM (Hayes et al., 2006; Li et al., 2009). Quercitrin has antiproliferative and apoptotic effect on colon cancer cells (Cincin et al., 2015). Given the cytotoxic properties reported in literature for xanthones (Bennet and Lee, 1989; Vieira and Kijjoa, 2005; Demirkiran, 2007), 1,2,3,5-tetrahydroxyxanthone may also contribute to the final effect observed on tumor cells. Our data confirm the properties of *H. androsaemum* to inhibit the proliferation of colon tumor

TABLE 4 | Cytotoxicity on tumor cells of the methanolic extracts from *H. androsaemum* berries.

Extracts	Cell line (IC_{50} $\mu\text{g/mL}$) ^a		
	A375 ^b	MDA-MB 231 ^c	HCT116 ^d
Black berries	19.31	12.88	8.40
95% C.I. ^e	18.77-19.86	12.33-13.45	8.07-8.74
Red berries	32.29	30.05	19.40
95% C.I. ^e	31.45-33.16	26.77-33.74	18.43-20.42
POSITIVE CONTROL			
Cisplatin	0.38	2.57	2.42
95% C.I. ^e	0.31-0.47	2.23-3.05	2.08-2.91

^a IC_{50} = The concentration of compound that affords a 50% reduction in cell growth (after 72 h of incubation).

^b Human malignant melanoma cell line.

^c Human breast adenocarcinoma cell line.

^d Human colon carcinoma cell line.

^e Confidence interval.

cell lines as reported by Xavier et al. (2012). Aqueous extract of *H. androsaemum* leaves, tested on two human colon cancer-derived cell lines, HCT15 and CO115, inhibits proliferation and induced apoptosis through MAP kinases and PI3K/Akt pathway. The phenolic components of the *H. androsaemum* fruits methanolic extracts could explain the cytotoxic activity on tumor cells. Although polyphenols are generally recognized as antioxidants, they also act as prooxidants inducing DNA degradation in the presence of metal ions such as copper. Copper-dependent prooxidant mechanism of action of polyphenols accounts for their observed chemopreventive properties, as also for their preferential cytotoxicity toward cancer cells (Khan et al., 2012).

In accordance with the US NCI criterion of anticancer activities (Boik, 2001), the *H. androsaemum* berries extracts may be considered as a potential source of cytotoxic drug, as they showed IC_{50} values below 20 $\mu\text{g/mL}$.

Immunomodulatory Activity

The immunomodulatory activity of *H. androsaemum* red berries was evaluated by the *in vitro* proliferation assay of pig's PBMC which were stimulated with decreasing dilutions of red berries extract. In the first experiment, the two higher concentrations of red berries methanolic extracts tested (20 and 10 $\mu\text{g/mL}$, respectively), after 5 days of culture, revealed a cytotoxic effect that destroyed all the cells. Whereas, as shown in Figure 2, an immunomodulatory effect started to be seen by using concentrations from 6 to 0.4 $\mu\text{g/mL}$.

Indeed, at the latter concentrations, while the addition of fruit extract to the unstimulated cells continued to elicit an inhibitory/cytotoxic (apoptosis has not been investigated in this study) effect on their proliferation, on the cells activated by PHA and PWM, the fruit extract elicited an increased proliferation response.

The dosage of 6 $\mu\text{g/mL}$ of fruit extract gave the highest proliferative response on cells co-stimulated by PWM, possibly B cells. However, by decreasing the dosage of *H. androsaemum*

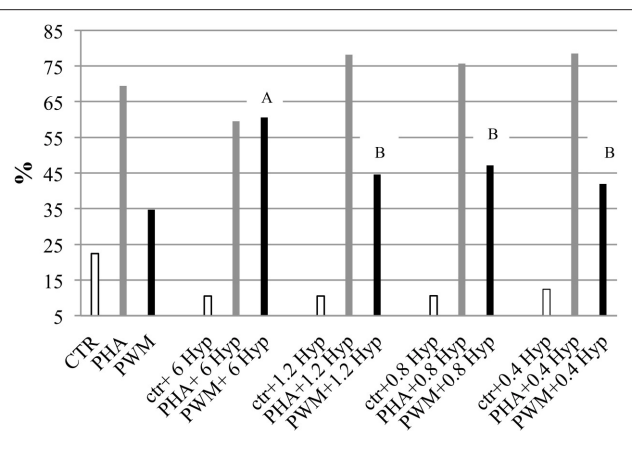


FIGURE 2 | Pig peripheral blood mononuclear cells (PBMC) proliferation assay monitored by CFSE labeling in response to *in vitro* stimulation with different dosage of *H. androsaemum* methanolic fruit extracts (expressed in $\mu\text{g}/\text{mL}$) \pm mitogen or activator. Data are shown as means (standard error: 6.27) and it was observed a significant effect of interaction between mitogen/activator and fruit extract dosages ($P < 0.006$). A,B: different letters denote the significant differences of increased proliferation vs. the basal values (CTR, PHA, and PWM cells cultured without fruit extracts, but only mitogen/activator) obtained by adding different concentrations of *H. androsaemum* methanolic fruit extracts, $P < 0.005$.

fruits, the cells co-stimulated by PHA too increased their proliferation responses vs. control ones (CTR + PHA). The polyclonal activator of T cells (PHA) induced the higher PBMC proliferation response when combined with the lower fruit extract dosages investigated. Although, the treatment (different fruit extract concentrations) did not show a significant effect on the mean percentages resulted by the proliferative assay, a significant interaction between fruit extract dosage and mitogen/activator was observed ($P < 0.01$). Indeed, the PI of cells stimulated with PWM and 6 $\mu\text{g}/\text{mL}$ of *H. androsaemum* extract was significantly higher than those obtained by cells cultured with PWM and 1.2, 0.8, and 0.4 $\mu\text{g}/\text{mL}$ of fruit extract, respectively.

At the dosage of 6 $\mu\text{g}/\text{mL}$, the methanolic extract of red berries seemed to induce an immune deviation from cellular immunity to humoral responses that has been already observed by other authors in mice treated with hydroalcoholic extract of *H. perforatum* (Abhtai Froushani et al., 2015). The observed results may be correlated with the high levels of shikimic acid found in red berries. Shikimic acid was found effective, even in low doses, in the modulation of leukocyte activity (Bertelli et al., 2008). This compound, either alone or in combination with quercitin, was able to modulate the release of IL-6 and IL-8 from PBMCs. Since xanthones are molecules capable to modulate anti-inflammatory and anti-bacterial activities (Bennet and Lee, 1989), also the presence of 1,2,3,5-tetrahydroxyxanthone in the fruits of *H. androsaemum* may be taken into account for the observed activity.

The possibility to modulate the immune responses represents a very important goal when situations of immunodeficiency

should be activated or a selective immunosuppression has to be induced, for example, in autoimmune disorders.

CONCLUSION

The present study represents a comprehensive phytochemical and biological investigation of fruits of *H. androsaemum*, a wild medicinal plant of the Mediterranean region. On the above, the balsamic period was identified as the plant produces red berries. The latter were proven to be rich in shikimic acid and in phenolic compounds, especially chlorogenic acids. Moreover, the pigment giving the red color to the fruit pericarp was structurally determined as 1,2,3,5-tetrahydroxyxanthone that is reported for the first time for *Hypericum* species. Hence, *H. androsaemum* berries can be a good source of this molecule with potential applications at industrial level. Overall, the high antioxidant potential of tutsan berries was demonstrated and could be achieved directly by consumption of infusions or by incorporating polar extracts in antioxidant formulations. The cytotoxicity of methanolic extracts on tumor cell lines, especially on colon carcinoma, make *H. androsaemum* berries a potential candidate as a functional food having beneficial effects against tumors correlated with a life style characterized by the so-called “western diet.” Data from immunomodulatory assay suggest that red berries of *H. androsaemum* may represent a promising and natural strategy to modulate the immune system, although the mechanisms of action remain to be clarified. The obtained results could explain the past and current usage of *H. androsaemum* as food and in folk medicine; also they may support its further uses in health and in nutrition as a functional food.

AUTHOR CONTRIBUTIONS

GC, HPLC analysis; AA, immunomodulatory assay; DB, immunomodulatory assay; AB, column chromatography and NMR; MB, MTT assay; CF, column chromatography and NMR; RI, HPLC analysis; FP, plant collection; LQ, MTT assay; GS, HPLC analysis; BT, antioxidant experiments; AV, column chromatography and NMR; SV, HPLC analysis.

ACKNOWLEDGMENTS

This work was supported by the FAR 2014-2015 (FPI000044-Fondo di Ateneo per la Ricerca) of the University of Camerino. Authors thank Dr. Marzia Innocenti from the University of Florence for her support in the chemical analysis, and Dr. Kevin Cianfaglione from the University of Camerino for his help in sample collections.

SUPPLEMENTARY MATERIAL

The Supplementary Material for this article can be found online at: <http://journal.frontiersin.org/article/10.3389/fpls.2016.00232>

REFERENCES

- Abtai Froushani, S. M., Galee, H. E. G., Khamisabadi, M., and Lotfallahzades, B. (2015). Immunomodulatory effects of hydroalcoholic extract of *Hypericum perforatum*. *Avicenna J. Phytomed.* 5, 62–68.
- Allen, D. A., and Hatfield, G. (2004). *Medicinal Plants in Folk Tradition. An Ethnobotany of Britain and Ireland*. Portland, OR: Timber Press, Inc.
- Aziz, N., Sauve, R. J., Long, D., and Cherry, M. (2006). Genetic and Phytochemical Diversity Assessment Among Eleven *Hypericum* Accessions via AFLP and HPLC Analyses. *J. Herbs Spices Med. Plants* 12, 97–105. doi: 10.1300/J044v12n01_09
- Bennet, G. J., and Lee, H.-H. (1989). Xanthones from Guttiferae. *Phytochemistry* 28, 967–998. doi: 10.1016/0031-9422(89)80170-0
- Bertelli, A. A. E., Mannari, C., Santini, S., Filippi, C., Migliori, M., and Giovannini, L. (2008). Immunomodulatory activity of shikimic acid and quercitin in comparison with oseltamivir (Tamiflu) in an “in vitro” model. *J. Med. Virol.* 80, 741–745. doi: 10.1002/jmv.21072
- Boik, J. (2001). *Natural Compounds in Cancer Therapy*. Princeton, MN: Oregon Medical Press.
- Bonkanka, C. X., Smelcerovic, A., Zuehlke, S., Rabanal, R. M., Spiteller, M., and Sánchez-Mateo, C. C. (2008). HPLC-MS analysis of anti-oedematogenic activity of *Hypericum grandifolium* Choisy (Hypericaceae). *Planta Med.* 74, 719–725. doi: 10.1055/s-2008-1074526
- Caprioli, G., Cortese, M., Odello, L., Ricciutelli, M., Sagratini, G., Tomassoni, G., et al. (2013). Importance of Espresso coffee machine parameters on the extraction of chlorogenic acids in a certified Italian Espresso by Using SPE-HPLC-DAD. *J. Food Res.* 2, 55–64. doi: 10.5539/jfr.v2n3p55
- Chen, W.-C., Liou, S.-S., Tzeng, T.-F., Lee, S.-L., and Liu, I.-M. (2013). Effect of topical application of chlorogenic acid on excision wound healing in rats. *Planta Med.* 79, 616–621. doi: 10.1055/s-0032-1328364
- Cho, A.-S., Jeon, S.-M., Kim, M.-J., Yeo, J., Seo, K.-I., Choi, M.-S., et al. (2010). Chlorogenic acid exhibits anti-obesity property and improves lipid metabolism in high-fat diet-induced-obese mice. *Food Chem. Toxicol.* 48, 937–943. doi: 10.1016/j.fct.2010.01.003
- Chung, H. S. (2003). Inhibition of monamine oxidase by a flavone and its glycoside from *Ixeris dentata* Nakai. *Nutr. Food* 8, 141–144. doi: 10.3746/jfn.2003.8.2.141
- Cincin, Z. B., Unlu, M., Kiran, B., Bireller, E. S., Baran, Y., and Cakmakoglu, B. (2015). Apoptotic effects of quercitrin on DLD-1 colon cancer cell line. *Pathol. Oncol. Res.* 21, 333–338. doi: 10.1007/s12253-014-9825-3
- Clifford, M. N. (1999). Chlorogenic acids and other cinnamates – nature, occurrence and dietary burden. *J. Sci. Food Agric.* 79, 362–372.
- Dapkevicius, A., Venskutonis, R., Van Beek, T. A., and Linssen, P. H. (1998). Antioxidant activity of extracts obtained by different isolation procedures from some aromatic herbs grown in Lithuania. *J. Sci. Food Agric.* 77, 140–146.
- Demirkiran, O. (2007). Xanthones in *Hypericum*: synthesis and biological activities. *Top. Heterocycl. Chem.* 9, 139–178. doi: 10.1007/7081_2007_079
- Dias, A. C. P., Seabra, R. M., Andrade, P. B., Ferreres, F., and Fernandes-Ferreira, M. (2000). Xanthone biosynthesis and accumulation in calli and suspended cells of *Hypericum androsaemum*. *Plant Sci.* 150, 93–101. doi: 10.1016/S0168-9452(99)00178-8
- Dopico-Garcia, M. S., Castro-Lopez, M. M., Lopez-Vilarino, J. M., Gonzalez-Rodriguez, M. V., Valenta, P., Andrade, P. B., et al. (2011). Natural extracts as potential source of antioxidants to stabilize polyolefins. *J. Appl. Polym. Sci.* 119, 3553–3559. doi: 10.1002/app.33022
- Dragović-Uzelac, V., Bursać Kovačević, D., Levaj, B., Pedisić, S., Mezak, M., and Tomljenović, A. (2009). Polyphenols and antioxidant capacity in fruits and vegetables common in the croatian diet. *Agric. Conspectus Scientificus* 74, 175–179.
- Han, J.-T., Bang, M.-H., Chun, O.-K., Kim, D.-O., Lee, C.-Y., and Baek, N.-I. (2004). Flavonol glycosides from the aerial parts of *Aceriphyllum rossii* and their antioxidant activities. *Arch. Pharm. Res.* 27, P390–P395. doi: 10.1007/BF02980079
- Han, T., Li, H., Zhang, Q., Zheng, H., and Qin, L. (2006). New thiazinediones and other components from *Xanthium strumarium*. *Chem. Nat. Comp.* 42, 567–570. doi: 10.1007/s10600-006-0215-2
- Hayes, C. J., Whittaker, B. P., Watson, S. A., and Grabowska, A. M. (2006). Synthesis and preliminary anticancer activity studies of C4 and C8-modified derivatives of catechin gallate (CG) and epicatechin gallate (ECG). *J. Org. Chem.* 71, 9701–9712. doi: 10.1021/jo061740e
- Hu, T., He, X. W., and Jiang, J. G. (2014). Functional analyses on antioxidant, anti-inflammatory, and antiproliferative effects of extracts and compounds from *Ilex latifolia* Thunb., a Chinese bitter tea. *J. Agric. Food Chem.* 62, 8608–8615. doi: 10.1021/jf501670v
- Jiang, Y., Kusama, K., Satoh, K., Takayama, F., Watanabe, S., and Sakagami, H. (2000). Induction of cytotoxicity by chlorogenic acid in human oral tumor cell lines. *Phytomedicine* 7, 483–491. doi: 10.1016/S0944-7113(00)80034-3
- Khan, H. Y., Zubair, H., Ullah, M. F., Ahmad, A., and Hadi, S. M. (2012). A prooxidant mechanism for the anticancer and chemopreventive properties of plant polyphenols. *Curr. Drug Targets* 13, 1738–1749. doi: 10.2174/138945012804545560
- Kitanov, G. M. (2001). Hypericin and pseudohypericin in some *Hypericum* species. *Biochem. Syst. Ecol.* 29, 171–178. doi: 10.1016/S0305-1978(00)00032-6
- Lamaison, J. L., and Carnat, A. (1990). Teneurs en principaux flavonoïdes des fleurset des feuilles de *Crataegus monogyna* Jacq. et de *Crataegus laevigata* (Poiret) DC. *Pharm. Acta Helv.* 65, 315–320.
- Li, L., Henry, G. E., and Seeram, N. P. (2009). Identification and bioactivities of resveratrol oligomers and flavonoids from *Carex folliculata* seeds. *J. Agric. Food Chem.* 57, 7282–7287. doi: 10.1021/jf901716j
- Liu, F. C., Coimbra, R., Hoyt, D. B., and Junger, W. G. (1996). Proliferation assays with human, rabbit, rat, and mouse lymphocytes. *In Vitro Cell. Dev. Biol. Anim.* 32, 420–523. doi: 10.1007/BF02722976
- Lu, Y., and Foo, L. Y. (2000). Flavonoid and phenolic glycosides from *Salvia officinalis*. *Phytochemistry* 55, 263–267. doi: 10.1016/S0031-9422(00)00309-5
- Manguro, L. O. A., Ugi, I., Lemmen, P., and Hermann, R. (2003). Flavonol glycosides of *Warburgia ugandensis* leaves. *Phytochemistry* 64, 891–896. doi: 10.1016/S0031-9422(03)00374-1
- Mulinacci, N., Ieri, F., Giaccherini, C., Innocenti, M., Andrenelli, L., Canova, G., et al. (2008). Effect of cooking on the anthocyanins, phenolic acids, glycoalkaloids and resistant starch content in two pigmented cultivars of *Solanum tuberosum* L. *J. Agric. Food Chem.* 56, 11830–11837. doi: 10.1021/jf8012021e
- Ngomuo, A. J., and Jones, R. S. (1996). Cytotoxicity studies of quercetin, shikimate, cyclohexanecarboxylate and ptaquiloside. *Vet. Hum. Toxicol.* 38, 14–18.
- Nielsen, H., and Arends, P. (1979). Xanthone constituents of *Hypericum androsaemum*. *J. Nat. Prod.* 42, 301–304. doi: 10.1021/np50003a012
- Perrone, R., De Rosa, P., De Castro, O., and Colombo, P. (2013). Leaf and stem anatomy in eight *Hypericum* species (Clusiaceae). *Turk. J. Bot.* 37, 847–858. doi: 10.3906/bot-1206-22
- Peterson, D. M., Hahn, M. J., and Emmons, C. L. (2002). Oat avenanthramides exhibit antioxidant activities *in vitro*. *Food Chem.* 79, 473–478. doi: 10.1016/S0308-8146(02)00219-4
- Phillips, R. (1977). *Wild Flowers of Britain*. London, UK: Pan Books.
- Quassinti, L., Lupidi, G., Maggi, F., Sagratini, G., Papa, F., Vittori, S., et al. (2013). Antioxidant and antiproliferative activity of *Hypericum hircinum* L. subsp. *majus* (Aiton) N. Robson essential oil. *Nat. Prod. Res.* 27, 865–868. doi: 10.1080/14786419.2012.677044
- Sagratini, G., Ricciutelli, M., Vittori, S., ÖzTÜRK, N., ÖzTÜRK, Y., and Maggi, F. (2008). Phytochemical and antioxidant analysis of eight *Hypericum* taxa from Central Italy. *Fitoterapia* 79, 210–213. doi: 10.1016/j.fitote.2007.11.011
- Scarpati, M. L., Oriente, G., and Panizzi, L. (1957). Sui costituenti caffeiici del carciofo. *Ann. Chim.* 47, 150.
- Schmidt, W., El-Mawla, A. M. A., Wolfender, J.-L., Hostettmann, K., and Beerhues, L. (2000). Xanthones in cell cultures of *Hypericum androsaemum*. *Planta Med.* 66, 380–381. doi: 10.1055/s-2000-8542
- Singleton, V. L., and Rossi, J. A. J. (1965). Colorimetry of total phenolics with phosphomolybdic-phosphotungstic acid reagents. *Am. J. Enol. Vit.* 16, 144–153.
- Trong Tuan, D., Thai Trung, D., Phi Hung, N., Eunhee, K., Phuong, T. T., and Won, K. O. (2012). Xanthones from *Polygala karense* inhibit neuraminidases from influenza A viruses. *Bioorg. Med. Chem. Lett.* 22, 3688–3692. doi: 10.1016/j.bmcl.2012.04.028
- Valentão, P., Carvalho, M., Fernandes, E., Carvalho, F., Andrade, P. B., Seabra, R. M., et al. (2004). Protective activity of *Hypericum androsaemum* infusion

- against *tert*-butyl hydroperoxide-induced oxidative damage in isolated rat hepatocytes. *J. Ethnopharmacol.* 92, 79–84. doi: 10.1016/j.jep.2004.02.004
- Valentão, P., Fernandes, E., Carvalho, F., Andrade, P. B., Seabra, R. M., Bastos, M. D. L. (2002). Antioxidant Activity of *Hypericum androsaemum* infusion: scavenging activity against superoxide radical, hydroxyl radical and hypochlorous acid. *Biol. Pharm. Bull.* 25, 1320–1323. doi: 10.1248/bpb.25.1320
- Vieira, L. M. M., and Kijjoa, A. (2005). Naturally-Occurring Xanthones: recent developments. *Curr. Med. Chem.* 12, 2413–2446. doi: 10.2174/092986705774370682
- Weiss, S. J., Klein, R., Slivka, A., and Wei, M. J. (1982). Chlorination of Taurine by Human Neutrophils. *J. Clin. Investig.* 70, 598–607. doi: 10.1172/JCI110652
- Xavier, C. P., Lima, C. F., Fernandes-Ferreira, M., and Pereira-Wilson, C. (2012). *Hypericum androsaemum* water extract inhibits proliferation in human colorectal cancer cells through effects on MAP kinases and PI3K/Akt pathway. *Food Funct.* 3, 844–852. doi: 10.1039/c2fo10226a
- Xiao, C., Dai, H., Liu, H., Wang, Y., and Tang, H. (2008). Revealing the metabolomic variation of rosemary extracts using ^1H NMR spectroscopy and multivariate data analysis. *J. Agric. Food Chem.* 56, 10142–10153. doi: 10.1021/jf8016833
- Zorzetto, C., Sánchez-Mateo, C. C., Rabanal, R. M., Lupidi, G., Petrelli, D., Vitali, L. A., et al. (2015). Phytochemical analysis and *in vitro* biological activity of three *Hypericum* specie from the Canary Islands (*Hypericum reflexum*, *Hypericum canariense* and *Hypericum grandifolium*). *Fitoterapia* 100, 95–109. doi: 10.1016/j.fitote.2014.11.013

Conflict of Interest Statement: The authors declare that the research was conducted in the absence of any commercial or financial relationships that could be construed as a potential conflict of interest.

Copyright © 2016 Caprioli, Alunno, Beghelli, Bianco, Bramucci, Frezza, Iannarelli, Papa, Quassinti, Sagratini, Tirillini, Venditti, Vittori and Maggi. This is an open-access article distributed under the terms of the Creative Commons Attribution License (CC BY). The use, distribution or reproduction in other forums is permitted, provided the original author(s) or licensor are credited and that the original publication in this journal is cited, in accordance with accepted academic practice. No use, distribution or reproduction is permitted which does not comply with these terms.



Metabolic Profile and Root Development of *Hypericum perforatum* L. *In vitro* Roots under Stress Conditions Due to Chitosan Treatment and Culture Time

Elisa Brasili¹, Alfredo Miccheli², Federico Marini², Giulia Praticò², Fabio Sciubba², Maria E. Di Cocco², Valdir Filho Cechinel³, Noemi Tocci¹, Alessio Valletta^{1*} and Gabriella Pasqua¹

OPEN ACCESS

Edited by:

Gregory Franklin,
Polish Academy of Sciences, Poland

Reviewed by:

Ute Roessner,
The University of Melbourne, Australia

Marta R. M. Lima,
University of California Davis, USA

*Correspondence:

Alessio Valletta
alessio.valletta@uniroma1.it

Specialty section:

This article was submitted to
Plant Metabolism and Chemodiversity,
a section of the journal
Frontiers in Plant Science

Received: 09 February 2016

Accepted: 30 March 2016

Published: 19 April 2016

Citation:

Brasili E, Miccheli A, Marini F, Praticò G, Sciubba F, Di Cocco ME, Cechinel VF, Tocci N, Valletta A and Pasqua G (2016) Metabolic Profile and Root Development of *Hypericum perforatum* L. *In vitro* Roots under Stress Conditions Due to Chitosan Treatment and Culture Time. *Front. Plant Sci.* 7:507. doi: 10.3389/fpls.2016.00507

The responses of *Hypericum perforatum* root cultures to chitosan elicitation had been investigated through ¹H-NMR-based metabolomics associated with morpho-anatomical analyses. The root metabolome was influenced by two factors, i.e., time of culture (associated with biomass growth and related “overcrowding stress”) and chitosan elicitation. ANOVA simultaneous component analysis (ASCA) modeling showed that these factors act independently. In response to the increase of biomass density over time, a decrease in the synthesis of isoleucine, valine, pyruvate, methylamine, ethanolamine, trigonelline, glutamine and fatty acids, and an increase in the synthesis of phenolic compounds, such as xanthones, epicatechin, gallic, and shikimic acid were observed. Among the xanthones, brasiliyanthone B has been identified for the first time in chitosan-elicited root cultures of *H. perforatum*. Chitosan treatment associated to a slowdown of root biomass growth caused an increase in DMAPP and a decrease in stigmasterol, shikimic acid, and tryptophan levels. The histological analysis of chitosan-treated roots revealed a marked swelling of the root apex, mainly due to the hypertrophy of the first two sub-epidermal cell layers. In addition, periclinal divisions in hypertrophic cortical cells, resulting in an increase of cortical layers, were frequently observed. Most of the metabolic variations as well as the morpho-anatomical alterations occurred within 72 h from the elicitation, suggesting an early response of *H. perforatum* roots to chitosan elicitation. The obtained results improve the knowledge of the root responses to biotic stress and provide useful information to optimize the biotechnological production of plant compounds of industrial interest.

Keywords: *Hypericum perforatum*, root culture, metabolomics, ASCA modeling, NMR spectroscopy, chitosan elicitation

INTRODUCTION

The development of alternative methods to whole plant cultivation for the production of pharmaceutically valuable compounds of commercial interest is an issue of considerable socio-economic importance. Current advancement in biotechnological research has made the plant cell, tissue, and organ culture an attractive alternative to whole plant for the production of biologically important compounds (Rao and Ravishankar, 2002). In particular, root cultures characterized by a high growth rate and active secondary metabolism provides an efficient system to produce great amounts of secondary metabolites highly valued in pharmaceutical industry (Sivakumar, 2006). As an example, root cultures of *Morinda citrifolia*, *Echinacea purpurea*, and *Panax ginseng* were successfully used to produce bioactive molecules such as anthraquinones, rubiadin, phenolics and flavonoids with antioxidative, antibacterial, antiviral, and antifungal properties (Baque et al., 2012). Among medicinal plants, *Hypericum perforatum* (L.) (Hypericaceae) has received a global attention, owing to its variety of structurally diverse bioactive compounds such as flavonols, naphthodianthrone, and phloroglucinols, which have been reported to have antidepressant activity in different antidepressive model systems (Barnes et al., 2001; Walker et al., 2002; Cirak et al., 2007). Research on *H. perforatum* has focused primarily on hypericin and pseudohypericin as the major constituents responsible for the antidepressant activity (Walker et al., 2002). Moreover, clinical studies underscored the possible role of flavonoids in several kinds of cancer (Maheep et al., 2011). Recently much attention has been paid to another class of bioactive polyphenols, namely xanthones whose high antifungal activity against human pathogens has been demonstrated (Tocci et al., 2013a,b; Simonetti et al., 2015). Root cultures of *H. perforatum* L. are considered an effective system for the biotechnological production of flavonols, xanthones, essential oils, and other secondary metabolites, with interesting pharmacological activities (Mulinacci et al., 2008; Crockett et al., 2011; Tocci et al., 2011, 2012, 2013b; Zubrická et al., 2015). One of the major obstacles to the use of organ cultures for the pharmaceutical industry is the low yield of the metabolites of interest. For this reason, several strategies have been adopted to improve the production of plant-derived secondary metabolites such as two-phase culture system, genetic transformation, metabolic and bioreactor engineering (Georgiev et al., 2012; Tocci et al., 2012; Wilson et al., 2014; Simonetti et al., 2015). Among the various efforts, chitosan elicitation proved to be one of the most effective strategy to enhance the production of bioactive compounds both in *in planta* and in *in vitro* root systems (Tocci et al., 2011; Yin et al., 2012). In particular, chitosan treatment has been shown to increase the production of xanthones in *H. perforatum* root cultures (Tocci et al., 2011, 2012, 2013a).

Xanthone compounds include a group of structurally diverse, biologically active, and synthetically challenging natural products with a wide range of pharmacological properties, e.g., antioxidant, anti-inflammatory, antimicrobial, and cytotoxic

activities (Franklin et al., 2009; Naldoni et al., 2009; Al-Shagdari et al., 2013; Nontakham et al., 2014; Zubrická et al., 2015).

It is well-known that the production of bioactive compounds in *H. perforatum* *in vitro* roots is greatly affected by various parameters such as inoculum density, culture medium composition, time of culture, type and concentration of growth regulators, and other physico-chemical factors that need to be optimized to maximize the growth of biomass and the production of natural compounds (Cui et al., 2010, 2011; Jin et al., 2012; Zubrická et al., 2015; Valletta et al., 2016).

However, the impact of culture conditions on the root metabolism is not limited to single biochemical pathways. Furthermore, the knowledge of biosynthetic pathways of desired compounds in root cultures is still in its infancy, and consequently, the understanding of the regulation of primary and secondary metabolic pathways is required. An omics approach in which a great number of primary and secondary metabolites are identified and quantified is needed to elucidate the function of a whole pathway or intersecting pathways as well as to understand how to increase metabolic fluxes into pathways involved in the production of plant pharmaceuticals (Giddings et al., 2000). With the recent developments in plant metabolomics techniques, it is now possible to detect several hundred metabolites simultaneously and to compare samples reliably to identify differences and similarities in an untargeted manner. On the other hand, the chemical analyses that are based on the whole composition of metabolites, rather than detection of a single constituent, are favored as they cover additionally or synergistically relevant components and can confirm the efficacy of *H. perforatum* medical preparations (Porzel et al., 2014).

So far the effects of chitosan elicitation and culture time on the whole metabolism of root cultures of *H. perforatum* have not been completely elucidated. Further studies are desirable to understand the relationships between primary and secondary metabolism with the aim to optimize the biomass growth and the production of bioactive compounds.

Recently, for the first time, a NMR-based metabolomic approach has been applied to study the primary and secondary metabolic changes of *H. perforatum* *in vitro* roots after a short period of chitosan treatment (24 and 72 h) and growth in a confined environment (Brasili et al., 2014). This approach has proved useful to demonstrate that root cultures are able to direct the shikimate pathway toward the biosynthesis of tryptophan and epicatechin in response to a high biomass density and toward the synthesis of xanthones, and epicatechin in response to the chitosan elicitation. The chitosan treatment also stimulated the mevalonate pathway toward isoprenoid intermediate production, such as dimethylallyl-pyrophosphate (DMAPP) and stigmasterol. These latter can function as primary metabolites, participating in essential plant cellular processes, and as secondary metabolites, of which many have substantial commercial, pharmacological, and agricultural value (Vranová et al., 2012). These metabolic variations have been observed after having subjected the roots to two renewals of the culture medium and within 72 h from chitosan elicitation.

In the present study, we have applied a non-targeted NMR-based metabolomics associated to ANOVA simultaneous

component analysis (ASCA) to explore the response of primary and secondary metabolism of roots to a longer culture time and a prolonged time of exposure to chitosan, until 192 h, in an attempt to improve the yield of xanthones and to obtain more information about the isoprenoid metabolism. Furthermore, the effect of chitosan treatment on the biomass growth and on the morpho-anatomical features of *H. perforatum* roots was investigated during the time course.

This metabolomic approach can provide a new platform for global analyses of *Hypericum* pharmaceuticals and/or other phytomedicines and it can be applied to define suitable protocols to produce the desired secondary metabolites with different bioactivities.

MATERIALS AND METHODS

Plant Material, Root Cultures, and Experimental Design

The experiment was designed to evaluate the changes of primary and secondary metabolism in *H. perforatum* *in vitro* roots after 72, 96, and 192 h of chitosan elicitation. To increase the time period of chitosan treatment, maintaining the root culture in the exponential growth phase, a necessary condition to assume the metabolic steady-state, the culture medium was renewed at day 4 and chitosan elicitation was performed at day 8 of the growth curve. Liquid root cultures were established inoculating 1 g fresh weight (FW) of roots in magenta vessels containing 80 ml liquid MS medium supplemented with glucose (2.2 g/l) and IBA (1 mg/l). The magenta vessels were shaken at 100 rpm at 25 ± 1°C and maintained in the continuous darkness. The culture medium was renewed after 4 days, the time necessary for biomass duplication. The roots were elicited using chitosan (medium molecular weight; Sigma-Aldrich, Milan, Italy) dissolved in water acidified with HCl (1 M) up to a final concentration of 200 mg/l. A volume of 1 ml of chitosan solution or acidified water (at the same pH of chitosan solution) was added at the 8th day of culture using a 0.22 µm sterile filter to the treated and control roots, respectively (Tocci et al., 2011). The growth curve of root biomass was recorded during a period of 16 days from inoculum.

Regenerated roots were harvested at 8th day (time 0), at 11th day (72 h), 13th day (96 h), and 16th day (192 h) and divided into following groups: control and treated at time 0, control and treated to 72 h after elicitation, control and treated at 96 h after elicitation, and control and treated at 192 h after elicitation. Five samples for each group were considered.

Determination of the Root Weight, Growth Ratio, and Growth Rate

Roots were separated from the liquid medium and the fresh weight (FW) was measured. Growth ratio and growth rate were calculated as follows:

$$\text{Growth ratio} = \frac{\text{Harvested fresh weight (g)} - \text{Inoculated fresh weight (g)}}{\text{Inoculated fresh weight (g)}}$$

$$\text{Growth rate} = \left[\frac{\text{Harvested fresh weight (g)} - \text{Inoculated fresh weight (g)}}{\text{Inoculated fresh weight}} \right] \frac{1}{\text{Day}}$$

Metabolite Extraction and ¹H-NMR Spectroscopy

The metabolic quenching of the roots was performed by rapidly freezing in liquid N₂. The frozen biomass (1.5 g of fresh weight) was ground up in a steel mortar in liquid N₂ and extracted by a solvent mixture of methanol, chloroform and distilled water at 2:2:1.2 (v/v ratio), according to the Bligh-Dyer procedure previously described by Brasili et al. (2014). The samples were mixed by vortex for 1 min, stored overnight at 4°C and then centrifuged for 30 min at 11,000 × g at 4°C. The resulting upper hydro-alcoholic and lower organic phases were then carefully separated and dried under N₂ flow. The dried residue of the hydro-alcoholic phase was dissolved in 0.6 ml CD₃OD/D₂O (1:2 v/v ratio) containing 3-(trimethylsilyl)- propionic-2,2,3,3,-d₄ acid sodium salt (TSP, 2 mM) as internal standard (chemical shift and concentration reference). The dried residue of the chloroformic phase was dissolved in 0.6 ml CDCl₃, (Cambridge Isotope Laboratories, Inc.), (99.8%) containing 1,1,3,3,5,5-hexamethylcyclo-tri-siloxane (HMS) (Sigma-Aldrich, USA) as internal standard (2 mM). NMR spectroscopy was carried out using a Bruker Avance III 400 spectrometer operating at a frequency of 400.13 MHz for the proton. One dimensional proton spectra were acquired according to the procedures previously described (Brasili et al., 2014). The univocal assignment of proton resonances was achieved by means of Human Metabolome Database (HMDB; Wishart et al., 2013), bidimensional ¹H homonuclear total correlation spectroscopy (TOCSY) experiments and by bidimensional ¹H-¹³C heteronuclear single quantum coherence (HSQC) experiments as described by Brasili et al. (2014). 1D-NMR spectra were processed using ACD Lab 1D-NMR Manager ver. 12.0 software (Advanced Chemistry Development, Inc., Toronto, Ontario, Canada), whereas 2D-NMR spectra were processed using Bruker Top Spin (Bruker, Karlsruhe, Germany). All assigned metabolites were quantified calculating the integral ratio of metabolite signal with respect to TSP and HMS.

Statistical Data Analysis

Multivariate data analysis was carried out using in house written functions operating under Matlab R2012b environment (The MathWorks, Inc., Natick, MA, USA).

Spectral data were mean-centered and Pareto-scaled before analysis. To assess whether the two controlled factors (time and treatment) and their interaction could have an effect on the multivariate signal recorded by NMR, ASCA was used as described in Brasili et al. (2014). ASCA is an exploratory technique proposed originally by Jansen et al. (2005) to deal with multivariate profiles coming from designed studies. In particular, it couples an ANOVA-like partitioning of the total variance present in the data matrix into the contributions of main effects and interactions, with the analysis of the resulting effect matrices by means of Simultaneous Component Analysis (SCA), a bilinear

modeling technique analogous to Principal Component Analysis (Smilde et al., 2005)

In the present study, a full factorial experimental design involving two factors (time and treatment) and their binary interaction was adopted. As a consequence, ASCA operates by partitioning the matrix X, collecting the concentration of the metabolites recorded in the NMR experiments, according to:

$$X_c = X - 1m^T = X_{treatment} + X_{time} + X_{time \times treatment} + X_{res}$$

where 1 is a vector of ones, m is the average signal recorded (grand mean), X_c indicates the mean centered data matrix, X_{time} , $X_{treatment}$ are the matrices accounting for the main effects, $X_{time \times treatment}$ the matrix corresponding to the interaction while the unmodeled variation is collected in the matrix X_{res} . Although all the effect matrices have the same dimensions as the original data array X, they are built so that the number of unique profiles (rows) matches the number of levels for the particular factor. For instance, the matrix $X_{treatment}$, accounting for the effect of the factor treatment, which has only two levels ("control" and "treated") is defined as follows: all the rows corresponding to the experiments on control roots will contain the average profile measured on control sample, while the other half (i.e., the positions associated to the treated ones) will all be replicates of the average signal recorded on the treated roots. The entity of the effect is then quantified by the sum of squares of the elements of the corresponding matrix, and its statistical significance is evaluated by means of permutation tests (Vis et al., 2007).

In the successive stage, each of the individual effect matrices is modeled by SCA which, under the constraints normally adopted in ASCA, is totally equivalent to PCA:

$$X_i = T_i P_i^T$$

where i can be either time, treatment or time \times treatment, while T and P are the scores and loadings matrices for the effect, respectively.

Two-Way Analysis of Variance (ANOVA) was applied to confirm the result of multivariate analysis on single metabolites; a multiple comparison procedure (Holm–Sidak method) was carried out to evaluate the differences between treatment groups and time points. A p -value of 0.05 was considered significant. Prior comparison, Shapiro–Wilk test was performed to assess the normal distribution of the data. Non normal distributed data were normalized by \log_{10} transformation.

Histological Analysis

To investigate the effect of biomass growth and chitosan elicitation on root morphology, whole root samples were analyzed by a Zeiss stereomicroscope (Zeiss Stemi 2000C, Carl Zeiss, Milan, Italy) equipped with reflected and transmitted light.

To investigate the effect of biomass growth and chitosan elicitation on root anatomy, sections of fixed samples embedded in resin were analyzed. To obtain resin sections, root samples were fixed for 24 h in 70% ethanol and dehydrated for 12 h through two soak in absolute ethanol. Pre-infiltration phase was carried out by transferring root samples in a mixture (basic

solution) composed by equal parts of absolute ethanol and base liquid Technovit (Heraeus Kulzer GmbH & Co. KG—Wehrheim—Germany) 7100 (1:1 v/v) at 4°C, for 2–3 h. Samples were infiltrated for 24 h in a working solution constituted by 1 g hardener I (=1 bag) dissolved in 100 ml base liquid Technovit 7100 and mixed for 10 min. Polymerization phase was carried out in a mixture composed by 1 ml hardener II added to 15 ml of working solution. Root samples were embedded into 1–3 ml of polymerization solution and poured in histoforms, at room temperature (23°C) for 24 h. To mount samples, a mixture of Technovit 3040 in a volume ratio of 2 parts powder to 1 part liquid was used. The mixture was poured into the recess at the back of the histoblocs to a level of about 2 mm above the base of the histoblocs. After about 10 min, the histoblocs together with the fixed roots were removed from the histoforms. Fixed roots were longitudinally and transversely sectioned at 7 μ m with a microtome (Microm HM 350 SV microtome, Microm, Germany), stained with 0.1% toluidine blue and observed under a light microscope (Zeiss Axioscop 2 Plus).

RESULTS

Effect of Chitosan Treatment on Biomass Growth and on Root Morpho-Anatomical Features

The growth curve of both treated and untreated *H. perforatum* roots is shown in Figure 1. The untreated roots, exponentially grew up to day 12 with a biomass doubling time of 4 days. The growth rate greatly decreased from 0.32 to 0.17 (1/day) between days 12 and 16. The biomass density reached 8.2 ± 2.2 g FW/flask at the last day of culture (day 16).

Chitosan addition at day 8 caused a sudden slowdown of biomass growth from day 12 to 16. The final biomass density was 3.5 ± 0.5 g FW/flask, less than half than that reached in untreated samples.

Chitosan elicitation strongly affected the root morphology and anatomy. Chitosan-treated roots at 72, 96, and 192 h showed

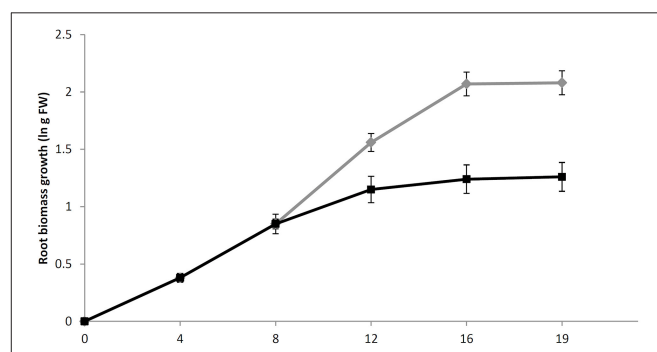
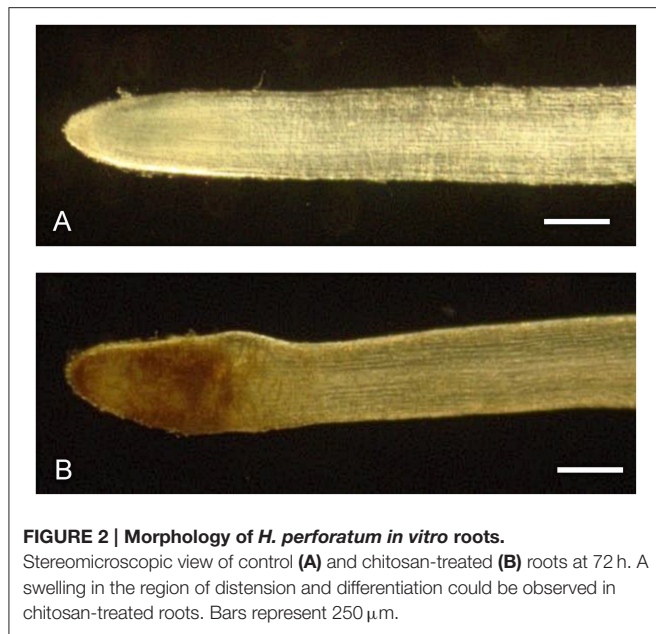


FIGURE 1 | The growth curve of *H. perforatum* in vitro roots over a period of 16 days. Growth is expressed as a natural logarithm (ln) of fresh weight biomass. Chitosan solution or an equal volume of water was added at day 8 for elicited (black line) or untreated (green line) root cultures, respectively. Data are presented as the mean \pm standard deviation (SD) of five biological repeats.



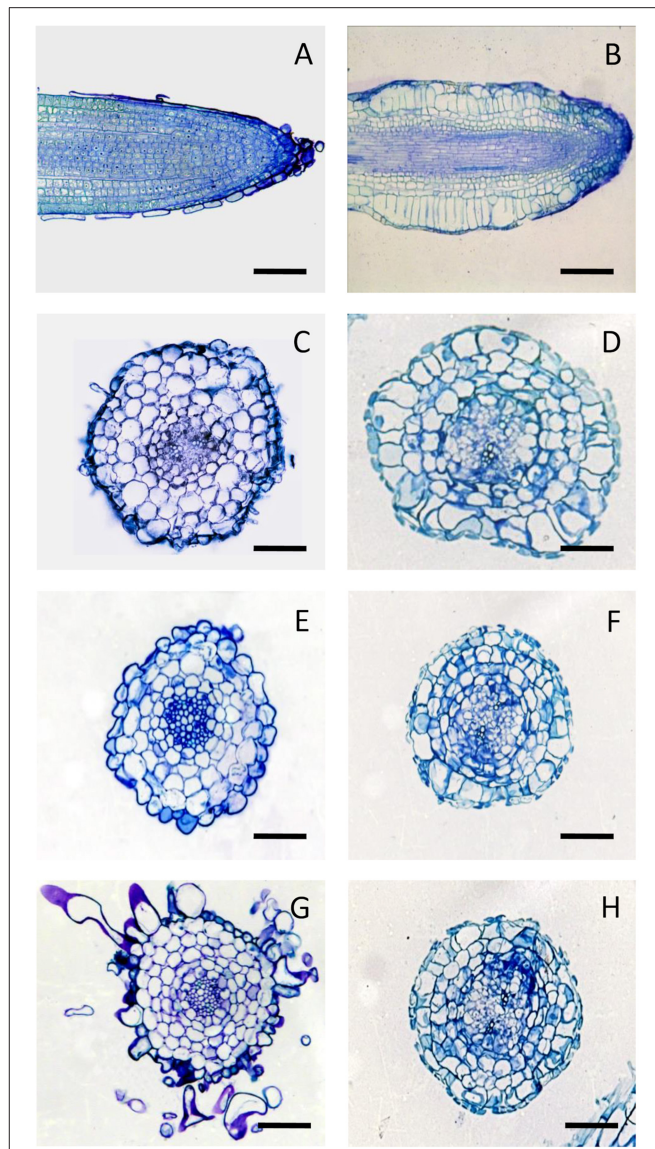
morpho-anatomical alterations with respect to the untreated roots. Morphological analysis after 72 h from chitosan treatment showed a remarkable swelling and browning in the region of distension and differentiation of the root (Figure 2), that remained unchanged up to 96 and 192 h.

The anatomical structure of the untreated *in vitro* roots appeared similar to that of the primary root of the plant. In particular, they showed mono-layered epidermis, three-layered cortex, endodermis, pericycle, and central cylinder with a diarch stele near the apex and a triarch stele at greater distance from the apex (Figure S1).

The analysis of chitosan-treated roots revealed that the swelling of the root apex was mainly due to the hypertrophy of the first two sub-epidermal cell layers. The cell expansion did not involve the root epidermis, which consequently was subjected to tensile forces that caused the thinning and often the breakage of this tissue. Furthermore, the direction of cell expansion in the cortex of the elicited roots took place predominantly in the radial direction, thus opposite than normal. Finally, in addition to the normal anticlinal divisions, periclinal divisions in hypertrophic cortical cells resulting in an increase of cortical layers were frequently observed (Figure 3). These alterations occurred in the early stages of post-elicitation period (within 72 h after chitosan addition) and did not proceed further in the following period. During the culture period, both in control and treated cultures, a progressive browning of the roots and culture medium has been observed.

NMR-Based Metabolic Profiling of *H. perforatum* Root Cultures

The hydroalcoholic and chloroformic extracts obtained from chitosan-treated and untreated roots were investigated by ^1H -NMR spectroscopy and 71 metabolites were assigned (Table S1). ^1H -NMR spectra of elicited and non-elicited roots



were characterized by a complex pattern of resonances, due to the presence of a vast array of metabolites (Figure S2). The hydroalcoholic extract was characterized by the presence of amino acids, small organic acids, polyphenols and other secondary metabolites, such as trigonelline and the isoprene unit, dymethylallyl pyrophosphate (DMAPP). The pattern of resonances at δ 8.10, δ 7.69, and δ 7.54 has been tentatively attributed to the benzyl ring of a phenolic unit, while the singlet at δ 8.58 was ascribed to the presence of a purine derivative based on the comparison with an analogous structure in the web database HMDB (<http://www.hmdb.ca>). Fifteen peaks have been quantified, but not identified and have been

classified as unknown (U0-U14). The ^1H -NMR spectrum of the chlorophormic extract resulted in more simple resonance patterns, associated with the presence of fatty acids, free and conjugated with a glycerol backbone, sterols, and xanthones. The method allowed the identification of the major classes of fatty acids, based on the presence of the resonances of olefinic (δ 5.35), acyl (δ 2.33), allylic (δ 2.04), and di-allylic (δ 2.77–2.85) groups. We identified and quantified saturated fatty acids (SFA), monounsaturated fatty acids (MUFA) and polyunsaturated fatty acids (PUFA). Particularly, we were able to discriminate the contribution of omega-3 (ω -3), measured as linolenic acid, and omega-6 (ω -6), measured as linoleic acid, to the total amount of PUFA, based on the resonances of the methylene between each pair of adjacent double bonds (δ 2.82 and δ 2.77, respectively). Six other resonances were quantified but not yet attributed (U17-U22).

The non-polar extract was also characterized by the resonances of a series of coupled doublets (CH at δ 7.95, δ 8.04, and δ 8.05), which were ascribed to the 2,2-dimethylpyran ring of a series of xanthone derivatives. In particular, from the comparison with the literature (Marques et al., 2000), it was possible to identify signals belonging to brasilixitone B [1,6-dihydroxy-6',6'-dimethylpyrano(2',3':2,3)-6'',6''-dimethylpyrano(2'',3'':7,8)xanthone] (Table S2), while the other two pairs of doublets were ascribed to analogs of brasilixitone B that have been named Compound-1 and Compound-2. The cumulative integral of such resonances has been defined as “total brasilixitones.” The pattern of signals at δ 4.55 (quartet) and 1.43 (doublet), and the two singlets at δ 1.60 and 1.34 were tentatively attributed to the 4',5'-dihydro-4',4',5'-trimethylfurane unit of 2-deprendyl-rheediaxanthone B, as reported in literature (Rath et al., 1996) and has been named Compound-3. However, the univocal assignment of this compound was hindered due to extreme signal overlapping. Nevertheless, these resonances were quantified by integration and considered for multivariate analysis.

The concentrations of 58 metabolites measured at the experimental times 0 (day 8), 72 h (day 11), 96 h (day 12), and 192 h (day 16) both in the control and in the chitosan-treated roots are reported in Figures S3–S7. The concentrations of unknown compounds are reported in Table S3.

Metabolic Responses to Chitosan Treatment and Culture Time

In order to investigate the metabolic response to chitosan treatment and culture time and/or to the interaction between them, ASCA modeling to ^1H -NMR spectroscopy data has been applied.

ASCA modeling showed that only the effects of culture time and chitosan treatment were significant ($p = 0.036$ and 0.002 , respectively, as estimated by permutation tests with 50,000 randomizations), while the effect of their interaction was not statistically different from zero ($p > 0.87$).

Having verified that time and treatment had a significant effect on the metabolic profiles of *H. perforatum* roots, SCA (after Pareto scaling) to model the variation in the two corresponding matrices $X_{\text{treatment}}$ and X_{time} has been used.

Effect of Chitosan Treatment

A single component (SC1), explaining 100% of total variance, was calculated by ASCA model for the treatment factor and the corresponding score plot is shown in Figure 4A. As described in Section Statistical Data Analysis, since the factor was investigated at two levels, scores along SC1 can only assume two different values for the investigated samples. In particular, the score plot shows that along SC1 untreated samples were placed at negative values, whereas the treated samples were placed at positive values of SC1. The interpretation of the observed differences in terms of chemical (metabolic) variation is then possible by analysing the SCA loadings. Indeed, since treated samples fall at positive values of SC1, variables having a positive loadings on the component will have higher concentration in the treated roots with respect to the untreated ones, while the concentration of the metabolites having negative loadings will be higher in the controls. The distribution of the variable loadings (blue line) and their 95% confidence intervals (red line) are represented in Figure 4B. To allow a rapid identification of significant metabolites a heatmap with the significant variables for the treatment model is displayed in Figure 5. In this figure, the colors represent the direction of metabolic changes (blue = decrease; red = increase; white = not significant changes). As displayed by ASCA model for the treatment factor, in treated roots the levels of shikimic acid, tryptophan, stigmasterol, and a series of unknown compounds (U0, U2, U11, U12, U20) decreased, whereas the levels of pyruvate, dimethylallyl pyrophosphate (DMAPP), and U5 increased.

In order to support the obtained data by ASCA model, we have also considered the metabolites that were significant by means two-way ANOVA test. In chitosan-treated roots, the increase in DMAPP was also significant in all experimental times and was associated to a decrease in stigmasterol, shikimic acid, and tryptophan levels in all experimental times. An exception was represented by the shikimic acid that increased at 72 h and then decreased at successive times. The univariate analysis also showed that the levels of primary metabolites, such as GABA, sucrose, and raffinose were significantly higher ($p = 0.02$, $p = 0.03$, and $p = 0.02$, respectively) in chitosan-treated roots than in control roots at 72 h after elicitation as well as the levels of secondary metabolites, such as gallic acid and compound-2 ($p = 0.03$ and $p = 0.01$, respectively), (Figures S3–S7). At 96 h after elicitation, the main metabolic variations were observed in primary metabolites such as GABA, leucine, alanine, and threonine that increased in treated roots, while isoleucine, trigonelline decreased.

Effect of Time

The SCA showed two significant components (SC1 and SC2) for the “time effect” model. The scores for each of the two components are shown in Figure 4C. The two components SC1 and SC2 showed that two coexistent metabolic phenomena contributed to the total variance, explaining the 60.3 and 23.6%, respectively.

The component SC1 displayed a monotonous trajectory as a function of time in which the scores increased during the time course until reaching a maximum. Along this component,

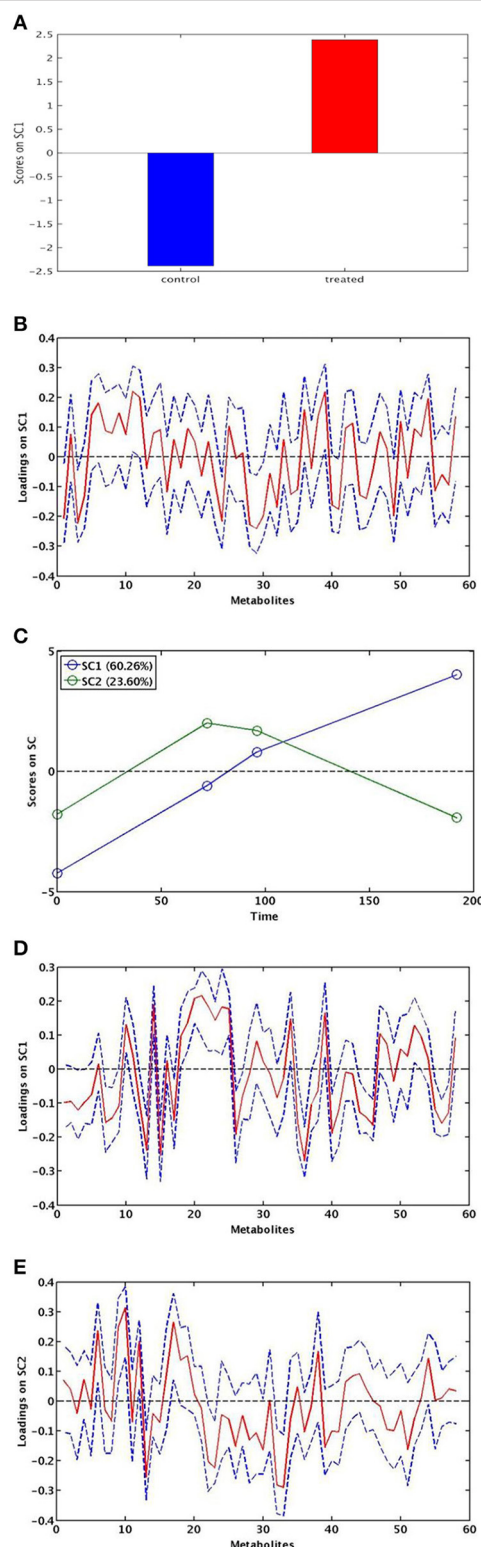


FIGURE 4 | ASCA modeling. SCA score plot for the effect of chitosan treatment (**A**). SCA score plot for the effect of time: SC1 and SC2 show the significant effect of time (**C**). SCA analysis on the effect matrix for treatment along SC1 (**B**) and for time along SC1 (**D**) and SC2 (**E**) and: variable loadings for the one-component SCA model (blue line) and their 95% confidence intervals (red).

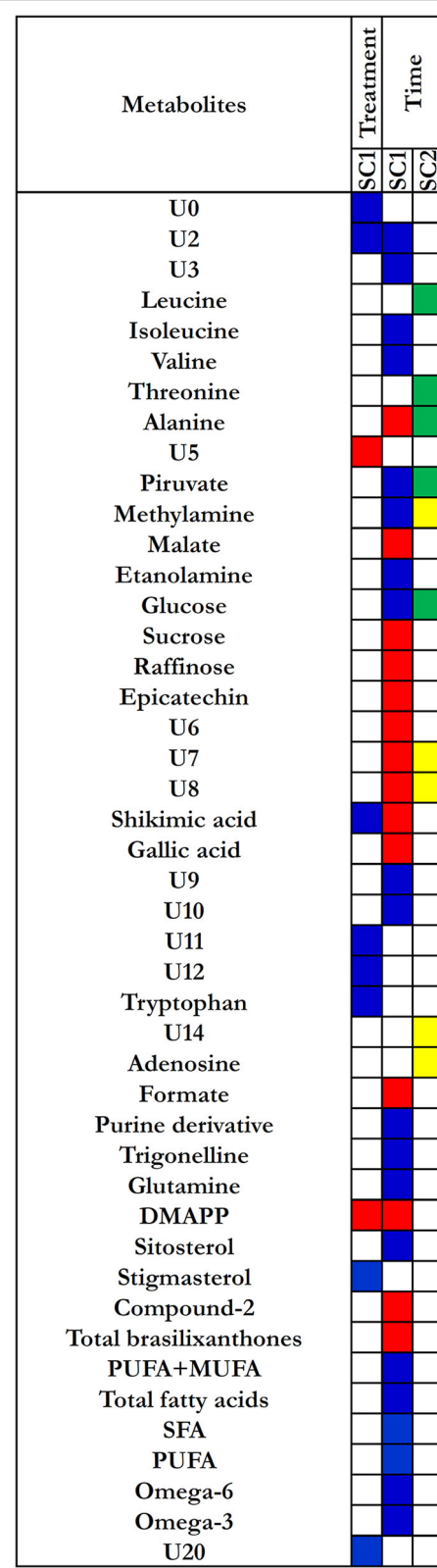


FIGURE 5 | Heatmap for loadings metabolites that contribute significantly to the model for time and treatment effects. Treatment effect: blue corresponds to the loading with positive direction (increase) in (Continued)

FIGURE 5 | Continued

control roots; red corresponds to the loadings with negative direction (increase) in treated roots. Time effect: for the SC1, blue corresponds to the loading with positive direction (decrease); red corresponds to the loading with negative direction (increase). For the SC2, yellow corresponds to the loading with positive direction (decreased and then increased); green corresponds to the loading with negative direction (increased and then decrease).

the significant metabolites such as alanine, malate, sucrose, raffinose, epicatechin, shikimic acid, gallic acid, formate, DMAPP, compound-2, total brasiliyanthones, and a series of unknown compounds (U6, U7, U8) increased, whereas isoleucine, valine, pyruvate, methylamine, ethanolamine, glucose, purine derivative, trigonelline, glutamine, sitosterol, and a series of unknown compounds (U2, U3, U9, U10) decreased. In addition, a decrease of fatty acids levels, both saturated and unsaturated fatty acids, was observed (**Figures 4D, 5**). Differently, SC2 displayed a metabolic perturbation that evolved over the time course, returning to the starting point. Along this component, the scores decreased until 72 h and then progressively increased, returning to the initial values. The metabolites leucine, threonine, alanine, pyruvate, and glucose increased and then progressively returned to the initial values. The levels of methylamine, adenosine, and a series of unknown compounds (U7, U8, U14) decreased and then returned nearly to their original values (**Figures 4E, 5**). The SC2 scores mainly describe the time-dependent changes of the metabolite levels occurring in the chitosan-treated roots before and after 72 h.

DISCUSSION

Effects of Chitosan Treatment and Culture Conditions on Biomass Growth and Morpho-Anatomical Features of *H. perforatum* Root Cultures

It is well-known that the production of secondary metabolites depends on plant genotype and culture conditions such as inoculum mass, culture age, elicitor's exposure time, and its concentration (Valletta et al., 2016). In order to develop and optimize a protocol for the production of bioactive compounds, *H. perforatum* root cultures were maintained for 16 days with only one renewal of the medium on day 4 and 8 days of exposure to chitosan (from day 8 to 16).

Our results reveal that chitosan elicitation induces a decrease of biomass growth accompanied by a browning and a notable swelling of the apex root; in parallel, a higher accumulation of secondary metabolites were observed. These results are consistent with previous reports and confirm that chitosan strongly affects both the secondary metabolism and root biomass growth and development (Sivanandhan et al., 2012; Brasili et al., 2014; Zubrická et al., 2015; Valletta et al., 2016). In non-elicited roots, the biomass density reached at day 16 of culture (8.2 ± 2.2 g FW/flask) was similar to that previously observed by Brasili et al. (2014) at day 15 (7.8 ± 1.2 g FW/flask) and after two renewals of culture medium. The comparison between the growth curves

obtained from the two independent experiments shows that the biomass density is not affected by the number of subcultures, suggesting that the medium components are not limiting factors for the root growth rate in the considered experimental time.

Metabolic Responses to Chitosan Treatment and Culture Conditions

Effect of Chitosan Treatment

To the best of our knowledge, for the first time an increase in brasiliyanthone B level was observed in response to chitosan elicitation in *H. perforatum* *in vitro* roots. This compound, that was previously isolated from root and stem of *Tovomita brasiliensis* Mart. Marques et al. (2000), has been recently identified in adventitious roots of *H. perforatum* (Li et al., 2013). Antibacterial activity of brasiliyanthone B, isolated from twigs of *Garcinia nigrolineata* Planch. ex T. Anderson, has been demonstrated against *Staphylococcus aureus* (Rukachaisirikul et al., 2005). Recently, the antioxidant and cytotoxic activities of brasiliyanthone B have been demonstrated against the HL-60 human promyelocytic leukemia cells (Li et al., 2013), suggesting that this secondary metabolite could be an interesting bioactive compound for pharmaceutical purposes. Eight days (192 h) after chitosan elicitation, *H. perforatum* roots showed the highest DMAPP levels ($0.28 \mu\text{mol/g} \pm 0.06$). DMAPP and its isomer isopentenyl pyrophosphate (IPP), are the universal precursors for the biosynthesis of isoprenoids, including sterols and terpenes (Kuzuyama and Seto, 2003). Our results suggest that chitosan stimulates the isoprenoid pathway. However, the increase in DMAPP level was not associated to an increase of sitosterol or stigmasterol, therefore its intracellular storage could be better explained by a reduced utilization of this intermediate in the synthesis of these specific isoprenoids, even though an increase in other highly volatile low molecular weight isoprenoids cannot be excluded. In fact, although the $^1\text{H-NMR}$ technique has been unable to detect terpenoid compounds, the presence of mono- and sesquiterpenes has been observed in *H. perforatum* L. roots by GC-MS (Motavalizadehkakhky, 2012).

Surprisingly, ASCA modeling shows that chitosan (SC1) do not significantly affect the production of phenolic compounds (**Figure 5**), as previously found (Brasili et al., 2014). In this work, the chitosan-dependent changes of both primary and secondary metabolites (GABA, sucrose, gallic acid, and compound-2) were significant only at 72 h after elicitation and not at the following experimental times, as revealed by ANOVA analysis (**Figures S3–S7**). These results are consistent with the observed morpho-anatomical alterations that occurred within 72 h after the elicitation, confirming that the main responses to chitosan elicitation take place in the first 3 days after treatment. These evidences show that the effects caused by chitosan are independent of the number of culture medium renewals.

Effect of Time

Along SC1 of time factor, the ASCA model describes the changes in the phenylpropanoid metabolism, as revealed by the increase in total brasiliyanthones, compound-2, epicatechin, gallic acid, and shikimic acid levels. Although, these findings are the sum of the contributes originating from both treated and untreated

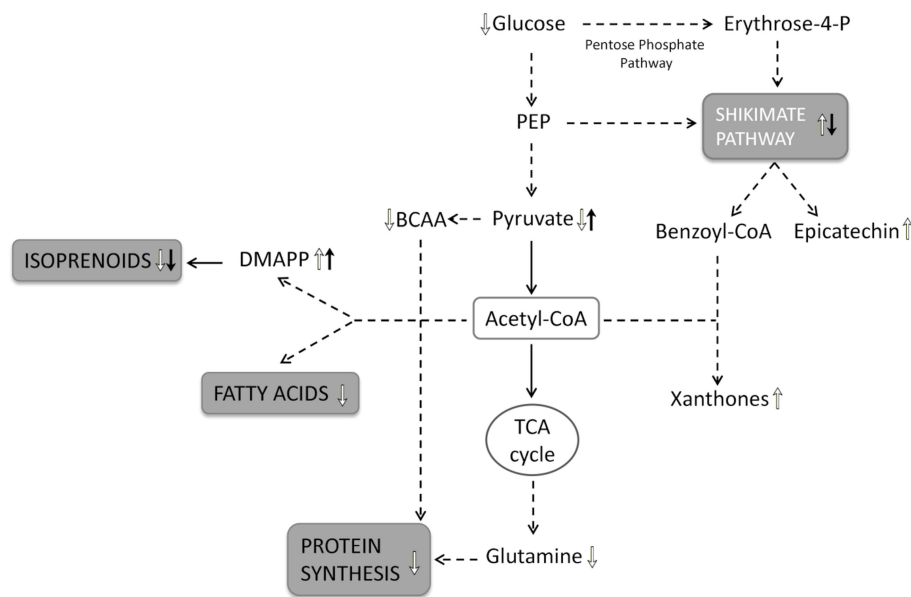


FIGURE 6 | Schematic representation of root metabolic network. The metabolic pathway involved in time-dependent response of root cultures to the stress condition are shown in gray boxes: the upward arrows indicate a positive regulation and the downward arrows a negative regulation of metabolic pathways as well as the significantly increase and the decrease in metabolite levels. The white arrows indicate the metabolic variations depending on the culture time; the black arrows indicate the metabolic variations depending on the chitosan treatment. PEP, phosphoenolpyruvate; BCAA, branched-chain aminoacids; DMAPP, dimethylallyl-pyrophosphate.

roots during the time course, examining the metabolic changes by two-way ANOVA it is possible to observe different metabolic trends in treated and untreated roots. The levels of epicatechin, gallic and shikimic acid, compound-2, and total brasiliyanthones reached the higher levels at 72 h (day 12) in chitosan treated roots. On the other hand, the levels of epicatechin, gallic and shikimic acid reached the higher values at 192 h (day 16) in untreated roots (Figures S3–S7), suggesting that the culture-age stimulate the secondary metabolism of the roots, regardless of the presence of the elicitor.

At 192 h, a significant increase in DMAPP and a decrease in sitosterol levels were only observed in the treated roots (Figures S3–S7).

The time factor also affects primary metabolic pathways involved in the biosynthesis of branches chain amino acid, glutamine, fatty acid, sterols, and low-molecular-weight organic acids. The increase in sucrose and shikimic acid levels is in agreement with the increased flux in pentose phosphate pathway that leads to fructose and erythrose-4-phosphate, the latter precursor of phenylpropanoids. The decrease in isoleucine, valine, and glutamine levels can be related to a decreased pool of free aminoacids, suggesting a down-regulation of primary metabolism toward protein synthesis that occurs during a slowdown or arrest of biomass growth.

During the time course, both control and chitosan-treated roots showed a common trend of decrease in ethanolamine and total fatty acids levels, including PUFA, MUFA, and SFA. It is well-known that ethanolamine that is mainly synthesized from serine through serine decarboxylase in mitochondria is

involved in the synthesis of membrane phospholipids, such as phosphatidylcholines and phosphatidylethanolamines. The decrease in ethanolamine levels, as well as in total fatty acid levels, could be linked to membrane remodeling that naturally occurs under stress conditions (Upchurch, 2008).

The increase in malate levels can be also related to metabolic processes associated to an altered lipid metabolism as a specific stress response (Fernie and Martinoia, 2009). Malate can be alternatively produced in the cytosol from phosphoenolpyruvate (PEP) through phosphoenolpyruvate carboxylase and malate dehydrogenase or through the malic enzyme that catalyses the reversible conversion between malate and pyruvate with a production of NADPH or NADP+, respectively (Sweetman et al., 2009). The production of NADPH through the malic enzyme is fundamental for the fatty acid synthesis (Alonso et al., 2010). The accumulation of malate in roots has been observed in response to heavy-metal stress, water stress, micronutrient disorders, as well as in pathogen response (Fernie and Martinoia, 2009; Libik-Konieczny et al., 2012; Sicher et al., 2012; Dresler et al., 2014).

Therefore, the changes in ethanolamine, fatty acids and malate levels appeared to be a common response of the roots to different stresses. Considering that a reduction in the lipid turnover is among the early and the major manifestations of aging and senescence (Troncoso-Ponce et al., 2013), the decrease in ethanolamine and total fatty acid synthesis could be associated to the root aging. The increase in malate levels could be interpreted as a decreased NADPH production, mediated by malic enzyme activity, for the fatty acid synthesis during stress conditions.

Furthermore, the observation of a browning of the biomass and the culture medium, accompanied to the slowdown of biomass growth in both treated and untreated roots, suggests that these stress responses could be referred to aging phenomena (Comas et al., 2010). In treated roots, aging processes could be linked to the stress caused by chitosan, whereas in control roots it could be related to the stress caused by the high biomass density (overcrowding stress). It should be stressed that, the SC1 loadings for the “time effect” highlighted the relationship among the changes in primary and secondary metabolism due to common phenomena occurring in both untreated and treated roots and depending on two different stresses, i.e., high biomass density and chitosan treatment. These metabolic variations suggest that two stresses affected the utilization of glycolytic intermediates and acetyl-CoA for the synthesis of amino acids and fatty acids, shifting the glucose metabolism from the glycolysis to the pentose phosphate pathway for the production of secondary metabolites. The response of root cultures to the stress conditions is displayed in **Figure 6**. Along the SC2, the significant metabolic variations regarding leucine, threonine, alanine, pyruvate, and glucose, as well as methylamine and adenosine displayed a biphasic pattern, mainly pronounced in chitosan-treated roots. Since these metabolites increased or decreased until to 72 h after chitosan elicitation and then progressively returned to their original level, a transient effect of chitosan on primary metabolism can be suggested. In other words the SC2 scores mainly describe the time-dependent changes of the metabolite levels occurring in the chitosan-treated roots before and after 72 h.

In this study, the ^1H -NMR-based metabolomics associated to ASCA modeling was used to investigate the metabolic response of *H. perforatum* *in vitro* roots to culture time and to chitosan elicitation proving a powerful tool to simultaneously analyse both primary and secondary metabolites. An up-regulation of shikimate pathway and a down-regulation of isoprenoids, fatty acids and protein metabolism was observed in response to culture time, whereas chitosan-treated roots down-regulated the shikimate and isoprenoid pathways increasing the total brasiliyanthones, particularly compound-2, and DMAPP levels. In the adopted culture conditions, it has been possible to isolate and identify for the first time in *H. perforatum* chitosan-elicited roots the brasiliyanthone B and to obtain a yield of total xanthones ten-times higher compared to previous study (Brasili et al., 2014). In untreated roots, the relative amounts of total xanthones in different days of culture were: 0.35 $\mu\text{mol/g}$ (day 11), 0.38 $\mu\text{mol/g}$ (day 12), and 0.44 $\mu\text{mol/g}$ (day 16) differently from what was observed in the previous study (0.02 $\mu\text{mol/g}$ at day 12 and 0.03 $\mu\text{mol/g}$ at day 15). In treated roots, total xanthones reached the higher levels at 72 h after chitosan addition with a yield of 0.66 $\mu\text{mol/g}$ differently from what was observed in the previous study (0.20 $\mu\text{mol/g}$; Brasili et al., 2014).

Since, most of the metabolic variations take place within 72 h from the chitosan elicitation, this culture time should be taken into account for the development of bioreactor technologies involving the use of chitosan as elicitor with the aim to maximize the production of biomass and bioactive compounds.

AUTHOR CONTRIBUTIONS

AV and GP designed the research and made the revision of the manuscript; EB and AV conducted the research; FM and GP performed the statistical analyses; FS, GP, and MD, analyzed the ^1H -NMR spectroscopy data; NT, AM, and VF, contributed to chemical data interpretation; EB, AM, and AV, wrote the manuscript and had primary responsibility for the final content. All authors read and approved the final manuscript.

ACKNOWLEDGMENTS

The present study has been supported by research grants of Sapienza University of Rome (Italy) n. C26A11XLZ5 (2011) and n. C26A14RP98 (2014).

SUPPLEMENTARY MATERIAL

The Supplementary Material for this article can be found online at: <http://journal.frontiersin.org/article/10.3389/fpls.2016.00507>

Table S1 | ^1H chemical shifts of metabolite signals in hydroalcoholic and chloroformic root extracts. Signals used for quantitative analysis by integration are highlighted in bold. d, doublet; dd, double doublet; dt, double triplet; m, multiplet; q, quartet; s, singlet; t, triplet; U0-U22, unassigned signals.

Table S2 | ^1H and ^{13}C data of Brasiliyanthone B in chloroformic extracts of chitosan-treated roots.

Table S3 | Metabolic trends of unknown compounds.

Figure S1 | Fresh cross sections of *H. perforatum* *in vitro* roots with diarch stele (A) and triarch stele (B) collected at 0.5 and 1.0 cm from the apex, respectively. The white arrows indicate xylematic arches.

Figure S2 | Typical ^1H -NMR spectra of hydroalcoholic phase of control and treated roots. (A) Control sample at time 0; (B) Control sample at time 72 h; (C) elicited sample at time 72 h; (D) Control sample at time 96 h; (E) elicited sample at time 96 h; (F) Control sample at time 192 h; (G) elicited sample at time 192 h.

Figure S3-S7 | Metabolic composition of the root extracts. The scatter plots represent the variation of each assigned metabolite over time, in both control and elicited samples. Data are expressed in $\mu\text{mol/g}$ of fresh weight and are presented as the mean \pm standard error (SEM) of five samples in five independent experiments. Gray and black dots represent control and chitosan elicited samples, respectively, at various experimental times. (a) Statistically significant difference between control and chitosan elicited samples at the same experimental time. Statistically significant difference in control or treated samples between 72 and 96 h (b), 72 and 192 h (c), and 96 and 192 h. Statistical significance was assessed by Two-Way ANOVA ($p < 0.05$).

REFERENCES

- Alonso, A. P., Dale, V. L., and Shachar-Hill, Y. (2010). Understanding fatty acid synthesis in developing maize embryos using metabolic flux analysis. *Metab. Eng.* 12, 488–497. doi: 10.1016/j.ymben.2010.04.002
- Al-Shagdari, A., Alarcón, A. B., Cuesta-Rubio, O., Piccinelli, A. L., and Rastrelli, L. (2013). Biflavonoids, main constituents from *Garcinia bakeriana* leaves. *Nat. Prod. Commun.* 8, 1237–1240.
- Baque, M. A., Moh, S. H., Lee, E. J., Zhong, J. J., and Paek, K. Y. (2012). Production of biomass and useful compounds from adventitious roots of high-value added medicinal plants using bioreactor. *Biotechnol. Adv.* 30, 1255–1267. doi: 10.1016/j.biotechadv.2011.11.004
- Barnes, J., Anderson, L. A., and Phillipson, J. D. (2001). St. John's wort (*Hypericum perforatum* L): a review of its chemistry, pharmacology, and clinical properties. *J. Pharm. Pharmacol.* 53, 583–600. doi: 10.1211/0022357011775910
- Brasili, E., Praticò, G., Marini, F., Valletta, A., Capuani, G., Sciubba, F., et al. (2014). A non-targeted metabolomics approach to evaluate the effects of biomass growth and chitosan elicitation on primary and secondary metabolism of *Hypericum perforatum* *in vitro* roots. *Metabolomics* 10, 1186–1196. doi: 10.1007/s11306-014-0660-z
- Cirak, C., Radusiene, J., Ivanauskas, L., and Janulis, V. (2007). Variation of bioactive secondary metabolites in *Hypericum origanifolium* during its phenological cycle. *Acta Physiol. Plant.* 29, 197–203. doi: 10.1007/s11738-007-0024-7
- Comas, L. H., Bauerle, T. L., and Eissenstat, D. M. (2010). Biological and environmental factors controlling root dynamics and function: effects of root ageing and soil moisture. *Aust. J. Grape Wine Res.* 16, 131–137. doi: 10.1111/j.1755-0238.2009.00078.x
- Crockett, S. L., Poller, B., Tabanca, N., Pferschy-Wenzig, E. M., Kunert, O., Wedge, D. E., et al. (2011). Bioactive xanthones from the roots of *Hypericum perforatum* (common St John's wort). *J. Sci. Food Agric.* 91, 428–434. doi: 10.1002/jsfa.4202
- Cui, X. H., Chakrabarty, D., Lee, E. J., and Paek, K. Y. (2010). Production of adventitious roots and secondary metabolites by *Hypericum perforatum* L. in a bioreactor. *Bioresour. Technol.* 101, 4708–4716. doi: 10.1016/j.biortech.2010.01.115
- Cui, X. H., Murthy, H. N., Jin, Y. X., Yim, Y. H., Kim, J. Y., and Paek, K. Y. (2011). Production of adventitious root biomass and secondary metabolites of *Hypericum perforatum* L. in a balloon type airlift reactor. *Bioresour. Technol.* 102, 10072–10079. doi: 10.1016/j.biortech.2011.08.044
- Dresler, S., Hanaka, A., Bednarek, W., and Maksymiec, W. (2014). Accumulation of low-molecular-weight organic acids in roots and leaf segments of *Zea mays* plants treated with cadmium and copper. *Acta Physiol. Plant.* 36, 1565–1575. doi: 10.1007/s11738-014-1532-x
- Fernie, A. R., and Martinoia, E. (2009). Malate. Jack of all trades or master of a few? *Phytochemistry* 70, 828–832. doi: 10.1016/j.phytochem.2009.04.023
- Franklin, G., Conceição, L. F., Kombrink, E., and Dias, A. C. (2009). Xanthone biosynthesis in *Hypericum perforatum* cells provides antioxidant and antimicrobial protection upon biotic stress. *Phytochemistry* 70, 60–68. doi: 10.1016/j.phytochem.2008.10.016
- Georgiev, M. I., Agostini, E., Ludwig-Müller, J., and Xu, J. (2012). Genetically transformed roots: from plant disease to biotechnological resource. *Trends Biotechnol.* 30, 528–537. doi: 10.1016/j.tibtech.2012.07.001
- Giddings, G., Allison, G., Brooks, D., and Carter, A. (2000). Transgenic plants as factories for biopharmaceuticals. *Nat. Biotechnol.* 18, 1151–1155. doi: 10.1038/81132
- Jansen, J. J., Hoefsloot, H. C., van der Greef, J., Timmerman, M. E., Westerhuis, J. A., and Smilde, A. K. (2005). ASCA: analysis of multivariate data obtained from an experimental design. *J. Chemom.* 19, 469–481. doi: 10.1002/cem.952
- Jin, Y. X., Cui, X. H., Paek, K. Y., and Yim, Y. H. (2012). A strategy for enrichment of the bioactive sphingoid base-1-phosphates produced by *Hypericum perforatum* L. in a balloon type airlift reactor. *Bioresour. Technol.* 123, 284–289. doi: 10.1016/j.biortech.2012.07.042
- Kuzuyama, T., and Seto, H. (2003). Diversity of the biosynthesis of the isoprene units. *Nat. Prod. Rep.* 20, 171–183. doi: 10.1039/B109860H
- Li, W., Sun, Y. N., Yan, X. T., Yang, S. Y., Choi, C. W., Hyun, J. W., et al. (2013). Isolation of xanthones from adventitious roots of St. John's Wort (*Hypericum perforatum* L.) and their antioxidant and cytotoxic activities. *Food Sci. Biotechnol.* 22, 945–949. doi: 10.1007/s10068-013-0168-8
- Libik-Konieczny, M., Surówka, E., Nosek, M., Goraj, S., and Miszalski, Z. (2012). Pathogen-induced changes in malate content and NADP dependent malic enzyme activity in C3 or CAM performing *Mesembryanthemum crystallinum* L. plants. *Acta Physiol. Plant.* 34, 1471–1477. doi: 10.1007/s11738-012-0945-7
- Maheep, K. C., Neelu, S., Mahabeer, P. D., and Yogesh, C. J. (2011). Flavonoids: a versatile source of anticancer drugs. *Pharmacogn. Rev.* 5, 1–12. doi: 10.4103/0973-7847.79093
- Marques, V. L., De Oliveira, F. M., Conserva, L. M., Brito, R. G., and Guilhon, G. M. (2000). Dichromenoxyxanthones from *Tovomita brasiliensis*. *Phytochemistry* 55, 815–818. doi: 10.1016/S0031-9422(00)00296-X
- Motavalizadehkakhky, A. (2012). Antimicrobial activity and chemical composition of essential oils of four *Hypericum* from Khorasan, Iran. *J. Med. Plant Res.* 6, 2478–2487. doi: 10.5897/jmpr11.1753
- Mulinacci, N., Giaccherini, C., Santamaria, A. R., Caniato, R., Ferrari, F., Valletta, A., et al. (2008). Anthocyanins and xanthones in the calli and regenerated shoots of *Hypericum perforatum* var. *angustifolium* (sin. Fröhlich) Borkh. *Plant Physiol. Biochem.* 46, 414–420. doi: 10.1016/j.plaphy.2007.12.005
- Naldoni, F. J., Claudino, A. L., Cruz, J. W. Jr., Chavasco, J. K., Faria e Silva, P. M., Veloso, M. P., et al. (2009). Antimicrobial activity of benzophenones and extracts from the fruits of *Garcinia brasiliensis*. *J. Med. Food* 12, 403–407. doi: 10.1089/jmf.2007.0622
- Nontakham, J., Charoenram, N., Upamai, W., Taweechotipatr, M., and Suksamrarn, S. (2014). Anti-*Helicobacter pylori* xanthones of *Garcinia fusca*. *Arch. Pharm. Res.* 8, 972–977. doi: 10.1007/s12272-013-0266-4
- Porzel, A., Farag, M. A., Mühlradt, J., and Wessjohann, L. A. (2014). Metabolite profiling and fingerprinting of *Hypericum* species: a comparison of MS and NMR metabolomics. *Metabolomics* 10, 574–588. doi: 10.1007/s11306-013-0609-7
- Rao, S. R., and Ravishankar, G. A. (2002). Plant cell cultures: chemical factories of secondary metabolites. *Biotechnol. Adv.* 20, 101–153. doi: 10.1016/S0734-9750(02)00007-1
- Rath, G., Potterat, O., Mavi, S., and Hostettmann, K. (1996). Xanthones from *Hypericum roeperanum*. *Phytochemistry* 43, 513–520. doi: 10.1016/S0031-9422(96)00284-1
- Rukachaisirikul, V., Tadpetch, K., Watthanaphanit, A., Saengsanae, N., and Phongpaichit, S. (2005). Benzopyran, biphenyl, and tetraoxxygenated xanthone derivatives from the twigs of *Garcinia nigrolineata*. *J. Nat. Prod.* 68, 1218–1221. doi: 10.1021/np058050a
- Sicher, R. C., Timlin, D., and Bailey, B. (2012). Responses of growth and primary metabolism of water-stressed barley roots to rehydration. *J. Plant Physiol.* 169, 686–695. doi: 10.1016/j.jplph.2012.01.002
- Simonetti, G., Tocci, N., Valletta, A., Brasili, E., D'Auria, F. D., Idoux, A., et al. (2015). *In vitro* antifungal activity of extracts obtained from *Hypericum perforatum* adventitious roots cultured in a mist bioreactor against planktonic cells and biofilm of *Malassezia furfur*. *Nat. Prod. Res.* 30, 544–550. doi: 10.1080/14786419.2015.1028059
- Sivakumar, G. (2006). Bioreactor technology: a novel industrial tool for high-tech production of bioactive molecules and biopharmaceuticals from plant roots. *Biotechnol. J.* 1, 1419–1427. doi: 10.1002/biot.200600117
- Sivanandhan, G., Arun, M., Mayavan, S., Rajesh, M., Mariashibu, T. S., Manickavasagam, M., et al. (2012). Chitosan enhances withanolides production in adventitious root cultures of *Withania somnifera* (L.) Dunal. *Industr. Crops Prod.* 37, 124–129. doi: 10.1016/j.indcrop.2011.11.022
- Smilde, A. K., Jansen, J. J., Hoefsloot, H. C., Lamers, R. J., van der Greef, J., and Timmerman, M. E. (2005). ANOVA-simultaneous component analysis (ASCA): a new tool for analyzing designed metabolomics data. *Bioinformatics* 21, 3043–3048. doi: 10.1093/bioinformatics/bti476
- Sweetman, C., Deluc, L. G., Cramer, G. R., Ford, C. M., and Soole, K. L. (2009). Regulation of malate metabolism in grape berry and other developing fruits. *Phytochemistry* 70, 1329–1344. doi: 10.1016/j.phytochem.2009.08.006
- Tocci, N., D'Auria, F. D., Simonetti, G., Panella, S., Palamara, A. T., Debrassi, A., et al. (2013a). Bioassay-guided fractionation of extracts from *Hypericum perforatum* *in vitro* roots treated with carboxymethylchitosans and determination of antifungal activity against human fungal pathogens. *Plant Physiol. Biochem.* 70, 342–347. doi: 10.1016/j.plaphy.2013.05.046
- Tocci, N., D'Auria, F. D., Simonetti, G., Panella, S., Palamara, A. T., and Pasqua, G. (2012). A three-step culture system to increase the xanthone production and

- antifungal activity of *Hypericum perforatum* subsp. *angustifolium* *in vitro* roots. *Plant Physiol Biochem.* 57, 54–58. doi: 10.1016/j.plaphy.2012.04.014
- Tocci, N., Simonetti, G., D'Auria, F. D., Panella, S., Palamara, A. T., Ferrari, F., et al. (2013b). Chemical composition and antifungal activity of *Hypericum perforatum* subsp. *angustifolium* roots from wild plants and plants grown under controlled conditions. *Plant Biosyst.* 147, 557–562. doi: 10.1080/11263504.2013.806964
- Tocci, N., Simonetti, G., D'Auria, F. D., Panella, S., Palamara, A. T., Valletta, A., et al. (2011). Root cultures of *Hypericum perforatum* subsp. *angustifolium* elicited with chitosan and production of xanthone-rich extracts with antifungal activity. *Appl. Microbiol. Biotechnol.* 91, 977–987. doi: 10.1007/s00253-011-3303-6
- Troncoso-Ponce, M. A., Cao, X., Yang, Z., and Ohlrogge, J. B. (2013). Lipid turnover during senescence. *Plant Sci.* 205–206, 13–19. doi: 10.1016/j.plantsci.2013.01.004
- Upchurch, R. G. (2008). Fatty acid unsaturation, mobilization, and regulation in the response of plants to stress. *Biotechnol. Lett.* 30, 967–977. doi: 10.1007/s10529-008-9639-z
- Valletta, A., De Angelis, G., Badiali, C., Brasili, E., Miccheli, A., Di Cocco, M. E., et al. (2016). Acetic acid acts as an elicitor exerting a chitosan-like effect on xanthone biosynthesis in *Hypericum perforatum* L. root cultures. *Plant Cell Rep.* doi: 10.1007/s00299-016-1934-x. [Epub ahead of print].
- Vis, D. J., Westerhuis, J. A., Smilde, A. K., and van der Greef, J. (2007). Statistical validation of megavariate effects in ASCA. *BMC Bioinformatics* 8:322. doi: 10.1186/1471-2105-8-322
- Vranová, E., Coman, D., and Grussem, W. (2012). Structure and dynamics of the isoprenoid pathway network. *Mol. Plant* 5, 318–333. doi: 10.1093/mp/sss015
- Walker, T. S., Bais, H. P., and Vivanco, J. M. (2002). Jasmonic acid-induced hypericin production in cell suspension cultures of *Hypericum perforatum* L. (St. John's wort). *Phytochemistry* 60, 289–293. doi: 10.1016/S0031-9422(02)00074-2
- Wilson, S. A., Cummings, E. M., and Roberts, S. C. (2014). Multi-scale engineering of plant cell cultures for production of specialized metabolism. *Curr. Opin. Biotechnol.* 29, 163–170. doi: 10.1016/j.copbio.2014.07.001
- Wishart, D. S., Jewison, T., Guo, A. C., Wilson, M., Knox, C., Liu, Y., et al. (2013). HMDB 3.0—the human metabolome database in 2013. *Nucleic Acids Res.* 41(Database issue), D801–D807. doi: 10.1093/nar/gks1065
- Yin, H., Fretté, X. C., Christensen, L. P., and Grevesen, K. (2012). Chitosan oligosaccharides polyphenols in Greek oregano (*Origanum vulgare* ssp. *hirtum*). *J. Agric. Food Chem.* 60, 136–143. doi: 10.1021/jf204376j
- Zubrická, D., Mišianiková, A., Henzelyová, J., Valletta, A., De Angelis, G., D'Auria, F. D., et al. (2015). Xanthones from roots, hairy roots and cell suspension cultures of selected *Hypericum* species and their antifungal activity against *Candida albicans*. *Plant Cell Rep.* 34, 1953–1962. doi: 10.1007/s00299-015-1842-5

Conflict of Interest Statement: The authors declare that the research was conducted in the absence of any commercial or financial relationships that could be construed as a potential conflict of interest.

Copyright © 2016 Brasili, Miccheli, Marini, Praticò, Sciubba, Di Cocco, Cechinel, Tocci, Valletta and Pasqua. This is an open-access article distributed under the terms of the Creative Commons Attribution License (CC BY). The use, distribution or reproduction in other forums is permitted, provided the original author(s) or licensor are credited and that the original publication in this journal is cited, in accordance with accepted academic practice. No use, distribution or reproduction is permitted which does not comply with these terms.



Molecular Cloning and Expression Analysis of *hyp-1* Type PR-10 Family Genes in *Hypericum perforatum*

Katja Karppinen¹, Emese Derzsó^{1†}, Laura Jaakola^{2,3*} and Anja Hohtola¹

¹ Genetics and Physiology Unit, University of Oulu, Oulu, Finland, ² Climate laboratory Holt, Department of Arctic and Marine Biology, UiT the Arctic University of Norway, Tromsø, Norway, ³ NIBIO, Norwegian Institute of Bioeconomy Research, Ås, Norway

OPEN ACCESS

Edited by:

Gregory Franklin,
Institute of Plant Genetics, Polish
Academy of Sciences, Poland

Reviewed by:

Anton R. Schäffner,
Helmholtz Zentrum München,
Germany
Zhi-Yuan Chen,
Louisiana State University, USA

*Correspondence:

Laura Jaakola
laura.jaakola@uit.no

†Present address:

Emese Derzsó,
Plant Developmental Biology
and Plant Physiology, University
of Kiel, Kiel, Germany

Specialty section:

This article was submitted to
Plant Metabolism
and Chemodiversity,
a section of the journal
Frontiers in Plant Science

Received: 14 February 2016

Accepted: 04 April 2016

Published: 21 April 2016

Citation:

Karppinen K, Derzsó E, Jaakola L and Hohtola A (2016) Molecular Cloning and Expression Analysis of *hyp-1* Type PR-10 Family Genes in *Hypericum perforatum*. *Front. Plant Sci.* 7:526.
doi: 10.3389/fpls.2016.00526

Hypericum perforatum L. is an important medicinal plant for the treatment of depression. The plant contains bioactive hypericins that accumulate in dark glands present especially in reproductive parts of the plant. In this study, pathogenesis-related class 10 (PR-10) family genes were identified in *H. perforatum*, including three previously unidentified members with sequence homology to *hyp-1*, a phenolic coupling protein that has earlier been suggested to participate in biosynthesis and binding/transportation of hypericin. The PR-10 genes showed constitutive but variable expression patterns in different *H. perforatum* tissues. They were all expressed at relatively high levels in leaves, variably in roots and low levels in stem and reproductive parts of the plant with no specific association with dark glands. The gene expression was up-regulated in leaves after salicylic acid, abscisic acid and wounding treatments but with variable levels. To study exact location of the gene expression, *in situ* hybridization of *hyp-1* transcripts was performed and the accumulation of the Hyp-1 protein was examined in various tissues. The presence of Hyp-1 protein in *H. perforatum* tissues mostly paralleled with the mRNA levels. *In situ* RNA hybridization localized the *hyp-1* transcripts predominantly in vascular tissues in root and stem, while in leaf the mRNA levels were high also in mesophyll cells in addition to vasculature. Our results indicate that the studied PR-10 genes are likely to contribute to the defense responses in *H. perforatum*. Furthermore, despite the location of the *hyp-1* transcripts in vasculature, no support for the transportation of the Hyp-1 protein to dark glands was found in the current study. The present results together with earlier data question the role of the *hyp-1* as a key gene responsible for the hypericin biosynthesis in dark glands of *H. perforatum*.

Keywords: St. John's wort, pathogenesis-related, PR proteins, defense response, gene expression, abscisic acid, salicylic acid, wounding

INTRODUCTION

Pathogenesis-related (PR) proteins constitute of a large group of proteins in higher plants often associated in plant defense responses. Based on sequence homology and biological activities, these proteins are classified into 17 different families (van Loon et al., 2006; Agarwal and Agarwal, 2014). The PR-10 subfamily is the largest family with members reported in numerous plant species and it includes major food and tree pollen allergens (Radauer and Breiteneder, 2007; Fernandes et al., 2013; Nakamura and Teshima, 2013). The members of the PR-10 protein family share

common features such as low-molecular weight (15–20 kDa) with typically acidic *pI*, similar three-dimensional structure as well as conserved P-loop region, and usually cytosolic location (Liu and Ekramoddoullah, 2006; Fernandes et al., 2013; Agarwal and Agarwal, 2014).

The biological significance of the PR-10 proteins is not well understood but they are proposed to have a wide range of roles in plants. Association of the PR-10 proteins in plant defense has been suggested since many of the proteins are induced or their expression is up-regulated under various biotic or abiotic stress conditions, and some members exhibit antimicrobial or ribonuclease activity (Liu and Ekramoddoullah, 2006; Fernandes et al., 2013; Agarwal and Agarwal, 2014). There are also several reports of the up-regulation of the PR-10 gene expression by plant hormones and other signaling molecules transmitting plant defense responses (Pulla et al., 2010; Takeuchi et al., 2011; Jain et al., 2012; Agarwal and Agarwal, 2014). Structural studies have implied that the role of PR-10 proteins could be related to the binding and transportation of various hydrophobic ligands involved in plant development and defense-related signaling (Radauer et al., 2008; Fernandes et al., 2009, 2013). Few PR-10 members have also been proposed to perform an enzymatic condensation reaction between the ligands they bind (Bais et al., 2003; Lee and Facchini, 2010).

Many plant species have been reported to contain more than one PR-10 protein (Schenk et al., 2009; Bahramnejad et al., 2010; Lebel et al., 2010; Xie et al., 2010; Lee et al., 2012). The significance of the multiple closely related genes in a single plant species is not clear but they may contribute to the diversification of functions between the PR-10 genes (Lebel et al., 2010). For example in peach, two Pru p 1 protein isoforms have been reported to differ in their RNA hydrolysis and ligand binding activities (Zubini et al., 2009). In lupin, birch, grapevine, and ginseng, the members of the PR-10 gene family showed variable expression patterns in various tissues or in response to stress conditions indicating functional diversification between the family members (Pinto et al., 2005; Schenk et al., 2006; Lebel et al., 2010; Lee et al., 2012; He et al., 2013).

Hypericum perforatum L., commonly known as St. John's wort, is a herbaceous perennial plant that has received considerable interest due to its medicinal properties. The plant is widely utilized for the treatment of mild to moderate depression, and the efficacy of the plant crude extracts has been confirmed by several clinical and pharmacological studies (reviewed in Russo et al., 2014). The medicinal properties of the plant are attributed to secondary metabolites called hypericins and hyperforins that are accumulating in dark and translucent glands, respectively, in the aerial parts of the plant, especially in reproductive parts (Karppinen and Hohtola, 2008). There are also evidences supporting the biosynthesis of hypericins in the dark glands (Zobayed et al., 2006; Kornfeld et al., 2007; Karppinen et al., 2008; Košuth et al., 2011). To date, one PR-10 gene from *H. perforatum*, called *hyp-1*, has been described, and its function has been suggested to be related with the biosynthesis and binding/transportation of hypericin (Bais et al., 2003; Michalska et al., 2010) as well as plant defense under stress conditions (Košuth et al., 2013). The objective of the present

study was to investigate the presence of PR-10 family genes in *H. perforatum*. Here we report molecular cloning and expression analysis of three previously unidentified *H. perforatum* cDNAs with sequence homology to *hyp-1* and genes encoding class PR-10 proteins of other species. The expression of the three *PR-10* genes along with *hyp-1* were examined in various *H. perforatum* tissues as well as following wounding and treatments with stress-related signaling molecules to assess their potential contribution in plant defense. Furthermore, the *hyp-1* expression was analyzed at protein and cellular levels in order to obtain more detailed information of its location in the plant.

MATERIALS AND METHODS

Plant Material

The *H. perforatum* L. plants of Finnish origin were grown in field conditions in the Botanical Gardens of the University of Oulu, Finland. Tissue samples (stem, root, leaf, and flower bud) were collected from the plants at the early stage of flowering. The collected leaves were dissected into leaf margins that contained dark glands and into leaf interior parts that were free of dark glands. Immediately after excision, all tissues were frozen in liquid nitrogen and stored at -80°C until they were used for RNA isolation, protein extraction and the determination of hypericins. Alternatively, tissues were fixed overnight at 4°C in 4% (w/v) paraformaldehyde and 0.25% (v/v) glutaraldehyde in 0.1 M sodium phosphate buffer (pH 7.0) for *in situ* RNA hybridization analysis. For stress treatments, the leaves of the plants were either wounded or sprayed with solutions of stress-related phytohormones (\pm -abscisic acid (ABA; Sigma, St. Louis, MO, USA) or salicylic acid (SA; Sigma). Concentrations of the phytohormones, 100 μM of ABA and 10 mM of SA, were selected based on previously reported studies (Bahramnejad et al., 2010; Pulla et al., 2010). Wounding of the leaves was carried out by making parallel incisions with a razor blade lengthwise on leaves. The leaf samples were collected at 0, 3, 6, 10, 24, and 48 h after each treatment, immediately frozen in liquid nitrogen and stored at -80°C until they were used for RNA isolation.

Isolation of RNA and cDNA Preparation

Total RNA was isolated from different tissues of *H. perforatum* according to Jaakola et al. (2001). The cDNA was synthesized from the total RNA using SuperScript III reverse transcriptase (Invitrogen, Carlsbad, CA, USA) with random primers according to the manufacturer's instructions. The cDNA was purified from contaminating genomic DNA by using the method described by Jaakola et al. (2004).

Isolation of *H. perforatum* PR-10 Genes

To isolate *H. perforatum* PR-10 genes, previously identified plant *PR-10* family genes were aligned and degenerate oligonucleotide primers were designed based on identified conserved regions. Degenerate primers 5'-ARATHATHGARGNGAYG-3' (forward primer) and 5'-RRTAYTCYTCNACYTGYT-3' (reverse primer) were used for amplification of *PR-10* genes from *H. perforatum* cDNA. PCR reactions were performed

with DyNzyme™ II DNA polymerase (Finnzymes, Espoo, Finland) under conditions: initial denaturation at 94°C for 4 min, followed by 7 cycles at 94°C for 1 min, 70°C for 3 min, ramp rate of 0,1°C/s to 36°C and 72°C for 2 min, followed by 35 cycles at 94°C for 1 min, 40°C for 2 min, and 72°C for 2 min, and final extension at 72°C for 5 min. The amplified PCR products were gel-purified using a Montage® DNA Gel Extraction Kit (Millipore, Bedford, MA, USA) and ligated into a pGEM-T Easy vector (Promega, Madison, WI, USA). Sequencing was performed by using an ABI 3730 DNA sequencer (Applied Biosystems, Foster City, CA, USA) with a BigDye Terminator Cycle Sequencing Kit (Applied Biosystems). The 3' and 5' cDNA ends were isolated using a SMART™ RACE cDNA Amplification Kit (Clontech, Palo Alto, CA, USA). The nucleotide sequences of *HpPR10.1* (*hyp-1*), *HpPR10.2*, *HpPR10.3*, and *HpPR10.4* were deposited to GenBank under accession numbers KU565780, KU565781, KU565782, and KU565783, respectively.

Sequence Analysis

For alignment and phylogenetic analysis of the *H. perforatum* PR-10 sequences, amino acid sequences of previously characterized PR-10 family proteins of other species were obtained from GenBank and aligned with *H. perforatum* PR-10 sequences by using Clustal Omega program. A phylogenetic tree was constructed by using the neighbor-joining method with the MEGA software, version 6.06. The reliability of the tree was evaluated by a bootstrap analysis with 1000 replicates. The predicted protein molecular weight was calculated using Compute PI/Mw tool (ExPASy Server). Signal peptide prediction was carried out using online tools SignalP 4.1 Server (Petersen et al., 2011) and Signal-BLAST, and the prediction of transmembrane domains was performed by using TMHMM Server v 2.0.

Relative Quantification by Real-Time PCR

Real-time quantitative reverse transcription PCR (qRT-PCR) analyses were performed with a LightCycler® 480 instrument and software (Roche, Basel, Switzerland). The transcript abundance of the isolated *H. perforatum* PR-10 genes was detected using a LightCycler SYBR Green I Master qPCR Kit (Roche). The PCR conditions were an initial incubation at 95°C for 10 min followed by 45 cycles at 95°C for 10 s, 60°C for 20 s, and 72°C for 10 s. The gene-specific primer sequences used for the qRT-PCR analysis are shown in Table 1. For relative quantification of the PCR products, glyceraldehyde-3-phosphate dehydrogenase (*GAPDH*; GenBank Accession No. GU014528) was employed as a control gene. The results were verified by using 18S rRNA (GenBank Accession No. AF206934) as a control gene. The results were calculated with LightCycler® 480 software (Roche), using the calibrator-normalized PCR efficiency-corrected method (Technical note No. LC 13/2001, Roche).

The specificities of the amplified qRT-PCR products were verified by a melting curve analysis. The obtained PCR products

were further subjected to agarose electrophoresis, followed by gel extraction using a Montage® DNA Gel Extraction Kit (Millipore) and sequenced as described above to confirm the amplification of the desired product.

In Situ RNA Hybridization Analysis

Fixed *H. perforatum* tissues were embedded in paraffin, sectioned, de-paraffined and rehydrated as described earlier (Karppinen et al., 2008). Digoxigenin (DIG)-labeled *hyp-1* sense and antisense RNA probes were obtained by *in vitro* transcription from a linearized plasmid containing a fragment of *hyp-1* cDNA. For the plasmid construction, a 312-bp fragment from the coding region of *hyp-1* was amplified from *H. perforatum* cDNA by PCR with DyNzyme™ II DNA polymerase (Finnzymes) using primers 5'-AGGCATTGGTCCTGAACG-3' (forward) and 5'-CAGGCTTGGGATGATAGGAG-3' (reverse) under standard PCR conditions. The PCR product was gel-purified, ligated into a pGEM-T Easy vector (Promega), and sequenced as described above to confirm the amplification of the desired product. *In vitro* transcription of the probes was performed from the linearized plasmid with either T7 or SP6 RNA polymerase using a DIG RNA Labeling Kit (Roche) according to the manufacturer's instructions.

In situ RNA hybridization analysis was performed as described previously (Karppinen et al., 2008) with the exception that the hybridization with the RNA probes was carried out at 54°C. The *hyp-1* sense probe was used in negative control sections. The sections were examined and photographed under a light microscope (Nikon Optiphot-2; Nikon Corporation, Tokyo, Japan) or scanned with a confocal laser scanning microscope (LSM-5 Pascal; Zeiss, Jena, Germany).

Immunoblotting Analysis

Proteins were isolated from *H. perforatum* tissues using a method described by Karppinen et al. (2010). The protein concentration of the extracts was determined according to Bradford (1976), using bovine serum albumin (Sigma) as a standard. Samples containing 30 µg of proteins were separated with sodium dodecyl sulfate-polyacrylamide gel electrophoresis (SDS-PAGE), using 12% resolving and 3% stacking gels. The separation was conducted using a Mini-Protean II electrophoresis system

TABLE 1 | Gene-specific primers used for quantitative reverse transcription PCR (qRT-PCR) analyses.

Gene	Primer sequence 5'-3'
<i>HpPR10.1</i> (<i>hyp-1</i>)	CAGGCTTAAAGGCATTGGTC (forward) GGGATGTCCATCAACGAAAGTG (reverse)
<i>HpPR10.2</i>	AGAAAATCAAGGTGGACAAGAG (forward) CGAGGAAACAAGACCATAAAC (reverse)
<i>HpPR10.3</i>	GAGGAAATCAAGCTAGGGCAAG (forward) TGACGACGACTATTGCACACAC (reverse)
<i>HpPR10.4</i>	GGCACAGGAAGCAAGGGTAAG (forward) GGGTAAACAAGGCCACCTCAG (reverse)
<i>HpGAPDH</i>	ATGGACCACATCAAGCAAGGACTG (forward) GAAGGCCATTCCAGTCAACTTC (reverse)

(Bio-Rad, Hercules, CA, USA) at 200 V. After electrophoresis, the proteins were either visualized with Coomassie Brilliant Blue R-250 (Merck, Darmstadt, Germany) or electroblotted for immunodetection onto polyvinylidene difluoride (PVDF) membrane (Bio-Rad) by using a Mini Trans-Blot Electrophoretic Transfer Cell (Bio-Rad) at 100 V for 2 h. The immunological detection of Hyp-1 protein was performed as described previously (Karppinen et al., 2010). Intensities of each protein band were quantified using Quantity One software (Bio-Rad). Samples from three independent plants were employed for analyses.

Production of Recombinant Hyp-1 Protein

The coding region of the *hyp-1* gene was amplified from *H. perforatum* cDNA by PCR, using forward primer 5'-CTATTTAACATTGGATCCATGGCGCGTA-3' (the translation start codon is in bold and the *Bam*HI site is underlined) and reverse primer 5'-GCAAAGGGTACCTTAAGCGAAAACTTCAGGA-3' (the translation stop codon is in bold and the *Kpn*I site is underlined) under standard PCR conditions. The PCR product was gel-purified and ligated into *Bam*HI/*Kpn*I site of a pQE30 expression vector (Qiagen GmbH, Hilden, Germany). The obtained recombinant plasmid was transferred into *Escherichia coli* host strain M15 [pREP4] (Qiagen). The *E. coli* cells were grown in Luria-Bertani liquid medium in the presence of ampicillin (100 µg mL⁻¹) and kanamycin (25 µg mL⁻¹) at 37°C until the *D*₆₀₀ of the culture reached 0.6. The cells were induced by 0.5 mM isopropyl thio-β-D-galactoside (IPTG) for 4 h at 37°C. The recombinant Hyp-1 protein containing an additional hexahistidine tag at the N-terminus was purified from the *E. coli* cells as described previously (Karppinen et al., 2008).

Determination of Hypericins

HPLC-DAD was used for the determination of hypericin, pseudohypericin, protohypericin, and protopseudohypericin from different *H. perforatum* tissues as described previously (Karppinen and Hohtola, 2008). Samples from three individual plants were employed for analyses.

Statistical Analysis

Quantitative results of analyses of gene expression, protein levels and content of hypericins are presented in terms of

means ± SEs of at least three biological replicates. The effects of stress treatments on gene expression were analyzed with Student's *t*-Test by using SPSS Statistics program, version 22 (IBM, New York, NY, USA).

RESULTS

Cloning and Sequence Analysis of PR-10 Genes

In a search for *H. perforatum* PR-10 genes, four different nucleotide sequences were obtained with a homology-based PCR-method designated to target conserved regions of the PR-10 genes. The first sequence (*HpPR10.1*) was identified as *hyp-1* gene that was first described and indicated for hypericin biosynthesis in *H. perforatum* by Bais et al. (2003). The other three genes, named according to usual nomenclature as *HpPR10.2*, *HpPR10.3*, and *HpPR10.4*, were isolated in full-length and they showed 79, 80, and 80% sequence identity, respectively, at nucleotide level to *hyp-1* gene (Table 2). All the isolated genes had a coding sequence (CDS) of 480 bp predicted to encode protein of 159 amino acids with a calculated molecular mass of 17.75–17.84 kDa and a theoretical *pI* ranging from 5.54 to 6.16 (Table 2). These protein features coincide well with those typically reported for PR-10 family proteins (Liu and Ekramoddoullah, 2006; van Loon et al., 2006; Fernandes et al., 2013) and earlier for *hyp-1* (Bais et al., 2003; Michalska et al., 2010). The proteins are likely to be cytoplasmic as no signal peptides or trans-membrane domains were detected in their sequences.

Multiple sequence alignment analysis showed that the predicted amino acid sequences of the isolated *H. perforatum* PR-10 genes (*HpPR10.1*, *HpPR10.2*, *HpPR10.3*, and *HpPR10.4*) had high homologies with other members of the PR-10 family proteins (Figure 1). All the four *H. perforatum* PR-10 sequences were found to contain a glycine-rich P-loop region (G-X-G-G-X-G) that is reported to be conserved among PR-10 proteins (Fernandes et al., 2013) and share similar Bet v 1 family signature motif region as described earlier for Hyp-1 by Bais et al. (2003). Phylogenetic analysis demonstrated that *H. perforatum* PR-10 sequences grouped as their own cluster similarly to other PR-10 proteins that also tended to cluster together with the homologs of the same taxonomic group (Figure 1). This type of clustering has been reported typical among PR-10 proteins and suggest gene duplication events

TABLE 2 | Characteristics of the sequences of *H. perforatum* PR-10 genes and their coding sequence (CDS) identity to each other.

Gene	GenBank no.	Characteristics				Sequence identity at nucleotide level (%) ¹			
		CDS (bp)	Amino acids	Protein mass (kDa)	<i>pI</i>	<i>HpPR10.1</i>	<i>HpPR10.2</i>	<i>HpPR10.3</i>	<i>HpPR10.4</i>
<i>HpPR10.1</i> (<i>hyp-1</i>)	KU565780	480	159	17.84	5.54	100	79	80	80
<i>HpPR10.2</i>	KU565781	480	159	17.75	5.80		100	91	91
<i>HpPR10.3</i>	KU565782	480	159	17.77	5.89			100	90
<i>HpPR10.4</i>	KU565783	480	159	17.81	6.16				100

¹The values were obtained from sequence alignments on Clustal Omega. CDS, coding sequence.

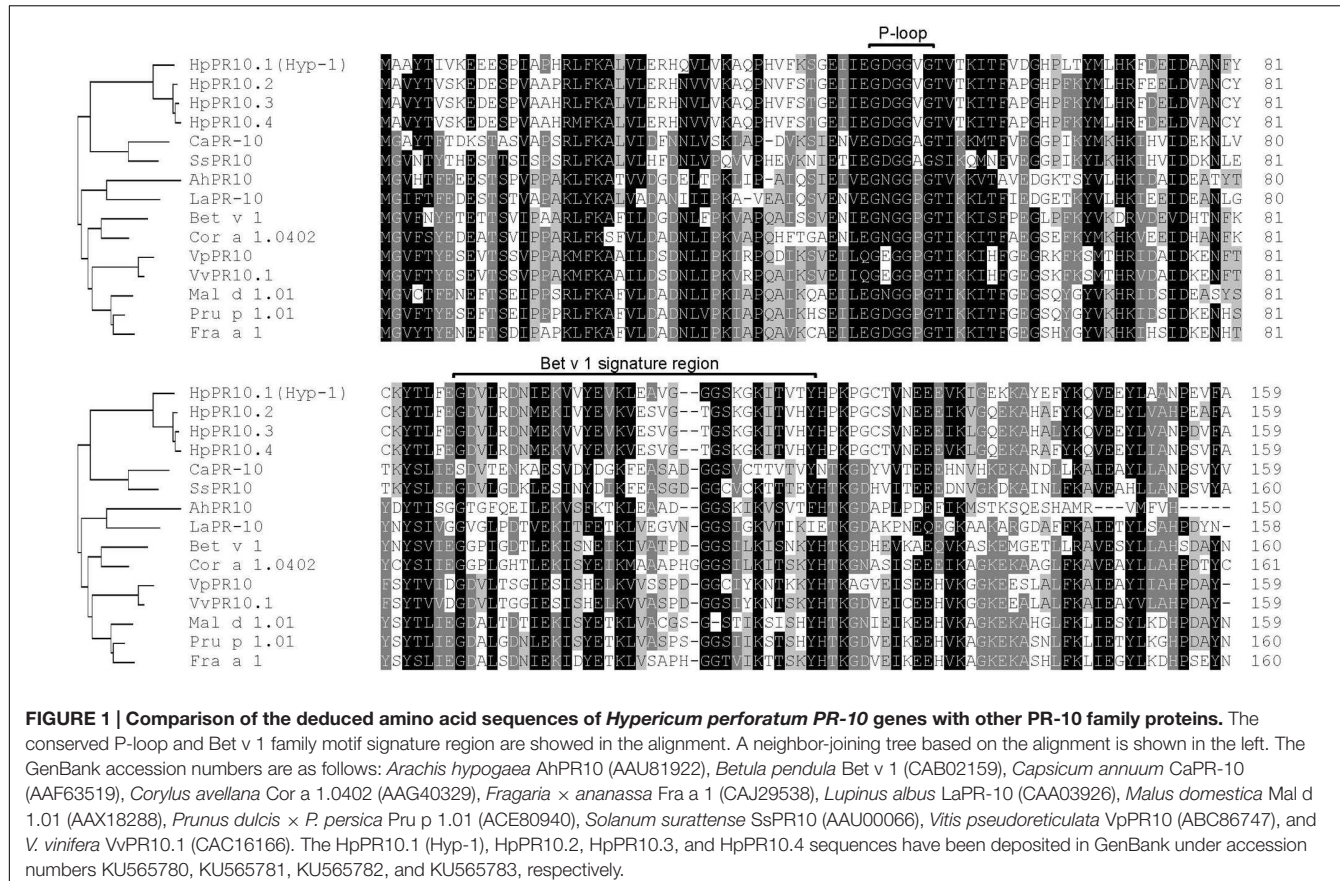


FIGURE 1 | Comparison of the deduced amino acid sequences of *Hypericum perforatum* PR-10 genes with other PR-10 family proteins. The conserved P-loop and Bet v 1 family motif signature region are showed in the alignment. A neighbor-joining tree based on the alignment is shown in the left. The GenBank accession numbers are as follows: *Arachis hypogaea* AhPR10 (AAU81922), *Betula pendula* Bet v 1 (CAB02159), *Capsicum annuum* CaPR-10 (AAF63519), *Corylus avellana* Cor a 1.0402 (AAG40329), *Fragaria × ananassa* Fra a 1 (CAJ29538), *Lupinus albus* LaPR-10 (CAA03926), *Malus domestica* Mal d 1.01 (AAC18288), *Prunus dulcis* × *P. persica* Pru p 1.01 (ACE80940), *Solanum tuberosum* SsPR10 (AAU00066), *Vitis pseudoreticulata* VpPR10 (ABC86747), and *V. vinifera* VvPR10.1 (CAC16166). The HpPR10.1 (Hyp-1), HpPR10.2, HpPR10.3, and HpPR10.4 sequences have been deposited in GenBank under accession numbers KU565780, KU565781, KU565782, and KU565783, respectively.

during evolution (Radauer and Breiteneder, 2007; Lebel et al., 2010).

Expression of PR-10 Genes in *H. perforatum* Tissues

The transcript levels of the isolated PR-10 genes were examined in different *H. perforatum* tissues with a qRT-PCR. All the genes were expressed at detectable levels in all tissues but with slightly variable expression patterns. Generally, the expression of all the genes was relatively high in leaf tissues, with no marked difference between leaf margin that contained dark glands and leaf interior part free of dark glands (Figure 2). Furthermore, the expression of all the genes was relatively low in stem tissue in comparison to leaf tissues and especially low in flower buds (Figure 2), the primary site for the accumulation of hypericins (Supplementary Figure S1). Instead, the expression levels of *HpPR10.1* (*hyp-1*; Figure 2A) and *HpPR10.4* (Figure 2D) were relatively low in root tissues while *HpPR10.2* (Figure 2B) and *HpPR10.3* (Figure 2C) had higher relative transcript levels in root. All the genes showed higher expression levels in younger parts of root closer to root tip compared to upper parts of root (data not shown).

In Situ RNA Localization of *hyp-1*

The exact localization of the *hyp-1* gene expression in *H. perforatum* tissues was studied by *in situ* RNA hybridization.

The study revealed that the *hyp-1* transcripts were mainly associated with leaf mesophyll as well as with the differentiated cells of vascular tissue in leaf, stem, and root. In stem, a blue signal for transcripts was mainly localized in both phloem and xylem cells in the area of vascular tissue but a weak signal was also present in the parenchyma cells under the stem epidermis (Figure 3A). The probe specificity was confirmed by the absence of any signal in the negative control sections of the stem hybridized with sense probe (Figure 3B). In the stem xylem, the signal was associated with xylem parenchyma cells in both the secondary and the primary xylem (Figure 3C). In the stem phloem, the signal was associated with parenchyma cells (Figure 3C) and small companion cells next to larger sieve elements (Figure 3D). The sieve elements showed no apparent signal. The mRNA was also apparent in cells surrounding specific secretory canals (Figure 3D), named type A canals earlier by Ciccarelli et al. (2001). In root, the transcripts were present in xylem parenchyma cells, in pericycle cells as well as in cells within the phloem (Figure 3E). No signal was detected in the corresponding areas of the negative control sections of roots (Figure 3F). In leaves, the mRNA was associated with both palisade and spongy parenchyma cells (Figure 3G). The signal was also detected in vascular tissues of leaves and was mostly associated with the cells surrounding the type A canals of the phloem (Figure 3H). No detectable signal was found in the cells of dark glands.

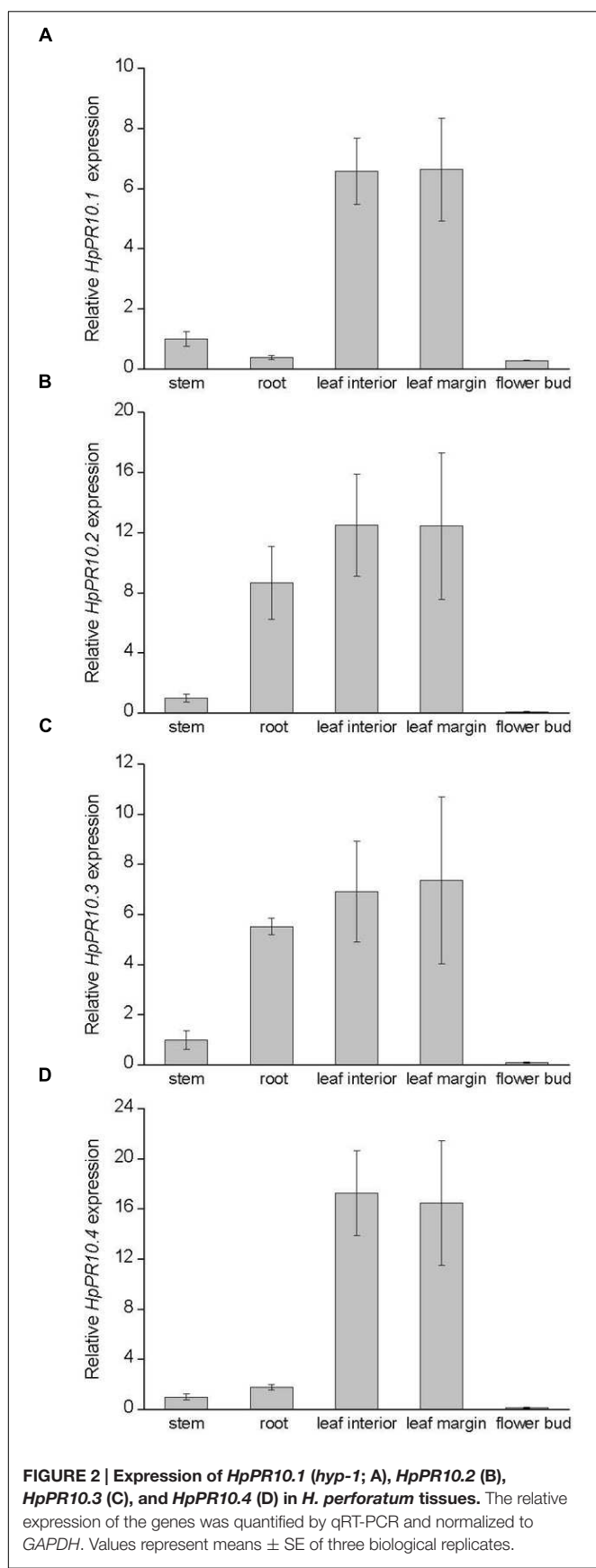


FIGURE 2 | Expression of *HpPR10.1* (*hyp-1*; A), *HpPR10.2* (B), *HpPR10.3* (C), and *HpPR10.4* (D) in *H. perforatum* tissues. The relative expression of the genes was quantified by qRT-PCR and normalized to GAPDH. Values represent means \pm SE of three biological replicates.

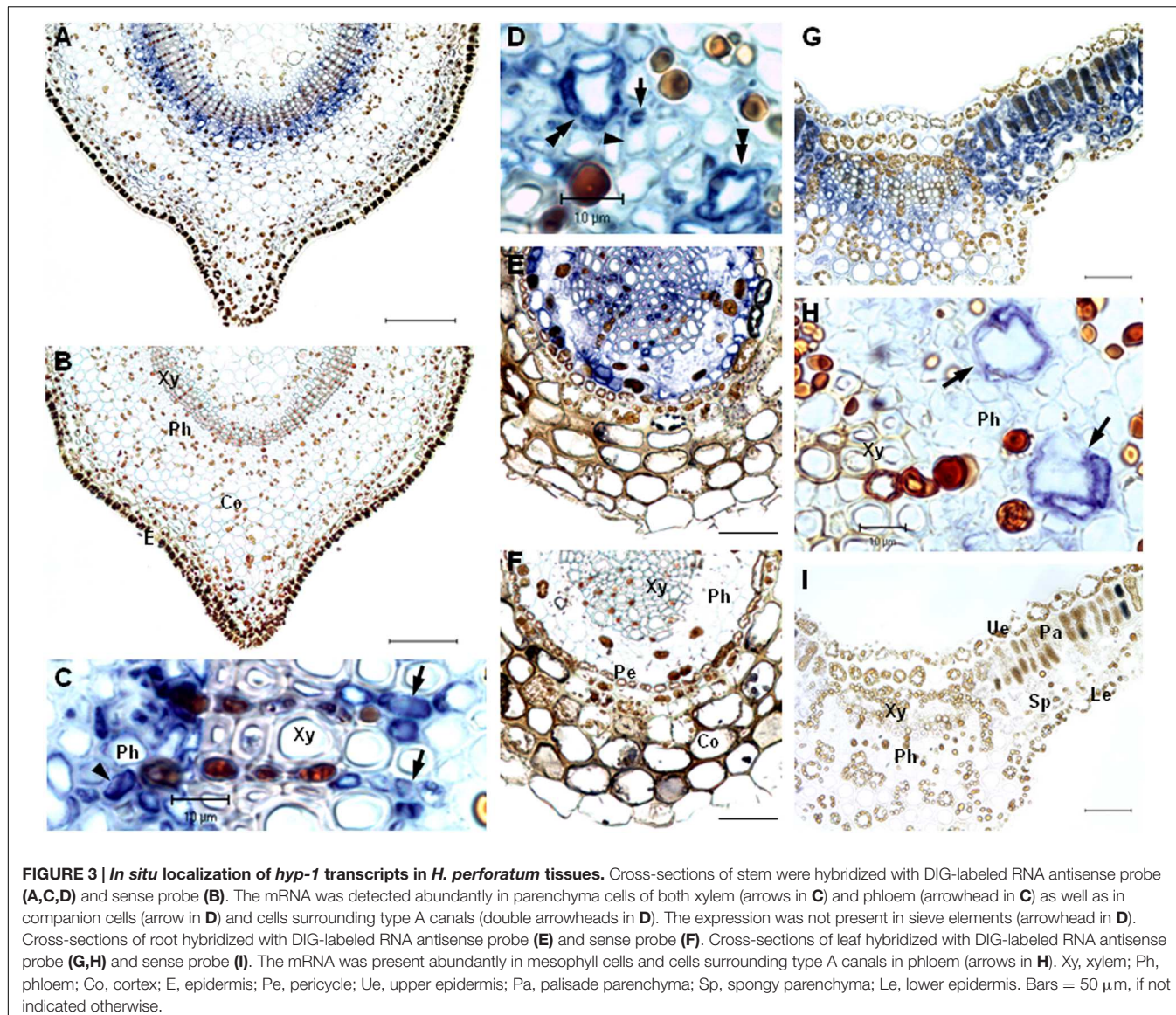
Neither signal was detected in negative controls of leaf sections (Figure 3I).

Immunoblotting Analysis of Hyp-1 Protein in *H. perforatum* Tissues

We also examined the presence of Hyp-1 at protein level by immunoblotting analysis in the same *H. perforatum* tissues used for qRT-PCR analysis. In immunoblots, the antibody raised against Hyp-1 reacted with a purified recombinant Hyp-1 protein of about 18.5 kDa (Figure 4A) and a polypeptide of approximately 18 kDa in extracts of *H. perforatum* tissues (Figure 4B). The size coincides with the predicted molecular mass of 17.8 kDa for natural Hyp-1 protein that was calculated using bioinformatics tools and with the size that has previously been reported for Hyp-1 protein by other authors (Bais et al., 2003; Michalska et al., 2010). The small increase in the recombinant Hyp-1 protein size compared with the natural Hyp-1 protein is due to the presence of a His-tag at the N-terminus of the recombinant protein (12 additional amino acids). Immunoblotting analysis of *H. perforatum* tissues showed the highest level of Hyp-1 protein to be present in stem and leaf tissues while markedly lower levels were detected in root and especially flower buds (Figure 4B). Leaf margin containing dark glands and leaf interior part free of dark glands contained equal amounts of Hyp-1 protein (Figure 4B). The SDS-PAGE analysis demonstrated an equal loading of proteins to the gel with equal amounts of Rubisco subunits between the samples of leaf margin and leaf interior. The portion of the Rubisco subunits in the total protein loaded to the gel is high in stem and leaf samples but in flower buds and especially in root the Rubisco subunits form lower portion in the total proteins. This may cause some elevation in the level of Hyp-1 protein in immunoblot in these tissues relative to the green tissues.

Expression of PR-10 Genes in Response to Stress Treatments

To examine whether the expression of the *HpPR10* genes are affected by different stress treatments, *H. perforatum* leaves were either wounded or treated with stress-related signaling molecules salicylic acid (SA; 10 mM) or abscisic acid (ABA; 100 μ M). As shown in Figure 5, the treatment with SA significantly up-regulated the expression of *HpPR10.2*, *HpPR10.3*, and *HpPR10.4* in *H. perforatum* leaves. Especially the transcripts of *HpPR10.4* were highly induced by SA already 3 h after the treatment, and the expression gradually declined after that. The expression of *HpPR10.2* peaked at 6 h and *HpPR10.3* at 10 h after the SA treatment. Also the treatment with ABA significantly elevated *HpPR10.2*, *HpPR10.3*, and *HpPR10.4* expression after 6 h of the treatment with declining trend in the expression detected thereafter. Mechanical wounding of leaves significantly up-regulated the expression of *HpPR10.3* and *HpPR10.4* peaking 6 h after the treatment. Also *HpPR10.2* expression was elevated by the wounding but there seemed to be high variation between individual plants in the level of response to the treatment. None of the treatments significantly increased the expression



of *HpPR10.1* (*hyp-1*) in *H. perforatum* leaves in the present study.

DISCUSSION

Many plant species have been found to contain several proteins belonging to the PR-10 family. Although the role of the PR-10 genes is not entirely known, functional diversification between the genes in plant development and protein-based defense has been suggested (Lebel et al., 2010). The presence of PR-10 genes has also been reported in genus *Hypericum* (Bais et al., 2003; Jin et al., 2010). In the present study, the search for sequences encoding PR-10 proteins in *H. perforatum* revealed three previously unidentified members that were closely related to earlier described *hyp-1*, a phenolic coupling protein suggested to be involved in biosynthesis and binding/transportation of

hypericin (Bais et al., 2003; Michalska et al., 2010). The isolated *H. perforatum* PR-10 genes shared 79 to 80% identity at nucleotide level with *hyp-1*. The characteristics of the proteins, which were predicted to be small, acidic and cytosol-located, coincide well with those typically reported for PR-10 family proteins (Liu and Ekramoddoullah, 2006; Fernandes et al., 2013; Agarwal and Agarwal, 2014). Furthermore, their sequences contained features common to PR-10 family proteins, such as a glycine-rich P-loop conserved among PR-10 proteins (Fernandes et al., 2013) and shared similar Bet v 1 family signature motif region as described earlier for Hyp-1 (Bais et al., 2003).

The expression of some PR-10 proteins is known to be induced under certain stress conditions or expressed only in some tissues while some are constitutively expressed (Agarwal and Agarwal, 2014). Based on our results, all the studied *H. perforatum* PR-10 genes were expressed in all analyzed

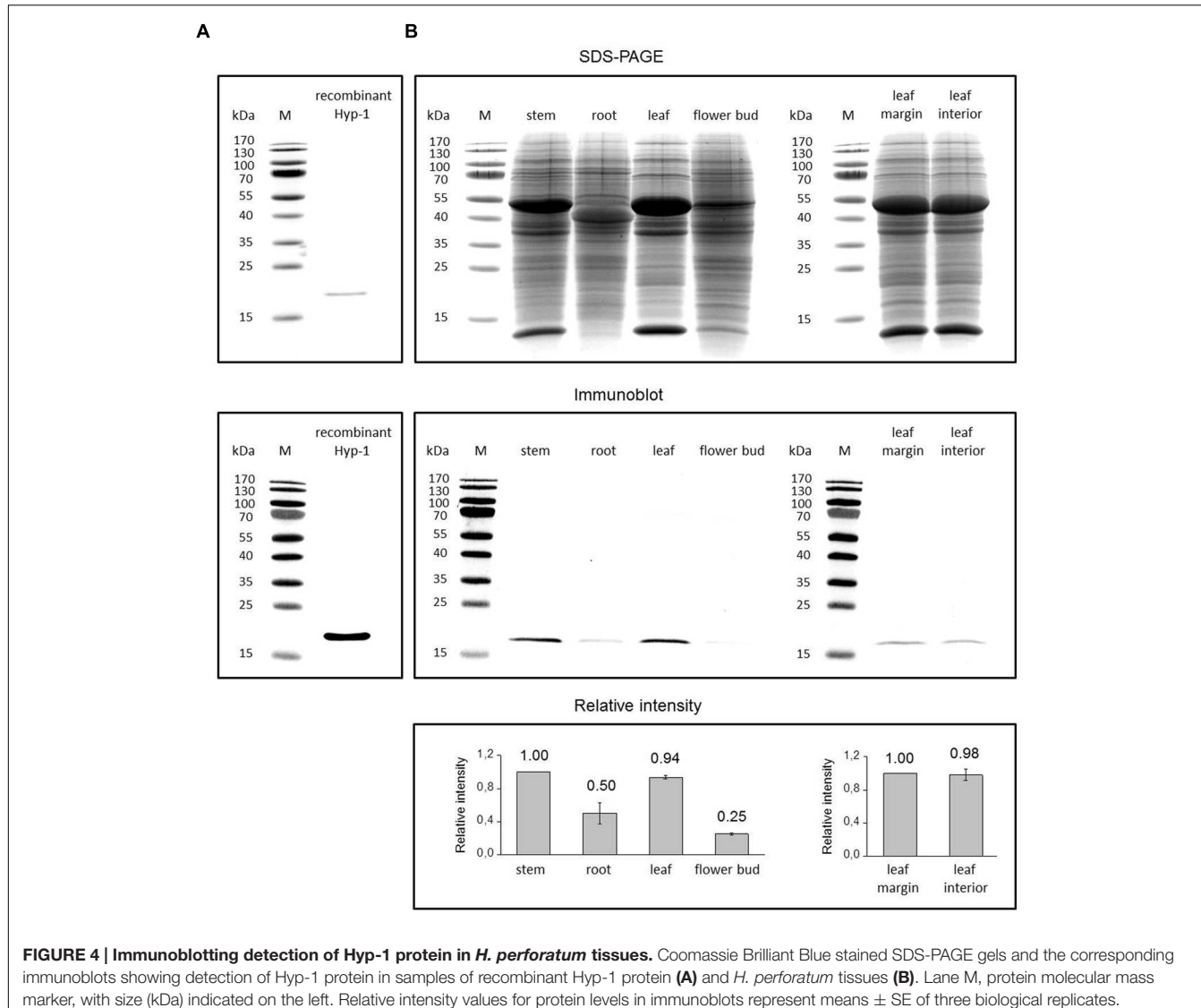


FIGURE 4 | Immunoblotting detection of Hyp-1 protein in *H. perforatum* tissues. Coomassie Brilliant Blue stained SDS-PAGE gels and the corresponding immunoblots showing detection of Hyp-1 protein in samples of recombinant Hyp-1 protein (**A**) and *H. perforatum* tissues (**B**). Lane M, protein molecular mass marker, with size (kDa) indicated on the left. Relative intensity values for protein levels in immunoblots represent means \pm SE of three biological replicates.

tissues. Their expression was most highly associated with leaf tissues with lower transcript amounts found in stem and root tissues. Their expression differed from each other mostly in root tissue where expression of *HpPR10.2* and *HpPR10.3* was relatively high compared to relatively low expression of *HpPR10.1* (*hyp-1*) and *HpPR10.4* indicating possible specialization in their function between organs. We also found that the expression of all the *H. perforatum* PR-10 genes was higher closer to the root tip. Earlier, Košuth et al. (2007) have reported that the *hyp-1* expression pattern of *ex vitro* plants differ from the pattern of young *in vitro* seedlings, which showed a high level of expression in roots. We have also demonstrated earlier that the developmental stage of leaf affects the presence of Hyp-1 protein (Karppinen et al., 2010) supporting the suggestion that the *H. perforatum* PR-10 genes are likely to be developmentally regulated similarly to many other PR-10 genes (Liu and Ekramoddoullah, 2006; Kim et al., 2008; Pulla et al., 2010).

The expression of the *HpPR10* genes was analyzed in this study for the first time in reproductive parts of *H. perforatum* which are rich with dark glands which form the primary accumulation sites of hypericins. All the genes were expressed relatively low levels in flower buds with no relation to analyzed content of hypericins. The lack of correlation between the *HpPR10* gene expression and the presence of dark glands was also confirmed by the similar expression levels of all the *HpPR10* genes in both leaf margin rich with dark glands and leaf interior parts lacking dark glands. Neither in earlier studies the *hyp-1* expression has been found to parallel with the presence of hypericins in the vegetative tissues of *H. perforatum* (Bais et al., 2003; Košuth et al., 2007) or in other species of genus *Hypericum* (Košuth et al., 2011).

Despite of numerous studies of *hyp-1* expression in genus *Hypericum*, the expression has not previously been studied at a cellular level. In the present study, we examined for the first time the expression of *hyp-1* gene in a cellular level by *in situ* RNA localization. The *hyp-1* transcripts in *H. perforatum* stem

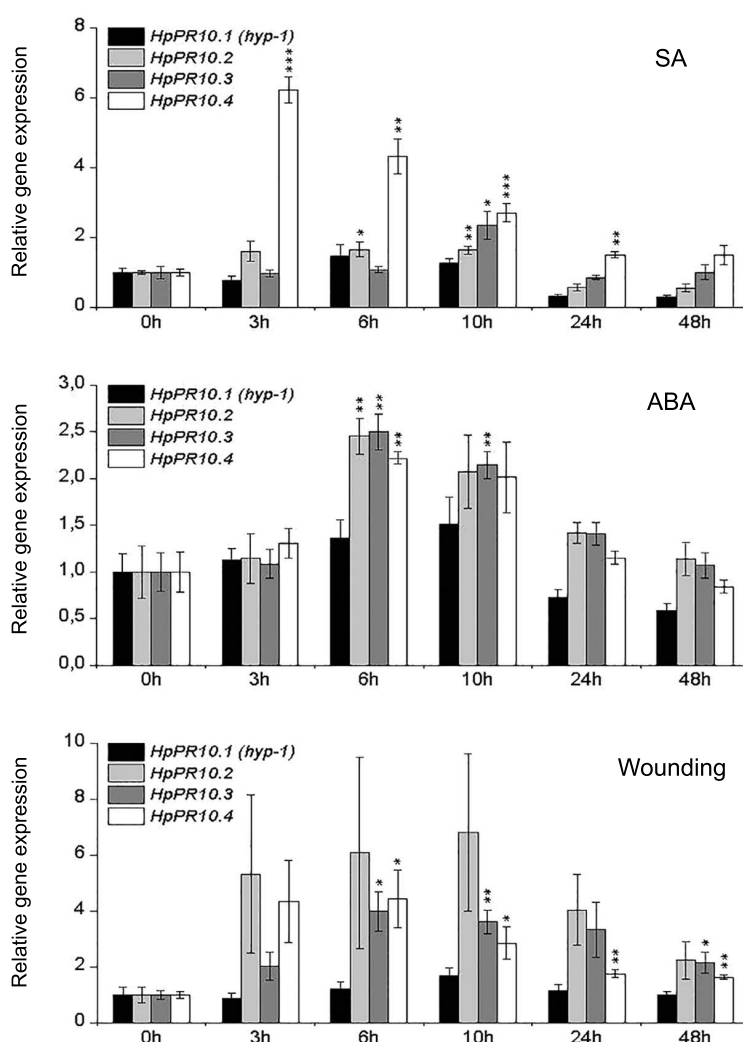


FIGURE 5 | Temporal expression patterns of *HpPR10.1 (hyp-1)*, *HpPR10.2*, *HpPR10.3*, and *HpPR10.4* in *H. perforatum* leaf tissues in response to treatments with SA (10 mM), ABA (100 μ M) or wounding. The relative expression of the genes was quantified by qRT-PCR and normalized to GAPDH. Values represent means \pm SE of at least three biological replicates. Asterisks indicate statistically significant difference in comparison to untreated control (0 h) in Student's *t*-Test at * $P \leq 0.05$, ** $P \leq 0.01$, *** $P \leq 0.001$.

and root were found to be present in vascular tissues while in leaves the transcripts were also highly associated with mesophyll cells in addition to vascular tissues but not in dark glands. In the vascular tissues, the expression was present in both xylem and phloem cells as well as type A canals. Type A canals have been described earlier for *H. perforatum* by Ciccarelli et al. (2001) but the meaning of the canals for the plant is unknown, although a function in transportation of photosynthates and phloem protectants were suggested. In root and stem, the *hyp-1* expression was highly associated with both xylem and phloem parenchyma cells and companion cells next to sieve elements as well as pericycle cells in root. The parenchyma cells in vascular tissue attend to the lateral transport of compounds, while the pericycle cells are known to be metabolically active and involved in the transport of compounds to and from the vascular bundle that they surround. Our results of the *hyp-1*

transcript localization are in agreement with the data obtained by Qian et al. (2012) who studied the cellular location at protein level in *H. perforatum* tissues and found the Hyp-1 protein to be present mainly in vascular tissues of both root and stem as well as in leaf mesophyll with no obvious signal in dark glands.

The expression and location of many PR-10 family proteins of various plant species have been found to be associated with vascular tissues (Breda et al., 1996; Pinto et al., 2005; Kim et al., 2008; Bahramnejad et al., 2010). The biological role of these proteins in the vasculature is not known although defensive role under stress conditions or binding/transportation of hydrophobic ligands have been suggested (Kim et al., 2008; Radauer et al., 2008; Fernandes et al., 2013). The location of the *hyp-1* transcripts in cells of vasculature suggests a similar role. The inconsistent results of *hyp-1* mRNA level with Hyp-1 protein

level in *H. perforatum* stem found in the current study can be due to the higher stability of the Hyp-1 protein in stem or indicate the movement of the protein between organs through vasculature. However, the sequences of *H. perforatum* PR-10 proteins, like those of most identified PR-10 proteins, contain no recognizable amino-terminal signal peptide sequence for apoplastic secretion specific to xylem sap proteins (Liu and Ekramoddoullah, 2006; Agarwal and Agarwal, 2014). Since there are suggestions of the role of Hyp-1 in binding and transportation of ligand molecules related to defense and developmental processes (Michalska et al., 2010; Košuth et al., 2013), the possible symplastic mobility of the protein by via plasmodesmata into phloem sap of mature sieve elements needs to be investigated in the future.

Previous studies have evidenced that hypericin biosynthesis is likely to take place in dark glands of *H. perforatum* (Zobayed et al., 2006; Kornfeld et al., 2007; Karppinen et al., 2008; Košuth et al., 2011). However, as discussed above, the *hyp-1* expression does not correlate with hypericin content or presence of dark glands in tissues of *H. perforatum* or other *Hypericum* species. In the present study, equal amounts of the Hyp-1 protein were found in leaf margin and leaf interior parts and, thus, neither our results provide any evidence that the Hyp-1 protein would be specifically associated or accumulating via transportation to the dark glands for its activity in the final stages of hypericin biosynthesis as suggested earlier (Bais et al., 2003). Our results are in agreement with the earlier study of Qian et al. (2012) who reported the presence of the Hyp-1 protein in leaf, stem and root of *H. perforatum* with no association in dark glands in leaves. These findings question the role of the *hyp-1* as a key gene in the hypericin biosynthesis. However, our results cannot exclude the possibility that the Hyp-1 would attend to the biosynthesis/transportation/binding of toxic hypericin (Bais et al., 2003; Michalska et al., 2010) in tissues outside dark glands that also contain minor amounts of hypericins as detected in the current and previous studies (Bais et al., 2002; Gadzovska et al., 2007; Karppinen and Hohtola, 2008; Cui et al., 2010).

Plants are continuously exposed to various stresses in their natural environment. The function of PR-10 proteins is often associated in plant defense because many PR-10 genes are induced or their expression is up-regulated by different types of biotic and abiotic stresses, such as drought, cold, wounding, and pathogens, as well as stress-related signaling molecules (Pulla et al., 2010; Takeuchi et al., 2011; Agarwal and Agarwal, 2014). Thus, PR-10 family proteins are considered as potentially useful genes for crop improvement. Previously Košuth et al. (2013) described increased expression of *hyp-1* in *H. perforatum* after wounding and treatment with *Agrobacterium* or ABA. ABA-mediated signaling is known to play an important role in plant responses to environmental stresses and plant pathogens (Lee and Luan, 2012). Wounding of plants induces defense responses that resemble those induced by herbivores or pathogen attack. In the current study, we found that all the three newly isolated PR-10 genes were up-regulated in leaves of *H. perforatum* by wounding as well as by treatment with ABA and SA suggesting a role for the genes in plant defense. The role of SA is established in defense responses against plant pathogens as well as many types of abiotic stresses (Miura and Tada, 2014). In our study, especially

the expression of *HpPR10.4* was rapidly and highly induced by SA indicating its special role in SA mediated defense responses. The differential gene expression patterns of the *HpPR10* genes in response to stress-related treatments may imply that they have gene-specific functions under different types of stress conditions. In the present study, *hyp-1* levels were only slightly but not significantly induced by the tested stress treatments which is different to the results of Košuth et al. (2013). The inconsistency in results between the two studies can be due to the differences in the applied treatments (ABA concentration or ABA application method and extent of wounding) or differences in plant material. Depending on the developmental stage of the plant, responses can differ as discussed above.

CONCLUSION

We have isolated three previously unidentified PR-10 family genes from *H. perforatum* and studied their expression along with closely related *hyp-1* in *H. perforatum* tissues and under various stress treatments. Our results show that these genes are constitutively but differently expressed in various *H. perforatum* tissues and their expression is also variably up-regulated by wounding and defense-related signaling molecules. The results suggest a role for these genes in contribution to the defense responses in *H. perforatum* with various functions. Since some PR-10 genes in other species have been reported to be expressed only in certain specific tissues or under certain stress conditions it cannot be excluded that *H. perforatum* would not have more PR-10 proteins which are to be discovered in the future. Furthermore, the results of the current study do not support the location of the *hyp-1* mRNA or Hyp-1 protein in dark glands or accumulation of the protein via transportation to the dark glands and, thus, question the role of *hyp-1* as a key gene in the hypericin biosynthesis in dark glands of *H. perforatum*.

AUTHOR CONTRIBUTIONS

KK and ED performed the analyses. All authors (KK, ED, LJ, and AH) have participated in preparation of the manuscript and have accepted the final version of the manuscript.

ACKNOWLEDGMENTS

This work was financially supported by the grants from the Finnish Cultural Foundation (Northern Ostrobothnia fund) and Oulu University Scholarship Foundation to KK.

SUPPLEMENTARY MATERIAL

The Supplementary Material for this article can be found online at: <http://journal.frontiersin.org/article/10.3389/fpls.2016.00526>

FIGURE S1 | The contents of hypericins (mg g^{-1} DW) in *H. perforatum* tissues. Values represent means \pm SE of three biological replicates.

REFERENCES

- Agarwal, P., and Agarwal, P. K. (2014). Pathogenesis related-10 proteins are small, structurally similar but with diverse role in stress signaling. *Mol. Biol. Rep.* 41, 599–611. doi: 10.1007/s11033-013-2897-4
- Bahramnejad, B., Goodwin, P. H., Zhang, J., Atnaseo, C., and Erickson, L. R. (2010). A comparison of two class 10 pathogenesis-related genes from alfalfa and their activation by multiple stresses and stress-related signaling molecules. *Plant Cell Rep.* 29, 1235–1250. doi: 10.1007/s00299-010-0909-6
- Bais, H. P., Vepachedu, R., Lawrence, C. B., Stermitz, F. R., and Vivanco, J. M. (2003). Molecular and biochemical characterization of an enzyme responsible for the formation of hypericin in St. John's wort (*Hypericum perforatum* L.). *J. Biol. Chem.* 278, 32413–32422. doi: 10.1074/jbc.M301681200
- Bais, H. P., Walker, T. S., McGrew, J. J., and Vivanco, J. M. (2002). Factors affecting growth of cell suspension cultures of *Hypericum perforatum* L. (St. John's wort) and production of hypericin. *In Vitro Cell. Dev. Biol. Plant* 38, 58–65. doi: 10.1079/IV2001253
- Bradford, M. M. (1976). A rapid and sensitive method for the quantitation of microgram quantities of protein utilizing the principle of protein-dye binding. *Anal. Biochem.* 72, 248–254. doi: 10.1016/0003-2697(76)90527-3
- Breda, C., Sallaud, C., El-Turk, J., Buffard, D., de Kozak, I., Esnault, R., et al. (1996). Defense reaction in *Medicago sativa*: a gene encoding a class 10 PR protein is expressed in vascular bundles. *Mol. Plant Microbe Interact.* 9, 713–719. doi: 10.1094/MPMI-9-0713
- Ciccarelli, D., Andreucci, A. C., and Pagni, A. M. (2001). Translucent glands and secretory canals in *Hypericum perforatum* L. (Hypericaceae): morphological, anatomical and histochemical studies during the course of ontogenesis. *Ann. Bot.* 88, 637–644. doi: 10.1006/anbo.2001.1514
- Cui, X. H., Chakrabarty, D., Lee, E. J., and Paek, K. Y. (2010). Production of adventitious roots and secondary metabolites by *Hypericum perforatum* L. in a bioreactor. *Bioresour. Technol.* 101, 4708–4716. doi: 10.1016/j.biortech.2010.01.115
- Fernandes, H., Bujacz, A., Bujacz, G., Jelen, F., Jasinski, M., Kachlicki, P., et al. (2009). Cytokinin-induced structural adaptability of a *Lupinus luteus* PR-10 protein. *FEBS J.* 276, 1596–1609. doi: 10.1111/j.1742-4658.2009.06892.x
- Fernandes, H., Michalska, K., Sikorski, M., and Jaskolski, M. (2013). Structural and functional aspects of PR-10 proteins. *FEBS J.* 280, 1169–1199. doi: 10.1111/febs.12114
- Gadzovska, S., Maury, S., Delaunay, A., Spasenoski, M., Joseph, C., and Hagège, D. (2007). Jasmonic acid elicitation of *Hypericum perforatum* L. cell suspensions and effects on the production of phenylpropanoids and naphthodianthrones. *Plant Cell Tiss. Organ Cult.* 89, 1–13. doi: 10.1007/s11240-007-9203-x
- He, M., Xu, Y., Cao, J., Zhu, Z., Jiao, Y., Wang, Y., et al. (2013). Subcellular localization and functional analyses of a PR10 protein gene from *Vitis pseudoreticulata* in response to *Plasmopara viticola* infection. *Protoplasma* 250, 129–140. doi: 10.1007/s00709-012-0384-8
- Jaakola, L., Pirttilä, A. M., Halonen, M., and Hohtola, A. (2001). Isolation of high quality RNA from bilberry (*Vaccinium myrtillus* L.) fruit. *Mol. Biotechnol.* 19, 201–203. doi: 10.1385/MB:19:2:201
- Jaakola, L., Pirttilä, A. M., Vuosku, J., and Hohtola, A. (2004). Method based on electrophoresis and gel extraction for obtaining genomic DNA-free cDNA without DNase treatment. *Biotechniques* 37, 744–748.
- Jain, S., Kumar, D., Jain, M., Chaudhary, P., Deswal, R., and Sarin, N. B. (2012). Ectopic overexpression of a salt stress-induced pathogenesis-related class 10 protein (PR10) gene from peanut (*Arachis hypogaea* L.) affords broad spectrum abiotic stress tolerance in transgenic tobacco. *Plant Cell Tiss. Organ Cult.* 109, 19–31. doi: 10.1007/s11240-011-0069-6
- Jin, M. L., Ahn, J. C., Hwang, B., Park, H. S., Lee, H. S., and Choi, D. W. (2010). Isolation and functional analysis of cDNAs similar to Hyp-1 involved in hypericin biosynthesis from *Hypericum erectum*. *Biol. Plant.* 54, 725–729. doi: 10.1007/s10535-010-0129-5
- Karppinen, K., and Hohtola, A. (2008). Molecular cloning and tissue-specific expression of two cDNAs encoding polyketide synthases from *Hypericum perforatum*. *J. Plant Physiol.* 165, 1079–1086. doi: 10.1016/j.jplph.2007.04.008
- Karppinen, K., Hokkanen, J., Mattila, S., Neubauer, P., and Hohtola, A. (2008). Octaketide-producing type III polyketide synthase from *Hypericum perforatum* is expressed in dark glands accumulating hypericins. *FEBS J.* 275, 4329–4342. doi: 10.1111/j.1742-4658.2008.06576.x
- Karppinen, K., Taulavuori, E., and Hohtola, A. (2010). Optimization of protein extraction from *Hypericum perforatum* tissues and immunoblotting detection of Hyp-1 at different stages of leaf development. *Mol. Biotechnol.* 46, 219–226. doi: 10.1007/s12033-010-9299-9
- Kim, S. T., Yu, S., Kang, Y. H., Kim, S. G., Kim, J. Y., Kim, S. H., et al. (2008). The rice pathogen-related protein 10 (JIOsPR10) is induced by abiotic and biotic stresses and exhibits ribonuclease activity. *Plant Cell Rep.* 27, 593–603. doi: 10.1007/s00299-007-0485-6
- Kornfeld, A., Kaufman, P. B., Lu, C. R., Gibson, D. M., Bolling, S. F., Warber, S. L., et al. (2007). The production of hypericins in two selected *Hypericum perforatum* shoot cultures is related to differences in black gland structure. *Plant Physiol. Biochem.* 45, 24–32. doi: 10.1016/j.plaphy.2006.12.009
- Košuth, J., Hrehorová, D., Jaskolski, M., and Čellárová, E. (2013). Stress-induced expression and structure of the putative gene hyp-1 for hypericin biosynthesis. *Plant Cell Tiss. Organ Cult.* 114, 207–216. doi: 10.1007/s11240-013-0316-0
- Košuth, J., Katkovčinová, Z., Olešová, P., and Čellárová, E. (2007). Expression of the hyp-1 gene in early stages of development of *Hypericum perforatum* L. *Plant Cell Rep.* 26, 211–217. doi: 10.1007/s00299-006-0240-4
- Košuth, J., Smelcerovic, A., Borsch, T., Zuehlke, S., Karppinen, K., Spiteller, M., et al. (2011). The hyp-1 gene is not a limiting factor for hypericin biosynthesis in the genus *Hypericum*. *Funct. Plant Biol.* 38, 35–43. doi: 10.1071/FP10144
- Lebel, S., Schellenbaum, P., Walter, B., and Maillot, P. (2010). Characterisation of the *Vitis vinifera* PR10 multigene family. *BMC Plant Biol.* 10:184. doi: 10.1186/1471-2229-10-184
- Lee, E. J., and Facchini, P. (2010). Norcoclaurine synthase is a member of the pathogenesis-related 10/Bet v1 protein family. *Plant Cell* 22, 3489–3503. doi: 10.1105/tpc.110.077958
- Lee, O. R., Pulla, R. K., Kim, Y. J., Balusamy, S. R. D., and Yang, D. C. (2012). Expression and stress tolerance of PR10 genes from *Panax ginseng* C. A. Meyer. *Plant Biol. Rep.* 39, 2365–2374. doi: 10.1007/s11033-011-0987-8
- Lee, S. C., and Luan, S. (2012). ABA signal transduction at the crossroad of biotic and abiotic stress responses. *Plant Cell Environ.* 35, 53–60. doi: 10.1111/j.1365-3040.2011.02426.x
- Liu, J. J., and Ekramoddoullah, A. K. M. (2006). The family 10 of plant pathogenesis-related proteins: their structure, regulation, and function in response to biotic and abiotic stresses. *Physiol. Mol. Plant Pathol.* 68, 3–13. doi: 10.1016/j.pmp.2006.06.004
- Michalska, K., Fernandes, H., Sikorski, M., and Jaskolski, M. (2010). Crystal structure of Hyp-1, a St. John's wort protein implicated in the biosynthesis of hypericin. *J. Struct. Biol.* 169, 161–171. doi: 10.1016/j.jsb.2009.10.008
- Miura, K., and Tada, Y. (2014). Regulation of water, salinity, and cold stress responses by salicylic acid. *Front. Plant Sci.* 5:4. doi: 10.3389/fpls.2014.00004
- Nakamura, R., and Teshima, R. (2013). Proteomics-based allergen analysis in plants. *J. Proteomics* 93, 40–49. doi: 10.1016/j.jprot.2013.03.018
- Petersen, T. N., Brunak, S., von Heijne, G., and Nielsen, H. (2011). SignalP 4.0: discriminating signal peptides from transmembrane regions. *Nat. Methods* 8, 785–786. doi: 10.1038/nmeth.1701
- Pinto, M. P., Ribeiro, A., Regalado, A. P., Rodrigues-Pousada, C., and Ricardo, C. P. P. (2005). Expression of *Lupinus albus* PR-10 proteins during root and leaf development. *Biol. Plant.* 49, 187–193. doi: 10.1007/s10535-005-7193-2
- Pulla, R. K., Lee, O. R., In, J. G., Kim, Y. J., Senthil, K., and Yang, D. C. (2010). Expression and functional characterization of pathogenesis-related protein family 10 gene, PgPR10-2, from *Panax ginseng* C.A. Meyer. *Physiol. Mol. Plant Pathol.* 74, 323–329. doi: 10.1016/j.pmp.2010.05.001
- Qian, J., Wu, J., Yao, B., and Lu, Y. (2012). Preparation of a polyclonal antibody against hypericin synthase and localization of the enzyme in red-pigmented *Hypericum perforatum* L. plantlets. *Acta Biochim. Pol.* 59, 639–645.
- Radauer, C., and Breiteneder, H. (2007). Evolutionary biology of plant food allergens. *J. Allergy Clin. Immunol.* 120, 518–525. doi: 10.1016/j.jaci.2007.07.024
- Radauer, C., Lackner, P., and Breiteneder, H. (2008). The Bet v 1 fold: an ancient, versatile scaffold for binding of large, hydrophobic ligands. *BMC Evol. Biol.* 8:286. doi: 10.1186/1471-2148-8-286

- Russo, E., Scicchitano, F., Whalley, B. J., Mazzitello, C., Ciriaco, M., Esposito, S., et al. (2014). *Hypericum perforatum*: pharmacokinetic, mechanism of action, tolerability, and clinical drug-drug interactions. *Phytother. Res.* 28, 643–655. doi: 10.1002/ptr.5050
- Schenk, M. F., Cordewener, J. H. G., America, A. H. P., van't Westende, W. P. C., Smulders, M. J. M., and Gilissen, L. J. W. J. (2009). Characterization of PR-10 genes from eight *Betula* species and detection of Bet v 1 isoforms in birch pollen. *BMC Plant Biol.* 9:24. doi: 10.1186/1471-2229-9-24
- Schenk, M. F., Gilissen, L. J. W. J., Esselink, G. D., and Smulders, M. J. M. (2006). Seven different genes encode a diverse mixture of isoforms of Bet v 1, the major birch pollen allergen. *BMC Genomics* 7:168. doi: 10.1186/1471-2164-7-168
- Takeuchi, K., Gyohda, A., Tominaga, M., Kawakatsu, M., Hatakeyama, A., Ishii, N., et al. (2011). RSOsPR10 expression in response to environmental stresses is regulated antagonistically by jasmonate/ethylene and salicylic acid signaling pathways in rice roots. *Plant Cell Physiol.* 52, 1686–1696. doi: 10.1093/pcp/pcp105
- van Loon, L. C., Rep, M., and Pieterse, C. M. J. (2006). Significance of inducible defense-related proteins in infected plants. *Annu. Rev. Phytopathol.* 44, 135–162. doi: 10.1146/annurev.phyto.44.070505.143425
- Xie, Y.-R., Chen, Z.-Y., Brown, R. L., and Bhatnagar, D. (2010). Expression and functional characterization of two pathogenesis-related protein 10 genes from *Zea mays*. *J. Plant Physiol.* 167, 121–130. doi: 10.1016/j.jplph.2009.07.004
- Zobayed, S. M. A., Afreen, F., Goto, E., and Kozai, T. (2006). Plant-environment interactions: accumulation of hypericin in dark glands of *Hypericum perforatum*. *Ann. Bot.* 98, 793–804. doi: 10.1093/aob/mcl169
- Zubini, P., Zambelli, B., Musiani, F., Ciurli, S., Bertolini, P., and Baraldi, E. (2009). The RNA hydrolysis and the cytokinin binding activities of PR-10 proteins are differently performed by two isoforms of the Pru p 1 peach major allergen and are possibly functionally related. *Plant Physiol.* 150, 12351247. doi: 10.1104/pp.109.139543

Conflict of Interest Statement: The authors declare that the research was conducted in the absence of any commercial or financial relationships that could be construed as a potential conflict of interest.

Copyright © 2016 Karppinen, Derzsó, Jaakola and Hohtola. This is an open-access article distributed under the terms of the Creative Commons Attribution License (CC BY). The use, distribution or reproduction in other forums is permitted, provided the original author(s) or licensor are credited and that the original publication in this journal is cited, in accordance with accepted academic practice. No use, distribution or reproduction is permitted which does not comply with these terms.



Crystal Structure of Hyp-1, a *Hypericum perforatum* PR-10 Protein, in Complex with Melatonin

Joanna Sliwiak¹, Zbigniew Dauter² and Mariusz Jaskolski^{1,3*}

¹ Center for Biocrystallographic Research, Institute of Bioorganic Chemistry, Polish Academy of Sciences, Poznań, Poland,

² Synchrotron Radiation Research Section, National Cancer Institute, Argonne National Laboratory, Argonne, IL, USA,

³ Department of Crystallography, Faculty of Chemistry, Adam Mickiewicz University in Poznań, Poznań, Poland

OPEN ACCESS

Edited by:

Gregory Franklin,
Polish Academy of Sciences, Poland

Reviewed by:

Kathrin Schrick,
Kansas State University, USA
Doriano Lamba,
Consiglio Nazionale delle Ricerche,
Italy

*Correspondence:

Mariusz Jaskolski
mariusz@amu.edu.pl

Specialty section:

This article was submitted to
Plant Metabolism
and Chemodiversity,
a section of the journal
Frontiers in Plant Science

Received: 19 February 2016

Accepted: 01 May 2016

Published: 18 May 2016

Citation:

Sliwiak J, Dauter Z and Jaskolski M (2016) Crystal Structure of Hyp-1, a *Hypericum perforatum* PR-10 Protein, in Complex with Melatonin. *Front. Plant Sci.* 7:668.
doi: 10.3389/fpls.2016.00668

Hyp-1, a PR-10-fold protein from *Hypericum perforatum*, was crystallized in complex with melatonin (MEL). The structure confirms the conserved protein fold and the presence of three unusual ligand binding sites, two of which are internal chambers (1,2), while the third one (3) is formed as an invagination of the protein surface. The MEL ligand in site 1 is well defined while that in site 3 seems to be rotating between the side chains of Lys33 and Tyr150 that act as a molecular vise. The patch of electron density in site 2 does not allow unambiguous modeling of a melatonin molecule but suggests a possible presence of its degradation product. This pattern of ligand occupation is reproducible in repeated crystallization/structure determination experiments. Although the binding of melatonin by Hyp-1 does not appear to be very strong (for example, MEL cannot displace the artificial fluorescence probe ANS), it is strong enough to suggest a physiological role of this interaction. For example, *trans*-zeatin, which is a common ligand of PR-10 proteins, does not overcompete melatonin for binding to Hyp-1 as it does not affect the crystallization process of the Hyp-1/MEL complex, and among a number of potential natural mediators tested, melatonin was the only one to form a crystalline complex with Hyp-1 with the use of standard crystallization screens. Hyp-1 is the second protein in the Protein Data Bank for which melatonin binding has been demonstrated crystallographically, the first one being human quinone reductase.

Keywords: pathogenesis-related protein, PR-10, phytohormone, ligand binding, cytokinin

INTRODUCTION

Hyp-1, the protein product (comprised of 159 residues) of the *hyp-1* gene in *Hypericum perforatum* has a picturesque history. It was first described as the enzyme catalyzing the biosynthesis of the pharmacological ingredient of this plant, the dianthrone hypericin, from two molecules of emodin (Bais et al., 2003). That study, however, could never be replicated and instead the crystal structure of the Hyp-1 protein revealed the canonical PR-10-fold (Michalska et al., 2010) strongly suggesting classification in class 10 of the superfamily of plant Pathogenesis-Related (PR-10) proteins. The latter hypothesis was corroborated by genetic data, which showed that *hyp-1* has gene structure analogous to typical *pr-10* genes (Kosuth et al., 2013), but it has to be underlined that Hyp-1 has not been demonstrated so far to be involved in stress response of *H. perforatum*. With regard to the localization in the plant, it was shown that Hyp-1 mRNA expression occurs in all organs of *Hypericum* seedlings with the highest levels in roots (Kosuth et al., 2007), whereas

immunofluorescence assays of plantlets revealed wide distribution of the Hyp-1 protein in different tissues, including roots, stem, and leaves (Qian et al., 2012).

The characteristic PR-10-fold (Fernandes et al., 2013), also known as the Betv1 fold according to the first protein from this class, a birch (*Betula verucosa*) pollen allergen to have its crystal structure determined (Gajhede et al., 1996), consists of a large seven-stranded antiparallel β -sheet forming a baseball-glove grip over a long C-terminal helix α 3, which is the most variable element of the PR-10 structure (Biesiadka et al., 2002; Pasternak et al., 2006). The consecutive β -strands are connected by loops, except for strands β 1 (first) and β 2 (last) at the edges of the β -sheet, which are connected by a V-shaped fork of two α -helices (α 1 and α 2) that provides a support for the C-terminal end of helix α 3. At its N-terminal end, helix α 3 is connected to the protein scaffold by loop L9. A conspicuous feature of the PR-10-fold is a large hydrophobic cavity formed between the main structural elements, i.e., the β -sheet and helix α 3, with the participation of other secondary structures, such as the odd-numbered loops (L3, L5, L7, L9), which are the fingertips of the gripping hand (Figure 1A). The cavity has two entrances connecting it to the outer environment: E1 surrounded by the odd numbered loops (L3, L5, L7) and helix α 3, and entrance E2 located between helix α 3 and strand β 1. Despite the hollow core, the PR-10 proteins are robust, resistant to proteases and have mechanical stability that even surpasses that of average globular proteins (Chwastyk et al., 2014). The properties, size and shape of the internal cavity are mostly modulated by the character of the α 3 helix.

The presence of such an intriguing cavity has led to the hypothesis that PR-10 proteins might have evolved in plants to bind/store/transport important small-molecule mediators, such as plant hormones (Fernandes et al., 2013). Along these lines, a number of PR-10 (or at least PR-10-fold) proteins have been characterized structurally in complex with phytohormones (or their analogs), such as cytokinins (Pasternak et al., 2006; Fernandes et al., 2008, 2009; Kofler et al., 2012; Ruszkowski et al., 2013; Sliwiak et al., 2016), gibberellin (Ruszkowski et al., 2014), brassinosteroids (Markovic-Housley et al., 2003), or abscisic acid (Sheard and Zheng, 2009). Moreover, other plant metabolites, such as flavonoids (Mogensen et al., 2002; Kofler et al., 2012; Casañal et al., 2013) or their glycosylated forms (Seutter von Loetzen et al., 2014, 2015), are also bound by PR-10 proteins.

On the list of recognized plant hormones, melatonin (*N*-acetyl-5-methoxytryptamine, MEL, Figure 2A) is a relatively new addition. Apart from the discovery of the presence of this conservative molecule in plants (Dubbels et al., 1995), relatively little has been learned about phytomelatonin function over the last decade. Melatonin appears to regulate plant growth in an auxin-like manner, regulate the response to photoperiod and increase tolerance to abiotic stress. It is also one of the most efficient antioxidants (Arnao and Hernández-Ruiz, 2015). *H. perforatum*, alongside *Tanacetum parthenium* or the Chinese herb *Scutellaria baicalensis*, appears to contain very high MEL concentrations (Murch et al., 1997) that reach 2 $\mu\text{g/g}$ of dried weight in leaves and are above 4 $\mu\text{g/g}$ in flowers. In the case of *H. perforatum*, this could be responsible for the

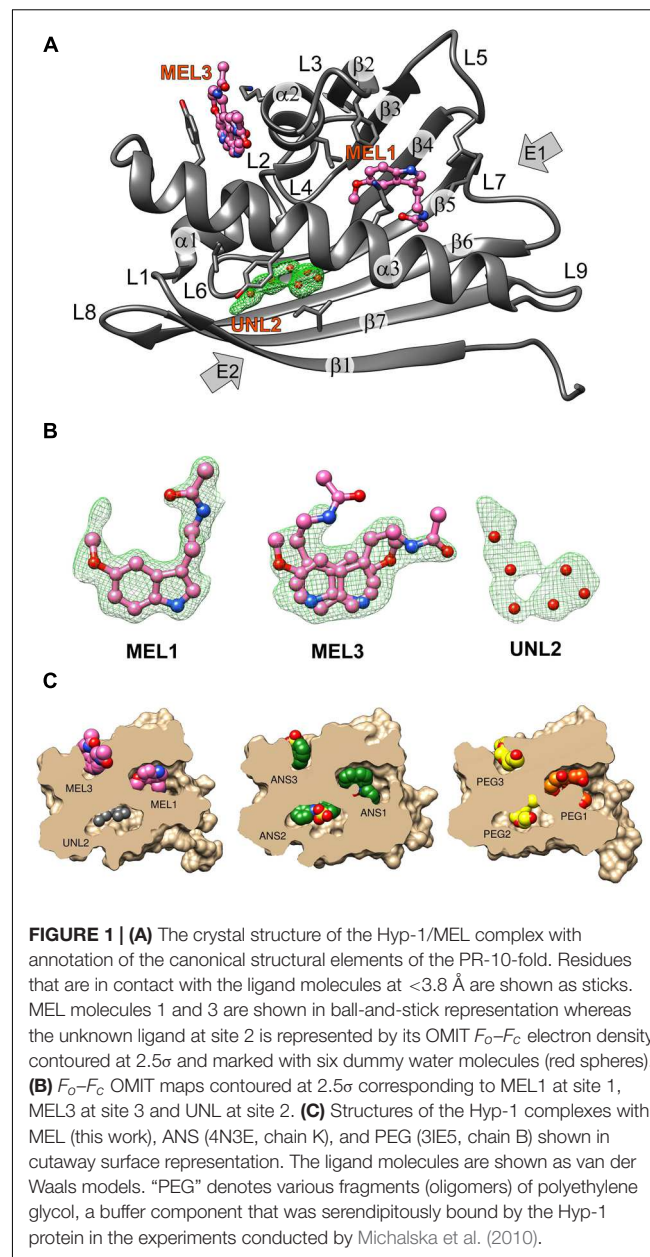


FIGURE 1 | (A) The crystal structure of the Hyp-1/MEL complex with annotation of the canonical structural elements of the PR-10-fold. Residues that are in contact with the ligand molecules at $<3.8 \text{ \AA}$ are shown as sticks. MEL molecules 1 and 3 are shown in ball-and-stick representation whereas the unknown ligand at site 2 is represented by its OMIT $F_o - F_c$ electron density contoured at 2.5σ and marked with six dummy water molecules (red spheres). **(B)** $F_o - F_c$ OMIT maps contoured at 2.5σ corresponding to MEL1 at site 1, MEL3 at site 3 and UNL at site 2. **(C)** Structures of the Hyp-1 complexes with MEL (this work), ANS (4N3E, chain K), and PEG (3IE5, chain B) shown in cutaway surface representation. The ligand molecules are shown as van der Waals models. “PEG” denotes various fragments (oligomers) of polyethylene glycol, a buffer component that was serendipitously bound by the Hyp-1 protein in the experiments conducted by Michalska et al. (2010).

medicinal effects of St John’s wort preparations. Apart from tissue content determinations and studies of the tryptophan-dependent biosynthetic pathway (Murch et al., 2000), studies also focused on the role of melatonin in *H. perforatum*, demonstrating that increased light intensity elevates melatonin synthesis, thus confirming its free radical scavenging function (Murch et al., 2000). It was shown that MEL is able to induce rhizogenesis (Murch et al., 2001), an observation that has been recently confirmed in other plant species (Arnao and Hernández-Ruiz, 2015).

Biophysical and kinetic studies of PR-10/phytohormone complexes are often difficult because of problems with ligand solubility, low heat effect upon binding (in calorimetry) and/or unsuitable spectroscopic properties. A frequently used assay

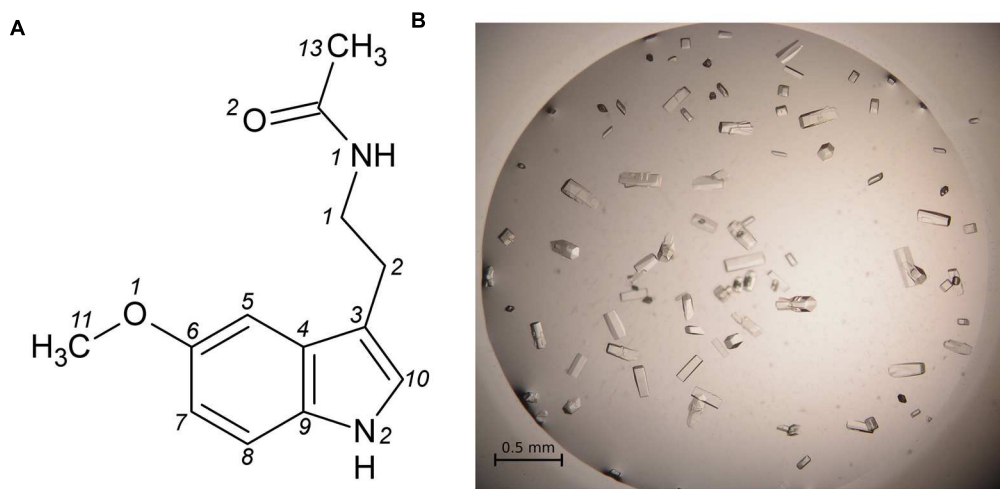


FIGURE 2 | (A) Melatonin with atom numbering according to Quarles et al. (1974). **(B)** Single crystals of the Hyp-1/MEL complex grown in 1 M citrate and 20% glycerol.

in such studies is ADA (ANS Displacement Assay), in which the fluorescent dye 8-anilinonaphthalene-1 sulfonate (ANS) is displaced by the ligand of interest (Mogensen et al., 2002). Our investigations of ligand-binding properties of the Hyp-1 protein started in fact with the crystallization of a Hyp-1/ANS complex, which turned out to have a complex modulated crystal structure with as many as 28 copies of the protein in the asymmetric unit (Sliwiak et al., 2014, 2015). At the same time, that structure revealed an unprecedented among PR-10-fold proteins ligand binding mode, with two ANS molecules (at sites 1, 2) bound in two tight internal chambers (instead of one large cavity) and another one (3) docked in a deep invagination of the protein surface.

In this work we present high resolution crystal structure of Hyp-1 in complex with melatonin, demonstrating that this physiological ligand utilizes the same internal docking sites as ANS. The Hyp-1/MEL structure is the first example reported in the Protein Data Bank (PDB) of melatonin bound to a plant protein, and the second case with any protein, the first one being human quinone reductase (Calamini et al., 2008). It is also important to stress that among many different phytohormones and hypothetical biologically relevant substrate/product molecules (e.g., emodin, hypericin) tested, melatonin was the only ligand that formed crystalline complex with the Hyp-1 protein.

MATERIALS AND METHODS

Protein Preparation, Complex Formation, and Crystallization

Hyp-1 was produced as described before (Sliwiak et al., 2015). Prior to crystallization, the protein solution was concentrated to 15 mg/ml and pre-incubated at 292 K for 1 h with 10-fold molar

excess of melatonin (Sigma-Aldrich) added from a 0.1 M stock solution in methanol, or with MEL powder. Screening for Crystal Screen, PEG/Ion I and II (Hampton Research) crystallization conditions was performed by the sitting drop vapor diffusion method against 120 μ L well solution with the use of a Mosquito Crystallization Robot. The crystallization drops were mixed from 0.2 μ L protein/ligand solution and 0.2 μ L well solution. Small crystals, which appeared the same day in 1.6 M tribasic sodium citrate, pH 6.5, were used for seeding in a gradient of PEG 400 or glycerol and tribasic sodium citrate in hanging drops. Large, prismatic crystals of dimensions 0.08 mm \times 0.08 mm \times 0.2 mm (Figure 2B) grew in 1 M citrate and 20% glycerol.

Competitive Crystallization Assays

Hyp-1 protein was pre-incubated for 1 h with an equimolar solution of MEL (from 0.1 M methanol stock) and *trans*-zeatin (from 0.1 M stock in DMSO), as well as with a solution mixture of MEL and ANS (from 0.1 M stock in DMSO), mixed at the following MEL:ANS ratios: 1:1, 2:1, and 3:1. The Hyp-1:MEL molar ratio was 1:10 in all conditions. Crystallization was performed in all these cases using the final growth conditions established for the crystals of the Hyp-1/MEL complex. In these competition assays, crystals were obtained only in the presence of *trans*-zeatin but they had the prismatic morphology of the Hyp-1/MEL crystals.

Data Collection, Structure Solution, and Refinement

X-Ray diffraction data extending to 1.30 Å resolution were collected at the SER-CAT 22ID beamline of the Advanced Photon Source (APS/ANL) and were processed with HKL-2000 (Otwinowski and Minor, 1997). The data were merged in space group C222₁ with R_{merge} of 5.7% (Table 1). For molecular replacement in Phaser (McCoy et al., 2007), the PDB model 3IE5

TABLE 1 | Data collection and refinement statistics.

Data collection	
Space group	C222 ₁
Unitcell parameters <i>a</i> , <i>b</i> , <i>c</i> (Å)	60.86, 89.64, 76.41
Beamline	SER-CAT 22ID (APS)
Wavelength (Å)	1.0000
Data collection temperature (K)	100
Resolution (Å)	30.0–1.30 (1.32–1.30) ^a
<i>R</i> _{merge} (%)	5.7 (51.4)
< <i>I</i> / <i>σI</i> >	28.9 (2.5)
CC _{1/2} /CC* (%) ^b	(86.3)/(96.2)
Completeness (%)	99.9 (99.6)
Redundancy	4.9 (3.9)
Refinement	
Resolution (Å)	25.31–1.30
Reflections work/test	49014/2630
<i>R</i> _{work} / <i>R</i> _{free} (%)	12.8/15.3
Protein/ligand/solvent/water/metal atoms	1405/51(MEL), 12(GOL), 6(UNL)/204/3
< <i>B</i> > protein/ligand/water/metal (Å ²)	22.8/45.3(MEL), 58.8(GOL), 59.8(UNL)/45.2/37.8
R.M.S.D. from ideal geometry	
Bond lengths (Å)/bond angles (°)	0.017/1.6
Ramachandran statistics (%) ^c	
Favored/outliers	98.3/0
PDB code	5I8F

^aValues in parentheses correspond to the last resolution shell. ^bCorrelation coefficients, as defined by Karplus and Diederichs (2012), given for the last resolution shell. ^cAssessed with MolProbity (Chen et al., 2010).

(Michalska et al., 2010) was used. Manual rebuilding was carried out in Coot (Emsley et al., 2010) and anisotropic maximum-likelihood refinement was carried out in phenix.refine (Afonine et al., 2012). Stereochemical restraints for the melatonin molecule were generated from the coordinates found in the CSD deposit MELATN01 of melatonin crystal structure (Quarles et al., 1974). X-Ray diffraction data collected for identical crystals, obtained upon co-crystallization with melatonin added in pulverized form or in the presence of equimolar concentration of *trans*-zeatin, extended to 1.34 Å and 1.40 Å resolution, respectively, and were also merged in the C222₁ space group with *R*_{merge} of 7.8 and 9.6%, respectively.

Other Software

For Cα superpositions and R.M.S.D. calculations the ALIGN program (Cohen, 1997) was used. Figures were prepared in UCSF Chimera (Pettersen et al., 2004).

Deposition Note

Atomic coordinates and processed structure factors corresponding to the final model of the Hyp-1/melatonin complex have been deposited with the PDB under the accession code 5I8F. The corresponding raw X-ray diffraction images have been deposited in the RepOD Repository at the Interdisciplinary Centre for Mathematical and Computational Modelling (ICM) of the University of Warsaw, Poland, and are available for

download with the following Digital Object Identifier (DOI): <http://dx.doi.org/10.18150/repol.4711822>.

RESULTS AND DISCUSSION

Crystallization Trials

Hyp-1 co-crystallization experiments were carried out with phytohormones from different classes, including auxin, *trans*-zeatin, gibberellic acid, abscisic acid, and melatonin; and additionally with the flavonoid quercetin, the fluorescence probe ANS, as well as with the hypothetical substrate (emodin) and product (hypericin) molecules. All these trials were performed using the same commercial screens and with similar protein:ligand ratios as for the present complex. The ultimate result of those crystallizations was that crystalline complexes of Hyp-1 could be obtained only with ANS (Sliwiak et al., 2015) or with MEL (added in solution or in powder form). In this context, it is interesting to note that crystallography emerges as a superior approach to the detection of protein-ligand complexes when standard biophysical methods fail (Schiebel et al., 2016).

Competitive crystallization with MEL and *trans*-zeatin resulted in crystals of the same Hyp-1/MEL complex. Thus one can conclude that *trans*-zeatin does not perturb Hyp-1/MEL complex formation under the conditions of Hyp-1/MEL crystal growth.

On the other hand, the presence of ANS in the Hyp-1/MEL crystallization conditions, even at lower concentration than that used for *trans*-zeatin, suppressed the crystal growth entirely. Moreover, addition of melatonin (even at 1:1 ANS:MEL ratio) to Hyp-1/ANS crystallization conditions (Sliwiak et al., 2015) resulted in crystals of the Hyp-1/ANS complex with a new type of modulation (Sliwiak, Unpublished Data). This suggests that ANS blocks the MEL binding sites of Hyp-1 with higher affinity, explaining why it was not possible to detect any signal with MEL titration in ANS Displacement Assays (ADA) performed according to a well-established procedure (Pasternak et al., 2006). On the other hand, it has to be noted that unlike in the Hyp-1/MEL complex, in the crystal structure of the Hyp-1/ANS complex, in addition to the internal binding sites 1,2,3, there are numerous ANS molecules bound at conserved sites on the surface of the Hyp-1 protein (Sliwiak et al., 2015). Since those superficial ANS molecules (which are most likely responsible for the modulation of the crystal structure) are not exchangeable for MEL even at high melatonin concentration, they could additionally mask the ADA signal.

Overall Features of the Crystal Structure

The structure of Hyp-1 described in this work is of the highest resolution (1.30 Å) among all Hyp-1 structures available in the PDB (3IE5, 1.69 Å; 4N3E, 2.43 Å) and therefore provides the most accurate model of this protein. Moreover, as the protein was purified in reducing condition, in variance with the 3IE5 model, in the present structure there are no accidental disulfide bonds bridging the Hyp-1 molecules in the crystals structure. In agreement with this, PISA (Krissinel and Henrick, 2007) analysis did not detect any stable quaternary structure. The

solvent content of the crystal is 56.4% with Matthews volume equal to $2.82 \text{ \AA}^3/\text{Da}$. Thanks to the high resolution of the diffraction data, all atoms in the structure were refined with anisotropic atomic displacement parameters (*B*-factors). Careful examination of difference electron density maps revealed the positions of 204 water molecules as well as of two molecules of MEL (Figure 1B), one of which (modeled in two orientations, with average *B*-factor of 54.5 \AA^2) is most likely endowed with rotational degrees of freedom within the surface invagination, and another one (modeled in one orientation with $\langle B \rangle$ of 36.1 \AA^2) is well stabilized in the internal cavity of the protein. Two glycerol molecules with low *B*-factors were modeled at the protein surface. In addition, there are three Na^+ ions included in the model, two of which are octahedrally coordinated by the protein (one by loop L5 and another one by strand $\beta 1$ and the C-end of helix $\alpha 3$), and a third one partially occupied within the protein cavity. Within the cavity, there is also an ambiguous patch of electron density which could not be assigned to any of the components of the crystallization solution. Since there is an indication of an indole ring with a short side chain (Figure 1B), it could be a poorly occupied MEL molecule or a product of its degradation. In view of these doubts, we decided to model this density with several water molecules marked as UNL (Unknown Ligand).

The main chain of the protein model could be traced in electron density without any brakes and it was possible to determine the rotamers of all side chains. Only the last two, one and three atoms, respectively, of three lysine side chains, Lys21, Lys40, and Lys113, which are directed toward bulk solvent, were omitted from the model due to their high mobility and lack of electron density. For 13 residues two rotamers of the side chain could be determined. The structure was refined to R/R_{free} of 12.8/15.3% and *MolProbity* (Chen et al., 2010) analysis emphasizes the high stereochemical quality of the model (Table 1).

Overall Fold and Three New PR-10 Binding Sites

As already established by Michalska et al. (2010), Hyp-1 has the canonical PR-10-fold with all its structural motifs (Figure 1A). The residue ranges of each structural motif are given in Table 2. Although the protein main chain creates the typical “baseball glove” framework, the peculiarity of the Hyp-1 protein lies in the side chains, which are responsible for shaping a very interesting and unusual internal cavity, quite different from the cavities known from other PR-10 proteins. As discussed before (Sliwiak et al., 2016), the PR-10 proteins of known structure appear to possess two types of cavities; type I, which is small, shallow, opened at the E1 entrance and capable of binding one ligand molecule in a specific manner; and type II, which resembles a spacious bag and spans the entire hydrophobic core between entrances E1 and E2, and is capable of accommodating more than two ligands of different chemical nature at different positions. In the case of Hyp-1, we observe two separated internal chambers (1 and 2), each with its own entrance (E1 and E2, respectively), and a third site (3) which is formed as a deep invagination of the

protein surface. A very unusual feature of the Hyp-1 binding sites as compared to other PR-10 proteins is the amazing conservation of the ligand position; regardless of their chemical character, the ligand molecules always take the same position in the three sites, as clearly illustrated by the cut-away sections of the protein interior in Figure 1C.

The binding site 3 is quite mysterious. Although the residues stabilizing the ligand in a vise-type manner (Lys33 and Tyr150) are conserved among almost all PR-10 proteins, Hyp-1 is the only protein where ligand binding is found at this site and is seen there in all available structures of Hyp-1 complexes. An explanation of this observation may lie in the interaction between the unstructured C-terminal end of Hyp-1 and helix $\alpha 1$. Among the aligned sequences (Figure 3A) of PR-10 proteins studied structurally in our laboratory, Hyp-1 is the only one to have a long C-terminal peptide forming a C-terminal loop that interacts with helix $\alpha 1$ (Figure 3B). This interaction involves hydrogen bonds between the $\text{N}\varepsilon 2$ atom of His17 and the C-terminal carboxylate group (of Ala159) and between the $\text{N}\varepsilon$ and $\text{N}\eta 2$ atoms of Arg18 and the O atom of Val157, as well as hydrophobic interactions of the aromatic ring of Phe158 with Lys21 and the main chain of helix $\alpha 1$ (Figure 3C). His17 is unique to the Hyp-1 protein, as in other PR-10 proteins there is a negatively charged Glu or hydrophobic Ala residue at this position (Figure 3A). Although the C-terminal sequence of MtN13 is even longer than in Hyp-1 (Figure 3A), in all crystal structures of MtN13/cytokinin complexes (4GY9, 4JHG, 4JHH, 4JHI; Ruszkowski et al., 2013), this end of the protein is disordered, indicating the absence of such C-terminal stabilization. The interactions mentioned above stabilize the surface invagination of Hyp-1, thereby creating the new ligand binding site 3. The above interactions between the

TABLE 2 | Residue ranges of PR-10 canonical motifs in Hyp-1 protein.

Secondary structure element	No	Residue range
α -helix	1	Pro16–Leu23
	2	Arg27–Ala34
	3	Glu130–Asn154
β -sheet	1	Ala2–Ser12
	2	Ser41–Glu46
	3	Val54–Thr58
	4	Tyr67–Asp76
	5	Tyr81–Glu88
	6	Lys98–Leu105
	7	Lys113–His121
Loop	1	Pro13–Ala15
	2	Val24–Glu26
	3	Gln35–Lys40
	4	Gly47–Thr53
	5	Phe59–Thr66
	6	Ala77–Phe80
	7	Gly89–Glu97
Unstructured	8	Glu106–Ser112
	9	Pro122–Asn129
	–	Pro155–Ala159

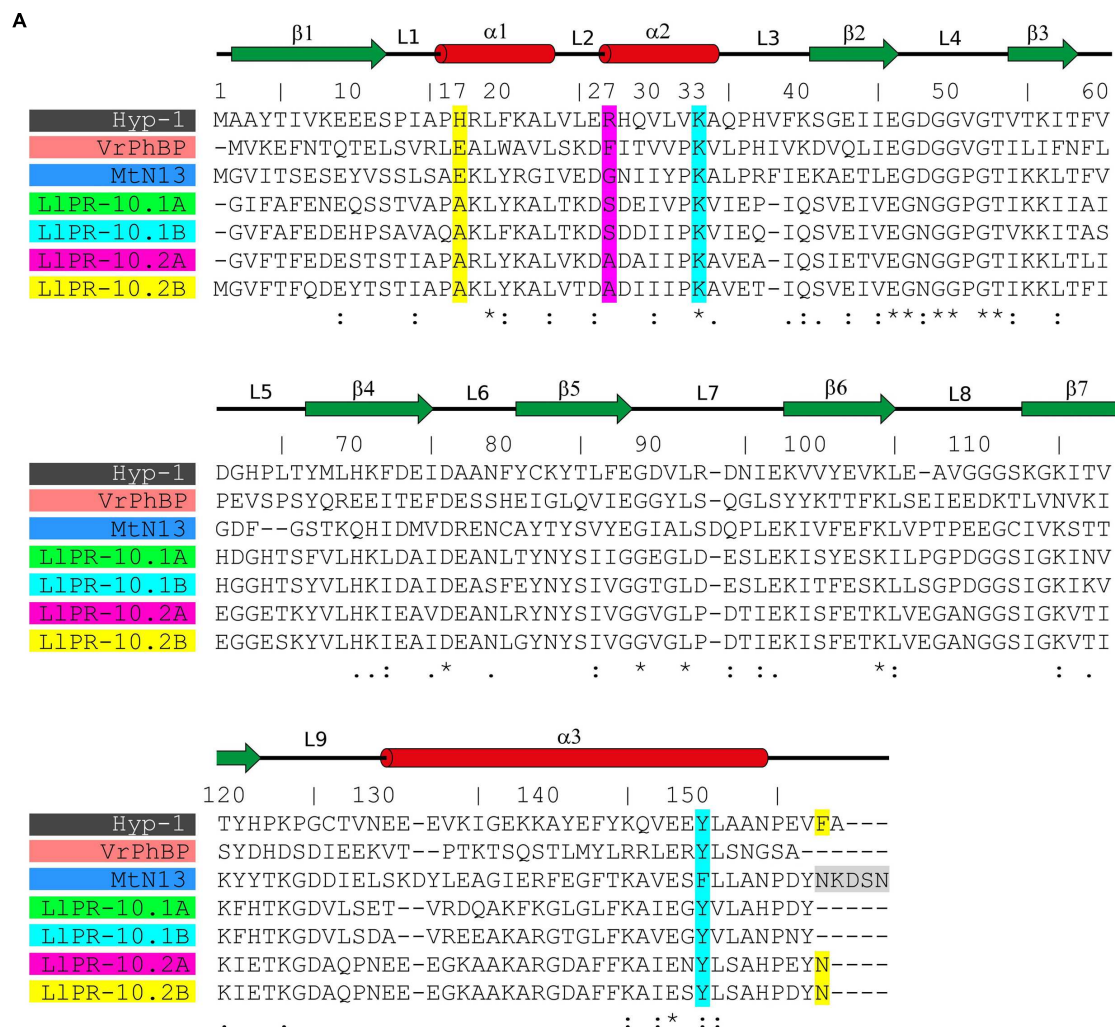


FIGURE 3 | (A) Multiple sequence alignment and **(B)** superposition of PR-10 models (identified by their PDB codes and color) with zoom on the area of the Lys33-Tyr150 invagination of Hyp-1. Green, LIPR-10.1A (4RYV); cyan, LIPR-10.1B (1IFV, chain A); magenta, LIPR-10.2A (1XDF, chain B); yellow, LIPR-10.2B (2QIM); salmon, VrPhBP (2FLH, chain B); blue, MtN13 (4JHG); dark gray, the present model. In the sequence alignment **(A)**, the positions corresponding to Hyp-1 Pro17, Arg27, Lys33, Tyr150 and Phe158 are highlighted as follows: cyan, conservative residues creating the surface invagination; yellow, unique Hyp-1 residues that are involved in C-end stabilization; magenta, the cavity separator Arg27. The disordered C-terminal pentapeptide of MtN13 is highlighted in gray. Identical (*) as well as more (:) and less (.) similar residues are marked at the bottom, while the pictograms above the Hyp-1 sequence numbers illustrate the secondary structure elements (green arrows, β-strands; red cylinders, α-helices) and their annotation. **(C)** Interaction of the C-end of Hyp-1 with α1, stabilizing the novel binding site 3. **(D)** Ca superposition of different PR-10 models as in **(B)** with zoom on the α2 structural element, with residues corresponding to Hyp-1 Arg27 shown in stick representation.

C-terminus and helix α 1 are present in all experimental models of Hyp-1.

As discussed before (Sliwiak et al., 2015), the main partition between the chambers 1 and 2 in Hyp-1 is the long side chain of Arg27 from helix α 2, with further contribution from Tyr84, Tyr101, Ala140, and Phe143. A structural superposition of the α 2 helix of different PR-10 proteins (**Figure 3D**) reveals not only that the Hyp-1-specific Arg27 residue is replaced in other PR-10 sequences by Gly, Ala or Ser, but also that the α 2 helix of Hyp-1 penetrates the hydrophobic core in an exceptionally high degree, contributing to this unique partitioning into two separate internal chambers.

Ligand Identification in Electron Density

As mentioned above, MEL1 is the best stabilized ligand in the structure. Its electron density (**Figure 1B**) clearly indicates the position of each atom. A similar situation was found in the Hyp-1/ANS complex, where the superposition of the 28 Hyp-1 molecules in the asymmetric unit produced an exceptionally consistent overlay of the ligand molecules at site 1 (Sliwiak et al., 2015). We note, however, that there is a strange positive electron density peak less than 2 Å from the MEL1 methoxy group (**Figure 1B**), for which we do not have a plausible explanation.

Although we did not model melatonin at site 2, it is quite obvious that the electron density there is consistent with the shape of the indole ring. However, we were unable to build a satisfactory model of MEL or 5-methoxyindole there. One possibility is that the ligand at site 2 is very mobile. Alternatively, a melatonin degradation product could be bound there. As a free radical scavenger, melatonin is rather unstable and could undergo X-ray-induced degradation. To test this possibility, we irradiated an NMR probe containing 0.6 M solution of melatonin in deuterated methanol with a synchrotron X-ray dose \sim 10 times higher than that used in the diffraction experiment. However, the NMR spectrum after irradiation was unchanged, suggesting that photodegradation was not a likely mechanism of the observed effect. Notwithstanding this result, we were also unable to model N1-acetyl-N2-formyl-5-methoxykynuramine (AFMK) or 6-hydroxymelatonin at this site, the two known photodegradation products of melatonin (Maharaj et al., 2002).

MEL3 has flat electron density, indicating in-plane rotation of the ligand. To account for this effect, we modeled MEL3 in two orientations. It is interesting to note that rotation of the flat ANS molecule at site 3 site was also observed in the Hyp-1/ANS complex, with the caveat that the rotation could be deduced from the superposition of the 28 copies of the Hyp-1 molecule, whereas in each individual case the ANS3 ligand could be modeled in a unique orientation. Nevertheless, despite the rotation of MEL3, it is safe to conclude that the ligand molecule is firmly docked between the jaws of the Lys33-Tyr150 vise.

It is very important to stress that the ligand electron densities described above were perfectly reproducible in several independent structure determinations utilizing differently produced Hyp-1/MEL crystals, namely either in the presence of solid (pulverized) melatonin or in the presence of equimolar concentration of *trans*-zeatin. The reproducibility includes

even the inexplicable electron density peak near the MEL1 molecule.

Ligand Binding

The MEL molecule at site 1 that has the best definition in electron density, makes direct contacts with the protein only via weak (3.6–3.8 Å) hydrophobic interactions with Phe39, Leu31, Leu65, Val91, Gly136, and Lys139, as well as via water-mediated hydrogen bonds of its O₂¹ atom with Gly136 (O), Ala140 (N), and Met68 (S), and of its N1 atom with Arg93 (N η 2) and Glu132 (O).

Interestingly, the MEL1 ligand is additionally stabilized and pushed to its binding site by a direct hydrogen bond of its N2 atom with the carboxylate group of Asp48 from loop L4 of an adjacent Hyp-1 molecule. This interaction is additionally stabilized by a hydrogen bond between the “intruding” Asp48 carboxylate and the N ϵ atom of His63 from loop L5 of the MEL1-binding protein molecule (**Figure 4**). Such a situation is not new among PR-10 proteins. In the structures of *Medicago truncatula* Nodulin 13 (MtN13) in complex with cytokinins (Ruszkowski et al., 2013), there is a similar interaction with Asp62 from loop L5 of another copy of MtN13, which forms a fork of hydrogen bonds with the N6 and N7 atoms of the cytokinin molecule. In variance with the Hyp-1 situation, however, the cytokinin...Asp62 interaction in MtN13 is mutual, leading to (quite exceptional) dimer formation of that PR-10 protein.

As mentioned above, the MEL3 ligand is evidently rotating between the jaws of the vise formed by the side chains of Lys33 and Tyr150. Its stacking interactions with these residues have van der Waals character.

¹The atom numbering scheme of melatonin (**Figure 2A**) follows that of Quarles et al. (1974) because the system used by the PDB is quite irrational and inconsistent with established rules, as also noted for other ligands (Jaskolski, 2013).

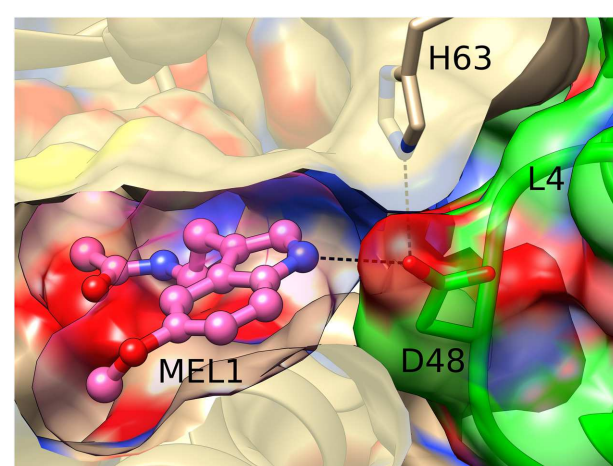


FIGURE 4 | Hydrogen bonding between MEL1 and Asp48 from loop L4 of an adjacent Hyp-1 molecule (green). MEL1 is shown as a ball-and-stick model surrounded by its (semitransparent) van der Waals surface, and the two interacting Hyp-1 molecules (sand and green) are presented with their semitransparent van der Waals surfaces.

The unidentified ligand marked by dummy (UNL) water molecules at site 2 is in van der Waals distance to residues Leu19, Ile116, and Tyr144. The same residues stabilize the ANS2 ligand in the binding site 2 of the Hyp-1/ANS complex (Sliwiak et al., 2015).

Conformational Differences between the Available Hyp-1 Complexes

We note at the outset that there is no truly ligand-free structure of Hyp-1 in the PDB. The closest case of a protein crystallized without any intentional ligand is 3IE5 (Michalska et al., 2010) but even in that structure there are serendipitous PEG molecules found in the binding sites of the two protein chains A and B. A superposition of the C α atoms revealed that the structures of Hyp-1 complexed with melatonin, ANS (4N3E, represented by chain K) and PEG (3IE5, chains A and B) are quite similar, with R.M.S.D. values within $\sim 1 \text{ \AA}$ (Table 3). That means that the chemical character of the ligand does not influence the Hyp-1-fold to a significant degree and that the three conserved binding sites are capable of accommodating different hydrophobic and amphiphilic ligands from the aqueous environment. Interestingly, chain A of the 3IE5 structure seems to differ most significantly from all the remaining Hyp-1 models, even when compared with chain B from the same structure (Figure 5). This difference can be correlated with the fact that in chain A of 3IE5 the binding site 3 is empty, allowing Tyr150 and Lys33 to form a direct stacking contact. This interaction brings the end of helix α 3 closer to helix α 2 and, in consequence, pulls the loops L3 and L5 toward α 3. One can speculate that binding of a ligand molecule at site 3 of Hyp-1 widens the E1 entrance, facilitating access of another ligand molecule to site 1. We can therefore hypothesize that the ligand binding mechanism of Hyp-1 has a cooperative character. Moreover the PEG molecules in 3IE5 (Figure 5) seem to pull the main cavity separator (Arg27) away from the hydrophobic core, resulting in a less solid separation between chambers 1 and 2.

CONCLUSION

Hyp-1, a protein from *H. perforatum*, has the characteristic PR-10-fold. However, despite the overall similarity, it has three highly unique and characteristic ligand binding sites, which may suggest a unique ligand-binding mechanism among the PR-10 proteins. Although the interaction of Hyp-1 with melatonin

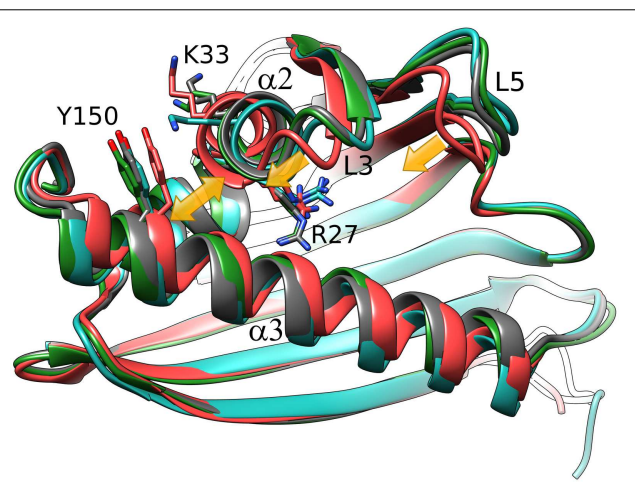


FIGURE 5 | C α superposition of the available models of Hyp-1. Color code: Hyp-1/MEL (this work), dark gray; Hyp-1/ANS (4N3E, chain K), green; Hyp-1/PEG (3IE5), chain A – red, chain B – blue. Yellow arrows indicate the conformational rearrangements in chain A of 3IE5, which has an empty site 3, in particular the approach of helices α 2 and α 3 (highlighted by Tyr150) leading to a tighter grip of the fingertip loops L3 and L5.

does not appear to be particularly strong, the structure of the Hyp-1/MEL complex is quite robust and reproducible in a number of crystal structure determination experiments. The reproducibility regards also the unidentified electron density at site 2 and an unattributed peak near the methoxy group of MEL1. Moreover, co-crystallization trials with other phytohormones and natural ligands using the same crystallization screens as in the Hyp-1/MEL experiments, produced no results. The three binding sites identified in the Hyp-1/MEL complex are exactly the same as in the Hyp-1/ANS complex. They comprise a well ordered MEL (site 1), a rotationally disordered one (3) and possibly an unidentified melatonin degradation product (2). Considering all the facts together, one can conclude that Hyp-1 may be capable of melatonin storage/transport under stress conditions in *H. perforatum*. A shortlist of the supporting observations is as follows: (i) Hyp-1, as a probable pathogenesis-related protein (a superfamily, whose members are expressed *inter alia* during abiotic and biotic stress) was detected in the roots and other parts of *Hypericum* plantlets and its mRNA expression has the highest level in the roots. (ii) Melatonin concentration is very high in vulnerable parts, like seedlings, as well as in the leaves and flowers of mature *Hypericum* plants, and it is further elevated during, e.g., radiation stress, and thus it could be bound by Hyp-1 despite of a relatively low affinity. (iii) Melatonin and its precursor tryptophan have been reported to be absorbed by plant roots from soil and media (Tan et al., 2007). (iv) *trans*-Zeatin, which is frequently reported as a natural ligand of PR-10 proteins, did not affect Hyp-1/MEL crystallization, while the artificial fluorescent probe ANS - did. However, taking into account that some PR-10 proteins show pleiotropic binding capacity (Sliwiak et al., 2016), it should not be ruled out that Hyp-1 may also play other role(s) in *H. perforatum*.

TABLE 3 | R.M.S.D. (\AA) values of C α superpositions of the following Hyp-1 models: Hyp-1/MEL complex (this work), Hyp-1/ANS complex (4N3E, chain K), and chains A/B from the “ligand free” (i.e., Hyp-1/PEG) form (3IE5).

	3IE5, chain A	3IE5, chain B	4N3E, chain K
Hyp-1/MEL	1.01	0.72	0.61
4N3E, chain K	1.04	0.75	
3IE5, chain B	1.07		

AUTHOR CONTRIBUTIONS

JS designed the experiments, conducted the experiments and calculations, analyzed the results, drafted the manuscript. ZD supervised initial experiments, conducted X-ray diffraction experiments and data processing, participated in ms preparation. MJ supervised the project, analyzed the results, wrote the paper.

FUNDING

X-Ray diffraction data were collected at the Southeast Regional Collaborative Access Team (SER-CAT) beamline of the APS/ANL. Use of the Advanced Photon Source was supported by the US Department of Energy, Office of Science, Office of

Basic Energy Sciences, under Contract No. W-31-109-Eng-38. Financial support of the project was provided by the European Union within the European Regional Developmental Fund and by the Polish National Science Centre (grant No. 2013/10/M/NZ1/00251). This publication was supported by the Polish Ministry of Science and Higher Education under the KNOW program.

REFERENCES

- Afonine, P. V., Grosse-Kunstleve, R. W., Echols, N., Headd, J. J., Moriarty, N. W., Mustyakimov, M., et al. (2012). Towards automated crystallographic structure refinement with phenix refine. *Acta Crystallogr. D68*, 352–367. doi: 10.1107/S0907444912001308
- Arnao, M., and Hernández-Ruiz, J. (2015). Functions of melatonin in plants: a review. *J. Pineal Res.* 59, 133–150. doi: 10.1111/jpi.12253
- Bais, H. P., Vepachedu, R., Lawrence, C. B., Stermitz, F. R., and Vivanco, J. M. (2003). Molecular and biochemical characterization of an enzyme responsible for the formation of hypericin in St. John's wort (*Hypericum perforatum* L.). *J. Biol. Chem.* 278, 32413–32422. doi: 10.1074/jbc.M301681200
- Biesiadka, J., Bujacz, G., Sikorski, M. M., and Jaskolski, M. (2002). Crystal structures of two homologous pathogenesis-related proteins from yellow lupine. *J. Mol. Biol.* 319, 1223–1234. doi: 10.1016/S0022-2836(02)00385-6
- Calamini, B., Santarsiero, B. D., Boutin, J. A., and Mesecar, A. D. (2008). Kinetic, thermodynamic and X-ray structural insights into the interaction of melatonin and analogues with quinone reductase 2. *Biochem. J.* 413, 81–91. doi: 10.1042/BJ20071373
- Casañal, A., Zander, U., Muñoz, C., Dupeux, F., Luque, I., Botella, M. A., et al. (2013). The strawberry pathogenesis-related 10 (PR-10) Fra a proteins control flavonoid biosynthesis metabolic intermediates. *J. Biol. Chem.* 288, 35322–35332. doi: 10.1074/jbc.M113.501528
- Chen, V. B., Arendall, W. B., Headd, J. J., Keedy, D. A., Immormino, R. M., Kapral, G. J., et al. (2010). MolProbity: all-atom structure validation for macromolecular crystallography. *Acta Crystallogr. D66*, 12–21. doi: 10.1107/s0907444909042073
- Chwastyk, M., Jaskolski, M., and Cieplak, M. (2014). Structure-based thermodynamic and mechanical stability of plant PR-10 proteins. *FEBS J.* 281, 416–429. doi: 10.1111/febs.12611
- Cohen, G. H. (1997). ALIGN: a program to superimpose protein coordinates, accounting for insertions and deletions. *J. Appl. Crystallogr.* 30, 1160–1161. doi: 10.1107/S0021889897006729
- Dubbels, R., Reiter, R. J., Klenke, E., Goebel, A., Schnakenberg, E., Ehlers, C., et al. (1995). Melatonin in edible plants identified by radioimmunoassay and by high performance liquid chromatography-mass spectrometry. *J. Pineal Res.* 18, 28–31. doi: 10.1111/j.1600-079X.1995.tb00136.x
- Emsley, P., Lohkamp, B., Scott, W., and Cowtan, K. (2010). Features and development of Coot. *Acta Crystallogr. D66*, 486–501. doi: 10.1107/S0907444910007493
- Fernandes, H., Bujacz, G., Bujacz, A., Jelen, F., Jasinski, M., Kachlicki, P., et al. (2009). Cytokinin-induced structural adaptability of a *Lupinus luteus* PR-10 protein. *FEBS J.* 276, 1596–1609. doi: 10.1111/j.1742-4658.2009.06892.x
- Fernandes, H., Michalska, K., Sikorski, M., and Jaskolski, M. (2013). Structural and functional aspects of PR-10 proteins. *FEBS J.* 280, 1169–1199. doi: 10.1111/febs.12114
- Fernandes, H., Pasternak, O., Bujacz, G., Bujacz, A., Sikorski, M. M., and Jaskolski, M. (2008). *L. luteus* pathogenesis-related protein as a reservoir for cytokinins. *J. Mol. Biol.* 378, 1040–1051. doi: 10.1016/j.jmb.2008.03.027
- Gajhede, M., Osmark, P., Poulsen, F. M., Ipsen, H., Larsen, J. N., Joost van Neerven, R. J., et al. (1996). X-ray and NMR structure of Bet v 1, the origin of birch pollen allergy. *Nat. Struct. Biol.* 3, 1040–1045. doi: 10.1038/nsb1296-1040
- Jaskolski, M. (2013). On the propagation of errors. *Acta Crystallogr. D69*, 1865–1866. doi: 10.1107/s090744491301528x
- Karplus, P. A., and Diederichs, K. (2012). Linking crystallographic model and data quality. *Science* 336, 1030–1033. doi: 10.1126/science.1218231
- Kofler, S., Asam, C., Eckhard, U., Wallner, M., Ferreira, F., and Brandstetter H. (2012). Crystallographically mapped ligand binding differs in high and low IgE binding isoforms of birch pollen allergen bet v 1. *J. Mol. Biol.* 422, 109–123. doi: 10.1016/j.jmb.2012.05.016
- Kosuth, J., Hrehorova, D., Jaskolski, M., and Cellarova, E. (2013). Stress-induced expression and structure of the putative gene hyp-1 for hypericin biosynthesis. *Plant Cell Tiss. Organ Cult.* 114, 207–216. doi: 10.1007/s11240-013-0316-0
- Kosuth, J., Katkovcinová, Z., Olexová, P., and Cellárová, E. (2007). Expression of the hyp-1 gene in early stages of development of *Hypericum perforatum* L. *Plant Cell Rep.* 26, 211–217. doi: 10.1007/s00299-006-0240-4
- Krissinel, E., and Henrick, K. (2007). Inference of macromolecular assemblies from crystalline state. *J. Mol. Biol.* 372, 774–797. doi: 10.1016/j.jmb.2007.05.022
- Maharaj, D. S., Anoopkumar-Dukai, S., Glass, B. D., Antunes, E. M., Lack, B., Walker, R. N., et al. (2002). The identification of the UV degradants of melatonin and their ability to scavenge free radicals. *J. Pineal Res.* 32, 257–261. doi: 10.1034/j.1600-079X.2002.01866.x
- Markovic-Housley, Z., Degano, M., Lamba, D., von Roepenack-Lahaye, E., Clemens, S., Susani, M., et al. (2003). Crystal structure of a hypoallergenic isoform of the major birch pollen allergen Bet v 1 and its likely biological function as a plant steroid carrier. *J. Mol. Biol.* 325, 123–133. doi: 10.1016/S0022-2836(02)01197-X
- McCoy, A. J., Grosse-Kunstleve, R. W., Adams, P. D., Winn, M. D., Storoni, L. C., and Read, R. J. (2007). Phaser crystallographic software. *J. Appl. Crystallogr.* 40, 658–674. doi: 10.1107/S0021889807021206
- Michalska, K., Fernandes, H., Sikorski, M. M., and Jaskolski, M. (2010). Crystal structure of Hyp-1, a St John's wort protein with implication in the biosynthesis of hypericin. *J. Struct. Biol.* 169, 161–171. doi: 10.1016/j.jsb.2009.10.008
- Mogensen, J. E., Wimmer, R., Larsen, J. N., Spangfort, M. D., and Otzen, D. E. (2002). The major birch allergen, Bet v 1, shows affinity for a broad spectrum of physiological ligands. *J. Biol. Chem.* 277, 23684–13692. doi: 10.1074/jbc.M202065200
- Murch, S. J., Campbell, S. S. B., and Saxena, P. K. (2001). The role of serotonin and melatonin in plant morphogenesis: regulation of auxin-induced root organogenesis in in vitro-cultured explants of St. John's Wort (*Hypericum perforatum* L.). *In Vitro Cell. Dev. Biol. Plant* 37, 786–793. doi: 10.1007/s11627-001-0130-y
- Murch, S. J., KrishnaRaj, S., and Saxena, P. K. (2000). Tryptophan is a precursor for melatonin and serotonin biosynthesis in in vitro regenerated St. John's wort (*Hypericum perforatum* L. cv. Anthos) plants. *Plant Cell Rep.* 19, 698–704. doi: 10.1007/s002990000206

- Murch, S. J., Simmons, C. B., and Saxena, P. K. (1997). Melatonin in feverfew and other medicinal plants. *Lancet* 359, 1598–1599. doi: 10.1016/S0140-6736(05)64014-7
- Otwinowski, Z., and Minor, W. (1997). Processing of X-ray diffraction data collected in oscillation mode. *Methods Enzymol.* 276, 307–326. doi: 10.1016/S0076-6879(97)76066-X
- Pasternak, O., Bujacz, G. D., Fujimoto, Y., Hashimoto, Y., Jelen, F., Otlewski, J., et al. (2006). Crystal structure of *Vigna radiata* cytokinin-specific binding protein in complex with zeatin. *Plant Cell* 18, 2622–2634. doi: 10.1105/tpc.105.037119
- Pettersen, E. F., Goddard, T. D., Huang, C. C., Couch, G. S., Greenblatt, D. M., Meng, E. C., et al. (2004). UCSF Chimera – a visualization system for exploratory research and analysis. *J. Comput. Chem.* 25, 1605–1612. doi: 10.1002/jcc.20084
- Qian, J., Wu, J., Yao, B., and Lu, Y. (2012). Preparation of a polyclonal antibody against hypericin synthase and localization of the enzyme in red-pigmented *Hypericum perforatum* L. plantlets. *Acta Biochim. Polon.* 59, 639–645.
- Quarles, W. G., Templeton, D. H., and Zalkin, A. (1974). The crystal and molecular structure of melatonin. *Acta Crystallogr. B30*, 99–103. doi: 10.1107/S0567740874002287
- Ruszkowski, M., Sliwiak, J., Ciesielska, A., Barciszewski, J., Sikorski, M. M., and Jaskolski, M. (2014). Specific binding of gibberellin acid by Cytokinin-Specific Binding Proteins: a new aspect of plant hormone-binding proteins with PR-10 fold. *Acta Crystallogr. D70*, 2032–2041. doi: 10.1107/s1399004714010578
- Ruszkowski, M., Szpotkowski, K., Sikorski, M. M., and Jaskolski, M. (2013). The landscape of cytokinin binding by a plant nodulin. *Acta Crystallogr. D69*, 2365–2380. doi: 10.1107/s0907444913021975
- Schiebel, J., Radeva, N., Krimmer, S. G., Wang, X., Stieler, M., Ehrmann, F. R., et al. (2016). Six biophysical screening methods miss a large proportion of crystallographically discovered fragment hits: a case study. *Chem. Biol.* doi: 10.1021/acschembio.5b01034 [Epub ahead of print].
- Seutter von Loetzen, C., Hoffmann, T., Hartl, M. J., Schweimer, K., Schwab, W., Rosch, P., et al. (2014). Secret of the major birch pollen allergen Bet v 1: identification of the physiological ligand. *Biochem. J.* 457, 379–390. doi: 10.1042/BJ20130413
- Seutter von Loetzen, C., Jacob, T., Hartl-Spiegelhauer, O., Vogel, L., Schiller, D., Spörlein-Güttler, C., et al. (2015). Ligand recognition of the major birch pollen allergen bet v 1 is isoform dependent. *PLoS ONE* 10:e0128677. doi: 10.1371/journal.pone.0128677
- Sheard, L. B., and Zheng, N. (2009). Plant biology: Signal advance for abscisic acid. *Nature* 462, 575–576. doi: 10.1038/462575a
- Sliwiak, J., Dauter, Z., Kowiel, M., McCoy, A. J., Read, R. J., and Jaskolski, M. (2015). ANS complex of St John's wort PR-10 protein with 28 copies in the asymmetric unit: a fiendish combination of pseudosymmetry with tetartohedral twinning. *Acta Crystallogr. D71*, 829–843. doi: 10.1107/s139900471501388
- Sliwiak, J., Dolot, R., Michalska, K., Szpotkowski, K., Bujacz, G., Sikorski, M. M., et al. (2016). Crystallographic and CD probing of ligand-induced conformational changes in a plant PR-10 protein. *J. Struct. Biol.* 193, 55–66. doi: 10.1016/j.jsb.2015.11.008
- Sliwiak, J., Jaskolski, M., Dauter, Z., McCoy, A. J., and Read, R. J. (2014). Likelihood-based molecular-replacement solution for a highly pathological crystal with tetartohedral twinning and sevenfold translational noncrystallographic symmetry. *Acta Crystallogr. D70*, 471–480. doi: 10.1107/s1399004713030319
- Tan, D., Manchester, L. C., Helton, P., and Reiter, R. J. (2007). Phytoremediatve capacity of plants enriched with melatonin. *Plant Signal. Behav.* 2, 514–516. doi: 10.4161/psb.2.6.4639
- Conflict of Interest Statement:** The authors declare that the research was conducted in the absence of any commercial or financial relationships that could be construed as a potential conflict of interest.
- Copyright © 2016 Sliwiak, Dauter and Jaskolski. This is an open-access article distributed under the terms of the Creative Commons Attribution License (CC BY). The use, distribution or reproduction in other forums is permitted, provided the original author(s) or licensor are credited and that the original publication in this journal is cited, in accordance with accepted academic practice. No use, distribution or reproduction is permitted which does not comply with these terms.



Benzophenone Synthase and Chalcone Synthase Accumulate in the Mesophyll of *Hypericum perforatum* Leaves at Different Developmental Stages

Asma K. Belkheir^{1†}, Mariam Gaid¹, Benye Liu¹, Robert Hänsch² and Ludger Beerhues^{1*}

¹ Institute of Pharmaceutical Biology, Technische Universität Braunschweig, Braunschweig, Germany, ² Institute of Plant Biology, Technische Universität Braunschweig, Braunschweig, Germany

OPEN ACCESS

Edited by:

Kazufumi Yazaki,
Kyoto University, Japan

Reviewed by:

Vinay Kumar,
Central University of Punjab, India
Michal Oren-Shamir,
Agricultural Research Organization,
Volcani Center, Israel

***Correspondence:**

Ludger Beerhues
l.beerhues@tu-bs.de

†Present address:

Asma K. Belkheir,
Department of Pharmacognosy,
Faculty of Pharmacy, Garyounis
University, Benghazi, Libya

Specialty section:

This article was submitted to
Plant Metabolism
and Chemodiversity,
a section of the journal
Frontiers in Plant Science

Received: 15 March 2016

Accepted: 10 June 2016

Published: 29 June 2016

Citation:

Belkheir AK, Gaid M, Liu B,
Hänsch R and Beerhues L (2016)
Benzophenone Synthase
and Chalcone Synthase Accumulate
in the Mesophyll of *Hypericum perforatum* Leaves at Different
Developmental Stages.
Front. Plant Sci. 7:921.
doi: 10.3389/fpls.2016.00921

The active medicinal constituents in *Hypericum perforatum*, used to treat depression and skin irritation, include flavonoids and xanthones. The carbon skeletons of these compounds are formed by chalcone synthase (CHS) and benzophenone synthase (BPS), respectively. Polyclonal antisera were raised against the polyketide synthases from *Hypericum androsaemum* and their IgG fractions were isolated. Immunoblotting and immunotitration were used to test the IgGs for crossreactivity and monospecificity in *H. perforatum* leaf protein extract. Immunofluorescence localization revealed that both CHS and BPS are located in the mesophyll. The maximum fluorescence levels were observed in approx. 0.5 and 1 cm long leaves, respectively. The fluorescence intensity observed for CHS significantly exceeded that for BPS. Using histochemical staining, flavonoids were detected in the mesophyll, indicating that the sites of biosynthesis and accumulation coincide. Our results help understand the biosynthesis and underlying regulation of active *H. perforatum* constituents.

Keywords: *Hypericum perforatum*, chalcone synthase, benzophenone synthase, polyketide synthases, immunofluorescence localization, histochemical localization, flavonoids, xanthones

INTRODUCTION

Medications containing extracts from the flowering upper parts of the medicinal plant *Hypericum perforatum* (St. John's wort; Hypericaceae) are used for the treatment of mild to moderate depressions as well as skin irritations and infected wounds (Linde et al., 2008; Wölfle et al., 2014). Due to the additive and synergistic effects of the ingredients, the entire extract is commonly used for therapy. The major active constituents involve hyperforins, hypericins, flavonoids, and xanthones (Beerhues, 2011). All these four classes of compounds are polyketide derivatives. Crucial steps of their biosynthetic pathways are catalyzed by polyketide synthase (PKS) enzymes. Plant PKSs (type III) are homodimers. Either subunit has an independent active site, which accommodates the starter and extender substrates (Austin and Noel, 2003). Variations in the starter molecule, the number of extender units and the mode of cyclization result in the formation of an amazing array of PKS products.

The PKSs that are involved in hyperforin, hypericin, flavonoid, and xanthone biosyntheses are isobutyrophenone, octaketide, chalcone, and benzophenone synthases, respectively

(Beerhues, 2011). cDNAs encoding benzophenone synthase (BPS) and chalcone synthase (CHS) were cloned from elicitor-treated *Hypericum androsaemum* cell cultures and greenhouse-grown *H. sampsonii* plants and were functionally expressed in *Escherichia coli* (Liu et al., 2003; Huang et al., 2012). BPS and CHS catalyze decarboxylative condensations of benzoyl-CoA and 4-coumaroyl-CoA, respectively, with three molecules of malonyl-CoA. While benzoyl-CoA is also preferred by BPS from *Garcinia mangostana*, the enzyme from *Centaurium erythraea* uses 3-hydroxybenzoyl-CoA (Beerhues, 1996; Nualkaew et al., 2012). The products of the BPS and CHS reactions are benzophenones and chalcones, which are metabolized to xanthones and flavonoids, respectively (Winkel-Shirley, 2001; El-Awaad et al., 2016). Upon mutation in a single active site position, *H. androsaemum* BPS formed phenylpyrones (Klundt et al., 2009). Xanthones and flavonoids contribute to the medicinal effects of *H. perforatum* extracts. Understanding their biosynthetic pathways in *H. perforatum* requires, in addition to the knowledge of the individual biochemical reactions, information about the spatial and temporal regulation, which underlies the metabolic routes. Here, immunofluorescence localization of BPS and CHS in leaves of *H. perforatum* is reported.

The two other PKSs, isobutyrophenone and octaketide synthases, were not included in this study. No cDNA encoding isobutyrophenone synthase, the key enzyme of hyperforin biosynthesis, has so far been isolated. For octaketide synthase, cDNAs were cloned from various species, including *H. perforatum* (Abe et al., 2005; Karppinen et al., 2008; Mizuuchi et al., 2009). However, all the recombinant proteins form an incorrectly cyclized octaketide derivative. Correct cyclization leading to formation of emodin anthrone has recently been observed in elicitor-treated *Cassia bicapsularis* cell cultures (Abdel-Rahman et al., 2013). Octaketide synthase transcripts in *H. perforatum* leaves were localized by *in situ* hybridization, indicating their exclusive presence in hypericin-containing dark nodules (Karppinen et al., 2008). Therefore, octaketide synthase was not considered here.

In the present study, we focus on the localization of BPS and CHS. Antibodies were raised, tested for their specificities and used for immunofluorescence detection of the PKSs in the mesophyll of *H. perforatum* leaves. Furthermore, biosynthetic products were histochemically localized. While a specific stain for xanthones was not available, flavonoids were detected in the mesophyll.

MATERIALS AND METHODS

Plants

Hypericum perforatum L. (Hypericaceae) was grown in the medicinal plants garden of the Institute of Pharmaceutical Biology, Technische Universität Braunschweig, Germany.

Chemicals and Materials

Solvents and chemicals were of either analytical or high performance liquid chromatography (HPLC) grade.

Polyvinylidene difluoride (PVDF) blotting membranes (Immobilon P) were purchased from Millipore (Bedford, USA). Enhanced chemiluminescence (ECL) Western blotting detection reagents were ordered from GE Healthcare (Freiburg, Germany). Peroxidase-conjugated AffinPure goat anti-rabbit IgG (H + L) and Alexa Fluor 488-goat anti-rabbit IgG (H + L) were obtained from Dianova (Hamburg, Germany) and Invitrogen (Karlsruhe, Germany), respectively. Cryo-embedding material and poly-L-lysine-coated slides were purchased from Plano (Marburg, Germany) and Roth (Karlsruhe, Germany), respectively. Polyclar AT and diphenylboric acid 2-aminoethyl ester (DPBA) were ordered from Serva (Heidelberg, Germany) and Sigma-Aldrich (Taufkirchen, Germany), respectively.

Generation of Polyclonal Antisera and Purification of IgG Fractions

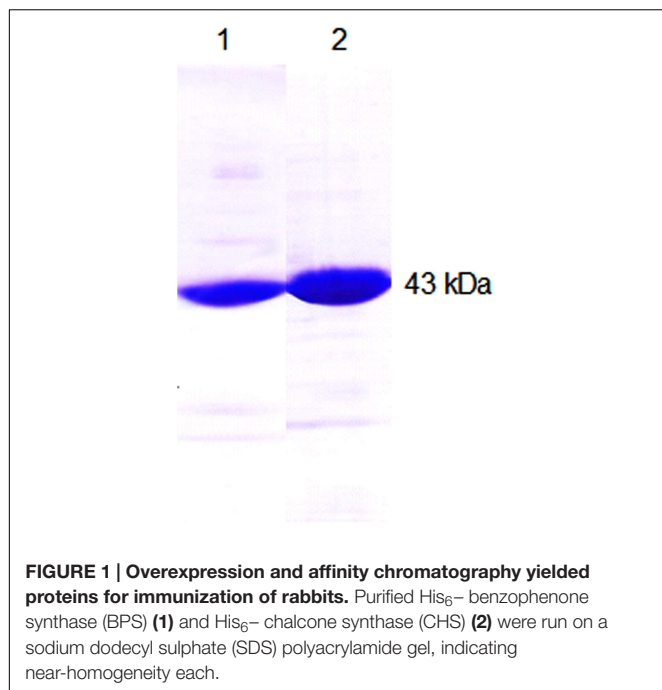
The BPS and CHS sequences used were from *H. androsaemum* (Liu et al., 2003). They were expressed as both His₆-tag and GST-fusion proteins using pRSET B (Invitrogen, Karlsruhe, Germany) and pGEX (Görlach and Schmid, 1996) expression vectors, respectively. The proteins were purified by affinity chromatography using Ni-NTA agarose and GSTrap matrices, respectively (Liu et al., 2003, 2007). The His₆-tag proteins were used for immunization of rabbits, which was carried out by SEQLAB Sequence Laboratories (Göttingen, Germany). The IgG fractions of the antisera and the pre-immune sera were isolated and stored, as described previously (Chizzali et al., 2012).

Protein Extraction and Immunoblotting

Fresh leaves (1 g) of varying size (0.3, 0.5, 0.8, 1.5, and 2.0 cm) were frozen in liquid nitrogen, ground in a mortar, mixed with 10% (w/v) Polyclar AT and extracted on ice for 10 min with 1 ml 50 mM Tris-HCl pH 7.4 containing 10 mM 1,4-dithiothreitol (DTT), 0.5 mM sucrose and 1 mM phenylmethane sulphonyl fluoride (protease inhibitor). The homogenate was centrifuged at 8,900 g for 25 min and the supernatant was used for immunoblotting. Protein concentration was determined by the method of Bradford (1976). Soluble proteins were separated on a 12% (w/v) sodium dodecyl sulphate (SDS) polyacrylamide gel and electroblotted on a PVDF membrane, as described previously (Chizzali et al., 2012). After blocking, the membrane was incubated with anti-His₆-BPS IgG (1:100,000 v/v) and anti-His₆-CHS IgG (1:10,000 v/v). Incubation with peroxidase-conjugated goat anti-rabbit IgG and further processing were carried out, as described previously (Chizzali et al., 2012). As control for efficient blotting, the membrane and the gel were stained with Indian ink and Coomassie blue solutions, respectively.

Enzyme Assays

The incubation mixtures (250 µL) consisted of 0.1 M potassium phosphate pH 7.0, 324 µM malonyl-CoA and 2 µg protein. In addition, the BPS and CHS assays contained 54 µM benzoyl-CoA and 4-coumaroyl-CoA, respectively. After



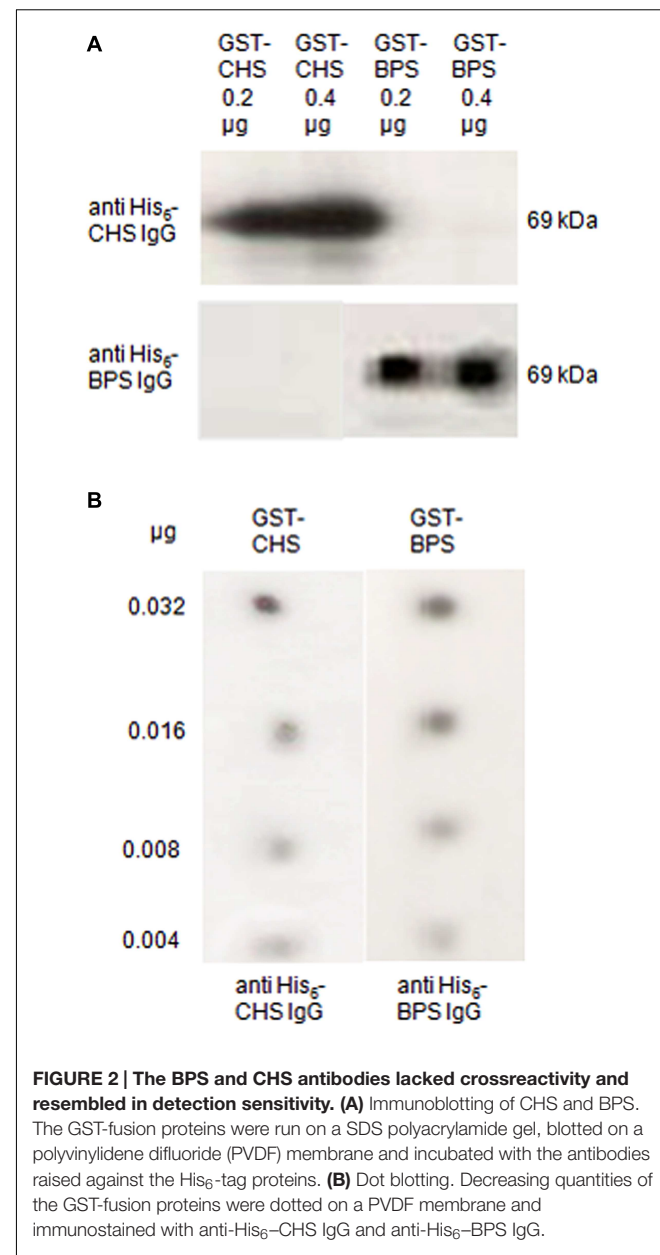
incubation at 30°C for 10 min, the enzymatic products were extracted and analyzed by high performance liquid chromatography (HPLC), as described previously (Liu et al., 2003).

Immunotitration

Mixtures of enzyme solution (50 µl) and IgG solution (50 µl of 1:2 to 1:512 dilutions) were incubated for 20 min at room temperature (Beerhues and Wiermann, 1988). Phosphate-buffered saline (PBS) (50 µl) containing 6% (w/v) polyethylene glycol 8000 was added. Following incubation at 4°C over night, the mixtures were centrifuged for 10 min at 8,700g. An aliquot of the supernatant (100 µl) was used to determine the non-precipitated enzyme activity that remained in the supernatant. Controls without antibody and with 1:2 to 1:512 dilutions of the pre-immune IgG were included.

Immunofluorescence Localization of BPS and CHS

For tissue fixation, the method of Moll et al. (2002) was used, except for slight modifications adapted to *H. perforatum* tissue. Small segments (1.2 mm²) were immediately fixed for 2 h under reduced pressure (0.3 mbar) in ice-cold buffered fixative solution, which consisted of 2% w/v formaldehyde (freshly prepared from paraformaldehyde), 0.1% v/v glutaraldehyde and 0.1% v/v Triton X-100 in 0.1 M phosphate buffer pH 7.2. After washing with PBS (2 × 10 min), the samples were dehydrated in a graded ethanol series (30, 50, 70, and 90% for 30 min each at room temperature). For cryosectioning, fixed and PBS-washed tissue was embedded in a cryo-embedding matrix and stored in a cool and dry place. The specimens were cut to thin segments (18–20 µm) using a



cryomicrotome (HM 500 O cryostate, Microme). The sections were transferred to poly-L-lysine-coated slides, dried and further treated, as described previously (Chizzali et al., 2012). The pre-immune IgG and His₆-tag IgG fractions were used in 1:10 to 1:100 dilutions. Goat anti-rabbit secondary antibody was conjugated with Alexa Fluor 488, which exhibits absorbance of blue light at 494 nm and emission of green light at 517 nm.

Histochemical Localization of Flavonoids

Fresh hand-sectioned leaves were stained for 5 min with 0.125% (w/v) diphenylboric acid 2-aminoethyl ester (DPBA) in 0.005% (v/v) Triton X-100 and washed in water for 2 min. Images were taken using the confocal laser scanning microscope

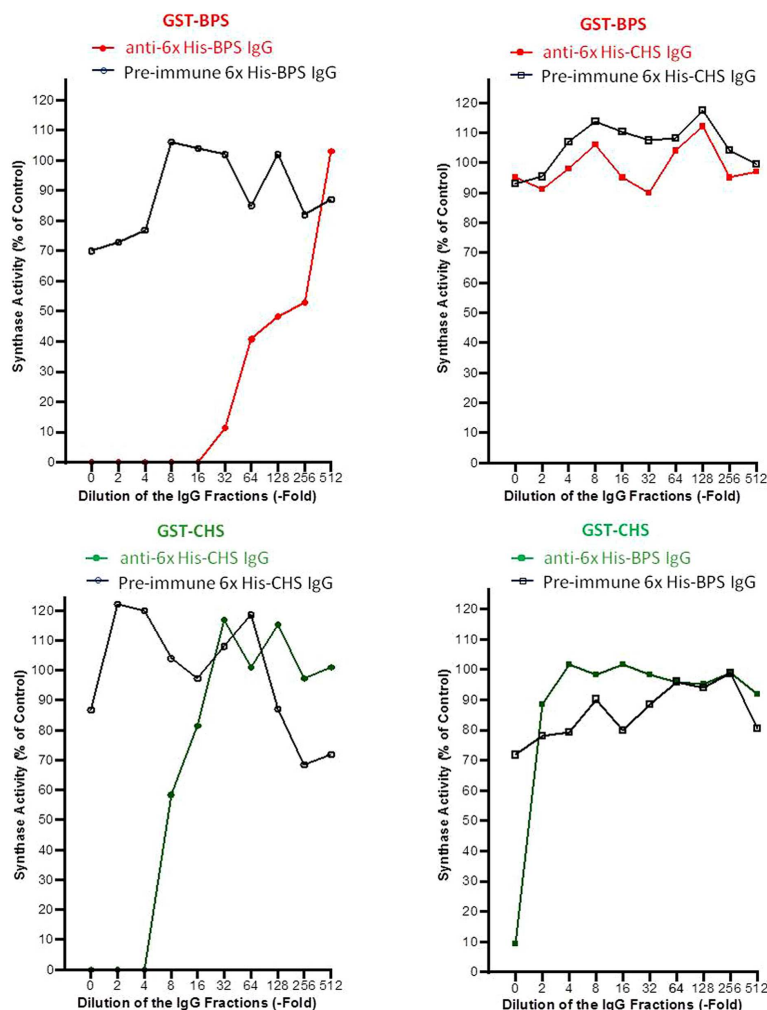


FIGURE 3 | The specific recognition of the antigens was confirmed by immunotitration. GST-BPS and GST-CHS were used as antigens in constant quantities (2 µg). Decreasing amounts of the anti-His₆ and pre-immune IgG fractions (1:2–1:512 dilutions) were added. The BPS and CHS activities that were not precipitated and remained in the supernatants of the titration mixtures were determined.

CLSM-510META (Release Version 4.2 SP1), connected to an Axiovert 200M (Carl Zeiss). The specimens were examined either using the Plan-Neofluar 10×/0.3 for overview or the C-Apochromat 40×/1.2 water-immersion objective for detailed pictures. The settings were as follows. Flavonoid staining was recorded using the 488 nm argon-laser (14% intensity) and chlorophyll autofluorescence was recorded using the 633 nm Helium laser (45% intensity) for excitation in the multi-tracking mode. The emitted light passed the primary beam splitting mirrors UV/488/543/633 and was detected after splitting with the NFT-545 on BP 505–550 for flavonoid staining and LP 650 for chlorophyll detection, respectively. When appropriate, the bright-field images of samples were visualized using the transmitted light photomultiplier. The lambda-mode was used to examine the spectral signature of fluorophores. All images were processed using the LSM Image Browser Release 4.2 (Carl Zeiss).

RESULTS

Antisera and Isolated IgG Fractions

To raise antibodies against BPS and CHS, the coding sequences of the proteins from *H. androsaemum* (Liu et al., 2003) were expressed in *E. coli* to yield both His₆-tag and GST-fusion proteins. Affinity chromatography on Ni-NTA and GSTrap matrices, respectively, resulted in proteins of near-homogeneity each, as indicated by SDS-polyacrylamide gel electrophoresis (PAGE) (Figure 1). The His₆-tag proteins served to raise polyclonal antisera in rabbits and the IgG fractions were isolated from both the pre-immune sera and the antisera. When studied by SDS-PAGE, the heavy and light chains at 50 and 25 kDa, respectively, were the only bands detectable. The isolated IgG fractions were tested for crossreactivity and monospecificity.

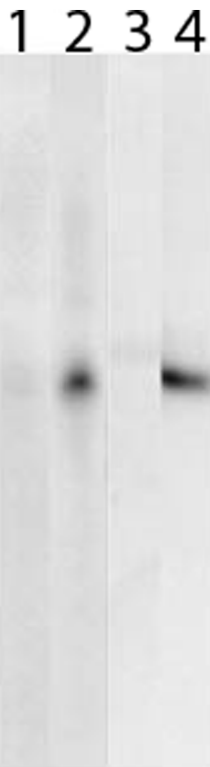


FIGURE 4 | Both BPS and CHS antibodies reacted monospecifically in leaf protein extract. Leaf proteins were separated by SDS-PAGE, blotted on a PVDF membrane and incubated with BPS pre-immune IgG (1), anti-His₆-BPS IgG (2), CHS pre-immune IgG (3) and anti-His₆-CHS IgG (4).

Lack of Crossreactivity between BPS and CHS Antibodies

Parallel immunolocalization of BPS and CHS requires that the antibodies do not crossreact with the respectively other antigen. Immunoblotting and immunotitration were used to study the specificities of the IgG fractions isolated. To rule out that cross-reactions in the polyclonal antisera occur between the His₆ tag and His₆-tag-directed antibodies, the GST-fusion proteins were used as antigens.

In immunoblotting after SDS-PAGE of the affinity-purified GST-fusion proteins, anti-His₆-CHS detected GST-CHS (69 kDa) but anti-His₆-BPS did not (**Figure 2A**). Conversely, anti-His₆-BPS stained GST-BPS (69 kDa) but anti-His₆-CHS did not. Thus, no crossreactivity was observed in immunoblotting. The pre-immune IgG fractions failed to cause any immunoreactions.

Parallel immunolocalization also requires that the two IgG fractions have similar detection capacities. For dot blotting, decreasing quantities of the GST-fusion proteins were dotted on a membrane and immunostained. Both anti-His₆-BPS and anti-His₆-CHS detected their antigens down to 0.004 µg, indicating similar sensitivities (**Figure 2B**).

For immunotitration coupled with the determination of enzyme activity, first the stability of the PKSs was studied. BPS

and CHS lost approx. 20 and 55%, respectively, of their activities within a day, however, the residual activities were sufficient for carrying out immunotitration. Constant quantities of the GST fusion proteins (2 µg) were mixed with decreasing quantities (1:2 to 1:512 dilutions) of the pre-immune and His₆-IgG fractions. The PKS activities that remained in the supernatants of the titration mixtures were determined (**Figure 3**). Anti-His₆-CHS IgG precipitated GST-CHS and did not crossreact with GST-BPS. Anti-His₆-BPS IgG precipitated GST-BPS and exhibited, when undiluted, crossreactivity with GST-CHS. However, the undiluted IgG fractions were not used for immunolocalization. Pre-immune His₆-CHS IgG did not recognize the PKSs, whereas pre-immune His₆-BPS IgG resulted in weak precipitation of the proteins.

Antibody Monospecificity in Leaf Extract

For use in immunolocalization, the BPS and CHS antibodies must (i) not crossreact with each other and (ii) not crossreact with foreign proteins, which occur in the leaf. Therefore, protein extracts from *H. perforatum* leaves at different developmental stages were subjected to SDS-PAGE and subsequent immunoblotting (**Figure 4**). Both anti-His₆-BPS IgG and anti-His₆-CHS IgG detected a single protein band at approx. 43 kDa, which corresponds to the subunit molecular mass of BPS and CHS. Thus, monospecificity in leaf protein extract was demonstrated for both IgG fractions. No staining of protein bands was observed when the two pre-immune IgG fractions were used.

Immunolocalization of BPS and CHS to the Mesophyll

Localization by immunofluorescence was carried out with leaves of field-grown plants, using green fluorescent labeling (Alexa Fluor 488) and laser scanning confocal microscopy. Two alternative procedures of section preparation were examined, the resin (Technovit) and the cryo-sectioning techniques. Since resin-embedded sections exhibited strongly decreased PKS antigenicities and strong unspecific background labeling, cryo-sectioning was preferred. Best results, i.e., high level of specific detection and low level of background staining, were obtained with 1:25 dilutions of the IgG fractions. In addition, this dilution failed to cause any crossreactivity between the BPS and CHS IgG preparations, as described above.

For CHS, bright immunofluorescence was observed in the mesophyll (**Figure 5A**). Palisade and sponge cells exhibited similar staining intensities. The lambda signature of the Alexa Fluor 488-labeled sections verified the correct emission wavelength (520 nm). Epidermal tissue was devoid of immunostaining. No labeling was observed in control sections incubated with pre-immune IgG (**Figure 5B**).

BPS was also present in the mesophyll, however, the intensity of immunofluorescence was markedly lower than for CHS (**Figure 5C**). The upper and the lower epidermis were devoid of staining. No labeling was observed with pre-immune IgG (**Figure 5D**).

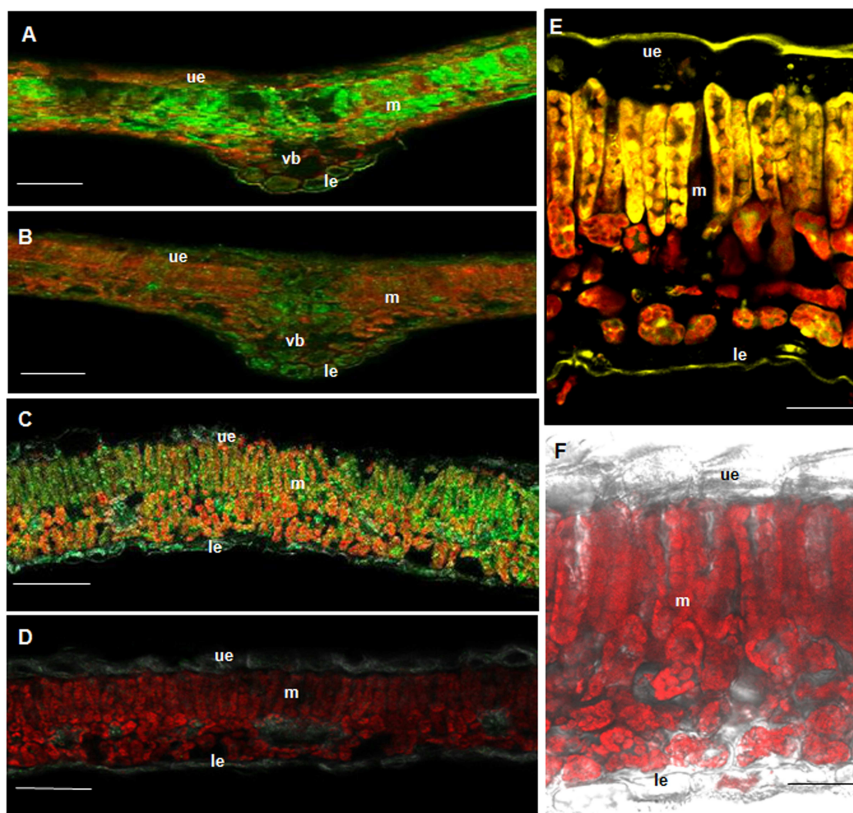


FIGURE 5 | BPS and CHS as well as flavonoids are located in the mesophyll. Immunofluorescence localization of CHS (A,B) and BPS (C,D) using a green fluorescent dye. (A,C) Cross-sections incubated with anti-His₆-CHS IgG and anti-His₆-BPS IgG, respectively. (B,D) Cross-sections incubated with the pre-immune IgGs. Localization of flavonoids (E,F) using histochemical detection. (E) Staining of flavonoids with diphenylboric acid 2-aminoethyl ester (DPBA). (F) Control section exhibiting only the red autofluorescence of chlorophyll. ue, upper epidermis; le, lower epidermis; m, mesophyll; vb, vascular bundle. Bar, 100 μm (A–D), 20 μm (E,F).

Histochemical Localization of Flavonoids to the Mesophyll

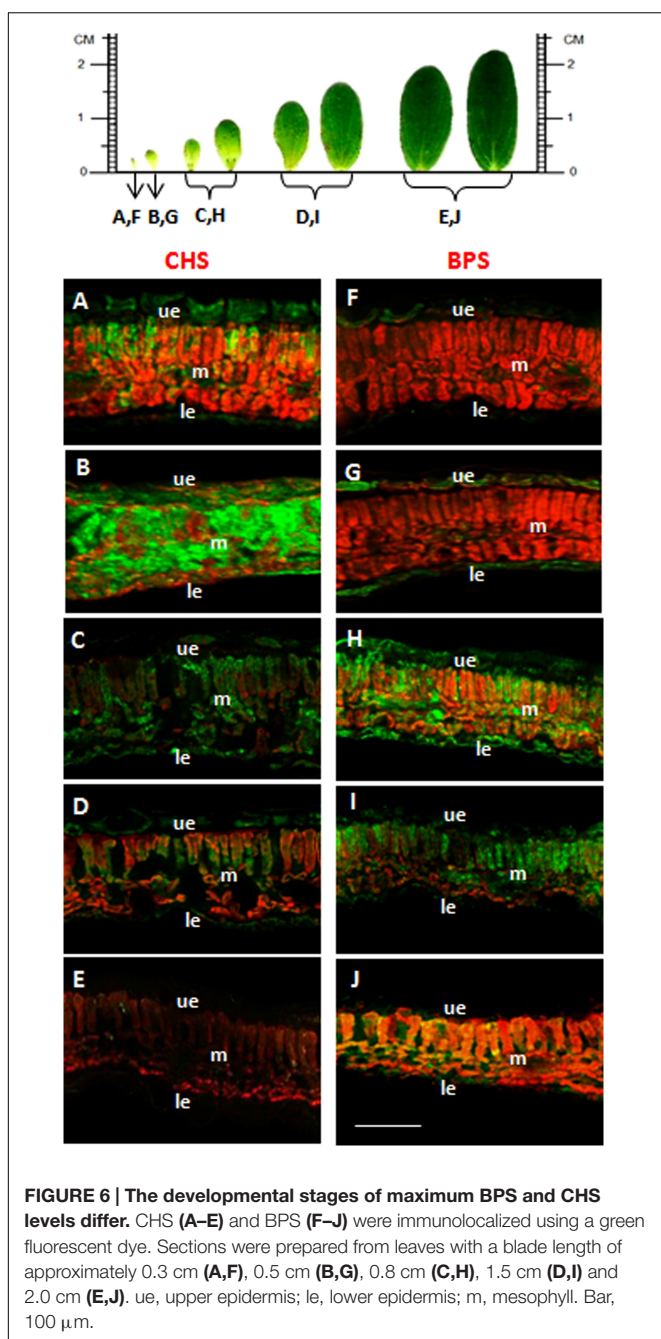
To stain the CHS products in *H. perforatum* leaf cross-sections, diphenylboric acid 2-aminoethyl ester (DPBA) was used (Figure 5E). Flavonoids were present in the mesophyll, palisade cells exhibiting stronger staining than sponge cells. The epidermal layers were devoid of labeling. No staining was observed in control sections (Figure 5F). For histochemical localization of xanthones, no specific stain was available.

Distinct Developmental Regulation of BPS and CHS

Leaves at various developmental stages were cross-sectioned and incubated with anti-His₆-BPS IgG and anti-His₆-CHS IgG in different sets of experiments. The intensity of immunofluorescence in the mesophyll changed with leaf age, which held true for both CHS and BPS (Figure 6). Maximum immunolabeling of CHS was observed in approx. 0.5 cm long leaves, which lacked detectable BPS quantities. The CHS-specific fluorescence rapidly decreased to a basal level in approx. 1 cm long leaves which, however, exhibited a high level of BPS immunofluorescence. In elder leaves, BPS fluorescence declined.

DISCUSSION

In the medicinal plant *H. perforatum*, the major active metabolites are formed by polyketide synthases, two of which are BPS and CHS. Demonstrated herein is that both BPS and CHS are located in *H. perforatum* leaves in the mesophyll tissue. Given the comparable detection capacities of the antibodies used, the immunofluorescence intensities for BPS and CHS differed significantly. The CHS level markedly exceeded the BPS level, which is in accordance with the previously detected quantities of flavonoids as CHS products and xanthones as BPS products. The flavonoid content in the aerial parts was 2–4%, the major compounds being quercetin derivatives, such as hyperoside and rutin (Nahrstedt and Butterweck, 1997; Hörlz and Petersen, 2003). In contrast, only traces of xanthones, such as 1,3,6,7-tetrahydroxyxanthone and mangiferin, were detected. As an exception, the aerial parts of Indian *H. perforatum* contained 2–4% xanthones (Muruganandam et al., 2000). Commonly, xanthones are abundant in roots of *Hypericum* species, which is consistent with the high BPS transcript level found in *H. sampsonii* roots (Pasqua et al., 2003; Huang et al., 2012; Zubrická et al., 2015). Therefore, immunohistochemical studies of these organs will be interesting.



CHS and BPS accumulated at different stages of leaf development, with CHS accumulation occurring earlier than that of BPS. Consistently, relatively high BPS transcript levels were detected in older leaves of *H. sampsonii*, whereas younger leaves had relatively high CHS transcript levels (Huang et al., 2012). Expression of *CHS* in young leaves is physiologically explainable. Due to absorption at 280–315 nm, flavonoids efficiently protect photosynthetically active tissue from damaging UV-B radiation, which can penetrate the ozone layer in the stratosphere (Harborne and Williams, 2000). Flavonoids also function as a preformed barrier against herbivore attack (Winkel-Shirley,

2001). As a consequence, flavonoid accumulation has to be initiated at an early stage of leaf development. In contrast, xanthones in *Hypericum* species serve as inducible defense compounds against microbial pathogens, i.e., phytoalexins (Abd El-Mawla et al., 2001; Franklin et al., 2009). Cell cultures of *H. perforatum* accumulated xanthones in response to the addition of a fungal elicitor prepared from *Colletotrichum gloeosporioides*, the causal agent of St. John's wort wilt (Gärber and Schenk, 2003; Conceição et al., 2006). Furthermore, *H. androsaemum* and *H. calycinum* cell cultures accumulated prenylated xanthones upon challenge with elicitors and a cDNA encoding the prenyltransferase involved was isolated (Abd El-Mawla et al., 2001; Gaid et al., 2012; Fiesel et al., 2015).

In *H. perforatum* leaves, the CHS products were located in the mesophyll tissue, as indicated by histochemical staining. Thus, the sites of biosynthesis and storage of flavonoids are identical. No transport process takes place at the tissue level. Previously, a similar tissue distribution of flavonoid biosynthetic enzymes was observed in primary leaves of oat (*Avena sativa*) by peeling the epidermal layers (Knogge and Weissenböck, 1986). The entire pathway, including CHS, chalcone-flavanone isomerase and methyl- and glycosyltransferase activities, was located in the leaf mesophyll. However, flavonoids, in this case flavones, were found in both epidermis and mesophyll tissues, with up to 70% being detected in the two epidermal layers (Weissenböck and Sachs, 1977). Therefore, intercellular translocation of individual products was proposed. While vitexin derivatives are transported to the epidermis, isovitexin derivatives remain in the mesophyll. Alternatively, the epidermal product pattern may reflect flavonoid biosynthesis in the subepidermal mesophyll cells.

Strict compartmentation of flavonoids between tissues and a close correlation between leaf development and flavonoid metabolism were also observed in primary leaves of rye (*Secale cereale*; Schulz et al., 1985; Schulz and Weissenböck, 1986; Hutzler et al., 1998). While two C-glucosylapigenin-O-glycosides were accumulated in the two epidermal layers, two anthocyanins and two luteolin O-glucuronides were exclusively located in the mesophyll, as shown by isolation and separation of epidermal and mesophyll protoplasts. Maximum product accumulation coincided with maximum activities of selected flavonoid biosynthetic enzymes, such as glucuronosyltransferases (Schulz and Weissenböck, 1988).

A different tissue distribution of CHS and flavonoids than in primary leaves of grass seedlings was found in leaves of spinach (*Spinacia oleracea*), pea (*Pisum sativum*), and bean (*Vicia faba*), using immunofluorescence localization (Beerhues and Wiermann, 1988; Beerhues et al., 1988). CHS was present in the upper and the lower epidermis and to a minor extent in the subepidermal layers at an early developmental stage. CHS in leaves of spinach, pea and bean was restricted to the epidermal tissue and flavonoids were either exclusively or predominantly present in the epidermal layers, indicating that the sites of biosynthesis and storage were identical (Tissut and Ravanel, 1980; Hrazdina et al., 1982; Weissenböck et al., 1984, 1986). This was also true for parsley (*Petroselinum crispum*) leaves (Jahnen and Hahlbrock, 1988;

Schmelzer et al., 1988). Using *in situ* hybridization, immunohistochemistry, and microspectrophotometry, light-induced CHS mRNA, CHS protein, and flavonoid products, respectively, were localized to epidermal cells, which thus contained the entire sequence of product formation. In leaves of *Catharanthus roseus*, CHS transcripts and flavonoids were also co-localized by *in situ* hybridization and histochemistry to the epidermis, mainly the adaxial layer (Mahroug et al., 2006). Furthermore, epidermal tissue of needles of Scots pine (*Pinus sylvestris*) contained both CHS mRNA and products (Schnitzler et al., 1996).

For localization of xanthones, no specific staining was available and, even if, the low xanthone level was likely to be below the detection limit. *In vitro* regenerated shoots of *H. perforatum* even lacked detectable quantities of xanthones (Pasqua et al., 2003). An interesting alternative for xanthone

localization may be leaves of Indian *H. perforatum*, which contain a high level of 1,3,5-trihydroxyxanthone derivatives (Muruganandam et al., 2000).

AUTHOR CONTRIBUTIONS

AB, MG, BL, RH, and LB designed the research and analyzed data; AB carried out the immunochemical studies; MG performed the histochemical analysis; MG and LB prepared the manuscript.

ACKNOWLEDGMENTS

This work was supported by the Deutsche Forschungsgemeinschaft (DFG). AB thanks the Libyan government for a Ph.D. scholarship.

REFERENCES

- Abd El-Mawla, A. M. A., Schmidt, W., and Beerhues, L. (2001). Cinnamic acid is a precursor of benzoic acids in cell cultures of *Hypericum androsaemum* L. but not in cell cultures of *Centaurium erythraea* RAFN. *Planta* 212, 288–293. doi: 10.1007/s004250000394
- Abdel-Rahman, I. A., Beuerle, T., Ernst, L., Abdel-Baky, A. M., Desoky Eel, D., Ahmed, A. S., et al. (2013). *In vitro* formation of the anthranoid scaffold by cell-free extracts from yeast-extract-treated *Cassia bicapsularis* cell cultures. *Phytochemistry* 88, 15–24. doi: 10.1016/j.phytochem.2013.01.001
- Abé, I., Oguro, S., Utsumi, Y., Sano, Y., and Noguchi, H. (2005). Engineered biosynthesis of plant polyketides: chain length control in an octaketide-producing plant type III polyketide synthase. *J. Am. Chem. Soc.* 127, 12709–12716. doi: 10.1021/ja053945v
- Austin, M. B., and Noel, J. P. (2003). The chalcone synthase superfamily of type III polyketide synthases. *Nat. Prod. Rep.* 20, 79–110. doi: 10.1039/b100917f
- Beerhues, L. (1996). Benzophenone synthase from cultured cells of *Centaurium erythraea*. *FEBS Lett.* 383, 264–266. doi: 10.1016/0014-5793(96)00265-7
- Beerhues, L. (2011). “Biosynthesis of the active *Hypericum perforatum* constituents,” in *Medicinal and Aromatic Plant Science and Biotechnology 5 (Special Issue 1): Hypericum*, ed. C. Cirak (Isleworth: Global Science Books), 70–77.
- Beerhues, L., Robenek, H., and Wiermann, R. (1988). Chalcone synthases from spinach (*Spinacia oleracea* L.) II. Immunofluorescence and immunogold localization. *Planta* 173, 544–553. doi: 10.1007/BF00958968
- Beerhues, L., and Wiermann, R. (1988). Chalcone synthases from spinach (*Spinacia oleracea* L.) I. Purification, peptide patterns, and immunological properties of different forms. *Planta* 173, 532–543. doi: 10.1007/BF00958967
- Bradford, M. M. (1976). A rapid and sensitive method for the quantitation of microgram quantities of protein utilizing the principle of protein-dye binding. *Anal. Biochem.* 72, 248–254. doi: 10.1016/0003-2697(76)90527-3
- Chizzali, C., Gaid, M. M., Belkheir, A. K., Hänsch, R., Richter, K., Flachowsky, H., et al. (2012). Differential expression of biphenyl synthase gene family members in fire blight-infected apple ‘Holsteiner Cox’. *Plant Physiol.* 158, 864–875. doi: 10.1104/pp.111.190918
- Conceição, L. F. R., Ferreres, F., Tavares, R. M., and Dias, A. C. P. (2006). Induction of phenolic compounds in *Hypericum perforatum* L. cells by *Colletotrichum gloeosporioides* elicitation. *Phytochemistry* 67, 149–155. doi: 10.1016/j.phytochem.2005.10.017
- El-Awaad, I., Bocola, M., Beuerle, T., Liu, B., and Beerhues, L. (2016). Bifunctional CYP81AA proteins catalyse identical hydroxylations but alternative regioselective phenol couplings in plant xanthone biosynthesis. *Nat. Commun.* 7, 11472. doi: 10.1038/ncomms11472
- Fiesel, T., Gaid, M., Müller, A., Bartels, J., El-Awaad, I., Beuerle, T., et al. (2015). Molecular cloning and characterization of a xanthone prenyltransferase from *Hypericum calycinum* cell cultures. *Molecules* 20, 15616–15630. doi: 10.3390/molecules200915616
- Franklin, G., Conceição, L. F. R., Kombrink, E., and Dias, A. C. P. (2009). Xanthone biosynthesis in *Hypericum perforatum* cells provides antioxidant and antimicrobial protection upon biotic stress. *Phytochemistry* 70, 60–68. doi: 10.1016/j.phytochem.2008.10.016
- Gaid, M. M., Sircar, D., Müller, A., Beuerle, T., Liu, B., Ernst, L., et al. (2012). Cinnamate:CoA ligase initiates the biosynthesis of a benzoate-derived xanthone phytalexin in *Hypericum calycinum* cell cultures. *Plant Physiol.* 160, 1267–1280. doi: 10.1104/pp.112.204180
- Gärber, U., and Schenk, R. (2003). Colletotrichum-wilt of St. John’s wort – Overview of results of examinations of several years. *Drogenreport* 16, 23–28.
- Görlich, J., and Schmid, J. (1996). Introducing *StuI* sites improves vectors for the expression of fusion proteins with factor Xa cleavage sites. *Gene* 170, 145–146. doi: 10.1016/0378-1119(95)00825-X
- Harborne, J. B., and Williams, C. A. (2000). Advances in flavonoid research since 1992. *Phytochemistry* 55, 481–504. doi: 10.1016/S0031-9422(00)00235-1
- Hölzl, J., and Petersen, M. (2003). “Chemical constituents of *Hypericum* spp,” in *Hypericum – The Genus Hypericum*, ed. E. Ernst (London: Taylor & Francis), 77–93.
- Hrazdina, G., Marx, G. A., and Hoch, H. C. (1982). Distribution of secondary plant metabolites and their biosynthetic enzymes in pea (*Pisum sativum* L.) leaves. *Plant Physiol.* 70, 745–748. doi: 10.1104/pp.70.3.745
- Huang, L., Wang, H., Ye, H., Du, Z., Zhang, Y., Beerhues, L., et al. (2012). Differential expression of benzophenone synthase and chalcone synthase in *Hypericum sampsonii*. *Nat. Prod. Commun.* 7, 1615–1618.
- Hutzler, P., Fischbach, R., Heller, W., Jungblut, T. P., Reuber, S., Schmitz, R., et al. (1998). Tissue localization of phenolic compounds in plants by confocal laser scanning microscopy. *J. Exp. Bot.* 49, 953–965. doi: 10.1093/jxb/49.323.953
- Jahnens, W., and Hahlbrock, K. (1988). Differential regulation and tissue-specific distribution of enzymes of phenylpropanoid pathways in developing parsley seedlings. *Planta* 173, 453–458. doi: 10.1007/BF00958957
- Karppinen, K., Hokkanen, J., Mattila, S., Neubauer, P., and Hohtola, A. (2008). Octaketide-producing type III polyketide synthase from *Hypericum perforatum* is expressed in dark glands accumulating hypericins. *FEBS J.* 275, 4329–4342. doi: 10.1111/j.1742-4658.2008.06576.x
- Klundt, T., Bocola, M., Lütge, M., Beuerle, T., Liu, B., and Beerhues, L. (2009). A single amino acid substitution converts benzophenone synthase into phenylpyrone synthase. *J. Biol. Chem.* 284, 30957–30964. doi: 10.1074/jbc.M109.038927

- Knogge, W., and Weissenböck, G. (1986). Tissue-distribution of secondary phenolic biosynthesis in developing primary leaves of *Avena sativa* L. *Planta* 167, 196–205. doi: 10.1007/BF00391415
- Linde, K., Berner, M. M., and Kriston, L. (2008). St John's wort for major depression. *Cochrane Database Syst. Rev.* 4:CD000448. doi: 10.1002/14651858.CD000448.pub3
- Liu, B., Falkenstein-Paul, H., Schmidt, W., and Beerhues, L. (2003). Benzophenone synthase and chalcone synthase from *Hypericum androsaemum* cell cultures: cDNA cloning, functional expression, and site-directed mutagenesis of two polyketide synthases. *Plant J.* 34, 847–855. doi: 10.1046/j.1365-313X.2003.01771.x
- Liu, B., Raeth, T., Beuerle, T., and Beerhues, L. (2007). Biphenyl synthase, a novel type III polyketide synthase. *Planta* 225, 1495–1503. doi: 10.1007/s00425-006-0435-5
- Mahroug, S., Courdavault, V., Thiersault, M., St-Pierre, B., and Burlat, V. (2006). Epidermis is a pivotal site of at least four secondary metabolic pathways in *Catharanthus roseus* aerial organs. *Planta* 223, 1191–1200. doi: 10.1007/s00425-005-0167-y
- Mizuuchi, Y., Shi, S. P., Wanibuchi, K., Kojima, A., Morita, H., Noguchi, H., et al. (2009). Novel type III polyketide synthases from *Aloe arborescens*. *FEBS J.* 276, 2391–2401. doi: 10.1111/j.1742-4658.2009.06971.x
- Moll, S., Anke, S., Kahmann, U., Hänsch, R., Hartmann, T., and Ober, D. (2002). Cell-specific expression of homospermidine synthase, the entry enzyme of the pyrrolizidine alkaloid pathway in *Senecio vernalis*, in comparison with its ancestor, deoxyhypusine synthase. *Plant Physiol.* 130, 47–57. doi: 10.1104/pp.004259
- Muruganandam, A. V., Ghosal, S., and Bhattacharya, S. K. (2000). The role of xanthones in the antidepressant activity of *Hypericum perforatum* involving dopaminergic and serotonergic systems. *Biog. Amines* 15, 553–567.
- Nahrstedt, A., and Butterweck, V. (1997). Biologically active and other chemical constituents of the herb of *Hypericum perforatum*. *Pharmacopsychiatry* 30(Suppl.), 129–134. doi: 10.1055/s-2007-979533
- Nualkaew, N., Morita, H., Shimokawa, Y., Kinjo, K., Kushiro, T., De-Eknamkul, W., et al. (2012). Benzophenone synthase from *Garcinia mangostana* L. pericarps. *Phytochemistry* 77, 60–69. doi: 10.1016/j.phytochem.2012.02.002
- Pasqua, G., Avato, P., Monacelli, B., Santamaria, A. R., and Argentieri, M. P. (2003). Metabolites in cell suspension cultures, calli, and in vitro regenerated organs of *Hypericum perforatum* cv. Topas. *Plant Sci.* 165, 977–982. doi: 10.1016/S0168-9452(03)00275-9
- Schmelzer, E., Jähnen, W., and Hahlbrock, K. (1988). In situ localization of light-induced chalcone synthase mRNA, chalcone synthase, and flavonoid end products in epidermal cells of parsley leaves. *Proc. Natl. Acad. Sci. U.S.A.* 85, 2989–2993. doi: 10.1073/pnas.85.9.2989
- Schnitzler, J. P., Jungblut, T. P., Heller, W., Köfferlein, M., Hutzler, P., Heinemann, U., et al. (1996). Tissue localization of UV-B-screening pigments and of chalcone synthase mRNA in needles of scots pine seedlings. *New Phytol.* 132, 247–258. doi: 10.1111/j.1469-8137.1996.tb01844.x
- Schulz, M., Strack, D., Weissenböck, G., Markham, K. R., Dellamonica, G., and Chopins, J. (1985). Two luteolin O-glucuronides from primary leaves of *Secale cereale*. *Phytochemistry* 24, 343–345. doi: 10.1016/S0031-9422(00)83549-9
- Schulz, M., and Weissenböck, G. (1986). Isolation and separation of epidermal and mesophyll protoplasts from rye primary leaves – tissue-specific characteristics of secondary phenolic product accumulation. *Z. Naturforsch.* 41c, 22–27.
- Schulz, M., and Weissenböck, G. (1988). Dynamics of the tissue-specific metabolism of luteolin glucuronides in the mesophyll of rye primary leaves (*Secale cereale*). *Z. Naturforsch.* 43c, 187–193.
- Tissut, M., and Ravanel, P. (1980). Répartition des flavonols dans l'épaisseur des feuilles de quelques végétaux vasculaires. *Phytochemistry* 19, 2077–2081. doi: 10.1016/S0031-9422(00)82197-4
- Weissenböck, G., Hedrich, R., and Sachs, G. (1986). Secondary phenolic products in isolated guard cell, epidermal cell and mesophyll cell protoplasts from pea (*Pisum sativum* L.) leaves: distribution and determination. *Protoplasma* 134, 141–148. doi: 10.1007/BF01275712
- Weissenböck, G., and Sachs, G. (1977). On the localization of enzymes related to flavonoid metabolism in sections and tissues of oat primary leaves. *Planta* 137, 49–52. doi: 10.1007/BF00394434
- Weissenböck, G., Schnabl, H., Sachs, G., Elbert, C., and Heller, F. O. (1984). Flavonol content of guard cell and mesophyll cell protoplasts isolated from *Vicia faba* leaves. *Physiol. Plant.* 62, 356–362. doi: 10.1111/j.1399-3054.1984.tb04586.x
- Winkel-Shirley, B. (2001). Flavonoid biosynthesis. A colorful model for genetics, biochemistry, cell biology, and biotechnology. *Plant Physiol.* 126, 485–493. doi: 10.1104/pp.126.2.485
- Wölflé, U., Seelinger, G., and Schempp, C. M. (2014). Topical application of St. John's wort (*Hypericum perforatum*). *Planta Med.* 80, 109–120. doi: 10.1055/s-0033-1351019
- Zubrická, D., Mišianiková, A., Henzelyová, J., Valletta, A., De Angelis, G., D'Auria, F. D., et al. (2015). Xanthones from roots, hairy roots and cell suspension cultures of selected *Hypericum* species and their antifungal activity against *Candida albicans*. *Plant Cell Rep.* 34, 1953–1962. doi: 10.1007/s00299-015-1842-5

Conflict of Interest Statement: The authors declare that the research was conducted in the absence of any commercial or financial relationships that could be construed as a potential conflict of interest.

Copyright © 2016 Belkheir, Gaid, Liu, Hänsch and Beerhues. This is an open-access article distributed under the terms of the Creative Commons Attribution License (CC BY). The use, distribution or reproduction in other forums is permitted, provided the original author(s) or licensor are credited and that the original publication in this journal is cited, in accordance with accepted academic practice. No use, distribution or reproduction is permitted which does not comply with these terms.



Alternative Oxidase Gene Family in *Hypericum perforatum* L.: Characterization and Expression at the Post-germinative Phase

Isabel Velada^{1†}, Hélia G. Cardoso^{1*†}, Carla Ragonezi¹, Amaia Nogales², Alexandre Ferreira¹, Vera Valadas¹ and Birgit Arnholdt-Schmitt^{3*}

¹ ICAAM - Instituto de Ciências Agrárias e Ambientais Mediterrânicas, Laboratório de Biologia Molecular, Universidade de Évora, Pólo da Mira, Évora, Portugal, ² Linking Landscape, Environment, Agriculture and Food, Instituto Superior de Agronomia-Universidade de Lisboa, Lisboa, Portugal, ³ EU Marie Curie Chair, ICAAM - Instituto de Ciências Agrárias e Ambientais Mediterrânicas, Universidade de Évora, Pólo da Mira, Évora, Portugal

OPEN ACCESS

Edited by:

Gregory Franklin,

Institute of Plant Genetics of the Polish Academy of Science, Poland

Reviewed by:

Marina Gavilanes-Ruiz,

Universidad Nacional Autónoma de México, Mexico

Daniel H. Gonzalez,

Universidad Nacional del Litoral, Argentina

*Correspondence:

Hélia G. Cardoso

hcardoso@uevora.pt

Birgit Arnholdt-Schmitt

eu_chair@uevora.pt

[†]These authors have contributed equally to this work.

Specialty section:

This article was submitted to
Plant Metabolism and Chemodiversity,
a section of the journal
Frontiers in Plant Science

Received: 16 March 2016

Accepted: 04 July 2016

Published: 11 August 2016

Citation:

Velada I, Cardoso HG, Ragonezi C, Nogales A, Ferreira A, Valadas V and Arnholdt-Schmitt B (2016) Alternative Oxidase Gene Family in *Hypericum perforatum* L.: Characterization and Expression at the Post-germinative Phase. *Front. Plant Sci.* 7:1043.
doi: 10.3389/fpls.2016.01043

Alternative oxidase (AOX) protein is located in the inner mitochondrial membrane and is encoded in the nuclear genome being involved in plant response upon a diversity of environmental stresses and also in normal plant growth and development. Here we report the characterization of the AOX gene family of *Hypericum perforatum* L. Two AOX genes were identified, both with a structure of four exons (*HpAOX1*, acc. KU674355 and *HpAOX2*, acc. KU674356). High variability was found at the N-terminal region of the protein coincident with the high variability identified at the mitochondrial transit peptide. *In silico* analysis of regulatory elements located at intronic regions identified putative sequences coding for miRNA precursors and trace elements of a transposon. Simple sequence repeats were also identified. Additionally, the mRNA levels for the *HpAOX1* and *HpAOX2*, along with the ones for the *HpGAPA* (glyceraldehyde-3-phosphate dehydrogenase A subunit) and the *HpCAT1* (catalase 1), were evaluated during the post-germinative development. Gene expression analysis was performed by RT-qPCR with accurate data normalization, pointing out *HpHYP1* (chamba phenolic oxidative coupling protein 1) and *HpH2A* (histone 2A) as the most suitable reference genes (RGs) according to GeNorm algorithm. The *HpAOX2* transcript demonstrated larger stability during the process with a slight down-regulation in its expression. Contrarily, *HpAOX1* and *HpGAPA* (the corresponding protein is homolog to the chloroplast isoform involved in the photosynthetic carbon assimilation in other plant species) transcripts showed a marked increase, with a similar expression pattern between them, during the post-germinative development. On the other hand, the *HpCAT1* (the corresponding protein is homolog to the major H₂O₂-scavenging enzyme in other plant species) transcripts showed an opposite behavior with a down-regulation during the process. In summary, our findings, although preliminary, highlight the importance to investigate in more detail the participation of AOX genes during the post-germinative development in *H. perforatum*, in order to explore their functional role in optimizing photosynthesis and in the control of reactive oxygen species (ROS) levels during the process.

Keywords: cyanide-resistant pathway, St. John's Wort, plant development, gene expression, transposable elements, miRNAs, alternative oxidase, post-germination

INTRODUCTION

Hypericum perforatum L., (St. John's Wort) is a wide spread species found throughout all temperate regions of north and south hemispheres (Robson, 1977). Natural populations are usually observed in abandoned fields, along roadsides or in overgrazed rangelands (Maron et al., 2007). Its high interest for the pharmaceutical industry, due to its medicinal properties attributed to the presence of metabolites with an antidepressive, anticancer, and antiviral action (Zanolli, 2004; Gartner et al., 2005; Kubin et al., 2005), leads to a gradual re-expanding of field cultivation in Western Europe since the nineties.

Nevertheless, breeding of medicinal plants was neglected for a long time and has been initiated only about 20 years ago with special efforts in North-Europe. Homogeneous plantations are expected to provide farmers not only with higher yield stability, but also with increased homogeneity in product quality which in terms of medicinal plants would correspond to the composition of effective plant extracts. In this view, adequate technologies are being requested, especially the ones related with the control of seed germination, seedling development, and growth. Thus, fundamental and applied research can help to identify efficient strategies to reach this goal.

Marker assisted selection (MAS) is a process commonly used in plant breeding programs by which the selection of desirable phenotypic characteristics with agronomic interest, known as agronomic traits, is achieved indirectly by using DNA markers, closely linked to underlying gene(s), or developed from a specific gene(s). The last ones, named functional markers (FM), can be used to find out allelic variation in the genes underlying a trait, contributing to increase efficiency and accuracy of plant breeding programs, reason why have been gaining increasing attention during the last years (Andersen and Lübbertedt, 2003; Neale and Savolainen, 2004; Arnholdt-Schmitt, 2005). The identification of candidate genes is recognized as the first step for FM development. These genes can be found out by high-through-put differential gene expression analyses or by hypothesis-driven research approaches, which actually represent the most promising strategies in molecular plant breeding (Arnholdt-Schmitt, 2005; Collins et al., 2008). Alternative oxidase (AOX) was previously pointed out as a potential source for FM development related with plant plasticity under environmental stress, which means genotypes able to better succeed across variable conditions (Arnholdt-Schmitt et al., 2006; Clifton et al., 2006; Cardoso and Arnholdt-Schmitt, 2013) and have been also related to plant developmental processes (Campos et al., 2009, 2016; Santos Macedo et al., 2009).

AOX is a mitochondrial membrane protein acting as a terminal oxidase in the alternative (cyanide-resistant) respiratory pathway, where it reduces oxygen to water (Umbach et al., 2002). AOX allows continued turnover of carbon skeletons through glycolysis and the tricarboxylic acid (TCA) cycle when the cytochrome pathway is saturated, functioning as an overflow enzyme in the electron transport chain (ETC). However, even when the cytochrome pathway is not saturated, AOX may be activated in order to maintain balanced oxidation/reduction

reactions and a balanced carbon metabolism (Rhoads et al., 1998 and references therein). AOX controls the formation of mitochondrial reactive oxygen species (ROS) and prevents specific components of the respiratory chain from over-reduction, thereby relieving oxygen species (OS) originated from environmental stresses (Popov et al., 1997; Amirsadeghi et al., 2007). Many reports show the involvement of AOX in plant response upon a diversity of biotic and abiotic stresses establishing the link between AOX and its role on the control of cellular ROS levels (see review Vanlerberghe, 2013). Other antioxidative enzymes are also implicated in the control of cellular ROS levels. Catalase (CAT), the major H_2O_2 -scavenging enzyme in all aerobic organisms (Mhamdi et al., 2010), performs the rapid removal of H_2O_2 from the cell by oxidation of H_2O_2 to H_2O and O_2 (Møller et al., 2007). Nevertheless, ROS are not only involved in plant response upon stress conditions, they have also an active play in normal physiological processes such as in seed germination and in dormancy alleviation (Kwak et al., 2006; Bailly et al., 2008; Oracz et al., 2009). The ability of seeds to germinate might be related to their capacity to regulate ROS levels produced during mitochondrial oxygen consumption, and to neutralize the pro-oxidant activities of allelochemicals present in the medium (Pergo and Ishii-Iwamoto, 2011). It is expected that AOX, like other antioxidative enzymes, would be involved in the process of seed germination and seedling development by the control of ROS produced during the germination process, and besides also in the promotion of cellular homeostasis under the large metabolic changes that take place during germination and post-germination development. The process of seed germination starts when dry seeds get in touch with water under favorable conditions (imbibition), and it ends when radicle penetrates seed covering layers and is observable, followed by seedling establishment (Weitbrecht et al., 2011).

The step forward corresponds to seedling development (growth and differentiation). AOX has been implicated in the regulation of the mechanism of cell-reprogramming by improving metabolic transitions associated to the flexible carbon balance (Arnholdt-Schmitt et al., 2006; Rasmusson et al., 2009). Several authors have shown that regulation of soybean AOX genes depend on the post-germinative development of soybean cotyledons (Finnegan et al., 1997; McCabe et al., 1998). In some plants, cyanide-insensitive respiration is required for germination (reviewed by Botha et al., 1992). For example, in cocklebur, the alternative pathway was activated after imbibition of seeds (Esashi et al., 1981; Saisho et al., 2001).

Considering this previous knowledge, this study aimed to isolate and characterize the *H. perforatum* AOX gene family to then be able to explore, by *in silico* analysis, the existence of regulatory elements located at intronic regions. Also, to investigate at the mRNA level the expression of the AOX gene family members during the post-germinative development along with two other proteins known to be involved, in other plant species, in different pathways: CAT1 involved in the control of ROS levels and chloroplast glyceraldehyde-3-phosphate dehydrogenase A subunit (GAPA) involved in the photosynthetic carbon assimilation.

MATERIALS AND METHODS

HpAOX Gene Member's Identification and Isolation

Isolation of Complete *HpAOX* Genes

Complete *AOX* gene isolation was performed in several steps. First, partial gene isolation was performed using degenerated P1 and P2 primers following the protocol previously described by Saisho et al. (1997). Genomic DNA (gDNA) used as template in the PCR was extracted from 1 month old seedlings (bulked of eight seedlings previously established under *in vitro* conditions) using the DNeasy Plant Mini Kit (Qiagen, Hilden, Germany) according to the manufacturer's protocol. PCR was conducted with the Ready-To-Go PCR Beads (GE Healthcare, Little Chalfont, England) using 10 ng of gDNA and 0.2 μ M of each primer. PCR was carried out for 35 cycles in the 2770 thermocycler (Applied Biosystems, Foster City, CA, USA).

In a second step, the 5' and 3' ends of the isolated *HpAOX* gene fragments were determined by 5' and 3' RACE-PCRs. For this, total RNA was extracted, from the same material used for gDNA extraction, using the RNeasy Plant Mini Kit (Qiagen, Hilden, Germany) with on-column digestion of DNA applying the RNase-Free DNase Set (Qiagen, Hilden, Germany), according to manufacturer's protocol.

For 3' end isolation, a cDNA single strand was produced by RevertAidTM HMinus First Strand cDNA Synthesis kit (Fermentas, Ontario, Canada) according to manufacturer's instructions with oligo d(T) primer (Roche, Mannheim, Germany) and 5 μ g of total RNA. 3'RACE-PCR was conducted using 1 μ l of cDNA single strand as template with the reverse primer VIAL 9 (Roche, Mannheim, Germany) and a gene-specific forward primer (see sequence on Table S1).

For 5' end isolation, 1 μ g of total RNA was used to synthesize the first-strand cDNA using the SMARTerTM RACE cDNA Amplification kit (Clontech Laboratories, Inc., Mountain View, CA, USA) according to manufacturer's instructions. 5'RACE-PCR was carried out using 0.2 μ M of the reverse gene specific primer (Table S1) following protocol provided with the kit.

Finally, for the complete gene isolation, gDNA and total RNA were isolated from a single *in vitro* growing plantlet following the procedures described above. One gene-specific primer set was designed for each *HpAOX* gene (see Table S1) based on the previously isolated 5' and 3'-UTR sequences. Ten nanograms of gDNA or 1 μ l of oligo d(T) first strand cDNA were used as template with 0.2 μ M of each specific primer. PCRs were performed using PhusionTM High-Fidelity DNA Polymerase (Finnzymes, Espoo, Finland) according to the manufacturer's protocol (see annealing temperatures at Table S1).

Cloning and Sequence Analysis

PCR fragments were separately cloned into a pGem[®]-T Easy vector (Promega, Madison, USA) and used to transform *E. coli* JM109 (Promega Madison, WI, USA) competent cells. Plasmid DNA was further extracted from putative recombinant clones by alkaline lysis protocol (Bimboim and Doly, 1979) and sense and antisense strands were sequenced (Macrogen company:

www.macrogen.com) using primers T7 and SP6 (Promega, Madison, USA).

Sequence homology was searched in the NCBI databases (National Center for Biotechnology Information, Bethesda, MD) using BLAST algorithm (Karlin and Altschul, 1993; <http://www.ncbi.nlm.nih.gov/>; BLASTn and BLASTp).

CLC Main Workbench 7.5.1 software (CLCbio, Aarhus N, Denmark) was used to edit *HpAOX* sequences (cDNA, gDNA and putative translated peptide). Intron location was made using the software Spidey (<http://www.ncbi.nlm.nih.gov/IEB/Research/Ostell/Spidey/>). Gene draw was performed in FancyGene 1.4 (Rambaldi and Ciccarelli, 2009), freely available at <http://bio.ieo.eu/fancygene/>.

Sequences were aligned in MUSCLE (<http://www.ebi.ac.uk/Tools/msa/muscle/>) following the standard parameters. Phylogenetic reconstruction was performed in MEGA software (Tamura et al., 2007) by Neighbor-Joining (NJ) and the inferred tree was tested by bootstrap analysis using 1000 replicates. Graphical view was edited in the Fig Tree v14.0 software (<http://tree.bio.ed.ac.uk/software/figtree/>). The free available TargetP software (Emanuelsson et al., 2000) was used to predict the protein subcellular localization and the position of the cleavage sites of mitochondrial targeting signals (<http://www.cbs.dtu.dk/services/TargetP/>).

In silico Identification of Regulatory Elements Located at the *HpAOX* Intronic Regions

For the identification of putative miRNA precursor sequences located at the *HpAOX* introns, the publicly available software miR-abela (http://www.mirz.unibas.ch/cgi/pred_miRNA_genes.cgi) was used. MiPred software was used (<http://server.malab.cn/MiPred/>; Jiang et al., 2007) to validate potential pre-miRNAs and the web-based software Mfold, (available at <http://mfold.rit.albany.edu/?q=mfold/RNA-Folding-Form>; Zuker, 2003) applied in the prediction of the secondary structure of pre-miRNA. To screen potential miRNAs candidates, the previous validated pre-miRNA sequences were analyzed with the software miRBase (<http://www.mirbase.org/search.shtml>). BLASTx from NCBI database (<http://www.ncbi.nlm.nih.gov/BLAST/>) was used to find the potential target genes (Mathews et al., 1999; Zuker, 2003).

For identification of transposable elements (TE) putatively located at the intronic regions of *HpAOX*, the CENSOR software tool from the Genetic Information Research Institute—GIRI (<http://www.girinst.org/censor/index.php>) was used (Kohany et al., 2006). For identification of simple sequence repeats (SSRs) the RepeatMasker platform was used (<http://www.repeatmasker.org/>; Smit et al., 2013–2015).

HpAOX Transcript Quantification

Plant Material and Experimental Conditions

In order to evaluate the role of *AOX* genes in *H. perforatum* post-germinative development an experiment was conducted. Seeds were collected from the achenes of a mother plant growing in the field (Viana do Alentejo, Portugal, 38°21'37"N, 7°59'13"W).

No specific licenses were needed for achene harvesting since *H. perforatum* is not a protected species. Seeds were inoculated *in vitro* after their disinfection (see details in Ferreira et al., 2009) and maintained during a period of 14 days under 16 h photoperiod, constant day/night temperature of 25°C, and 80 $\mu\text{mol m}^{-2}\text{s}^{-1}$ of light intensity (Philips fluorescent lamps).

Samples were collected at different time points: 4, 6, 8, 10, 12, and 14 days after sowing (Figure 1). Samples collected between 4 and 8 days consisted in a bulked sample of \sim 50 explants. Samples collected between 10 and 14 days represented a set of \sim 10 seedlings for each time point.

RNA Isolation and First-Strand cDNA Synthesis

Total RNA was extracted with the RNeasy Plant Mini Kit (Qiagen, Hilden, Germany), according to the manufacturer's instructions, and eluted in 30 μl volume of RNase-free water. Possible residual genomic DNA present in RNA samples was digested with the DNase I (RNase-Free DNase Set, Qiagen, Hilden, Germany), following the manufacturer's instructions. The RNA concentration was assessed with the NanoDrop-2000C spectrophotometer (Thermo Scientific, Wilmington, DE, USA), and the RNA integrity was checked, based on the presence of the two ribosomal subunits, by agarose gel electrophoresis in a Gene Flash Bio Imaging system (Syngene, Cambridge, UK). Maxima First Strand cDNA Synthesis Kit for RT-qPCR (Thermo Scientific, Wilmington, DE, USA) was used to synthesize complementary DNA (cDNA) from RNA samples (using 1 μg of total RNA), according to the manufacturer's instructions.

Quantitative Real-Time PCR

Real-time PCR was performed in the Applied Biosystems 7500 Real-Time PCR System (Applied Biosystems, Foster City, CA, USA). Real-time PCR reactions were carried out using 1X Maxima SYBR Green qPCR Master Mix, 300 nM of forward and reverse primers, and 1.25 ng of cDNA in a total volume of 18

μl . Primers for the 11 genes analyzed here were designed based on the *H. perforatum* sequences deposited in the NCBI with the Primer Express v3.0 (Applied Biosystems, Foster City, CA, USA), using the default parameters of the software (Table 1). All primer pairs were evaluated for their probability to form dimers and secondary structures using the proper tool of the software for the purpose. The following thermal profile was applied: 10 min at 95°C, and 40 cycles of 15 s at 95°C and 60 s at 60°C. Possible contaminations and primer dimers formation were discarded by using no-template controls (NTCs). A standard curve with four points was performed using the undiluted pool containing all cDNA samples and three 5-fold serial dilutions. All samples were run in duplicate. A melting curve analysis was performed to guarantee amplification of specific products. The values of quantification cycles (C_q) were obtained for each sample with the Applied Biosystems 7500 software (Applied Biosystems, Foster City, CA, USA).

Determination of Reference Gene Expression Stability Using GeNorm Algorithm

GeNorm algorithm was used to determine the expression stability of each candidate reference gene (RG). The input data for GeNorm algorithm were the relative quantities (RQ) calculated with the C_q value for each sample by the delta-Ct method using the formula $RQ = E^{\Delta C_q}$, where E is the amplification efficiency calculated for each primer pair and $\Delta C_q = \text{lowest } C_q - \text{sample } C_q$ (Vandesompele et al., 2002). Amplification efficiency (E) was calculated using the formula $E = 10^{(-1/\text{slope})}$ where the slope value was given by the Applied Biosystems (AB) software. GeNorm determines the pairwise variation (V ; Vandesompele et al., 2002) and in the present study V values were determined for the candidate RGs using a cut-off value of 0.15, below which the inclusion of an additional RG is not required for normalization. In this way, GeNorm also determines the optimal number of genes required to calculate a reliable normalization factor.

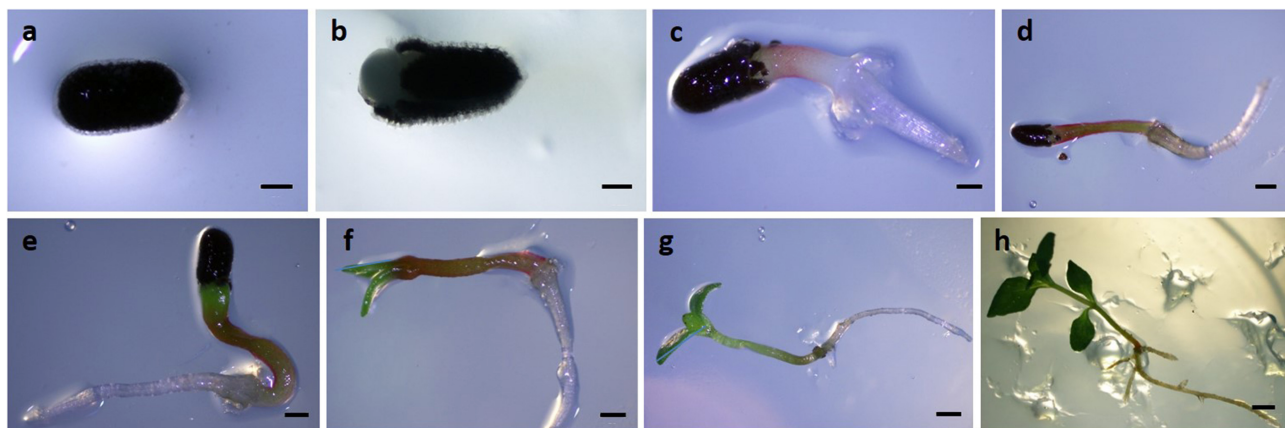


FIGURE 1 | Seed germination and post-germinative development of seedlings in *Hypericum perforatum*. (A) 0 days, **(B)** 2 days, **(C)** 4 days, **(D)** 6 days, **(E)** 8 days, **(F)** 10 days, **(G)** 12 days, **(H)** 14 days post-sowing. Bars: **(A–C)** = 0, 5 mm; **(D–G)** = 1 mm; **(H)** = 5 mm.

TABLE 1 | Primer sequences and other parameters for the genes used in this study.

Gene (acc. no.)	Primer Sequence (5'-3')	AL (bp)	Tm (°C)	r ² /E (%)
H _p 18SrRNA (AF206934)	Fw: CGTCCCTGCCCTTGTACAC	72	80.23	0.999/94.50
	Rv: CGAACACTTCACCGGACCAT			
H _p 26SrRNA (DQ110887)	Fw: GCGTTCGAATTGAGTCTGAAGAA	65	80.79	0.999/90.65
	Rv: CGGCACCCCCCTTCAA			
H _p GAPA (EU301783)	Fw: GGTGCACTTCAGGTGCAGTGA	76	81.04	0.999/83.88
	Rv: CACCATGTCGTCCTCCATCA			
H _p GSA (KJ624985)	Fw: GCAATAATCCTTGAACCTGTTGTG	78	78.35	0.992/94.30
	Rv: CCTGCGGAGAGCGTTGA			
H _p HYP1 (JF774163)	Fw: GGAGGAAGCAAGGGTAAGATTACA	81	77.18	0.997/93.97
	Rv: CCCGATCTTGAECTTCTTCTTATT			
H _p H2A (EU034009)	Fw: CCGGTTGGGAGGGTTCA	63	79.64	0.995/95.01
	Rv: TGCACCGACCCTTCCATT			
H _p RBCL (HM850066)	Fw: CGCGGTGGGCTTGATT	71	76.86	0.999/98.95
	Rv: CGATCCCTCCATCGCATAAA			
H _p TUB (KJ669725)	Fw: GGAGTACCCCTGACAGAAATGATGCT	80	77.89	0.990/93.48
	Rv: TTGTACGGCTCAACAAACAGTATCC			
H _p AOX1 (EU330415)	Fw: TTGGACAATGGCAACATCGA	69	80.11	0.995/90.46
	Rv: GGGAGGTAGGCGCCAGTAGT			
H _p AOX2 (EU330413)	Fw: TCAACGCCTACTTGTATCTATCTC	80	78.47	0.998/95.03
	Rv: AATGGCCTCTCTTCCAAATAGC			
H _p CAT1 (AY173073)	Fw: CGCTTCTCAACAGATGGATTAG	71	79.10	0.996/96.45
	Rv: ACCCAGATGGCTCTGATTCA			

acc. no., NCBI accession number; AL, amplicon length; Tm, melting temperature for each amplicon; r², correlation coefficient; E, PCR efficiency.

Analysis of Transcript Expression

For expression levels normalization of the genes under study, C_q values were converted into RQ by the delta-Ct method, as described in previous section. The normalization factor was determined by the GeNorm algorithm and corresponds to the geometric mean between the relative quantities of the selected RGs, for each sample. For each gene of interest, the normalized value of gene expression is obtained by doing the ratio between the relative quantities and the corresponding normalization factor, for each sample. Graphics indicate the mean ± standard deviation of three biological replicates. The control group (4 dps) was set to 1 and the bars corresponding to the other time points show the fold-change with respect to 4 dps. The t-test method [IBM® SPSS® Statistics version 22.0 (SPSS Inc., USA)] was used to ascertain statistical significances ($p \leq 0.05$ and $p \leq 0.01$ between means).

RESULTS

Characterization of the Full-Length Sequences of H_pAOX Gene Family

The use of P1/P2 primers allowed the isolation of amplicons with 444 bp length showing high homology with AOX genes from other plant species, which was expected considering the previous identification of AOX genes using this degenerated primer pair not only in *Arabidopsis thaliana* (Saisho et al., 1997) but also in several other plant species (Campos et al., 2009; Costa et al., 2009; Frederico et al., 2009; Santos Macedo et al., 2009) where it

is included *H. perforatum* with three AOX1 gene members and a single AOX2 (Ferreira et al., 2009). However, the use of amplicon-specific primers located at 5' and 3' ends allowed the isolation of the full-length cDNA sequences from only two *HpAOX* genes. After several attempts it was possible to confirm the existence of only two AOX gene members in *H. perforatum*, one belonging to the AOX1-subfamily and another to the AOX2-subfamily.

Gene size variability was identified at cDNA level in both genes. 5' end showed variability among sequences of the same gene. In the case of *HpAOX1*, the length of 5' end ranged between 26 and 116 bp (Figure S1), and in *HpAOX2* it ranged between 56 and 111 bp (Figure S2). Sequence size variability was also detected at 3' end of the *HpAOX1* ranging between 159 and 227 bp (Figure S3). The larger sequences are presented in Figures S4, S5.

The AOX1 gene at cDNA level isolated from *H. perforatum* (deposited at the NCBI with the acc. EU330415.2) has 1415 bp (Figure S4) and presents an open reading frame (ORF) of 1056 bp, which encodes a putative polypeptide with 351 amino acid residues. The AOX2-subfamily member, *HpAOX2* (acc. EU330413.2), presents 1311 bp and an ORF of 1017 bp encoding a putative polypeptide with 338 amino acid residues (Figure S5). The first ATG codon found in the beginning of the resultant ORF of *HpAOX1* represents the correct initiation of translation. In the *HpAOX2* two putative start codons were detected, one generating a larger peptide (with more 18 amino acid residues, see Figure S2). However, no similarity with other plant species was observed on that region which lead us to select a sequence encoding the shorter sequence. Figures S4, S5 indicate the cDNA sequences

for both genes including the putative translated peptide and the conserved sites for intron positions. The difference in the overall length for the complete ORF sequences is mostly due to the size variability at exon 1 in the N-terminal region. Exon 1 has a size of 378 bp for *HpAOX1* and 339 bp for *HpAOX2*.

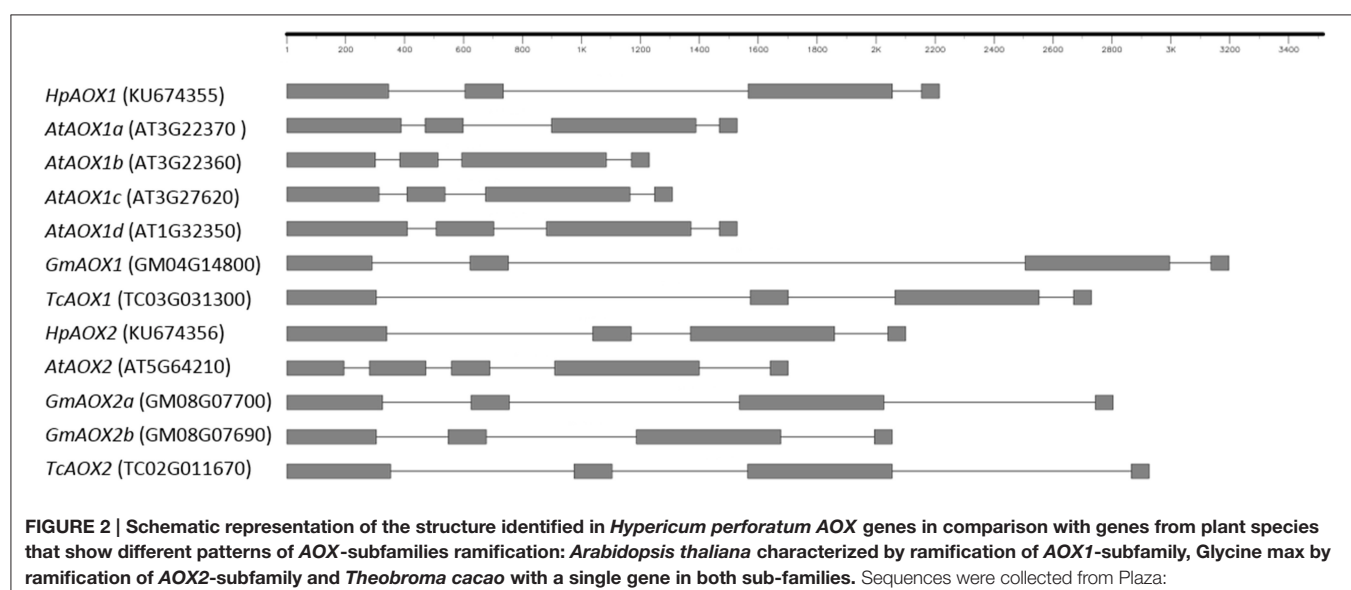
Forward and reverse primers located at 5' and 3' gene ends, respectively, were used at genomic level and allowed the isolation of *HpAOX1* gene with 2825 bp and *HpAOX2* with 2213 bp. Gene structure, common to both *HpAOX* genes, is composed by four exons interrupted by three introns (Figure 2). The conservation of exons size is here confirmed for the three last exons (exon 2: 129, exon 3: 489, and exon 4: 57 bp). Contrarily to this conservation at the exons, high level of variability in intronic regions was observed. Intron 1, intron 2, and intron 3 of *HpAOX1* are 261, 831, and 99 bp long, respectively, while in *HpAOX2* they are 699, 202, and 181 bp long, respectively. This variability was observed within a gene and across gene members from the AOX subfamily/family at species level and across species (Figure 2).

The homologous identity score obtained with the deduced amino acid residue sequence revealed that both *HpAOX1* and *HpAOX2* share a great similarity with other AOX proteins, like AOX1a from *Arabidopsis thaliana* (acc. NP_188876.1, 70%) and AOX2 from *Vitis vinifera* (acc. NP_001268001.1, 71%), respectively. To determine the relationship between both *HpAOX* genes and AOX from other eudicot plant species a NJ tree was constructed using the 153 translated AOX sequences from both eudicot and monocot plant species (Figure 3). A clear separation between both AOX-subfamilies could be seen forming the two main clusters (in blue the AOX1-subfamily and in green the AOX2-subfamily). Each *HpAOX* member was grouped in each AOX-subfamily. Monocot AOX1 members form a separated group within the cluster of the AOX1-subfamily. Gene members from species that belong to the same family also group in separated clusters within each subfamily. A synteny plot to the AOX gene family (HOM03D001776) across whole genomes

available at PLAZA 3.0 and Phytozome v11.0 showed that AOX genes occur mainly as a single copy gene in sense or reverse orientation. Some cases of tandem duplication events are also reported. In the NJ tree it is possible to see that translated peptides corresponding to those duplicated events are not always grouped together (examples are highlighted in blue). Sequences of *Salix purpurea* are tandem repeats in which two sequences group together (SapurV1A.1470s0080.1 and SapurV1A.0346s0170.1) and another not (SapurV1A.0377s0140.1.p and SapurV1A.0377s0150.1.p). A second example are the sequences of *A. thaliana* (AT3G22360.1 and AT3G22370.1) which share more similarity with sequences of other plant species.

A multiple sequence alignment, constructed using complete AOX sequences from plant species including both *HpAOX* deduced sequences (*HpAOX1* and *HpAOX2*), allowed us to highlight similarities and differences in the protein sequences (Figure S6). The predicted cleavage site length of the mitochondrial transit peptide (mTP) from the start of the protein is highlighted in blue boxes for all sequences included in the alignment. A great variation on the predicted length of this region can be seen, going from 8 amino acids in AtAOX1b (acc. AT3G22360) to 72 amino acids in AtAOX2 (acc. AT5G64210). Both *HpAOX* proteins were predicted to be located in the mitochondria (mit score of 76% for *HpAOX1* and 87% for *HpAOX2*).

Helices $\alpha 1$ and $\alpha 4$ (in red in Figure S6) that make part of the hydrophobic region of the AOX molecular surface demonstrated high degree of variability when compared with helices $\alpha 2$, $\alpha 3$, $\alpha 5$, and $\alpha 6$ (in green in Figure S6) which form the four-helix bundle. The helix $\alpha 4$ is slightly more conserved than $\alpha 1$. In fact, low level of similarity can be seen at the N-terminal region, not only related with differences in size (shown by the presence of minus signs) due to exon 1 variability reported above, but also due to different amino acid composition (shown by the presence



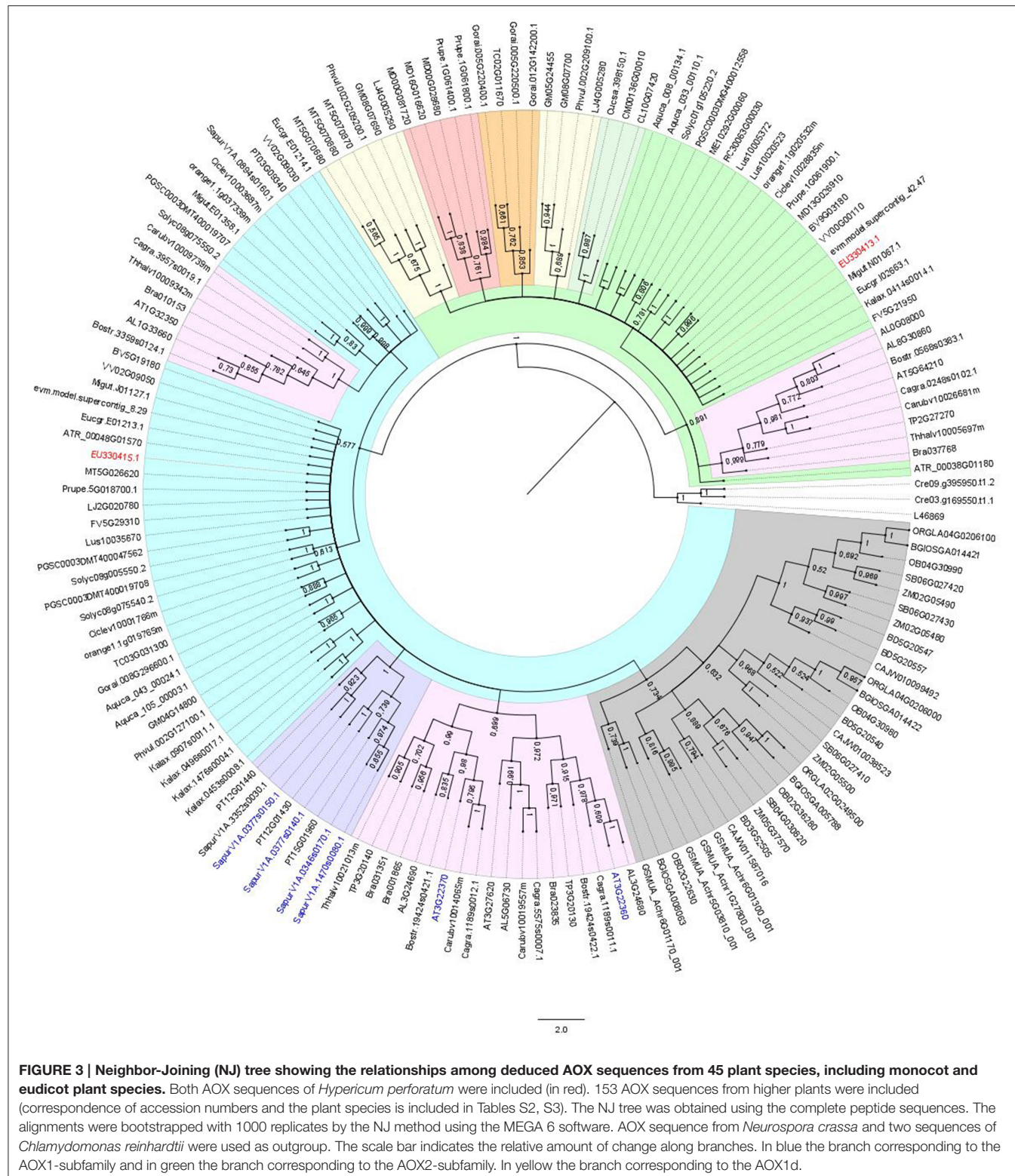


FIGURE 3 | Neighbor-Joining (NJ) tree showing the relationships among deduced AOX sequences from 45 plant species, including monocot and eudicot plant species. Both AOX sequences of *Hypericum perforatum* were included (in red). 153 AOX sequences from higher plants were included (correspondence of accession numbers and the plant species is included in Tables S2, S3). The NJ tree was obtained using the complete peptide sequences. The alignments were bootstrapped with 1000 replicates by the NJ method using the MEGA 6 software. AOX sequence from *Neurospora crassa* and two sequences of *Chlamydomonas reinhardtii* were used as outgroup. The scale bar indicates the relative amount of change along branches. In blue the branch corresponding to the AOX1-subfamily and in green the branch corresponding to the AOX2-subfamily. In yellow the branch corresponding to the AOX1d.

of amino acids colored in red). Increase in the similarity, at both levels (sequence composition and size conservation), starts near the conserved regulatory cysteine residue I (CysI). All main features that characterize AOX proteins are equally conserved

at both *H_p*AOX peptide sequences. There are examples, the four universally conserved glutamate residues (E) and the two universally conserved histidine (H) residues, and the amino acid residues that interact with the protein inhibitor located

at helix $\alpha 5$. *In silico* analysis searching for regulatory elements lead us to the identification of simple sequence repeats (SSR) in intronic regions of *HpAOX1*: a 59 bp long TTTAT motif in intron 1 and a 32 bp long AT motif in intron 2, and of *HpAOX2*: a 44 bp long CGGAGG motif located at exon 1 (location of SSRs are presented in Figures S7, S8 of Supplementary material). CENSOR software detected a region of 119 bp in the *HpAOX2* sequence with similarity to the LTR region of a *Cassandra* MT-LTR retrotransposon from *Medicago truncatula*. RepeatMasker software also found a positive match of this fragment with a *Cassandra* LTR from *Zea mays*. A blast search in the NCBI databases using that previous identified sequence revealed a 72% homology to a *Pisum sativum* *Cassandra*-like LTR.

Additionally, a search for putative miRNA precursor sequences (pre-miRNAs) identified one putative pre-miRNA located at intron 1 and two pre-miRNAs at intron 2 of *HpAOX1* (**Table 2**). Potential candidates for miRNAs were identified with homology with miRNAs previously described in other plant species. The pre-miRNA at intron 1 revealed homology with the gma-miR5780c; the pre-miRNAs at intron 2 revealed

homology with vvi-miR3637-5p and gra-miR7484n. These homologous miRNAs seem to be encoded by pre-miRNA sequences located also at intronic regions (see Figure S9). No target genes were identified for any of the predicted miRNAs.

Selection of Reference Genes

The analysis of expression stability was performed with the following candidate reference genes: glyceraldehyde-3-phosphate dehydrogenase A subunit (*GAPA*), 18S (18SrRNA) and 26S (26SrRNA) ribosomal RNAs, beta-tubulin (*TUB*), ribulose-1,5-bisphosphate carboxylase/oxygenase large subunit (*RBCL*), glutamate-1-semialdehyde 2,1-aminomutase (*GSA*), chama phenolic oxidative coupling protein (*HYP1*), and histone 2A (*H2A*). This analysis was performed to select the most suitable ones to be used to normalize the expression levels of target genes. GeNorm algorithm selected *HpHYP1* and *HpH2A* ($M = 0.347$) simultaneously as the most stable genes (Figure S10A) with no need to include a third RG for normalization (Figure S10B). *HYP1* is involved in plant defense and *H2A* participates in nucleosome assembly.

TABLE 2 | Computational prediction of intronic miRNA precursors in AOX genes of *Hypericum perforatum* determined at miR-abela software (http://www.mirz.unibas.ch/cgi/pred_miRNA_genes.cgi) using as prediction threshold-10.

Intron	Score	Putative pre-miRNA sequence and structure	bp	MFE	Candidates of potential miRNAs
1	-2.48	p-value: 0.022 UUUAUAAAUAUUGAUAAUGAUUUAGAUGGUUCUAAUAAUAGGGAA 10 20 30 40 A UG G A GUUCUA G UUU UUUAUAAA U AAU AUUU GAU AUUAUUA GGAA \ AGUGUAAA G UAUG AAAA UUA UAUGUAGU UUUU U ^ - GU - A AUUUA- G UGU 90 80 70 60 50	94	-16.60	Coordinates (v1.0): chr14: 33572228-33572414 [-] >gma-miR5780c: UUUAAUAUAUCAGGGACUUGGA score: 68 e-value: 1.9 UserSeq 29 ucuaauauauuagggaauu 47 gma-miR5780c 1 uuuaauauaucaggcacuu 19
2	-1.51	p-value: 0.003 UUUACUUAGAUGAGAACUGGUUUUUGGUUGGUUUUACACAA ACUCUAUGGACUAAAAGACUCCAUUAGAGUAUGA 10 20 30 - A - --- U- UU UUUACUU AGAUG GAA UCU GGUUUAU GUUUGUG U AGUAUGAG UUUAC CUU AGA UCAGGUA CAAACAC U A - C AAAU UCU^ UA 80 70 60 50 40	83	-24.80	Coordinates (Genoscope-20100122): chr16: 20659651-20659852 [-] >vvi-miR3637-5p: AUUUAAUGUAUUGUGUUUUGUCGGA score: 64 e-value: 5.4 UserSeq 23 uuuauuguuuuguguuuuauc 42 vvi-miR3637-5p 2 uuuaugauuuguguuuuguc 21
2	-1.47	p-value: 0.001 GUAUGAGAUUUACCUUCAGAAAAAUUCAGGUACUCAACACAUUUUGUG UUUGGUUAAAUGGUUCUAGAGUAGAUUCAAU 10 20 30 40 A - C AAAU UCU UA GUAUGAG UUUAC CUU AGA UCAGGUA CAAACAC U UUAUCUU AGAUG GAA UCU GGUUUAU GUUUGUG U ^ - A - --- U-- UU 80 70 60 50	81	-23.70	Coordinates (Graimondi2_0): chr6: 49675651-49675852 [+] >gra-miR7484n: CUAGUUUGCUCUUUGAUCAUAAUGU score: 63 e-value: 6.3 UserSeq 50 guuuguuauuuggucuua 67 gra-miR7484n 4 guuugcucuuuugaucua 21

Score, given at miR-abela software to the identified pre-miRNA sequence; bp, length of the pre-miRNA sequence in bp; MFE, minimal free energy in kcal/mol. Prediction confidence to be a pseudo microRNA precursor was calculated at MiPred software (shuffle times: 1000) as 100% (<http://server.malab.cn/MiPred/>; Jiang et al., 2007). For screening the candidates of potential miRNAs the validated pre-miRNA were run in the software miRBase (<http://www.mirbase.org/search.shtml>).

The amplification specificity for each gene was confirmed by the melting curve analysis, observing amplification of the expected specific product and no formation of primer dimers (Figure S11). The slope and correlation coefficient (r^2) values were given by the AB software. The r^2 ranged from 0.990 to 0.999 and the slope values ranged between -3.780 (PCR efficiency = 83.9%) for *HpGAPA* and -3.347 (PCR efficiency = 98.9%) for *HpRBCL* (Table 1). The PCR efficiency for *HpGAPA* revealed to be low, nevertheless, and due to the fact the corresponding r^2 was high (0.999), the gene was not discarded from the analysis. The PCR efficiency value for *HpGAPA* was taken into account in the formula for the RQ calculation.

Analysis of Transcript Expression

The transcript expression profiles of *HpAOX1*, *HpAOX2*, *HpCAT1*, and also *HpGAPA* were analyzed in the present work. The amplification specificity of the genes was verified by the melting curve analysis (Figure S11). The geometric mean of the 2 top-ranked RGs (*HpHYP1* and *HpH2A*), given by the GeNorm algorithm, was used in gene expression data normalization, as described above in the “Selection of reference genes” section.

The mRNA of *HpAOX1* was maintained constant from day 4 after seed *in vitro* sowing (dps, days post-sowing) up to day 8, nevertheless, after this time point, an accumulation of the transcript was observed up to 14 dps with an increase of approximately 10-fold ($p \leq 0.05$; Figure 4A). The mRNA expression of *HpAOX2* did not differ statistically over time in the post-germination process, even if a slight tendency to decrease (1.8-fold-change) from day 4 to 6 after seeds sowing was observed. This expression was maintained up to day 10 post-sowing and a subsequent complete recovery was observed up to day 14, demonstrating high stability of this gene during the developmental process (Figure 4B). The expression of *HpCAT1* transcript showed a gradual down-regulation over the 12 dps of about 3.8-fold ($p \leq 0.05$) which was maintained up to 14 dps (Figure 4C). The *HpGAPA* transcript increased drastically about 64-fold ($p \leq 0.01$) from day 4 up to day 12, maintaining the expression at elevated levels up to day 14 (Figure 4D).

DISCUSSION

HpAOX Genes Sequence Analysis

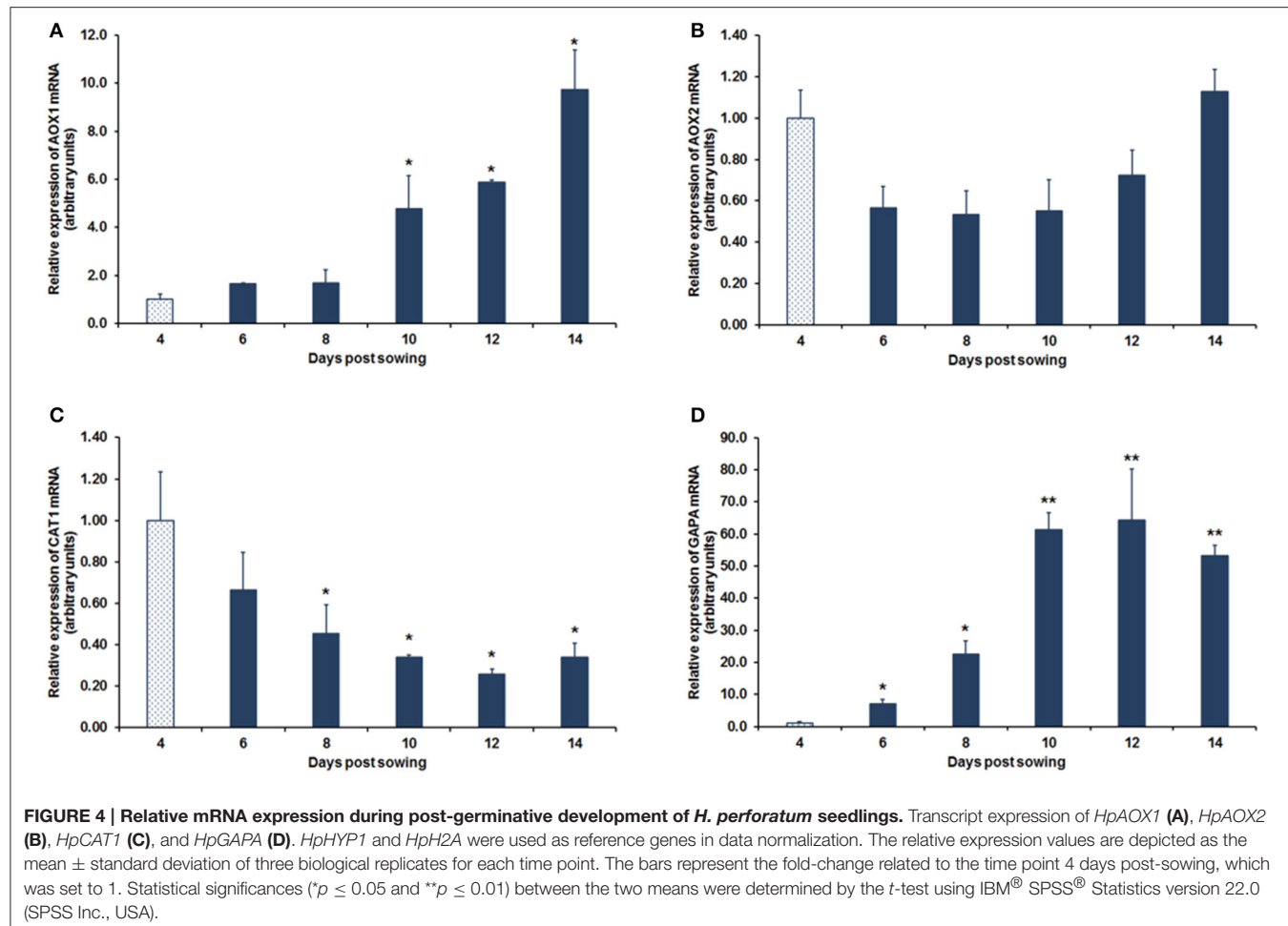
Mitochondrial AOX proteins are encoded by a small nuclear gene family, with a maximum of six gene members (Cardoso et al., 2015) distributed in 2 subfamilies, AOX1 and AOX2 (Considine et al., 2002; Borecky et al., 2006). In higher plants AOX1 is found in all studied monocot and eudicot plant species while AOX2 is only present in eudicots (Considine et al., 2002). The number of AOX gene members and its pattern of expansion is highly variable across eudicot plant species (Cardoso et al., 2015). At genome level, AOX genes appear usually as single copy genes. Nevertheless, 17 cases of duplication events can also be seen in different plant species. The majority of these duplicated copies are adjacent to the original (tandem repeats,

e.g., SapurV1A.0377s0140.1.p and SapurV1A. 0377s0150.1.p). Three exceptions appear with the duplicated sequence located somewhere along the chromosome (e.g., SapurV1A.1470s0080.1 and SapurV1A.0346s0170.1). Tandem duplication events have been described as one of the major mechanisms that creates new genes, particularly in cases where genes are clustered into a gene family (Fan et al., 2008). In *H. perforatum* it was identified the complete sequence of two AOX genes, one belonging to the AOX1-subfamily and the other to the AOX2-subfamily. Considering the efforts made to isolate the complete sequence of all the previous reported *HpAOX* genes (Ferreira et al., 2009) it is here hypothesized that the AOX gene family in *H. perforatum* is composed by only two gene members.

Alternative oxidase is a diiron carboxylate protein composed by two monomers (dimeric protein). Each monomer is composed by six long helices ($\alpha 1$ to $\alpha 6$) and four short helices ($\alpha S1$ to $\alpha S4$) arranged in an antiparallel fashion. Helices $\alpha 2$, $\alpha 3$, $\alpha 5$, and $\alpha 6$ forming a four-helix bundle (Moore et al., 2013) accommodate the active site composed by the diiron center, four universally conserved glutamate residues, and two universally conserved histidine residues. The alignment made across deduced AOX sequences, including both *HpAOX* sequences, shows not only the high conservation on the regions of the long helices, but also the complete conservation of the four glutamate (Glu-201, Glu-240, Glu-291, and Glu-342) and the two histidine (His-243 and His-345) residues.

Nevertheless, an exception can be seen at the *HpAOX2* sequence where the Ile-230 is substituted by a Val. This position corresponds to the Ile-207 in *Sauromatum guttatum* and to the Ile-152 in *Trypanosoma brucei* previously investigated by mutagenesis approach (see review at Moore et al., 2013). In an attempt to elucidate about the occurrence of this change, an alignment was constructed including high number of AOX sequences available at different Gene Banks (not shown). This allowed the identification of the same amino acid change in a sequence of *V. vinifera* (acc. VV00G00110). Nevertheless, no data are available about the effect of this mutation on the inhibition of respiration.

Besides the effect that those changes at gene sequence level could have on protein functionality (see review at Moore et al. (2013)), post-transcriptional events have also a role on AOX regulation. In plants, AOX is controlled at post-transcriptional level by two interrelated mechanisms, being one of them dependent of α -keto acid regulation in which two cysteine residues are involved, CysI-145 and CysII-195 (Umbach et al., 2002), both conserved in *HpAOX* sequences. Nevertheless, some plant AOX lack the conserved CysI, having a SerI residue instead (Umbach and Siedow, 1993; Costa et al., 2009) which change the regulation from pyruvate to succinate (Holtzapffel et al., 2003; Grant et al., 2009). Recently, Moore et al. (2013) suggested that AOX regulation might also occur via phosphorylation of the N-terminal extension through charge-induced conformational changes and/or an interaction with other mitochondrial proteins. AOX N-terminal region is known as the less conserved region at size and sequence level, with the exception of the CysI, and has been considered independently from the structural defined



four-helix bundle (Moore et al., 2013). The distance between CysI and CysII is 50 amino acids, as previously reported by Moore et al. (2013), but the distance between the predicted N-terminal sequence and CysI varies. This variation can be explained by the variability at genomic level observed at the level of exon 1 since the other exons show a conservation in size across genes with the four exons structure (exon 2: 129, exon 3: 489, exon 4: 57). The prediction of the mitochondrial signal peptide located at N-terminal region revealed no conservation at sequence and size level, going from very short mTP (AtAOX1b, acc. AT3G22360) to much longer (AtAOX2, acc. AT5G64210) although from the same plant species. This region determines the interaction of the peptide with the protein transport system to the organelle, and in many cases, amino acids comprising the signal peptide are cleaved off the protein once they reach their final destination. Finnegan et al. (1997) referred that proteins requiring N-terminal signals for mitochondrial import typically present a lack in overall sequence conservation at the N terminus. Huang et al. (2009) also reported a high variability in this region in a comparison between *Arabidopsis* and rice using a high set of proteins, describing that this region varied greatly from 19 to 109 amino acids in *Arabidopsis*, and from 18 to 117 amino acids in rice. Specifically related with AOX, Campos

et al. (2009, 2016) described length variability at the mTP across plant species and also between carrot protein isoforms. More recently, Nogales et al. (2016) reported the presence of single nucleotide polymorphisms (SNPs) within the mTP sequence in *AOX1* sequences across carrot genotypes.

The effect of those differences in the N-terminal region for the regulation of gene expression, protein transport or activity is still unknown. Concerning the effect of the mTP sequence composition, structural studies revealed the importance of hydrophobic residues for mTP binding (Huang et al., 2009), and several studies on yeast, mammals, and plants revealed also that positively charged residues in mTP have a relevant role in protein import into mitochondria (Lister et al., 2005; Neupert and Herrmann, 2007). In plants, AOX are encoded by genes commonly composed by four exons interrupted by three size variable introns. Both *HpAOX* genes present the four exons structure, with the three last exons showing size conservation. Nevertheless, events of intron loss and gain, responsible by the variability in gene structure and consequently in exons size variation, were previously reported in *AOX* genes. A detailed description about *AOX* gene structure variation can be found in different reports (Polidoros et al., 2009; Cardoso et al., 2015; Campos et al., 2016).

In an attempt to search for putative motifs in *HpAOX* genes that could be further used to develop molecular markers, the intronic regions were explored *in silico*. Previous reports pointed out the existence of intron length polymorphism at individual plant level in *HpAOX1*, thus, pointing to the possibility for allelic discrimination (Ferreira et al., 2009). More recently Velada et al. (2014) pointed out the response of both *HpAOX* genes upon temperature stress. These observations are highly promising for a perspective toward FM development. Sequence variability at intron level in AOX genes has been suggested as a good source for functional polymorphisms that could be useful for FM development (Cardoso et al., 2009, 2011; Santos Macedo et al., 2009; Hedayati et al., 2015). In the present study, the identification of SSRs located at intronic regions of both *HpAOX* genes makes them genes of interest for further search for variability among genotypes that could be used for FM development. Besides its abundance, SSRs are highly polymorphic compared with other genetic markers, as well as being species-specific and co-dominant. For these reasons, they have become increasingly important genetic markers ideal for detecting differences between and within species of genes of all eukaryotes (Farooq and Azam, 2002). Nevertheless, variation in the length of microsatellite motifs in protein non-coding gene sequences (i.e., promoters, UTRs, and introns) may affect the process of transcription and translation through slippage, gene silencing and pre-mRNA splicing as has been observed for many human disorders (e.g., Kim et al., 2001), and also in some plant species (Tan and Zhang, 2001; Bao et al., 2006; Wang et al., 2011). Therefore, SSR markers generated from those sequence motifs can be of great use in terms of FM selection for genomic studies and crop breeding applications (Parida et al., 2009). However, the development of SSR markers located in potentially functional genic sequences in plants has been scarce, and the unique example known is in *Eucalyptus globulus* for wood quality traits (Acuña et al., 2012). The identification of SSRs within AOX gene sequences was firstly reported by Nogales et al. (2016) with the recognition of TTCTT tandem repeats in intron 1 of carrot *AOX1* gene.

The increasing knowledge on the involvement of introns in the regulation of gene expression (Rose et al., 2008; Goebels et al., 2013; Heyn et al., 2015), particularly the encoding of important regulatory elements, makes introns of great interest for the identification of polymorphisms that can be responsible for phenotypical differences. MicroRNAs are an example of regulatory elements that can be encoded at intronic regions, playing its control by negatively regulating gene expression at post-transcriptional level. In plants, miRNAs play a critical role in almost all biological and metabolic processes, including plant development (Chen et al., 2015) and plant stress response (Bej and Basak, 2014). The identification of homologous miRNAs in distinct plant species is facilitated since many families of miRNAs are evolutionarily conserved across all principal lineages of plants (Axtell and Bartel, 2005; Zhang et al., 2006). Considering this knowledge, putative locations coding for precursors of miRNAs were identified at intronic regions of both *HpAOX* genes. In all cases, a high homology with previously described miRNAs was found.

In the same way, also transposable elements (TE), which includes intact TEs, degenerate TEs and sequence residues of mobile elements (TE remnants), can also influence the regulation of gene expression (McDonald, 1993; Brosius, 2000; Bowen and McDonald, 2001; Ganko et al., 2001; Nekrutenko and Li, 2001), which leads to a significant effect in functional genome diversity and phenotypic variations (Yadav et al., 2015). The *in silico* analysis searching for TEs allowed us to identify a 119 bp sequence in intron 1 of *HpAOX2* gene that showed similarity to the long terminal repeat region of a LTR retrotransposon (*Cassandra* MT-LTR) from *Medicago truncatula*. Whether this LTR remnant has any role in the regulation of AOX expression still needs to be elucidated, but the fact that several TEs and their evolved sequences are highly polymorphic in sequence and in genome location facilitates development of TE-based markers for various genotyping purposes.

Analysis of Transcript Expression

The germination process involves many metabolic activities including a marked development of the photosynthetic and respiratory metabolisms. Thus, it is expected that AOX, like other antioxidative enzymes, would be involved in the process of seed germination and seedling development by the control of ROS produced during the germination process, and also in the promotion of the cellular homeostasis under the large metabolic changes that take place during germination and post-germination development.

To the best of our knowledge, this is the first report on the involvement of AOX genes in the post-germinative development of seedlings in *H. perforatum*. In the present study, a high increase for *HpAOX1* transcript was observed from 8 dps on. On the contrary, *HpAOX2* showed less variation in the expression of its transcript even if a slight tendency to decrease was observed right from day 4. These results are in agreement with other studies showing, for example, a decrease in the relative abundance of *AOX2* transcripts during seedling development in soybean, whereas the transcripts of the other *AOX* genes increased (McCabe et al., 1998). Other example are the findings from Saisho et al. (2001) demonstrating that the expression of *AOX2* in *Arabidopsis* was high in dry seeds and subsequently decreased during early germination, whereas *AOX1a* was less abundant at the beginning of the process, increasing only in a later stage. Several examples illustrate, as well, the involvement of AOX on plant vegetative growth and reproductive performance. In general, *AOX1* sub-family members are reported as more responsive genes upon stress factors, whereas *AOX2* members were considered during years not being affected by stress conditions, being more involved in developmental and growth processes events (Considine et al., 2002; Chai et al., 2012). Nevertheless, further studies have showed that *AOX2* members are also involved in plastid-dependent signaling (Clifton et al., 2005) and in plant stress response (Costa et al., 2010; Campos et al., 2016).

Interestingly, the increment in *HpAOX1* mRNA levels was accompanied by also a marked increase of the chloroplast *HpGAPA* transcript, having both transcripts a similar expression pattern during the post-germinative process of seedlings.

HpGAPA was first used in our study in the expression stability analysis to select the most suitable RGs because it is commonly used as reference gene in data normalization of RT-qPCR studies, and particularly in studies involving gene expression during growth and development of seedlings, like in *Zea mays* (Sytykiewicz, 2014), *Arabidopsis thaliana* (Rigas et al., 2009), *Oryza sativa* (Ismail et al., 2009), or *Triticum* sp. (Boutrot et al., 2005). However, in our study, *HpGAPA* showed to be the most unstable gene among all tested candidate reference genes, and therefore, it seems not to be appropriate to be used as RG in the experimental conditions of the present study. Our findings are in accordance with other recent studies demonstrating also the unsuitability of this gene for data normalization purposes involving gene expression in seedlings, such as in *Sasha inchi* (Niu et al., 2015), or in *Oryza sativa* (Moraes et al., 2015). The gene product of *GAPA* is a key enzyme in the photosynthetic carbon fixation pathway (Cerff, 1982), and therefore, the marked increase of its transcript observed in our study might indicate an increment of the photosynthetic activity during the post-germinative process. In fact, green tissues started to be more apparent at that time (Figure 1). Dewdney et al. (1993) found that the expression of the *GAPA* gene is regulated by light in *Arabidopsis* seedlings. In the same line, other works showed that the increase of total photosynthetic activity was accompanied by an increase in the GAPDH activity in response to light (Shih and Goodman, 1988 and references therein).

Taken together, it could be hypothesized that the increment in *GAPA* gene expression, and possibly in the photosynthetic activity, is closely related to an increased need of the *HpAOX1* enzyme during the post-germinative process of *H. perforatum*. This would be in accordance with previous reports about the role of AOX in optimizing photosynthesis (Dinakar et al., 2016). Indeed, it has been reported that AOX has a role in optimizing photosynthesis, e.g., by maintaining a balanced carbon and energy metabolism (Watanabe et al., 2008), by keeping up the light activation of chloroplastic enzymes (Padmasree and Raghavendra, 2001), by functioning as a sink for the excess reducing equivalents generated by photosynthesis (Yoshida et al., 2006, 2007), or by regulating ROS levels (Dinakar et al., 2016). With regard to the latter, during active photosynthesis there are four major types of ROS being produced in green tissues, such as, singlet oxygen (O_2^+), superoxide (O_2^-), hydrogen peroxide (H_2O_2), and hydroxyl radicals (OH^-) (Apel and Hirt, 2004). AOX has been described as a potential means to dampen O_2^- production by the ETC (Purvis and Shewfelt, 1993) and catalase, other antioxidative enzyme also analyzed in our study, as having a role in the hydrogen peroxide scavenging (Puntarulo et al., 1988; Møller, 2001; Mittler, 2002; Dinakar et al., 2010).

Unlike *HpAOX1* and *HpGAPA*, *HpCAT1* revealed a gradual down-regulation in its transcript levels reaching the peak of down-regulation at 12 dps, which suggests an involvement of *HpCAT1* during the post-germinative process in *H. perforatum*. Several studies imply that CAT activity is necessary for seed germination and early seedling growth and its measurement may be used as a parameter to examine seed viability and germination (Ak et al., 2012 and references therein). Indeed, most of these works revealed higher levels of catalase activity related to germination, whereas our data revealed a down-regulated

expression for this gene. It should not rule out the possibility that other catalase isoforms may be present in this process, having a different behavior. However, they were not included in this study since no information about their nucleotide sequence are available in databases. Additionally, it must be noticed that in our study the germination process has already finished at the first time point considered (4 dps), since the radicle emerging from the seed coat was already observable. The subsequent steps consisted in the post-germinative process with the development of seedlings. Therefore, it would be plausible that the peak observed on *HpCAT1* expression might have occurred earlier during the first stages of *H. perforatum* seeds germination (before 4 dps), when *HpCAT1* is more required, and that the subsequent decrease on transcript accumulation that we observed might be related to the necessity of maintaining ROS at adequate levels for cellular survival. Indeed, it has been reported that excessive removal of hydrogen peroxide free radicals might reduce the inhibition of the cellular cycle, which is important for DNA repair (Santos et al., 2013). In the same line, cellular biology studies have clearly described the beneficial functions of hydrogen peroxide to the cell, beyond causing oxidative stress. One of these beneficial functions is stopping the cellular cycle during DNA repair after certain types of stress and aging (Santos et al., 2013). Accordingly to our results, Mhamdi et al. (2012) reported that a transcriptional down-regulation of *CAT* could be important to induce or sustain increased H_2O_2 availability necessary for certain environmental responses or developmental processes.

Taken together, we suggest that fluctuations in the expression between *HpAOX1* and *HpCAT1* might occur in order to control ROS levels during the germination process in *H. perforatum*.

In summary, to the best of our knowledge, this is the first study in which the characterization of the AOX gene family is reported in *H. perforatum* and the expression of their transcripts are analyzed during the post-germinative development of seedlings. Two *HpAOX* genes were identified, one belonging to the AOX1-subfamily and another to the AOX2-subfamily. Sequence variability was observed at 3' and 5' ends. At the N-terminal region, the variability was reported across AOX gene members within a species and among species. Besides, SSR, a TE remnant and putative miRNA coding sequences were detected in intronic regions of *HpAOX* genes, whose variability could be explored across genotypes to identify polymorphisms with functional significance that would allow functional marker development. Our findings, although preliminary, lead us to consider *HpAOX* members, in particular *HpAOX1*, as relevant to investigate further, also at the protein level (e.g., amount, activity and capacity), in post-germinative processes in order to explore its role in optimizing photosynthesis and in the control of ROS levels. This would help making the link between gene function and the desired phenotype related to better germination rates and consequently to develop a functional marker for it.

AUTHOR CONTRIBUTIONS

HC contributed to the conception and design of the work; to the acquisition, analysis, and interpretation of data; to the drafting and critical revision of the work; and to the final approval of the manuscript; IV contributed to the acquisition, analysis, and

interpretation of data; to the drafting and critical revision of the work, and to the final approval of the manuscript; CR contributed to the conception and design of the work; to the acquisition of data; to the drafting and revision of the work; and to the final approval of the manuscript; AN contributed to the analysis and interpretation of data; to the drafting and critical revision of the work; and to the final approval of the manuscript; AF contributed to the conception and design of the work; to the acquisition of data; to the drafting of the work and to the final approval of the manuscript; VV contributed to the acquisition of data; to the drafting of the work; and to the final approval of the manuscript; BA contributed to the interpretation of data; to the critical revision of the work; and to the final approval of the manuscript. All authors are responsible for all the work.

FUNDING

This work was funded by the European Commission (MEXC-CT-2004-006669) through providing the EU Marie Curie Chair and by the National Funds through FCT - Foundation for Science and Technology under the Project UID/AGR/00115/2013, and

under the project PTDC/AGR-GPL/099263/2008. The authors are also thankful to FCT for the support provided under the program POPH-Programa Operacional Potencial Humano to BA and HC (Ciéncia 2007 and Ciéncia 2008: C2008-UE/ICAM/06), and also to ICAAM and UEvora for the support given to HC (BPD UEvora ICAAM INCENTIVO AGR UI0115 and BI_PosDoc_UEVORA_Calorespirometria_2).

ACKNOWLEDGMENTS

The authors are very grateful to Tânia Nobre for valuable suggestions and the help on the AOX phylogenetic analysis. The authors especially thank Dariusz Grzebelus for great help in the analysis of AOX sequences to search for SSR and TE elements. The authors also thank to Virginia Sobral for technical assistance.

SUPPLEMENTARY MATERIAL

The Supplementary Material for this article can be found online at: <http://journal.frontiersin.org/article/10.3389/fpls.2016.01043>

REFERENCES

- Acuña, C. V., Villalba, P. V., García, M., Pathauer, P., Hopp, H. E., and Marcucci Poltri, S. N. (2012). Microsatellite markers in candidate genes for wood properties and its application in functional diversity assessment in eucalyptus globules. *Electron. J. Biotechnol.* 15, 1–17. doi: 10.2225/vol15-issue2-fulltext-3
- Ak, A., Yücel, E., and Ayan, S. (2012). Relationship between seed germination and catalase enzyme activity of *abies* taxa from Turkey. *J. For. Fac.* 12, 185–188. doi: 10.17475/kuofd.74547
- Amirsadeghi, S., Robson, C., and Vanlerberghe, G. C. (2007). The role of the mitochondrion in plant responses to biotic stress. *Physiol. Plant.* 129, 253–266. doi: 10.1111/j.1399-3054.2006.00775.x
- Andersen, J. R., and Lübbertedt, T. (2003). Functional markers in plants. *Trends Plant Sci.* 8, 554–560. doi: 10.1016/j.tplants.2003.09.010
- Apel, K., and Hirt, H. (2004). Reactive oxygen species: metabolism, oxidative stress, and signal transduction. *Annu. Rev. Plant Biol.* 55, 373–399. doi: 10.1146/annurev.arplant.55.031903.141701
- Arnholdt-Schmitt, B. (2005). Efficient cell reprogramming as a target for functional marker strategies? Towards new perspectives in applied plant nutrition research. *J. Plant Nutr. Soil. Sci.* 168, 617–624. doi: 10.1002/jpln.200420493
- Arnholdt-Schmitt, B., Costa, J. H., and Fernandes de Melo, D. (2006). AOX - a functional marker for efficient cell reprogramming under stress? *Trends Plant Sci.* 11, 281–287. doi: 10.1016/j.tplants.2006.05.001
- Axtell, M. J., and Bartel, D. P. (2005). Antiquity of microRNAs and their targets in land plants. *Plant Cell* 17, 1658–1673. doi: 10.1105/tpc.105.032185
- Bailly, C., El-Maarouf-Bouteau, H., and Corbineau, F. (2008). From intracellular signaling networks to cell death: the dual role of reactive oxygen species in seed physiology. *C. R. Biol.* 331, 806–814. doi: 10.1016/j.crvi.2008.07.022
- Bao, J. S., Corke, H., and Sun, M. (2006). Microsatellite, single nucleotide polymorphisms and a sequence tagged site in starch-synthesizing genes in relation to starch physicochemical properties in nonwaxy rice (*Oryza sativa* L.). *Theor. Appl. Genet.* 113, 1185–1196. doi: 10.1007/s00122-006-0394-z
- Bej, S., and Basak, J. (2014). MicroRNAs: the potential biomarkers in plant stress response. *Am. J. Plant Sci.* 5, 748–759. doi: 10.4236/ajps.2014.55089
- Bimboim, H. C., and Doly, J. (1979). A rapid alkaline extraction procedure for screening recombinant plasmid DNA. *Nucleic Acids Res.* 7, 1513–1523. doi: 10.1093/nar/7.6.1513
- Borecky, J., Nogueira, F. T., de Oliveira, K. A., Maia, I. G., Vercesi, A. E., and Arruda, P. (2006). The plant energy-dissipating mitochondrial systems: depicting the genomic structure and the expression profiles of the gene families of uncoupling protein and alternative oxidase in monocots and dicots. *J. Exp. Bot.* 57, 849–864. doi: 10.1093/jxb/erj070
- Botha, F. C., Potgieter, G. P., and Botha, A. M. (1992). Respiratory metabolism and gene expression during seed germination. *Plant Growth Regul.* 11, 211–224. doi: 10.1007/BF00024560
- Boutrot, F., Guirao, A., Alary, R., Joudrier, P., and Gautier, M.-F. (2005). Wheat non-specific lipid transfer protein genes display a complex pattern of expression in developing seeds. *Biochim. Biophys. Acta* 1730, 114–125. doi: 10.1016/j.bbapex.2005.06.010
- Bowen, N. J., and McDonald, J. F. (2001). Drosophila euchromatic LTR retrotransposons are much younger than the host species in which they reside. *Genome Res.* 11, 1527–1540. doi: 10.1101/gr.164201
- Brosius, J. (2000). “Genomes were forged by massive bombardments with retroelements and retrosequences,” in *Transposable Elements and Genome Evolution*, ed J. F. McDonald (Dordrecht: Kluwer Academic Publishers), 209–238.
- Campos, M. D., Cardoso, H. G., Linke, B., Costa, J. H., Fernandes de Melo, D., Justo, L., et al. (2009). Differential expression and coregulation of carrot AOX genes (*Daucus carota* L.). *Physiol. Plant.* 137, 578–591. doi: 10.1111/j.1399-3054.2009.01282.x
- Campos, M. D., Nogales, A., Cardoso, H. G., Sarma, R. K., Nobre, T., Sathishkumar, R., et al. (2016). Stress-induced accumulation of DcAOX1 and DcAOX2a transcripts coincides with critical time point for structural biomass prediction in carrot primary cultures (*Daucus carota* L.). *Front. Genet.* 7:1. doi: 10.3389/fgene.2016.00001
- Cardoso, H., Campos, M. D., Nothnagel, T., and Arnholdt-Schmitt, B. (2011). Polymorphisms in intron 1 of carrot AOX2b - a useful tool to develop a functional marker? *Plant Genet. Resour.* C. 9, 177–180. doi: 10.1017/S1479262111000591
- Cardoso, H. G., and Arnholdt-Schmitt, B. (2013). “Functional marker development across species in selected traits” in *Diagnostics in Plant Breeding*, eds T. Lübbertedt and R. K. Varshney (Dordrecht: Springer), 467–515.
- Cardoso, H. G., Campos, M. D., Costa, A. R., Campos, M. C., Nothnagel, T., and Arnholdt-Schmitt, B. (2009). Carrot alternative oxidase

- gene *AOX2a* demonstrates allelic and genotypic polymorphisms in intron 3. *Physiol. Plant.* 137, 592–608. doi: 10.1111/j.1399-3054.2009.01299.x
- Cardoso, H. G., Nogales, A., Frederico, A. M., Svensson, J. T., Santos Macedo, E., Valadas, V., et al. (2015). “Natural AOX gene diversity” in *Alternative Respiratory Pathways in Higher Plants*, eds K. J. Gupta, L. A. J. Mur, and B. Neelwarne (Chichester, UK: John Wiley & Sons Inc, Oxford), 241–254.
- Cerff, R. (1982). “Separation and purification of NAD- and NADP linked glyceraldehyde-3-phosphate dehydrogenases from higher plants,” in *Methods in Chloroplast Molecular Biology*, eds N. -H. C. M. Edelman and R. B. Hallick (Amsterdam: Elsevier-North Holland), 683–694.
- Chai, T. T., Simmonds, D., Day, D. A., Colmer, T. D., and Finnegan, P. M. (2012). A GmAOX2b antisense gene compromises vegetative growth and seed production in soybean. *Planta* 236, 199–207. doi: 10.1007/s00425-012-1601-6
- Chen, Y., Gao, D. Y., and Huang, L. (2015). *In vivo* delivery of miRNAs for cancer therapy: challenges and strategies. *Adv. Drug Deliv. Rev.* 81, 128–141. doi: 10.1016/j.addr.2014.05.009
- Clifton, R., Lister, R., Parker, K. L., Sappl, P. G., Elhafey, D., Millar, A. H., et al. (2005). Stress-induced co-expression of alternative respiratory chain components in *Arabidopsis thaliana*. *Plant Mol. Biol.* 58, 193–212. doi: 10.1007/s11103-005-5514-7
- Clifton, R., Millar, A. H., and Whelan, J. (2006). Alternative oxidases in *Arabidopsis*: a comparative analysis of differential expression in the gene family provides new insights into function of non-phosphorylating bypasses. *Biochim. Biophys. Acta* 1757, 730–741. doi: 10.1016/j.bbabi.2006.03.009
- Collins, N. C., Tardieu, F., and Tuberrosa, R. (2008). Quantitative trait loci and crop performance under abiotic stress: where do we stand? *Plant Physiol.* 147, 469–486. doi: 10.1104/pp.108.118117
- Considine, M. J., Holtzapffel, R. C., Day, D. A., Whelan, J., and Millar, A. H. (2002). Molecular distinction between alternative oxidase from monocots and dicots. *Plant Physiol.* 129, 949–953. doi: 10.1104/pp.004150
- Costa, J. H., Fernandes de Melo, D., Gouveia, Z., Cardoso, H. G., Peixe, A., and Arnholdt-Schmitt, B. (2009). The alternative oxidase family of *Vitis vinifera* reveals an attractive model to study the importance of genomic design. *Physiol. Plant.* 137, 553–565. doi: 10.1111/j.1399-3054.2009.01267.x
- Costa, J. H., Mota, E. F., Cambursano, M. V., Lauxmann, M. A., de Oliveira, L. M. N., Silva Lima Mda, G., et al. (2010). Stress-induced co-expression of two alternative oxidase (*VuAOx1* and *2b*) genes in *Vigna unguiculata*. *J. Plant Physiol.* 167, 561–570. doi: 10.1016/j.jplph.2009.11.001
- Dewdney, J., Conley, T. R., Shih, M. C., and Goodman, H. M. (1993). Effects of blue and red light on expression of nuclear genes encoding chloroplast glyceraldehyde-3-phosphate dehydrogenase of *Arabidopsis thaliana*. *Plant Physiol.* 103, 1115–1121. doi: 10.1104/pp.103.4.1115
- Dinakar, C., Abhaypratap, V., Yearla, S. R., Raghavendra, A. S., and Padmasree, K. (2010). Importance of ROS and antioxidant system during the beneficial interactions of mitochondrial metabolism with photosynthetic carbon assimilation. *Planta* 231, 461–474. doi: 10.1007/s00425-009-1067-3
- Dinakar, C., Vishwakarma, A., Raghavendra, A. S., and Padmasree, K. (2016). Alternative oxidase pathway optimizes photosynthesis during osmotic and temperature stress by regulating cellular ROS, malate valve and antioxidative systems. *Front. Plant Sci.* 7:68. doi: 10.3389/fpls.2016.00068
- Emanuelsson, O., Nielsen, H., Brunak, S., and von Heijne, G. (2000). Predicting subcellular localization of proteins based on their N-terminal amino acid sequence. *J. Mol. Biol.* 300, 1005–1016. doi: 10.1006/jmbi.2000.3903
- Esashi, Y., Sakai, Y., and Ushizawa, R. (1981). Cyanide-sensitive and cyanide-resistant respiration in the germination of cocklebur seeds. *Plant Physiol.* 67, 503–508. doi: 10.1104/pp.67.3.503
- Fan, C., Chen, Y., and Long, M. (2008). Recurrent tandem gene duplication gave rise to functionally divergent genes in *Drosophila*. *Mol. Biol. Evol.* 25, 1451–1458. doi: 10.1093/molbev/msn089
- Farooq, S., and Azam, F. (2002). Molecular markers in plant breeding—I: concepts and characterization. *Pak. J. Biol. Sci.* 5, 1135–1140. doi: 10.3923/pjbs.2002.1135.1140
- Ferreira, A. O., Cardoso, H. G., Macedo, E. S., Breviaro, D., and Arnholdt-Schmitt, B. (2009). Intron polymorphism pattern in AOX1b of wild St John’s wort (*Hypericum perforatum*) allows discrimination between individual plants. *Physiol. Plant.* 137, 520–531. doi: 10.1111/j.1399-3054.2009.01291.x
- Finnegan, P. M., Whelan, J., Millar, A. H., Zhang, Q., Smith, M. K., Wiskich, J. T., et al. (1997). Differential expression of the multigene family encoding the soybean mitochondrial alternative oxidase. *Plant Physiol.* 114, 455–466. doi: 10.1104/pp.114.2.455
- Frederico, A. M., Campos, M. D., Cardoso, H. G., Imani, J., and Arnholdt-Schmitt, B. (2009). Alternative oxidase involvement in *Daucus carota* somatic embryogenesis. *Physiol. Plant.* 137, 498–508. doi: 10.1111/j.1399-3054.2009.01278.x
- Ganko, E. W., Fielman, K. T., and McDonald, J. F. (2001). Evolutionary history of cer elements and their impact on the *C. elegans* genome. *Genome Res.* 11, 2066–2074. doi: 10.1101/gr.196201
- Gartner, M., Müller, T., Simon, J. C., Giannis, A., and Sleeman, J. P. (2005). Aristoforin, a novel stable derivative of hyperforin, is a potent anticancer agent. *ChemBioChem* 6, 171–177. doi: 10.1002/cbic.200400195
- Goebels, C., Thonn, A., Gonzalez-Hilarion, S., Rolland, O., Moyrand, F., Beilharz, T. H., et al. (2013). Introns regulate gene expression in *Cryptococcus neoformans* in a Pab2p dependent pathway. *PLoS Genet.* 9:e1003686. doi: 10.1371/journal.pgen.1003686
- Grant, N., Onda, Y., Kakizaki, Y., Ito, K., Watling, J., and Robinson, S. (2009). Two cys or not two cys? That is the question; alternative oxidase in the thermogenic plant sacred lotus. *Plant Physiol.* 150, 987–995. doi: 10.1104/pp.109.139394
- Hedayati, V., Mousavi, A., Razavi, K., Cultrera, N., Alagna, F., Mariotti, R., et al. (2015). Polymorphisms in the AOX2 gene are associated with the rooting ability of olive cuttings. *Plant Cell Rep.* 34, 1151–1164. doi: 10.1007/s00299-015-1774-0
- Heyn, P., Kalinka, A. T., Tomancak, P., and Neugebauer, K. M. (2015). Introns and gene expression: cellular constraints, transcriptional regulation, and evolutionary consequences. *Bioessays* 37, 148–154. doi: 10.1002/bies.201400138
- Holtzapffel, R. C., Castelli, J., Finnegan, P. M., Millar, A. H., Whelan, J., and Day, D. A. (2003). A tomato alternative oxidase protein with altered regulatory properties. *Biochim. Biophys. Acta* 1606, 153–162. doi: 10.1016/S0006-2728(03)00112-9
- Huang, S., Taylor, N. L., Whelan, J., and Millar, A. H. (2009). Refining the definition of plant mitochondrial presequences through analysis of sorting signals, N-terminal modifications, and cleavage motifs. *Plant Physiol.* 150, 1272–1285. doi: 10.1104/pp.109.137885
- Ismail, A. M., Ella, E. S., Vergara, G. V., and Mackill, D. J. (2009). Mechanisms associated with tolerance to flooding during germination and early seedling growth in rice (*Oryza sativa*). *Ann. Bot.* 103, 197–209. doi: 10.1093/aob/mcn211
- Jiang, P., Wu, H., Wang, W., Ma, W., Sun, X., and Lu, Z. (2007). MiPred: classification of real and pseudo microRNA precursors using random forest prediction model with combined features. *Nucleic Acids Res.* 35, 339–344. doi: 10.1093/nar/gkm368
- Karlin, S., and Altschul, S. F. (1993). Applications and statistics for multiple high-scoring segments in molecular sequences. *Proc. Natl. Acad. Sci. U.S.A.* 90, 5873–5877. doi: 10.1073/pnas.90.12.5873
- Kim, G. P., Colangelo, L., Allegra, C., Glebov, O., Parr, A., Hooper, S., et al. (2001). Prognostic role of microsatellite instability in colon cancer. *Proc. Am. Soc. Clin. Oncol.* 20:1666.
- Kohany, O., Gentles, A. J., Hankus, L., and Jurka, J. (2006). Annotation, submission and screening of repetitive elements in Repbase: RepbaseSubmitter and Censor. *BMC Bioinformatics* 7:474. doi: 10.1186/1471-2105-7-474
- Kubin, A., Wierrani, F., Burner, U., Alth, G., and Grunberger, W. (2005). Hypericin—the facts about a controversial agent. *Curr. Pharm. Des.* 11, 233–253. doi: 10.2174/1381612053382287
- Kwak, J. M., Nguyen, V., and Schoeder, J. I. (2006). The role of reactive oxygen species in hormonal responses. *Plant Physiol.* 141, 323–329. doi: 10.1104/pp.106.079004
- Lister, R., Hulett, J. M., Lithgow, T., and Whelan, J. (2005). Protein import into mitochondria: origins and functions today. *Mol. Membr. Biol.* 22, 87–100. doi: 10.1080/09687860500041247
- Maron, J. L., Elmendorf, S. C., and Vilà, M. (2007). Contrasting plant physiological adaptation to climate in the native and introduced range of *Hypericum perforatum*. *Evolution* 61, 1912–1924. doi: 10.1111/j.1558-5646.2007.00153.x
- Mathews, D. H., Sabina, J., Zuker, M., and Turner, D. H. (1999). Expanded sequence dependence of thermodynamic parameters improves

- prediction of RNA secondary structure. *J. Mol. Biol.* 288, 911–940. doi: 10.1006/jmbi.1999.2700
- McCabe, T. C., Finnegan, P. M., Millar, A. H., Day, D. A., and Whelan, J. (1998). Differential expression of alternative oxidase genes in soybean cotyledons during postgerminative development. *Plant Physiol.* 118, 675–682. doi: 10.1104/pp.118.2.675
- McDonald, J. F. (1993). Evolution and consequences of transposable elements. *Curr. Opin. Genet. Dev.* 3, 855–864. doi: 10.1016/0959-437X(93)90005-A
- Mhamdi, A., Noctor, G., and Baker, A. (2012). Plant catalases: peroxisomal redox guardians. *Arch. Biochem. Biophys.* 525, 181–194. doi: 10.1016/j.abb.2012.04.015
- Mhamdi, A., Queval, G., Chaouch, S., Vanderauwera, S., Van Breusegem, F., and Noctor, G. (2010). Catalase function in plants: a focus on *Arabidopsis* mutants as stress-mimic models. *J. Exp. Bot.* 61, 4197–4220. doi: 10.1093/jxb/erq282
- Mittler, R. (2002). Oxidative stress, antioxidants and stress tolerance. *Trends Plant Sci.* 7, 405–410. doi: 10.1016/S1360-1385(02)02312-9
- Möller, I. M. (2001). Plant mitochondria and oxidative stress: electron transport, NADPH turnover, and metabolism of reactive oxygen species. *Annu. Rev. Plant Biol.* 52, 561–591. doi: 10.1146/annurev.arplant.52.1.561
- Möller, I. M., Jensen, P. E., and Hansson, A. (2007). Oxidative modifications to cellular components in plants. *Annu. Rev. Plant Biol.* 58, 459–481. doi: 10.1146/annurev.arplant.58.032806.103946
- Moore, A. L., Shiba, T., Young, L., Harada, S., Kita, K., and Ito, K. (2013). Unraveling the heater-new insights into the structure of the alternative. *Annu. Rev. Plant Biol.* 64, 637–663. doi: 10.1146/annurev-arplant-042811-105432
- Moraes, G. P., Benitez, L. C., do Amaral, M. N., Vighi, I. L., Auler, P. A., da Maia, L. C., et al. (2015). Evaluation of reference genes for RT-qPCR studies in the leaves of rice seedlings under salt stress. *Genet. Mol. Res.* 14, 2384–2398. doi: 10.4238/2015.March.27.24
- Neale, D. B., and Savolainen, O. (2004). Association genetics of complex traits in conifers. *Trends Plant Sci.* 9, 325–330. doi: 10.1016/j.tplants.2004.05.006
- Nekrutenko, A., and Li, W. H. (2001). Transposable elements are found in a large number of human protein-coding genes. *Trends Genet.* 17, 619–621. doi: 10.1016/S0168-9525(01)02445-3
- Neupert, W., and Herrmann, J. M. (2007). Translocation of proteins into mitochondria. *Annu. Rev. Biochem.* 76, 723–749. doi: 10.1146/annurev.biochem.76.052705.163409
- Niu, L., Tao, Y.-B., Chen, M.-S., Fu, Q., Li, C., Dong, Y., et al. (2015). Selection of reliable reference genes for gene expression studies of a promising oilseed crop, *Plukenetia volubilis*, by real-time quantitative PCR. *Int. J. Mol. Sci.* 16, 12513–12530. doi: 10.3390/ijms160612513
- Nogales, A., Nobre, T., Cardoso, H. G., Muñoz-Sanhueza, L., Valadas, V., Campos, M. D., et al. (2016). Allelic variation on DcAOX1 gene in carrot (*Daucus carota* L.): An interesting simple sequence repeat in a highly variable intron. *Plant Gene* 5, 49–55. doi: 10.1016/j.pglene.2015.11.001
- Oracz, K., El-Maarouf-Bouteau, H., Kranner, I., Bogatek, R., Corbineau, F., and Bailly, C. (2009). The mechanisms involved in seed dormancy alleviation by hydrogen cyanide unravel the role of reactive oxygen species as key factors of cellular signaling during germination. *Plant Physiol.* 150, 494–505. doi: 10.1104/pp.109.138107
- Padmasree, K., and Raghavendra, A. S. (2001). Restriction of mitochondrial oxidative metabolism leads to suppression of photosynthetic carbon assimilation but not of photochemical electron transport in pea mesophyll protoplasts. *Curr. Sci.* 81, 680–684.
- Parida, S. K., Dalal, V., Singh, A. K., Singh, N. K., and Mohapatra, T. (2009). Genic non-coding microsatellites in the rice genome: characterization, marker design and use in assessing genetic and evolutionary relationships among domesticated groups. *BMC Genomics* 10:140. doi: 10.1186/1471-2164-10-140
- Pergo, É. M., and Ishii-Iwamoto, E. L. (2011). Changes in energy metabolism and antioxidant defense systems during seed germination of the weed species *Ipomoea triloba* L. and the responses to allelochemicals. *J. Chemi. Ecol.* 37, 500–513. doi: 10.1007/s10886-011-9945-0
- Polidoros, A. N., Mylona, P. V., and Arnholdt-Schmitt, B. (2009). AOX gene structure, transcript variation and expression in plants. *Physiol. Plant.* 137, 342–353. doi: 10.1111/j.1399-3054.2009.01284.x
- Popov, V., Simonian, R., Skulachev, V., and Starkov, A. (1997). Inhibition of the alternative oxidase stimulates H2O2 production in plant mitochondria. *FEBS Lett.* 415, 87–90. doi: 10.1016/S0014-5793(97)01099-5
- Puntarulo, S., Sánchez, R. A., and Boveris, A. (1988). Hydrogen peroxide metabolism in soybean embryonic axes at the onset of germination. *Plant Physiol.* 86, 626–630. doi: 10.1104/pp.86.2.626
- Purvis, A. C., and Shewfelt, R. L. (1993). Does the alternative pathway ameliorate chilling injury in sensitive plant tissues? *Physiol. Plant.* 88, 712–718. doi: 10.1111/j.1399-3054.1993.tb01393.x
- Rambaldi, D., and Ciccarelli, F. D. (2009). FancyGene: dynamic visualization of gene structures and protein domain architectures on genomic loci. *Bioinformatics* 25, 2281–2282. doi: 10.1093/bioinformatics/btp381
- Rasmussen, A. G., Fernie, A. R., and van Dongen, J. T. (2009). Alternative oxidase: a defence against metabolic fluctuations? *Physiol. Plant.* 137, 371–382. doi: 10.1111/j.1399-3054.2009.01252.x
- Rhoads, D. M., Umbach, A. L., Sweet, C. R., Lennon, A. M., Rauch, G. S., and Siedow, J. N. (1998). Regulation of the cyanide-resistant alternative oxidase of plant mitochondria - Identification of the cysteine residue involved in alpha-keto acid stimulation and intersubunit disulfide bond formation. *J. Biol. Chem.* 273, 30750–30756. doi: 10.1074/jbc.273.46.30750
- Rigas, S., Daras, G., Laxa, M., Marathias, N., Fasseas, C., Sweetlove, L. J., et al. (2009). Role of Lon1 protease in post-germinative growth and maintenance of mitochondrial function in *Arabidopsis thaliana*. *New Phytol.* 181, 588–600. doi: 10.1111/j.1469-8137.2008.02701.x
- Robson, N. K. B. (1977). Studies in the genus *Hypericum* L. (Guttiferae): 1. Infrageneric classification. *Bull. Br. Mus. Bot.* 5, 291–355.
- Rose, A. B., Elfersi, T., Parra, G., and Korff, I. (2008). Promoter-proximal introns in *Arabidopsis thaliana* are enriched in dispersed signals that elevate gene expression. *Plant Cell* 20, 543–551. doi: 10.1105/tpc.107.057190
- Saisho, D., Nakazono, M., Lee, K. H., Tsutsumi, N., Akita, S., and Hirai, A. (2001). The gene for alternative oxidase-2 (AOX2) from *Arabidopsis thaliana* consists of five exons unlike other AOX genes and is transcribed at an early stage during germination. *Genes Genet. Syst.* 76, 89–97. doi: 10.1266/ggs.76.89
- Saisho, D., Nambara, E., Naito, S., Tsutsumi, N., Hirai, A., and Nakazono, M. (1997). Characterization of the gene family for alternative oxidase from *Arabidopsis thaliana*. *Plant Mol. Biol.* 35, 585–596. doi: 10.1023/A:1005818507743
- Santos, G. C., von Pinho, E. V. R., and Rosa, S. D. V. F. (2013). Gene expression of coffee seed oxidation and germination processes during drying. *Genet. Mol. Res.* 12, 6968–6982. doi: 10.4238/2013.December.19.16
- Santos Macedo, E. S., Cardoso, H. G., Hernandez, A., Peixe, A. A., Polidoros, A., Ferreira, A., et al. (2009). Physiologic responses and gene diversity indicate olive alternative oxidase as a potential source for markers involved in efficient adventitious root induction. *Physiol. Plant.* 137, 532–552. doi: 10.1111/j.1399-3054.2009.01302.x
- Shih, M., and Goodman, H. M. (1988). Differential light regulated expression of nuclear genes encoding chloroplast and cytosolic glyceraldehyde-3-phosphate dehydrogenase in *Nicotiana tabacum*. *EMBO J.* 7, 893–898.
- Smit A.F. A., Hubley, R., and Green, P. (2013–2015). RepeatMasker Open-4.0. Available online at: <http://www.repeatmasker.org>
- Szytkiewicz, H. (2014). Differential expression of superoxide dismutase genes in aphid-stressed maize (*Zea mays* L.) seedlings. *PLoS ONE* 9:e94847. doi: 10.1371/journal.pone.0094847
- Tamura, K., Dudley, J., Nei, M., and Kumar, S. (2007). MEGA4: Molecular Evolutionary Genetics Analysis (MEGA) software version 4.0. *Mol. Biol. Evol.* 24, 1596–1599. doi: 10.1093/molbev/msm092
- Tan, Y. F., and Zhang, Q. F. (2001). Correlation of simple sequence repeat (SSR) variants in the leader sequence of the waxy gene with amylose content of the grain in rice. *Acta Bot. Sin.* 43, 146–150.
- Umbach, A. L., Gonzalez-Meler, M. A., Sweet, C. R., and Siedow, J. N. (2002). Activation of the plant mitochondrial alternative oxidase: insights from site-directed mutagenesis. *Biochim. Biophys. Acta* 1554, 118–128. doi: 10.1016/S0006-2728(02)00219-0
- Umbach, A. L., and Siedow, J. N. (1993). Covalent and noncovalent dimers of the cyanide-resistant alternative oxidase protein in higher plant mitochondria and their relationship to enzyme activity. *Plant Physiol.* 103, 845–854.
- Vandesompele, J., De Preter, K., Pattyn, F., Poppe, B., Van Roy, N., De Paepe, A., et al. (2002). Accurate normalization of real-time quantitative RT-PCR

- data by geometric averaging of multiple internal control genes. *Genome Biol.* 3:RESEARCH0034. doi: 10.1186/gb-2002-3-7-research0034
- Vanlerberghe, G. C. (2013). Alternative oxidase: a mitochondrial respiratory pathway to maintain metabolic and signaling homeostasis during abiotic and biotic stress in plants. *Int. J. Mol. Sci.* 14, 6805–6847. doi: 10.3390/ijms14046805
- Velada, I., Ragonezi, C., Arnholdt-Schmitt, B., and Cardoso, H. G. (2014). Reference genes selection and normalization of oxidative stress responsive genes upon different temperature stress conditions in *Hypericum perforatum* L. *PLoS ONE* 9:e115206. doi: 10.1371/journal.pone.0115206
- Wang, C., Chen, S., and Yu, S. (2011). Functional markers developed from multiple loci in GS3 for fine marker-assisted selection of grain length in rice. *Theor. Appl. Genet.* 122, 905–913. doi: 10.1007/s00122-010-1497-0
- Watanabe, C. K., Hachiya, T., Terashima, I., and Noguchi, K. O. (2008). The lack of alternative oxidase at low temperature leads to a disruption of the balance in carbon and nitrogen metabolism, and to an up-regulation of antioxidant defence systems in *Arabidopsis thaliana* leaves Identification of the T-DNA insertion in the. *Plant Cell Environ.* 31, 1190–1202. doi: 10.1111/j.1365-3040.2008.01834.x
- Weitbrecht, K., Müller, K., and Leubner-Metzger, G. (2011). First off the mark: early seed germination. *J. Exp. Bot.* 62, 3289–3309. doi: 10.1093/jxb/err030
- Yadav, C. B., Bonthala, V. S., Muthamilarasan, M., Pandey, G., Khan, Y., and Prasad, M. (2015). Genome-wide development of transposable elements-based markers in foxtail millet and construction of an integrated database. *DNA Res.* 22, 79–90. doi: 10.1093/dnares/dsu039
- Yoshida, K., Terashima, I., and Noguchi, K. (2006). Distinct roles of the cytochrome pathway and alternative oxidase in leaf photosynthesis. *Plant Cell Physiol.* 47, 22–31. doi: 10.1093/pcp/pcp219
- Yoshida, K., Terashima, I., and Noguchi, K. (2007). Up-regulation of mitochondrial alternative oxidase concomitant with chloroplast over-reduction by excess light. *Plant Cell Physiol.* 48, 606–614. doi: 10.1093/pcp/pcm033
- Zanolli, P. (2004). Role of hyperforin in the pharmacological activities of St. John's Wort. *CNS Drug Rev.* 10, 203–218. doi: 10.1111/j.1527-3458.2004.tb00022.x
- Zhang, L., Huang, J., Yang, N., Greshock, J., Megraw, M. S., Giannakakis, A., et al. (2006). microRNAs exhibit high frequency genomic alterations in human cancer. *Proc. Natl. Acad. Sci. U.S.A.* 103, 9136–9141. doi: 10.1073/pnas.0508889103
- Zuker, M. (2003). Mfold web server for nucleic acid folding and hybridization prediction. *Nucleic Acids. Res.* 31, 3406–3415. doi: 10.1093/nar/gkg595

Conflict of Interest Statement: The authors declare that the research was conducted in the absence of any commercial or financial relationships that could be construed as a potential conflict of interest.

Copyright © 2016 Velada, Cardoso, Ragonezi, Nogales, Ferreira, Valadas and Arnholdt-Schmitt. This is an open-access article distributed under the terms of the Creative Commons Attribution License (CC BY). The use, distribution or reproduction in other forums is permitted, provided the original author(s) or licensor are credited and that the original publication in this journal is cited, in accordance with accepted academic practice. No use, distribution or reproduction is permitted which does not comply with these terms.



Comparative Transcriptome Reconstruction of Four *Hypericum* Species Focused on Hypericin Biosynthesis

Miroslav Soták^{1*}, Odetta Czeranková¹, Daniel Klein², Zuzana Jurčacková¹, Ling Li^{3,4} and Eva Čellárová¹

¹ Department of Genetics, Institute of Biology and Ecology, Faculty of Science, Pavol Jozef Šafárik University, Košice, Slovakia, ² Institute of Mathematics, Faculty of Science, Pavol Jozef Šafárik University, Košice, Slovakia, ³ Department of Genetics, Development, and Cell Biology, Iowa State University, Ames, IA, USA, ⁴ Center for Metabolic Biology, Iowa State University, Ames, IA, USA

OPEN ACCESS

Edited by:

Ludger Beerhues,
Technische Universität Braunschweig,
Germany

Reviewed by:

Hubert Schaller,
Institut de Biologie Moléculaire des
Plantes—CNRS, France
Kexuan Tang,
Shanghai Jiao Tong University, China

***Correspondence:**

Miroslav Soták
miroslav.sotak@upjs.sk

Specialty section:

This article was submitted to
Plant Metabolism
and Chemodiversity,
a section of the journal
Frontiers in Plant Science

Received: 26 February 2016

Accepted: 01 July 2016

Published: 13 July 2016

Citation:

Soták M, Czeranková O, Klein D, Jurčacková Z, Li L and Čellárová E (2016) Comparative Transcriptome Reconstruction of Four *Hypericum* Species Focused on Hypericin Biosynthesis. *Front. Plant Sci.* 7:1039.
doi: 10.3389/fpls.2016.01039

Next generation sequencing technology rapidly developed research applications in the field of plant functional genomics. Several *Hypericum* spp. with an aim to generate and enhance gene annotations especially for genes coding the enzymes supposedly included in biosynthesis of valuable bioactive compounds were analyzed. The first *de novo* transcriptome profiling of *Hypericum annulatum* Moris, *H. tomentosum* L., *H. kalmianum* L., and *H. androsaemum* L. leaves cultivated *in vitro* was accomplished. All four species with only limited genomic information were selected on the basis of differences in ability to synthesize hypericins and presence of dark nodules accumulating these metabolites with purpose to enrich genomic background of *Hypericum* spp. *H. annulatum* was chosen because of high number of the dark nodules and high content of hypericin. *H. tomentosum* leaves are typical for the presence of only 1–2 dark nodules localized in the apical part. Both *H. kalmianum* and *H. androsaemum* lack hypericin and have no dark nodules. Four separated datasets of the pair-end reads were gathered and used for *de novo* assembly by Trinity program. Assembled transcriptomes were annotated to the public databases Swiss-Prot and non-redundant protein database (NCBI-nr). Gene ontology analysis was performed. Differences of expression levels in the marginal tissues with dark nodules and inner part of leaves lacking these nodules indicate a potential genetic background for hypericin formation as the presumed site of hypericin biosynthesis is in the cells adjacent to these structures. Altogether 165 contigs in *H. annulatum* and 100 contigs in *H. tomentosum* were detected as significantly differentially expressed ($P < 0.05$) and upregulated in the leaf rim tissues containing the dark nodules. The new sequences homologous to octaketide synthase and enzymes catalyzing phenolic oxidative coupling reactions indispensable for hypericin biosynthesis were discovered. The presented transcriptomic sequence data will improve current knowledge about the selected *Hypericum* spp. with proposed relation to hypericin biosynthesis and will provide a useful resource of genomic information for consequential studies in the field of functional genomics, proteomics and metabolomics.

Keywords: *Hypericum* spp., RNA-Seq, *de novo* assembly, differential expression analysis, hypericin

INTRODUCTION

Hypericum is the genus with 496 species of plants spread worldwide (Nürk et al., 2013). The most of them are typical for compounds with anti-cancer (Agostinis et al., 2002), antioxidant (Silva et al., 2005), anti-viral (Birt et al., 2009), and anti-depressive (Butterweck, 2003) properties. Dark nodules (glands), the sites of hypericin accumulation are characteristic for approximately 2/3 of the taxonomic sections and are limited to particular organs (Robson, 2003). The metabolome of leaf tissue samples of *ex vitro* grown plants from the proximity to the dark nodules in *Hypericum perforatum* containing hypericin was visualized by the use of matrix-assisted laser desorption/ionization high-resolution mass spectrometry (MALDI-HRMS; Kusari et al., 2015). This study suggested the site of hypericin biosynthesis is in dark nodules and adjacent leaf tissues. The localization of hypericin in dark nodules of the leaves of *Hypericum* spp. cultured *in vitro* was also qualitatively assessed by desorption electrospray ionization mass spectrometry imaging (DESI-MSI). The presence of hypericin in closeness of the dark nodules was confirmed in *H. annulatum*, *H. perforatum*, and *H. tomentosum*, while in *H. androsaemum* and *H. kalmianum* it was not detected (Kucharíková et al., 2016). Hypericin biosynthesis consists of experimentally not yet proven subsequent reactions (Figure 1). Acetyl-CoA is condensed with seven molecules of malonyl-CoA to form the octaketide chain. This undergoes specific cyclization to form emodin anthrone, the immediate precursor of hypericin, catalyzed by the octaketide synthase (OKS). Emodin is converted to protohypericin, followed by condensation and transformation reaction leading to hypericin under visible light irradiation (Bais et al., 2003; Zobayed et al., 2006). This study was dedicated to identify new genes involved in the hypericin biosynthesis pathway by approach of functional genomics. Next generation sequencing (NGS) method, especially RNA-Seq (RNA sequencing) used for cDNA identification enables deeper view into biological mechanisms with a potential to reveal unprecedented complexity of the transcriptomes in non-model plants.

To-date, the only available NGS data of the genus *Hypericum* are from *H. perforatum* (St John's Wort), as the model representative of genus with 39 SRA-NCBI archive entries. The aim of our work was to create new transcriptomic resources for four *Hypericum* spp. (*H. annulatum* and *H. tomentosum* as hypericin-producing and *H. androsaemum* and *H. kalmianum* as hypericin-lacking spp.). Interspecific approach and differential gene expression in leaf tissues with/without dark nodules and hypericin content were performed to approve already identified differentially expressed genes (DEGs) associated with hypericin biosynthesis from *H. perforatum* (Soták et al., 2016). We concentrated especially on verification of the occurrence and expression levels of octaketide synthase *HpPKS2* (OKS; Karppinen et al., 2008) and phenolic oxidative coupling like proteins (POCP) including *hyp-1* sequences (Bais et al.,

2003) in leaves. The group of genes coding POCPs belongs to PR-10 genes family (Fernandes et al., 2013). Phenolic oxidative coupling proteins share sequences of SRPBCC (START/RHO_alpha_C/PITP/Bet_v1/CoxG/CalC) domain superfamily.

MATERIALS AND METHODS

Plant Material and RNA Extraction

Hypericum annulatum Moris, *H. tomentosum* L., *H. androsaemum* L., and *H. kalmianum* L. plants were cultivated *in vitro* on basal medium containing salts according to Murashige and Skoog (1962), Gamborg's B5 vitamins (Gamborg et al., 1968), 30 g.l⁻¹ sucrose, 100 mg.l⁻¹ myoinositol, 2 mg.l⁻¹ glycine, and 7 g.l⁻¹ agar. The plants were grown in the chamber at 23°C, 40% relative humidity, 16/8 h day/night photoperiod and artificial irradiation of 80 μmol m⁻² s⁻¹. Leaf tissues from 4-week old seedlings were processed on ice under sterile conditions, frozen rapidly in liquid nitrogen and kept at -80°C till the RNA extraction.

The marginal parts of the leaves with dark nodules (*H. annulatum*) and apical part of leaves with 1–2 dark nodules (*H. tomentosum*) were separated from the inner part leaf tissues lacking dark nodules (Figure 2). Whole leaves were collected from *H. androsaemum* and *H. kalmianum* seedlings. Each sample contained approximately 10 individual genetically identical plants representing biological replicates from one specimen. The frozen tissues were homogenized by TissueLyser II (Qiagen) and total RNA was extracted with SpectrumTM Plant Total RNA Kit (Sigma-Aldrich) according to manufacturer's protocol. The quality of total RNA was analyzed on the basis of UV absorption ratios by NanoDrop spectrophotometer 2000 (Thermo Scientific) and the RNA integrity was determined on 2100 Bioanalyzer (Agilent Technologies).

Determination of Polyketides Content in *Hypericum* spp. Leaves

The experimental design of current transcriptomic paper was based on qualitative metabolomic data of the same *in vitro* cultivated clones by desorption electrospray ionization mass spectrometry imaging (DESI-MSI) published by Kucharíková et al. (2016). The content of phloroglucinol (hyperforin), naphtodianthrone (protopseudohypericin, pseudohypericin, protohypericin, and hypericin) and their putative precursor emodin in the leaves of *Hypericum* species was determined by high-performance liquid chromatography (HPLC). The extracts were prepared and analyzed according to Bruňáková and Čellárová (2016) in three replicates. The compounds were identified and quantified by the Agilent Infinity 1,260 HPLC system (Agilent Technologies, Palo Alto, CA, USA) equipped by a diode array detector. The separation was performed with Agilent Poroshell 120, EC-C18 (3.0 mm × 50 mm, 2.7 μm).

Illumina Transcriptome Sequencing

Oligo(dT) magnetic beads were used for enrichment of the mRNA from total RNA. The fragmentation of mRNA into short

Abbreviations: DEGs, differentially expressed genes; HpPKS2, *Hypericum perforatum* polyketide synthase 2; OKS, octaketide synthase; POCP, phenolic oxidative coupling protein; PR-10, pathogenesis-related class 10.

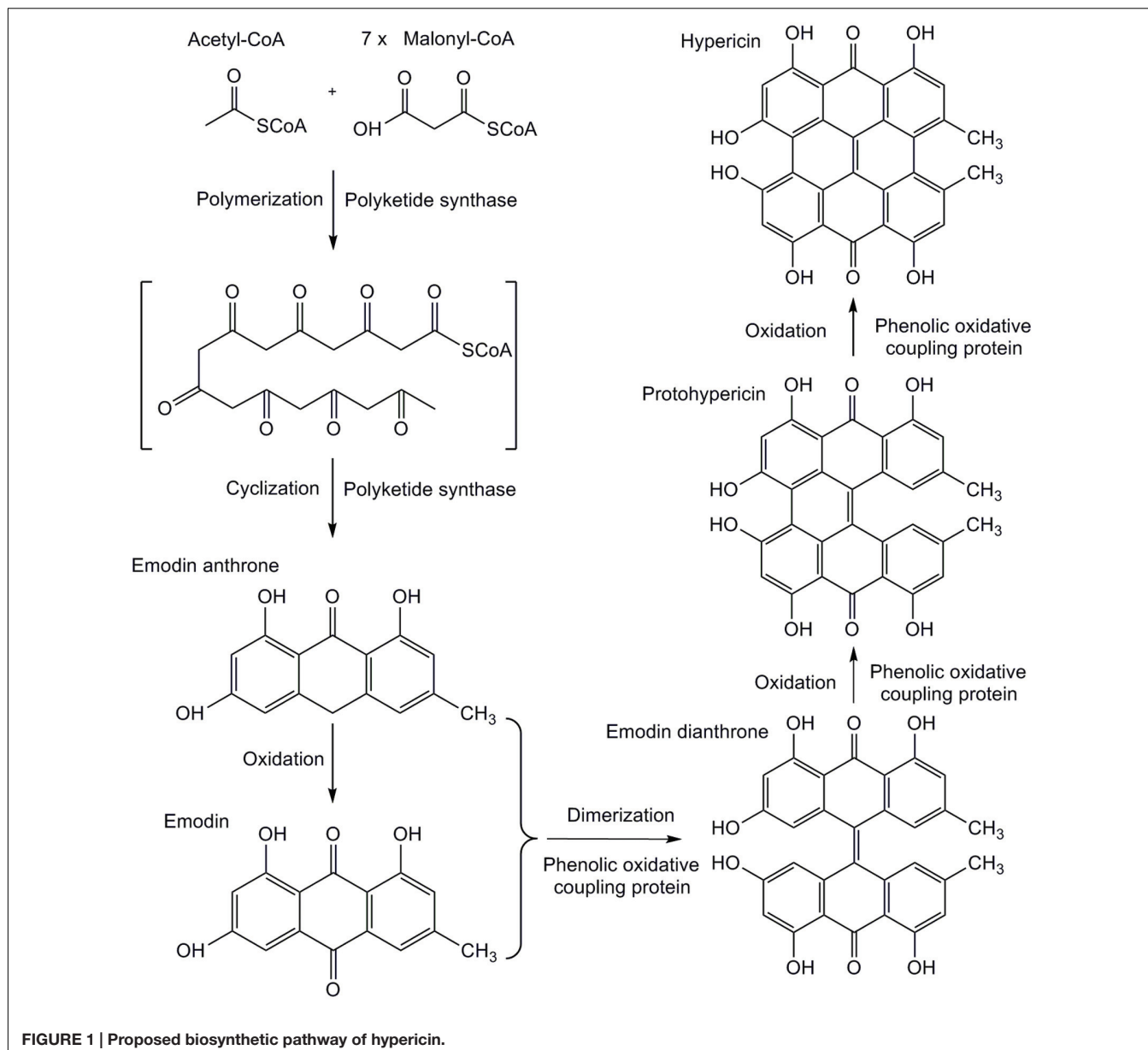
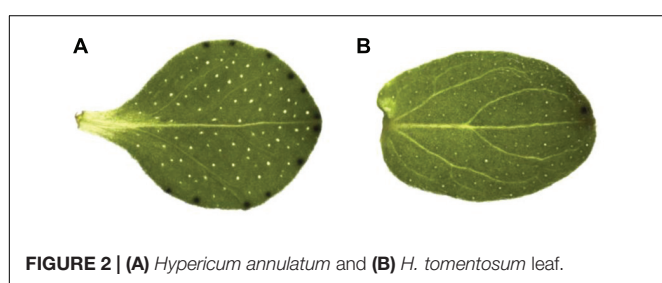


FIGURE 1 | Proposed biosynthetic pathway of hypericin.

FIGURE 2 | (A) *Hypericum annulatum* and (B) *H. tomentosum* leaf.

fragments ($200 \sim 500$ bp) was conducted by the fragment buffer treatment. The first-strand cDNA was synthesized by random hexamer-primer with the mRNA fragments as templates. Buffer, dNTPs, RNase H, and DNA polymerase I were used

to synthesize the second strand. The double strand cDNAs, purified with QiaQuick PCR extraction kit, were used for end repair and base A addition. Short fragments were purified by agarose gel electrophoresis after connecting short fragments to sequencing adapters, and enriched by PCR to create the final cDNA library. The libraries were subjected to RNA-Seq using an Illumina HiSeqTM 2000 platform (BGI Americas, USA). Sequencing was performed in paired-end mode with the read length of 100 bp.

Quality Control and De Novo Assembly Without the Reference Genome

Using the BGI in house software program (BGI Americas, USA), high-quality clean reads were filtered from the raw reads

by removing adaptor sequences, low-quality reads with the percentage of unknown nucleotides 'N' higher than 5% and reads with the percentage of low quality bases higher than 20% (PHRED quality scores lower than 10). Transcriptome *de novo* assembly was conducted using the program Trinity (v2.0.6; Grabherr et al., 2011) with default settings. The reads were firstly combined based on nucleotide complementarity with certain lengths of overlap to form longer fragments, known as contigs. Contigs redundancy was decreased by the program CD-HIT-EST (Fu et al., 2012), the sequence identity threshold was set to 0.98, word length to 10 and both strands were compared. Sequence Cleaner software (SeqClean) processed and cleaned the contigs at default settings¹.

Differential Expression and qRT-PCR Validation

The sequence reads filtered by the quality control were aligned to the assembled contigs using Bowtie2 (Langmead and Salzberg, 2012) to obtain counts of mapped reads. The relative abundances and expected read counts for the contigs were estimated with RNA-Seq by Expectation-Maximization (RSEM; Li and Dewey, 2011). Three different Bioconductor R packages were used to gage important differences in the marginal parts of the leaves with dark nodules and in the inner part leaf tissues without dark nodules of *H. annulatum* and *H. tomentosum*: EdgeR (Robinson et al., 2010), DESeq (Anders and Huber, 2010), and NOISeq (Tarazona et al., 2011), a novel non-parametric approach for the identification of DEGs from count data with the ability to simulate replicates. The variance of 0.05 and the *P*-value of 0.05 were set as the thresholds for the significance of the differential gene expression between two types of tissue samples in hypericin producing species.

Five of DEGs upregulated in the leaf rim tissues, namely OKS and four different forms of predicted genes coding POCP were selected to verify differential expression analysis by quantitative real-time polymerase chain reaction (qRT-PCR). The RNA extraction process followed the same protocol as described for RNA-Seq. Degenerative primers were constructed for the reference gene, translation elongation factor 1α (EF-1α; Košuth et al., 2007). The first-strand cDNAs were synthesized from 1 μg of total RNAs using RevertAid Reverse Transcriptase (Thermo Fisher Scientific). NCBI primer-BLAST and Primer3 (Untergasser et al., 2012), a tools for finding specific primers were applied (Table 1). LightCycler® Nano Instrument (Roche) was utilized for qRT-PCR reaction and ran on SYBR Green Supermix chemistry. Amplification was performed as follows: first denaturation at 95°C for 10 min, followed by 40 cycles of denaturation at 95°C for 15 s, annealing at 60°C for 10 s and extension at 72°C for 60 s with a single fluorescence measurement. Melting curve program (60–95°C with a heating rate of 0.1°C per second and a continuous fluorescence measurement) and finally a cooling step to 40°C. All the PCR reactions were carried out in three replicates. The relative expression levels for each gene were calculated using the $\Delta\Delta C_t$ method.

¹<https://sourceforge.net/projects/seqclean>

Functional Annotation and Similarity Search

The transcriptomes of the studied *Hypericum* spp. were annotated against the SwissProt database (Swiss Institute of Bioinformatics databases²) and the NCBI non-redundant protein database³ using blastx at the *E*-value cut-off of 10^{-5} . The results of five best hits were extracted and the hits of lower *E*-value than 10^{-5} were considered to be significant. Functional annotation was performed with the Blast2GO software (Conesa and Götz, 2008). Gene ontology (GO) terms were taxonomically specified to green plants (*Viriplantae*) and Enzyme Commission (EC) codes were achieved. The annotation was improved by the Augment Annotation by ANNEX function (Myhre et al., 2006), Validate annotation and Remove first level annotation to erase all the redundant GO terms for a given sequence and to assign only the most specific GO terms. Sequence alignments of candidate genes were performed and phylogenetic tree was constructed by the neighbor-joining method with the MEGA 6 program (Tamura et al., 2013).

RESULTS

Determination of Polyketides Content by HPLC

High-performance liquid chromatography analysis confirmed the presence of hypericins and emodin in hypericin producing spp., *H. annulatum*, *H. tomentosum*, and *H. perforatum*. The phloroglucinol hyperforin was detected in *H. androsaemum* and *H. perforatum* (Supplementary Table S1).

Sequencing and De Novo Assembly

Six cDNA libraries from the marginal parts of the leaves with dark nodules and from the inner part leaf tissue lacking dark nodules from *H. annulatum* and *H. tomentosum*, and whole leaves from *H. androsaemum* and *H. kalmianum*, were subjected to Illumina sequencing. Paired-end read technology was preferred to increase the depth and improve *de novo* assembly efficiency. Sequencing using the Illumina HiSeq™ 2000 platform resulted in the generation of 74.4 G raw reads. The samples were deposited in NCBI Sequence Read Archive (SRA) with accession numbers SRX1528960 (*H. annulatum* leaves with dark nodules), SRX1528962 (*H. annulatum* leaves without dark nodules), SRX1528963 (*H. tomentosum* leaves with dark nodules), SRX1528964 (*H. tomentosum* leaves without dark nodules), SRX1528157 (*H. androsaemum*) and SRX1528958 (*H. kalmianum*). After removing reads with adapters, reads with unknown nucleotides, and low-quality reads, we gained 312.4 million clean reads with the average GC content of 50.56% and more than 98% of the bases had PHRED quality scores higher than Q20 (error rate < 0.01%; Table 2).

The clean reads were assembled by the Trinity program to obtain the *de novo* reference transcriptome sequence. The

²<http://www.uniprot.org/downloads>

³<ftp://ftp.ncbi.nlm.nih.gov/blast/db/>

TABLE 1 | Gene-specific primers used for quantitative RT-PCR analyses.

Species	Gene	Contig	Accession number	Primer sequence 5'-3'
<i>H. annulatum</i>	<i>POCP1</i>	TR34666	KU744672	F CCGATTCTCCGAGTTGAA R CTCAGGTTCTCCATCTCAA
	<i>POCP2</i>	TR36949	KU744673	F CCAGTGACCCATTATAACCTCAA R CCACACAATACAGCCCTCAA
	<i>POCP3</i>	TR41545	KU744674	F CTTGGCTCAAACCCGAAATA R GCAAGCCAAGGTGAAACTC
	<i>POCP4</i>	TR45083	—NA—	F GAGGTTCACTTCTCCCTGT R CACCCGGCGATTACACTAC
<i>H. perforatum</i>	<i>POCP1</i>	TR93881	KU744669	F CCGATTCTCCGAGTTGAA R CTCAGGTTCTCCATCTCAA
	<i>POCP2</i>	TR82269	KU744670	F CCAGTGACCCATTATAACCACAA R GCAACACGATAACATCCCTCA
	<i>POCP3</i>	TR24220	KU744671	F CTTGGCTCAAACCCGAAATA R AAAGGCGAAGTCGAACCTCAA
	<i>POCP4</i>	TR1044	—NA—	F GAGGTTCACTTCTCCCTGT R CACCCGGCGATTACACTAC
<i>H. tomentosum</i>	<i>POCP1</i>	TR47529	KU744675	F CCGATTCTCCGAGTTGAA R CACTCAGATTCTCCATCTCAA
	<i>POCP2</i>	TR38948	KU744676	F AACCAAGTGACCCATTACACCA R GCAACACAATACAGCCCTCA
	<i>POCP3</i>	TR8620	KU744677	F CTTGGCTCAAACCCGAAATA R GCAAGCCAAGGTGAAACTC
	<i>POCP4</i>	TR5871	—NA—	F TCTCCCCTAACCCACAAAAAA R GACTTCCACGACACGATTCA

TABLE 2 | Statistics of the sequencing output and preprocessed data.

Sample description		Read quality							
Hypericum species	Material	Total reads (Gb)	%Q20 before filter	%Q20 after filter	%GC before filter	%GC after filter	Filter adapter	Filter low quality	Clean reads (Gb)
<i>H. annulatum</i>	Marginal parts of the leaves with dark nodules	5.75	96.88	98.25	50.23	50.21	3.24	2.79	5.4
<i>H. annulatum</i>	Inner part of leaves without dark nodules	5.83	96.63	98.15	50.93	50.87	3.2	2.97	5.47
<i>H. tomentosum</i>	Apical parts of the leaves with dark nodules	4.56	96.58	98.24	50.18	50.13	4.04	2.91	4.24
<i>H. tomentosum</i>	Inner parts of the leaves without dark nodules	6.42	96.67	98.16	50.35	50.3	3.88	3.05	5.98
<i>H. androsaemum</i>	Whole leaves	5.6	96.76	98.16	54.49	51.45	3.19	2.94	5.26
<i>H. kalmianum</i>	Whole leaves	5.21	96.94	98.27	50.46	50.42	3.49	2.71	4.89

first leaf transcriptome of *H. androsaemum*, *H. annulatum*, *H. kalmianum*, and *H. tomentosum* was generated. The CD-HIT program followed by SeqClean removed redundant and similar isoforms. The high-quality transcriptomes of different *Hypericum* ssp. were created and described in **Table 3**.

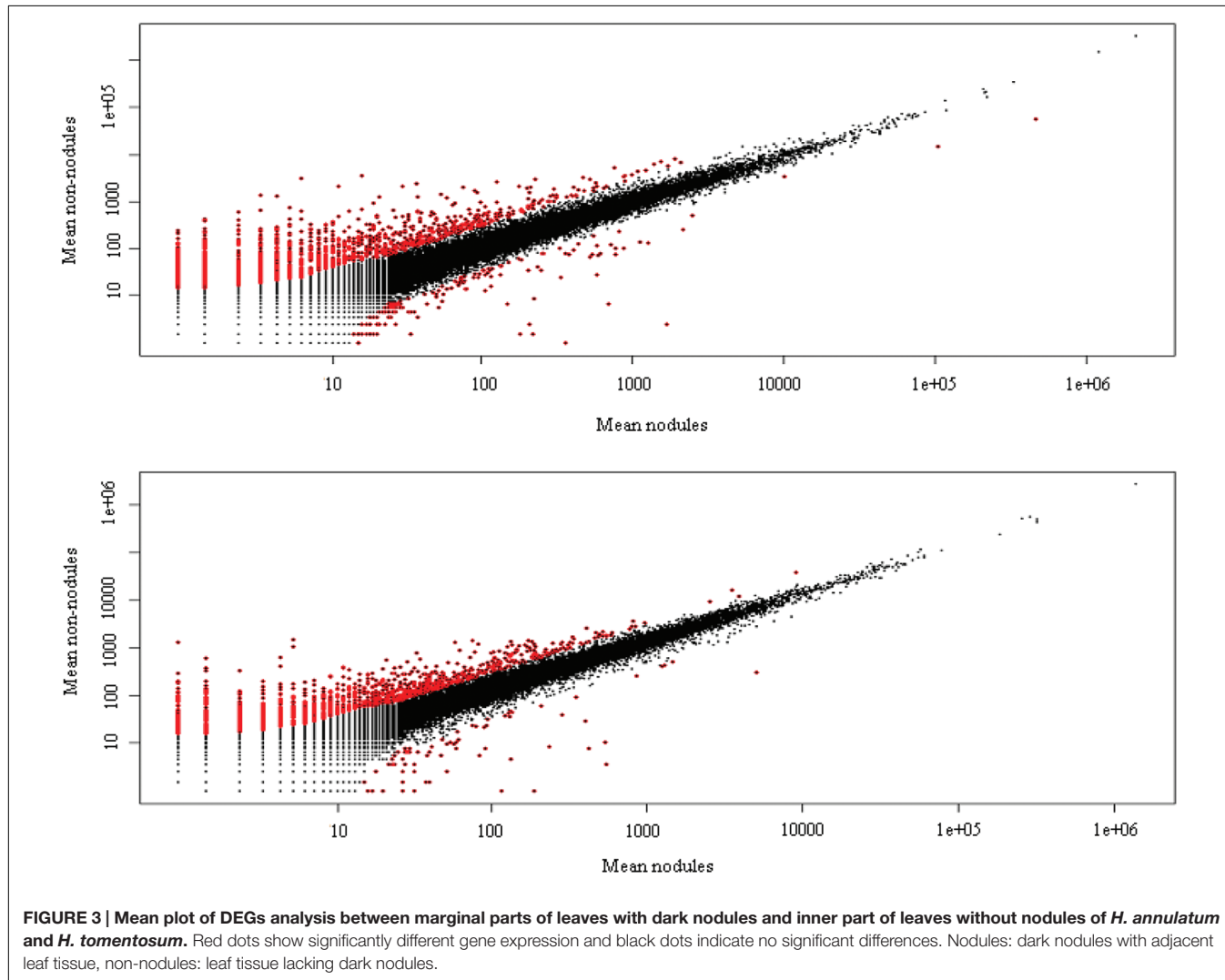
Identification and Validation of Differentially Expressed Contigs

Cleaned reads of *H. annulatum* and *H. tomentosum* as the hypericin producers were separately aligned (Bowtie2) to *de novo* assembled transcriptomes. Transcripts abundances were

normalized using RSEM package and fragments per kilobase of transcript per million fragments mapped value (FPKM) were estimated. Differential expression analyses between the parts of the leaves with dark nodules and the inner part leaf tissues without dark nodules were performed for both species separately. DE analysis ran on the basis of three different R packages (DESeq, edgeR, and NOISeq) at the values of var = 0.05 and P < 0.05 (**Figure 3**). We attained 165 contigs (135 DEGs) for *H. annulatum* and 100 contigs (72 DEGs) for *H. tomentosum* upregulated in the leaf tissues containing dark nodules (**Supplementary Tables S2 and S3**). The qRT-PCR was applied for experimental

TABLE 3 | Statistics of transcriptome de novo assembly.

<i>Hypericum</i> species	Total assembled bases	Total trinity genes	Contig N50	Average contig	Percent GC (%)
<i>H. annulatum</i>	91,602,062	60,611	1771	1077.27	45.04
<i>H. tomentosum</i>	92,533,952	59,872	1851	1131.87	44.89
<i>H. androsaemum</i>	84,822,534	60,041	1602	991.01	46.08
<i>H. kalmianum</i>	74,609,783	51,244	1642	1018.51	45.19

**FIGURE 3 | Mean plot of DEGs analysis between marginal parts of leaves with dark nodules and inner part of leaves without nodules of *H. annulatum* and *H. tomentosum*.** Red dots show significantly different gene expression and black dots indicate no significant differences. Nodules: dark nodules with adjacent leaf tissue, non-nodules: leaf tissue lacking dark nodules.

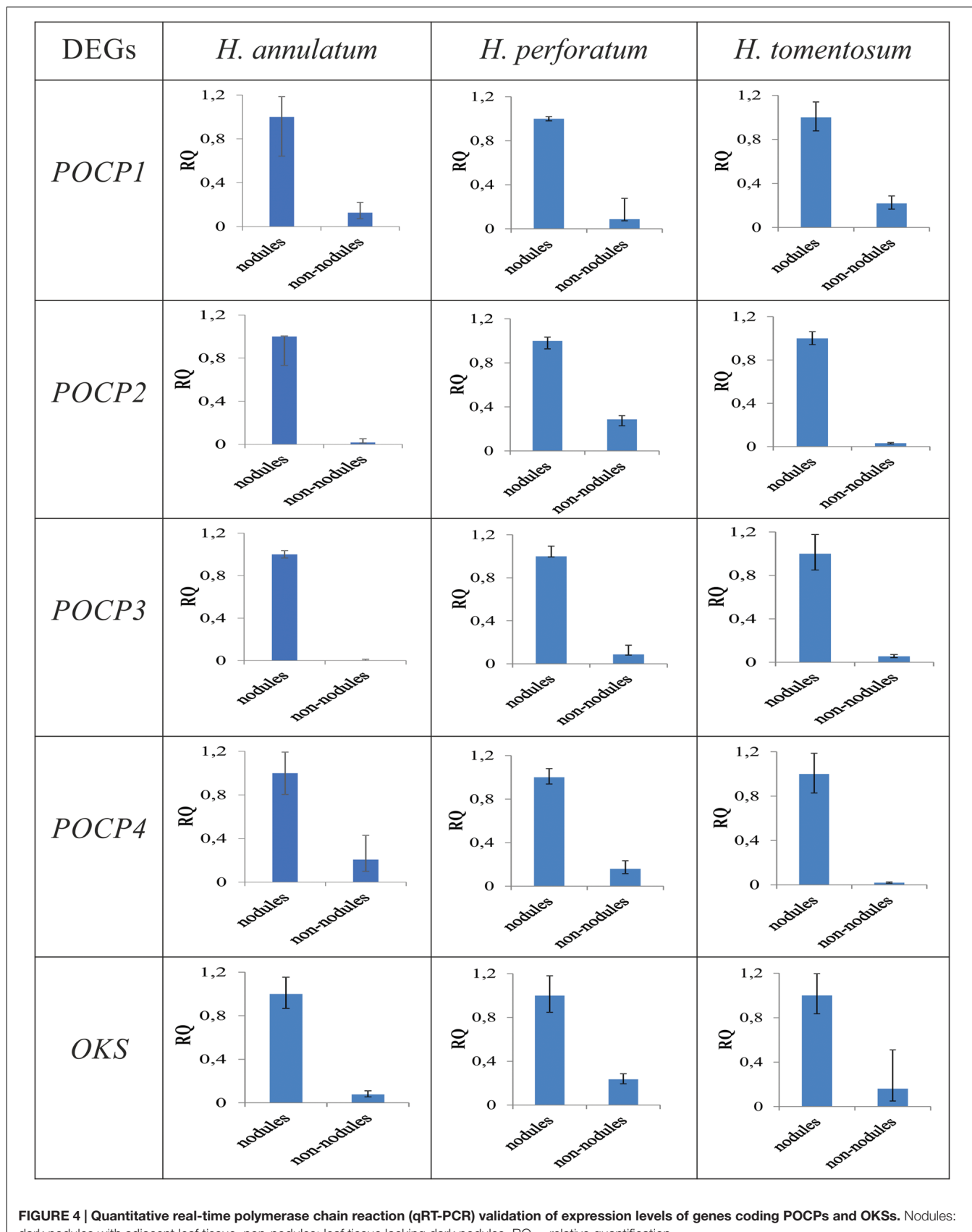
confirmation of the computational analysis. Five DEGs with significant transcript abundance changes were subjected to the validation. Normalized relative ratios based on $\Delta\Delta C_t$ method were calculated to estimate relative quantification of the expression level. The expression patterns in qRT-PCR were in agreement with the transcriptomic data for all the detected genes (Figure 4).

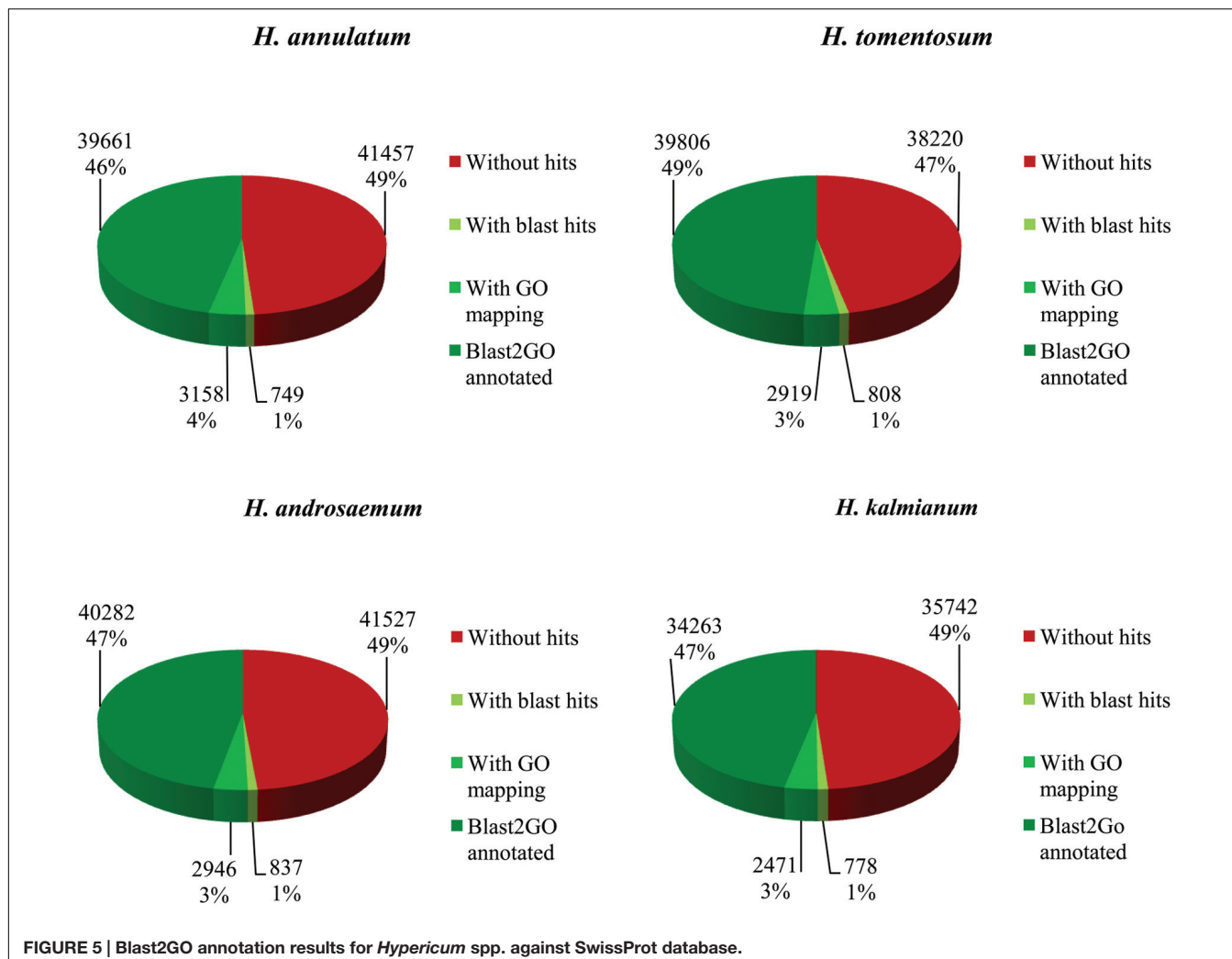
Functional Annotation and Classification

Gene categorization was conducted by homology search blastx against SwissProt and NCBI non-redundant protein database (NCBI-nr) with a cut-off E -value of 1×10^{-5} . SwissProt

database was used to process basic functional information for the transcriptomes from all four species. Due to limited genomic information about the selected *Hypericum* spp. only lower coverage of annotated data was achieved. Approximately 50% of contigs showed blastx hit to SwissProt (Figure 5).

We presume the key enzymes for most of the processes including secondary metabolism of specific compounds share similar coding sequences. GO classification was carried out to show cellular component, molecular function and biological process primary distribution (Figure 6). Highly similar numbers of GO terms for all four studied *Hypericum* spp. were discovered. The most frequent subcategories in Biological Process section





were cellular, metabolic and single organism processes. The most common terms in Molecular Function were binding and catalytic activities.

The transcriptomes of *H. androsaemum* and *H. kalmianum* were annotated also to NCBI-nr and used as the negative control to contigs originated from hypericin producing *H. annulatum* and *H. tomentosum* DEGs. Almost 70% of contigs showed blastx hit to NCBI-nr (Figure 7). Hypericin producing species *H. annulatum* and *H. tomentosum* DEGs upregulated in leaf rim containing dark nodules were blasted against NCBI-nr additionally. Functional annotation was improved as the SwissProt database did not cover rich variety of not yet verified genes from non-model species. The most frequent GO subcategories for DEGs were metabolic process and catalytic activity. The distribution of the major GO subcategories in all of the *Hypericum* spp. for NCBI-nr annotated transcriptomes was comparable (Figure 8).

Blast2GO analysis of species distribution showed unexpected transcriptome similarity of *Hypericum* spp. to *Jatropha curcas* L. despite of considerable taxonomical distance. *Hypericum* spp. are known for its similarity to genera *Populus*, *Ricinus*, and *Vitis*

vinifera of which rRNAs sequences are used to mRNA set clean up (Figure 9).

Contigs Supposedly Related to Hypericin Biosynthesis

The genetic and metabolomic background of hypericin biosynthesis led us to lay our interest in two groups of crucial enzymes, OKSs and POCPs. *HpPKS2*, the gene coding OKS was expressed in dark nodules (Karppinen et al., 2008). OKSs are supposed to play key role in the reaction of emodin anthrone formation. The gene coding POCP (*hyp-1*) has been originally reckoned as the gene capable to catalyze conversion of precursor emodin to hypericin (Bais et al., 2003). Although this presumption has never been proved, it is possible, the different gene variant coding POCP homologous to *hyp-1* may catalyze this reaction.

The sequence alignment of the *HpPKS2* (EU635882.1) to transcriptomes discovered presence of five contigs in *H. perforatum* (Soták et al., 2016), six contigs in *H. annulatum*, two contigs in *H. tomentosum*, three contigs in *H. androsaemum*

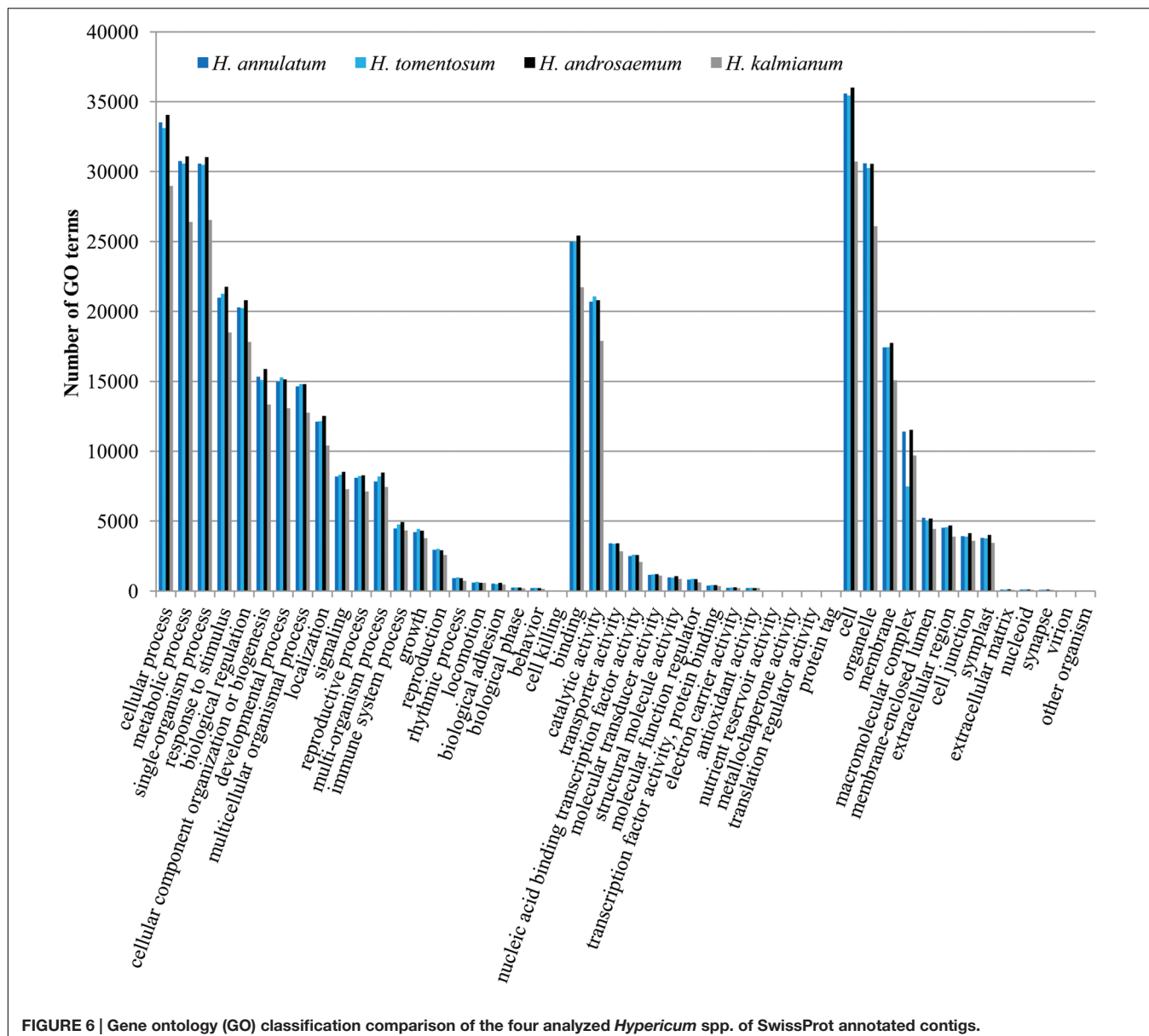
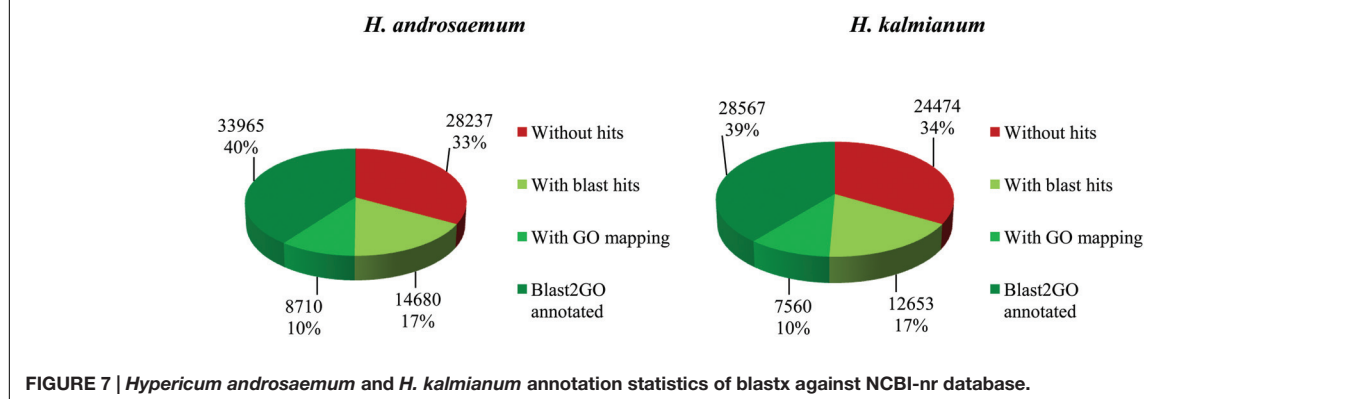


FIGURE 6 | Gene ontology (GO) classification comparison of the four analyzed *Hypericum* spp. of SwissProt annotated contigs.



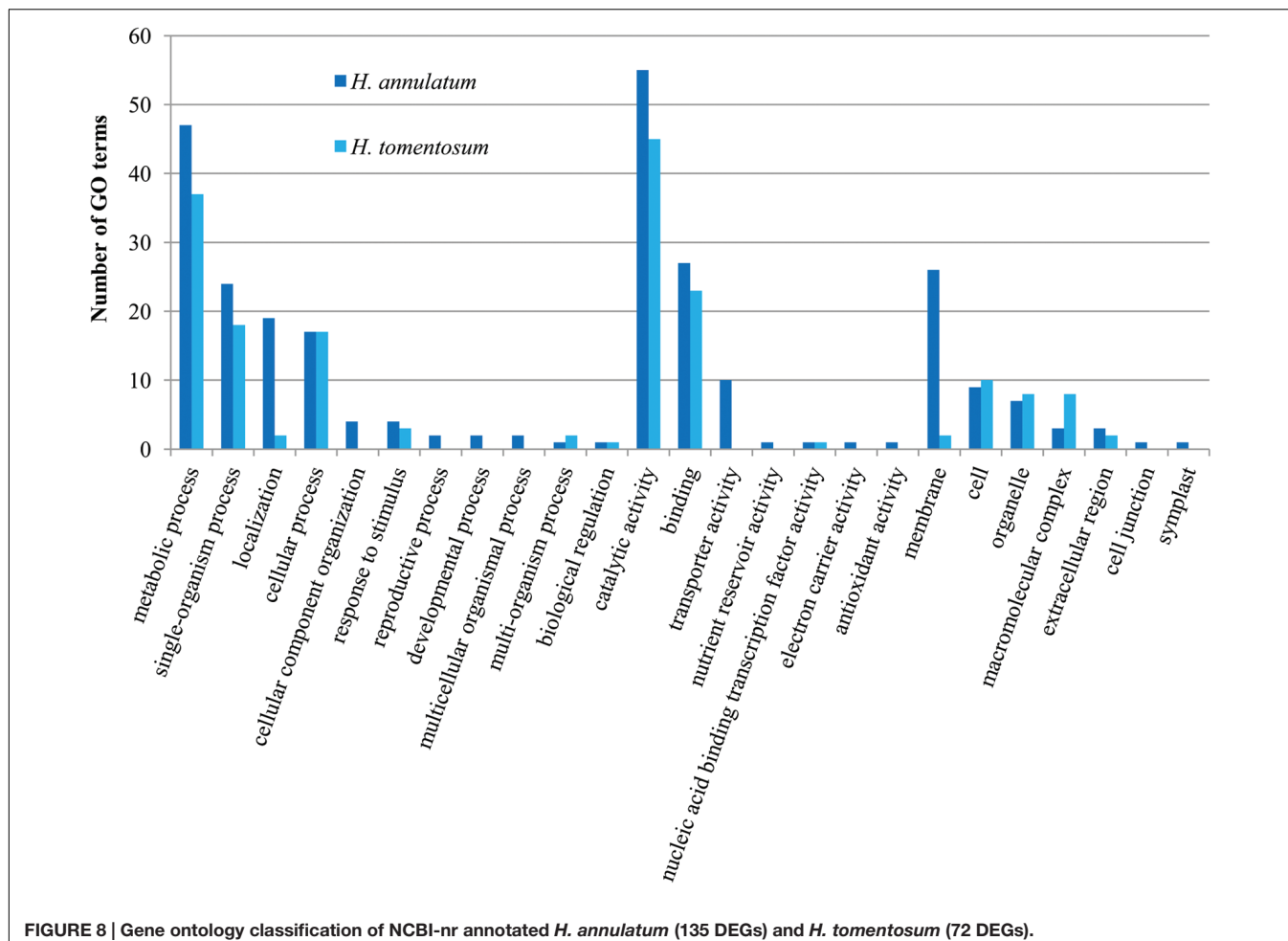


FIGURE 8 | Gene ontology classification of NCBI-nr annotated *H. annulatum* (135 DEGs) and *H. tomentosum* (72 DEGs).

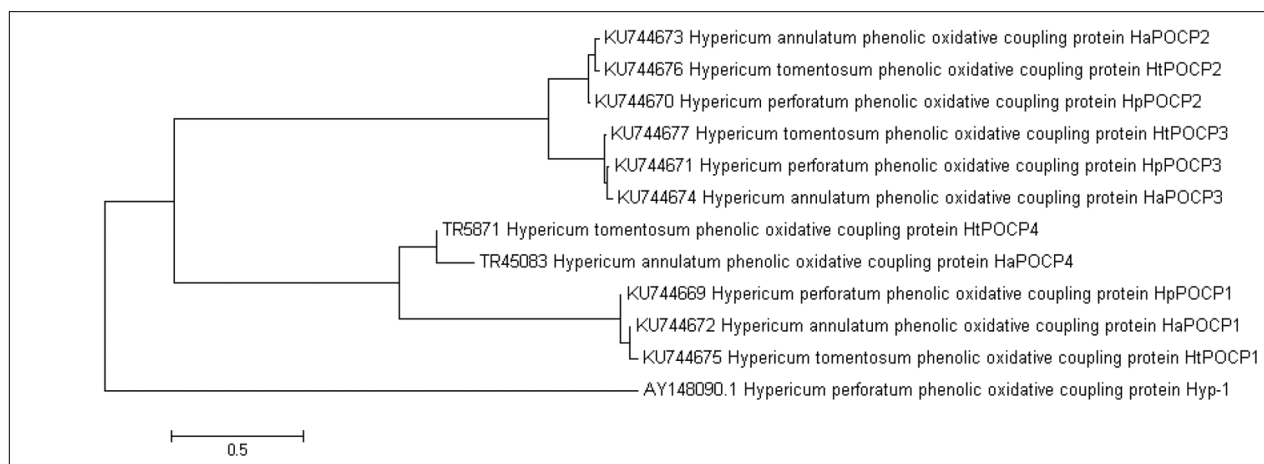
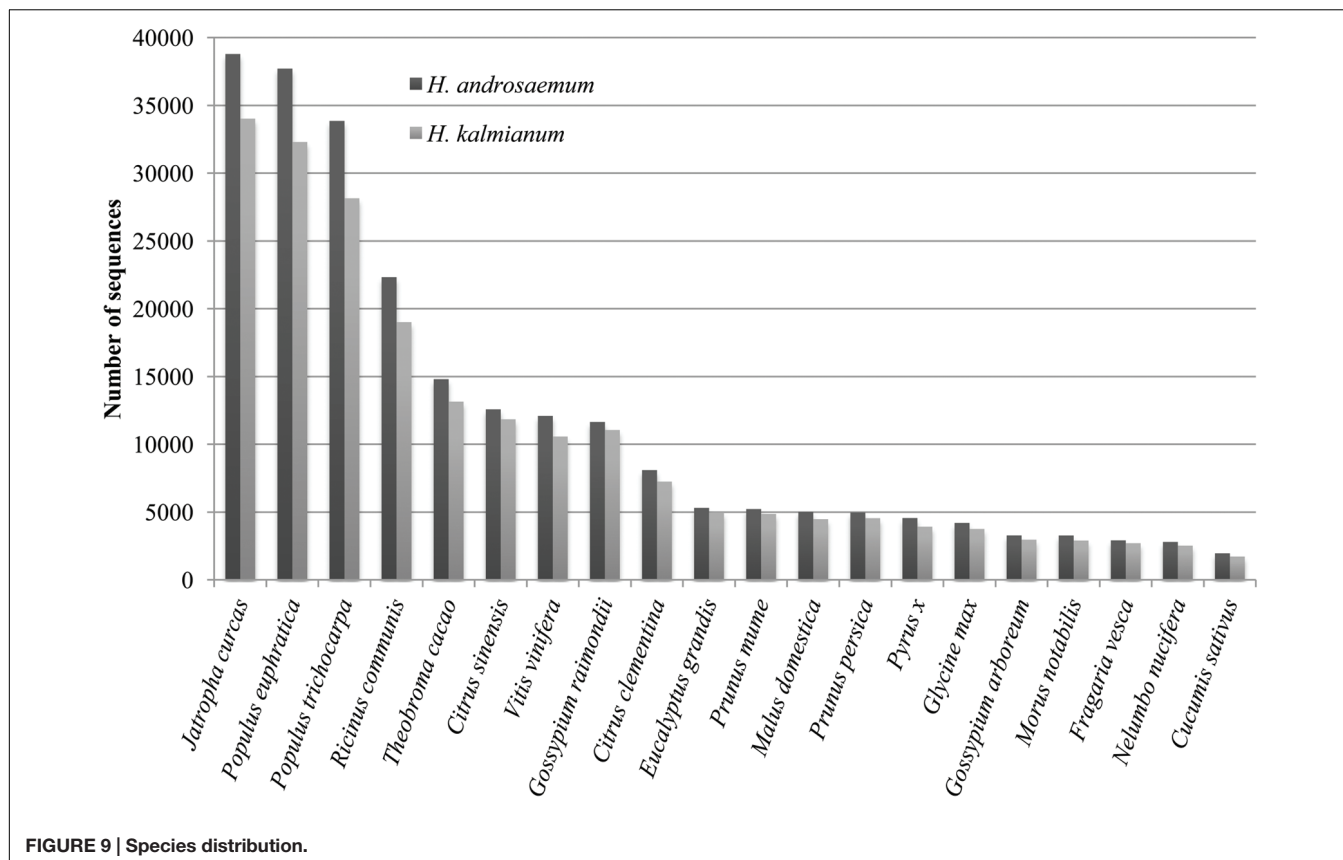
and one single contig in *H. kalmianum*. The sequence homology search identified DEGs annotated as genes coding OKS in *H. annulatum* (3 contigs), *H. perforatum* (1 contig), and *H. tomentosum* (2 contigs). The sequence alignment of hypericin producing *Hypericum* spp. discovered one particular OKS DEG with only little variation and meaningful match to *HpPKS2* published by Karppinen et al. (2008) with sequence identity higher than 97%. *H. kalmianum* and *H. androsaemum* shared one similar gene coding OKS with sequence different from OKS genes found in hypericin producing species and Karppinen's *HpPKS2* with the sequence identity about 70%.

This transcriptomic study demonstrated the existence of more genes and isoforms resembling to POCP *hyp-1* sequence (AY148090.1). Blast2GO annotation of leaf transcriptomes against NCBI-nr database revealed genes supposedly coding POCPs in both hypericin producing and non-producing species: *H. annulatum* (8 genes, 9 isoforms), *H. perforatum* (14 genes, 21 isoforms) and *H. tomentosum* (15 genes, 17 isoforms), *H. androsaemum* (14 genes, 20 isoforms), *H. kalmianum* (8 genes, 16 isoforms), highly similar to *hyp-1*. The sequence homology analysis of DEGs in hypericin producing species detected three different gene forms supposedly coding POCPs common for *H. perforatum* (KU744669, KU744670, and KU744671),

H. annulatum (KU744672, KU744673, and KU744674) and *H. tomentosum* (KU744675, KU744676, and KU744677) and one form common for *H. annulatum* and *H. tomentosum* (Figure 10). NCBI Open Reading Frame Finder identified the coding sequences of the same length in predicted POCP gene forms: POCP1 (471 bp), POCP2 (483 bp), POCP3 (477 bp), and POCP4 (480 bp). These lengths corresponded to the length of *hyp-1* coding sequence from *H. perforatum* (480 bp). The sequence identity within each proposed gene coding POCP varied from 95 to 98% and showed significant divergence to *hyp-1* sequence. *Hyp-1* did not occur among DEGs upregulated in tissues containing dark nodules.

DISCUSSION

The presented paper contributes to fill the blank space in transcriptome profiling of *Hypericum* spp. Nowadays, the only transcriptomic information within the genus *Hypericum* is available for *H. perforatum*, representing the “model” species of the genus. This is the first high throughput RNA-Seq description of *H. annulatum*, *H. tomentosum*, *H. androsaemum*, and *H. kalmianum* transcriptomes. Our major interest was aimed

**FIGURE 10 | Neighbor joining tree of POCP sequences.**

at identification of secondary metabolites coding genes especially those associated to naphtodianthrone hypericin. Differential expression analysis on RNA-Seq data was selected to uncover contigs upregulated in the leaf parts containing dark nodules and adjacent tissues. The experimental selection of contrasting leaf tissues with/without dark nodules (leaf rim vs. leaf middle) for differential gene expression analysis was based on the latest metabolomic results. Kusari et al. (2015) analyzed leaves excised from *ex vitro* cultivated *H. perforatum* plants by MALDI-HRMS

method. Kucharíková et al. (2016) used DESI-MSI for qualitative characterization of metabolome of the leaf tissues from 17 *Hypericum* spp. including same *in vitro* cultured clones as in the current transcriptomic study. The occurrence of hypericin in proximity of dark nodules was approved in *H. annulatum*, *H. perforatum*, and *H. tomentosum*, while in *H. androsaemum* and *H. kalmianum* it was not detected. According to metabolomic data it is predicted that at least the final steps of hypericin biosynthesis are situated to the leaf parts containing nodules

and adjacent tissues. HPLC analysis added quantitative values of polyketides content of selected *Hypericum* spp. leaves.

Three different Bioconductor packages listed 165 contigs in *H. annulatum* and 100 contigs in *H. tomentosum* as significantly differentially expressed ($P < 0.05$) and upregulated in the leaf rim tissues containing the dark nodules. The number of DEGs upregulated in leaf tissues containing dark nodules was significantly lower in comparison to DESeq2 analysis of two technical replicates *H. perforatum* revealing 799 DEGs sequences with 2058 isoforms (Soták et al., 2016). As the current analysis ran solely on the biological replicates, NOISeq-sim script from the NOISeq package simulated technical replicates in this interspecific approach survey and the final results showed only a smaller number of highly significant DEGs hits.

According to the GO classification of the contigs, the section Biological Process, subcategory Metabolic Process represented the second largest group for all four *Hypericum* spp. and for DEGs upregulated in leaf tissues containing dark nodules appeared as the most frequent group. These classification findings highly correspond to the recent studies on *H. perforatum* transcriptome from the whole plant (He et al., 2012) and the transcriptome from leaf tissues (Soták et al., 2016). On the other hand, a comparison between hyperforin-producing *H. annulatum* and hyperforin-lacking *H. tomentosum* revealed a significant difference in the section Macromolecular complex.

The sequence analysis of DEGs in *H. perforatum*, *H. annulatum*, *H. tomentosum*, and hypericin non-producing *H. kalmianum* and *H. androsaemum* (NCBI-nr annotated) including already published sequences in NCBI-nr database showed meaningful inter and intra species variations for both of focused enzymes. We investigated the presence and expression levels of the *HpPKS2* (Karppinen et al., 2008) and *hyp-1* (Bais et al., 2003). Contigs coding OKSs were found in all *Hypericum* transcriptomes but OKS gene sequences from hypericin non-producing species were more different from *HpPKS2*. We suppose that OKS gene sequences identified among DEGs in hypericin producing species may play a role in hypericin biosynthesis. Differential gene expression analysis revealed four novel genes supposedly coding POCP belonging to PR-10 class proteins. Although four different gene forms of the proposed POCPs were annotated in DEGs, none of them was highly similar to *hyp-1*. The whole transcriptome annotation of *H. perforatum* against NCBI-nr discovered 14 genes, 21 isoforms coding PR-10 proteins. Karppinen et al. (2016) identified four different genes coding PR-10: *HpPR10.2*, *HpPR10.3*, *HpPR10.4*, and *HpPR10.1* representing *hyp-1* sequence. The transcriptomic study of *H. perforatum* validated the presence of all sequences published by Karppinen et al. (2016).

The *hyp-1* was also expressed in the other 15 *Hypericum* species regardless of whether hypericins and emodin were detected in the plants (Košuth et al., 2011). We assume, though the *hyp-1* was not found in DEGs of hypericin producing species but was present only in the transcriptome datasets of all four studied *Hypericum* spp. regardless they synthesize hypericin or not, the probability of *hyp-1* to represent the crucial component of emodin to hypericin conversion is doubtful.

CONCLUSION

This study was objected to elucidate hypericin biosynthesis pathway by approach of interspecific differential gene expression analysis of leaf tissues with/without dark nodules and hypericin-producing and hypericin-lacking species. We have generated six new RNA-Seq libraries of *Hypericum* spp. followed by sequencing and bioinformatic analysis with the focus on biological properties to reveal unknown features of genes, proteins, metabolites, and biological pathways. The results proved existence of the most of differentially expressed contigs in *H. annulatum*, *H. perforatum*, and *H. tomentosum*, as they supposedly share the same hypericin biosynthetic pathway steps. Sequence alignment homology of DEGs upregulated in tissues containing dark nodules identified presence of contigs highly similar to *HpPKS2*. Hypericin non-producing species uncovered contigs with only low homology to *HpPKS2*. New variants of cDNAs coding enzyme catalyzing phenolic oxidative coupling reactions were recognized in the dataset of DEGs from the tested hypericin producing species. We suppose that different variant of proposed POCP may play a role in hypericin biosynthesis. This presumption will be further verified by functional validation experimental approaches.

AVAILABILITY OF SUPPORTING DATA

The RNA sequence dataset supporting the results in this article are available in the NCBI Sequence Read Archive. The accession number are SRX1528960 (*H. annulatum* leaves with dark nodules), SRX1528962 (*H. annulatum* leaves without dark nodules), SRX1528963 (*H. tomentosum* leaves with dark nodules), SRX1528964 (*H. tomentosum* leaves without dark nodules), SRX1528157 (*H. androsaemum*) and SRX1528958 (*H. kalmianum*). The nucleotide sequence of genes coding POCPs are available in the NCBI GenBank submitted through BankIt for *H. annulatum* (KU744672, KU744673, and KU744674), *H. perforatum* (KU744669, KU744670, and KU744671) and *H. tomentosum* (KU744675, KU744676, and KU744677).

AUTHOR CONTRIBUTIONS

MS designed the study, concluded the analyses and drafted the manuscript. OC prepared samples, analyzed the data, performed the validations, and drafted the manuscript. DK conducted the DEG analysis. ZJ analyzed the data and performed the validations. LL participated on Illumina sequencing, revised the manuscript. EC designed the study, directed on the study and revised the manuscript. All authors read and approved the final manuscript.

ACKNOWLEDGMENTS

This research was supported by the Slovak Research and Development Agency APVV-14-0154, the Scientific Grant Agency of Slovak Republic VEGA 1/0090/15 and the grant

project SOFOS-knowledge and skill development of staff, students of P. J. Šafárik University in Košice (contract number: 003/2013/1.2/OPV, ITMS code: 26110230088), funded by the European Social Fund through the Operational Program Education. We thank Linda Petijová and Katarína Nigutová from Department of Genetics, Institute of Biology and Ecology, Faculty of Science, Pavol Jozef Šafárik University in Košice and Tomáš Horváth, Pavol Sokol, Maroš Andrejko from Institute of Computer Sciences, Faculty of Science, Pavol Jozef Šafárik University in Košice and Libuše Brachová from Roy J. Carver Department of Biochemistry, Biophysics and Molecular Biology, Iowa State University for support. We thank BGI Americas for contributing its expertise in genomic sequencing and bioinformatics analysis to provide processed sequencing data. Part of the calculations were performed in the Computing Centre of the Slovak Academy of Sciences

using the supercomputing infrastructure acquired in project ITMS 26230120002 and 26210120002 (Slovak infrastructure for high-performance computing) supported by the Research & Development Operational Programme funded by the ERDF.

SUPPLEMENTARY MATERIAL

The Supplementary Material for this article can be found online at: <http://journal.frontiersin.org/article/10.3389/fpls.2016.01039>

TABLE S1 | Polyketides content measured by HPLC ($\mu\text{g.mg}^{-1}$).

TABLE S2 | Counts and FPKM values of *H. annulatum* DEGs annotated on NCBI-nr.

TABLE S3 | Counts and FPKM values of *H. tomentosum* DEGs annotated on NCBI-nr.

REFERENCES

- Agostinis, P., Vantieghem, A., Merlevede, W., and de Witte, P. A. (2002). Hypericin in cancer treatment: more light on the way. *Int. J. Biochem. Cell Biol.* 34, 221–241. doi: 10.1016/S1357-2725(01)00126-1
- Anders, S., and Huber, W. (2010). Differential expression analysis for sequence count data. *Genome Biol.* 11:R106. doi: 10.1186/gb-2010-11-10-r106
- Bais, H. P., Vepachedu, R., Lawrence, C. B., Sternitz, F. R., and Vivanco, J. M. (2003). Molecular and biochemical characterization of an enzyme responsible for the formation of hypericin in St. John's wort (*Hypericum perforatum* L.). *J. Biol. Chem.* 278, 32413–32422. doi: 10.1074/jbc.M301681200
- Birt, D. F., Widrlechner, M. P., Hammer, K. D., Hillwig, M. L., Wei, J., Kraus, G. A., et al. (2009). Hypericum in infection: identification of anti-viral and anti-inflammatory constituents. *Pharm. Biol.* 47, 774–782. doi: 10.1080/13880200902988645
- Bruňáková, K., and Čellárová, E. (2016). Conservation strategies in the genus *Hypericum* via cryogenic treatment. *Front. Plant Sci.* 7:558. doi: 10.3389/fpls.2016.00558
- Butterweck, V. (2003). Mechanism of action of St John's wort in depression: what is known? *CNS Drugs* 17, 539–562. doi: 10.2165/00023210-200317080-00001
- Conesa, A., and Götz, S. (2008). Blast2GO: a comprehensive suite for functional analysis in plant genomics. *Int. J. Plant Genomics* 2008:619832. doi: 10.1155/2008/619832
- Fernandes, H., Michalska, K., Sikorski, M., and Jaskolski, M. (2013). Structural and functional aspects of PR-10 proteins. *FEBS J.* 5, 1169–1199. doi: 10.1111/febs.12114
- Fu, L., Niu, B., Zhu, Z., Wu, S., and Li, W. (2012). CD-HIT: accelerated for clustering the next generation sequencing data. *Bioinformatics* 28, 3150–3152. doi: 10.1093/bioinformatics/bts565
- Gamborg, O. L., Miller, R. A., and Ojima, K. (1968). Nutrient requirements of suspension cultures of soybean root cells. *Exp. Cell Res.* 50, 151–158. doi: 10.1016/0014-4827(68)90403-5
- Grabher, M. G., Haas, B. J., Yassour, M., Levin, J. Z., Thompson, D. A., Amit, I., et al. (2011). Full-length transcriptome assembly from RNA-Seq data without a reference genome. *Nat. Biotechnol.* 29, 644–652. doi: 10.1038/nbt.1883
- He, M., Wang, Y., Hua, W., Zhang, Y., and Wang, Z. (2012). De novo sequencing of *Hypericum perforatum* transcriptome to identify potential genes involved in the biosynthesis of active metabolites. *PLoS ONE* 7:e42081. doi: 10.1371/journal.pone.0042081
- Karppinen, K., Derzsó, E., Jaakola, L., and Hohtola, A. (2016). Molecular cloning and expression analysis of *hyp-1* type PR-10 family genes in *Hypericum perforatum*. *Front. Plant Sci.* 7:526. doi: 10.3389/fpls.2016.00526
- Karppinen, K., Hokkanen, J., Mattila, S., Neubauer, P., and Hohtola, A. (2008). Octaketide-producing type III polyketide synthase from *Hypericum perforatum* is expressed in dark glands accumulating hypericin. *FEBS J.* 275, 4329–4342. doi: 10.1111/j.1742-4658.2008.06576.x
- Košuth, J., Katkovčinová, Z., Oleksová, P., and Čellárová, E. (2007). Expression of the *hyp-1* gene in early stages of development of *Hypericum perforatum* L. *Plant Cell. Rep.* 26, 211–217. doi: 10.1007/s00299-006-0240-4
- Košuth, J., Smelcerovič, A., Borsch, T., Zuehlke, S., Karppinen, K., Spiteller, M., et al. (2011). The *hyp-1* gene is not a limiting factor for hypericin biosynthesis in the genus *Hypericum*. *Funct. Plant Biol.* 38, 35–43. doi: org/10.1071/FP10144
- Kucharíková, A., Kimáková, K., Janfelt, C., and Čellárová, E. (2016). Interspecific variation in localization of hypericins and phloroglucinols in the genus *Hypericum* as revealed by desorption electrospray ionization mass spectrometry imaging. *Physiol. Plant.* 157, 2–12. doi: 10.1111/plp.12422
- Kusari, S., Selahaddin, S., Nigutova, K., Cellarova, E., and Spiteller, M. (2015). Spatial chemo-profiling of hypericin and related phytochemicals in *Hypericum* species using MALDI-HRMS imaging. *Anal. Bioanal. Chem.* 407, 4779–4791. doi: 10.1007/s00216-015-8682-6
- Langmead, B., and Salzberg, S. L. (2012). Fast gapped-read alignment with Bowtie2. *Nat. Methods* 4, 357–359. doi: 10.1038/NMETH.1923
- Li, B., and Dewey, C. N. (2011). RSEM: accurate transcript quantification from RNA seq data with or without a reference genome. *BMC Bioinformatics* 12:323. doi: 10.1186/1471-2105-12-323
- Murashige, T., and Skoog, F. (1962). A revised medium for rapid growth and bioassays with tobacco tissue cultures. *Plant Physiol.* 15, 473–497. doi: 10.1111/j.1399-3054.1962.tb08052.x
- Myhre, S., Tveit, H., Mollestad, T., and Laegreid, A. (2006). Additional gene ontology structure for improved biological reasoning. *Bioinformatics* 22, 2020–2027. doi: 10.1093/bioinformatics/btl334
- Nürk, N. M., Uribe-Convers, S., Gehrke, B., Tank, D. C., and Blattner, F. R. (2013). Molecular phylogenetics and morphological evolution of St. John's wort (*Hypericum*; Hypericaceae). *Mol. Phylogenet. Evol.* 66, 1–16. doi: 10.1186/s12862-015-0359-4
- Robinson, M. D., McCarthy, D. J., and Smyth, G. K. (2010). edgeR: a bioconductor package for differential expression analysis of digital gene expression data. *Bioinformatics* 26, 139–140. doi: 10.1093/bioinformatics/btp616
- Robson, N. K. B. (2003). "Hypericum botany," in *Hypericum – The Genus Hypericum*, ed. E. Ernst (London: Taylor and Francis), 1–22. doi: 10.1016/j.ymprev.2012.08.022
- Silva, B. A., Ferreres, F., Malva, J. O., and Dias, A. C. P. (2005). Phytochemical and antioxidant characterization of *Hypericum perforatum* alcoholic extracts. *Food Chem.* 90, 57–167. doi: 10.1016/j.foodchem.2004.03.049
- Soták, M., Czeranková, O., Klein, D., Nigutová, K., Altschmied, L., Li, L., et al. (2016). Differentially expressed genes in hypericin-containing

- Hypericum perforatum* leaf tissues as revealed by de novo assembly of RNA-Seq. *Plant Mol. Biol. Rep.* (in press). doi 10.1007/s11105-016-0982-2
- Tamura, K., Stecher, G., Peterson, D., Filipski, A., and Kumar, S. (2013). MEGA6: molecular evolutionary genetics analysis version 6.0. *Mol. Biol. Evol.* 30, 2725–2729. doi: 10.1093/molbev/mst197
- Tarazona, S., García-Alcalde, F., Ferrer, A., Dopazo, J., and Conesa, A. (2011). Differential expression in RNA-Seq: a matter of depth. *Genome Res.* 12, 2213–2223. doi: 10.1101/gr.124321.111
- Untergasser, A., Cutcutache, I., Koressaar, T., Ye, J., Faircloth, B. C., Remm, M., et al. (2012). Primer3 - new capabilities and interfaces. *Nucleic Acids Res.* 40:e115. doi: 10.1093/nar/gks596
- Zobayed, S. M., Afreen, F., Goto, E., and Kozai, T. (2006). Plant-environment interactions: accumulation of hypericin in dark glands of *Hypericum perforatum*. *Ann. Bot.* 98, 793–804. doi: 10.1093/aob/mcl169

Conflict of Interest Statement: The authors declare that the research was conducted in the absence of any commercial or financial relationships that could be construed as a potential conflict of interest.

The handling Editor declared an ongoing collaboration, the co-editing of a Frontiers Research Topic, with one of the authors EC, but states that no other conflict of interest exists and that the review process was nevertheless fair and objective.

Copyright © 2016 Soták, Czeranková, Klein, Jurčácková, Li and Čellárová. This is an open-access article distributed under the terms of the Creative Commons Attribution License (CC BY). The use, distribution or reproduction in other forums is permitted, provided the original author(s) or licensor are credited and that the original publication in this journal is cited, in accordance with accepted academic practice. No use, distribution or reproduction is permitted which does not comply with these terms.



A Perspective on *Hypericum perforatum* Genetic Transformation

Weina Hou^{1†}, Preeti Shakya^{2†} and Gregory Franklin^{1,2*}

¹ Centre for the Research and Technology of Agro-Environment and Biological Sciences, University of Minho, Braga, Portugal,

² Department of Integrative Plant Biology, Institute of Plant Genetics of the Polish Academy of Sciences, Poznan, Poland

OPEN ACCESS

Edited by:

Thomas Vogt,
Leibniz Institute of Plant Biochemistry,
Germany

Reviewed by:

Qing Liu,
Commonwealth Scientific and
Industrial Research Organisation,
Australia
Gary John Loake,
University of Edinburgh, UK

***Correspondence:**

Gregory Franklin
fgre@igr.poznan.pl

[†]These authors have contributed
equally to this work.

Specialty section:

This article was submitted to
Plant Metabolism and Chemodiversity,
a section of the journal
Frontiers in Plant Science

Received: 15 March 2016

Accepted: 03 June 2016

Published: 24 June 2016

Citation:

Hou W, Shakya P and Franklin G
(2016) A Perspective on *Hypericum perforatum* Genetic Transformation.
Front. Plant Sci. 7:879.
doi: 10.3389/fpls.2016.00879

Hypericum perforatum (St John's wort) is a reservoir of diverse classes of biologically active and high value secondary metabolites, which captured the interest of both researchers and the pharmaceutical industry alike. Several studies and clinical trials have shown that *H. perforatum* extracts possess an astounding array of pharmacological properties. These properties include antidepressant, anti-inflammatory, antiviral, anti-cancer, and antibacterial activities; and are largely attributed to the naphtodianthrone and xanthones found in the genus. Hence, improving their production via genetic manipulation is an important strategy. In spite of the presence of contemporary genome editing tools, genetic improvement of this genus remains challenging without robust transformation methods in place. In the recent past, we found that *H. perforatum* remains recalcitrant to *Agrobacterium tumefaciens* mediated transformation partly due to the induction of plant defense responses coming into play. However, *H. perforatum* transformation is possible via a non-biological method, biolistic bombardment. Some research groups have observed the induction of hairy roots in *H. perforatum* after *Agrobacterium rhizogenes* co-cultivation. In this review, we aim at updating the available methods for regeneration and transformation of *H. perforatum*. In addition, we also propose a brief perspective on certain novel strategies to improve transformation efficiency in order to meet the demands of the pharmaceutical industry via metabolic engineering.

Keywords: *Agrobacterium tumefaciens*, *A. rhizogenes*, *Hypericum perforatum*, hairy root culture, biolistic bombardment, metabolic engineering, regeneration

INTRODUCTION

Hypericum perforatum is one of the most important and well-known species of the *Hypericum* genus, which has been appreciated by Greek herbalists for its medicinal value since the first century A.D. Several studies and clinical trials have shown that *H. perforatum* extracts possess an astounding array of pharmacological properties. The clinical efficacies of *H. perforatum* extracts in the therapy of mild to moderate depression have been confirmed in many studies (Lecrubier et al., 2002; Butterweck, 2003). Many other important pharmaceutical properties of *H. perforatum* including antiviral (Schinazi et al., 1990), anticancer (Agostinis et al., 2002), neuroprotective (Silva et al., 2004), antioxidant (Silva et al., 2005), and wound healing (Yadollah-Damavandi et al., 2015) activities have also been reported. Since treating humans and animals with *H. perforatum* extracts does not result in any serious adverse side effects (Trautmann-Sponsel and Dienel, 2004), use of this medicinal herb has increased dramatically during the past decade. Because of its well-established market position, popularity, and efficacy, *H. perforatum*

is reputed as one of the best-selling herbs today. *H. perforatum* products are currently sold as dietary supplements, anti-depressive agents, relaxants, and mood enhancers in many countries.

H. perforatum cell and tissue cultures have been attempted with the main focus being to produce pharmaceutically important compounds under controlled conditions. However, large-scale production of secondary metabolites could not be achieved so far using *in vitro* cultures due to low performance and unreliable yield of the products. Although, significant improvements in product yields have been achieved through conventional biochemical approaches combined with the manipulation of culture process, the results are not reproducible. Plant metabolic pathway engineering would allow us to improve the production of major compounds in *H. perforatum* by overexpressing specific genes. However, metabolic engineering of this genus has so far not been attempted due to the lack of an efficient transformation method.

Plant transformation is an indispensable tool for crop improvement, plant functional genomics, genome editing, synthetic biology, etc. (Sainsbury and Lomonosoff, 2014; Xu et al., 2014; Hwang et al., 2015; Nester, 2015). Success of transformation in non-model plants is generally based on two important principles: (1) foreign genes could be introduced into a plant cell through various methods and its genetic makeup could be altered and (2) plant cells are totipotent, which means in principle that every cell contains all the genetic information necessary to regenerate into a complete plant under optimal conditions. Therefore, the efficiency of gene delivery into target cells and the ability to recover plants from those transformed cells are the two major factors critically contributing to the recovery of transgenic plants. In spite of the availability of excellent regeneration methods via organogenesis and somatic embryogenesis in *H. perforatum*, the recovery of transgenic plants remains challenging. Although *Agrobacterium rhizogenes* and biolistics mediated transformation of *H. perforatum* has been reported, these protocols could not meet the vast needs of functional genomic research. *Agrobacterium tumefaciens* mediated transformation is the most preferred method of gene transfer due to frequent single copy transgene integration into the plant genome and low incidence of transgene silencing. The advantages of simplicity, affordable costs, lower transgenic rearrangement, ability for long DNA segment transfer, and preferential integration of foreign genes into transcriptionally active regions make *A. tumefaciens*-mediated transformation an attractive method (Kumar et al., 2013). Although this method could be useful for metabolic engineering and functional genomic studies in *H. perforatum*, plant recalcitrance against *A. tumefaciens* mediated transformation is a major concern. In this article, we discuss the present status and future perspectives of genetic transformation of *H. perforatum*.

CELLULAR TOTIPOTENCY OF *H. PERFORATUM*

Cellular totipotency of *H. perforatum* has been demonstrated in several reports. Originally, *in vitro* regeneration of *H. perforatum* has been investigated as an option for multiplication

of elite plants and production of valuable phytopharmaceuticals. In particular, the effect of plant growth regulator (PGR) combinations on secondary metabolite concentration has been intensively studied in cell and tissue culture. As a result, several methods of plant regeneration and micropropagation are available today.

Basically, *in vitro* plant regeneration of *H. perforatum* is relatively simple and quick. *In vitro* regeneration of *H. perforatum* has been achieved from several types of explants (Table 1), including whole seedlings (Cellarova et al., 1992), leaves (Pretto and Santarem, 2000; Pasqua et al., 2003; Franklin and Dias, 2006), nodal segments (Santarém and Astarita, 2003), root segments (Zobayed and Saxena, 2003; Franklin and Dias, 2006), hypocotyls (Murch et al., 2000; Franklin and Dias, 2006), stems (Zobayed and Saxena, 2003), shoot tips (Zobayed and Saxena, 2003), organogenic nodules derived from cell suspension culture (Franklin et al., 2007), and thin cell layers (Franklin and Dias, 2011). Root explants responded better than the shoot tip, leaf, hypocotyl, or stem explants in terms of thidiazuron-induced shoot organogenesis, whereas, the lowest number of regenerants was found in shoot tip explants (Zobayed and Saxena, 2003). Plants could be produced on medium augmented with various PGR combinations. Although the general requirement for shoot regeneration is a high cytokinin/auxin ratio in most species, *H. perforatum* showed efficient direct shoot regeneration on a low cytokinin/auxin ratio (Pasqua et al., 2003; Franklin and Dias, 2006). On the other hand, for callus mediated indirect shoot regeneration, *H. perforatum* needs a high cytokinin/auxin ratio. Interestingly, plants could be efficiently regenerated from root explants on basal medium (Franklin and Dias, 2006) and on medium supplemented with IAA (Goel et al., 2008).

Most of the regeneration studies are restricted to a single genotype (Murch et al., 2000; Pretto and Santarem, 2000; Zobayed and Saxena, 2003; Zobayed et al., 2004). We have established a genotype-independent plant regeneration protocol and elucidated the specific pathway of plant regeneration in *H. perforatum* (Franklin and Dias, 2006). There was no significant difference in the percentage of regeneration and number of shoots/explants between the tested genotypes indicating regeneration in *H. perforatum* is genotype independent. On the other hand, the explant type (hypocotyl, leaf, or root) had a significant effect on the regeneration of shoots (Franklin and Dias, 2006). Similar variation in the regeneration frequency of shoots based on explant types on the same thidiazuron concentration was also reported previously in *H. perforatum* (Zobayed and Saxena, 2003). Hence, from the results reported in the literature, *H. perforatum* regeneration response is clearly a PGR-driven explant-dependent phenomenon.

Age of the explant source also affected the regeneration potential of leaf, hypocotyl, and petal explants (Franklin and Dias, 2006; Goel et al., 2008). In contrast, age did not affect the morphogenetic potential of root segment explants (Franklin and Dias, 2006). Age-independent regeneration of root segments might be due to the high metabolic activity and faster cell division of roots due to continuous meristematic activity nearer to the root tip. Orientation of leaf explants on the medium also had a distinct effect on regeneration. While leaves with their adaxial side touching the medium exhibited high frequencies

TABLE 1 | *In vitro* plant regeneration of *H. perforatum*.

Explant	PGRs tested	Major result	References
Seedling	BA	Plant regeneration	Cellarova et al., 1992
Halved leaves	2,4-D, BA, KIN, IBA	Callus initiation and shoot organogenesis	Pretto and Santarem, 2000
Isolated anther	NAA, BA	Plant regeneration from isolated anthers	Murch and Saxena, 2002
Shoot tip, hypocotyl, root, and whole seedling	Thidiazuron, NAA, IBA, IAA	Best regeneration potential of root explants	Zobayed and Saxena, 2003
Leaf discs and stem segments	2,4-D, KIN	Leaf disks are better than stem segments for shoot regeneration	Ayan et al., 2005
Root, hypocotyl, and leaves from <i>in vitro</i> grown seedlings	BA, IAA	Organogenesis and embryogenesis in several genotypes	Franklin and Dias, 2006
Organogenic nodules obtained from cell suspension culture	BA, NAA	Plant regeneration	Franklin et al., 2007
<i>In vitro</i> grown roots	IAA, IBA, NAA, KIN	Established liquid culture medium most suitable for culturing roots	Goel et al., 2008
Nodal segments from <i>in vitro</i> grown shoots	BA	Used different liquid cultures, semisolid, partial immersion, paper bridge, and total immersion for shoot organogenesis	Savio et al., 2011
Petals	IAA, IBA, KIN	Shoot regeneration from petals dependent on age of buds	Palmer and Keller, 2011
Thin cell layers of organogenic nodules	BA, NAA	Regulation of shoot, root and root hair development by chlorogenic acid	Franklin and Dias, 2011

of regeneration, leaves with the opposite surface contacting the medium failed to show any response.

Generally, there are two important pathways leading to regeneration of a new plant from cultured explants, organogenesis, and somatic embryogenesis (**Figure 1**). A process in which an organ (e.g., shoot or root) is initiated and developed is known as organogenesis. On the other hand, the process of formation of an embryo, which is developed from somatic cells, is called somatic embryogenesis. While the emergence of a unipolar primordium or a bipolar embryo are the typical characteristics of organogenesis and somatic embryogenesis, respectively. During the above processes, if de-differentiation (callus formation) is involved, they are termed indirect regeneration.

In *H. perforatum* regeneration has been demonstrated *via* both embryogenesis and organogenesis in the same culture (Franklin and Dias, 2006). In this study, meristematic cells formed from the sub-epidermal layer developed into two functionally different globular structures simultaneously. The globular structures, which were attached to the explant developed into shoots, while the others detached from the explant underwent embryogenesis. Embryogenesis progressed from the globular embryos to the cotyledon stage *via* heart-shaped and torpedo-stage embryos. Cotyledonary embryos did not develop into plants as they failed to establish root systems. It should be noted that indirect regeneration is better suited for generating transgenic plants than direct regeneration, as the selection of transgenic callus is usually straightforward and allows efficient enrichment of transformed tissue before regeneration.

DNA DELIVERY INTO *H. PERFORATUM* PLANT CELLS

Agrobacterium Mediated Transformation

A. tumefaciens-mediated transformation is the most efficient and commonly used technique in plant genetic engineering. On the

other hand, hairy root cultures established by *A. rhizogenes*-mediated transformation often sustain stable productivity in hormone-free culture conditions resulting in large amounts of secondary metabolites accumulating (Oksman-Caldentey and Sévon, 2002).

Agrobacterium is called the “natural genetic engineer” because of its natural capacity to infect plants and introduce a piece of DNA (T-DNA) from its tumor inducing (Ti) or root inducing (Ri) plasmid into plant cells *via* a process known as “T-DNA transfer.” Once inside the plant cell, the T-DNA (transferred DNA) is transported into the nucleus where it stably integrates into the plant genome. T-DNA encodes genes for the synthesis of auxin, cytokinin, and opine. Hence, T-DNA integration into the host genome results in an imbalance of host cell auxin–cytokinin ratios, which leads to uncontrolled cell division and the development of crown gall or hairy roots and opine synthesis. Opines are used as the main food resource by *Agrobacterium*. With neither the T-DNA able to be transcribed in *Agrobacterium* nor opines metabolized by plants the T-DNA transfer process is a molecular niche for *Agrobacterium*’s survival. This natural process is evidenced in several plant species (e.g., rose, grape, stone fruit, pome, tomato) and considered as a disease. This disease causing T-DNA transfer process has been exploited as a tool to introduce genes into plants. Today, *A. tumefaciens*-mediated transformation is the preferred method for functional genomics because of its simplicity and frequent single copy transgene integration into the host genome.

Although *A. tumefaciens* mediated *H. perforatum* transformation has not yet been reported, induction of hairy roots after co-cultivation with *A. rhizogenes* has been reported (**Table 2**). Although strains ATCC 15834 and A4 strains could produce hairy roots, *A. rhizogenes* strain K599 did not induce hairy root formation (Santarem et al., 2008). On the other hand, *A. rhizogenes* strain like A4, LBA9402, could not induce hairy roots in *H. perforatum* cv. Helos (Franklin et al., 2007). The seemingly contradictory results between groups

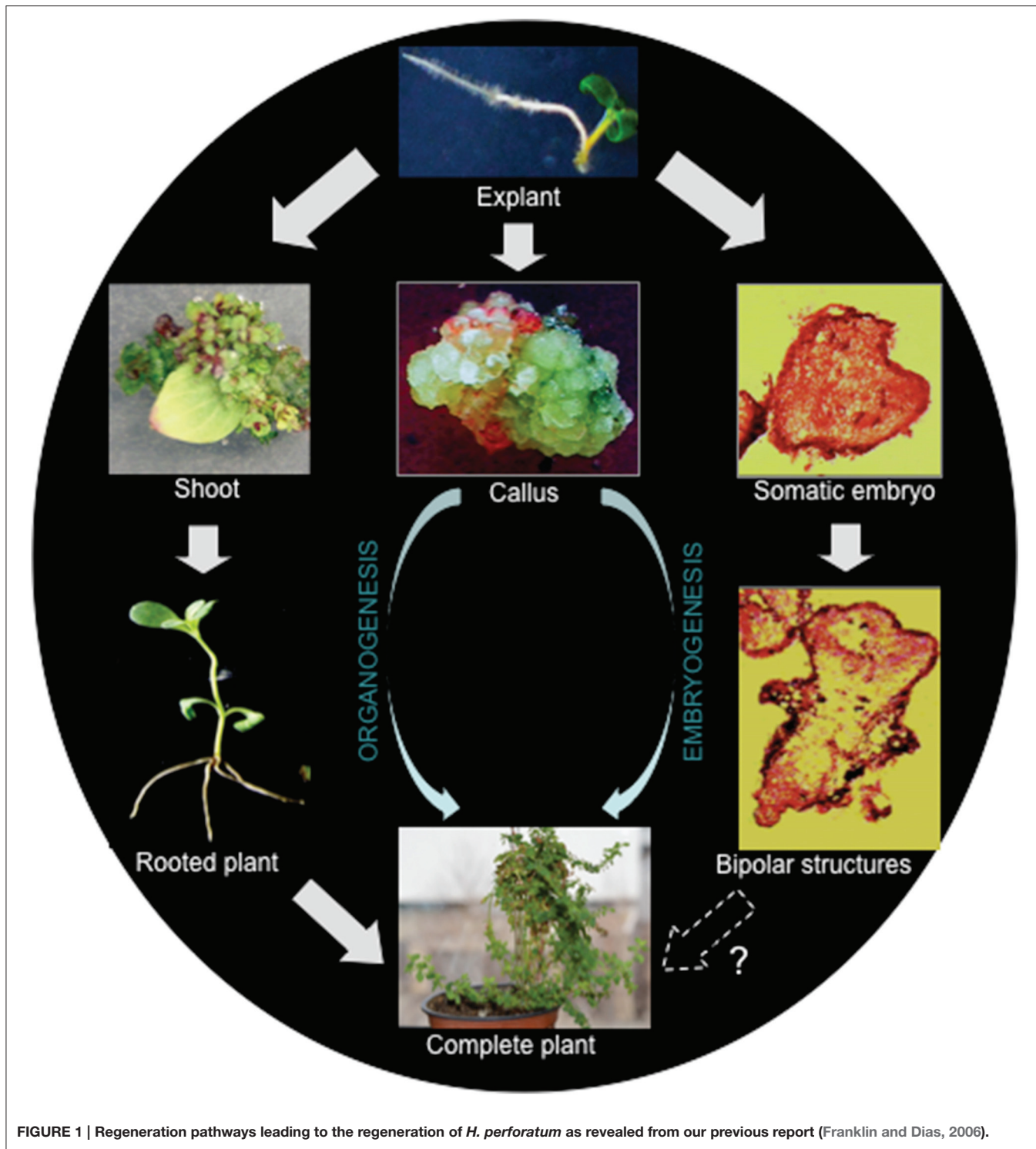


FIGURE 1 | Regeneration pathways leading to the regeneration of *H. perforatum* as revealed from our previous report (Franklin and Dias, 2006).

clearly emphasize the complexity of *A. rhizogenes* mediated transformation of *H. perforatum*.

Hairy root cultures could be established from *H. perforatum* epicotyls co-cultivated with *A. rhizogenes* strain A4 containing GUS (β -glucuronidase) gene inserted into the Ri plasmid pRiA4 (Vinterhalter et al., 2006). These hairy roots exhibited high

potential for spontaneous regeneration into whole transgenic plants. The presence of GUS gene in the hairy root and shoot cultures was determined by PCR analysis. Recently, this group studied the effect of sucrose concentration on shoot regeneration potential of *H. perforatum* hairy roots clones obtained from their previous study (Vinterhalter et al., 2006) and found that up to 2%

TABLE 2 | A. rhizogenes mediated transformation of *H. perforatum*.

<i>A. rhizogenes</i> strain	Explant	Molecular confirmation	References
ATCC 15834	Root and leaf	PCR and southern blot analysis of rolC gene	Di Guardo et al., 2003
A4	Epicotyls	PCR amplification of GUS gene	Vinterhalter et al., 2006
LBA9402 and A4	Root, leaf, epicotyl, and organogenic nodules	No hairy root induction	Franklin et al., 2007
ATCC 15834	Leaf and root fragments	PCR amplification of rolC gene	Bertoli et al., 2008
K599	Adventitious shoots	No hairy root induction	Santarem et al., 2008, 2010
A4	Root segments	PCR amplification of rolB and rolC genes	Tusevski et al., 2013b, 2014

sucrose promoted intense shoot regeneration (Vinterhalter et al., 2015).

Co-cultivation of root segments with *A. rhizogenes* strain A4 resulted in hairy root production of *H. perforatum* (Tusevski et al., 2013b, 2014). Transgenic nature of the hairy root cultures was demonstrated by PCR amplification of rolB gene in DNA isolated from the roots. These authors have also found several important secondary metabolites (phenolic acids, flavonol glycosides, flavonoid aglycones, flavan-3-ols, and xanthones) in hairy roots of *H. perforatum* (Tusevski et al., 2013b, 2014). This group has also compared the production of phenolic compounds between dark-grown hairy root cultures and those grown with a 16 h photoperiod, which revealed marked differences in phenolic acids, flavonols, flavan-3-ols, and xanthones between those cultures (Tusevski et al., 2013a). Similarly, hairy root clones with elevated levels of hyperoside, chlorogenic acid, and hypericin were obtained from leaf and root fragments co-cultivated with *A. rhizogenes* strain ATCC 15834 (Bertoli et al., 2008). Furthermore, hypericin was found at elevated levels in adventitious shoots of *H. perforatum* after co-cultivation with *A. rhizogenes* strain K599, despite the co-cultivation not resulting in hairy root formation (Santarem et al., 2008, 2010). Similarly, co-cultivation with *A. tumefaciens* and *A. rhizogenes* enhanced secondary metabolite production in *H. perforatum* cell suspension culture (Tusevski et al., 2015).

***H. perforatum* Recalcitrance to Agrobacterium Infection**

Neither *A. rhizogenes* (LBA9402 and A4) nor *A. tumefaciens* (LBA4404 and EHA105) could infect *H. perforatum* tissues in our studies. Various explants (leaf blade, petiole, stem, and root segments) were co-cultivated with *A. tumefaciens* and *A. rhizogenes* carrying a binary vector pCAMBIA1301 which carries the HPT (hygromycin phosphotransferase) gene as the selection marker and GUS interrupted with a eukaryotic intron (GUS-INT) as the reporter gene. The presence of an intron in the GUS gene permits gene expression only in eukaryotic cells such as plant cells. When assayed for transient GUS gene expression, none of the explants showed blue foci (Franklin et al., 2007). This was irrespective of vir gene induction or addition of an antioxidant (butylated hydroxytoluene, BHT), thiol compounds (cysteine), or ethylene inhibitors (AgNO_3 and aminoethoxyvinylglycine) to the co-cultivation medium. We presumed that antimicrobial secondary metabolites might be the reason for the inability of *Agrobacterium* to infect these explants.

In order to avoid antimicrobial compounds such as hypericins in the explants, we used organogenic nodule explants derived from cell suspension culture that lack hypericin glands (Franklin et al., 2007). Upon co-cultivation with *A. tumefaciens* or *A. rhizogenes*, these explants started to become brown within one day and subsequently become necrotic within 10 days. They did not show any transient GUS expression or callus formation when grown on selection medium containing antibiotic. On the other hand, under non-selective conditions, all the explants co-cultivated with *A. tumefaciens* and *A. rhizogenes* regained their normal growth within 5 days and produced calluses comparable to the control explants. In spite of the browning occurring after *Agrobacterium* co-cultivation, genomic DNA isolated from the explants did not show any fragmentation indicating that the incompatibility of *Agrobacterium*-mediated transformation in *H. perforatum* is not due to necrosis induced by programmed cell death as reported in maize (Hansen, 2000).

When the co-cultivation medium was augmented with BHT, two explants co-cultivated with *A. tumefaciens* strain EHA105 and one explant co-cultivated with *A. tumefaciens* strain LBA4404 showed blue foci in the GUS assay. Whereas, explants co-cultivated in the presence of other antioxidants and ethylene inhibitors as well as the shoots obtained from the calluses maintained in non-selective medium after co-cultivation did not show GUS gene expression. Even though the calluses obtained under non-selective conditions regenerated shoots as the control, none of them were transgenic. A number of plant species previously considered recalcitrant to *A. tumefaciens* became transformable upon supplementing antioxidants (Das et al., 2002; Frame et al., 2002) and ethylene inhibitors (Han et al., 2005; Petri et al., 2005; Seong et al., 2005) in the co-cultivation medium. This is mainly because of the fact that these scavengers could suppress the oxidative burst or ethylene production during plant-*Agrobacterium* interactions. However, in our case the tested antioxidants and ethylene inhibitors added to the co-cultivation medium neither prevented tissue browning nor favored transformation.

***H. perforatum* Plant Defense Response against Agrobacterium**

The mechanism of *H. perforatum* recalcitrance against *Agrobacterium* infection was studied using cell suspension cultures (Franklin et al., 2008, 2009a). Briefly, *H. perforatum* cell suspension culture was challenged with *A. tumefaciens* strain EHA105 and *A. rhizogenes* strain A4 both containing plasmid

pCAMBIA1301. After different post inoculation periods (0, 6, 12, and 24 h), both the plant cells and bacteria were analyzed. A typical biphasic ROS (reactive oxygen species) burst followed by darkening of *H. perforatum* cells was observed. In spite of ROS production *H. perforatum* cells did not undergo an obvious apoptotic process, while both *A. tumefaciens* and *A. rhizogenes* reached 99% mortality within 12 h of co-cultivation (Franklin et al., 2008). On the other hand, *A. tumefaciens* co-cultivation with tobacco BY2 cells under the same conditions lead to successful T-DNA transfer.

In addition to ROS production, genes encoding important enzymes of the phenylpropanoid pathway such as phenylalanine ammonia lyase (PAL), 4-coumarate:CoA ligase (4CL), and benzophenone synthase (BPS) were upregulated which would eventually lead to alteration of the profile of secondary metabolites. Analysis of the soluble phenolic fraction revealed an enormous increase in xanthone concentration and the emergence of many xanthones in *H. perforatum* cells after *Agrobacterium* co-cultivation was observed, while flavonoid content remained unaffected (Franklin et al., 2009a). Recently, we studied changes in *H. perforatum* cell wall fractions and cell wall bound phenolic compounds in response to *A. tumefaciens* elicitation (Singh et al., 2014). This study revealed that lignin content was significantly increased in *H. perforatum* cell walls after *A. tumefaciens* elicitation (0.085–0.24 mg/mg dry weight cell wall) implying that *H. perforatum* reinforced its cell wall as a protective measure against *A. tumefaciens* infection. Similarly, flavonoid (e.g., quercetin, quercetin etc.) content was also significantly higher in the cell walls of elicited cells compared to controls. Hence, in addition to PAL, 4CL, and BPS (Franklin et al., 2009a), chalcone synthase (CHS) is also upregulated after elicitation (Singh et al., 2014). While those xanthones produced in response to *A. tumefaciens* elicitation were incorporated into the soluble phenolic fraction, flavonoids were actually incorporated into the cell wall. This swift change in the secondary metabolites increased the cellular antioxidant and antimicrobial competence compared to the control cells revealing that this change plays a dual role in the plant cells; as antioxidants to protect the cells from oxidative damage and as phytoalexins to impair the pathogen growth upon *Agrobacterium* interaction.

Thus, we provided the first evidence for a typical oxidative burst combined with the upregulation of phenylpropanoid pathway genes in response to *Agrobacterium* co-cultivation, which could prevent T-DNA transfer. Recently, upregulation of a pathogenesis related 10 (PR10) gene (Sliwiak et al., 2015) in *H. perforatum* upon *A. tumefaciens* co-cultivation has been reported (Kosuth et al., 2013). Based on the above observations, we believe that recalcitrant plants could mobilize their antioxidant, antimicrobial and PR defense machinery against *Agrobacterium* (Figure 2).

Considering all the studies conducted so far in our laboratory and by others, the emerging depiction is that in both compatible and incompatible plant-*Agrobacterium* interactions, an initial defense response is induced. In the case of compatible interactions, despite the initial transient activation of basal host defense, the subsequent transfer of virulence factors might lead to the suppression of plant defense, resulting in successful

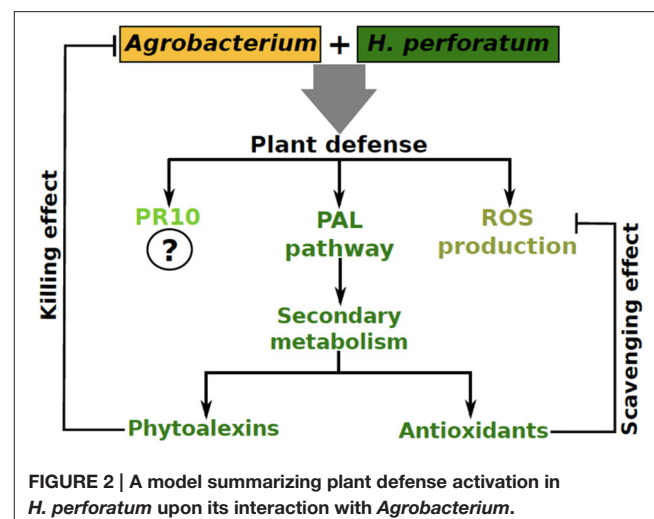


FIGURE 2 | A model summarizing plant defense activation in *H. perforatum* upon its interaction with *Agrobacterium*.

transformation as observed in tobacco (Veena et al., 2003; Franklin et al., 2008). By contrast, in incompatible interactions the initially evoked plant defense response is long lasting (and successful), therefore, affecting the bacterium and preventing T-DNA transfer into plant cells, as observed in *H. perforatum* (Franklin et al., 2008), making these plants recalcitrant to *Agrobacterium*-mediated transformation.

Biostatic-Mediated Transformation of *H. perforatum*

Biostatic technology (particle bombardment) is a useful technique used in the genetic manipulation of many crop improvement programs. In this method, the vector carrying the gene of interest is coated on metal particles and bombarded on target tissues with a high force/pressure by a biostatic device or gene gun (Kikkert et al., 2005). The biostatic method not only allows the expression of multiple transgenes in the target tissue, which can be achieved by fusion of genes within the same plasmid that is then bombarded into the target tissues, but also serves as an alternative method to achieve transient or stable transformation in *Agrobacterium* resistant plant species. In recent years, gene expression cassettes have been successfully transferred into many recalcitrant plant species (Guirimand et al., 2009; Liu et al., 2014; Sparks and Jones, 2014; Carqueijeiro et al., 2015; Zhang et al., 2015). The use of bombardment has made it easy to transfer large DNA fragments into the plant genome, though DNA integrity is a concern (Barampuram and Zhang, 2011).

With the biostatic technology, DNA-coated microparticles (gold or platinum) are accelerated directly into intact tissues by a physical process, thus avoiding the negative influence of *A. tumefaciens* components (elicitors), and genes can be delivered literally into any cell type. Upon reaching the nucleus, the DNA may be integrated, randomly, into the host genome. Since *H. perforatum* remains highly recalcitrant to *A. tumefaciens*-mediated genetic transformation (Franklin et al., 2007, 2008), we have used biostatic bombardment to transform this species (Figure 3). In this work, organogenic nodule explants obtained from cell suspension culture were used as the target

materials. The PDS-1000/He particle delivery system (Bio-Rad) was employed to introduce the HPT and GUS genes from the binary vector pCAMBIA1301 into *H. perforatum* tissue. After the selection of bombarded explants, hygromycin-resistant transgenic callus cultures and subsequently GUS positive plants were obtained. Molecular biology methods such as PCR and Southern blot analysis were used to analyze the transgenic nature of resulting plants. The results demonstrated for the first time that *H. perforatum* could be transformed and transgenic plants could be produced via biolistic bombardment of novel organogenic cell suspension cultures.

Genotype, physiological age, type of explant, culture period prior to and after gene transfer, culture medium composition, and osmotic pre-treatment were the key parameters affecting efficiency of particle bombardment-mediated transformation. Concerning the biolistic device, the acceleration pressure, the distance between rupture disc, macrocarrier, stopping screen, and target plate, the vacuum pressure in the bombardment chamber, number of bombardments as well as size and density of micro-particles, DNA-micro-particle mixing protocols, and physical configuration of transforming DNA all affected transformation efficiency.

FUTURE PERSPECTIVES AND STRATEGIES FOR *H. PERFORATUM* TRANSFORMATION

Improving the content of existing bioactive compounds (hypericin, hyperforin, xanthones, etc.) and the production of novel variants are the major targets of *H. perforatum* genetic engineering. Although overexpression of genes involved in the rate limiting biosynthetic steps would allow us to achieve the above goals, pathway engineering in this species is still in its infancy mainly due to the lack of genetic information about these biosynthetic pathways and due to the absence of an efficient transformation method. For instance, although hypericin was identified centuries ago, its biosynthetic pathway is not yet understood. Studies on the genes involved in hypericin biosynthesis have begun only recently and a systematic analysis of genes involved in hypericin biosynthesis has not yet been reported. A decade ago, hypericin biosynthesis was presumed to occur through the polyketide pathway in which type-III polyketide synthases act as key enzymes (Bais et al., 2003). Although a gene termed hyp1 was cloned from red suspension cells and claimed to be involved in the final steps of hypericin biosynthesis (Bais et al., 2003) recent studies contradict its involvement (Karppinen et al., 2008, 2010; Kosuth et al., 2011). The expression pattern of this gene does not correlate with hypericin production, as this gene is constitutively expressed in tissues (roots) and *Hypericum* species that do not produce hypericin (Kosuth et al., 2007). A recent study reported that hyp1 expression is not a limiting factor of hypericin biosynthesis in species that generally produce hypericin (Kosuth et al., 2011). Recently, *de novo* sequencing of *H. perforatum* transcriptomes generated a huge amount of genic data (He et al., 2012; Galla et al., 2015; Soták et al., 2016). In addition, taking advantage

of the strong correlation between the presence of dark glands and hypericin accumulation, we performed subtraction between cDNAs of tissues with and without hypericin glands to construct a hypericin gland-specific cDNA library (Singh et al., 2016).

Generally, gene functions can be predicted via both forward and reverse genetic approaches. *H. perforatum* possess a polyploid (tetraploid or hexaploid) genome in which genes are usually represented by two or three homoeologous copies with high sequence similarity. Since the effect of single-gene knockouts can generally be nullified by the functional redundancy of homoeologous genes present in the other genomes, forward genetic approaches such as mutagenesis would be inefficient. In plants with polyploid genomes, RNA interference (RNAi) is a valuable technique in which multiple homoeologs can be simultaneously down regulated. RNAi is a double-stranded RNA (dsRNA) induced gene-silencing phenomenon, conserved among various organisms, including animals and plants. RNAi technology has potential to block the activity of enzymes that are not only encoded by a multigene family but are also expressed across a number of tissues and developmental stages. This technology has been successfully used in the dissection of secondary metabolic pathways (Lin et al., 2015). Alternatively, short palindromic repeat (CRISPR)/CRISPR-associated protein (Cas9) system can be used to knockdown gene function (Xing et al., 2014). This system employs an RNA-guided nuclease, Cas9, to induce double-strand breaks. The Cas9-mediated breaks are repaired by cellular DNA repair mechanisms and mediate gene/genome modifications. Although employing the above techniques in *H. perforatum* would be useful to understand gene functions, the RNAi and CRISPR-Cas cassettes need to be introduced into *H. perforatum* genome, which necessitates a robust genetic transformation method. Another powerful reverse genetics approach, which combines chemical mutagenesis with a high-throughput screen for mutations, known as TILLING (Targeting Induced Local Lesions in Genomes) does not require genetic transformation. Although polyploids are well-suited for TILLING due to their tolerance to high mutation densities, this approach is time consuming, laborious and complicated in *H. perforatum* as seed formation in this species proved to be highly polymorphic (Matzke et al., 2001).

Although heterologous expression of secondary metabolic pathway genes has led to the successful production of many secondary metabolites in microbial systems, heterologous expression of *Hypericum*-specific pathways (e.g., hypericin biosynthesis) is currently limited by the lack of cloned genes encoding enzymes involved in the pathways of interest. Moreover, due to the potential toxicity of these compounds to plant tissues, they are accumulated in specialized dark glands. Hence, analyzing the functions of genes related to hypericin synthesis will only be possible in a system, which contain these glands.

Because of the above reasons, establishing an efficient *A. tumefaciens* mediated transformation protocol is unavoidable in order to promote *H. perforatum* functional genomics and metabolic engineering.

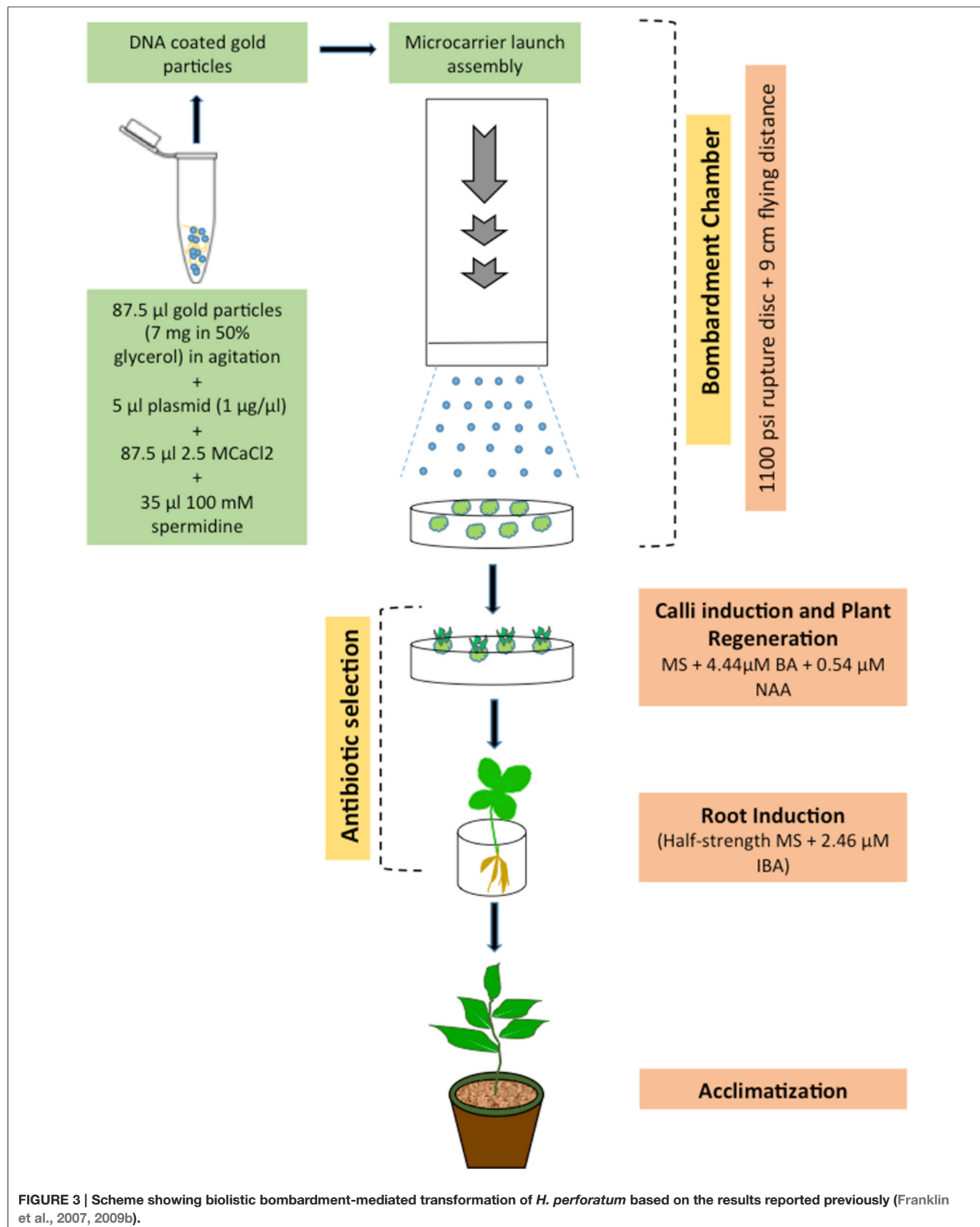


FIGURE 3 | Scheme showing biolistic bombardment-mediated transformation of *H. perforatum* based on the results reported previously (Franklin et al., 2007, 2009b).

Activation of plant defense is considered as a prevailing cause of plant recalcitrance against *Agrobacterium* infection (Franklin et al., 2008; Pitzschke, 2013). Hence, to achieve optimum gene delivery into *H. perforatum* cells via *Agrobacterium*, either suppressing or avoiding the elicitation of defense responses is essential.

A. tumefaciens-*H. perforatum* interaction results in the production of ROS. The consequences of the oxidative burst in plant defense responses could be suppressed by the addition of antioxidants such as ascorbic acid, cysteine, citric acid, polyvinylpolypyrrolidone (PVPP), polyvinylpyrrolidone (PVP), dithiothreitol (DTT), BHT, tocopherol, etc. However, it should be recalled that use of these compounds individually did not help in *H. perforatum* transformation in our previous attempts (Franklin et al., 2007). Nevertheless, application of a mixture of antioxidants could be useful, as it has been shown to improve the efficiency of *Agrobacterium*-mediated transformation in a number of other recalcitrant plant species (Dan, 2008; Dan et al., 2010, 2015). It is also important to understand the signaling events that trigger *H. perforatum* defense activation upon *Agrobacterium* interaction. Plant signaling pathways related to systemic resistance and secondary metabolism are involved in the successful activation of defense responses against *A. tumefaciens* (Yuan et al., 2007; Franklin et al., 2008). It should be noted that the involvement of salicylic acid (SA) in shutting down the expression of *A. tumefaciens vir* regulon and thereby directly impairing the infection process has been demonstrated (Yuan et al., 2007; Anand et al., 2008). Therefore, inhibiting the signaling pathways such as SA, methyl jasmonate (MeJ), jasmonic acid (JA), nitric oxide (NO), and the phenylpropanoid pathway using inhibitors [paclobutrazol,2-4-carboxyphenyl-4,4,5,5-tetramethylimidazoline-1-oxyl-3-oxide (cPTIO), 2-aminoindan-2-phosphonic acid (AIP), or diethyldithiocarbamate] would be able to improve the transformation rate.

In addition to the above plant defense suppressing strategies, plant defense response against *A. tumefaciens* could be bypassed by applying the following principles. Although *H. perforatum* remains recalcitrant to *Agrobacterium* mediated transformation (Franklin et al., 2007, 2008), we could successfully transform this plant and obtain transgenic plants via particle-bombardment-mediated transformation (Franklin et al., 2007, 2009b) suggesting that *H. perforatum* recalcitrance toward *A. tumefaciens* mediated transformation is conferred by the bacterial components. In spite of the presence of well-characterized pathogen-associated molecular patterns (PAMPs) in *A. tumefaciens* such as flagellin and EF-Tu, it is also known that not all plants respond to all elicitors (Felix and Boller, 2003; Kunze et al., 2004). Hence, it is crucial to identify the specific *A. tumefaciens* elicitors/PAMPs that are recognized by *H. perforatum* to activate its defense machinery, since *A. tumefaciens* devoid of elicitor function would be able to transform *H. perforatum* efficiently. However, it may not be possible to obtain elicitor mutants, if this mutation is lethal.

The plant cell wall plays a crucial role in sensing signals (e.g., wall associated receptor kinases), establishing basal host

defense, and serves as a major site of defense activation (Yeom et al., 2012). Presence of plant cell walls can be avoided by using protoplast transformation. Efficient isolation of viable protoplasts from *H. perforatum* and subsequent regeneration is possible (Pan et al., 2004). Taking advantage of the intimate lateral contact of *A. tumefaciens* with plant protoplasts via multiple virulent type IV secretion systems (Aguilar et al., 2011), *A. tumefaciens*-mediated T-DNA transfer can be performed (Wang et al., 2005). However, it is possible that protoplasts can produce ROS and soluble phenolics during the maceration process and in response to *A. tumefaciens*. Hence, the chemical inhibitors of the defense pathways and ROS scavengers can be used here, if required. Therefore, it may be possible to transform isolated protoplasts with *A. tumefaciens* at high efficiency. In addition, making use of the fluid-mosaic characteristics of protoplasts, naked DNA uptake methods such as polyethylene glycol (PEG) transfection and electroporation can be achieved (Hassanein et al., 2009), where both the plant cell walls as well as bacterial components are excluded.

Besides the above strategies, virus mediated transformation may be also employed. Viruses infecting *H. perforatum* (Kegler et al., 1999) and *H. japonicum* (Du et al., 2013) have been identified and characterized. Furthermore, nanoparticle mediated DNA delivery into plant cells is gaining momentum (Rai et al., 2015), which would also offer potential benefits in the genetic transformation of *H. perforatum* in the future.

Progress in the areas of *H. perforatum*-*Agrobacterium* interaction such as understanding the molecular mechanisms of *Agrobacterium* recognition and defense activation together with the novel strategies discussed here will allow us fully exploit and maximize the potential of this tremendously useful source of biotherapeutics.

AUTHOR CONTRIBUTIONS

GF conceived the idea of this review, designed the overall concept, and participated in the writing. WH and PS participated in the writing of the article and design tables and figures. All the authors approved the final version.

ACKNOWLEDGMENTS

GF and PS are financed from the BIOTALENT project (GA621321) funded by the European Union Seventh Framework Programme (FP7) ERA Chairs Pilot Call and co-financed by funds allocated for education through project no W26/7.PR/2015 [GA 3413/7.PR/2015/2] for the years 2015–2019. This work was partially supported by Fundação para a Ciência e a Tecnologia (FCT) project (PTDC/AGR-GPL/119211/2010). WH acknowledges the financial support provided by the FCT (SFRH/BD/52561/2014), under the Doctoral Programme “Agricultural Production Chains—from fork to farm” (PD/00122/2012).

REFERENCES

- Agostinis, P., Vantieghem, A., Merlevede, W., and De Witte, P. A. (2002). Hypericin in cancer treatment: more light on the way. *Int. J. Biochem. Cell Biol.* 34, 221–241. doi: 10.1016/S1357-2725(01)00126-1
- Aguilar, J., Cameron, T. A., Zupan, J., and Zambryski, P. (2011). Membrane and core periplasmic *Agrobacterium tumefaciens* virulence type IV secretion system components localize to multiple sites around the bacterial perimeter during lateral attachment to plant cells. *MBio* 2, e00218–e00211. doi: 10.1128/mBio.00218-11
- Anand, A., Uppalapati, S. R., Ryu, C. M., Allen, S. N., Kang, L., Tang, Y. H., et al. (2008). Salicylic acid and systemic acquired resistance play a role in attenuating crown gall disease caused by *Agrobacterium tumefaciens*. *Plant Physiol.* 146, 703–715. doi: 10.1104/pp.107.111302
- Ayan, A. K., Çirak, C., Kewseroglu, K., and Sökmen, A. (2005). Effects of explant types and different concentrations of sucrose and phytohormones on plant regeneration and hypericin content in *Hypericum perforatum* L. *Turkish J. Agric. Forestry* 29, 197–204.
- Bais, H. P., Vepachedu, R., Lawrence, C. B., Stermitz, F. R., and Vivanco, J. M. (2003). Molecular and biochemical characterization of an enzyme responsible for the formation of hypericin in St. John's Wort (*Hypericum perforatum* L.). *J. Biol. Chem.* 278, 32413–32422. doi: 10.1074/jbc.M301681200
- Barampuram, S., and Zhang, Z. J. (2011). Recent advances in plant transformation. *Methods Mol. Biol.* 701, 1–35. doi: 10.1007/978-1-61737-957-4_1
- Bertoli, A., Giovannini, A., Ruffoni, B., Guardo, A. D., Spinelli, G., Mazzetti, M., et al. (2008). Bioactive constituent production in St. John's wort *in vitro* hairy roots. Regenerated plant lines. *J. Agric. Food Chem.* 56, 5078–5082. doi: 10.1021/jf0729107
- Butterweck, V. (2003). Mechanism of action of St John's wort in depression - what is known? *CNS Drugs* 17, 539–562. doi: 10.2165/00023210-200317080-00001
- Carqueijeiro, I., Masini, E., Foureau, E., Sepulveda, L. J., Marais, E., Lanoue, A., et al. (2015). Virus-induced gene silencing in *Catharanthus roseus* by biolistic inoculation of tobacco rattle virus vectors. *Plant Biol. (Stuttgart)* 17, 1242–1246. doi: 10.1111/plb.12380
- Cellarova, E., Kimakova, K., and Brutovska, R. (1992). Multiple shoot formation and phenotypic changes of R0 regenerants in *Hypericum perforatum* L. *Acta Biotechnol.* 12, 445–452. doi: 10.1002/abio.370120602
- Dan, Y. (2008). Biological functions of antioxidants in plant transformation. *In Vitro Cell. Dev. Biol. Plant* 44, 149–161. doi: 10.1007/s11627-008-9110-9
- Dan, Y., Baxter, A., Zhang, S., Pantazis, C. J., and Veilleux, R. E. (2010). Development of efficient plant regeneration and transformation system for impatiens using *Agrobacterium tumefaciens* and multiple bud cultures as explants. *BMC Plant Biol.* 10:165. doi: 10.1186/1471-2229-10-165
- Dan, Y., Zhang, S., Zhong, H., Yi, H., and Sainz, M. B. (2015). Novel compounds that enhance *Agrobacterium*-mediated plant transformation by mitigating oxidative stress. *Plant Cell Rep.* 34, 291–309. doi: 10.1007/s00299-014-1707-3
- Das, D. K., Reddy, M. K., Upadhyaya, K. C., and Sopory, S. K. (2002). An efficient leaf-disc culture method for the regeneration via somatic embryogenesis and transformation of grape (*Vitis vinifera* L.). *Plant Cell Rep.* 20, 999–1005. doi: 10.1007/s00299-002-0441-4
- Di Guardo, A., Cellarova, E., Koperdáková, J., Pistelli, L., Ruffoni, B., Allavena, A., et al. (2003). Hairy root induction and plant regeneration in *Hypericum perforatum* L. *J. Genet. Breed.* 57, 269–278.
- Du, Z., Tang, Y., Zhang, S., She, X., Lan, G., Varsani, A., et al. (2013). Identification and molecular characterization of a single-stranded circular DNA virus with similarities to *Sclerotinia sclerotiorum* hypovirulence-associated DNA virus 1. *Arch. Virol.* 159, 1527–1531. doi: 10.1007/s00705-013-1890-5
- Felix, G., and Boller, T. (2003). Molecular sensing of bacteria in plants - the highly conserved RNA-binding motif RNP-1 of bacterial cold shock proteins is recognized as an elicitor signal in tobacco. *J. Biol. Chem.* 278, 6201–6208. doi: 10.1074/jbc.M209880200
- Frame, B. R., Shou, H. X., Chikwamba, R. K., Zhang, Z. Y., Xiang, C. B., Fonger, T. M., et al. (2002). *Agrobacterium tumefaciens*-mediated transformation of maize embryos using a standard binary vector system. *Plant Physiol.* 129, 13–22. doi: 10.1104/pp.000653
- Franklin, G., Conceição, L. F. R., Kombrink, E., and Dias, A. C. P. (2008). *Hypericum perforatum* plant cells reduce *Agrobacterium* viability during co-cultivation. *Planta* 227, 1401–1408. doi: 10.1007/s00425-008-0691-7
- Franklin, G., Conceição, L. F. R., Kombrink, E., and Dias, A. C. P. (2009a). Xanthone biosynthesis in *Hypericum perforatum* cells provides antioxidant and antimicrobial protection upon biotic stress. *Phytochemistry* 70, 60–68. doi: 10.1016/j.phytochem.2008.10.016
- Franklin, G., and Dias, A. C. P. (2006). Organogenesis and embryogenesis in several *Hypericum perforatum* genotypes. *In Vitro Cell. Dev. Biol. Plant* 42, 324–330. doi: 10.1079/IVP2006787
- Franklin, G., and Dias, A. C. P. (2011). Chlorogenic acid participates in the regulation of shoot, root and root hair development in *Hypericum perforatum*. *Plant Physiol. Biochem.* 49, 835–842. doi: 10.1016/j.plaphy.2011.05.009
- Franklin, G., Oliveira, M., and Dias, A. C. P. (2007). Production of transgenic *Hypericum perforatum* plants via particle bombardment-mediated transformation of novel organogenic cell suspension cultures. *Plant Sci.* 172, 1193–1203. doi: 10.1016/j.plantsci.2007.02.017
- Franklin, G., Oliveira, M. M., and Dias, A. C. (2009b). Transgenic *Hypericum perforatum*. *Methods Mol. Biol.* 547, 217–234. doi: 10.1007/978-1-60327-287-2_18
- Galla, G., Vogel, H., Sharbel, T. F., and Barcaccia, G. (2015). *De novo* sequencing of the *Hypericum perforatum* L. flower transcriptome to identify potential genes that are related to plant reproduction sensu lato. *BMC Genomics* 16:254. doi: 10.1186/s12864-015-1439-y
- Goel, M. K., Kukreja, A. K., and Bisht, N. S. (2008). *In vitro* manipulations in St. John's wort (*Hypericum perforatum* L.) for incessant and scale up micropropagation using adventitious roots in liquid medium and assessment of clonal fidelity using RAPD analysis. *Plant Cell Tissue Organ Cult.* 96, 1–9. doi: 10.1007/s11240-008-9453-2
- Guirimand, G., Burlat, V., Oudin, A., Lanoue, A., St-Pierre, B., and Courdavault, V. (2009). Optimization of the transient transformation of *Catharanthus roseus* cells by particle bombardment and its application to the subcellular localization of hydroxymethylbutenyl 4-diphosphate synthase and geraniol 10-hydroxylase. *Plant Cell Rep.* 28, 1215–1234. doi: 10.1007/s00299-009-0722-2
- Han, J. S., Kim, C. K., Park, S. H., Hirschi, K. D., and Mok, I. (2005). Agrobacterium-mediated transformation of bottle gourd (*Lagenaria siceraria* Standl.). *Plant Cell Rep.* 23, 692–698. doi: 10.1007/s00299-004-0874-z
- Hansen, G. (2000). Evidence for *Agrobacterium*-induced apoptosis in maize cells. *Mol. Plant Microbe Interact.* 13, 649–657. doi: 10.1094/MPMI.2000.13.6.649
- Hassanein, A., Hamama, L., Loridon, K., and Dorion, N. (2009). Direct gene transfer study and transgenic plant regeneration after electroporation into mesophyll protoplasts of *Pelargonium x hortorum*, 'Panache Sud'. *Plant Cell Rep.* 28, 1521–1530. doi: 10.1007/s00299-009-0751-x
- He, M., Wang, Y., Hua, W., Zhang, Y., and Wang, Z. (2012). *De novo* sequencing of *Hypericum perforatum* transcriptome to identify potential genes involved in the biosynthesis of active metabolites. *PLoS ONE* 7:e42081. doi: 10.1371/journal.pone.0042081
- Hwang, H. H., Galvin, S. B., and Lai, E. M. (2015). Editorial: "Agrobacterium biology and its application to transgenic plant production." *Front. Plant Sci.* 6:265. doi: 10.3389/fpls.2015.00265
- Karppinen, K., Hokkanen, J., Mattila, S., Neubauer, P., and Hohtola, A. (2008). Octaketide-producing type III polyketide synthase from *Hypericum perforatum* is expressed in dark glands accumulating hypericins. *FEBS J.* 275, 4329–4342. doi: 10.1111/j.1742-4658.2008.06576.x
- Karppinen, K., Taulavuori, E., and Hohtola, A. (2010). Optimization of protein extraction from *Hypericum perforatum* tissues and immunoblotting detection of Hyp-1 at different stages of leaf development. *Mol. Biotechnol.* 46, 219–226. doi: 10.1007/s12033-010-9299-9
- Kegler, H., Fuchs, E., Plescher, A., Ehrig, F., Schliephake, E., and Grünzig, M. (1999). Evidence and characterization of a virus of St John's Wort (*Hypericum perforatum* L.). *Arch. Phytopathol. Plant Prot.* 32, 205–221. doi: 10.1080/03235409909383290
- Kikkert, J. R., Vidal, J. R., and Reisch, B. I. (2005). Application of the biolistic method for grapevine genetic transformation. *Acta Hortic.* 689, 459–462. doi: 10.17660/ActaHortic.2005.689.54
- Kosuth, J., Hrehorova, D., Jaskolski, M., and Cellarova, E. (2013). Stress-induced expression and structure of the putative gene hyp-1 for hypericin biosynthesis. *Plant Cell Tissue Organ Cult.* 114, 207–216. doi: 10.1007/s11240-013-0316-0
- Kosuth, J., Katkovčinová, Z., Olešová, P., and Čellárová, E. (2007). Expression of the hyp-1 gene in early stages of development of *Hypericum perforatum* L. *Plant Cell Rep.* 26, 211–217. doi: 10.1007/s00299-006-0240-4

- Kosuth, J., Smelcerovic, A., Borsch, T., Zuehlke, S., Karppinen, K., Spiteller, M., et al. (2011). The *hyp-1* gene is not a limiting factor for hypericin biosynthesis in the genus *Hypericum*. *Funct. Plant Biol.* 38, 35–43. doi: 10.1071/FP10144
- Kumar, N., Gulati, A., and Bhattacharya, A. (2013). L-glutamine and L-glutamic acid facilitate successful Agrobacterium infection of recalcitrant tea cultivars. *Appl. Biochem. Biotechnol.* 170, 1649–1664. doi: 10.1007/s12010-013-0286-z
- Kunze, G., Zipfel, C., Robatzek, S., Niehaus, K., Boller, T., and Felix, G. (2004). The N terminus of bacterial elongation factor Tu elicits innate immunity in *Arabidopsis* plants. *Plant Cell* 16, 3496–3507. doi: 10.1105/tpc.104.026765
- Lecrubier, Y., Clerc, G., Didi, R., and Kieser, M. (2002). Efficacy of St. John's wort extract WS 5570 in major depression: a double-blind, placebo-controlled trial. *Am. J. Psychiatry* 159, 1361–1366. doi: 10.1176/appi.ajp.159.8.1361
- Lin, C. Y., Wang, J. P., Li, Q., Chen, H. C., Liu, J., Loziuk, P., et al. (2015). 4-coumaroyl and caffeoyl shikimic acids inhibit 4-coumaric acid:coenzyme A ligases and modulate metabolic flux for 3-hydroxylation in monolignol biosynthesis of *Populus trichocarpa*. *Mol. Plant* 8, 176–187. doi: 10.1016/j.molp.2014.12.003
- Liu, G., Campbell, B. C., and Godwin, I. D. (2014). Sorghum genetic transformation by particle bombardment. *Methods Mol. Biol.* 1099, 219–234. doi: 10.1007/978-1-62703-715-0_18
- Matzka, F., Meister, A., Brutovská, R., and Schubert, I. (2001). Reconstruction of reproductive diversity in *Hypericum perforatum* L. opens novel strategies to manage apomixis. *Plant J.* 26, 275–282. doi: 10.1046/j.1365-313x.2001.01026.x
- Murch, S. J., Choffe, K. L., Victor, J. M. R., Slimmon, T. Y., Krishnaraj, S., and Saxena, P. K. (2000). Thidiazuron-induced plant regeneration from hypocotyl cultures of St. John's wort (*Hypericum perforatum*, cv 'Anthos'). *Plant Cell Rep.* 19, 576–581. doi: 10.1007/s002990050776
- Murch, S. J., and Saxena, P. K. (2002). Mammalian neurohormones: potential significance in reproductive physiology of St. John's wort (*Hypericum perforatum* L.)? *Naturwissenschaften* 89, 555–560. doi: 10.1007/s00114-002-0376-1
- Nester, E. W. (2015). *Agrobacterium*: nature's genetic engineer. *Front. Plant Sci.* 5:730. doi: 10.3389/fpls.2014.00730
- Oksman-Caldentey, K. M., and Sévon, N. (2002). *Agrobacterium rhizogenes*-mediated transformation: root cultures as a source of alkaloids. *Planta Med.* 68, 859–868. doi: 10.1055/s-2002-34924
- Palmer, C. D., and Keller, W. A. (2011). Plant regeneration from petal explants of *Hypericum perforatum* L. *Plant Cell Tissue Organ Cult.* 105, 129–134. doi: 10.1007/s11240-010-9839-9
- Pan, Z. G., Liu, C. Z., Murch, S. J., and Saxena, P. K. (2004). 2004 SIVB congress symposium proceedings "Thinking Outside the Cell": optimized chemodiversity in protoplast-derived lines of St. John's Wort (*Hypericum perforatum* L.). *In Vitro Cell. Dev. Biol. Plant* 41, 226–231. doi: 10.1079/IVP2004635
- Pasqua, G., Avato, P., Monacelli, B., Santamaria, A. R., and Argentieri, M. P. (2003). Metabolites in cell suspension cultures, calli, and *in vitro* regenerated organs of *Hypericum perforatum* cv. Topas. *Plant Sci.* 165, 977–982. doi: 10.1016/S0168-9452(03)00275-9
- Petri, C., Alburquerque, N., Perez-Tornero, O., and Burgos, L. (2005). Auxin pulses and a synergistic interaction between polyamines and ethylene inhibitors improve adventitious regeneration from apricot leaves and *Agrobacterium*-mediated transformation of leaf tissues. *Plant Cell Tissue Organ Cult.* 82, 105–111. doi: 10.1007/s11240-004-7013-y
- Pitzschke, A. (2013). *Agrobacterium* infection and plant defense-transformation success hangs by a thread. *Front. Plant Sci.* 4:519. doi: 10.3389/fpls.2013.00519
- Pretto, F. R., and Santarem, E. R. (2000). Callus formation and plant regeneration from *Hypericum perforatum* leaves. *Plant Cell Tissue Organ Cult.* 62, 107–113. doi: 10.1023/A:1026534818574
- Rai, M., Bansod, S., Bawaskar, M., Gade, A., Santos, C. A., Seabra, A. B., et al. (2015). "Nanoparticles-based delivery systems in plant genetic transformation," in *Nanotechnologies in Food and Agriculture*, eds M. Rai, C. Ribeiro, L. Mattoso and N. Duran (Cham: Springer International Publishing), 209–239.
- Sainsbury, F., and Lomonossoff, G. P. (2014). Transient expressions of synthetic biology in plants. *Curr. Opin. Plant Biol.* 19, 1–7. doi: 10.1016/j.pbi.2014.02.003
- Santarém, E. R., and Astarita, L. V. (2003). Multiple shoot formation in *Hypericum perforatum* L. and hypericin production. *Brazilian J. Plant Physiol.* 15, 43–47. doi: 10.1590/S1677-04202003000100006
- Santarem, E. R., Zamban, D. C., Felix, L. M., and Astarita, L. V. (2008). Secondary metabolism of *Hypericum perforatum* induced by *Agrobacterium rhizogenes*. *In Vitro Cell. Dev. Biol. Anim.* 44, S52.
- Santarem, E., Silva, T., Freitas, K., Sartori, T., and Astarita, L. (2010). *Agrobacterium rhizogenes* and salicylic acid trigger defense responses in *Hypericum perforatum* shoots. *In Vitro Cell. Dev. Biol. Anim.* 46, S159–S160.
- Savio, L. E. B., Astarita, L. V., and Santarem, E. R. (2011). Secondary metabolism in micropropagated *Hypericum perforatum* L. grown in non-aerated liquid medium. *Plant Cell, Tissue Organ Cult. (PCTOC)* 108, 465–472. doi: 10.1007/s11240-011-0058-9
- Schinazi, R. F., Chu, C. K., Babu, J. R., Oswald, B. J., Saalmann, V., Cannon, D. L., et al. (1990). Anthraquinones as a new class of antiviral agents against human immunodeficiency virus. *Antiviral Res.* 13, 265–272. doi: 10.1016/0166-3542(90)90071-E
- Seong, E. S., Song, K. J., Jegal, S., Yu, C. Y., and Chung, I. M. (2005). Silver nitrate and aminoethoxyvinylglycine affect *Agrobacterium*-mediated apple transformation. *Plant Growth Regul.* 45, 75–82. doi: 10.1007/s10725-004-4126-y
- Silva, B. A., Dias, A. C., Ferreres, F., Malva, J. O., and Oliveira, C. R. (2004). Neuroprotective effect of *H. perforatum* extracts on beta-amyloid-induced neurotoxicity. *Neurotox Res.* 6, 119–130. doi: 10.1007/BF03033214
- Silva, B. A., Ferreres, F., Malva, J. O., and Dias, A. C. P. (2005). Phytochemical and antioxidant characterization of *Hypericum perforatum* alcoholic extracts. *Food Chem.* 90, 157–167. doi: 10.1016/j.foodchem.2004.03.049
- Singh, R. K., Hou, W., and Franklin, G. (2016). Hypericin gland-specific cDNA library via suppression subtractive hybridization. *Methods Mol. Biol.* 1391, 317–334. doi: 10.1007/978-1-4939-3332-7_22
- Singh, R. K., Hou, W., Marslin, G., Dias, A. C. P., and Franklin, G. (2014). Lignin and flavonoid content increases in *Hypericum perforatum* cell wall after *Agrobacterium tumefaciens* co-cultivation. *Planta Med.* 80, 1388–1388. doi: 10.1055/s-0034-1394589
- Sliwiak, J., Dauter, Z., Kowiel, M., McCoy, A. J., Read, R. J., and Jaskolski, M. (2015). ANS complex of St John's wort PR-10 protein with 28 copies in the asymmetric unit: a fiendish combination of pseudosymmetry with tetrahedral twinning. *Acta Crystallogr. D Biol. Crystallogr.* 71, 829–843. doi: 10.1107/S1399004715001388
- Soták, M., Czeranková, O., Klein, D., Nigutová, K., Altschmied, L., Li, L., et al. (2016). Differentially expressed genes in hypericin-containing *Hypericum perforatum* leaf tissues as revealed by *de novo* assembly of RNA-Seq. *Plant Mol. Biol. Rep.* doi: 10.1007/s11105-016-0982-2. [Epub ahead of print].
- Sparks, C. A., and Jones, H. D. (2014). Genetic transformation of wheat via particle bombardment. *Methods Mol. Biol.* 1099, 201–218. doi: 10.1007/978-1-62703-715-0_17
- Trautmann-Sponsel, R. D., and Dienel, A. (2004). Safety of *Hypericum* extract in mildly to moderately depressed outpatients - a review based on data from three randomized, placebo-controlled trials. *J. Affect. Disord.* 82, 303–307. doi: 10.1016/j.jad.2003.12.017
- Tusevski, O., Petreska Stanoeva, J., Stefova, M., Pavokovic, D., and Gadzovska Simic, S. (2014). Identification and quantification of phenolic compounds in *Hypericum perforatum* L. transgenic shoots. *Acta Physiol. Plant.* 36, 2555–2569. doi: 10.1007/s11738-014-1627-4
- Tusevski, O., Petreska Stanoeva, J., Stefova, M., and Simic, S. G. (2013a). Phenolic profile of dark-grown and photoperiod-exposed *Hypericum perforatum* L. hairy root cultures. *Scientific World J.* 2013, 9. doi: 10.1155/2013/602752
- Tusevski, O., Stanoeva, J. P., Stefova, M., Kungulovski, D., Pancevska, N. A., Sekulovski, N., et al. (2013b). Hairy roots of *Hypericum perforatum* L.: a promising system for xanthone production. *Cent. Eur. J. Biol.* 8, 1010–1022. doi: 10.2478/s11535-013-0224-7
- Tusevski, O., Stanoeva, J., Stefova, M., and Simic, S. G. (2015). Agrobacterium enhances xanthone production in *Hypericum perforatum* cell suspensions. *Plant Growth Regul.* 76, 199–210. doi: 10.1007/s10725-014-9989-6
- Veena, Jiang, H. M., Doerge, R. W., and Gelvin, S. B. (2003). Transfer of T-DNA and Vir proteins to plant cells by *Agrobacterium tumefaciens* induces expression of host genes involved in mediating transformation and suppresses host defense gene expression. *Plant J.* 35, 219–236. doi: 10.1046/j.1365-313X.2003.01796.x

- Vinterhalter, B., Ninkovic, S., Cingel, A., and Vinterhalter, D. (2006). Shoot and root culture of *Hypericum perforatum* L. transformed with *Agrobacterium rhizogenes* A4M70GUS. *Biol. Plant.* 50, 767–770. doi: 10.1007/s10535-006-0127-9
- Vinterhalter, B., Zdravković-Korač, S., Mitić, N., Bohanec, B., Vinterhalter, D., and Savić, J. (2015). Effect of sucrose on shoot regeneration in *Agrobacterium* transformed *Hypericum perforatum* L. roots. *Acta Physiol. Plant.* 37, 1–12. doi: 10.1007/s11738-015-1785-z
- Wang, Y. P., Sonntag, K., Rudloff, E., and Han, J. (2005). Production of fertile transgenic *Brassica napus* by *Agrobacterium*-mediated transformation of protoplasts. *Plant Breed.* 124, 1–4. doi: 10.1111/j.1439-0523.2004.01015.x
- Xing, H. L., Dong, L., Wang, Z. P., Zhang, H. Y., Han, C. Y., Liu, B., et al. (2014). A CRISPR/Cas9 toolkit for multiplex genome editing in plants. *BMC Plant Biol.* 14:327. doi: 10.1186/s12870-014-0327-y
- Xu, R. F., Li, H., Qin, R. Y., Wang, L., Li, L., Wei, P. C., et al. (2014). Gene targeting using the *Agrobacterium tumefaciens*-mediated CRISPR-Cas system in rice. *Rice* 7:5. doi: 10.1186/s12284-014-0005-6
- Yadollah-Damavandi, S., Chavoshi-Nejad, M., Jangholi, E., Nekouyan, N., Hosseini, S., Seifaei, A., et al. (2015). Topical *Hypericum perforatum* improves tissue regeneration in full-thickness excisional wounds in diabetic rat model. *Evid. Based Complement. Alternat. Med.* 2015:245328. doi: 10.1155/2015/245328
- Yeom, S. I., Seo, E., Oh, S. K., Kim, K. W., and Choi, D. (2012). A common plant cell-wall protein HyPRP1 has dual roles as a positive regulator of cell death and a negative regulator of basal defense against pathogens. *Plant J.* 69, 755–768. doi: 10.1111/j.1365-313X.2011.04828.x
- Yuan, Z. C., Edlind, M. P., Liu, P., Saenkham, P., Banta, L. M., Wise, A. A., et al. (2007). The plant signal salicylic acid shuts down expression of the vir regulon and activates quormone-quenching genes in *Agrobacterium*. *Proc. Natl. Acad. Sci. U.S.A.* 104, 11790–11795. doi: 10.1073/pnas.0704866104
- Zhang, K., Liu, J., Zhang, Y., Yang, Z., and Gao, C. (2015). Biolistic genetic transformation of a wide range of Chinese elite wheat (*Triticum aestivum* L) varieties. *J. Genet. Genomics* 42, 39–42. doi: 10.1016/j.jgg.2014.11.005
- Zobayed, S. M. A., Murch, S. J., Rupasinghe, H. P. V., and Saxena, P. K. (2004). *In vitro* production and chemical characterization of St. John's wort (*Hypericum perforatum* L. cv 'New Stem'). *Plant Sci.* 166, 333–340. doi: 10.1016/j.plantsci.2003.10.005
- Zobayed, S. M. A., and Saxena, P. K. (2003). *In vitro*-grown roots: a superior explant for prolific shoot regeneration of St. John's wort (*Hypericum perforatum* L. cv 'New Stem') in a temporary immersion bioreactor. *Plant Sci.* 165, 463–470. doi: 10.1016/S0168-9452(03)00064-5

Conflict of Interest Statement: The authors declare that the research was conducted in the absence of any commercial or financial relationships that could be construed as a potential conflict of interest.

Copyright © 2016 Hou, Shakya and Franklin. This is an open-access article distributed under the terms of the Creative Commons Attribution License (CC BY). The use, distribution or reproduction in other forums is permitted, provided the original author(s) or licensor are credited and that the original publication in this journal is cited, in accordance with accepted academic practice. No use, distribution or reproduction is permitted which does not comply with these terms.

Advantages of publishing in Frontiers



OPEN ACCESS

Articles are free to read,
for greatest visibility



COLLABORATIVE PEER-REVIEW

Designed to be rigorous
– yet also collaborative,
fair and constructive



FAST PUBLICATION

Average 85 days from
submission to publication
(across all journals)



COPYRIGHT TO AUTHORS

No limit to article
distribution and re-use



TRANSPARENT

Editors and reviewers
acknowledged by name
on published articles



SUPPORT

By our Swiss-based
editorial team



IMPACT METRICS

Advanced metrics
track your article's impact



GLOBAL SPREAD

5'100'000+ monthly
article views
and downloads



LOOP RESEARCH NETWORK

Our network
increases readership
for your article

Frontiers

EPFL Innovation Park, Building I • 1015 Lausanne • Switzerland
Tel +41 21 510 17 00 • Fax +41 21 510 17 01 • info@frontiersin.org
www.frontiersin.org

Find us on

